كلية العلوم و التقنيات فاس
ⵜⴰⵖⵉⵡⴰⵏⵜ ⵏ ⵜⵎⴰⵙⵙⴰⵏⵉⵏ ⴷ ⵜⵙⵏⵉⴳⵉⵜⵉⵏ
Faculté des Sciences et Techniques de Fès

جامعة سيدي محمد بن عبد الله
ⵜⴰⵙⴷⴰⵡⵉⵜ ⵙⵉⴷⵉ ⵎⵓⵃⵎⵎⴰⴷ ⴱⵏ ⵄⴱⴷⵓⵍⵍⴰⵀ
Université Sidi Mohamed Ben Abdellah

Centre d'Etudes Doctorales : Sciences et Techniques de l'Ingénieur

76 /2021

THESE DE DOCTORAT

Présentée par

Mr : DANOUCHE MOHAMMED

Spécialité : Biotechnologies

Sujet de la thèse : Bioremédiation des polluants (in)organiques par des microalgues et des levures : Caractérisation des interactions physico-chimiques, des réponses biochimiques et enzymatiques et profilage métabolomique.

Formation Doctorale : Sciences et Génie de la matière, de la Terre et de la Vie.

Thèse présentée et soutenue le samedi 23 octobre 2021 à 10h au Centre de conférences devant le jury composé de :

Nom Prénom	Titre	Etablissement	
Pr. IBNSOUDA KORAICHI Saad	PES	Faculté des Sciences et Techniques, Université Sidi Mohamed Ben Abdellah – Fès	Président
Pr. BOUKIR Abdellatif	PES	Faculté des Sciences et Techniques, Université Sidi Mohamed Ben Abdellah – Fès	Rapporteur
Pr. BOULARBAH Ali	PES	Faculté des Sciences et Techniques, Université Cadi Ayyad - Marrakech	Rapporteur
Pr. SMOUNI Abdelaziz	PH	Faculté des sciences, Université Mohamed V - Rabat	Rapporteur
Pr. OUKARROUM Abdallah	PH	Université Mohammed VI Polytechnique Ben-guérir	Examinateur
Pr. EL ABED Soumya	PH	Faculté des Sciences et Techniques, Université Sidi Mohamed Ben Abdellah – Fès	Examinateur
Pr. BAHAFID Wifak	PH	Faculté des Sciences et Techniques, Université Sidi Mohamed Ben Abdellah – Fès	Examinateur
Pr. EL GHACHTOULI Naïma	PES	Faculté des Sciences et Techniques, Université Sidi Mohamed Ben Abdellah – Fès	Directeur de thèse
Dr. EL ARROUSSI Hicham	Expert	Green Biotechnology, MAScIR Rabat	Invité

Laboratoire d'accueil : Biotechnologie Microbienne & Molécules Bioactives (BM2B)

Etablissement : Faculté des Sciences et Techniques de Fès

AVANT-PROPOS

Cette thèse a été co-dirigée par Pr. **EL GHACHTOULI Naïma** du Laboratoire de Biotechnologie Microbienne & Molécules Bioactives (LBM2B) de la Faculté des Sciences et Techniques de Fès, Université Sidi Mohammed ben Abdellah et par Dr. **EL ARROUSSI Hicham**, chercheur au centre de Biotechnologie Végétale (BioV) de la fondation MAScIR (Moroccan Foundation for Advanced Science, Innovation and Research). Les travaux de recherche qui font l'objet de cette thèse ont été effectués entre 2018 et 2021 dans les deux laboratoires.

CONTEXTE

De nos jours, la protection de l'environnement est devenue un enjeu économique et politique majeur. Un volet important et vital concerne la préservation des ressources en eaux. En effet, ces dernières sont menacées par une pollution diffuse et multiforme aggravée par le progrès dans le bien-être de l'homme, l'industrialisation et la démographie galopante. Le Maroc comme tous les pays du monde n'échappe pas à cette réalité. Au cours de ces dernières décennies, il a connu un développement exponentiel touchant tous les secteurs d'activités. Cette situation a entraîné en revanche plusieurs problèmes environnementaux, au premier rang desquels se place la pollution des eaux par des contaminants d'origine industrielle. Pour répondre à cette faille, le Maroc a l'instar des pays bien avancés au niveau de la protection de l'environnement, a promulgué des lois, qui contraindraient les industriels en fonction de leur activité à s'équiper d'unités de traitement des eaux usées afin de diminuer la charge polluante, ou bien de payer des redevances (Ecotaxe). Selon le ministère de l'industrie, du commerce et de l'économie verte, le secteur du textile comprend plus de 1075 entreprises, qui représentent 5 % de la production du secteur industriel marocain. Ce secteur est répertorié parmi les industries les plus consommatrices d'eau, générant ainsi de grands volumes de rejets liquides caractérisés par une charge élevée en polluants de nature organique et inorganique. A titre d'exemple, il est estimé qu'à partir du 70 % des colorants utilisé dans ce secteur, environ 10 à 15 % sont rejetés dans les effluents (Saratale et al. 2011). En outre, les métaux lourds sont souvent utilisés dans diverses applications industrielles, notamment dans la fabrication de textiles et de cuire, de par leur capacité à fixer les colorants sur les tissus en formant des complexes stables et résistants aux attaques chimiques et biologiques. Par conséquent, le rejet de ces xénobiotiques dans l'environnement naturel est une source alarmante de contamination.

Diverses méthodes physico-chimiques sont utilisées pour éliminer les colorants et/ou les métaux lourds de l'eau. Cependant, elles se sont avérées coûteuses et nécessitent généralement des équipements sophistiqués. De même, certains sous-produits de la transformation chimique des polluants organiques sont parfois plus toxiques que leurs molécules d'origine. Ce constat a poussé les chercheurs à évaluer l'utilisation potentielle des bioprocédés dans le traitement des eaux usées, vu qu'ils sont à la fois moins coûteux et respectueux de l'environnement. Le sujet de cette thèse s'inscrit dans ce contexte, tout en exploitant les potentialités biotechnologiques de la diversité microbienne des organismes autotrophes (microalgues) et hétérotrophes (levures) en vue de développement des bioprocédés de traitement des polluants organiques et/ou métalliques. Ce travail de thèse a permis de produire des publications dans des revues scientifiques de renommée, y compris quatre revues de littérature, quatre articles de recherche, deux chapitres de livres, ainsi que des communications orales et affichées dans des conférences nationales et internationales.

PUBLICATIONS

1. **Danouche, M**., El Ghachtouli, N., El Baouchi, A., Arroussi, H., (2020). Heavy metals phycoremediation using tolerant green microalgae: Enzymatic and non-enzymatic antioxidant systems for the management of oxidative stress. *J. Environ. Chem. Eng.* 104460. https://doi.org/10.1016/j.jece.2020.104460 (ISSN: 22133437; **Q1**, FI_{2020} = **5.7**, H-INDEX = 72; **Elsevier**)

2. **Danouche, M**., El Ghachtouli, N., El Arroussi, H., (2021). Phycoremediation mechanisms of heavy metals using living green microalgae: physicochemical and molecular approaches for enhancing selectivity and removal capacity. *Heliyon* 7, e07609. https://doi.org/10.1016/j.heliyon.2021.e07609 (ISSN: 2405844; **Q1**, FI_{2020} = **2.8**, H-INDEX =28; **CellPress**)

3. **Danouche, M.,** El Arroussi, H., Bahafid, W., & El Ghachtouli, N. (2021). An overview of the biosorption mechanism for the bioremediation of synthetic dyes using yeast cells. *Environmental Technology Reviews*,*10*(1), 58-76.https://doi.org/10.1080/21622515.2020.1869839 (ISSN: 21622515; **Q1**, FI_{2020} = **4.8**, H-INDEX =19; **Taylor & Francis**)

4. **Danouche, M.,** EL Arroussi, H., & El Ghachtouli, N. (2021). Mycoremediation of synthetic dyes by yeast cells: a sustainable biodegradation approach. *Environmental Sustainability*, 1-18. https://doi.org/10.1007/s42398-020-00150-w (ISSN: 2523-8922; FI_{2020} = NA, H-INDEX =NA; **Springer**)

5. **Danouche, M.,** Ferioun, M., Bahafid, W., & El Ghachtouli, N. (2020). Mycoremediation of azodyes using *Cyberlindnera fabianii* yeast strain: Application of designs of experiments for decolorization optimization. *Water Environment Research*. https://doi.org/10.1002/wer.1499 **(**ISSN:10614303; **Q3**; FI_{2020} = **1.7,** H-INDEX =73; **Wiley)**

6. Mutale-joan, C., Rachidi, F., Mohamed, H. A., Mernissi, N. E., Aasfar, A., Barakate, M., Sbabou, L., **Danouche, M** & Arroussi, H. E. (2021). Microalgae-cyanobacteria–based biostimulant effect on salinity tolerance mechanisms, nutrient uptake, and tomato plant growth under salt stress. *Journal of Applied Phycology*, https://doi.org/1-17. 10.1007/s10811-021-02559-0 (ISSN: 09218971; **Q2**, FI2020 = 3.9, H-INDEX = 108; **Springer**)

7. **Danouche, M.,** El Ghachtouli, N. & El Arroussi, H. (2021). Overview of the management of heavy metal toxicity by microalgae through biochemical, enzymatic and phycohormonal mechanisms. *Journal of Applied Phycology*. (ISSN: 09218971; **Q1**, FI_{2020} = 3**.1**, H-INDEX = 108; **Springer**).(Révision mineure).

8. **Danouche, M.,** El Ghachtouli, N., Aasfar, A., bennis I., & El Arroussi, H., (2021). Mechanisms of lead (II) phycoremediation using *Scenedesmus obliquus*: Cells physicochemical properties, biochemical composition and metabolomic profiling. *International journal of phytoremediation* (ISSN: 15226514; **Q2**, FI_{2020}= 3.2, H-INDEX =84;**Taylor & Francis**).(Sous révision)

9. **Danouche, M.,** El Arroussi, H., & El Ghachtouli, N. (2021). Mycoremediation of the azo dye Acid Red 14 by *Wickerhamomyces anomalus*: Physicochemical characterization, equilibrium, and kinetics studies. *Antonie van Leeuwenhoek*. (ISSN: 00036072; **Q1**, FI_{2020} = 3.08, H-INDEX = 107; **Springer**). (Sous révision)

CHAPITRE DE LIVRES

10. **Danouche M**., El Arroussi H., El Ghachtouli N., (2021). Biodegradation of environmental pollutants by marine yeasts in Marine Organisms: A Solution to Environmental Pollution? – Uses in Bioremediation and in Biorefinery. *Environmental Challenges and Solutions*. Springer. (ISSN: 2214-2827). (Soumis)

11. Encarnação T., **Danouche M.,** McDonald J., Lizzul M., Sobral A., da Graça Campos M., Bioremediation using microalgae and biomass valorisation. in Marine Organisms: A Solution to

Environmental Pollution? – Uses in Bioremediation and in Biorefinery. *Environmental Challenges and Solutions*. Springer. (ISSN: 2214-2827). (Soumis)

COMMUNICATIONS ORALES

1. **DANOUCHE M.,** FERIOUN M., BAHAFID W., AOUINE M., MISBAH A., EL GHACHTOULI N., Activity of *Cyberlindnera fabianii* reductase and oxidase enzymes for the decolourization of toxic azo dye at optimized conditions. 3éme congrès international "Biotechnologie au service de la société" (BIOTECH-2020). 27 au 29 Février 2020. FST-Fès.
2. **DANOUCHE M.,** BAHAFID W., AGZOUR K., EL GHACHTOULI N., Biosorption and Biodegradation mechanisms for the Bioremediation of textile dyes using yeast cells. International congress microbial technology for developments (Microbiod 4). 24-26 Avril 2019. UIZ-Agadir.
3. **DANOUCHE M.,** BAHAFID W., EL GHACHTOULI N., Bioremediation of various azo dyes by newly isolated bacterial monocultures and mixed consortium. 5éme édition du colloque internationale de valorisation des déchets pour un développement durable (V3D-2018). 12-13 Mai 2018. FSDM-Fès.
4. **DANOUCHE M.,** TIRRY N., EL GHACHTOULI S., EL GHACHTOULI N., BAHAFID W., Optimisation de la décoloration du colorant azoïque Rouge de Carmoisine et du rendement de la réduction du Chrome (VI) par des isolats bactériens. 1er Forum National "Biodiversité et Ressources Naturelles". 12-13 décembre 2017. FST-Fès.
5. AOUINE M., **DANOUCHE M.,** MISBAH A., HAGGOUD A., BARAKAT A., IBNSOUDA KORAICHI S., The potential of Pichia kudriavzevii for high-temperature ethanol production from chickpea straw. 3éme congrès international "Biotechnologie au service de la société" (BIOTECH-2020). 27 au 29 Février 2020. FST-Fès.
6. MISBAH A., AOUINE M., ER RAOUAN S., **DANOUCHE M**., IBNSOUDA KORAICHI S., TAHRI JOUTI M.A., Evaluation of Organic Solvent-Tolerant and Alkaline Crude Lipases from Serratia marcescens OM2 and Proteus vulgaris OR34 as Additives in Laundry Detergent Formulations. 3éme congrès international "Biotechnologie au service de la société" (BIOTECH-2020). 27 au 29 Février 2020. FST-Fès.

COMMUNICATIONS AFFICHEES

1. **DANOUCHE M.,** FIRENOUN M., AOUINE M., MISBAH A., BAHAFID W., EL GHACHTOULI N., Application of experimental designs for the optimization of biosorption of CI. AR14 azo dyes using yeast strain of *Candida tropicalis*. 3éme congrès international "Biotechnologie au service de la société" (BIOTECH-2020). 27 au 29 Février 2020. FST-Fès.

2. **DANOUCHE M.,** BAHAFID W. EL GHACHTOULI N.**,** Packed bed column studie for the bioremediation of synthetic azo dye using free and immobilised bacteria consortium biofilm**.** Symposium sur les Biofilms microbiens : Intérêts et applications. 21-23 Février 2019. FST-Fès.

3. **DANOUCHE M.,** BAHAFID W., EL GHACHTOULI S., TIRRY N., EL GHACHTOULI N., Treatment of Azo dye AR14 and Chromium (VI) in single and binary systems by using yeast cells with the purpose of managing polluted industrial wastewaters. 4éme édition du symposium international sur les biotechnologies "Biotechnologies environnementales : recherche, applications et enjeux pour le Maroc". 13-14 Février 2018. FMP-Fès.

4. **DANOUCHE M.,** BAHAFID W., TIRRY N., EL GHACHTOULI S., EL GHACHTOULI N. bio-dépollution du colorant Rouge Carmoisine en milieux aqueux. 2éme congrès international "Biotechnologie au service de la société". 22-25 novembre 2017 FST-Fès.

5. **DANOUCHE M.,** EL GHACHTOULI S., TIRRY N., EL GHACHTOULI N., BAHAFID W. Traitement du chrome (VI) et du colorant rouge carmoisine en milieux aqueux par des procédés biologique.1ère journée scientifique dédiée Aux doctorants "Biotechnologie, Ecologie et Valorisation des Phyto-ressources". 26 décembre 2017. FSDM- Fès.

6. **DANOUCHE M.,** TIRRY N., EL GHACHTOULI N., BAHAFID W., Etude de la phytotoxicité du colorant azoïque AR14 sur la germination et la croissance de *Medicago sativa*. 1er Forum National "Biodiversité et Ressources Naturelles" 12-13 décembre 2017. FST-Fès

7. AOUINE M., **DANOUCHE M.,** MISBAH A., HAGGOUD A., BARAKAT A., IBNSOUDA KORAICHI **S.,** Cellulase production from *Thielavia hyalocarpa* through solid-state tray fermentation, and its use for simultaneous saccharification and fermentation of *chickpea stover* for bioethanol production. 3éme congrès international "Biotechnologie au service de la société" (BIOTECH-2020). 27 au 29 Février 2020. FST-Fès.

REMERCIEMENTS

Je commence par remercier Allah de m'avoir entouré de personnes merveilleuses qui, chacune à sa manière, et à différentes étapes de mon parcours, ont contribué d'une manière directe ou indirecte à la réalisation de cette thèse de doctorat.

Mes premières pensées et ma reconnaissance la plus profonde se tournent vers mes deux encadrants Pr. ***Naïma EL GHACHTOULI*** *&* *Dr.* ***Hicham EL Arroussi****, qui ont conduit ces travaux de recherche avec une haute compétence et une grande disponibilité. Ils ont toujours été présents dans les moments difficiles, leurs encouragements m'ont beaucoup apporté et je les en remercie du fond du cœur.*

Je tiens ensuite à remercier les membres de mon jury d'avoir accepté de consacrer une partie de leur temps précieux à lire et évaluer ce travail. Je me réjouis de pouvoir échanger avec vous sur ce travail lors de sa défense orale.

Je tiens à remercier toute l'équipe du laboratoire LBM2B et green biotech pour leur disponibilité et leurs conseils.



DEDICACES

C'est avec un grand plaisir que je dédie ce modeste travail à la plus proche qui m'a beaucoup encouragé à poursuivre le bon chemin, qui m'a donnée l'amour, la tendresse et la volonté. C'est grâce à toi, chère maman…Merci et que Dieu te garde et te bénisse.

Je dédie ce travail à mon père, qui m'a donné tendresse et volonté

Mes sœurs : SANAE & YOUSSRA

Mon frère : YASSIR

Mes grand-mères

Mes amis

Et mes collègues.

RÉSUMÉ

La pollution de l'eau est un problème de haut niveau dont souffrent actuellement des millions de personnes dans le monde. Le sujet de recherche abordé dans cette thèse vise à mettre en évidence l'application de nouvelles stratégies pour le traitement des polluants organiques et métalliques, à travers la phycoremédiation des polluants inorganiques par les microalgues, et la mycoremédiation des contaminants organiques par les levures. Huit souches de microalgues ont été criblées en vue de leur utilisation dans la phycoremédiation des métaux lourds (MLs) Pb(II), Cd(II), Cu(II) et Cr(VI). La souche *Scenedesmus obliquus* a fait preuve d'une forte tolérance aux ions Pb(II), avec une EC50 de 141 ppm. Elle a été retenue pour l'étude des mécanismes impliqués. Lors de la phycoremédiation, les ions de Pb(II) à la concentration EC50 ont impacté la croissance de *S. obliquus*, en comparaison avec le témoin. Toutefois, la viabilité et la taille des cellules analysées respectivement par le cyrtométrie en flux et le Zetasizer n'ont montré aucune différence significative. Après traitement, la concentration de Pb(II) en solution, analysée par ICP-AES, a diminué de 58,42 % et l'analyse par thermogravimétrie des poids résiduels des cellules a montré une récupération des ions Pb(II) par *S. obliquus*. La discrimination entre les mécanismes de récupération extra et intracellulaires, via l'analyse des digests des cellules chargées en Pb(II) (lavés et non lavés) a révélé l'implication de la biosorption et de la bioaccumulation avec respectivement une contribution de 85,5% et 14,5%. La caractérisation physicochimique des interactions contrôlant la biosorption par le biais du MEB-EDX, de la FTIR, du potentiel zêta, du pH zéro charge, et de l'angle de contact ont confirmé l'implication des interactions de type chimiques et électrostatiques. Par ailleurs, la bioaccumulation du Pb(II) a induit des modifications biochimiques notamment l'augmentation des contenus en peroxyde d'hydrogène, malondialdéhyde, caroténoïdes et lipides. Cependant, les teneurs en chlorophylle, carbohydrates et protéines ont diminué sensiblement. Le profilage métabolomique par GS-MS des cellules stressées a révélé une augmentation des esters méthyliques d'acides gras, des alcanes, des aromatiques et des stérols. En revanche, les alcènes et les acides gras monoinsaturés ont diminué par rapport au témoin. L'évaluation des systèmes antioxydants enzymatiques et non enzymatiques dans la gestion du stress oxydatif a montré une augmentation significative de l'activité de piégeage des radicaux libres, des teneurs en proline et polyphénols, de même qu'une induction des activités de la superoxyde dismutase, catalase, guaiacol peroxydase, ascorbate peroxydase et glutathion réductase. Au regard de la mycoremédiation des colorants azoïques utilise comme model de polluant organique, trois levures ont ainsi été examinées. Le taux de décoloration le plus élevé a été atteint par la souche *Cyberlindnera fabianii* (97%). Ensuite, la couleur de la biomasse après décoloration du milieu a été évaluée pour anticiper les mécanismes impliqués dans la mycoremédiation de divers colorants synthétiques. Les résultats ont montré un couplage entre la structure chimique du colorant et la voie de son élimination. En effet, l'élimination du colorant AR14 a été accomplie principalement par des voies enzymatiques. Une augmentation significative de l'activité de laccase, de tyrosinase, de peroxydase de manganèse et d'azoréductase a été enregistrée dans la biomasse incolore ainsi obtenue. Sur le plan éco-toxicologique, la dégradation enzymatique de l'AR14 par *C. fabianii* a permis leur détoxification efficace. En effet, les sous-produits résultants n'ont montré aucun signe de phytotoxicité. D'un autre côté, le mécanisme de biosorption du colorant AR14 a également été abordé en utilisant des cellules inactivées. L'étude cinétique de la biosorption et sa modélisation ont montré que la biosorption de AR14 par la biomasse fongique répond à une chimiosorption sur une monocouche de sites homogènes. Ces prédictions ont été vérifiées en appliquant les mêmes techniques de caractérisation décrites ci-dessus. La biosorption de l'AR14 est médiée par des interactions chimiques avec les groupes fonctionnels de la paroi cellulaire, ainsi que par des interactions électrostatiques. Ces résultats ouvrent la voie au développement de bioprocédés de traitement des eaux usées basés sur des stratégies de phycoremédiation et de mycoremédiation en vue de répondre aux démarches de développement durable.

ABSTRACT

Water pollution is a high-level problem that millions of people in the world are currently suffering from. The research topic addressed in this thesis aims to highlight the application of new strategies for the treatment of organic and metallic pollutants, through the phycoremediation of inorganic pollutants by microalgae, and the mycoremediation of organic contaminants using yeasts cells.

Eight microalgae strains were screened for their potential application in the phycoremediation of heavy metals (HMs) Pb(II), Cd(II), Cu(II) and Cr(VI).. The strain of *Scenedesmus obliquus* exhibited a high tolerance towards Pb(II) ions, with an EC50 of 141 ppm. It was selected for the investigation of the involved mechanisms. Phycoremediation of Pb(II) ions at EC50 concentration impacted the growth of *S. obliquus* compared to the control cells. However, the viability and the cell size analyzed by flow cytometry and Zetasizer showed no significant difference. After the phycoremediation process, the concentration of Pb(II) ions in the solution, analyzed by ICP-AES, decreased by 58.42%. In addition, the residual weights of Pb(II)-loaded cells and controls cells analyzed by thermogravimetry, were 57.8% and 31.34%, respectively, indicating the uptake of Pb(II) ions by *S. obliquus*. Discrimination between extra and intracellular recovery mechanisms, via analysis of the digests Pb(II)-loaded cell (washed and unwashed) revealed the involvement of biosorption and bioaccumulation with a contribution of 85.5% and 14.5% respectively. Physicochemical characterization of interactions controlling biosorption through SEM-EDX, FTIR, zeta potential, zero charge pH, and contact angle, confirmed the involvement of chemicals and electrostatic interactions. On the other hand, the bioaccumulation of Pb(II) induces biochemical modifications, in particular the increase of the contents of: hydrogen peroxide, malondialdehyde, carotenoids and lipids. However, the chlorophyll, the carbohydrate and the protein contents decreased significantly. Metabolomic profiling by GS-MS revealed an increase in fatty acid methyl esters, alkanes, aromatics and sterols. In contrast, alkenes and monounsaturated fatty acids decreased in stressed cells compared to the control. Evaluation of enzymatic and non-enzymatic antioxidant systems in the management of oxidative stress showed a significant increase in free radical scavenging activity, proline and polyphenol levels, as well as induction of superoxide dismutase, catalase, guaiacol peroxidase, ascorbate peroxidase and glutathione reductase activities.

With respect to the mycoremediation of azo dyes used as model of organic pollutant, three yeast strains were examined. The highest decolorization rate was achieved by the strain *Cyberlindnera fabianii* (97%). The color of the biomass was then evaluated in order to anticipate the mechanisms involved in the mycoremediation of various synthetic dyes by this strain. The results showed a coupling between the chemical structure of the dye and the pathway of its removal. For example, the removal of AR14 by *C. fabianii* was performed mainly through an enzymatic pathway. A significant increase in the intracellular and extracellular activity of laccase, tyrosinase, manganese peroxidase and azoreductase was recorded in the resulting biomass. From an eco-toxicological point of view, the enzymatic degradation of AR14 by *C. fabianii* ensured an efficient detoxification. Indeed, the resulting by-products showed no sign of phytotoxicity. The mechanism of dye biosorption by yeast was also addressed using inactivated cells. The kinetic study of biosorption and their modeling showed that the biosorption of AR14 by fungal biomass responds to chemisorption on a monolayer of homogeneous sites. These predictions were verified by applying the same characterization techniques as described above. AR14 biosorption is mediated by both chemical interactions with cell wall functional groups, and electrostatic interactions. These results pave the way for the development of wastewater treatment bioprocesses based on phycoremediation and mycoremediation strategies in order to meet sustainable development requirements.

ملخص

يعتبر تلوث المياه من بين المشـــاكل الحالية التي تواجه الملايين من الناس حول العالم. موضـــوع بحث هذه الأطروحة يندرج ضمن هذا الإطار، حيث يسلط الضوء على تطبيق استراتيجيات بيئية جديدة في معالجة ملوثات المياه العضوية والمعدنية منها، وذلك باستعمال الطحالب والخمائر المجهرية.

أولاً تم فحص ثماني سلالات من الطحالب المجهرية لاستخدامها في إزالة المعادن الثقيلة ((Pb(II), Cd(II), Cu(II) , Cr(VI) من المياه. أظهرت النتائج المخبرية ان لسلالة "*Scenedesmus obliquus*" مقاومة عالية لأيونات الرصـاص، بتركيز فعال نصف أقصى يصل الى ١٤١ ميليجرام لكل لتر. ومنه تم اختيار هده السلالة لدراسة آلياتها في معالجة الرصاص. خلال عملية المعالجة، اثرت ايونات الرصاص سلبا على نمو السلالة، في حين لم تظهر معاينة نسبة البقاء، وكدا حجم الخلايا باستخدام جهاز قياس التدفق الخلوي (CMF) وجهاز"Zetasizer" أي فرق كبير. بعد عملية المعالجة البيولوجية للوسط الملوث بالرصاص، انخفض تركيز أيونات الرصـاص في المحلول بنسبة ٤٢,٥٨ ٪ والذي تم تحليله بواسطة جهاز التحليل الطيفي للانبعاث الذري للبلازما المقترن بالحث (ICP-AES). و بناء على اختبار التحليل الحراري الوزني (TGA) للخلايا بعد عملية المعالجة، تم التأكيد أن أيونات الرصـاص تم استخراجها من المحلول بواسطة خلايا الطحلب المجهري . للتمييز بين الآليات خارج الخلية أو داخل الخلايا المشـاركة في عملية معالجة الرصـاص، تم تحليل هضـم الخلايا المحملة بالرصـاص (المغسـولة وغير المغسـولة) والتي تم الحصول عليها، حيث أوضحت النتائج ان استخلاص الرصاص راجع الى الامتصاص الحيوي الخلوي بنسبة ٥,٨٥ ٪ وكدا عبر التراكم حيوي بداخل الخلية بنسبة ٥,١٤٪. في سياق هذه الملاحظات الأولية، أكد التوصيفات الفيزيوكيميائية باستخدام كل من المجهر الإلكتروني الماسـح إلى جانب مطيافية تشـتت الطاقة بالأشـعة السـينية"MEB-EDX"،تحويل فورييه للطيف بالأشـــعة تحت الحمراء "FTIR"،زيتا المحتملة "potentielzêta"،نقطة الصـــفر شـــحنة "pH zéro charge"،زاوية تلامس"l'angle de contact"،الى ان الامتصاص الحيوي للرصاص بخارج الخلايا تؤطره تأثيرات كيميائية و كهروستاتيكية متبادلة. وعلاوة على ذلك، أدى التراكم الأحيائي للرصاص إلى تغيرات كيميائية حيوية، ولا سيما الزيادة في محتويات بيروكسيد الهيدروجين و المالونديالديهيد"MDA" و الكاروتينات و الدهون. في حين أن محتوى اليخضـور والكربوهيدرات والبروتينات فقد انخفض بشكل كبير. كشف التنميط الأيضي بواسطة استشراب غازي-مطياف كتلة (GC-MS) عن تغيير في تكوين الخلايا المجهدة تحت تأثير الرصـاص، حيث لوحظت زيادة في استرات الميثيل والأحماض الدهنية والألكانات والعطريات والستيرول. من ناحية أخرى، انخفضـــت الألكينات والأحماض الدهنية الأحادية غير المشـــبعة مقارنة بالخلايا غير المجهدة. أظهر تقييم الأنظمة المضـــادات للأكســـدة الأنزيمية وغير الأنزيمية، زيادة كبيرة في نشـــاط مســـح الجذور الحرة، ومحتويات البرولين والبوليفينول. وكذلك تفعيل النشاط الانزيمي ل SOD،CAT،GPX، APX ، وGR.

فيما يتعلق بالمعالجة الفطرية للأصـبغة الآزوية باسـتخدام الخمائر، اوضـحت نتائج فحص ثلاث سـلالات ان أعلى معدل لإزالة التلوين من الوسط (٩٧٪) قد سجلت من قبل سلالة Cyberlindnera *fabianii* .لتوقع الآليات المشاركة في المعالجة الفطرية لمختلف الأصـــباغ الاصـــطناعية، تم تقييم لون الكتلة الحيوية بعد إزالة التلوين من الوســـط. أظهرت النتائج وجود اقتران بين التركيب الكيميائي للصـبغة وطريقة إزالتها. على سبيل المثال، تمت معالجة الصـبغة حمض أحمر ١٤ (ح أ ١٤) بشكل رئيسـي بفضـل الأنزيمات حيث لوحظ انه .بعد معالجة هده الصـبغة تم تسـجيل زيادة كبيرة في النشـاط الانزيمي داخل الخلايا وخارج الخلية لكل من ManP ,Lac, Tyr وAzoR.من وجهة نظر السـمية البيئية، فإن الهدم الإنزيمي لصـبغة (ح. أ١٤) بواسـطة الخميرة المختارة جعل من الممكن القضـاء على سـميتها، حيث لم تظهر المنتجات الثانوية الناتج عن هدم الصـبغة أي علامات على السمية. من ناحية أخرى، تم تناول آلية الامتصاص البيولوجي لهذه الصبغة باستخدام خلايا ميتة. أظهرت الدراسة الحركية للامتصاص الحيوي ونمذجته، أن الامتصاص الحيوي لـــلصبغة (ح. أ١٤) بواسطة الكتلة الحيوية الفطرية انه يستجيب لنموذج الامتصـــاص الكيميائي على مسـتوى طبقة أحادية من المواقع النشـيطة المتجانسـة. تم التحقق من هذه التنبؤات من خلال تطبيق نفس تقنيات التوصيف الموضحة أعلاه. والتي مكنت من استنتاج ان الامتصاص الحيوي لـصبغة (ح. أ١٤) يرجع إلى التأثيرات الكيميائية مع المجموعات الوظيفية لجدار الخلية وكذلك عن طريق بعض التفاعلات الكهروســـتاتيكية .في الختام يمكن القول ان هذه النتائج تمهد الطريق لتطوير وسـائل بيولوجية جديدة لمعالجة مياه الصـرف باسـتخدام كل من الطحالب والخمائر المجهرية، وذلك من أجل الاستجابة لنهج التنمية المستدامة.

SOMMAIRE

Avant-propos.....i
Remerciements.....vi
Dédicaces.....vii
Résumé.....viii
Abstract.....x
ملخص.....x
Introduction générale.....1

REVUE BIBLIOGRAPHIQUE

CHAPITRE I

Phycoremediation Mechanisms of Heavy Metals using Living Green Microalgae: Physicochemical and Molecular Approaches for Enhancing Selectivity and Removal Capacity

Résumé.....4
Abstract.....6
1. Introduction.....6
2. Mechanisms of HMs phycoremediation using living microalgae.....7
2.1 Extracellular HMs-bioremoval with living microalgae.....7
2.1.1 Cell walls composition and its role in HMs-biosorption.....7
2.1.2 Physicochemical interactions of HMs and cell surface.....8
2.1.3 Extracellular polymeric substances interactions with HMs.....8
2.2 HMs-Bioaccumulation mechanisms in microalgae.....8
2.2.1 Metal transporters in microalgae cell membrane.....9
2.2.2 Pathways of intracellular HMs detoxification.....10
2.2.3 HMs compartmentalization in the vacuole, chloroplast and mitochondria.....10
2.3 Biotransformation and mitigation of HMs by microalgae.....10
2.3.1 Enzymatic biotransformation.....10
2.3.2 Biochemical transformations of HMs.....11
2.3.3 Other biotransformation mechanisms of HMs.....11
3. Future outlook for enhancing the phycoremediation process.....11
3.1 Cell manipulation for enhancing the biosorption capacity and selectivity.....12
3.1.1 Physicochemical approaches.....12
3.1.2 Bioengineering of cell-surface approaches.....12
3.2 Microalgae genetically engineered for intracellular recovery of HMs.....13
3.2.1 Metal-transporters transition in microalgae.....13
3.2.2 Molecular manipulation for AA and PCs biosynthesis.....13
3.2.3 Genetic transformation for HMs enzyme biocatalysts.....14
4. Conclusion.....14
5. References.....14

CHAPITRE II

Overview of the management of heavy metal toxicity by microalgae through biochemical, enzymatic and phytohormonal mechanisms

Résumé....17
Abstract....18
1. Introduction....19
2. HMs-induced oxidative stress in microalgae....19
2.1 Lipid peroxidation....20
2.2 Protein oxidation....21
2.3 DNA oxidation....21
3. Enzymatic and non-enzymatic antioxidant defense systems in microalgae....22
3.1 Biochemical antioxidant defense systems....23
3.1.1 Glutathione....23
3.1.2 Phytochelatins....23
3.1.3 Ascorbate....24
3.1.4 Glutathione....24
3.1.5 Tocopherols....24
3.1.6 Phenolic compounds....24
3.1.7 Carotenoids....25
3.1.8 Proline....25
3.2 Enzymatic antioxidant defense systems in microalgae....26
3.2.1 Superoxide dismutase....26
3.2.2 Catalase....26
3.2.3 Peroxidases....27
3.2.4 Enzymes of Ascorbate-Glutathione Cycle....27
4. Roles of phytohormones in the management of oxidative stress....28
5. Conclusion....31
6. References....32

CHAPITRE III

Mycoremediation of synthetic dyes by yeast cells: a sustainable biodegradation approach.

Résumé....41
Abstract....42
1. Introduction....42
2. Adverse effects of synthetic dyes on aquatic ecosystems....43
3. Biodegradation of synthetic dyes by yeast....44
3.1 Enzymes involved in the biodegradation of dyes by yeast....44
3.1.1 Laccase (EC 1.10.3.2)....45
3.1.2 Tyrosinase (E.C. 1.14.18.1)....45
3.1.3 Lignin peroxidase (EC 1.11.1.14)....45

3.1.4 Manganese peroxidase (EC 1.11.1.13)....48
3.1.5 Azoreductase (EC 1.7.1.6)....48
3.1.6 NADH-DCIP reductase (EC 1.6.99.3)....49
3.1.7 Malachite green reductase....49
3.2 Factors affecting the biodegradation of dyes by yeast....49
3.2.1 Effects of temperature....49
3.2.2 Effects of pH....50
3.2.3 Effects of dye structure and concentration....50
3.2.4 Effects of oxygen and shaking....50
3.2.5 Effect of carbon and nitrogen sources....50
3.3 Chemical characterization and toxicity assessment of dye biodegradation by-products....51
4. Molecular aspects of dye degradation by yeasts....53
5. Future perspectives....54
6. Conclusion....54
7. References....55

CHAPITRE IV

An overview of the biosorption mechanism for the bioremediation of synthetic dyes using yeast cells

Résumé....60
Abstract....61
1. Introduction....61
2. Synthetic dyes: industrial use and environmental impacts....62
3. Biosorption for dye removal using yeast cells....64
3.1 Biosorption mechanisms....64
3.2 Analytical methods employed for biosorption studies....65
3.3 Kinetic study and equilibrium biosorption models....68
3.4 Factors affecting the biosorption of dyes....69
3.4.1 pH effect....69
3.4.2 Temperature effect....69
3.4.3 Dye concentration effect....70
3.4.4 Dye chemical structure effect....70
3.4.5 Biosorbent effect....71
3.4.6 Shaking rate effect....71
3.4.7 Ionic strength effect....71
4. Methods to improve the biosorption capacity of yeast cells....71
4.1 Physical pre-treatment approaches....72
4.2 Genetic and biomolecular approaches....72
5. Conclusion....73
6. References....74

PARTIE PRATIQUE

CHAPITRE I

Heavy metals phycoremediation using tolerant green microalgae: Enzymatic and non-enzymatic antioxidant systems for the management of oxidative stress

Résumé....80
Abstract....81
1. Introduction....81
2. Material and methods....82
2.1. Potential use of fresh water microalgae in phycoremediation....82
2.1.1. Screening of metal tolerant microalgae candidate....82
2.1.2. Half maximal effective concentration....82
2.1.3. Lead phycoremediation at scaling up microalgal cultures....82
2.2. Management of oxidative stress....83
2.2.1. Oxidative stress markers....83
2.2.1.1. Determination of hydrogen peroxide....83
2.2.1.2. Measurement of lipid peroxidation....83
2.2.2. Non-enzymatic scavenging pathways....83
2.2.2.1. Radical scavenging activity....83
2.2.2.2. Proline content....83
2.2.2.3. Ascorbate content....83
2.2.2.4. Phenolic compounds....83
2.2.3. Enzymatic scavenging pathways....83
2.2.4. Statistical analysis....83
3. Results and Discussion....84
3.1. Potential use of microalgae in phycoremediation....84
3.1.1. Screening of metal tolerant microalgae candidates....84
3.1.2. Half maximal effective concentration....85
3.1.3. Lead phycoremediation at scaling up microalgal cultures....86
3.2. Management of oxidative stress by *S. obliquus*....86
3.2.1. Oxidative stress markers....86
3.2.1.1. Hydrogen peroxide and lipid peroxidation....86
3.2.2. Non-enzymatic antioxidants pathways....86
3.2.3. Enzymatic scavenging pathways....87
4. Conclusion....89
5. References....89

CHAPITRE II

Mechanisms of lead (II) phycoremediation using Scenedesmus obliquus: Cells physicochemical properties, biochemical composition and metabolomic profiling

Résumé....92
Abstract....93
1. Introduction....94
2. Material and methods....95

2.1 Strain and culture condition....95
2.2 Growth inhibition, cells viability and size analysis....95
2.2.1 Growth inhibition....95
2.2.2 Cells viability....95
2.2.3 Cells size analyses....96
2.3 Pb(II)-phycoremediation mechanism with *S. obliquus*....96
2.3.1 Thermogravimetric analysis....96
2.3.2 Chemical extraction and ICP-AES analysis....96
2.4 Physicochemical characterization of Cells-metal interaction....96
2.4.1 Scanning electron microscopy with energy dispersive X-Ray analysis....96
2.4.2 Fourier-transform infrared spectroscopy analysis....97
2.4.3 Zeta potential and Zero-point charge measurement....97
2.4.4 Contact angle measurement....97
2.5 Effect of Pb(II) on the biochemical composition....97
2.5.1 Photosynthetic pigments analysis....97
2.5.2 Proteins, lipids, and carbohydrates determination....98
2.6 Metabolomics profiling of control and Pb(II)-loaded cells....98
2.6.1 Non-polar metabolites determination using transesterification reaction....98
2.6.2 Metabolite identification, data mining, normalization, and statistical analysis....99
2.7 Statistical analysis....99
3. Results and discussion....99
3.1 S. obliquus growth inhibition, cells viability and size....99
3.2 Pb(II)-phycoremediation mechanism with S. obliquus....101
3.3 Physicochemical characterization of Cells-metal interaction....102
3.4 Pb (II) influence on the biochemical composition of *S. obliquus*....106
3.5 Metabolomics profiling of control and Pb(II)-loade dcells....108
4. Conclusion....112
5. References....112

CHAPITRE III

Mycoremediation of azo dyes using *Cyberlindnera fabianii* yeast strain: Application of designs of experiments for decolorization optimization

Résumé....120
Abstract....121
1. Introduction....123
2. Material and methods....123
2.1 Chemicals....123
2.2 Yeast source and culture medium....123
2.3 Screening of yeast strains for dye decolorization....123
2.4 Growth measurement and biomass determination....123
2.5 Yeast decolorization performance of various synthetic dyes....123
2.6 Determination of yeast enzyme activities....123
2.7 Phytotoxicity assessment....124
2.8 Statistical analysis....124
2.9 Optimization of decolorization by using the design of experiments....124

3. Results and discussion.....125
3.1 Decolorization screening of the yeast strains.....125
3.2 Yeast decolorization performance of various synthetic dyes.....125
3.3 Determination of enzyme activities.....127
3.4 Phytotoxicity assessment.....128
3.5 Optimization of decolorization by using the design of experiments.....128
4. Conclusion.....132
5. References.....133

CHAPITRE IV

Mycoremediation of the azo dye Acid Red 14 by *Wickerhamomyces anomalus:* Physicochemical characterization, equilibrium, and kinetics studies

Résumé.....136
Abstract.....137
1. Introduction.....138
2. Material and methods.....138
1.1 Chemicals.....138
1.2 Yeast source, culture medium and biosorbent preparation.....139
1.3 Biosorption: kinetics and equilibrium study.....139
1.4 Characterization of yeast biomass.....140
2.4.1 Scanning electron microscopy with energy dispersive X-Ray analysis.....140
2.4.2 Fourier-transform infrared spectroscopy analysis.....140
2.4.3 Zeta potential and Zero-point charge measurement.....140
2.4.4 Contact angle measurement.....140
1.5 Statistical analysis.....140
1.6 Optimization of biosorption using the design of experiments.....141
2.6.1 Screening of factors using Plackett–Burman design.....141
2.6.2 Optimization of biosorption parameters using Box-Behnken design.....141
3. Results and discussion.....141
3.1 Biosorption: kinetics and equilibrium study.....141
3.2 Characterization of yeast biomass.....144
3.2.1 SEM coupled with EDX analysis.....144
3.2.3 FTIR spectroscopy analysis.....145
3.2.4 Zeta potential and Zero-point charge measurement.....146
3.2.5 Contact angle measurement.....147
3.3 Optimization of biosorption using the design of experiments.....148
3.3.1 Screening of factors using Plackett–Burman design.....148
3.3.2 Optimization of biosorption parameters using Box-Behnken design.....149
4. Conclusion.....151
5. References.....152

DISCUSSION GÉNÉRALE.....157
CONCLUSION ET PERSPECTIVES.....168
RÉFÉRENCES.....171

INTRODUCTION GÉNÉRALE

Depuis le début de la révolution industrielle au XIXe siècle, la solution à l'équation d'équilibre entre la croissance économique et la préservation de l'environnement n'a pas encore été trouvée. Les différentes activités anthropogéniques mènent sans cesse à la contamination des sols, de l'air, et de l'eau. En effet, presque tous les secteurs industriels utilisent des produits chimiques aussi bien organiques qu'inorganiques tels que les métaux lourds (MLs) et les colorants synthétiques. La pollution par de tels contaminants a des conséquences négatives sur les écosystèmes aquatiques (faune et flore), de même que sur la santé publique. Il s'agit d'un défi urgent auquel les scientifiques, les écologistes et les décideurs politiques se sont engagés à relever. De ce fait, un intérêt particulier a été porté au traitement des effluents industriels qui se trouve au centre de cette problématique. Pour répondre aux challenges environnementaux, de nombreuses lois ont été adoptées à l'échelle mondiale afin de réglementer et limiter les rejets des effluents industriels dans l'environnement. Au Maroc, plusieurs législations ont été mises en place pour la protection de l'environnement. C'est le cas de la loi n° 36-15 relative à l'eau, et la loi n°10-95 relative à la gestion des ressources en eau qui permet de doter les pouvoirs publics des outils leur permettant de faire face aux multiples défis posés. Il existe également, la loi n° 11-03 relative à la protection et à la mise en valeur de l'environnement et d'autre texte législatif qui ont comme vocation la préservation de l'environnement et la sante publique.

Techniquement, de nombreux procédés physico-chimiques (systèmes membranaires, procédés d'oxydation photochimique et électrochimique...) ont été proposés comme solutions pour traiter les eaux usées industrielles. Toutefois, ces procédés se sont avérés coûteux, car ils nécessitent des équipements et une expertise très pointue, ainsi qu'un travail d'entretien permanent. Ils peuvent également être à l'origine d'une pollution secondaire, dont témoigne la dégradation des colorants azoïques par des processus chimiques qui génèrent des sous-produits plus toxiques et mutagènes que leurs molécules d'origine. La bioremédiation est l'approche la plus recommandée en raison des avantages qu'elles offrent en termes d'efficacité du traitement, de coût approprié et de leur impact écologique minimal (Srinivasan et Viraraghavan 2010). L'émergence de cette nouvelle approche repose sur l'exploitation de la biodiversité d'espèces qui possèdent la capacité de tolérer, de s'adapter et de survivre dans des environnements extrêmes auxquelles elles sont confrontées dans leur habitat (Jafari et coll. 2014 ; Miranda et coll. 2013).

Les microalgues et plus spécifiquement les espèces de cyanobactéries sont les premiers organismes autotrophes qui ont apparus sur la terre il y a environ 3,5 milliards d'années. Au cours des siècles d'évolution, ces micro-organismes ont développé des mécanismes adaptatifs leur permettant de survivre aux conditions difficiles rencontrées sur terre, y compris l'apparition d'oxygène, et les autres gaz toxiques libéré par les activités volcaniques, les températures extrêmes, ainsi que l'exposition aux métaux ou d'autres composés toxiques. L'exploitation des fonctionnalités écologiques de ces microorganismes photoautotrophe pour le traitement des effluents gazeux ou liquides, ou la bioremédiation des écosystèmes contaminés, est désignée sous le terme de "Phycoremédiation".

Par ailleurs, les levures font partie des espèces hétérotrophes qui peuvent survivre dans des conditions environnementales défavorables. Ces organismes unicellulaires partagent avec d'autres espèces le phylum des champignons, avec des espèces appartenant à la division des basidiomycètes ou ascomycètes. Le rôle environnemental qu'ils jouent est identique à celui d'autres espèces de champignons. En effet, elles agissent comme des saprophytes qui transforment la matière organique végétale et animale en biomasse et en sous-produits (Kutty et Philip, 2008). L'exploitation de cette propriété écologique des levures a également incitée les scientifiques à évaluer leur capacité à dégrader des xénobiotiques de nature organique tels que les hydrocarbures aromatiques polycycliques, les composés phénoliques, les pesticides, les déchets pharmaceutiques, ainsi que les colorants synthétiques (Aksu, 2005). Pour distinguer l'utilisation des champignons des autres stratégies de bioremédiation, le terme mycoremédiation est souvent utilisé (Bosco et Mollea, 2019). La présente étude vise à exploiter le potentiel biotechnologique de microorganismes autotrophes (microalgues) et hétérotrophes (levures), isolés de biotopes marocains dans le traitement des MLs et des colorants synthétiques choisis comme modèle de polluants organiques du milieu aquatique.

Hypothèse du travail :

L'hypothèse générale de cette étude s'est basée sur les points suivants: (**i**) les microalgues tolérantes aux MLs possèdent un réel potentiel d'application en matière de traitement des effluents contaminés; (**ii**) Les mécanismes d'élimination extracellulaire et intracellulaire sont liés aux caractéristiques physico-chimiques, physiologiques, biochimiques et métabolomiques de la souche concernée; (**iii**) Le caractère saprophyte des champignons confère aux levures la faculté de

dégrader les polluants organiques dont les colorants synthétiques; (**iv**) La valorisation de la biomasse de levure offre également l'opportunité de servir en tant que biosorbant économique.

Objectifs du travail :

L'objectif de cette étude concerne le traitement des contaminants inorganiques (MLs) et organiques (colorants) par de micro-organismes autotrophes (microalgues), et hétérotrophes (levures) en vue de développer des bioprocédés de traitement des eaux usées. Dans cette optique, nous avons entrepris un travail pluridisciplinaire dont les objectifs spécifiques étaient les suivants :

I) Évaluer la tolérance des souches de microalgues aux MLs. Ainsi, examiner les performances de phycoremédiation de la souche la plus tolérante. Enfin, clarifier les mécanismes biochimiques et enzymatiques impliqués dans la gestion du stress oxydatif généré par les ions métalliques (**Chapitre I**).

II) Etudier les mécanismes impliqués dans la phycoremédiation du Pb(II) avec la souche présélectionnée, et souligner les changements dans les caractéristiques physicochimiques, la composition biochimique et le profilage métabolomique des cellules après la phycoremédiation de Pb(II) (**Chapitre II**).

III) Evaluer la capacité de décoloration des souches de levure, examiner les enzymes impliquées dans le mécanisme de biodégradation, et évaluer l'efficacité de la biodégradation sur le plan éco-toxicologique (**Chapitre III**).

IV) Mettre en évidence les propriétés de la biomasse fongique comme biosorbant naturel destiné à la biosorption des colorants toxiques, à travers un examen approfondi des interactions physico-chimique responsables du mécanisme de biosorption (**Chapitre IV**).

Articulation du mémoire :

Le présent document est subdivisé en deux sections, la première concerne une synthèse bibliographique présentée sous forme de quatre revues de la littérature, traitant chacune l'état de l'art et l'état des connaissances autour des quatre objectifs fixés. La deuxième section est consacrée aux travaux pratique réalisés dans le cadre de cette thèse pour répondre à la problématique des objectifs visés. Ces travaux sont présentés sous la forme de quatre articles originaux. Les deux premiers articles portent sur la phycoremédiation des MLs, tandis que les deux derniers articles portent sur la mycoremédiation des colorants azoïques. Avant la conclusion générale et les perspectives de ce travail, une discussion exposant l'ensemble des résultats obtenus et vérifiant les hypothèses posées est également détaillée à la fin de ce document.

Revue de la littérature

"On ne connait pas complètement une science tant qu'on n'en sait pas l'histoire"

Auguste Comte
Philosophe (1798 - 1857)

Chapitre I

Phycoremediation Mechanisms of Heavy Metals using Living Green Microalgae: Physicochemical and Molecular Approaches for Enhancing Selectivity and Removal Capacity

RESUME

La contamination des milieux aquatiques par les MLs est un grave problème environnemental à l'échelle mondiale. Les MLs ne sont pas biodégradables, ils ont par conséquent tendance à s'accumuler dans les chaînes trophiques, provoquant ainsi des signes de toxicité chez les organismes exposés, y compris l'homme. La phycoremédiation, ou l'exploitation des fonctions écologiques des microalgues pour le traitement des eaux usées contaminées par les MLs est l'une des méthodes les plus recommandées, en raison de son efficacité, de son faible coût, et de son aspect écologique.

La présente étude vise à examiner les mécanismes impliqués dans la phycoremédiation des métaux lourds par les microalgues vertes. Le premier axe de cette revue propose un examen détaillé des interactions contrôlant la biosorption des ions métalliques et les cellules. Le deuxième volet porte sur les transporteurs membranaires impliqués dans la bioaccumulation intracellulaire des MLs, les principaux sites de leur compartimentation, et les mécanismes biochimiques et enzymatiques de la biotransformation des ions métalliques d'un état d'oxydation à un autre. En effet, les souches de microalgues disposant de mécanismes à facettes multiples pour éliminer et/ou atténuer les effets toxiques des MLs, y compris la biosorption extracellulaire, la complexation avec les substances polymères extracellulaires, la bioaccumulation et la compartimentation intracellulaires dans les vacuoles, les chloroplastes et les mitochondries, la réduction enzymatique (tel que le chromate réductase qui permet la transformation du Cr(VI) en Cr(III)), la bio-méthylation et la volatilisation....etc. La dernière question abordée dans ce travail concerne les techniques de modification physico-chimique et génétique aux fins d'améliorer la capacité, la sélectivité et la rentabilité de ces bioprocédés de phycoremédiation.

Récemment, les modifications physicochimiques et moléculaires de la surface des cellules microbiennes ont démontré leur applicabilité en vue d'améliorer la performance de cette bioremédiation. En revanche, il n'existe que très peu d'exemples de manipulation génétique des microalgues pour l'amélioration de la capacité des souches à éliminer des MLs. La poursuite des recherches dans les domaines du génie génétique, des méthodes de prétraitement, et des techniques d'immobilisation permettront d'améliorer d'avantage les bioprocédés de phycoremediation pour une utilisation future à grande échelle.

Heliyon 7 (2021) e07609

Contents lists available at ScienceDirect

Heliyon

journal homepage: www.cell.com/heliyon

Review article

Phycoremediation mechanisms of heavy metals using living green microalgae: physicochemical and molecular approaches for enhancing selectivity and removal capacity

Mohammed Danouche [a,b,**], Naïma El Ghachtouli [b,*], Hicham El Arroussi [a,c]

[a] Green Biotechnology Center, Moroccan Foundation for Advanced Science, Innovation and Research (MAScIR), Rabat, Morocco
[b] Microbial Biotechnology and Bioactive Molecules Laboratory, Sciences and Technologies Faculty, Sidi Mohamed Ben Abdellah University, Fez, Morocco
[c] AgroBioScience (AgBS), Mohammed VI Polytechnic University (UM6P), Benguerir, Morocco

ARTICLE INFO

Keywords:
Microalgae
Heavy metal
Phycoremediation
Mechanisms
Bioengineering

ABSTRACT

Heavy metal (HM) contamination of water bodies is a serious global environmental problem. Because they are not biodegradable, they can accumulate in food chains, causing various signs of toxicity to exposed organisms, including humans. Due to its effectiveness, low cost, and ecological aspect, phycoremediation, or the use of microalgae's ecological functions in the treatment of HMs contaminated wastewater, is one of the most recommended processes. This study aims to examine in depth the mechanisms involved in the phycoremediation of HMs by microalgae, it also provides an overview of the prospects for improving the productivity, selectivity, and cost-effectiveness of this bioprocess through physicochemical and genetic engineering applications. Firstly, this review proposes a detailed examination of the biosorption interactions between cell wall functional groups and HMs, and their complexation with extracellular polymeric substances released by microalgae in the extracellular environment under stress conditions. Subsequently, the metal transporters involved in the intracellular bioaccumulation of HMs as well as the main intracellular mechanisms including compartmentalization in cell organelles, enzymatic biotransformation, or photoreduction of HMs were also extensively reviewed. In the last section, future perspectives of physicochemical and genetic approaches that could be used to improve the phytoremediation process in terms of removal efficiency, selectivity for a targeted metal, or reduction of treatment time and cost are discussed, which paves the way for large-scale application of phytoremediation processes.

1. Introduction

Except for a small amount that appeared through geologic time at Earth's impact events, metallic elements as they are known today, have been present on Earth since its formation. These elements have been naturally recycled between the environmental compartments, through different biotic and abiotic processes of the biogeochemical cycles (Garrett, 2000). As they are not biodegradable, metal elements are present at natural background levels in water, soil, sediment and living organisms (Dung et al., 2013). They are considered a contaminant when a particular metallic element is present in an inappropriate biotope at a concentration that exceeds the tolerance of the organisms that compose this ecosystem (Gałuszka, 2007). Indeed, inorganic pollution can be the result of a natural phenomenon (Erosion, infiltration, thermal springs activity, and volcanoes...), as well as of anthropogenic sources, such as the large-scale mining operations, irrational use of fertilizers in agriculture, non-hazardous waste management (Tchounwou et al., 2012). In order to distinguish the metallic elements necessary for the functioning of biological processes from those that cause signs of toxicity, a new terminology "Heavy Metal (HM)" was introduced. Among all the natural elements, 53 are considered as HMs, they represent the transition elements, the elements of actinides and lanthanides as well as some elements of the p block of the periodic table (Rahman and Singh, 2019). According to Wang and Chen (2009), HMs can also be classified into three categories: (i) toxic HMs, such as Hg, Cr, Pb, Zn, Cu, Ni, Cd, As, Co, Sn. (ii) precious metals mainly including Ag, Au, Ru, Pt and Pd, and (iii) radionuclides HMs such as Am, Ra, Th, and U. On the other hand, its commonly recognized that non-essential HMs have varying

* Corresponding author.
** Corresponding author.
E-mail addresses: mohammed.danouche@usmba.ac.ma (M. Danouche), naima.elghachtouli@usmba.ac (N. El Ghachtouli).

https://doi.org/10.1016/j.heliyon.2021.e07609
Received 21 May 2021; Received in revised form 2 July 2021; Accepted 14 July 2021
2405-8440/© 2021 Published by Elsevier Ltd. This is an open access article under the CC BY-NC-ND license (http://creativecommons.org/licenses/by-nc-nd/4.0/).

degrees of toxicity towards microorganisms, animals, plants, and humans even at very low concentrations (Ali et al., 2019). Thus, the treatment of HMs-contaminated water is a global issue that has piqued the attention of scientists, environmentalists, and legislators. Hence, to protect the environment and subsequently the public health, such contaminants should be removed from industrial wastewater and aquatic ecosystems. Various techniques have been applied to remove HMs, including hydroxide and sulfide precipitation, adsorption, nano-filtration, ultrafiltration and reverse osmosis, electrochemical treatment technologies and biological treatment approaches (Fu and Wang, 2011; Kumar et al., 2015). Indeed, because they are effective, environmentally friendly and inexpensive the use of bioremediation methods appear to be competitive and even advantageous compared to some conventional physicochemical techniques (Chibueze et al., 2016). Phycoremediation is a bioremediation subcategory proposed by John (2003), it refers to the use of algae in the removal or the mitigation of harmful pollutants. The phycoremediation could be mediated by different mechanisms, depending on the HM and its speciation, the used microalgae strain; living or non-living, and the operational condition (Gonzalez-dkila, 1995). The ability of living microalgae to remove and detoxify HMs is the result of several adaptive mechanisms developed over centuries of evolution (Monteiro et al., 2012). Harnessing this natural power in the treatment of HMs contaminated water seems to be a promising strategy. This review provides an in-depth understanding of the mechanisms involved by the living cells of green microalgae for the removal and mitigation of HMs toxicity. It also provides a future outlook for the physicochemical and the genetic modifications that can be applied with a view to improving the phycoremediation capacity, selectivity, and cost-effectiveness of this bioprocess.

2. Mechanisms of HMs phycoremediation using living microalgae

The application of living microalgae for the phycoremediation of HMs can include both extracellular and/or intracellular bioremediation strategies, Figure 1 summarizes the main pathways involved in the bioremediation and mitigation of HMs.

2.1. Extracellular HMs-bioremoval with living microalgae

The extracellular uptake of HMs by living cells of microalgae may occur by biosorption in the cell wall or in the extracellular polymeric substances (EPS) formed by microalgae in response to stress conditions. In the first case, HMs-biosorption refers to a physicochemical property of the microalgae cell surface that binds to HMs ions from the solution independently to the cellular metabolism. However, HMs-biosorption into the EPS is a metabolism-dependent process. In response to metallic stress, microalgae cells can not only regulate EPS synthesis, but also they can change the properties of these biopolymers as required (Naveed et al., 2019; Ubando et al., 2021).

2.1.1. Cell walls composition and its role in HMs-biosorption

The cell wall is the interface between the intracellular compartment and the external environment (Macfie and Welbourn, 2000). It contains multifunctional macromolecules such as lipids, proteins and carbohydrates, which offer on its surface different negatively charged functional groups such as amino, hydroxyl, carboxyl, sulfhydryl, sulfate, phosphate, phenol...etc. (Javanbakht et al., 2014). These negatively charged groups permit the binding of ions from the surrounding environment, making the outer layer of the cell wall as the first participator in the removal of HMs (Leong and Chang, 2020; Saavedra et al., 2018; Singh et al., 2021). Therefore, understanding the structure, composition, and properties of the cell wall is essential when studying biosorption mechanisms (Podder and Majumder, 2017). In addition, this non-metabolic mechanism depends closely on the operating conditions, the influence of the physicochemical conditions including pH, temperature, presence of other ions and the ratio of adsorbate adsorbent must be controlled (Zeraatkar et al., 2016). In recent years, the most frequently used microalgae strains in the phycoremediation belong to the Chlorophyta phylum, particularly species of genera *Chlorella* and *Scenedesmus* (Spain et al., 2021). Nevertheless, even under similar operating conditions, the sensitivity and the biosorption efficiency vary depending on genus and species of microalgae (Kumar et al., 2015). For instance, the growth *C. sorokiniana* and *S. obliquus* in media contaminated with Pb(II), Cd(II), Cu(II) and Cr(VI) was significantly different (Danouche et al., 2020). This can be attributed to the physiology of the strain, in particular the cell walls composition and structure. Depending on the species and the growth stage, different structures and compositions of the call wall have been reported. Within this phylum, it is ranging from a simple cell membrane as of *Dunaliella* and *Isochrysis* species, which consists of a lipid bilayer with integrated and peripheral proteins and sometimes a cap of glycoproteins and glycolipids envelops the outer of the cells surface. To complex multilayer structures with additional intracellular material in vesicles like that of Dinoflagellates strains, or that of euglenophytes and cryptophytes species

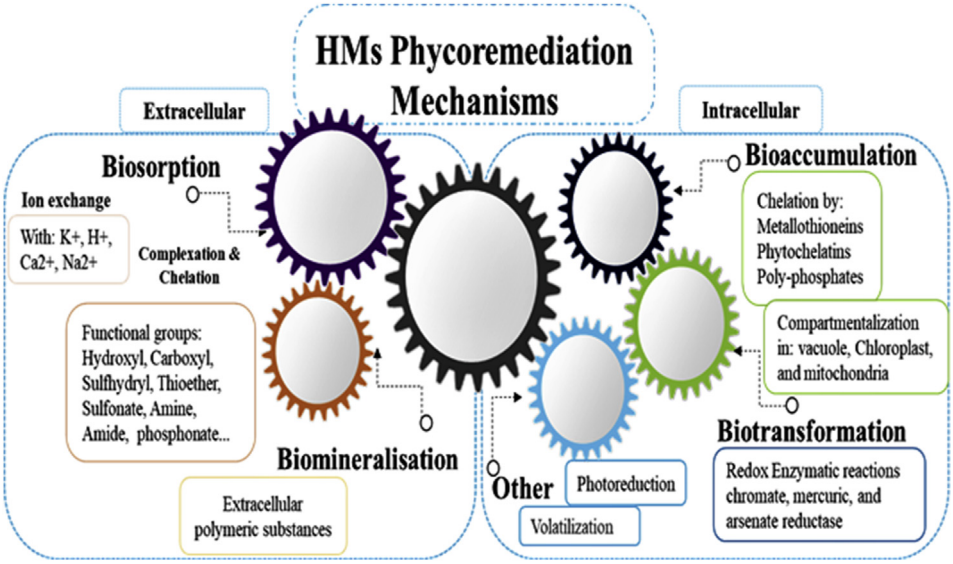

Figure 1. HMs-phycoremediation mechanisms (modified from (García-García et al., 2016; Kumar et al., 2015)).

that characterized by both intracellular and extracellular material associated to the cell membranes (D'Hondt et al., 2017). Figure 2 illustrates the structure of the cell wall of some microalgae species. Furthermore, species of the same genus may exhibit also variations in the composition of their cell walls. For example, *C. vulgaris* has an inner layer (Rashidi and Trindade, 2018), while, *C. homosphaera* and *C. zofingiensis* both have an inner and an outer layer, and also have the trilaminar version of the outer layer (Rodrigues and Pinto, 2011). In the case of *C. trilaminar,* the outermost layer is composed by sporopollenin, the middle layer is principally composed by mannose and chitin-like polysaccharides and the innermost layer is a phospholipid bilayer (Dixon and Wilken, 2018).

2.1.2. Physicochemical interactions of HMs and cell surface

Understanding the interaction of HMs ions and cell surface of microalgae are challenging, due to the complexity of the cell surface. Several chemical and physical interactions have been reported. The chelation and the complexation of HMs with active groups of the cell wall were the main involved mechanisms. Furthermore, the cell surface of microalgae incorporates ions such as Na^{+}, K^{+}, Ca^{2+} and Mg^{2+}, which can be reversibly substituted by other toxic HMs ions in solution, via a process called ion exchange. The physical forces principally van der Waals and electrostatic interactions, can in turn managed the physical adsorption mechanism of metal binding into the cell surface. On the other hand, the microprecipitation is a process that can be associated with both passive and active pathways of metal uptake (Navakoudis and Ververidis, 2018).

2.1.3. Extracellular polymeric substances interactions with HMs

EPS are high molecular weight extracellular biopolymers that can be produced by a diversity of microorganisms including microalgae species. They include nucleic acids, proteins, lipids, sugar, humic substances and other extracellular inorganic components that can bind to carbohydrates (Xiao and Zheng, 2016). Thus, we can divide the EPS of microalgae into three broad categories, soluble EPS in growth media (SL-EPS), attached EPS to the cells wall or Loosely Bound EPS (LB-EPS), as well as Tightly Bound EPS (TB-EPS), which are gel-like coatings of cells wall (Naveed et al., 2019). Microalgae are usually endangered in aquatic ecosystems by the presence of hazardous materials like toxic metals. One of the adaptive mechanisms developed by such organisms as a self-defense mechanism is the production of EPS. Generally, the EPS production increase under the metals stimulation. According to Yu et al. (2019), LB-EPS of *Chlamydomonas reinhardtii* had increased significantly after Cd-exposure. Recently, Li et al. (2021) indicted also an increase in EPS production by *C. reinhardtii* under Pb(II) and Cd(II) stresses. Similarly, Zhang et al. (2015) reported that the increase in EPS yields in Cu-enriched *Chlorella* sp. cultures indicates that Cu-uptake are carried out by EPS rather than intracellular chelation. Comparing EPS-free and EPS-covered cells of *C. pyrenoidosa*, Zhang et al. (2020) show that EPS improve adsorption capacity, reduce intracellular accumulation and increase the tolerance against As ions. EPS appear to be capable of forming an extracellular protective layer on the surface of the cell wall, preventing the harmful effect of HMs in intracellular environment. Therefore, their excretion is a survival mechanism, allowing a maintenance of cellular integrity (Hou et al., 2016; Naveed et al., 2019). Additionally, EPS have abundant charged hydrophobic groups, which are appropriate for an active binding to HMs (Zhang et al., 2020). According to Li et al. (2016), metal biosorption into EPS can be related to cell surface properties and functional groups. Figure 3 summarizes the interactions that can manage the biosorption mechanism of HMs into cells of microalgae.

2.2. HMs-bioaccumulation mechanisms in microalgae

In contrast to the biosorption process, bioaccumulation is a depending metabolic pathway. It refers to the intracellular accumulation of HMs through the cell membranes of living microalgae based on passive and/or active transport pathways (Chojnacka, 2010). It's characterized by two successive stages: first, a rapid, passive and non-specific absorption of metal ions on the cell wall. Followed by an active and/or passive transport across the cell wall and plasma membrane to the cytoplasm (Kumar et al., 2015). Indeed, Pérez-Rama et al. (2002) reported that the Cd(II)-uptake using *Tetraselmis suecica* was a biphasic process, assisted in the first phase by an adsorption to proteins or polysaccharides, followed by an energy-dependent accumulation to the cytosol. Furthermore, when the concentration of metal in the extracellular environment is significantly higher than the intracellular concentration, cations can be transported by the negative charged groups of the cell surface to reach the intracellular compartment via active transport across the plasma

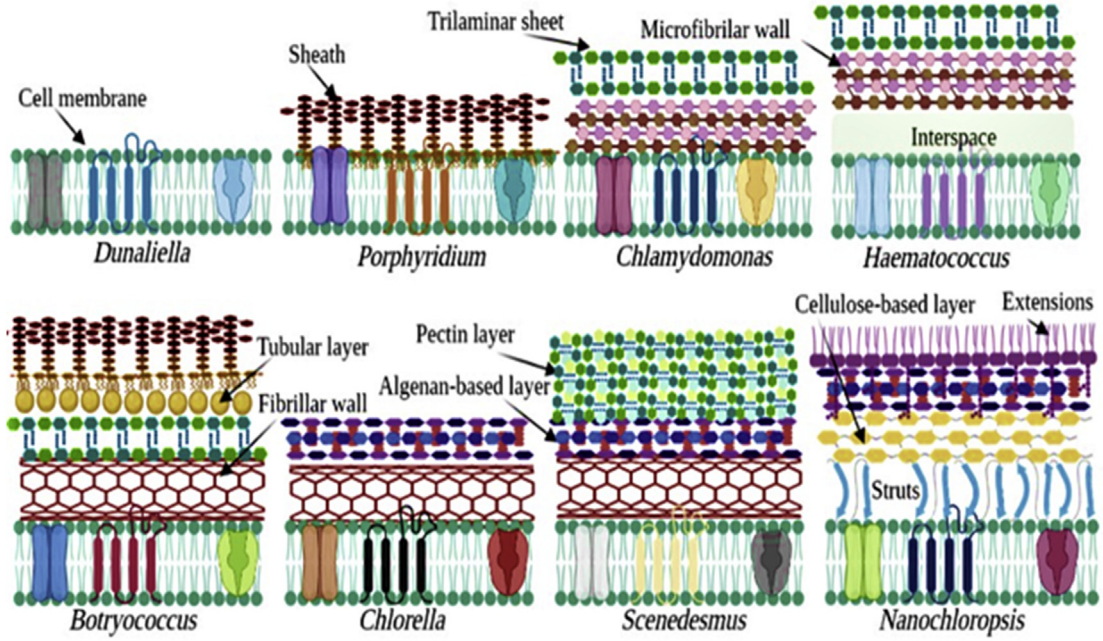

Figure 2. Schematic view of cell wall structures of some microalgae species (modified from (Baudelet et al., 2017; Carvalho et al., 2020), For better interpretation of the color figure, the reader could refer the web version of this article).

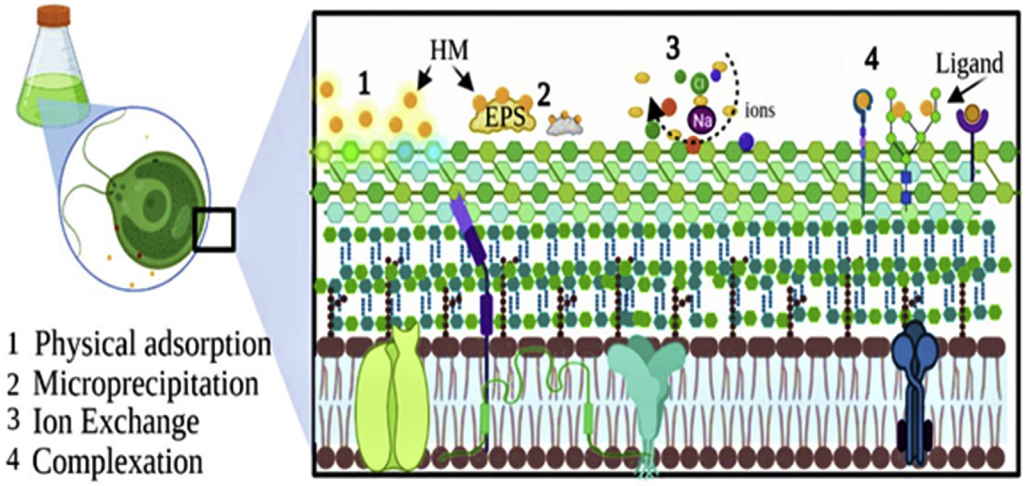

Figure 3. Extracellular bio-removal mechanisms of HMs using living cells of microalgae, modified from (Navakoudis and Ververidis, 2018).

membrane after binding to thiols molecules primarily cysteine (Monteiro et al., 2012). The other amino acids such as histidine, glutamate and proline can play also a crucial role in metal chelation and detoxification (Hayat et al., 2012; Kumar et al., 2015; Leszczyszyn et al., 2010). As most of the HMs are hydrophilic, their transport across the plasma membrane (lipophilic) is mediated mainly through a specific protein (Metal transporters). Thereafter, several detoxification pathways can take place in intracellular compartments (Leong and Chang, 2020; Monteiro et al., 2011).

2.2.1. *Metal transporters in microalgae cell membrane*

Metal transporters play an important role in the interaction of algae with their surroundings. They represent the first line of osmotic balances control, as well as they manage the intracellular concentration of essential ions for micronutrient homeostasis, in order to cope with the deleterious effects of nonessential HMs (Hanikenne et al., 2005). The involvement of membrane transporters have been characterized in various microalgae species (García-garcía et al., 2012; Rosakis and Köster, 2004). According to Blaby-haas and Merchant (2012), two transporter groups are responsible for the influx and efflux of each metal ions in the algal model *C. reinhardtii*. Indeed, the transporters group (A) ensures the traffic of HMs from the extracellular environment to the cytosol, including Natural Resistance-Associated Macrophage Proteins (NRAMP), Zrt-Irt-like proteins (ZIP), Fe-Transporter (FTR) and Cu-transporter (CTR) families. This group of transporters has been identified also in the vacuole membrane and has the same function as the assimilative transporters. The second group (B) includes members from the cation diffusion facilitator (CDF), P1B-type ATPases, FerroPortiN (FPN) and the families Ca (II)-sensitive cross-complementer$_1$/Vacuolar iron transporter$_1$ (Ccc$_1$/VIT$_1$) (Figure 4), they decrease the metal concentration in the cytoplasm through active mechanism of efflux of metal ions into the extracellular surroundings, This occurs when the metal concentration exceeds cellular requirements, or if the metal peptide complex starts to affect cellular metabolism (Tripathi et al., 2019). Very

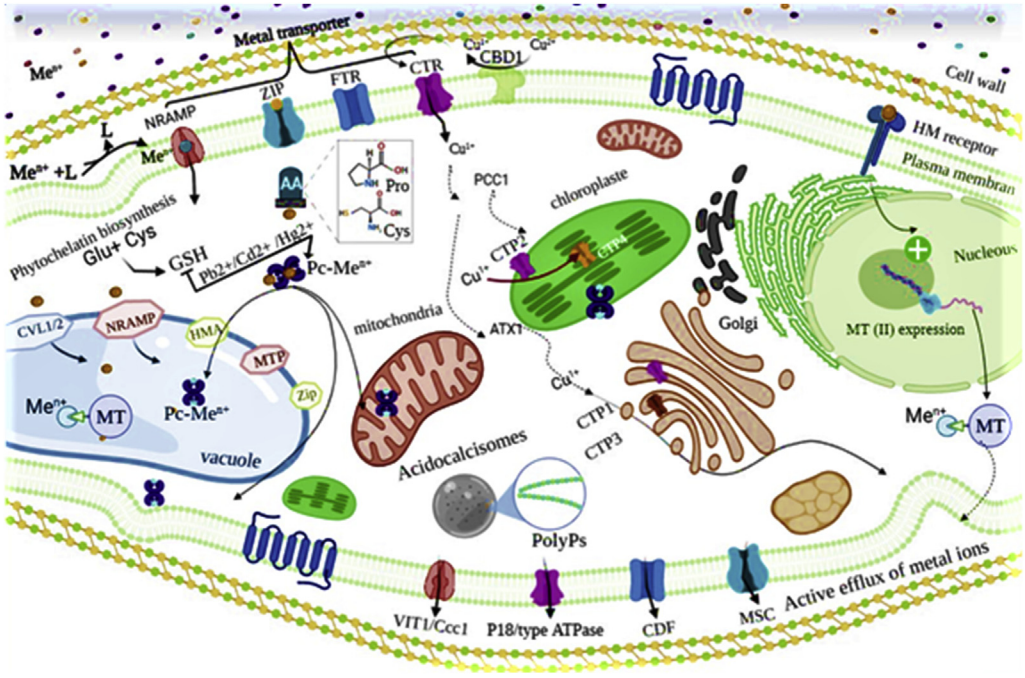

Figure 4. General scheme of intracellular detoxification of HMs in microalgae cells adapted from (Blaby-Haas and Merchant, 2012; Torres et al., 2008).

few studies have described the role of membrane transporters in HMs accumulation in microalgae. Thus, future research on this topic is crucial for a deeper understanding of the pathways of metal accumulation in cell of microalgae.

2.2.2. Pathways of intracellular HMs detoxification

Various strategies are used by microalgae to maintain intracellular ion concentrations at the optimal level and protect the cell from non-essential metals (Torres et al., 2008). These strategies include the modification of the permeability of plasma membrane and function of the cell wall, the activation of phytochelatins synthase, the formation of HMs-metallothioneins, HMs-poly-phosphates complexes, the compartmentalization into organelles, as well as the activation of metal efflux systems (García-García et al., 2016; Navakoudis and Ververidis, 2018).

2.2.2.1. Chelation by metallothioneins. MTs are small peptides that can be divided into two groups, gene-encoded proteins (MTs class I and II) and enzymatically synthesized polypeptides (MTs class III) commonly named phytochelatins (PCs) (Cobbett and Goldsbrough, 2002). The MTs class II are a super-rich cysteine family located in the cytosol, characterized by low molecular weight (6–7 kDa). These metal-binding proteins are primarily involved in the control of intracellular concentrations of metals at regular levels (Gaur and Rai, 2001). MTs-class II are little studied in microalgae compared to other organisms. The most known MTs from microalgae are of *Chlorella Aureococcus, Symbiodinium, Nannochloropsis, Thalassiosira,* and *Ostreococcus* genera (Balzano et al., 2020). Since microalgae can survive in habitats contaminated with HM, they have the potential for new forms of MTs. Therefore, future research should focus on the discovery of such new MTs using in silico experiment and experimental researches.

2.2.2.2. Chelation by phytochelatins. In response to metal exposure, microalgae like other organisms synthesize enzymatically PCs rather than MTs that are genetically encoded. The PCs are also thiol-containing peptides consisting of three amino acids: glutamate (Glu), cysteine (Cys) and glycine (Gly), with general structure (γ -Glu-Cys)n-Gly, the sulfhydryl group in the cysteine molecule is responsible for metal binding. Their biosynthetic pathway starts with the formation of γ–Glu–Cys by γ–glutamylcysteine synthetase (γ-GCS). Afterwards, the glutathione synthetase (GS) catalyzes the production of glutathione (GSH). Next, the transfer of γ-Glu-Cys from GSH to another GSH molecule is followed by the formation of (γ-Glu-Cys) 2-Gly (Hirata et al., 2005). Indeed, GSH has been reported to be the key ligand when intracellular metal concentrations are low, while metal detoxification is ensured by PCs when metal concentrations are high (Gaur and Rai, 2001). The synthesis of MTs class III in microalgae strains has been documented in several studies, it was first identified in *C. fusca* after exposure to Cd(II) ions (Gekeler et al., 1988). Subsequently, numerous researches were aiming to clarify PCs biosynthesis under HMs exposure such as Gómez-Jacinto et al. (2015) who identified Hg–PCs in *C. sorokiniana* under Hg-exposure. also in *S. bijugatus* Cu(II)-treated (Nagalakshmi and Prasad, 2001), and Pb (II)-treated *Stichococcus bacillaris* (Pawlik-skowron, 2002). Furthermore, it has been reported that Cd(II) was the most effective stimulator of PCs synthase of *Chlamydomonas* species, while other metals have shown less effectiveness in various degrees (Abboud and Wilkinson, 2013; Kobayashi et al., 2006; Li et al., 2021; Suárez et al., 2010). Nevertheless, PC synthesis was most strongly induced by Zn in *Dunaliella* species (Hirata et al., 2001; Tsuji et al., 2003). Recently, Wang et al. (2017) reported that GSH was the main non-protein sulfhydryl compound in *D. salina.* Its exposure to As(III) and As(V) has induced PCs synthesis indicating therefore their involvement in As-detoxification. The HMs-bound to PCs, they can be stored into organelles of microalgae cells as organometallic complexes.

2.2.2.3. Chelation by poly-phosphates. In nature, orthophosphate polymers (polyp) are abounding in both eukaryotic and prokaryotic organisms. Numerous algal research report the accumulation of polyp body in acidocalcisomes founded mainly in granules of specific vacuoles in the trans-Golgi that show diverse variants according to their disposition, composition, and consistency (Goodenough et al., 2019; Tsednee et al., 2019). However, polyp can also be localized in other cellular compartments including the cell wall, cytoplasm, mitochondria, and endoplasmic reticulum and nucleus (Sanz-luque et al., 2020; Werner et al., 2007). For instance, the metabolism of polyp in *C. reinhardtii* can be regulate via enzymatic reaction of exopolyphosphatase, or through compartmentalization mechanisms, mainly by the acidocalcisome membrane transporters (Ruiz et al., 2001). HMs sequestration and detoxification are among the various functions and cellular responses where polyp are implicated including cycling phosphorus (P) in oceans, P reservoir, acclimatation to nutrient deprivation as well as in response to osmotic and heat stress conditions (Sanz-luque et al., 2020). It has been reported that polyp formation facilitates the accumulation of HMs and storage (Wang and Dei, 2006). In fact, the crucial function of acidocalcisomes and polyps in maintaining cellular homeostasis of essential ions underlines the hypothesis that this role could be extended to the regulation of levels of toxic HMs in the intracellular compartment bioaccumulation via chelation and compartmentalization (García-García et al., 2016).

2.2.3. HMs compartmentalization in the vacuole, chloroplast and mitochondria

As previously mentioned, the sequestration of the MTs-HMs complex in particular cell organelles, especially vacuoles, chloroplasts, and mitochondria has prompted researchers to develop hypotheses about metal bioaccumulation pathways, and the tolerance mechanisms associated. Various biophysical techniques can be used for studding the intracellular localization and the analysis of HMs or their complex (Polyp-HMs, MT-HMs PCs-HMs), mainly by using transmission electron microscope (TEM) with added techniques and accessories, such as energy-dispersive X-ray spectroscopy (EDS), electron energy loss spectroscopy (EELS), electron spectroscopic imaging (ESI), and atomic force microscopy (AFM) (Tripathi et al., 2019). In plant species, vacuolar compartmentalization has been reported as an indispensable component of HMs detoxification (Sharma et al., 2016). In contrast, metal sequestration has been identified in different cell organelles. For example, Shanab et al. (2012) found by means of TEM analysis, an electron-dense dark spherical bodies accumulated in the vacuoles of *Pseudochlorococcum typicum* exposed to Pb ions. Volland et al. (2012) located also the accumulation of Cr (IV) using TEM coupled with EELS and ESI inside cells of *Micrasterias denticulata* as chromium-iron-oxygen compound and increased vacuolation. In contrast, Hanikenne et al. (2009), described that the main storage location of PCs–Cd(II) complexes in *C. reinhardtii* was in the chloroplast. Likewise, Mendoza-co and Moreno-sa, (2005) found that more than 60% of the accumulated Cd(II) resides inside the chloroplast of *Euglena gracilis*. Similarly, Soldo et al. (2005) reported that the intracellular Cu(II) was detected in the thylakoids and the pyrenoid of *O. nephrocytioides* cells. In addition, Mendoza-co et al. (2005) demonstrated the accumulation of Cd(II) and Cd(II)-Mt (III) complexes in chloroplast and mitochondria of *E. gracilis*.

2.3. Biotransformation and mitigation of HMs by microalgae

The broad sense of biotransformation refers to the pathway by which xenobiotic or endobiotic chemicals are metabolized into products, which vary in their activity (activation vs deactivation), excretability (hydrophobic vs hydrophilic), and toxicity (detoxification vs toxication) (Rourke and Sinal, 2014). In the context of HMs-phycoremediation, the term "biotransformation" may apply to a variety of detoxification pathways, primarily enzymatic and biochemical transformation of toxic HMs.

2.3.1. Enzymatic biotransformation

The enzymatic biotransformation of HMs can be defined as chemical transformation from a high toxic form to a less harmful through oxidation

reduction reactions. In fact, HMs cannot be degraded, but they can be transformed from one oxidation state to another an inorganic complex form, in order to mitigate their toxic impact. Only few studies have emphasized the role of oxidoreductase enzymes in the detoxification of HMs by microalgae. The main redox enzymes reported in microalgae are chromate reductases, mercuric reductase and arsenate reductase (Leong and Chang, 2020). It has been reported by Lee et al. (2017) and Yen et al. (2017) that *C. vulgaris* strains have the potential to convert Cr(VI) to Cr(III) through an enzymatic reaction catalyzed by the chromate reductase. Also, Kelly et al. (2007) reported that the microalgae strains of *Selenastrum minutum*, *C. fusca* and *Galdiera sulphuraria* have the ability to catalyze the bio-transformation of Hg^{2+} into elemental Hg0 and meta-cinnabar (β-HgS) through mercuric reductase. The arsenate reductase has also been found in the green microalgae *C. reinhardtii* (Yin et al., 2011). Figure 5 depicts the intracellular and extracellular mitigation pathways for Cr (VI) by microalgae.

2.3.2. Biochemical transformations of HMs

During the phytoremediation process, cells of microalgae may use biochemical mechanisms for HMs-mitigation. For example, the reaction of chromium reduction from the hexavalent oxidation state to the trivalent form is catalyzed by the transfer of electrons to the reduced form of GSH (Yen et al., 2017) (Figure 5). Moreover, the mitigation of the toxicity of inorganic arsenic can be the result of several other detoxification mechanisms (Hasegawa et al., 2019; Karadjova et al., 2008; Levy et al., 2005; Wang et al., 2015b). In fact, a variety of microalgae species seem to be able to reduce As(V) to As(III). For example, Karadjova et al. (2008) indicated that after 72 h of exposure of *C. salina* to As(V), 32% of total intracellular concentration of As(V) was converted to As (III). According to Hasegawa et al. (2001), the initial concentration of As(V) in the medium was firstly converted to As(III) by *C. aciculare*, and reached a peak concentration during the exponential growth. Generally, As-species are distributed among different cellular fractions of cells of microalgae including the lipid, cytosolic, cell membranes and debris fractions. The detoxification pathway begins with the reduction of As(V) into As(III) form, and then methylation to monomethylarsonate (MMA(V)) via oxidase and S-adenosylmethionine (SAM). The produced MMA is converted to dimethylarsinate (DMA(V)), that is further reduced to DMA(III), next its conversion to a range of organoarsenicals such as, arsenolipids, arsenosugars, arsenobetaine, and arsenoribosides (Arora et al., 2018; Wang et al., 2015b). Figure 6 shows the pathways of biotransformation of As(V and III) by microalgae.

2.3.3. Other biotransformation mechanisms of HMs

In addition to the intracellular HMs-biotransformation mechanism previously described, the biosynthesis of metal nanoparticles can occur both extracellularly and intracellularly, depending on the location of NP biosynthesis and the reductive agents (Hamida et al., 2020). It has been reported that microalgae have the potential to remodel toxic HMs into malleable forms, such as via their combination with protein, lipids, carbohydrate, pigments, and other antioxidants molecules which can reduce the charge of the metal ion to a zero-valence state (Chaudhary et al., 2020). Also in the extracellular surroundings, the charged functional groups of the cells surface as well as the EPS, the binding sites, organic ligands may contribute to speciation changes of the toxic HMs via redox reactions (Naveed et al., 2019). Indeed, Priyadarshini et al. (2019) reported that the extracellular biosynthesis of metal nanoparticles appears to be simpler compared to the intracellular environment, where the algae extract contains polysaccharides, proteins and pigments that act as reducing agents that stabilize metal ions and metal nanoparticles. On the other hand, biologically and non-biologically volatilization of mercury can be used by *E. gracilis* as another biotransformation mechanism for the mitigation of the toxic effect of mercury (Devars et al., 2000). Besides, Deng et al. (2006) reported that the Cr(VI)-biotransformation with *C. vulgaris* was managed by a photoreduction pathway.

3. Future outlook for enhancing the phycoremediation process

Numerous research studies have demonstrated the feasibility of using green microalgae in metal remediation, both technically and economically. In addition to optimizing the factors that influence the phycoremediation process, various physicochemical and biotechnological approaches can be used to (i) improve the extracellular uptake and selectivity for a target metal (Precious elements or rare earths), to (ii)

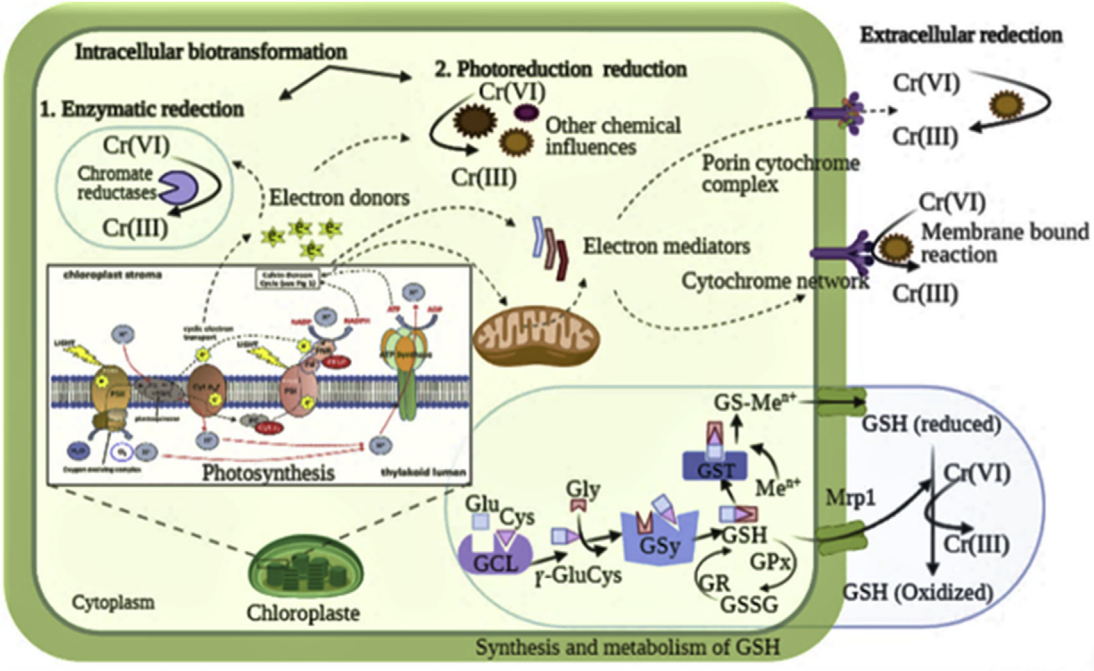

Figure 5. Proposed biotransformation pathways of Cr(VI) developed from the finding of (Deng et al., 2006; Lee et al., 2017; Rahman and Thomas, 2021; Yen et al., 2017).

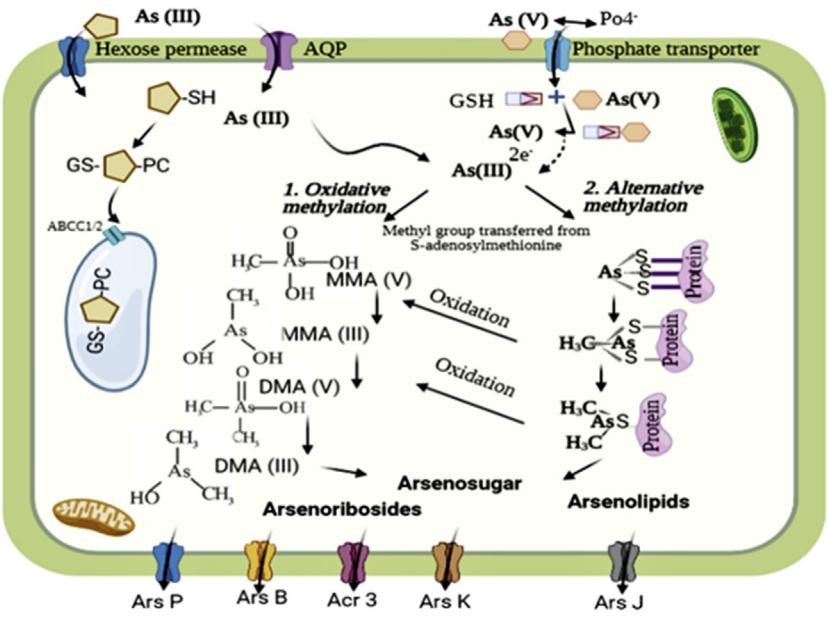

Figure 6. Proposed biotransformation pathways of As (V and III) developed from (Arora et al., 2018; Garbinski et al., 2019; Wang et al., 2015b).

increase the intracellular bioaccumulation capacity, or to (iii) enhance the biotransformation and mitigation capacity.

3.1. Cell manipulation for enhancing the biosorption capacity and selectivity

As detailed above, the biosorption of HMs occurs mainly in the cell surface. Thus, modifying their composition and their physicochemical properties can improve the interaction with ions of HMs, increasing thereby the biosorption performance.

3.1.1. Physicochemical approaches

3.1.1.1. Cell surface functionalization. According to Pearson acid-base concept, the affinity of the cell surface towards species of HMs considerably depends on the functional groups. For instance, the biosorption capacity of Pb(II), Cd(II), Zn(II), Cu(II), and Ni(II) into *Neochloris minuta* and *N. alveolaris* was related to the HSAB theory in terms of their biomass compositions and the type of hard or soft metal acid based (Giarikos et al., 2021). Indeed, changing the nature and density of functional groups at the cell surface, regulated the affinity and sorption behavior for specific metal species. The functionalization of the cell surface can be achieved by introduction of active functional groups (binding sites) using chemical reaction, or by inhibiting functional groups that have a negative impact on the target metal's biosorption (Yang et al., 2015).

3.1.1.2. Chemical pretreatment. Many pretreatment reagents can be used to change the physicochemical properties of the cell wall, and remove impurities on the surface, as well as to expose metal binding sites by eliminating blocking ions. These reagents include acid, alkali, organic solvents (alcohol, acetone and toluene), and inorganic salts (NaCl and Na_2CO_3) (Nagase et al., 2005). Besides the use of acid that may dissolve polysaccharides, an alkali washing can get rid of the liposome on the cell membrane. Both pretreatment processes can effectively remove the impurities and expose the binding sites by eliminating the blocking ions, thus improving the sorption capacity (Mehta et al., 2002).

3.1.1.3. Magnetic modification. The magnetically modification of microalgae with magnetic nano- and micro particles have been used in a variety of algae biotechnology research areas, including the removal of HMs ions (Safarik et al., 2020). According to Lalhmunsiama et al. (2017), cells of *C. vulgaris* coated with magnetic iron oxide NPs has successfully removed ions of Cd(II) and Pb(II) from aqueous solutions. Thus, their simultaneous biosorption was completed by distinguished binding sites. Pb(II) ions were chemically bound to amino groups, while Cd(II) ions were bound to dissociated hydroxyl or carboxyl groups through weak electrostatic forces. Likewise, Ferraro et al. (2018) reported that cells of native *Chlorella* sp. flocculated with polyethylenimine-coated magnetic have exhibited a high removal efficiency of Zn (II) ions. Although physicochemical modification can improve the binding performance of cellular metals, it can also present some drawbacks. Firstly, they can lead to a decrease in selectivity towards the targeted metal species. Secondly, washing the cells could lead to a loss of biomass, and finally, chemical and magnetic modifications are costly for large-scale applications (Cheng et al., 2019).

3.1.2. Bioengineering of cell-surface approaches

Adsorption-based processes have a high potential for HMs absorption, but their common weakness is a lack of selectivity for the absorption of target metal from heterogeneous metal ions solutions (Shen et al., 2017). The advancement of bioengineering of living microorganisms has recently enabled the construction of new biosorbents by adapting the metallosorption properties of the cell surfaces, in order to increase the adsorption selectivity for target metal species (Wang et al., 2021). This molecular technique is called cell surface engineering or cell surface display. It consists of expressing proteins of interest (passenger protein) such metal-binding proteins (MTs or PCs) on the cell surface by a translational fusion with anchoring motif (carrier protein), which allows the passenger protein to be exported across the cell envelope and anchors it to the cell surface (Kuroda and Ueda, 2011; Yang et al., 2015). Artificial proteins with new activities and/or imitative roles such as high metal-binding and pre-programmed properties for the removal of HMs in theory that can be located in any specific cellular compartment may be created through genetic and protein engineering (Agapakis and Silver, 2009). Figure 7 illustrates the cell surface engineering procedure for a target metal biosorption. First, the coding DNA of the target metal-binding peptide or protein previously was obtained via whole sequence synthesis or PCR amplification from genomic or plasmid DNA. Next it can be transformed to the host in the form of fusion of a protein

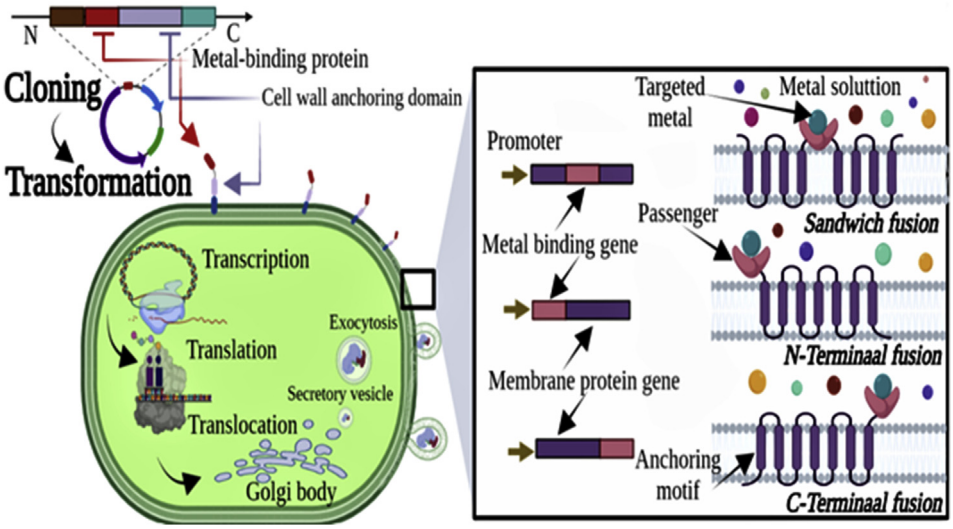

Figure 7. Procedure of cell surface engineering for a target metal biosorption.

under specific induction. The metal-binding protein/peptide can be displayed in the form of fusion of an anchor protein after transcription, translation and translocation. The secretory vesicles encompassing the passenger and carrier proteins pass through the cell membrane and anchor the passenger proteins to the surface of cell wall (Kuroda and Ueda, 2011; Li and Tao, 2013; Wang et al., 2021). There are considerable published works on genetically-engineered biosorbents for removal of HMs using bacteria, yeast and fungi (Wang et al., 2021; Yang et al., 2015). However, to our knowledge, there are not yet studies using microalgae as host cells for the surface display of target metal binding. He et al. (2011) showed that the removal capacity of Hg (II) using a transgenic *C. reinhardtii* (2AMT-2) designed to express a membrane-anchored MT polymer, was at high levels that could be released into the aqueous phase by sonication over a wide pH range of 2–9. Based on these preliminary studies, it's essential to emphasize the importance of future work on the bioengineering of the microalgae cell surface for the biosorption of HMs. Indeed, several benefits can be derived from overexpression of metal-binding-proteins into the cell surface of green microalgae. Firstly, due to the increase of the ligand on the surface of the cell, the processing time will be greatly shortened. Second, such a modification would increase the selectivity for a target metal. This adsorbed metal can thereby be easily recovered with mild pickling reagent, instead of breaking the cell wall to recover the metals inside the cell. This makes such biosorbent recyclable and economical. Finally, the surface adsorption is independent of metabolism and the dead biomass can therefore be used.

3.2. Microalgae genetically engineered for intracellular recovery of HMs

Application of genetic engineering strategy for the enhancement of the intra-cellular uptake of HMs encompass the genetic modification of genes encoding for: metals membrane transporters, high-affinity HM binding proteins such as genetically encoded chelators, enzymes that catalyze the reduction of toxic metals via redox transformations, and enzymes that scavenge reactive oxygen species (Rajamani et al., 2007). In fact, the genetic manipulation of microalgae for enhancing the bioaccumulation capacity typically comprises two techniques: gene overexpression and the construction of transgenic algae by introducing exogenous DNA into cells of microalgae (Cheng et al., 2019).

3.2.1. Metal-transporters transition in microalgae

Identification of microalgae genes encoding metalloregulatory proteins is critical for genetic engineering research for phytoremediation purposes. As detailed in the previous section (2.1.1), metal transporters play an important role in the interaction of microalgae with their surroundings. They constitute the second line of protection after the cell wall, via the control of the perturbations in cellular and subcellular homeostasis of metal (Blaby-Haas and Merchant, 2012). Despite the fact that this approach may allow both increased accumulation of metals in the cell and increased tolerance to metals, such as by transferring a toxic metal out of the cytosol and into an internal compartment, genetic manipulation of metal transporters towards HMs phycoremediation is still quite limited. Ibuot et al. (2017) reported that the overexpression of metal tolerance protein (MTP) in *C. reinhardtii* led to a significant increase in resistance to Cd(II) toxicity as well as bioaccumulation efficiency. This was proposed to be due to increased transfer and storage of Cd(II) into vacuoles. According to Ibuot et al. (2020), the expression of a plant Cd and Zn transporter ($AtHMA_4$) known to bind metals in *C. reinhardtii*, either as a full-length protein or only as the C-terminal tail, had led to increase the bioaccumulation and internalization of both Cd(II) and Zn(II) ions, with expression of either the FL protein or the CT domain. This suggests that the enhancement of metal bioaccumulation was primarily the result of increased metal binding rather than metal transport. Ramírez-rodríguez et al. (2019) evaluated the As-bioremoval capability of Acr_3-modified *C. reinhardtii* strain produced by transforming the wild-type strain with *Agrobacterium tumefaciens* using the construct $pARR_1$ including a synthetic, optimized acr3 gene from *Pteris vittata*, reported to have two homologs proteins $PvACR_{3;1}$ and $PvACR_3$ localized in the membrane of vacuolar possible ensure the sequestration of As(III) by effluxing into the vacuole (Indriolo et al., 2010). The result of this study indicates that the acr3-modified strain removed 1.5 to 3 times more arsenic compared to the wild-type.

3.2.1. Molecular manipulation for AA and PCs biosynthesis

As previously mentioned in the section (2.2.2), the metal chelator is primarily responsible for the intracellular bioaccumulation of HMs. Genetic manipulation of the biosynthesis and metabolism of certain AA, and PCs seems to be an optimal strategy to increase the capacity of HMs bioaccumulation into microalgal cultures. However, despite the great potential for involvement of AA and the PCs biosynthesis in the HMs-tolerance and detoxification, the number of microalgae mutants developed for this purpose is still limited. Zheng et al. (2013) reported that overexpressing of $HISN_3$ gene (Coding for phosphoribosylformimino-5-aminoimidazole carboxamide ribonucleotide isomerase) in *C. reinhardtii* induces a high tolerance towards Ni, with moderate increase of histidine accumulation in comparison to the wild type. Furthermore, Siripornadulsil et al. (2002) suggest that the expression of the P5CS (mothbean Δ 1 -pyrroline-5--carboxylate synthetase) gene in *C. reinhardtii* induces proline buildup compared to wild type, and increases their tolerance against Cd(II) ions. Similarly, the expression of the HAL_2 gene in *C. reinhardtii,* which regulates

cysteine synthesis increased the Cd-carrying capacity of transgenic cells compared to wild-type cells (Rajamani et al., 2007). Regarding the transgenic manipulation for the transformation of *C. reinhardtii* with a foreign MTs(II), it was firstly documented by Cai et al. (1999) that the cell density of *C. reinhardtii* cells expressing a foreign MTs(II) was higher compared to the wild type when exposed to Cd(II) ions.

3.2.3. Genetic transformation for HMs enzyme biocatalysts

The mitigation of toxic HMs by living microorganisms can also be improved using genetically engineered enzymes (Diep et al., 2018). For instance, the transformation of *Chlorella* spp. DT, by mercuric reductase (merA) gene from *Bacillus megaterium*, improved reduction of bioremoval Hg(II) up to twofold compared to the wild type (Huang et al., 2006). As previously noted in the section (2.2.2), the biosynthesis of GSH occurs via an enzymatic reaction catalyzed by γ -GCS. Recently, Piña-olavide et al. (2020) reported that the transformation of *C. reinhardtii* with a synthetic gene (gshA) encoding for γ-GCS had significantly increased Cd (II) bioaccumulation. Furthermore, Wang et al. (2015a) studied the transformation of *C. reinhardtii* with CrGNAT gene encoding for acetyltransferase, they reported also that such modification regulates excess Cu(II) bioaccumulation and tolerance. The acetyltransferase can be involved in the production of cysteine, glutathione and PCs under Cd(II) stress (Howarth et al., 2003).

4. Conclusion

Based on the above considerations, we can infer that the strains of green microalgae had multifaceted mechanisms for removing toxic HMs, including extracellular biosorption, EPS-complexation, intracellular bioaccumulation and compartmentalization, enzymatic reduction, biomethylation, and volatilization. Although the process of phycoremediation of HMs is still on the lab scale, the analysis of the involved mechanisms provides insights for improving efficiency, selectivity, and reduces processing costs. Recently, physicochemical and molecular modifications of the microbial cell surface have demonstrated their applicability for the enhancement of bioremediation performance. In fact, several microorganisms with innovative cell surface properties have been bioengineered. In contrast, there are still limited examples of genetic manipulation of microalgae for HMs-removal purposes. Further research in the fields of genetic engineering, pre-treatment, immobilization techniques and a combination of other physicochemical strategies will allow phycoremediation processes to be used on a large scale.

Declarations

Author contribution statement

All authors listed have significantly contributed to the development and the writing of this article.

Funding statement

This work was supported by Moroccan Foundation for Advanced Science, Innovation and Research (MAScIR), and Regional University Centre of Interface (CURI), Sidi Mohamed Ben Abdellah University.

Data availability statement

Data included in article/supplementary material/referenced in article.

Declaration of interests statement

The authors declare no conflict of interest.

Additional information

No additional information is available for this paper.

References

Abboud, P., Wilkinson, K.J., 2013. Role of metal mixtures (Ca, Cu, and Pb) on Cd bioaccumulation and phytochelatin production by *Chlamydomonas reinhardtii*. Environ. Pollut. 179, 33–38.
Agapakis, C.M., Silver, P.A., 2009. Molecular BioSystems the design of novel biological networks w. Mol. Biosyst. 5, 704–713.
Ali, H., Khan, E., Ilahi, I., 2019. Environmental chemistry and ecotoxicology of hazardous heavy metals: environmental persistence, toxicity, and bioaccumulation. J. Chem. 2019.
Arora, N., Gulati, K., Tripathi, S., Pruthi, V., 2018. Algae as a budding tool for mitigation of arsenic from aquatic systems. In: Mechanisms of Arsenic Toxicity and Tolerance in Plants, pp. 269–297.
Balzano, S., Sardo, A., Blasio, M., Chahine, T.B., Anno, F.D., Sansone, C., Brunet, C., 2020. Microalgal metallothioneins and phytochelatins and their potential use in bioremediation. Front. Microbiol. 11, 1–16.
Baudelet, P.H., Ricochon, G., Linder, M., Muniglia, L., 2017. A new insight into cell walls of Chlorophyta. Algal Res. 25, 333–371.
Blaby-Haas, C.E., Merchant, S.S., 2012. The ins and outs of algal metal transport. Biochim. Biophys. Acta 1823 (9), 1531–1552.
Cai, X., Brown, C., Adhiya, J., Traina, S.J., Sayre, R.T., 1999. Growth and heavy metal binding properties of transgenic *Chlamydomonas* expressing a foreign metallothionein gene growth and heavy metal binding properties of transgenic *Chlamydomonas* expressing a foreign. Int. J. Phytoremediation 1, 37–41.
Carvalho, J.C. De, Irineudo Jr., A.M., Vinicius, G., Pereira, D.M., Bianchi, A., Medeiros, P., Sydney, E.B., Rodrigues, C., Tatiana, D., Aulestia, M., Porto, L., Vandenberghe, D.S., Soccol, V.T., Soccol, C.R., 2020. Microalgal biomass pretreatment for integrated processing into biofuels, food, and feed. Bioresour. Technol. 300, 122719.
Chaudhary, R., Nawaz, K., K.A., K., Hano, C., Abbasi, B.H., Anjum, S., 2020. An overview of the algae-mediated biosynthesis of nanoparticles and their biomedical applications. Biomolecules 10, 1497.
Cheng, S.Y., Show, P., Lau, F., Chang, J., Ling, T.C., 2019. Review new prospects for modified algae in heavy metal adsorption. Trends Biotechnol. 37, 1255–1268.
Chibueze, C., Chioma, A., Chikere, B., 2016. Bioremediation techniques – classification based on site of application : principles , advantages , limitations and prospects. World J. Microbiol. Biotechnol. 32, 1–18.
Chojnacka, K., 2010. Biosorption and bioaccumulation–the prospects for practical applications. Environ. Int. 36 (3), 299–307.
Cobbett, C., Goldsbrough, P., 2002. Phytochelatins and metallothioneins: roles in heavy metal detoxification and homeostasis. Annu. Rev. Plant Biol. 53, 159–182.
D'Hondt, E., Martín-Juárez, J., Bolado, S., Kasperoviciene, J., Koreiviene, J., Sulcius, S., Elst, K., Bastiaens, L., 2017. Cell disruption technologies. In: Microalgae-Based Biofuels and Bioproducts: from Feedstock Cultivation to End-Products, pp. 133–154.
Danouche, M., El Ghachtouli, N., El Baouchi, A., El Arroussi, H., 2020. Heavy metals phycoremediation using tolerant green microalgae : enzymatic and non-enzymatic antioxidant systems for the management of oxidative stress. J. Environ. Chem. Eng. 8, 104460.
Deng, L., Wang, H., Deng, N., 2006. Photoreduction of chromium (VI) in the presence of algae *Chlorella vulgaris*. J. Hazard Mater. 138 (2), 288–292.
Devars, S., Avilés, C., Cervantes, C., Moreno-sánchez, R., 2000. Mercury uptake and removal by *Euglena gracilis*. Arch. Microbiol. 174, 175–180.
Diep, P., Mahadevan, R., Yakunin, A.F., 2018. Heavy metal removal by bioaccumulation using genetically engineered microorganisms. Front. Bioeng. Biotechnol. 6.
Dixon, C., Wilken, L.R., 2018. Green microalgae biomolecule separations and recovery. Bioresour. Bioprocess. 5 (1), 1–24.
Dung, T.T.T., Cappuyns, V., Swennen, R., Phung, N.K., 2013. From geochemical background determination to pollution assessment of heavy metals in sediments and soils. Rev. Environ. Sci. Biotechnol. 12, 335–353.
Ferraro, G., Toranzo, R.M., Castiglioni, M., Lima, E., Vasquez, M., Fellenz, N.A., Zysler, R.D., Pasquevich, D.M., Bagnato, C., 2018. Zinc removal by *Chlorella* sp. biomass and harvesting with low cost magnetic particles. Algal Res. 33, 266–276.
Fu, F., Wang, Q., 2011. Removal of heavy metal ions from wastewaters: a review. J. Environ. Manag. 92, 407–418.
Gałuszka, A., 2007. A review of geochemical background concepts and an example using data from Poland. Environ. Geol. 861–870.
Garbinski, L.D., Rosen, B.P., Chen, J., 2019. Pathways of arsenic uptake and efflux. Environ. Int. 126, 585–597.
García-garcía, J.D., Olin-sandoval, V., Saavedra, E., Girard, L., Hernández, G., Moreno-sánchez, R., 2012. Sulfate uptake in photosynthetic *Euglena gracilis*. Mechanisms of regulation and contribution to cysteine homeostasis. BBA - Gen. Subj. 1820, 1567–1575.
García-García, J.D., Sánchez-Thomas, R., Moreno-Sánchez, R., 2016. Bio-recovery of non-essential heavy metals by intra- and extracellular mechanisms in free-living microorganisms. Biotechnol. Adv. 34, 859–873.
Garrett, R.G., 2000. Natural sources of metals to the environment. Hum. Ecol. Risk Assess. 6, 945–963.
Gaur, J.P., Rai, L.C., 2001. Heavy metal tolerance in algae. In: Algal Adaptation to Environmental Stresses, pp. 363–388.
Gekeler, W., Grill, E., Winnacker, E.L., Zenk, M.H., 1988. Algae sequester heavy metals via synthesis of phytochelatin complexes. Arch. Microbiol. 150 (2), 197–202.
Giarikos, D.G., Brown, J., Razeghifard, R., Vo, D., Castillo, A., Nagabandi, N., 2021. Effects of nitrogen depletion on the biosorption capacities of *Neochloris minuta* and *Neochloris alveolaris* for five heavy metals. Appl. Water Sci. 11, 1–15.
Gómez-Jacinto, V., García-Barrera, T., Gómez-Ariza, J.L., Garbayo-Nores, I., Vílchez-Lobato, C., 2015. Elucidation of the defence mechanism in microalgae *Chlorella sorokiniana* under mercury exposure. Identification of Hg-phytochelatins. Chem. Biol. Interact. 238, 82–90.

Gonzalez-dkila, M., 1995. The role of phytoplankton cells on the control of heavy metal concentration in seawater. Mar. Chem. 48, 215–236.
Goodenough, U., Heiss, A.A., Roth, R., Rusch, J., Lee, J., 2019. Acidocalcisomes : ultrastructure, biogenesis, and distribution in microbial eukaryotes. Protist 170, 287–313.
Hamida, R.S., Ali, M.A., Redhwan, A., Bin-Meferij, M.M., 2020. Cyanobacteria–a promising platform in green nanotechnology: a review on nanoparticles fabrication and their prospective applications. Int. J. Nanomed. 15, 6033.
Hanikenne, M., Krämer, U., Demoulin, V., Baurain, D., 2005. Comparative inventory of metal transporters in the green alga *Chlamydomonas reinhardtii* and the red alga *Cyanidioschizon merolae*. Plant Physiol. 137, 428–446.
Hanikenne, M., Merchant, S.S., Hamel, P., 2009. Transition metal Nutrition : a balance between deficiency and toxicity. The *Chlamydomonas Sourcebook*, pp. 333–399.
Hasegawa, H., Papry, R.I., Ikeda, E., Omori, Y., Mashio, A.S., Maki, T., Rahman, M.A., 2019. Freshwater phytoplankton: biotransformation of inorganic arsenic to methylarsenic and organoarsenic. Sci. Rep. 9, 1–13.
Hasegawa, H., Sohrin, Y., Seki, K., Sato, M., Norisuye, K., Naito, K., Matsui, M., 2001. Biosynthesis and release of methylarsenic compounds during the growth of freshwater algae. Chemosphere 43, 265–272.
Hayat, S., Hayat, Q., Alyemeni, M.N., Wani, A.S., Pichtel, J., Ahmad, A., 2012. Role of proline under changing environments: a review. Plant Signal. Behav. 7, 1456–1466.
He, Z., Siripornadulsil, S., Sayre, R.T., Traina, S.J., Weavers, L.K., 2011. Removal of mercury from sediment by ultrasound combined with biomass (transgenic *Chlamydomonas reinhardtii*). Chemosphere 83, 1249–1254.
Hirata, K., Tsuji, N., Miyamoto, K., 2005. Biosynthetic regulation of phytochelatins, peptides, heavy metal-binding. J. Biosci. Bioeng. 100, 593–599.
Hirata, K., Tsujimoto, Y., Namba, T., Ohta, T., Hirayanagi, N., Miyasaka, H., Meinhart, H., Miyasaka, H., Miyamoto, K., 2001. Strong induction of phytochelatin synthesis by zinc in marine green alga, *Dunaliella tertiolecta*. J. Biosci. Bioeng. 92, 24–29.
Hou, J., Yang, Y., Wang, P., Wang, C., Miao, L., 2016. Effects of CeO_2 , CuO , and ZnO nanoparticles on physiological features of *Microcystis aeruginosa* and the production and composition of extracellular polymeric substances. Environ. Sci. Pollut. Res. 24 (1), 226–235.
Howarth, J.R., Dom, R., Guti, G., Wray, J.L., Romero, L.C., Gotor, C., 2003. The serine acetyltransferase gene family in *Arabidopsis thaliana* and the regulation of its expression by cadmium. Plant Mol. Biol. 51, 589–598.
Huang, C.C., Chen, M.W., Hsieh, J.L., Lin, W.H., Chen, P.C., Chien, L.F., 2006. Expression of mercuric reductase from *Bacillus megaterium* MB1 in eukaryotic microalga *Chlorella* sp. DT: an approach for mercury phytoremediation. Appl. Microbiol. Biotechnol. 72, 197–205.
Ibuot, A., Dean, A.P., McIntosh, O.A., Pittman, J.K., 2017. Metal bioremediation by CrMTP4 over-expressing *Chlamydomonas reinhardtii* in comparison to natural wastewater-tolerant microalgae strains. Algal Res. 24, 89–96.
Ibuot, A., Webster, R.E., Williams, L.E., Pittman, J.K., 2020. Increased metal tolerance and bioaccumulation of zinc and cadmium in *Chlamydomonas reinhardtii* expressing a AtHMA4 C - terminal domain protein. Biotechnol. Bioeng. 2996–3005.
Indriolo, E., Na, G., Ellis, D., Salt, D.E., Banks, J.A., 2010. A vacuolar arsenite transporter necessary for arsenic tolerance in the arsenic hyperaccumulating *fern Pteris vittata* is missing in flowering plants. Plant Cell 22, 2045–2057.
Javanbakht, V., Alavi, S.A., Zilouei, H., 2014. Mechanisms of heavy metal removal using microorganisms as biosorbent. Water Sci. Technol. 69, 1775–1787.
John, J., 2003. Phycoremediation: algae as tools for remediation of mine-void wetlands. In: Modern Trends in Applied Aquatic Ecology. Springer, Boston, MA, pp. 133–147.
Karadjova, I.B., Slaveykova, V.I., Tsalev, D.L., 2008. The biouptake and toxicity of arsenic species on the green microalga *Chlorella salina* in seawater. Aquat. Toxicol. 87, 264–271.
Kelly, D.J.A., Budd, K., Lefebvre, D.D., 2007. Biotransformation of mercury in pH-stat cultures of eukaryotic freshwater algae. Arch. Microbiol. 45–53.
Kobayashi, I., Fujiwara, S., Saegusa, H., Inouhe, M., Matsumoto, H., Tsuzuki, M., 2006. Relief of arsenate toxicity by Cd-stimulated phytochelatin synthesis in the green alga *Chlamydomonas reinhardtii*. Mar. Biotechnol. 8, 94–101.
Kumar, K.S., Dahms, H.U., Won, E.J., Lee, J.S., Shin, K.H., 2015. Microalgae - a promising tool for heavy metal remediation. Ecotoxicol. Environ. Saf. 113, 329–352.
Kuroda, K., Ueda, M., 2011. Molecular design of the microbial cell surface toward the recovery of metal ions. Curr. Opin. Biotechnol. 22, 427–433.
Lalhmunsiama, Gupta, Prabuddha L., Hyunhoon, J., Diwakar, T., Sung-Ho, K., Seung-Mok, L., 2017. Insight into the mechanism of Cd (II) and Pb (II) removal by sustainable magnetic biosorbent precursor to *Chlorella vulgaris*. J. Taiwan Inst. Chem. Eng. 71, 206–213.
Lee, L., Hsu, C.Y., Yen, H.W., 2017. The effects of hydraulic retention time (HRT) on chromium(VI) reduction using autotrophic cultivation of *Chlorella vulgaris*. Bioproc. Biosyst. Eng. 40, 1725–1731.
Leong, Y.K., Chang, J.S., 2020. Bioremediation of heavy metals using microalgae: recent advances and mechanisms. Bioresour. Technol. 303, 122886.
Leszczyszyn, O.I., White, C.R.J., Blindauer, C.A., 2010. The isolated Cys 2 His 2 site in E C metallothionein mediates metal-specific protein folding. Mol. Biosyst. 6, 1592–1603.
Levy, J.L., Stauber, J.L., Adams, M.S., Maher, W.A., Kirby, J.K., Jolley, D.F., 2005. Toxicity, biotransformation, and mode of action of arsenic in two freshwater microalgae (*Chlorella* sp. and *Monoraphidium arcuatum*). Environ. Toxicol. Chem. 24, 2630–2639.
Li, C., Zheng, C., Fu, H., Zhai, S., Hu, F., Naveed, S., Zhang, C., Ge, Y., 2021. Contrasting detoxification mechanisms of *Chlamydomonas reinhardtii* under Cd and Pb stress. Chemosphere 274, 129771.
Li, N., Wei, Dong, Wang, Shaotong, Hu, Lihua, Xu, Weiying, Du, Bin, Wei, Qin, Wei, D., Wang, S., Hu, L., Xu, W., Du, B., Wei, Q., 2016. Comparative study of the role of extracellular polymeric substances in biosorption of Ni (II) onto aerobic/anaerobic granular sludge. J. Colloid Interface Sci. 490, 754–761.
Li, P., Tao, H., 2013. Cell surface engineering of microorganisms towards adsorption of heavy metals. Crit. Rev. Microbiol. 41, 140–149.
Macfie, S.M., Welbourn, P.M., 2000. The cell wall as a barrier to uptake of metal ions in the unicellular green alga *Chlamydomonas reinhardtii* (Chlorophyceae). Arch. Environ. Contam. Toxicol. 39, 413–419.
Mehta, S.K., Tripathi, B.N., Gaur, J.P., 2002. Enhanced sorption of Cu 2+ and Ni 2+ by acid-pretreated. J. Appl. Phycol. 14, 267–274.
Mendoza-co, D., Loza-tavera, H., Herna, A., Moreno-sa, R., 2005. Sulfur assimilation and glutathione metabolism under cadmium stress in yeast , protists and plants. FEMS Microbiol. Rev. 29, 653–671.
Mendoza-co, D.G., Moreno-sa, R., 2005. Cd^{2+} transport and storage in the chloroplast of *Euglena gracilis*. Biochim. Biophys. Acta 1706, 88–97.
Monteiro, C.M., Castro, P.M.L., Malcata, F.X., 2011. Microalga-mediated bioremediation of heavy metal–contaminated surface waters. In: Biomanagement of Metal-Contaminated Soils. Springer, Dordrecht, pp. 365–385.
Monteiro, C.M., Castro, P.M.L., Malcata, F.X., Instituto, I., Carlos, A., Campos, O., Maia, C., Pedro, P.–A.S., 2012. Metal uptake by Microalgae : underlying mechanisms and practical applications. Biotechnol. Prog. 28 (2), 299–311.
Nagalakshmi, N., Prasad, M.N.V., 2001. Responses of glutathione cycle enzymes and glutathione metabolism to copper stress in *Scenedesmus bijugatus*. Plant Sci. 160, 291–299.
Nagase, H., Inthorn, D., Oda, A., Nishimura, J.U.N., Kajiwara, Y., Park, M., Hirata, K., 2005. Improvement of selective removal of heavy metals in cyanobacteria by NaOH treatment. J. Biosci. Bioeng. 99, 372–377.
Navakoudis, A.M.E., Ververidis, K.P.F., 2018. Microalgae: a potential tool for remediating aquatic environments from toxic metals. Int. J. Environ. Sci. Technol. 15 (8), 1815–1830.
Naveed, S., Li, C., Lu, X., Chen, S., Yin, B., Zhang, C., Ge, Y., 2019. Microalgal extracellular polymeric substances and their interactions with metal(loid)s: a review. Crit. Rev. Environ. Sci. Technol. 49, 1769–1802.
Pawlik-skowron, B., 2002. Correlations between toxic Pb effects and production of Pb-induced thiol peptides in the microalga *Stichococcus bacillaris*. Environ. Pollut. 119, 119–127.
Pérez-Rama, M., Abalde Alonso, J., Herrero López, C., Torres Vaamonde, E., 2002. Cadmium removal by living cells of the marine microalga *Tetraselmis suecica*. Bioresour. Technol. 84, 265–270.
Piña-olavide, R., Paz-maldonado, L.M.T., Torre, M.C.A. La, García-soto, M.J., Ramírez-rodríguez, A.E., Rosales, S., Bañuelos-hernández, B., De, R.F.G., Bañuelos-hernández, B., Fernando, R., Increased, G. De, 2020. Increased removal of cadmium by *Chlamydomonas reinhardtii* modified with a synthetic gene for γ - glutamylcysteine synthetase. Int. J. Phytoremediation 1–9.
Podder, M.S., Majumder, C.B., 2017. Prediction of phycoremediation of As(III) and As(V) from synthetic wastewater by *Chlorella pyrenoidosa* using artificial neural network. Appl. Water Sci. 7, 3949–3971.
Priyadarshini, E., Priyadarshini, S.S., Pradhan, N., 2019. Heavy metal resistance in algae and its application for metal nanoparticle synthesis. Appl. Microbiol. Biotechnol. 103 (8), 3297–3316.
Rahman, Z., Singh, V.P., 2019. The relative impact of toxic heavy metals (THMs) (arsenic (As), cadmium (Cd), chromium (Cr)(VI), mercury (Hg), and lead (Pb)) on the total environment: an overview. Environ. Monit. Assess. 191.
Rahman, Z., Thomas, L., 2021. Chemical-assisted microbially mediated chromium (Cr) (VI) reduction under the influence of various electron donors , redox mediators , and other Additives : an outlook on enhanced Cr(VI) removal. Front. Microbiol. 11, 1–19.
Rajamani, S., Siripornadulsil, S., Falcao, V., Torres, M., Colepicolo, P., Sayre, R., 2007. Phycoremediation of heavy metals. In: Transgenic Microalgae as Green Cell Factories, pp. 99–109.
Ramírez-rodríguez, A.E., Bañuelos-hernández, B., Mariano, J., Govea-alonso, D.G., Rosales-mendoza, S., Catalina, M., Torre, A. De, Monreal-escalante, E., Paz-maldonado, L.M.T., Bañuelos-hernández, B., Monreal-escalante, E., Arsenic, L.M.T.P., 2019. Arsenic removal using *Chlamydomonas reinhardtii* modified with the gene acr3 and enhancement of its performance by decreasing phosphate in the growing media. Int. J. Phytoremediation 1–7.
Rashidi, B., Trindade, L.M., 2018. Detailed biochemical and morphologic characteristics of the green microalga *Neochloris oleoabundans* cell wall. Algal Res. 35, 152–159.
Rodrigues, A., Pinto, E., 2011. Evaluation of *Chlorella* (Chlorophyta) as source of fermentable sugars via cell wall enzymatic hydrolysis. Enzym. Res. 2011.
Rosakis, A., Köster, W., 2004. Transition metal transport in the green microalga *Chlamydomonas reinhardtii* genomic sequence analysis. Res. Microbiol. 155, 201–210.
Rourke, J.L., Sinal, C.J., 2014. Biotransformation/metabolism In: Encyclopedia of Toxicology, third ed., 2. Elsevier, pp. 289–294.
Ruiz, F.A., Marchesini, N., Seufferheld, M., Docampo, R., 2001. The polyphosphate bodies of *Chlamydomonas reinhardtii* possess a proton-pumping pyrophosphatase and are similar to acidocalcisomes. J. Biol. Chem. 276 (49), 46196–46203.
Saavedra, R., Muñoz, R., Taboada, M.E., Vega, M., Bolado, S., 2018. Comparative uptake study of arsenic, boron, copper, manganese and zinc from water by different green microalgae. Bioresour. Technol. 263, 49–57.
Safarik, I., Baldikova, E., Prochazkova, J., Pospiskova, K., 2020. Magnetic particles in algae biotechnology : recent updates. J. Appl. Phycol.
Sanz-luque, E., Bhaya, D., Grossman, A.R., 2020. Polyphosphate : a multifunctional metabolite in cyanobacteria and algae. Front. Microbiol. 11, 1–21.
Shanab, S., Essa, A., Shalaby, E., 2012. Bioremoval capacity of three heavy metals by some microalgae species (Egyptian isolates). Plant Signal. Behav. 7.
Sharma, S.S., Dietz, K., Mimura, T., 2016. Vacuolar Compartmentalization as Indispensable Component of Heavy Metal Detoxification in Plants, pp. 1112–1126.
Shen, N., Birungi, Z.S., Chirwa, E.M.N., 2017. Selective biosorption of precious metals by cell-surface engineered selective biosorption of precious metals by cell-surface engineered microalgae. Chem. Eng. Trans. 61.

Singh, D.V., Bhat, R.A., Upadhyay, A.K., Singh, R., Singh, D.P., 2021. Microalgae in aquatic environs: a sustainable approach for remediation of heavy metals and emerging contaminants. Environ. Technol. Innov. 21, 101340.

Siripornadulsil, S., Traina, S., Verma, D.P.S., Sayre, R.T., 2002. Molecular mechanisms of proline-mediated tolerance to toxic heavy metals in transgenic microalgae. Plant Cell 14, 2837–2847.

Soldo, D., Hari, R., Sigg, L., Behra, R., 2005. Tolerance of *Oocystis nephrocytioides* to copper : intracellular distribution and extracellular complexation of copper. Aquat. Toxicol. 71, 307–317.

Spain, O., Plöhn, M., Funk, C., 2021. The cell wall of green microalgae and its role in heavy metal removal. Physiol. Plantarum 1–10.

Suárez, C., Torres, E., Pérez-Rama, M., Herrero, C., Abalde, J., 2010. Cadmium toxicity on the freshwater microalga *Chlamydomonas moewusii Gerloff*: biosynthesis of thiol compounds. Environ. Toxicol. Chem. 29, 2009–2015.

Tchounwou, P.B., Yedjou, C.G., Patlolla, A.K., Sutton, D.J., 2012. Heavy metals toxicity and the environment. Mol. Clin. Environ. Toxicol. 101, 133–164.

Torres, M.A., Barros, M.P., Campos, S.C.G., Pinto, E., Rajamani, S., Sayre, R.T., Colepicolo, P., 2008. Biochemical biomarkers in algae and marine pollution : a review. Ecotoxicol. Environ. Saf. 71, 1–15.

Tripathi, S., Arora, N., Gupta, P., Pruthi, P.A., Poluri, K.M., Pruthi, V., 2019. Microalgae: an Emerging Source for Mitigation of Heavy Metals and Their Potential Implications for Biodiesel Production, Advanced Biofuels: Applications, Technologies and Environmental Sustainability. Elsevier Ltd, pp. 97–128.

Tsednee, M., Castruita, M., Salomé, X.P.A., Sharma, A., Lewis, X.B.E., Schmollinger, S.R., Strenkert, D., Holbrook, K., Otegui, X.M.S., Khatua, K., Das, S., Datta, A., Chen, X.S., Ramon, C., Ralle, M., Weber, P.K., Stemmler, T.L., Pett-ridge, J., Hoffman, B.M., Merchant, S.S., 2019. Manganese co-localizes with calcium and phosphorus in *Chlamydomonas acidocalcisomes* and is mobilized in manganese-deficient conditions. J. Biol. Chem. 294, 17626–17641.

Tsuji, N., Hirayanagi, N., Iwabe, O., Namba, T., Tagawa, M., 2003. Regulation of phytochelatin synthesis by zinc and cadmium in marine green alga. Dunaliella tertiolecta 62, 453–459.

Ubando, A.T., Africa, A.D.M., Maniquiz-Redillas, M.C., Culaba, A.B., Chen, W.H., Chang, J.S., 2021. Microalgal biosorption of heavy metals: a comprehensive bibliometric review. J. Hazard Mater. 402, 123431.

Volland, S., Lütz, C., Michalke, B., Lütz-meindl, U., 2012. Intracellular chromium localization and cell physiological response in the unicellular alga Micrasterias. Aquat. Toxicol. 109, 59–69.

Wang, J., Chen, C., 2009. Biosorbents for heavy metals removal and their future. Biotechnol. Adv. 27, 195–226.

Wang, W., Dei, R.C.H., 2006. Metal stoichiometry in predicting Cd and Cu toxicity to a freshwater green alga *Chlamydomonas reinhardtii*. Environ. Pollut. 142, 303–312.

Wang, Ye, Cheng, Z.Z., Chen, X., Zheng, Q., Yang, Z.M., 2015a. CrGNAT gene regulates excess copper accumulation and tolerance in *Chlamydomonas reinhardtii*. Plant Sci. 240, 120–129.

Wang, Y., Selvamani, V., Yoo, I., Kim, T.W., Hong, S.H., 2021. A novel strategy for the microbial removal of heavy Metals : cell-surface display of peptides A novel strategy for the microbial removal of heavy Metals : cell-surface display of peptides. Biotechnol. Bioproc. Eng.

Wang, Y., Zhang, C., Zheng, Y., Ge, Y., 2017. Phytochelatin synthesis in *Dunaliella salina* induced by arsenite and arsenate under various phosphate regimes. Ecotoxicol. Environ. Saf. 136, 150–160.

Wang, Ya, Wang, S., Xu, P., Liu, C., Liu, M., Wang, Yulan, Wang, C., 2015b. Review of arsenic speciation , toxicity and metabolism in microalgae. Rev. Environ. Sci. Bio/Technol. 14, 427–451.

Werner, T.P., Amrhein, N., Freimoser, F.M., 2007. Inorganic polyphosphate occurs in the cell wall of *Chlamydomonas reinhardtii* and accumulates during cytokinesis. BMC Plant Biol. 11, 1–11.

Xiao, R., Zheng, Y., 2016. Overview of microalgal extracellular polymeric substances (EPS) and their applications. Biotechnol. Adv. 34 (7), 1225–1244.

Yang, T., Chen, M., Wang, J., 2015. Genetic and chemical modification of cells for selective separation and analysis of heavy metals of biological or environmental significance. Trends Anal. Chem. 66, 90–102.

Yen, H., Chen, P., Hsu, C., Lee, L., 2017. The use of autotrophic *Chlorella vulgaris* in chromium (VI) reduction under different reduction conditions. J. Taiwan Inst. Chem. Eng. 74, 1–6.

Yin, X., Wang, L., Duan, G., Sun, G., 2011. Characterization of arsenate transformation and identification of arsenate reductase in a green alga *Chlamydomonas reinhardtii*. J. Environ. Sci. 23, 1186–1193.

Yu, Z., Zhang, T., Hao, R., Zhu, Y., 2019. Sensitivity of *Chlamydomonas reinhardtii* to cadmium stress is associated with phototaxis. Environ. Sci. Process. Impacts 21, 1011–1020.

Zeraatkar, A.K., Ahmadzadeh, H., Talebi, A.F., Moheimani, N.R., McHenry, M.P., 2016. Potential use of algae for heavy metal bioremediation, a critical review. J. Environ. Manag. 181, 817–831.

Zhang, J., Zhou, F., Liu, Y., Huang, F., Zhang, C., 2020. Effect of extracellular polymeric substances on arsenic accumulation in *Chlorella pyrenoidosa*. Sci. Total Environ. 704, 135368.

Zhang, W., Tan, N.G.J., Fu, B., Li, S.F.Y., 2015. Metallomics and NMR-based metabolomics of *Chlorella* sp. reveal the synergistic role of copper and cadmium in multi-metal toxicity and oxidative stress. Metallomics 7, 426–438.

Zheng, Q., Cheng, Z.Z., Yang, Z.M., 2013. HISN3 mediates adaptive response of *Chlamydomonas reinhardtii* to excess nickel. Plant Cell Physiol. 54, 1951–1962.

Chapitre II

Overview of the management of heavy metal toxicity by microalgae through biochemical, enzymatic and phycohormonal mechanisms

RÉSUMÉ

Les microalgues, principalement les cyanophycées, sont les plus anciennes formes de vie qui ont colonisé la Terre. Au cours des siècles d'évolution, elles ont développé des mécanismes d'adaptation pour survivre aux conditions environnementales difficiles auxquelles elles sont confrontées, notamment l'exposition à des éléments toxiques tels que les MLs. Dans cette deuxième revue, nous abordons trois axes majeurs concernant le stress oxydatif induit par les MLs chez les microalgues. Il s'agit d'abord des effets néfastes des MLs sur les microalgues, pour ensuite discuter des réponses biochimiques et enzymatiques face au stress oxydatif, et souligner dans la dernière partie le rôle des phytohormones dans la régulation des stress oxydatifs. La réponse des microalgues aux effets toxiques des MLs est similaire à celle produite face à tous les autres types de stress abiotique. Elle conduit généralement à la production des ROS, tels que l'oxygène singulet ($^1O_2$), le radical anion superoxyde (O_2•.), le radical hydroxyle (HO•), le radical perhydroxy (HO_2•) et le peroxyde d'hydrogène (H_2O_2). En effet, l'augmentation des taux de ROS dans la cellule entraîne une altération de plusieurs fonctions vitales, telles que la peroxydation des lipides, l'oxydation des protéines et des sucres et la détérioration des acides nucléiques. Pour faire face à ces effets néfastes, plusieurs stratégies d'autodéfense sont adoptées par les cellules des microalgues, notamment l'engagement des enzymes de piégeage des ROS à savoir, la superoxyde dismutase, la catalase, la guaiacol peroxydase, l'ascorbate peroxydase, la glutathion réductase..., ainsi que via l'intervention des systèmes antioxydants non-enzymatiques dont les principaux composés antioxydants sont l'ascorbate, le glutathion, les tocophérols, les composés phénoliques, les pigments, ainsi que la production de certains acides aminés comme la proline. En outre, plusieurs classes de phytohormones sont présentes chez les microalgues, ils comprennent l'acide abscissique, les auxines, les brassinostéroïdes, les cytokinines et les gibbérellines. En effet, ces phytohormones influencent de manier direct ou indirect les réponses moléculaires et physiologiques des microalgues face à l'exposition aux MLs. Bien que plusieurs études suggèrent la phycoremédiation des MLs par les microalgues, les mécanismes moléculaires et les voies de signalisation via les phytohormones ne sont pas clairs. D'où la nécessité d'appliquer des approches omiques pour mieux comprendre les systèmes de défense contre les phénomènes de stress métallique.

Journal of Applied Phycology

Overview of the management of heavy metal toxicity by microalgae through biochemical, enzymatic and phycohormonal mechanisms

--Manuscript Draft--

Manuscript Number:	JAPH-D-21-00519
Full Title:	Overview of the management of heavy metal toxicity by microalgae through biochemical, enzymatic and phycohormonal mechanisms
Article Type:	Book Reviews
Keywords:	microalgae; Phycoremediation; Heavy Metals; Antioxidants; ROS-Enzymes; Phytohormones.
Corresponding Author:	Mohammed Danouche MASCIR: Moroccan Foundation for Advance Science Innovation and Research Rabat, MOROCCO
Corresponding Author Secondary Information:	
Corresponding Author's Institution:	MASCIR: Moroccan Foundation for Advance Science Innovation and Research
Corresponding Author's Secondary Institution:	
First Author:	Mohammed Danouche
First Author Secondary Information:	
Order of Authors:	Mohammed Danouche
	Naima El Ghachtouli
	Hicham El Arroussi
Order of Authors Secondary Information:	
Funding Information:	
Abstract:	Microalgae are among the oldest life forms to have colonized the Earth, and over centuries of evolution, they have developed adaptive mechanisms that allow them to survive harsh environmental conditions, including exposure to toxic xenobiotics such as heavy metals (HMs). The response of microalgae to HMs stress is like that occurring under any other stress conditions, generally leading to the formation of reactive oxygen species (ROS). An increase in ROS levels in algal cells causes alterations of various biological functions, mainly lipid peroxidation, protein oxidation and nucleic acid damage. To cope with these disturbances, cells of microalgae employ several self-defense mechanisms, based on the action of ROS-scavenging enzymes and non-enzymatic antioxidant systems. The contribution of phytohormones to the management of abiotic stress is also one of the most important mechanisms. Although several studies suggest that microalgae are potential organisms for phycoremediation of heavy metals, the mechanisms by which they cope with oxidative stress remain unclear. This review aims to: (i) highlight the adverse effects of HMs on microalgae, (ii) describe the enzymatic and biochemical mechanisms by which microalgae manage oxidative stress, and finally (iii) point out the roles of phycohormones in the regulation of oxidative stress caused by HMs.

Powered by Editorial Manager® and ProduXion Manager® from Aries Systems Corporation

Overview of the management of heavy metals toxicity by microalgae

Danouche Mohammed [a,b]*, El Ghachtouli Naïma[b], El Arroussi Hicham [a,c]

[a] *Green Biotechnology Center, Moroccan Foundation for Advanced Science, Innovation and Research (MAScIR), Rabat, Morocco.*
[b] *Microbial Biotechnology and Bioactive Molecules Laboratory, Sciences and Technologies Faculty, Sidi Mohamed Ben Abdellah University, Fez, Morocco.*
[c] *AgroBioScience (AgBS), Mohammed VI Polytechnic University (UM6P), Benguerir, Morocco.*

***Corresponding author**: Danouche Mohammed
Address: Microbial Biotechnology and Bioactive Molecules Laboratory, Faculty of Sciences and Techniques, Sidi Mohamed Ben Abdellah University, Route Immouzer, P. O. Box 2202, Fez, Morocco.
***E-mail Address:** mohammed.danouche@usmba.ac.ma

Abstract

Microalgae are among the oldest life forms to have colonized the Earth, and over centuries of evolution, they have developed adaptive mechanisms that allow them to survive harsh environmental conditions, including exposure to toxic xenobiotics such as heavy metals (HMs). The response of microalgae to HMs stress is like that occurring under any other stress conditions, it generally leads to the formation of reactive oxygen species (ROS). An increased ROS levels in algal cells causes alterations of various biological functions, primarily lipid peroxidation, protein oxidation and nucleic acid damage. To cope with these perturbations, microalgae cells employ several self-defense mechanisms, based on the action of ROS-scavenging enzymes and non-enzymatic antioxidant systems. The contribution of phytohormones to the management of oxidative stress is also one of the most important mechanisms. Although several studies suggest that microalgae are potential organisms for phycoremediation of HMs, the mechanisms by which they cope with oxidative stress remain unclear. This review aims to: (i) highlight the oxidative stress of HMs on cells of microalgae, (ii) describe the enzymatic and biochemical mechanisms by which microalgae manage oxidative stress, and finally (iii) point out the roles of phytohormones in the regulation of oxidative stress caused by HMs.

Graphical abstract

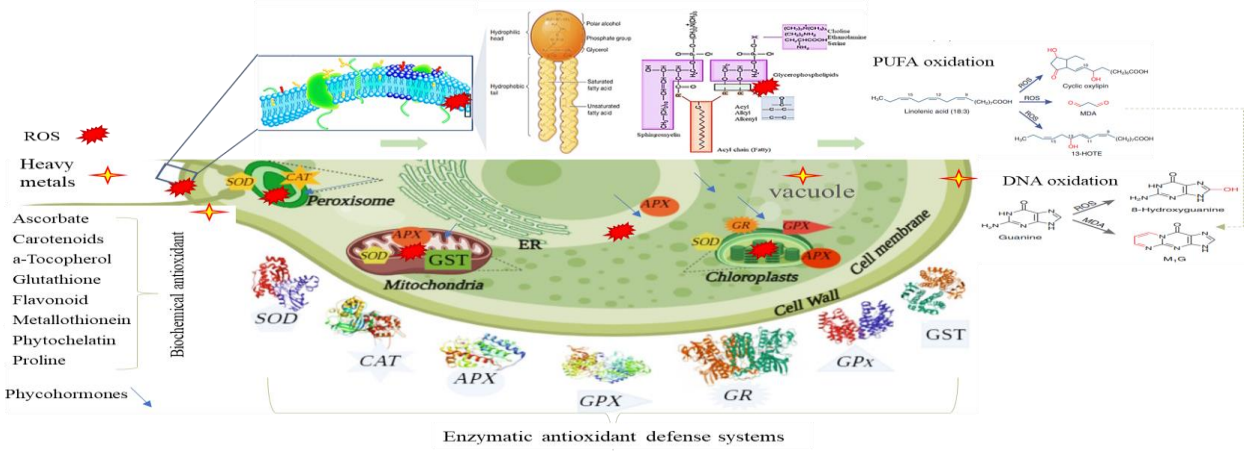

Keywords: Microalgae; Heavy Metals; Antioxidants; ROS-Enzymes; Phytochelatins; Phytohormones.

1. Introduction

Microalgae are among the primitive microorganisms of anoxygenic photosynthesis. According to Vishnivetskaya (2009), green microalgae have appeared on earth about 1.5 billion years ago, from a symbiosis of cyanobacteria and non-photosynthetic eukaryotic ancestors. Although oxygen is a vital element for many biological functions in aerobic organisms, the by-products of its metabolism are very harmful (Mallick and Mohn, 2000). Indeed, the aerobic metabolism is recognized as a constant generator of reactive oxygen species (ROS) which are confined in different intracellular compartments such as chloroplasts, mitochondria, peroxisomes... etc. Under natural conditions, the intracellular concentrations of ROS in cells of microalgae are constantly maintained at low equilibrium levels thanks to the ROS scavenging antioxidant systems (Ugya et al., 2019). The disturbances of the equilibrium between the production and the scavenging of ROS lead to an increase in the intracellular levels of ROS which can induce stress responses, and cause significant cellular damages (Huang et al., 2019). In addition to endogenous sources, several exogenous conditions can disrupt the redox balance of microalgae cells, including the high light intensity, nutrient deficiency, and exposure to xenobiotics…etc. (Cirulis et al., 2013). Although some heavy metals (HMs) are essential micronutrients for microalgae, the majority of them are toxic and they can stimulate the production of ROS even at very low concentrations (Pinto et al., 2003). Worldwide, the pollution of aquatic ecosystems by HMs has recently become a major environmental problem. Toxic HMs are widely used in many industrial activities (mining, fossil fuel combustion, electroplating, fertilizers....), leading to the discharge of large quantities of wastewater containing these pollutants (Leong and Chang, 2020). The treatment of such wastewater is a real challenge. Although traditional procedures such as chemical precipitation, ion exchange, membrane filtration, and electrochemical approaches are successful, they have the disadvantages of being expensive to operate and maintain, as well as causing secondary pollution (Fu and Wang, 2011). Because of their ecological aspect and low-cost. bioremediation of HMs has been widely applied as an emerging and promising approach. Indeed, several studies have shown the potential use of microalgae as effective remediators for many HMs. Yet, the mechanisms by which microalgae manage the stress induced by HMs exposure are not clearly understood. In fact, most of what is known about the responses of microalgae to HMs toxicity is based on fundamental knowledge of response mechanisms in plants. Although these two groups share some characteristics, but there are many differences in morphology, physiology, and metabolisms... etc. Therefore, the mechanisms by which plants manage ROS are not always the same for microalgae (Bajguz, 2011). The present study aims to (i) highlight the oxidative stress of HMs on cells of microalgae; (ii) outline the enzymatic and the biochemical mechanisms by which microalgae manage the oxidative stress; and (iii) define the role of phytohormones in regulating metal stress.

2. HMs-induced oxidative stress in microalgae

Contamination of aquatic ecosystems by HMs can be a natural consequence of erosion, seepage, and geodynamic phenomena, as well as, the result of anthropogenic activities such as mining, irrational use of fertilizers in agriculture, and poor management of industrial wastes (Ali et al., 2019; Tchounwou et al., 2012). Due to their wide distribution in different biotopes, including extreme areas and polluted environments, microalgae are subject to various types of environmental stresses, including exposure to HMs (Mallick and Mohn, 2000). The response of microalgae to such stress conditions leads to the production of O_2-mediated ROS via redox reactions such as the so-called Fenton reactions. Especially by the production of singlet oxygen ($^1O_2$), superoxide anion radical (O_2•), hydroxyl radical (OH•), perhydroxy radical (HO_2•), and hydrogen peroxide (H_2O_2)

(Pinto et al., 2003). The activity of ROS in all biological systems is related to the physicochemical properties of ROS, and the conditions under which the reaction takes place in a specific cellular compartment. The ROS activity decreases in the following order HO• $>^1O_2>$ $H_2O_2>$ O_2•. Indeed, the HO• has been reported to have strong oxidative activity towards several organic molecules. Nevertheless, its lifetime is very short compared to H_2O_2, which has relatively stable properties and low reactivity. Moreover, H_2O_2 can easily cross cell membranes and cleave various sites after conversion into HO•. In the presence of some transition HMs, it can also generate other radical species (Rezayian et al., 2019). That's why a numerous studies have focused on the assessment of H_2O_2 production in microalgae as a response to the exposure to HMs. For example, Hamed et al. (2017a) reported that the content of H_2O_2 was significantly increased in cells of *Scenedesmus acuminatus* and *Chlorella sorokiniana* exposed to Cu(II) ions. Correspondingly, Danouche et al. (2020) showed that the level of H_2O_2 increases significantly in *S. obliquus* exposed to Pb(II) ions versus unstressed cells. Likewise, Cheng et al., (2016) reported that H_2O_2 and O_2• levels in *C. vulgaris* increased with increasing Cd(II) concentration in the medium. Increased levels of ROS in the cell disrupt several vital functions, particularly lipid peroxidation (LOPs), protein and sugar oxidation, and nucleic acid damage. Fig. 1 describes the process of ROS generation in various cellular organelles, as well as their specific targets in the cells of microalgae.

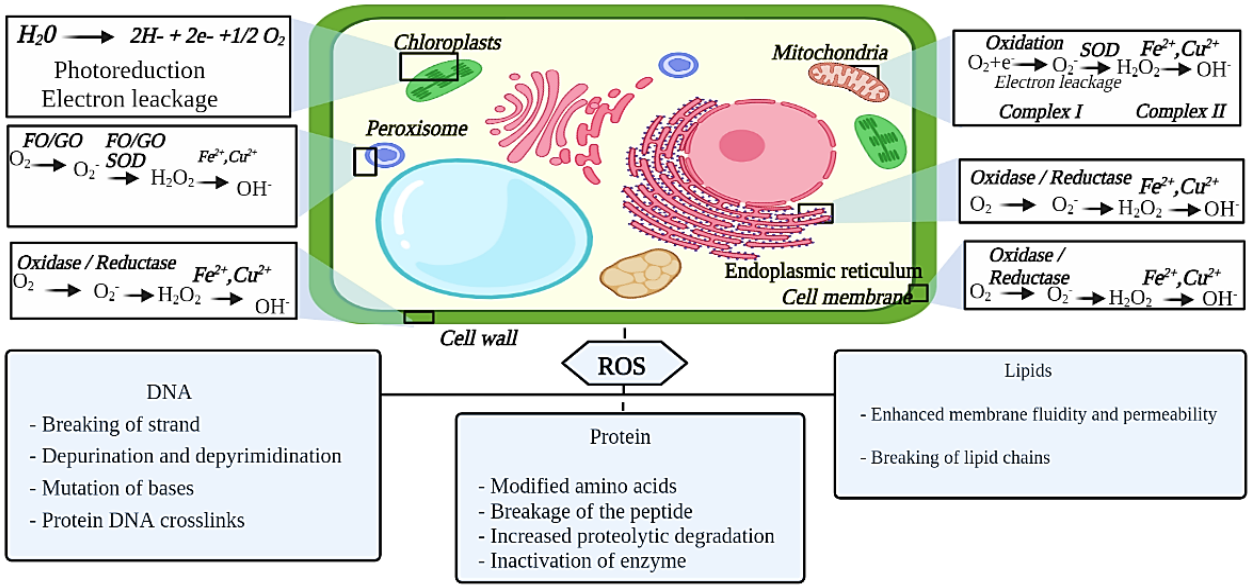

Fig. 1 Mechanism of ROS generation in microalgae cell organelles and their specific targets (Rezayian et al., 2019).

2.1 Lipid peroxidation

The plasma membrane enveloping the cell of microalgae is constituted of a lipidic bilayer, which ensures several essential functions, like the adaptation to the conditions of their environment (Harwood and Remarks, 1998). LOPs is a natural metabolic process, that occurs in cell membranes, mainly in glycolipids, phospholipids, and cholesterol, known as the target of LOPs (Ayala et al., 2014). However, under metal stress conditions, the increase of ROS level above the threshold value leads to LOPs become damaging (Blokhina et al., 2003). Among the different aldehydes that can be generated as by-products of LOPs. The malondialdehyde (MDA) has been extensively studied in microalgae in relation to the HMs-exposure. For example, Danouche et al. (2020) reported that the exposure of *S. obliquus* to Pb(II) ions at the EC_{50} concentration increased the MDA content.

Also, Cd(II) has the same effect on *S. quadricauda* (Çelekli et al., 2013). At the concentration above EC_{50}, Rocchetta et al. (2006) mention a high accumulation of MDA in *Euglena gracilis* exposed to Cr(VI). According to Rai et al. (2013), a concentration-dependent increase in the MDA content was noticed in *C. vulgaris* exposed to Cr(VI) at concentrations ranging from 0 to 15 µg mL^{-1}. Similarly, Sabatini et al. (2009) observed that the cells of *S. vacuolatus* had an increase in the MDA content as Cu(II) concentration increased. As shown in Fig. 2, the main $^1O_2$ and OH• hotspots at the membrane level are the double bonds between carbon atoms and the ester bond between glycerol and the polyunsaturated fatty acids (PUFAs) such as linoleic and linolenic acids. In fact, OH• is the most harmful compound, since it has the particularity of triggering the cyclic chain reaction and causing additional peroxidation of other PUFAs at the cell membrane (Das and Roychoudhury, 2014). Moreover, LOPs activate the chain reactions and exacerbates oxidative stress by creating lipidic radicals that damage in turn proteins and DNA.

2.2 Protein oxidation

As with LOPs, increased ROS production can lead to protein oxidation by causing direct or indirect reactions such as disulfide bond formation, nitrosylation, carboxylation and glutathionylation (Fig. 2) (Das and Roychoudhury, 2014). The protein carbonylation is the most widely used test to examine their oxidation. On the basis of the carbonyl content, Okamoto et al. (2001) reported that *Gonyaulax polyedra* proteins underwent oxidative damage after acute exposure to Pb(II), Cd(II), Cu(II), and Hg(II). Similar finding was also noticed in cells of *S. rotundus* exposed to Zn(II) (Shivaji and Dro, 2019). Indirect modifications of proteins occur as a result of interaction with LOPs products, or by specific modification of certain amino acids (AAs), such as Proline (Pro), Tryptophan (Trp), Arginine (Arg), Lysine (Lys) and Threonine (Thr), thereby leading to increasing sensitivity to proteolytic degradation (Møller et al., 2007). The sensitivity of AAs to ROS attack is highly variable, with thiolated and sulfur-containing AAs being the most vulnerable (Baba and Bhatnagar, 2018). Methionine (Met) and Cysteine (Cys) are both prone to damage by the reactive $^1O_2$ and OH•. According to Ahii et al. (2015), an increase in the concentrations of Pro, sarcosine (MeGly), valine (Val), phenylalanine (Phe), isoleucine (Ile) and Met was observed in *C. vulgaris* exposed to Cd(II). Furthermore, iron-sulfur center-containing enzymes are irreversibly inactivated when oxidized by O2•. These oxidized proteins thus become prime candidates for the proteolytic digestion process, as the first step in ubiquitination-mediated proteosomal degradation (Das and Roychoudhury, 2014). It has been reported that an increase in the composition of essential AAs (Ile, leucine (Leu), Lys, Phe, Thr, and Val) was noticed in *C. pyrenoidosa* after Se exposure. Also, Phe showed the greatest increase, indicating their implications in the detoxification mechanism of HMs. Indeed, it participates in the formation of glutathione (GSH) and other antioxidant thiols (Danouche et al., 2021; Zhong and Cheng, 2017).

2.3 DNA oxidation

In contrast to nuclear DNA, mitochondrial and chloroplast DNA are most vulnerable to ROS attack due to the absence of protective histones, and because of their proximity to the ROS-producing machinery in microalgae cells (Das and Roychoudhury, 2014). The directly damage caused by ROS include nucleotide base deletion, pyrimidine dimers, cross-linking, strand breaks, and base modification, such as alkylation and oxidation (Rezayian et al., 2019; Tuteja et al., 2001). Indeed, OH• may damages the deoxyribose sugar backbone by extracting H-atom, and reacts with double bonds of the purine and pyrimidine bases (Halliwell, 2006). Likewise, $^1O_2$ attacks mainly guanine (Gill and Tuteja, 2010). ROS can also indirectly damage DNA through the conjugation of MDA with guanine, producing an additional ring (Fig. 2) (Jeong et al., 2005). MohyEl-Din and

Abdel-Kareem (2020) studied the effects of Cu(II) and Cd(II) at EC_{50} concentration on DNA damage. Based on phylogenetic tree, they reported moderate genetic similarity between untreated and HMs-treated cells of *C. salina* and *Nannochloropsis salina* at 52% and 10% respectively. For DNA genetic pattern variability, the random amplified polymorphic DNA technique indicates that Cu(II) has a greater genotoxic influence than Cd(II).

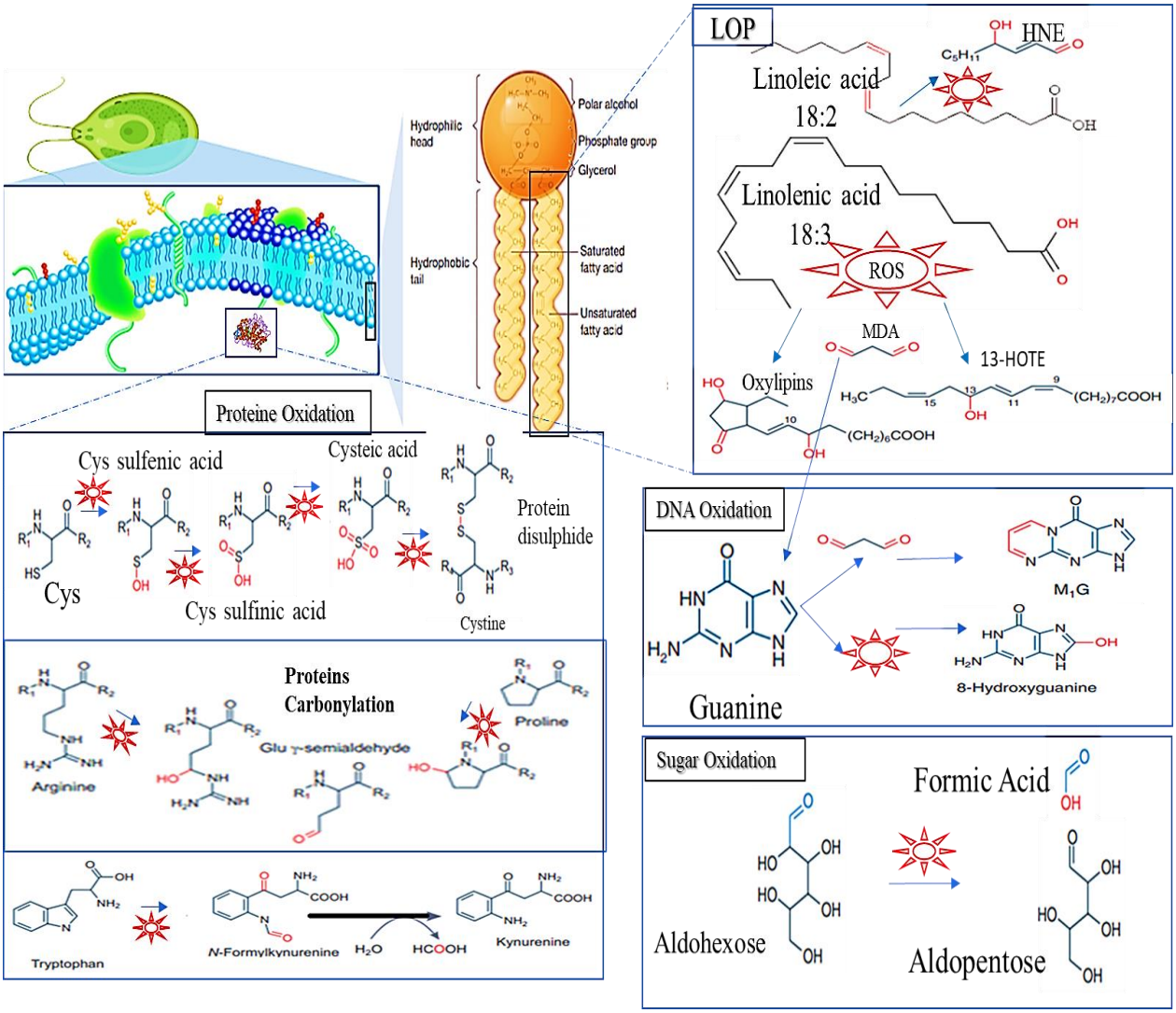

Fig. 2 Impact of ROS on the lipid peroxidation (Wang et al., 2017); protein, sugar and DNA oxidation (Gill and Tuteja, 2010; Vara and Pula, 2014).

3. Enzymatic and non-enzymatic antioxidant defense systems in microalgae

To cope with the adverse effects of HMs, several self-defense strategies have been developed by microalgae, which can be divided into two main pathways consisting of enzymatic and non-enzymatic antioxidant systems.

3.1 Biochemical antioxidant defense systems

The main antioxidant compounds detected in microalgae are ascorbate (AsA), GSH, tocopherols (TOCs), Phenolic compounds and carotenoids, as well as the production of mycosporinic amino acids (MAA) and Pro (Gauthier et al., 2020). Table 1 illustrates the cellular targets of these low molecular weight antioxidants.

Table 1. Antioxidants compounds and cellular targets (Pinto et al., 2003).

Compounds	Targets
Ascorbate	O_2 ($^1\Delta_g$), •OH, O_2•, and HO_2•
Carotenoids	O_2 ($^1\Delta_g$), RO_2•
a-Tocopherol	RO_2•
Glutathione	Nonspecific
Flavonoid	Antioxidant of OH and HOCL
Metallothionein	•OH, Metal chelator
Phytochelatin	Metal chelator
Proline	H_2O_2, Metal chelator

3.1.1 Glutathione

GSH is a low molecular tripeptide antioxidant consisting of three amino acids: glutamate (Glu), Cys and glycine (Gly) (γ-glutatamyl-cysteinyl-glycine), involved in several biological processes in cells of microalgae, through a direct transfer of a hydrogen atom from the thiol group and converted into the oxidized form (GSSG). As a response to HMs stress, GSH participates in the neutralization of oxidative damage through the direct scavenging of H_2O_2 or organic peroxides (ROOH), the adjustment of the redox potential of AAs and proteins, as well as acting as a substrate/cofactor for reactions catalyzed by ROS scavenging enzymes (Fig. 3) (Forman et al., 2010; Ulrich, K., & Jakob, 2019). There are different viewpoints regarding the level of GSH in the cells of microalgae following exposure to HMs. Rocchetta et al. (2012) showed a significant increase in the level of GSH in cells of *E. gracilis* with increasing concentrations of Cr(VI) ranging from 0 to 40 µM. Also, Li et al. (2006) reported that the level of GSH significantly increases in cells of *Pavlova viridis* under Cu(II), and Zn(II) exposure. In contrast to these statements, the majority of studies indicted the decrease of GSH level in cells of microalgae exposed to HMs, for instance in cells of *C. vulgaris* under ZnO NPs stress (Suman et al., 2015), and in *D. salina* exposed to Cd(II) (Zhu et al., 2019). Likewise, the effect of HMs on the GSH/GSSG ratio was also considered in some microalgae strain like *S. acutus* (Randhawa et al., 2001), *Phaeodactylum tricornutum* (Morelli and Scarano, 2004), as well as in cells of *S. quadricauda* (Strejckova et al., 2019). The GSH/GSSG ratio is an essential parameter to evaluate in microalgae cells after HMs exposure. It defines the intracellular redox potential, maintains oxidants in a reduced state and avoids protein denaturation (Strejckova et al., 2019).

3.1.2 Phytochelatins

In response to exposure to HMs, microalgae can also produce various metallothioneins (MTs) consisting of small thiol-containing peptides that are classified into two main groups: those genetically encoded known as class (I) and (II) MTs, and those enzymatically synthesized, called phytochelatins (PCs). The latter have the general structure (γ -Glu-Cys)n-Gly, where the sulfhydryl group of Cys is responsible for the binding with HMs ions (Danouche et al., 2021). Several studies have confirmed that PCs biosynthesis is a response of microalgae to HMs exposure. It is the case of green alga *Acutodesmus obliquus* under Pb(II) stress (Piotrowska-niczyporuk and Bajguz, 2017), in *S. bijugatus* under Cu(II) exposure (Nagalakshmi and Prasad, 2001), in *Stichococcus bacillaris* under Pb(II) exposure (Pawlik-skowron, 2002), in *C. vulgaris* underAs^{5+} stress (Jiang et al., 2011), and in *C. sorokiniana* under Hg exposure (Gómez-Jacinto et al., 2015). On the other hand, it was reported that PCs biosynthesis was dependent on microalgal species as well as HMs. For example, in *Dunaliella* species, PCs biosynthesis was more strongly induced by Zn(II) (Hirata et al., 2001; Tsuji et al., 2003). In *Chlamydomonas* species, Cd(II) ions were the most effective stimulator of

PCs biosynthesis compared to the other tested HMs (Abboud and Wilkinson, 2013; Kobayashi et al., 2006; Li et al., 2021; Suárez et al., 2010).

3.1.3 Ascorbate

AsA is naturally abundant compound in cells of microalgae as in plants, it has been detected in several strains of microalgae (Brown and Miller, 1992). The chemical structure of AsA is related to C_6 sugars. It is a 1,4-aldono-lactone of hexonic acid (either l-galacturonic acid or l-gulonic acid), with an enediol group in C_2 and C_3, allowing it to transfer one or two electrons, forming an oxidized first intermediate (monodehydroascorbate (MDHA)) followed by its oxidized form dehydroascorbic acid (DHA) (Tripathi et al., 2009). Several studies have demonstrated the stimulation the production of AsA by HMs as a key step in the response to oxidative stress (Piotrowska-Niczyporuk et al., 2015; Singh et al., 2006; Strejckova et al., 2019). It has been reported that AsA participate in the defense against oxidative stress by reacting with •OH, $^1O_2$, and $•O_2$, as a substrate for a variety of enzymatic and non-enzymatic reactions, as well as regenerates the carotenoids and the TOCs in thylakoid membranes (Blokhina et al., 2003; Mallick and Mohn, 2000). Indeed, in the chloroplasts, AsA acts as a cofactor of violaxantin de-epoxidase, sustaining thus the dissipation of excess excitation energy (Fig. 3) (Smirnoff, 2000). In addition, it can regulate the production of TOCs from tocopheroxyl radicals, thus protecting the thylakoid membranes (Thomas et al., 1992).

3.1.4 Tocopherols

TOCs and tocotrienols are essential components of biological membranes, it implicated in many metabolic pathways, among which they serve as lipophilic antioxidants against ROS and protect unsaturated fatty acids, that compose cell membranes. Indeed, it acts as captors of lipid peroxyl radicals to prevent these radicals to react with the side chains of adjacent fatty acids, thus finish the reaction of LOPs (Fig. 3) (Blokhina et al., 2003; Kagan, 1989). Lipophilic antioxidants, particularly TOCs, have been less studied than other antioxidants in microalgae response to HMs stress. Studies conducted by Hamed et al. (2017b) with *S. acuminatus* and *C. sorokiniana* demonstrated that the ratio α/β TOCs increased in both species under Zn(II) exposure. Furthermore, *C. sorokiniana* exhibited higher TOCs levels under Cu(II) stress (Hamed et al., 2017a). It has been observed that during the response to chronic stress induced by enhanced concentrations of Cu(II), the α-TOCs content also increased in *C. reinhardtii* (Luis et al., 2006).

3.1.5 Phenolic compounds

Despite the fact that microalgae have great potential as a source of polyphenols, which have well-known antioxidant properties due to their ability to transfer an electron or hydrogen to scavenge ROS, limited research has been conducted on their role in the response of microalgae to HMs stress (Blokhina et al., 2003; Cirulis et al., 2013; Rezayian et al., 2019). A study by Danouche et al. (2020) reported that the exposure of *S. obliquus* to Pb(II) results in a significant increase in the levels of the total of polyphenols. In addition to the phenolics compounds, Elleuch et al. (2021), and Hamed et al. (2017b) reported also the involvement of flavonoids and condensed tannins in the response of microalgal strains to HMs exposure. It has been shown that the protection of cells against oxidative stress associated with polyphenols can take place through different pathways (Hamed et al., 2017a; Kováčik et al., 2010). For instance, they can directly chelate HMs, scavenge ROS and alkoxylated lipid radicals, thus reduce the effect of LOPs (Rodrigo and Libuy, 2014).

3.1.6 Carotenoids

Most carotenoids groups have antioxidant properties, they act as an inhibitor of LOPs, they increase the stability of the photosynthetic apparatus and protect the integrity of the cell membranes (Pérez-Gálvez et al., 2020). Only a few researches have focused on the expression of pigments in microalgae cells in response to HMs stress. For instance, Piotrowska-Niczyporuk et al. (2015) reported that the total carotenoids in cells of *A. obliquus* was less influenced by Pb(II) compared to chlorophyll. Also, Dahmen-Ben Moussa et al. (2018) showed that Ni(II) negatively affects the chlorophyll content and positively increases carotenoids content in *Dunaliella* sp. According to Rai et al. (2013), the carotenoids provides protection to photosynthetic membranes against ROS generated following the accumulation of HMs in intracellular compartments.

3.1.7 Proline

The production of Pro is another way in which microalgae react to the toxicity of HMs, thus contribute to their detoxification (Zhang and Yang, 2008). The molecular mechanisms by which Pro protects the cells of microalgae under HMs stress are not fully understood. However, it has been reported that Pro, due to its chemical properties, can serve as signaling molecules, osmolytes, chemical chaperones, and ROS scavenger antioxidants (Fig. 3) (Hayat et al., 2012; Liang et al., 2013). The accumulation of Pro in cells of microalgae under HMs exposure has been documented in some research studies. For instance, a study by Çelekli et al. (2013) suggested that Cd(II) induces the production of Pro in cells of *S. quadricauda*. Similarly, Tripathi et al. (2006) point out that the accumulation of Pro in *S. acuminatus* may be an effective strategy to reduce oxidative stress induced by Cu(II) and Z(II). Also, Danouche et al. (2020) reported that *S. obliquus* under Pb(II) stress accumulated Pro. Likewise, Hamed et al. (2017b) showed that both strains *C. sorokiniana* and *S. acuminatus* accumulated Pro under Zn(II) stress.

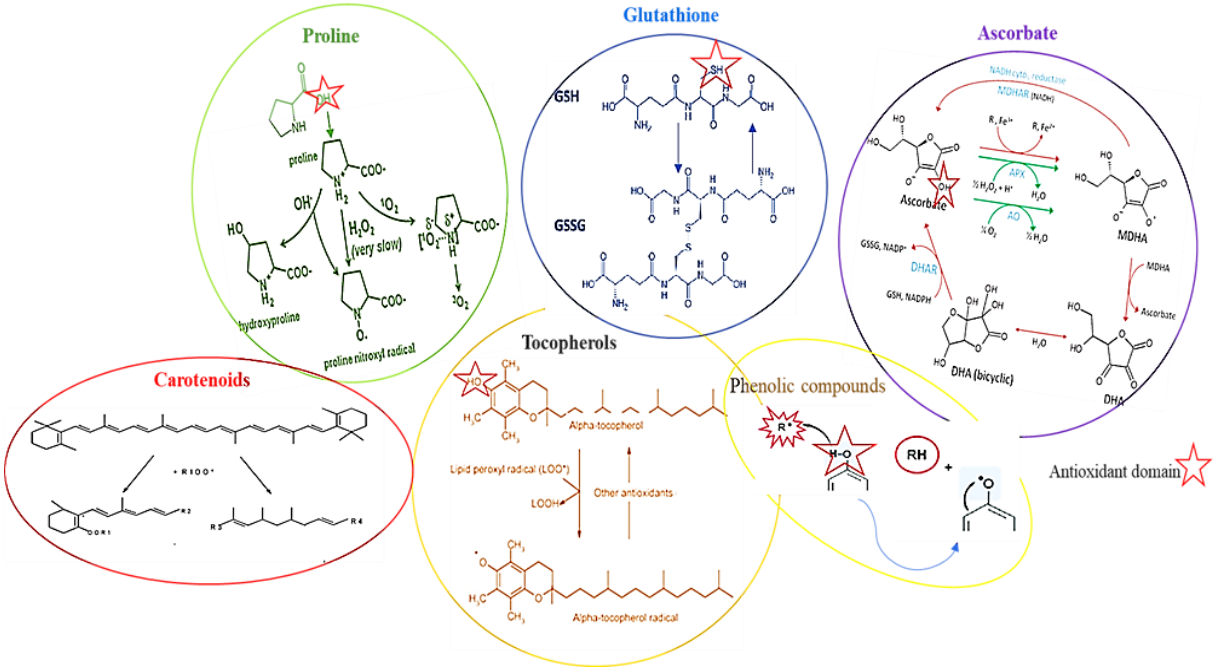

Fig. 3 Biochemical antioxidant defense systems: Role of GSH, AsA, TOCs, Pro, Phenolics, and carotenoids (Kagan, 1989; Liang et al., 2013).

3.2 Enzymatic antioxidant defense systems in microalgae

In cells of microalgae, several enzymes may be involved in enzymatic defense against ROS, including superoxide dismutase (SOD), catalase (CAT), various peroxidases (PODs), glutathione reductase (GR) and glutathione-S-transferase (GST) (Pikula et al., 2019). Fig. 4 shows the enzymatic antioxidant system in microalgae. Table 2 summarizes the enzymatic reactions catalyzed by these enzymes.

Table 2. ROS enzymes and their catalyzed reactions (Das and Roychoudhury, 2014).

Enzymes	Reactions
SOD	$O_2\bullet^- + 2H+ \rightarrow H_2O_2$
CAT	$H_2O_2 \rightarrow H_2O+1/2\ O_2$
POD	$H_2O_2 \rightarrow H_2O+1/2\ O_2$
APX	H_2O_2 + AsA → MDHA
MDAR	MDHA + NAD(P)H → AsA+ $NAD(P)^+$
DHAR	DHA + GSH → AsA+ GSSG
GR	GSSG+ NAD(P)H → GSH + $NAD(P)^+$
GPX	H_2O_2+ GSH → H_2O + GSSG

3.2.1 Superoxide dismutase

SOD (EC 1.15.1.1) is one of the main metalloenzymes of the antioxidant system, present in microalgae species. It catalyzes the dismutation reaction, i.e. reduction and oxidation occur on the same reactant such as $\bullet O_2^-$, via the addition of 2 H^+ ions giving rise to two compounds, one with a higher oxidation state (O_2), and the other with a lower oxidation state (H_2O_2) (Rajput et al., 2021). The expression of SOD isozymes in cytoplasm, peroxisomes, mitochondria, and chloroplasts varies among species. The common plant SOD isoforms such as iron (Fe-SOD), manganese (Mn-SOD) and copper-zinc (CuZn-SOD) have also been found in some microalgae species (Janknegt et al., 2009; Zbigniew and Wojciech, 2006). In addition, increased SOD activity in response to HMs stress has been reported in different microalgal species (Danouche et al., 2020; Hamed et al., 2017b; Lu et al., 2019; Zhu et al., 2019) (Table 3). The activity of SOD is closely related to exposure time and HMs concentration. Indeed, a concentration-dependent increase in SOD activity has been demonstrated with Zn(II) in *Scenedesmus* sp. (Tripathi et al., 2006), as well as with Cu(II) in *S. vacuolatus* (Sabatini et al., 2009), *Scenedesmus* sp. (Tripathi et al., 2006), and *P. viridis* (Li et al., 2006). The duration of HMs exposure also enhances SOD activity as reported by Tripathi et al. (2006) and Morelli and Scarano (2004) under Cu(II) exposure. However, Zhu et al. (2019) reported that there was a decrease in SOD activity in *D. salina* exposed to 2.5 mg L^{-1} of Cd(II).

3.2.2 Catalase

CAT (EC 1.11.1.6) is a tetrameric antioxidant enzyme containing porphyrin heme active sites, with high affinity for H_2O_2. It is located in all major sites of H_2O_2 production in the intracellular compartments of aerobic organisms. The typical reaction catalyzed by the CAT is the dismutation of two molecules of H_2O_2 to H_2O and O_2 (Mhamdi et al., 2010). The catalytic activity of CAT does not require any reductant. In the first step, H_2O_2 oxidizes the Fe present in the catalytic site of the enzyme, giving rise to an iron peroxide intermediate called compound I. The enzyme can remain in this quiescent state if the concentration of H_2O_2 is low. However, at high H_2O_2 concentration, the second H_2O_2 molecule serves as a reductant for this intermediate compound I, regenerating the enzyme and releasing H_2O and O_2 through this second step (Rajput et al., 2021). Similar to SOD, the enzymatic activity of CAT in microalgal cells can be stimulated when the

concentration of HMs increases (Qian et al., 2008; Sabatini et al., 2009). As well as by the duration of exposure (Morelli and Scarano, 2004). A time-dependent increase in the activity of CAT has been reported in *P. tricornutum* exposed to Cu(II) ions (Morelli and Scarano, 2004). However, at high levels of Zn(II) and Cu(II) stress, the CAT activity was inhibited in *Scenedesmus* sp. (Tripathi et al., 2006). Cheng et al. (2016) found that the activity of CAT in *C. vulgaris* peaked at a Cd(II) concentration of 0.5 mg L^{-1} and then declined above this concentration. Also, Lu et al. (2019) reported a decrease in the enzymatic activity of CAT of *Auxenochlorella protothecoides* under Cd(II) stress, and they concluded that the CAT contributes insignificantly to ROS removal at high concentrations compared to SOD activity and PODs.

3.2.3 Peroxidases

PODs (EC 1.11.1.x) are a class of enzymes that catalyze the oxidation of a substrate with H_2O_2. Among the known substrates of this enzymes class, we can mention AsA (APX; EC 1.11.1.11), phenolic substrates (EC 1.11.1.7) (Pyrogallol (PPX) and Guaiacol (GPX)) as well as glutathione (GPx ; EC 1.11.1.9) (Cirulis et al., 2013). PODs have been recognized as the most important enzymes for ROS capture in cells of microalgae under HMs stress. As presented in Table 3, several studies have shown the involvement of PODs in the management of ROS stress induced by HMs, as seen in *D. salina* under Cd(II) exposure (Zhu et al., 2019), in *E. gracilis* under exposure to Zn(II) and Cd(II), in *Dunaliella* sp. under Ni (II) exposure (Dahmen-Ben Moussa et al., 2018), as well in *S. obliquus* under Pb(II) exposure (Danouche et al., 2020). Moreover, the increase in POD activity also depends on the concentration and the duration of exposure. Indeed, a time-dependent increase has been showed in the PPX activity in cells of *A. protothecoides* under Cd(II) stress (Lu et al., 2019). Due to the wide distribution in the cytosol, the chloroplast and the mitochondria, as well as its high affinity towards H_2O_2, APX is more efficient in scavenging H_2O_2 under HMs stress conditions in several microalgal species, such as in *D. salina* under Cd(II) exposure (Zhu et al., 2019), in *C. sorokiniana* and *S. acuminatus* under Zn(II) exposure (Hamed et al., 2017b). Similarly, GPx has been identified as one of the important enzymatic antioxidant systems found in microalgae. Randhawa et al. (2001) reported that after 22 h of exposure to Ni(II) ions, the GPx activity of the Cu(II)-tolerant strain of *S. acutus* was enhanced significantly. Also, Li et al. (2006) showed a concentration-dependent increase in GPx activity under Cu(II) ion exposure. However, there was a concentration-dependent decrease in this activity under exposure to Zn(II) ions.

3.2.4 Enzymes of Ascorbate-Glutathione Cycle

As shown in Fig. 4, the GSH-AsA pathway involves both antioxidants (AsA, GSH, and NADPH), and also enzymes that catalyze their regeneration. In addition to APX activity, a variety of reductases with different substrates such as monodehydroascorbate (MDHAR; EC 1.6.5.4), dehydroascorbate (DHAR, EC 1.8.5.1), glutathione (GR; EC 1.6.4.2), are all essential for the functioning of this metabolism pathway. The APX catalyzes the neutralization of H_2O_2 using AsA as a reducing agent, thus producing H_2O and MDHA (Hasanuzzaman et al., 2019). The regeneration of the AsA used in the previous step by APX occurs through the action of monodehydroascorbate reductases (MDHAR) which catalyzes the reduction of MDHA, using NADH or NADPH as electron donor. Next the dehydroascorbate reductases (DHAR) catalyzes the reduction of the DHA to regenerates reduced AsA, thought a GSH-dependent reduction (Park et al., 2016). In cells of microalgae, the high ratio of GSH to GSSG is maintained by the enzymatic reaction catalyzed by GR (Al-rashed et al., 2016). GR is a flavoenzyme that contains an essential disulfide group. They catalyze the reduction of GSSG to GSH by using NAD(P)H as an electron

donor through two steps. In the first phase, NADPH reduces the flavin part is oxidized and a redox disulfide bridge, thereby reduced to produce a thiolate anion and a Cys. The second phase involves the reduction of GSSG via thiol-disulfide interchange reactions (Chisla and Massey, 1989). Several authors have reported the increased activity of GR in microalgae strains under different HMs stress, such as in *S. obliquus* under Pb(II) stress (Danouche et al., 2020), in *D. salina* under Cd(II) stress (Zhu et al., 2019), in *S. acutus* under Ni (II) stress (Randhawa et al., 2001), as well as in *C. sorokiniana* and *S. acuminatus* under Zn (II) stress (Hamed et al., 2017b). Its activity appears to be also time-dependent as reported in *P. tricornutum* exposed to Cu(II) (Morelli and Scarano, 2004). In contrast, Tripathi et al. (2006) showed that the activity of GR was reduced in *Scenedesmus* sp. after exposure to Cu(II) and Zn(II). Regarding the role of the GST (EC 2.5.1.18), it's involved in phase II of the detoxification, its catalyzing the conjugation of the GSH tripeptide with a variety of hydrophobic, and electrophilic substrates (Marrs, 1996). The involvement of GST in microalgae under HMs stress conditions has been reported in cell of *D. salina* under Cd(II) stress (Zhu et al., 2019), *C. sorokiniana*, *S. acuminatus* under Zn(II) stress (Hamed et al., 2017b), as well in *S. bijugatus* under Cu(II) stress (Nagalakshmi and Prasad, 2001).

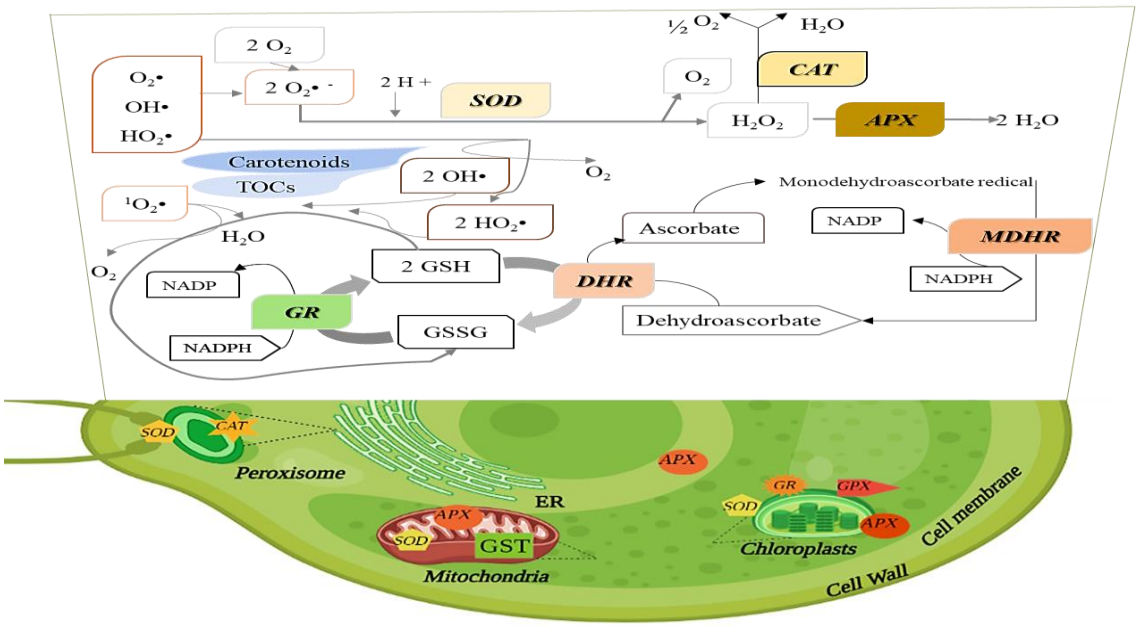

Fig. 4 General scheme of the enzymatic antioxidant defense systems of microalgae modified from (Pikula et al., 2019; Hajiboland, 2014).

4. Role of phytohormones in the management of oxidative stress

Phytohormones are among the main regulators of numerous biological processes in plants. They include several classes of chemicals that may be traditional or nontraditional, and are generally active at very low concentrations (Erland et al., 2019). in microalgae cells, "phytohormones", which can also be called "phycohormones", are involved in a wide spectrum of physiological processes (Lu and Xu, 2015). In fact, the most common phytohormones found in microalgae are: Abscisic acid (ABA), Auxins, Brassinosteroids (BR), Cytokinins (CK), Gibberellins (GA),Ethylene (ET), and Jasmonic Acid (JA) (H. N. Nguyen et al., 2020; Tarakhovskaya et al., 2007).

Table 3. Studies of phycoremediation of HMs using microalgae: markers of oxidative stress, and mechanism of ROS management through enzymatic and non-enzymatic pathways

Microalgae strains	HMs	Oxidative stress markers	antioxidant enzymes	Antioxidant's molecules	References
S. obliquus	Pb(II)	LOPs (MDA); H_2O_2	SOD; CAT; GPX; POX; GR	AsA; Phenolics and Pro	(Danouche et al., 2020)
D. salina	Cd(II)	LOPs (MDA)	SOD; APX; GST; GPX; GR	Carotenoids, GSH	(Zhu et al., 2019)
C. sorokiniana *S. acuminatus*	Zn(II)	LOPs (TBARS); H_2O_2	SOD; POX; APX; GST; GR	GSH; ASC; ASC/tASC; TOCs; Flavonoids; Phenolics and Pro	(Hamed et al., 2017c)
Dunaliella sp.	Zn(II)	----------	SOD; CAT; APX; GPX	GSH; Phenolics; Flavonoids and Tannins	(Elleuch et al., 2021)
E. gracilis	Zn(II); Cd(II)	----------	APX; GPX	Polyphosphates	(Sánchez-Thomas et al., 2016)
E. gracilis	Cr(VI)	LOPs (TBARS)	SOD	GSH	(Rocchetta et al., 2012)
Dunaliella sp.	Ni (II)	LOPs (TBARS)	SOD; GPX	Carotenoids and Phenolics	(Dahmen-Ben Moussa et al., 2018)
Pavlova viridis	Mn(II); Co(II); Cu(II); Zn(II)	LOPs (MDA)	SOD, CAT, GPX	GSH	(Li et al., 2006; LI et al., 2007)
C. pyrenoidosa *M. aeruginosa*	Cu(II)	LOPs (MDA)	SOD	----------	(Lu et al., 2015)
S. vacuolatus *C. kessleri*	Cu(II)	LOPs (MDA)	SOD; CAT	GSH	(Sabatini et al., 2009)
C. vulgaris	CdSe NPs		SOD; CAT; POD	Phenol	(Movafeghi et al., 2019)
C. vulgaris	ZnO NPs	LOPs (MDA)	SOD	GSH	(Suman et al., 2015)
S. acutus	Ni (II)	LOPs (TBARS)	SOD; CAT; GR; GPx	GSH and GSSG	(Randhawa et al., 2001)
P. tricornutum	Cu(II)	LOPs (TBARS)	SOD; CAT; GR; APX; PPX	GSH and GSSG	(Morelli and Scarano, 2004)
A. protothecoides	Cd(II)		SOD; POD	GSH, Carotenoids, and metal-chelating thioredoxin (Trx)	(Lu et al., 2019)
S. quadricauda	Cd(II); Cu(II);Ni(II)		SOD; APX, CAT, GR	AsA, GSH and PCs	(Kováčika et al., 2017)
S. obliquus	Cd(II)	----------	SOD; CAT,	GSH	(Ma et al., 2021)
C. sorokiniana	Cd(II)	----------	CAT, APX, glutamine synthetase, Glutamate dehydrogenase, O-acetylserine (thiol) lyase, and NAD-isocitrate dehydrogenase	----------	(León-Vaz et al., 2021)
C. vulgaris	Cr(VI)	LOPs (MDA)	SOD and CAT,	----------	(Lu et al., 2021)
Scenedesmus sp.	Cu(II); Zn(II)	LOPs (MDA);	SOD; CAT; APX and GR	Pro	(Tripathi et al., 2006; Tripathi and Gaur, 2004)
Micrasterias denticulata	Cr(VI); Cr(III)	ROS (H_2DCFDA dye and CLSM-microscopy)	SOD and CAT	GSH	(Volland et al., 2012)
C. vulgaris	Zn(II);Hg(II)	ROS generation	SOD and CAT	----------	(Ajitha et al., 2021)

Indeed, microalgae shares much of the biosynthetic pathways of phytohormones with higher plant species. Nevertheless, their function is not fully understood, particularly under HMs stress conditions. It is therefore essential to understand how these phytohormones influence physiological and metabolic responses of microalgae under HMs stress (T. Q. Nguyen et al., 2020). The mechanisms of HMs stress regulation by phytohormones have been mainly characterized through their exogenic equivalents. Based on the available literature on the contribution of phytohormones in mitigating HMs and the tolerance of microalgae to their stress. It has been reported that the content of ABA increased in cells of microalgae strain of *A. obliquus* (Talarek-Karwel et al., 2020), and *C. vulgaris* (Bajguz, 2010), with increasing the intracellular accumulation of Pb(II). According to Maillard et al. (1993), the level of ET increased in cells of *Haematococcous pluvialis* at high concentrations of cobalt (Co), manganese (Mn) and silver (Ag). Meanwhile, Cu(II) caused an inhibition of ET production. In contrast, Zn(II), Fe(II) and (Mg) had no effect. There are few reports on the involvement of GAs in regulation of HMs in microalgae. For example, the study of Piotrowska-Niczyporuk et al. (2012) as well as that of Falkowska et al. (2011)showed that exogenously applied GA_3 positively influences the growth rate, protein, pigment, and monosaccharide contents in *C. vulgaris* cells exposed to HMs. According to Piotrowska-niczyporuk et al. (2018), the exogenous Auxin and CKs significantly alleviated the Pb(II) toxicity in *A. obliquus* through the activation of non-enzymatic, and enzymatic defense systems. Also, Piotrowska-Niczyporuk et al. (2020) described that exogenous auxins cause the activation of Pb(II) tolerance mechanisms through increased PCs synthase activity, the accumulation of PCs, and their precursors. Regarding the effect of BRs, it has been reported that they are involved in a number of HMs detoxification pathways. The exogenous supply of BRs in *C. vulgaris* significantly reduces the effects of HMs on growth, and increases chlorophyll, sugar, and protein contents. It ensures also a precise regulation of the ROS level, through an increase of the activity of non-enzymatic and enzymatic detoxification pathways. As well as by the acceleration of the biosynthesis of PCs (Bajguz, 2019, 2011, 2010, 2002). In contrast, the presence of exogenous JA exacerbated Cd(II), Cu(II), or Pb(II) toxicity accompanied by an increase in metal biosorption, and the level of LOPs and H_2O_2 in *C. vulgaris*. Indeed, the response to JA treatment significantly reduced cell number, pigment, monosaccharide, soluble protein, AsA, and GSH levels, as well as ROS-scavenging enzyme activity (Piotrowska-Niczyporuk et al., 2012). Fig. 5 illustrates the phytohormones signaling pathways and their actions in microalgae cells in response to HMs stress.

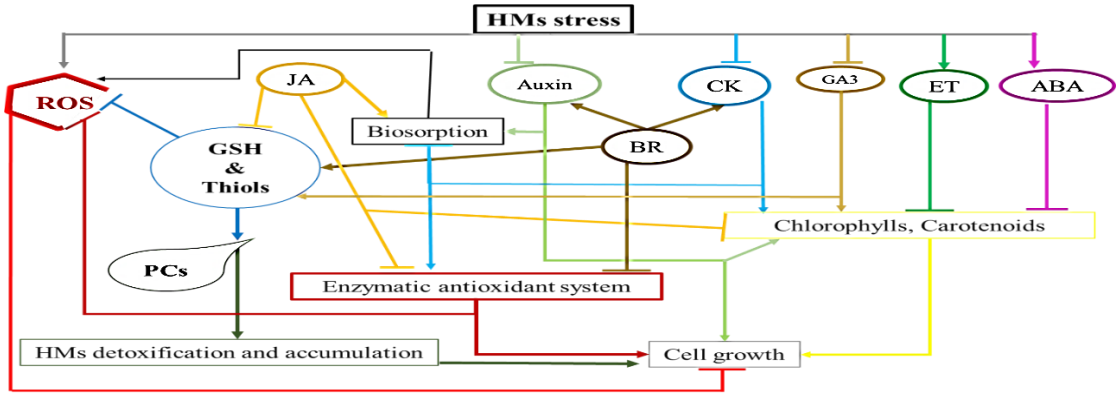

Fig. 5 Proposed model of phytohormone signaling response to oxidative stress induced by HMs in cell of microalgae. The arrow symbol (→) demonstrates the promoting and/or increasing effects, Whereas the symbol (–|) indicates a negative effect from (T. Q. Nguyen et al., 2020).

5. Conclusion

When microalgae cells are exposed to HMs ions, either under natural conditions or during phycoremediation of HMs-contaminated wastewater, they are often affected by the high level of ROS generated under such stress conditions. In fact, the disruption of the balance between ROS production and suppression leads to the peroxidation of lipids, oxidation of proteins and sugars, as well as damaging of nucleic acids. To overcome this oxidative damage, microalgae dispose of complex defense mechanisms including physiological, biochemical, and enzymatic systems, as well as numerous signaling pathways involving phytohormones. The future challenge concerning the use of microalgae in the phycoremediation of HMs will consist first of all in deepening the knowledge on the basic components of the various oxidative stress management systems, at the genomic, transcriptomic, proteomic, metabolomic and metallomic levels. This will be done with the aim of optimizing these bioprocesses and the valorization of the resulting biomass in a biorefinery perspective.

Declaration of competing interest

The authors declare that they have no known competing financial interests or personal relationships that could have appeared to influence the work reported in this paper.

Funding

No funding was received to assist with the preparation of this manuscript

Acknowledgements

Authors gratefully acknowledge the Moroccan Foundation for Advanced Science, Innovation and Research (MAScIR)for their financial and technical support.

References

Abboud, P., Wilkinson, K.J., 2013. Role of metal mixtures (Ca , Cu and Pb) on Cd bioaccumulation and phytochelatin production by *Chlamydomonas reinhardtii*. Environ. Pollut. 179, 33–38. https://doi.org/10.1016/j.envpol.2013.03.047

Ahii, M., Teresa, A., Grac, M., Parrish, C.C., 2015. Combined nitrogen limitation and cadmium stress stimulate total carbohydrates , lipids , protein and amino acid accumulation in *Chlorella vulgaris* (Trebouxiophyceae). Aquat. Toxicol. 160, 87–95. https://doi.org/10.1016/j.aquatox.2015.01.002

Ajitha, V., Sreevidya, C.P., Sarasan, M., Park, J.C., Mohandas, A., Sarojini, I., Singh, B., Puthumana, J., Lee, J., 2021. Effects of zinc and mercury on ROS-mediated oxidative stress-induced physiological impairments and antioxidant responses in the microalga *Chlorella vulgaris*. Environ. Sci. Pollut. Res.https://doi.org/10.1007/s11356-021-12950-6

Al-rashed, S.A., Ibrahim, M.M., El-gaaly, G.A., Al-shehri, S., Mostafa, A., 2016. Evaluation of radical scavenging system in two microalgae in response to interactive stresses of UV-B radiation and nitrogen starvation. Saudi J. Biol. Sci. 23, 706–712. https://doi.org/10.1016/j.sjbs.2016.06.010

Ali, H., Khan, E., Ilahi, I., 2019. Environmental chemistry and ecotoxicology of hazardous heavy metals: Environmental persistence, toxicity, and bioaccumulation. J. Chem. 2019. https://doi.org/10.1155/2019/6730305

Ayala, A., Muñoz, M.F., Argüelles, S., 2014. Lipid Peroxidation : Production , Metabolism , and Signaling Mechanisms of Malondialdehyde and 4-Hydroxy-2-Nonenal. Oxid. Med. Cell. Longev. 2014. https://doi.org/10.1155/2014/360438

Baba, S.P., Bhatnagar, A., 2018. Role of thiols in oxidative stress. Curr. Opin. Toxicol. 7, 133–

139. https://doi.org/10.1016/j.cotox.2018.03.005.
Bajguz, A., 2019. Brassinosteroids in Microalgae : Application for Growth Improvement and Protection Against Abiotic Stresses, in: Brassinosteroids: Plant Growth and Development. pp. 45–58. https://doi.org/10.1007/978-981-13-6058-9
Bajguz, A., 2011. Suppression of *Chlorella vulgaris* Growth by Cadmium , Lead , and Copper Stress and Its Restoration by Endogenous Brassinolide. Arch Env. Contam Toxicol 60, 406–416. https://doi.org/10.1007/s00244-010-9551-0
Bajguz, A., 2010. An enhancing effect of exogenous brassinolide on the growth and antioxidant activity in Chlorella vulgaris cultures under heavy metals stress. Environ. Exp. Bot. 68, 175–179. https://doi.org/10.1016/j.envexpbot.2009.11.003
Bajguz, A., 2002. Brassinosteroids and lead as stimulators of phytochelatins synthesis in *Chlorella vulgaris*. J. Plant Physiol. 324, 321–324.4. https://doi.org/10.1078/0176-1617-00654
Blokhina, O., Virolainen, E., Fagerstedt, K. V., 2003. Antioxidants, oxidative damage and oxygen deprivation stress: A review. Ann. Bot. 91, 179–194. https://doi.org/10.1093/aob/mcf118
Brown, M.R., Miller, K.A., 1992. The ascorbic acid content of eleven species of microalgae used in mariculture. J. Appl. Phycol. 4, 205–215. https://doi.org/https://doi.org/10.1007/BF02161206
Çelekli, A., Kapi, M., Bozkurt, H., 2013. Effect of cadmium on biomass, pigmentation, malondialdehyde, and proline of *Scenedesmus quadricauda* var. longispina. Bull. Environ. Contam. Toxicol. 91, 571–576. https://doi.org/10.1007/s00128-013-1100-x
Cheng, J., Qiu, H., Chang, Z., Jiang, Z., Yin, W., 2016. The effect of cadmium on the growth and antioxidant response for freshwater algae *Chlorella vulgaris*. Springerplus 5, 1–8. https://doi.org/10.1186/s40064-016-2963-1
Chisla, S., Massey, V., 1989. Mechanisms of flavoprotein-catalyzed reactions. Eur. J. Biochem. 181, 1–17. https://doi.org/https://doi.org/10.1111/j.1432-1033.1989.tb14688.x
Cirulis, J.T., Scott, J.A., Ross, G.M., 2013. Management of oxidative stress by microalgae. Can. J. Physiol. Pharmacol. 91, 15–21. https://doi.org/10.1139/cjpp-2012-0249
Dahmen-Ben Moussa, I., Athmouni, K., Chtourou, H., Ayadi, H., Sayadi, S., Dhouib, A., 2018. Phycoremediation potential, physiological, and biochemical response of *Amphora subtropica* and *Dunaliella* sp. to nickel pollution. J. Appl. Phycol. 30, 931–941. https://doi.org/10.1007/s10811-017-1315-z
Danouche, M., El Ghachtouli, N., El Arroussi, H., 2021. Phycoremediation mechanisms of heavy metals using living green microalgae : physicochemical and molecular approaches for enhancing selectivity and removal capacity. Heliyon 7, e07609. https://doi.org/10.1016/j.heliyon.2021.e07609
Danouche, M., Ghachtouli, N. El, Baouchi, A. El, Arroussi, H. El, 2020. Heavy metals phycoremediation using tolerant green microalgae : Enzymatic and non-enzymatic antioxidant systems for the management of oxidative stress. J. Environ. Chem. Eng. 8, 104460. https://doi.org/10.1016/j.jece.2020.104460
Das, K., Roychoudhury, A., 2014. Reactive oxygen species (ROS) and response of antioxidants as ROS-scavengers during environmental stress in plants. Front. Environ. Sci. 2, 1–13. https://doi.org/10.3389/fenvs.2014.00053
Elleuch, J., Ben Amor, F., Chaaben, Z., Frikha, F., Michaud, P., Fendri, I., Abdelkafi, S., 2021. Zinc biosorption by *Dunaliella* sp. AL-1: Mechanism and effects on cell metabolism. Sci. Total Environ. 773. https://doi.org/10.1016/j.scitotenv.2021.145024
Erland, L.A.E., Turi, C.E., Saxena, P.K., 2019. Chapter 2 - Serotonin in Plants: Origin, Functions, and Implications, in: Serotonin. Elsevier Inc., pp. 23–46. https://doi.org/10.1016/B978-0-12-

800050-2.00002-4
Falkowska, M., Pietryczuk, A., Piotrowska, A., Bajguz, A., Grygoruk, A., Czerpak, R., 2011. The Effect of Gibberellic Acid (GA_3) on Growth, Metal Biosorption and Metabolism of the Green Algae *Chlorella vulgaris* (Chlorophyceae) Beijerinck Exposed to Cadmium and Lead Stress. Polish J. Environ. Stud. 20, 53–59.
Forman, H.J., Zhang, H., Rinna, A., 2010. Glutathione: overview of its protective roles, measurement, and biosynthesis. Mol. Aspects Med. 30, 1–12. https://doi.org/10.1016/j.mam.2008.08.006.
Fu, F., Wang, Q., 2011. Removal of heavy metal ions from wastewaters: A review. J. Environ. Manage. 92, 407–418. https://doi.org/10.1016/j.jenvman.2010.11.011
Gauthier, M.R., Senhorinho, G.N.A., Scott, J.A., 2020. Microalgae under environmental stress as a source of antioxidants. Algal Res. 52, 102104. https://doi.org/10.1016/j.algal.2020.102104
Gill, S.S., Tuteja, N., 2010. Reactive oxygen species and antioxidant machinery in abiotic stress tolerance in crop plants. Plant Physiol. Biochem. 48, 909–930. https://doi.org/10.1016/j.plaphy.2010.08.016
Gómez-Jacinto, V., García-Barrera, T., Gómez-Ariza, J.L., Garbayo-Nores, I., Vílchez-Lobato, C., 2015. Elucidation of the defence mechanism in microalgae *Chlorella sorokiniana* under mercury exposure. Identification of Hg-phytochelatins. Chem. Biol. Interact. 238, 82–90. https://doi.org/10.1016/j.cbi.2015.06.013
Hajiboland, R., 2014. Reactive Oxygen Species and Photosynthesis, in: Oxidative Damage to Plants. Elsevier Inc., pp. 1–64. https://doi.org/10.1016/B978-0-12-799963-0.00001-0
Halliwell, B., 2006. Reactive Species and Antioxidants . Redox Biology Is a Fundamental Theme of Aerobic Life. Plant Physiol. 141, 312–322. https://doi.org/10.1104/pp.106.077073.312
Hamed, S.M., Selim, S., Klöck, G., AbdElgawad, H., 2017a. Sensitivity of two green microalgae to copper stress: Growth, oxidative and antioxidants analyses. Ecotoxicol. Environ. Saf. 144, 19–25. https://doi.org/10.1016/j.ecoenv.2017.05.048
Hamed, S.M., Zinta, G., Klöck, G., Asard, H., Selim, S., AbdElgawad, H., 2017b. Zinc-induced differential oxidative stress and antioxidant responses in *Chlorella sorokiniana* and *Scenedesmus acuminatus*. Ecotoxicol. Environ. Saf. 140, 256–263. https://doi.org/10.1016/j.ecoenv.2017.02.055
Harwood, J.L., Remarks, I.I., 1998. Membrane Lipids in Algae, in: In Lipids in Photosynthesis: Structure, Function and Genetics. Springer, Dordrecht, pp. 53–64.https://doi.org/10.1007/0-306-48087-5_3
Hasanuzzaman, M., Bhuyan, M.H.M.B., Anee, T.I., 2019. Regulation of ascorbate-glutathione pathway in mitigating oxidative damage in plants under abiotic stress. Antioxidants 8, 1–50.https://doi.org/10.3390/antiox8090384
Hayat, S., Hayat, Q., Alyemeni, M.N., Wani, A.S., Pichtel, J., Ahmad, A., 2012. Role of proline under changing environments: A review. Plant Signal. Behav. 7, 1456–1466. https://doi.org/10.4161/psb.21949
Hirata, K., Tsujimoto, Y., Namba, T., Ohta, T., Hirayanagi, N., Miyasaka, H., ... & Miyamoto, K, 2001. Strong induction of phytochelatin synthesis by zinc in marine green alga, *Dunaliella tertiolecta*. J. Biosci. Bioeng. 92, 24–29.https://doi.org/10.1016/S1389-1723(01)80193-6
Huang, H., Ullah, F., Zhou, D., Yi, M., Zhao, Y., Terzaghi, W.B., 2019. Mechanisms of ROS Regulation of Plant Development and Stress Responses 10, 1–10. https://doi.org/10.3389/fpls.2019.00800
Janknegt, P.J., Graaff, C.M. De, Poll, W.H. Van De, Visser, R.J.W., Rijstenbil, J.W., Buma, A.G.J., 2009. Short-term antioxidative responses of 15 microalgae exposed to excessive irradiance

including ultraviolet radiation. Eur. J. Phycol. 44, 37–41. https://doi.org/10.1080/09670260902943273
Jeong, Y., Nakamura, J., Upton, P.B., Swenberg, J.A., 2005. Pyrimido [1 ,2- a]-purin-10(3H)-one, M1G, is less prone to artifact than base oxidation. Nucleic Acids Res. 33, 6426–6434. https://doi.org/10.1093/nar/gki944
Jiang, Y., Purchase, D., Jones, H., Garelick, H., 2011. Technical note: Effects of arsenate (As5+) on growth and production of glutathione (GSH) and phytochelatins (PCS) in *Chlorella Vulgaris*. Int. J. Phytoremediation 13, 834–844. https://doi.org/10.1080/15226514.2010.525560
Kagan, V.E., 1989. Tocopherol Stabilizes Membrane against Phospholipase A, Free Fatty Acids, and Lysophospholipids. Ann. N. Y. Acad. Sci. 570, 121–135. https://doi.org/10.1111/j.1749-6632.1989.tb14913.
Kobayashi, I., Fujiwara, S., Saegusa, H., Inouhe, M., Matsumoto, H., Tsuzuki, M., 2006. Relief of Arsenate Toxicity by Cd-Stimulated Phytochelatin Synthesis in the Green Alga *Chlamydomonas reinhardtii*. Mar. Biotechnol. 8, 94–101. https://doi.org/10.1007/s10126-005-5092-3
Kováčik, J., Klejdus, B., Hedbavny, J., Bačkor, M., 2010. Effect of copper and salicylic acid on phenolic metabolites and free amino acids in *Scenedesmus quadricauda* (Chlorophyceae). Plant Sci. 178, 307–311. https://doi.org/10.1016/j.plantsci.2010.01.009
Kováčika, J., Klejdusb, B., Babulad, P., Hedbavny, J., 2017. Ascorbic acid affects short-term response of *Scenedesmus quadricauda* to cadmium excess. Algal Res. 24, 354–359. https://doi.org/10.1016/j.algal.2017.04.026
León-Vaz, A., León, R., Giráldez, I., Vega, J.M., Vigara, J., 2021. Impact of heavy metals in the microalga *Chlorella sorokiniana* and assessment of its potential use in cadmium bioremediation. Aquat. Toxicol. 239. https://doi.org/10.1016/j.aquatox.2021.105941
Leong, Y.K., Chang, J.S., 2020. Bioremediation of heavy metals using microalgae: Recent advances and mechanisms. Bioresour. Technol. 303, 122886. https://doi.org/10.1016/j.biortech.2020.122886
Li, C., Zheng, C., Fu, H., Zhai, S., Hu, F., Naveed, S., Zhang, C., Ge, Y., 2021. Contrasting detoxification mechanisms of *Chlamydomonas reinhardtii* under Cd and Pb stress. Chemosphere 274, 129771. https://doi.org/10.1016/j.chemosphere.2021.129771
Li, M., Hu, C., Zhu, Q., Chen, L., Kong, Z., Liu, Z., 2006. Copper and zinc induction of lipid peroxidation and effects on antioxidant enzyme activities in the microalga *Pavlova viridis* (Prymnesiophyceae). Chemosphere 62, 565–572. https://doi.org/10.1016/j.chemosphere.2005.06.029
LI, M., ZHU, Q., HU, C. wei, CHEN, L., LIU, Z. li, KONG, Z. ming, 2007. Cobalt and manganese stress in the microalga Pavlova viridis (Prymnesiophyceae): Effects on lipid peroxidation and antioxidant enzymes. J. Environ. Sci. 19, 1330–1335. https://doi.org/10.1016/S1001-0742(07)60217-4
Liang, X., Zhang, L., Natarajan, S.K., Becker, D.F., 2013. Proline Mechanisms of Stress Survival. Antioxid. Redox Signal. 19, 998–1011. https://doi.org/10.1089/ars.2012.5074
Lu, J., Ma, Y., Xing, G., Li, W., Kong, X., Li, J., Wang, L., Yuan, H., Yang, J., 2019. Revelation of microalgae ' s lipid production and resistance mechanism to ultra-high Cd stress by integrated transcriptome and physiochemical analyses. Environ. Pollut. 250, 186–195. https://doi.org/10.1016/j.envpol.2019.04.018
Lu, L., Wu, Y., Ding, H., Zhang, W., 2015. The combined and second exposure effect of copper (II) and chlortetracycline on fresh water algae, *Chlorella pyrenoidosa* and *Microcystis*

aeruginosa. Environ. Toxicol. Pharmacol. 40, 140–148. https://doi.org/10.1016/j.etap.2015.06.006
Lu, M., Gao, F., Li, C., Yang, H., 2021. Response of microalgae *Chlorella vulgaris* to Cr stress and continuous Cr removal in a membrane photobioreactor. Chemosphere 262, 128422. https://doi.org/10.1016/j.chemosphere.2020.128422
Lu, Y., Xu, J., 2015. Phytohormones in microalgae : a new opportunity for microalgal biotechnology ? Trends Plant Sci. 20, 1–10. https://doi.org/10.1016/j.tplants.2015.01.006
Luis, P., Behnke, K., Toepel, J., Wilhelm, C., 2006. Parallel analysis of transcript levels and physiological key parameters allows the identification of stress phase gene markers in *Chlamydomonas reinhardtii* under copper excess. Plant, Cell Environ. 29, 2043–2054. https://doi.org/10.1111/j.1365-3040.2006.01579.x
Ma, X., Chen, Y., Liu, F., Zhang, S., Wei, Q., 2021. Enhanced tolerance and resistance characteristics of *Scenedesmus obliquus* FACHB-12 with K3 carrier in cadmium polluted water. Algal Res. 55, 1–10.https://doi.org/10.1016/j.algal.2021.102267
Maillard, P., Thepenier, C., Gudin, C., Microalgues, D.B., Paul, S., Durance, L., 1993. Determination of an ethylene biosynthesis pathway in the unicellular green alga, *Haematococcus pluvialis* . Relationship between growth and ethylene production. J. Appl. Phycol. 5, 93–98. https://doi.org/10.1007/BF02182426
Mallick, N., Mohn, F.H., 2000. Reactive oxygen species: Response of algal cells. J. Plant Physiol. 157, 183–193. https://doi.org/10.1016/S0176-1617(00)80189-3
Marrs, K.A., 1996. The functions and regulation of glutathione S-transferases in plants. Annu. Rev. Plant Biol. 47, 127-158.https://doi.org/10.1146/annurev.arplant.47.1.127
Mhamdi, A., Queval, G., Chaouch, S., Vanderauwera, S., Breusegem, F. Van, Noctor, G., 2010. Catalase function in plants : a focus on *Arabidopsis* mutants as stress-mimic models 61, 4197–4220. https://doi.org/10.1093/jxb/erq282
Mohy El-Din, S.M., Abdel-Kareem, M.S., 2020. Effects of Copper and Cadmium on the Protein Profile and DNA Pattern of Marine Microalgae *Chlorella salina* and *Nannochloropsis salina*. Environ. Process. 7, 189–205. https://doi.org/10.1007/s40710-019-00419-1
Møller, I.M., Jensen, P.E., Hansson, A., 2007. Oxidative Modifications to Cellular Components in Plants. Annu. Rev. Plant Biol. 58, 459–483. https://doi.org/10.1146/annurev.arplant.58.032806.103946
Morelli, E., Scarano, G., 2004. Copper-induced changes of non-protein thiols and antioxidant enzymes in the marine microalga *Phaeodactylum tricornutum*. Plant Sci. 167, 289–296. https://doi.org/10.1016/j.plantsci.2004.04.001
Movafeghi, A., Khataee, A., Rezaee, A., Kosari-Nasab, M., Tarrahi, R., 2019. Toxicity of cadmium selenide nanoparticles on the green microalga *Chlorella vulgaris* : inducing antioxidative defense response. Environ. Sci. Pollut. Res. 26, 36380–36387. https://doi.org/10.1007/s11356-019-06675-w
Nagalakshmi, N., Prasad, M.N. V, 2001. Responses of glutathione cycle enzymes and glutathione metabolism to copper stress in *Scenedesmus bijugatus*. Plant Sci. 160 160, 291–299.
Nguyen, H.N., Kisiala, A.B., Emery, R.J.N., 2020. The roles of phytohormones in metal stress regulation in microalgae. J. Appl. Phycol. https://doi.org/10.1007/s10811-020-02271-5
Nguyen, T.Q., Sesin, V., Kisiala, A., Emery, R.J.N., 2020. The Role of Phytohormones in Enhancing Metal Remediation Capacity of Algae. Bull. Environ. Contam. Toxicol. https://doi.org/10.1007/s00128-020-02880-3
Okamoto, O.K., Pinto, E., Latorre, L.R., Bechara, E.J.H., Colepicolo, P., 2001. Antioxidant modulation in response to metal-induced oxidative stress in algal chloroplasts. Arch.

Environ. Contam. Toxicol. 40, 18–24. https://doi.org/10.1007/s002440010144
Park, A.K., Kim, I.S., Do, H., Jeon, B.W., Lee, C.W., Roh, S.J., ... & Kim, H.W., 2016. Structure and catalytic mechanism of monodehydroascorbate reductase, MDHAR, from *Oryza sativa* L. japonica. Sci. Rep. 6, 1–10. https://doi.org/10.1038/srep33903
Pawlik-skowron, B., 2002. Correlations between toxic Pb effects and production of Pb-induced thiol peptides in the microalga *Stichococcus bacillaris*. Environ. Pollut. 119, 119–127.https://doi.org/10.1016/S0269-7491(01)00280-9
Pérez-Gálvez, A., Viera, I., Roca, M., 2020. Carotenoids and Chlorophylls as Antioxidants. antioxidants 9, 1–34. https://doi.org/doi:10.3390/antiox9060505
Pikula, K.S., Zakharenko, A.M., Aruoja, V., Golokhvast, K.S., Tsatsakis, A.M., 2019. Toxicology Oxidative stress and its biomarkers in microalgal ecotoxicology. Curr. Opin. Toxicol. 13, 8–15. https://doi.org/10.1016/j.cotox.2018.12.006
Pinto, E., Sigaud-kutner, T.C., Leitao, M.A., Okamoto, O.K., Morse, D., Colepicolo, P., 2003. Heavy metal-induced oxidative stress in algae. J. Phycol. 39, 1008–1018. https://doi.org/10.1111/j.0022-3646.2003.02-193.x
Piotrowska-niczyporuk, A., Bajguz, A., 2017. Response and the detoxi fi cation strategies of green alga *Acutodesmus obliquus* (Chlorophyceae) under lead stress. Environ. Exp. Bot. 144, 25–36. https://doi.org/10.1016/j.envexpbot.2017.08.013
Piotrowska-Niczyporuk, A., Bajguz, A., Kotowska, U., Zambrzycka-Szelewa, E., Sienkiewicz, A., 2020. Auxins and Cytokinins Regulate Phytohormone Homeostasis and Thiol-Mediated Detoxification in the Green Alga *Acutodesmus obliquus* Exposed to Lead Stress. Sci. Rep. 10,1-14. https://doi.org/10.1038/s41598-020-67085-4
Piotrowska-Niczyporuk, A., Bajguz, A., Talarek, M., Bralska, M., Zambrzycka, E., 2015. The effect of lead on the growth, content of primary metabolites, and antioxidant response of green alga *Acutodesmus obliquus* (Chlorophyceae). Environ. Sci. Pollut. Res. 22, 19112–19123. https://doi.org/10.1007/s11356-015-5118-y
Piotrowska-niczyporuk, A., Bajguz, A., Zambrzycka-szelewa, E., Bralska, M., 2018. Exogenously applied auxins and cytokinins ameliorate lead toxicity by inducing antioxidant defence system in green alga *Acutodesmus obliquus*. Plant Physiol. Biochem. https://doi.org/10.1016/j.plaphy.2018.09.038
Piotrowska-Niczyporuk, A., Bajguz, A., Zambrzycka, E., Godlewska-żyłkiewicz, B., 2012. Phytohormones as regulators of heavy metal biosorption and toxicity in green alga *Chlorella vulgaris* (Chlorophyceae). Plant Physiol. Biochem. 52, 52–65. https://doi.org/10.1016/j.plaphy.2011.11.009
Qian, H., Chen, W., Sheng, G.D., Xu, X., Liu, W., Fu, Z., 2008. Effects of glufosinate on antioxidant enzymes , subcellular structure , and gene expression in the unicellular green alga *Chlorella vulgaris*. Aquat. Toxicol. 88, 301–307. https://doi.org/10.1016/j.aquatox.2008.05.009
Rai, U.N., Singh, N.K., Upadhyay, A.K., Verma, S., 2013. Chromate tolerance and accumulation in *Chlorella vulgaris* L.: Role of antioxidant enzymes and biochemical changes in detoxification of metals. Bioresour. Technol. 136, 604–609. https://doi.org/10.1016/j.biortech.2013.03.043
Rajput, V.D., Singh, R.K., Verma, K.K., Sharma, L., Sushkova, S., Mandzhieva, S., 2021. Recent Developments in Enzymatic Antioxidant Defence Mechanism in Plants with Special Reference to Abiotic Stress. Biology (Basel). 10, 1--28.
Randhawa, V.K., Zhou, F., Jin, X., Nalewajko, C., Kushner, D.J., 2001. Role of oxidative stress and thiol antioxidant enzymes in nickel toxicity and resistance in strains of the green alga

Scenedesmus acutus f. alternans. Can. J. Microbiol. 47, 987–993. https://doi.org/10.1139/cjm-47-11-987
Rezayian, M., Niknam, V., Ebrahimzadeh, H., 2019. Oxidative damage and antioxidative system in algae. Toxicol. Reports 6, 1309–1313. https://doi.org/10.1016/j.toxrep.2019.10.001
Rocchetta, I., Mazzuca, M., Conforti, V., Balzaretti, V., de Molina, M. del C.R., 2012. Chromium induced stress conditions in heterotrophic and auxotrophic strains of *Euglena gracilis*. Ecotoxicol. Environ. Saf. 84, 147–154. https://doi.org/10.1016/j.ecoenv.2012.07.020
Rocchetta, I., Mazzuca, M., Conforti, V., Ruiz, L., Balzaretti, V., De Molina, M.D.C.R., 2006. Effect of chromium on the fatty acid composition of two strains of *Euglena gracilis*. Environ. Pollut. 141, 353–358. https://doi.org/10.1016/j.envpol.2005.08.035
Rodrigo, R., Libuy, M., 2014. Modulation of Plant Endogenous Antioxidant Systems by Polyphenols, Polyphenols in Plants: Isolation, Purification and Extract Preparation. Elsevier. https://doi.org/10.1016/B978-0-12-397934-6.00005-X
Sabatini, S.E., Juárez, Á.B., Eppis, M.R., Bianchi, L., Luquet, C.M., Ríos de Molina, M. del C., 2009. Oxidative stress and antioxidant defenses in two green microalgae exposed to copper. Ecotoxicol. Environ. Saf. 72, 1200–1206. https://doi.org/10.1016/j.ecoenv.2009.01.003
Sánchez-Thomas, R., Moreno-Sánchez, R., García-García, J.D., 2016. Accumulation of zinc protects against cadmium stress in photosynthetic *Euglenagracilis*. Environ. Exp. Bot. 131, 19–31. https://doi.org/10.1016/j.envexpbot.2016.06.009
Shivaji, S., Dro, S.V.L., 2019. *Scenedesnus rotundus* isolated from the petroleum effluent employs alternate mechanisms of tolerance to elevated levels of Cadmium and Zinc. Sci. Rep. 1–15. https://doi.org/10.1038/s41598-019-44374-1
Singh, S., Eapen, S., D'Souza, S.F., 2006. Cadmium accumulation and its influence on lipid peroxidation and antioxidative system in an aquatic plant, *Bacopa monnieri* L. Chemosphere 62, 233–246. https://doi.org/10.1016/j.chemosphere.2005.05.017
Smirnoff, N., 2000. Ascorbic acid: metabolism and functions of a multi-facetted molecule. Curr. Opin. Plant Biol. 3, 229–235. https://doi.org/10.1016/s1369-5266(00)80070-9
Strejckova, A., Dvorak, M., Klejdus, B., Krystofova, O., Hedbavny, J., Adam, V., Huska, D., 2019. The strong reaction of simple phenolic acids during oxidative stress caused by nickel, cadmium and copper in the microalga *Scenedesmus quadricauda*. N. Biotechnol. 48, 66–75. https://doi.org/10.1016/j.nbt.2018.07.004
Suárez, C., Torres, E., Pérez-Rama, M., Herrero, C., Abalde, J., 2010. Cadmium toxicity on the freshwater microalga *Chlamydomonas moewusii* Gerloff: Biosynthesis of thiol compounds. Environ. Toxicol. Chem. 29, 2009–2015. https://doi.org/10.1002/etc.242
Suman, T.Y., Radhika Rajasree, S.R., Kirubagaran, R., 2015. Evaluation of zinc oxide nanoparticles toxicity on marine algae *chlorella vulgaris* through flow cytometric, cytotoxicity and oxidative stress analysis. Ecotoxicol. Environ. Saf. 113, 23–30. https://doi.org/10.1016/j.ecoenv.2014.11.015
Talarek-Karwel, M., Bajguz, A., Piotrowska-Niczyporuk, A., 2020. Hormonal response of *Acutodesmus obliquus* exposed to combined treatment with 24-epibrassinolide and lead. J. Appl. Phycol. 32, 2903–2914. https://doi.org/10.1007/s10811-020-02191-4
Tarakhovskaya, E.R., Maslov, Y.I., Shishova, M.F., 2007. Phytohormones in Algae. Russ. J. Plant Physiol. 54, 163–170. https://doi.org/10.1134/S1021443707020021
Tchounwou, P.B., Yedjou, C.G., Patlolla, A.K., Sutton, D.J., 2012. Heavy Metals Toxicity and the Environment. Mol. Clin. Environ. Toxicol. 101, 133–164. https://doi.org/10.1007/978-3-7643-8340-4
Thomas, C.E., McLean, L.R., Parker, R.A., Ohlweiler, D.F., 1992. Ascorbate and phenolic

antioxidant interactions in prevention of liposomal oxidation. Lipids 27, 543–550. https://doi.org/10.1007/BF02536138
Tripathi, B.N., Gaur, J.P., 2004. Relationship between copper- and zinc-induced oxidative stress and proline accumulation in *Scenedesmus* sp. Planta 219, 397–404. https://doi.org/10.1007/s00425-004-1237-2
Tripathi, B.N., Mehta, S.K., Amar, A., Gaur, J.P., 2006. Oxidative stress in *Scenedesmus* sp. during short- and long-term exposure to Cu2+ and Zn2+. Chemosphere 62, 538–544. https://doi.org/10.1016/j.chemosphere.2005.06.031
Tripathi, R.P., Singh, B., Bisht, S.S., Pandey, J., 2009. L-Ascorbic Acid in Organic Synthesis : An Overview. Curr. Org. Chem. 226001, 99–122.https://doi.org/10.2174/138527209787193792
Tsuji, N., Hirayanagi, N., Iwabe, O., Namba, T., Tagawa, M., 2003. Regulation of phytochelatin synthesis by zinc and cadmium in marine green alga , *Dunaliella tertiolecta* 62, 453–459.https://doi.org/10.1016/S0031-9422(02)00559-9
Tuteja, N., Singh, M.B., Misra, M.K., Bhalla, P.L., Tuteja, R., Mishra, R.N.C., Carolina, S., 2001. Molecular Mechanisms of DNA Damage and Repair : Progress in Plants. Crit. Rev. Biochem. Mol. Biol. 36, 337–397. https://doi.org/doi:10.1080/20014091074219
Ugya, A.Y., Imam, T.S., Li, A., Ma, J., Hua, X., 2019. Antioxidant response mechanism of freshwater microalgae species to reactive oxygen species production : a mini review species to reactive oxygen species production : a mini review. Chem. Ecol. 0, 1–20. https://doi.org/10.1080/02757540.2019.1688308
Ulrich, K., & Jakob, U., 2019. The role of thiols in antioxidant systems. Free Radic. Biol. Med. 140, 14–27. https://doi.org/10.1016/j.freeradbiomed.2019.05.035.
Vara, D., Pula, G., 2014. Reactive Oxygen Species : Physiological Roles in the Regulation of Vascular Cells Reactive Oxygen Species : Physiological Roles in the Regulation of Vascular Cells. Curr. Mol. Med. 13, 1–23. https://doi.org/10.2174/15665240146661406031140 10
Vishnivetskaya, T.A., 2009. Viable Cyanobacteria and Green Algae from the Permafrost Darkness, in: Permafrost Soils. pp. 73–84. https://doi.org/10.1007/978-3-540-69371-0
Volland, S., Lütz, C., Michalke, B., Lütz-meindl, U., 2012. Intracellular chromium localization and cell physiological response in the unicellular alga *Micrasterias*. Aquat. Toxicol. 109, 59–69. https://doi.org/10.1016/j.aquatox.2011.11.013
Wang, W., Yang, H., Johnson, D., Gensler, C., Decker, E., Zhang, G., 2017. Chemistry and biology of ω-3 PUFA peroxidation-derived compounds. Prostaglandins Other Lipid Mediat. 132, 84-91. https://doi.org/10.1016/j.prostaglandins.2016.12.004
Zbigniew, T., Wojciech, P., 2006. Individual and combined effect of anthracene , cadmium , and chloridazone on growth and activity of SOD izoformes in three *Scenedesmus* species. Ecotoxicol. Environ. Saf. 65, 323–331. https://doi.org/10.1016/j.ecoenv.2005.12.001
Zhang, L.P., Yang, Z.M., 2008. Copper-Induced Proline Synthesis is Associated with Nitric Oxide Generation in *Chlamydomonas reinhardtii*. Plant Cell Physiol 49, 411–419. https://doi.org/10.1093/pcp/pcn017
Zhong, Y., Cheng, J.J., 2017. Effects of selenite on unicellular green microalga *Chlorella pyrenoidosa*: bioaccumulation of selenium, enhancement of photosynthetic pigments, and amino acid production. J. Agric. Food Chem. 65, 10875-10883. https://doi.org/10.1021/acs.jafc.7b04246
Zhu, Q.L., Guo, S.N., Wen, F., Zhang, X.L., Wang, C.C., Si, L.F., Zheng, J.L., Liu, J., 2019. Transcriptional and physiological responses of *Dunaliella salina* to cadmium reveals time-dependent turnover of ribosome, photosystem, and ROS-scavenging pathways. Aquat. Toxicol. 207, 153–162. https://doi.org/10.1016/j.aquatox.2018.12.007

“ La science consiste à passer d 'un étonnement à un autre ”

Aristote

Philosophe (-384 -322 av JC)

Chapitre III

Mycoremediation of synthetic dyes by yeast cells: a sustainable biodegradation approach

RÉSUMÉ

Cette troisième revue de la littérature se concentre sur le pouvoir des levures à dégrader les colorants synthétiques. Tout d'abord, une synthèse détaillée des études de la biodégradation des colorants par les différentes espèces de levures a été présentée. L'accent a ensuite été mis sur les enzymes impliquées dans la biodégradation des colorants, et l'influence des facteurs opératoires sur la performance de la biodégradation. Par ailleurs, les méthodes analytiques utilisées dans la caractérisation chimique des sous-produits issues de la biodégradation des colorants et l'évaluation de leur toxicité ont fait l'objet de troisième volet de ce chapitre. Dans la dernière section, les aspects moléculaires de la biodégradation des colorants par les levures ont été évoqués.

Sur la base des études examinées dans cette revue, on peut conclure que la mycoremédiation des colorants par les cellules de levure peut être une stratégie prometteuse, efficace et respectueuse de l'environnement pour le traitement des effluents chargés en colorants. La capacité de biodégradation des levures a été liée à l'activité des oxydases à savoir la laccase, la tyrosinase, la manganèse peroxydase et la lignine peroxydase, ainsi qu'à celle des réductases, en particulier l'azo réductase, la NADH-DCIP réductase et le vert malachite réductase.

Pour la plupart des souches de levure, la capacité de biodégradation optimale a été atteinte dans des gammes de pH neutres ou acides, dans des cultures agitées à 30°C. L'ajout de sources d'azote ou de carbone appropriées améliore considérablement l'efficacité de la décoloration. De plus, la capacité de biodégradation des levures peut être affectée à la fois par les propriétés chimiques des molécules de colorants et par leur concentration. Par conséquent, les paramètres physico-chimiques doivent être optimisés pour une décoloration efficace.

Pa ailleurs, au cours du processus de biotransformation des colorants, la caractérisation chimique des intermédiaires de la dégradation fongique des colorants par les techniques de chromatographie et de spectroscopie, permet de déduire les voies de leur biodégradation. En outre, les tests éco-toxicologiques montrent que les métabolites intermédiaires résultant de la biodégradation des colorants par différents souches de levures sont généralement moins toxiques que la molécule d'origine. Cela fait de l'utilisation de cellules des levures ou de leurs enzymes dans le traitement des colorants synthétiques, une technologie prometteuse pour une détoxication efficace de ces polluants organiques.

Environmental Sustainability
https://doi.org/10.1007/s42398-020-00150-w

REVIEW

Mycoremediation of synthetic dyes by yeast cells: a sustainable biodegradation approach

M. Danouche[1,2] · H. EL Arroussi[1] · N. El Ghachtouli[2]

Received: 19 December 2019 / Revised: 25 October 2020 / Accepted: 20 November 2020
© Society for Environmental Sustainability 2021

Abstract

Dye effluents released from various industries, notably the textile sector, are hazardous, and can cause significant damage to the environment. Thus, treatment and detoxification of these toxic dyes are of major concern for compliance with environmental legislations. So far, a number of physicochemical dye-removal methods have been proposed. However, despite their effectiveness in dye decolorization, by-products of chemical degradation methods may be more toxic than their parent dye molecules. The cost of these processes is also very high, thereby limiting their large-scale application. The use of yeast cells for the removal of toxic dyes is a comparatively effective, eco-friendly and cost-effective method. In this review, we describe the adverse effects of synthetic dyes on living organisms and enzymatic biodegradation mechanisms involved in mycoremediation processes of synthetic dyes. In addition, the influence of various physico-chemical factors on the decolorization performance of yeast cells, the analytical techniques used to identify the intermediates of dye biodegradation, the assessment of their toxicity and the molecular aspects of their biodegradation are also highlighted. This study may provide a basis for the development of dye bio-removal methods using yeast cells.

Graphical abstract

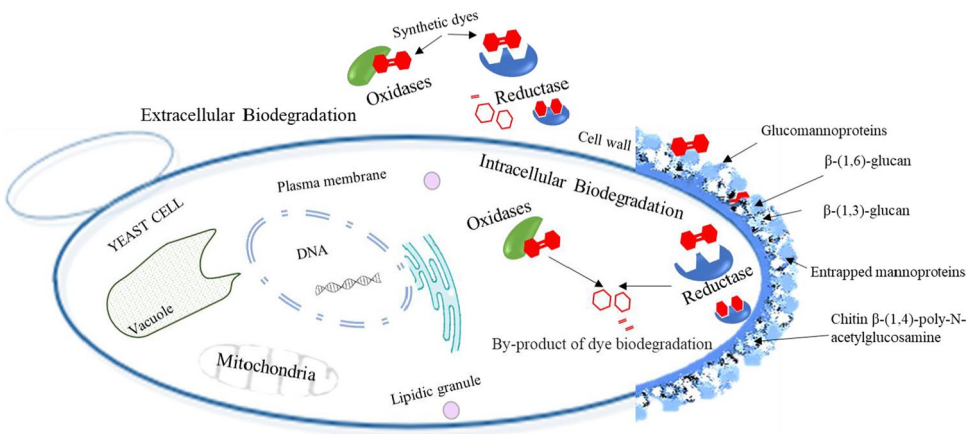

Keywords Yeast · Decolorization · Enzymatic biodegradation · By-product identification · Toxicity assessment

Introduction

Since the beginning of the industrial revolution in the nineteenth century, the equation for balanced economic growth while protecting the environment has not yet been resolved. In fact, soil, air, and water pollution are among the main global challenges facing the world today. More critical than

✉ M. Danouche
mohammed.danouche@usmba.ac.ma

Extended author information available on the last page of the article

Published online: 01 January 2021

ever, there is a growing concern about the impact of water contamination on aquatic life and public health. Compared to other industrial sectors, the textiles industry consumes large quantity of water; it was estimated that about 200–500 L of water is required to produce 1 kg of finished textile products (Waghmode et al. 2012a). Therefore, this sector generates significant volume of wastewater composed of suspended solids, surfactants, heavy metals and several synthetic dyes (Balapure et al. 2015; Chen et al. 2009). The exact amount of dyes released into the environment is uncertain, it has only been estimated that the overall use of dyes in the textile sector is more than 10 000 tons per year, and about 10–15% of this amount is lost as waste during the dyeing process, due to the low chemical affinity of the dyes used on textile fibers (Kunamneni et al. 2008; Saratale et al. 2011). Consequently, the release of such xenobiotics leads to significant pollution, which not only affects the aesthetic quality of water but also leads to serious impacts on exposed organisms including humans (Lellis et al. 2019; Puvaneswari et al. 2006). To cope with this issue, legislations have been enacted worldwide for the management and the treatment of these contaminants prior to their release into the environment. A variety of physicochemical methods have therefore been used, particularly membrane processes, photochemical oxidation, and electrochemical processes (Arslan et al. 2016). Although these methods are effective, they require a large amount of chemicals and energy-intensive facilities, which makes them expensive, thereby limiting their large-scale applications (Barakat 2011; Fu and Wang 2011). The most recommended approach is the use of biological techniques, due to their advantages, including treatment efficiency, appropriate cost, and a minimal ecological impact (Srinivasan and Viraraghavan 2010). The emergence of this promising solution is based on the exploitation of the ecological principles of bacteria, fungi, and microalgae in the treatment of toxic dyes (Chen et al. 2009; Jafari et al. 2014; Miranda et al. 2013). While bioprocesses have several advantages, some drawbacks may also be noted, such as the long time required for the bio-removal of dyes using filamentous fungi or microalgae (Singh and Arora 2011). Moreover, the decolorization of dyes using bacteria requires two phases; the anaerobic reduction of Azo bonds, followed by aerobic mineralization of the resultant aromatic amines (Abiri et al. 2017; Roșu et al. 2019). However, the use of yeast cells overcomes this drawback; they do not only grow rapidly like bacteria, but exhibit great plasticity and ability to adapt to adverse growth conditions like pH fluctuation or temperature changes. Also, yeast does not require special biphase growth conditions like bacteria. In addition, the biodegradation mechanisms of dyes using yeast cells involve different oxidases, that can directly break the azo dyes through non-specific free radical mechanisms, avoiding therefore the production of toxic intermediates like aromatic amines, that are typically produced after the specific cleavage of the azo bond of synthetic dyes by bacteria (Pandey et al. 2007; Dave et al. 2015). Furthermore, yeast have a special flocculating characteristic that allows them to aggregate into multicellular masses (flakes), facilitating, therefore, their recovery after treatment of colored effluents (Soares and Soares 2012). Hence, the use of yeast cells in the bioremoval of synthetic dyes has attracted more interest (Jafari et al. 2014; Sen et al. 2016). Several studies focusing on the decolorization mechanisms of the ascomycete and basidiomycete strains of yeast have demonstrated the involvement of three bioremoval strategies, with active and/or passive metabolism pathways, namely: extracellular biosorption (Dil et al. 2017; Mahmoud 2016), intracellular bioaccumulation (Das et al. 2010; Gönen and Aksu 2009) and/or intra and extracellular biodegradation (Martorell et al. 2018; Tan et al. 2019). The present review focuses on the harmful effects of synthetic dyes on aquatic environments and the state-of-the-art of the biodegradation mechanisms of synthetic dyes by yeast cells. Sequential summary studies on the biodegradation of synthetic dyes using different yeast species are also discussed. Much emphasis will be projected towards oxidoredactase enzymes involved in the biodegradation of dyes, as well as the influence of operating factors on this bioprocess. Besides, the analytical methods used in the chemical characterization of dye biodegradation by-products and the evaluation of their toxicity will be discussed. Throughout the last section, the molecular aspects of the degradation of dyes by yeast cells will be addressed in order to identify the future scope of this research.

Adverse effects of synthetic dyes on aquatic ecosystems

Since the dawn of human civilization, colorants have played a crucial role in different aspects of everyday life. Before the end of the nineteenth century, all dyes used were obtained from natural sources, until the first artificial dye was discovered by W.H Perkins (1838–1907) through an accidental production of Mauveine. This successful discovery paved the way for the synthesis of chemical dyes as we know them today. Since then, many chemical compounds have been identified as coloring substances (Rai et al. 2005). Thus, the use of these chemicals has continued to increase, notably in textile and leather industries. In addition to the type of color emitted by these chemicals, other physicochemical requirements have become more stringent in textile sectors including resistance to various environmental conditions, such as persistence of colored fabrics against washing, exposure to light, chemicals and biological attacks (Khan et al. 2013). However, the same requirements that confer higher resistance qualities,

could complicate the dye's removal from wastewater by traditional methods. Meanwhile, the release of untreated or inadequately treated colored wastewater into aquatic environments can lead to various signs of toxicity to exposed living organisms (Moopantakath and Kumavath 2018). The high concentration of dyes in aquatic ecosystems may prevent the penetration of light into the depths, thus disturbing the photosynthetic activity of autotrophic organisms, and impacting the re-oxygenation potential of the receiving waters (Carmen et al. 2009). Moreover, the toxicity of synthetic dyes may occur in aquatic ecosystems across the food chains. Numerous studies have focused on the adverse effect of dyes on species from various trophic levels, including producer and consumer species (Puvaneswari et al. 2006; Tkaczyk et al. 2020). For instance, the microalgae's morphological, biochemical, and metabolic properties can be influenced by increasing concentrations of dyes. Gita et al. (2019) reported that a concentration-dependent decrease in the specific growth rate and pigment contents of *Chlorella vulgaris* was observed after exposure to increasing concentrations of the textile dyes Drimarene Blue, Optilan Yellow and Lanasyn Brown. Similarly, Indigo dye induced a significant growth reduction of *Scenedesmus quadricauda*, and altered its morphological characteristics (Chia and Musa 2014). Likewise, zooplankton organisms can be directly or indirectly influenced by dyes. Hernández-Zamora et al. (2016) showed that exposure to low concentrations of Congo Red or feeding on microalgae that already accumulated this dye, induced adverse effects on the survival and reproduction of *Ceriodaphnia dubia.* Additionally, many toxic dyes have shown a direct effect on primary consumers like fish. For instance, Kaur and Kaur (2014) investigated Poikilocytosis occurrence in *Labeo rohita* fish as an indicator of stress caused by the azo dye Basic Violet-1, with a highly toxic effect (96-h LC_{50}) at 0.45 mg L^{-1} concentrations. Srivastava et al. (2017) also noted that the exposure of *L. rohita* to sublethal concentrations of Eriochrome Black T caused considerable histopathological abnormalities and altered antioxidant enzyme activities in the epidermis. Hence, the accumulation of these xenobiotics in aquatic organisms and their transmission to humans through the consumption of sea food from polluted sources may provoke many human health problems (Chung 2016; Mendes et al. 2011).

To prevent these environmental issues, it is necessary to introduce standards and framework laws to limit the use of hazardous dyes or to substitute them with new synthetic dyes that can meet industrial requirements, and that can also be easily biodegradable. Therefore, research in synthetic chemistry of dyes must not only compete with the criteria of resistance, but also their fate in nature. On the other hand, it is important to establish promising approaches for the treatment of these pollutants before their release into the environments.

Biodegradation of synthetic dyes by yeast

Biodegradation is defined as an energy-dependent process, involving the decomposition of organic compounds, into smaller and simpler by-products, through different enzymatic reactions (Kaushik and Malik 2009). When the biodegradation is completed, the bioprocess is called mineralization. This form of treatment produces simpler products, such as H_2O, CO_2, NH_3, CH_4, H_2S and PO_3, which are less harmful. The same process is defined as biotransformation if the organic compounds are not completely mineralized (Martorell et al. 2017a). Many microorganisms belonging to various taxonomic classes (bacteria, fungi, and microalgae) have shown the ability to decompose a broad variety of anthropogenic compounds, including synthetic dyes (Chen et al. 2009; El-Sheekh et al. 2009; Jafari et al. 2014; Miranda et al. 2013). In recent years, mycoremediation or the biotechnological application of fungi has become a model example for bioremoval of pollutants. It has been documented that a diversity of fungal species could be used for removing a variety of toxic dyes, mainly with white-rot fungi like *Trametes versicolor* and *Phanerochaete chrysosporium*. Other fungi species such as *Rhizopus oryzae* and *Aspergillus niger*, have also been reported (Sen et al. 2016). Regarding the use of yeast in the bioremediation of synthetic dyes, it was first mooted back in 1992, when the yeast strain of *Candida curvata* was used for the treatment of colored wastewater (Kakuta et al. 1992). Until today, reports on the biodegradation of synthetic dyes using yeast cells are limited compared to other investigations on the biodegradation of dyes using other microorganisms. The most studied yeast strains for the biodegradation of synthetic dyes are *Candida* sp., *Saccharomyces cerevisiae,* and *Pichia* sp. which belong to the Ascomycetes phylum, and only a few reports involve Basidiomycetous yeast strains, such as *Trichosporon* sp. and *Pseudozyma rugulosa* (Pajot et al. 2014).

Enzymes involved in the biodegradation of dyes by yeast

The biodegradation of synthetic dyes using yeast cells is performed with various intra-extracellular oxidase and reductase enzymes (Fig. 1). Oxidases are the most studied enzymes for the biodegradation of dyes by yeast. Moreover, the activity of certain reductases has also been reported in

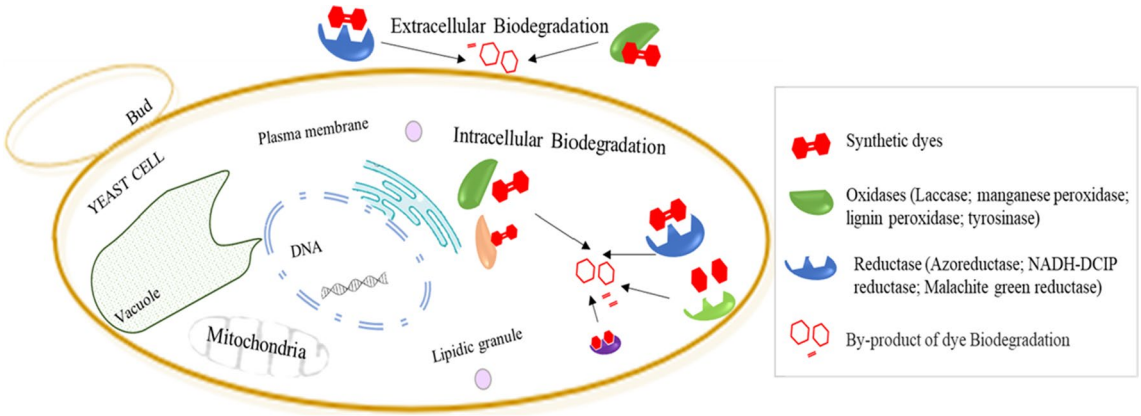

Fig. 1 Intracellular and extracellular enzymatic biodegradation of synthetic dyes in yeast cells

some yeast strains (Table 1). The suggested mechanism for the enzymatic biodegradation of azo dyes is shown in Fig. 2.

Oxidases are a class of enzymes that use O_2 as an electron acceptor to catalyze oxidation–reduction reaction, and thereby generating H_2O or H_2O_2 as products. The oxidases typically contain metal or Flavin coenzyme on their active site (Phale et al. 2019). It was reported that the biodegradation of synthetic dyes by yeast cells can be accomplished through lignin-modifying enzymes, particularly phenoloxidase like Laccase (Lac) and tyrosinase (Tyr) as well as peroxidase such as manganese peroxidase (MnP) and lignin peroxidase (LiP) (Martorell et al. 2012; Solís et al. 2012).

Laccase (EC 1.10.3.2) Lac is a benzenediol oxygen reductase that can be expressed in different species including lichens, bacteria and fungi. In fact, this enzyme belongs to the classes of urushiol and P-diphenol oxidase, distinguished by a multicopper atoms in their catalytic center (Arregui et al. 2019). A high redox potential (780 mV) allows these enzymes to oxidize many organic compounds, such as polyphenols, methoxy-substituted phenols, aromatic diamines, and several organic pollutants inclining dyes (Upadhyay et al. 2016). The fungal Lac was found present in Ascomycetes, Deuteromycetes, Basidiomycetes species, but is particularly abundant in white-rot fungi that degrade lignin (Brijwani et al. 2010). In addition, fungal Lac is an extracellular enzyme, this peculiarity facilitates their isolation and purification compared to Lac from other organisms. Therefore, they have gained particular commercial interest in organic syntheses, pulp/textile bleaching, bioremediation, chemical grafting, and surface modification of polymers (Jeon et al. 2012; Viswanath et al. 2014). As shown in the Table 1, a number of studies have documented the role of Lac in yeast cells in the biodegradation of synthetic dye. The use of Lac for the biodegradation of dyes does not require cofactors, since it directly breaks azo dyes via non-specific free radical mechanisms, which does not create toxic by-products, such as aromatic amines, typically produced after the specific cleavage of the azo bond of azo dye (Dave et al. 2015).

Tyrosinase (E.C. 1.14.18.1) Try is a copper-containing enzyme, known as polyphenol oxidase or monophenol mono-oxygenase. It has been found in plants, filamentous fungi, bacteria, and some yeast strains. This enzyme has a range of industrial interests, for example in the biosynthesis of melanin, the manufacture of L-dihydroxy phenylalanine, as well as several environmental biotechnologies like the detoxification of phenol-containing wastewater (Ates et al. 2007; Kim and Uyama 2005; Zaidi et al. 2014). With regard to the involvement of Try in the decolorization of synthetic dyes in yeast cells, only a few species revealed their role, notably *Galactomyces geotrichum* MTCC (Waghmode et al. 2012a, b), *S. cerevisiae* MTCC 463 (Jadhav et al. 2007) and *Candida krusei* strains (Charumathi and Das 2011). The catalytic reaction of dyes with Try is performed in two steps: The primary reaction catalyzing the o-hydroxylation of monophenols to the corresponding catechols (monophenolase activity), followed by the second oxidizing monophenols to the corresponding o-quinones (Diphenolase activity) (Duckworth and Coleman 1970).

Lignin peroxidase (EC 1.11.1.14) LiP is a glycosylated enzyme that belongs to the oxidoreductase family that acts on peroxide as an acceptor. This ligninolytic enzyme has a high redox potential (700–1400 mV), with optimum activity at acidic range (pH 3–4.5). Lip is a non-specific substrate enzyme, which means that this characteristic confers it the ability to catalyze the degradation of different phenolic and non-phenolic aromatic compounds, including β-O-4 linkage-type arylglycerol-aryl ethers with a redox potential of up to 1.4 V (in comparison with the normal hydrogen electrode) (Choinowski et al. 1999; Chowdhary et al. 2018). For example, the biodegradation mechanism of sulphonated azo

Table 1 Studies on the biodegradation of dyes by yeasts species

Yeasts species	Dyes	Conditions	D (%)/Time	Enzymatic activity	References
Sterigmatomyces halophilus SSA-1575	Reactive Black 5	50 mg L^{-1} 30 °C/0 rpm pH 5.0	98/24 h	Oxidase: LiP, MnP and Lac Reductase NADH-DCIP reductase	Al-Tohamy et al. (2020)
G. geotrichum GG	Acid Scarlet GR	100 mg L^{-1} 30 °C /180 rpm pH 7.0–8.0	92/10 h	Oxidase: LiP and Lac Reductase: NADH-DCIP reductase	Guo et al. (2019)
P. occidentalis G1	Acid Red B	50 mg L^{-1} 30 °C/160 rpm pH 5.0	98/16 h	Oxidase: LiP, MnP and Lac Reductase: NADH-DCIP reductase	Song et al. (2018a, b)
G. geotrichum MTCC 1360	Methyl Red	100 mg L^{-1} 30 °C/150 rpm pH 3.0	100/1 h	Oxidase: LiP and Lac Reductase: NADH–DCIP reductase, MG-reductase	Jadhav et al. (2008b)
S. cerevisiae MTCC 463	Methy Red	100 mg L^{-1} 30 °C/0 rpm pH 6.5–9.0	100/16 min	Oxidase: LiP, Tyr, Lac and Aminopyrine N-demethylase Reductase: NADH-DCIP reductase, AzoR	Jadhav et al. (2007)
G. geotrichum MTCC 1360	Remazol Red Rubine GFL	50 mg L^{-1} 30 °C /0 rpm pH 7.0	96/36 h 87/96 h	Oxidase: Tyr and Lac Reductase: NADH-DCIP reductase, AzoR, and Riboflavin reductase	Waghmode et al. (2012a, b)
S. cerevisiae MTCC 463	Malachite Green	100 mg L^{-1} 33 °C/150 rpm pH 7.2	95/23 h	Oxidase: LiP and Lac Reductase: NADH-DCIP reductase, MG-reductase	Jadhav and Govindwar (2006)
S. cerevisiae	Malachite Green	100 mg L^{-1} 30 °C/150 rpm pH 7.2	99/2 h	Oxidase: LiP and Lac Reductase: NADH-DCIP reductase, MG-reductase	Biradar et al. (2016)
C. krusei	Basic Violet 3	10 mg L^{-1} 28 °C/120 rpm pH 6.5	100/24 h	Oxidase: LiP, Tyr and Lac Reductase: NADH-DCIP reductase, MG-reductase and AzoR	Charumathi and Das (2011)
D. rugosa	Indigo	10 mg L^{-1} 30 °C/0 rpm pH 2.0	99.9/5 5 d	Oxidase: LiP Reductase: NADH-DCIP reductase	Bankole et al. (2017)
C. samutprakarnensis	Acid Red B	50 mg L^{-1} 30 °C/160 rpm pH 6.0	97/18 h	Oxidase: LiP Reductase: NADH-DCIP reductase	Song et al. (2018a, b)
Candida sp VITJASS	Reactive Green	100 mg L^{-1} 30 °C/120 rpm pH 5.0–6.0	84/96 h	Oxidase: Lac Reductase: NADH-DCIP reductase, AzoR	Sinha et al. (2018)

Table 1 (continued)

Yeasts species	Dyes	Conditions	D (%)/Time	Enzymatic activity	References
Candida sp MM 4035 *T. porosum* MM 4037 *C. satwnus* MM 4034 *Barnettozyma californica* MM 4018	Yellow 4R-HE Black B-V Blue RR-BB Red 7B-HE	200 mg L^{-1} 25 °C/250 rpm pH 4.0	64–96/24 h	Oxidase: LiP, MnP, Tyr, Lac and *N*-demethylase	Martorell et al. (2012)
D. polymorphus *C. tropicalis*	Reactive Black 5	200 mg L^{-1} 28 °C/200 rpm pH 5.0–6.0	100/18–24 h	Oxidase: MnP	Yang et al. (2008)
T. multisporum *T. laibachii*	Yellow 4R-HE Red 7B-HE Blue RR-BB Green RR-4B	200 mg L^{-1} 26 °C/200 rpm pH 4.5	63–98/36–72 h	Oxidase: LiP, MnP and Lac	Pajot et al. (2007)
C. boidinii MM 4035	Reactive Black 5	200 mg L^{-1} 25 °C/250 rpm pH 4.0	100/24 h	Oxidase: MnP, Lac and peroxidase	Martorell et al. (2017a)
T. akiyoshidainum HP2023	Reactive Black 5	200 mg L^{-1} 25 ºC/250 rpm pH 7.0	100/12 h	Oxidase: phenol oxidase and peroxidase enzymes	Martorell et al. (2018)
T. beigelii NCIM-3326	Reactive Blue 171	50 mg L^{-1} 37 °C/0 rpm pH 6.6	95/24 h	Reductase: NADH-DCIP reductase and AzoR	Saratale et al. (2009a)
P. kudriavzevii CR-Y103	Reactive Orange 16	400 mg L^{-1} 30 °C/120 rpm pH 6.0	95/72 h	Reductase: NADH-DCIP reductase and AzoR	Rosu et al. (2018)
C. oleophila	Reactive Black 5	200 mg L^{-1} 26 °C/120 rpm pH 7.6	100/24 h	Reductase: AzoR-like	Lucas et al. (2006)
I. occidentalis	Methyl Orange Orange II	0.2 mM dye 26 °C/120 rpm Acidic pH	80/15 h	Reductase: AzoR	Ramalho et al. (2004)
G. geotrichum KL20A	Methylene Blue	50 mg L^{-1} 35 °C pH 7.0	70/48 h	Biodegradation	Contreras et al. (2019)
C. tropicalis TL-F1	Acid Brilliant Red GR	100 mg L^{-1} 35 °C/160 rpm pH 5.0–6.0	95/24 h	Biodegradation	Tan et al. (2013)
P. rugulosa Y48 *C. kruseia* Gl	Reactive Brilliant Red K-2BP	200 mg L^{-1} 28 °C/200 rpm pH 5.0–6.0	99/24 h	Biodegradation	Yu and Wen (2005)

Table 1 (continued)

Yeasts species	Dyes	Conditions	D (%)/Time	Enzymatic activity	References
Magnusiomyces ingens LH-F1	Acid Red B	50 mg L^{-1} 30 °C/200 rpm pH 6.0	98/10 h	Biodegradation	Tan et al. (2014b)

D (%) percentage of decolorization

dyes by LiP may involve two consecutive one-electron oxidations of the H_2O_2-oxidized forms of LiP in the phenolic ring, where the corresponding carbonium ion carrying the azo link contributes to the formation of quinone and phenyldiazine through a nucleophilic attack by H_2O. The phenyldiazine product is then oxidized by O_2 to a phenyl radical and the azo bond is removed as N_2, and the phenyl radical extracts hydrogen from its environment to produce a stable aromatic compound (Chivukula et al. 1995). LiP activity was detected during the biodegradation of various dyes using Ascomycota yeast strains of *Pichia occidentalis* (Song et al. 2018a, b), *G. geotrichum* (Guo et al. 2019), *S. cerevisiae* (Jadhav et al. 2007), *C. krusei* (Charumathi and Das 2011), *Diutina rugosa* (Bankole et al. 2017), *Cyberlindnera samutprakarnensis* (Song et al. 2018a, b), as well as strains belonging to the Basidiomycota phylum like *Trichosporon laibachii and Trichosporon multisporum* (Pajot et al. 2007).

Manganese peroxidase (EC 1.11.1.13) MnP is a glycoprotein enzyme belonging to the oxidoreductase's family, having a molecular weight ranging from 38 to 62.5 kDa (~ 350 amino acid residue). It is a substrate specific enzyme that oxidizes Mn^{2+} to Mn^{3+}, which diffuses from the enzyme surface and in turn oxidizes the phenolic substrate, such as lignin model compounds or other organic contaminants (Zhou et al. 2013). It was reported by Hofrichter (2002), that MnP production is limited to certain soil litter decomposing and wood-decaying fungus. But some research on the biodegradation of synthetic dyes using yeast reported the involvement of MnP in yeast strains of *P. occidentalis* (L. Song et al. 2018a, b), *Debaryomyces polymorphus, Candida tropicalis* (Yang et al. 2008), *T. multisporum,* and *T. laibachii* (Pajot et al. 2007).

Reductases They are enzyme classes that catalyze the reduction of the azo bonds (–N=N–) of azo dyes to produce a colorless aromatic amine. The involvement of such enzymes in the biodegradation of dyes was mainly recorded in bacteria (Hu 2001). However, other studies demonstrated the biodegradation activity of this enzyme in microalgae (Sinha et al. 2016), filamentous fungi (Bankole et al. 2018) and yeast (Lucas et al. 2006). The main reductase enzymes described in yeast strains are:

Azoreductase (EC 1.7.1.6) AzoR is present in diverse microorganisms and higher eukaryotes. Although their structure and function are diverse, they have a common ability to reduce azo bonds of organic compounds including azo dyes, nitroaromatic and azoic drugs (Misal and Gawai 2018). The AzoR classification is primarily based on their secondary and tertiary structures. Thus, they can be divided into two classes: Flavin dependent and independent AzoR. The flavin-dependent AzoR can also be classified according to the required co-enzymes NADH, NADPH, or both (Saratale et al. 2011; Solís et al. 2012). Breaking the azo bond by AzoR act as a critical step in the dye biotransformation

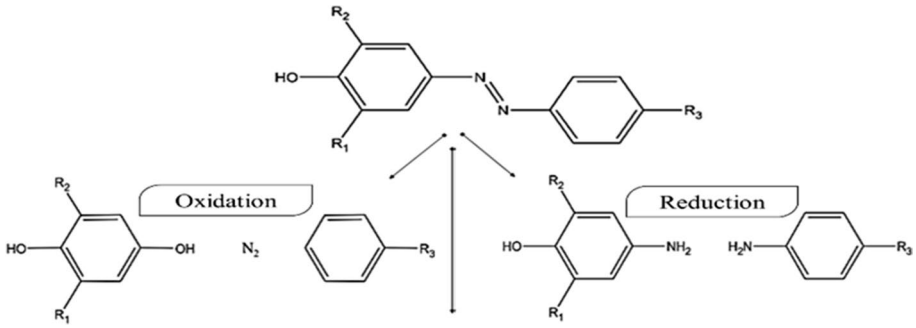

Fig. 2 Suggested azo bond cleavage via a reduction and oxidation, adapted from Kandelbauer and Guebitz (2005)

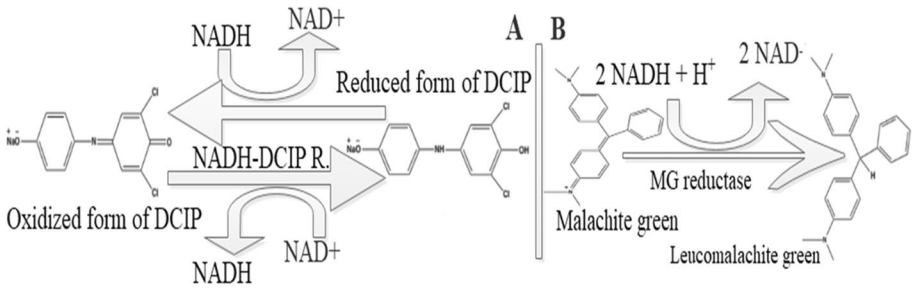

Fig. 3 Reactions catalyzed by NADH-DCIP reductase (**a**) and MG- reductase (**b**)

mechanisms (Elfarash et al. 2017). The involvement of AzoR during the dye biodegradation was detected in yeast strains of *S. cerevisiae* MTCC 463 (Jadhav et al. 2007), *C. krusei* (Charumathi and Das 2011), *Issatchenkia occidentalis* (Ramalho et al. 2004), *Trichosporon beigelii* NCIM-3326 (Saratale et al. 2009a).

NADH-DCIP reductase (EC 1.6.99.3) The NADH-preferring 2,6-dichloroindophenol reductase is an oxidoreductase that reduces 2,6-dichloroindo-phenol (DCIP) using NADH as an electron donor. DCIP is blue in its oxidized state and becomes colorless after reduction with reductase. This feature confers to this enzyme the ability to be useful in many clinical settings such as the determination of NADH and other dehydrogenases with a colorimetric reaction, when coupled to formazan dye-forming chromogens that act as hydrogen acceptors (Nishiya and Yamamoto 2007). Some studies have shown a significant increase in the activities of NADH-DCIP reductase, during the decolorization of azo dyes by yeast cells (Bankole et al. 2017; Rosu et al. 2018; Saratale et al. 2009a; Song et al. 2018a, b).

Malachite green reductase It is an enzyme that also uses NADH as an electron donor to convert green malachite to green Leucomalachite. Only few researchers reported (MG)-reductase as a marker enzyme for the reduction of synthetic dyes. The first study showing the role of (MG)-reductase in the biodegradation of green malachite dye was discovered in a yeast strain of *S. cerevisiae* MTCC 463 (Jadhav and Govindwar 2006). Two years later, Jadhav et al. (2008b) demonstrated that the biodegradation of methyl red by *G. geotrichum* MTCC 1360 strain involved also the (MG)-reductase. Thereafter, Charumathi and Das (2011), reported that (MG)-reductase activity was increased in *C. krusei* cells following the biodegradation of Basic Violet 3. Biradar et al. (2016) also, reported that the biodegradation of Malachite green by the *S. cerevisiae* yeast strain involved an increase in the enzymatic activity of (MG)-reductase. The reactions catalyzed by MG-reductase (B) and DCIP-reductase (A) are reflected in Fig. 3.

The enzymatic biodegradation of dyes using yeast cells can be improved through omics approaches, especially protein engineering, which would pave the way for further studies. In addition, the exploitation of enzymes from yeast cells after the dye mycoremediation process may be another form of valorization of the resulting biomass.

Factors affecting the biodegradation of dyes by yeast

The effective biodegradation of dye contaminants in wastewater remains a challenging process, due to many factors that influence this bioprocess. Therefore, it is important to evaluate and optimize the effect of physicochemical operating conditions, in order to make the process faster, more efficient and suitable for large-scale applications.

Effects of temperature In the microbial environment, temperature is a critical factor that plays several roles in cell viability, physiological status and metabolic performance. Optimal temperature for yeast growth is typically between 25 °C and 37 °C (Fu and Viraraghavan 2001). In fact, the optimum temperature for dye decolorization using yeast cells, is often correlated with the optimum growth temperature. Changes

in temperature can affect the biological response of yeast cells, especially enzyme activities (Ali 2010). Numerous studies (Table 1) have reported that the decolorization rate increases with increasing temperatures (from low to optimum temperature). However, a decolorization decline was noted at high temperatures (Tan et al. 2013, 2014b, 2016), which can be attributed to the loss of cell viability, or the denaturation of enzymes (Saratale et al. 2009b).

Effects of pH It's known that fungi, including yeast species show greater biodegradation behaviors in acidic or neutral mediums (Ali 2010). As showed in Table 1, almost all yeast decolorization studies demonstrated that the bioremoval of dyes is higher at optimum pH between 4 and 7 (Bankole et al. 2017; Jadhav et al. 2008b; Ramalho et al. 2004), and tended to decrease significantly when the pH of the medium was within the alkaline range. The pH effects are also related to cell viability, as shown by Peña et al. (2015), where the cell cycle of *S. cerevisiae* was interrupted at pH 9.0. This growth inhibition might be attributed to the decrease in cell transport of amino acids or the incorporation of proteins. On the other hand, the change in pH of the medium could also inhibit the transport of dye molecules through the cell membrane, which is considered as a limiting step for intracellular decolorization (Khan et al. 2013).

Effects of dye structure and concentration The chemical structure and concentration of dyes are among the influencing factors of decolonization efficiency. Research studies have suggested that increasing dye concentration gradually reduces their decolorization (Aksu 2003; Jadhav et al. 2007; Martorell et al. 2018), which could be attributed to an increase in dye toxicity. Moreover, at high concentrations, dyes can bind to the active site of enzymes mainly of AzoR, thereby preventing their activity (Jadhav et al. 2008a; Saratale et al. 2009a). Meanwhile, the chemical structure of dyes could also influence their degradation. In a comparative study on monoazo, diazo or triazo dyes, Franciscon et al. (2012) reported that simple-structured azo dyes with low molecular weight were easily biodegradable. Additionally, the azo bond is more susceptible to be broken when the substituent is in the para position of the phenyl ring relative to the ortho and meta position (Hsueh et al. 2009). For example, the substitution of electron withdrawal groups ($-SO_3H$) by ($-SO_2NH_2$) in the phenyl ring para position relative to the azo bond, increases the rate of reduction (Walker and Ryan 1971). Also, amino and hydroxyl-based dyes are more resistant to degradation than dyes with nitro, methyl, sulpho, and methoxy groups. This can be explained by the reduction mechanism that is conducted in two steps: a fast one-electron transfer reaction occurs to the radical anion, followed by a second, slower electron transfer process to create a stable dianion. The functional group of azo bond with a higher electronic density may not be suitable for this second electron transfer forming the dianion (Pearce et al. 2003; Rau et al. 2002). Metal-complex dyes might also have an adverse effect on the decolorization efficiency (Chen et al. 2003; Libra et al. 2004).

Effects of oxygen and shaking There are differing views on the effect of agitation on decolorization efficiency. According to results of several studies, the highest decolorization efficiency was observed in agitated cultures compared to static cultures. Shaking allows aeration to the medium, and equal distribution of nutrients, it also facilitates the exchange of gas formed by yeasts during the degradation of dyes (Martorell et al. 2017b; Pajot et al. 2007; Yang et al. 2008; Yu and Wen 2005). As mentioned above, several oxidative enzymes require oxygen (Shahid et al. 2015). Meanwhile, some researchers obtained the best decolorization results under static conditions (Table 1). The negative effect of medium agitation on the decolorization efficiency was attributed to the fact that oxygen acts as an electron acceptor with high redox potential, thereby preventing dye reduction (Li et al. 2004; Kalyani et al. 2008; Al-Tohamy et al. 2020).

Effect of carbon and nitrogen sources Despite the presence of dyes and other organic compounds in textile wastewater, no yeast strain can achieve an effective decolorization via the biodegradation mechanisms with dyes as the only carbon source, unless bioremoval is based on biosorption mechanisms with non-viable yeast biomass (Mahmoud 2016). It was mentioned that the addition of glucose to yeast culture medium stimulates the biodegradation of dyes (Chang et al. 2000; Waghmode et al. 2011). Other studies also showed a strong correlation between glucose depletion and the rate of dye removal (Lucas et al. 2006; Yang et al. 2008). Glucose can play many roles in metabolic pathways, including its role as regenerator of the redox mediators like NADH and FADH, that act as substrates for the production of H_2O_2, through an enzymatic reaction by glucose1oxidase and glucose-2-oxidase (Jafari et al. 2014). In turn, H_2O_2 acts as a co-substrate for extracellular peroxidase activity (Swamy and Ramsay 1999). Meanwhile, decolorization in a medium containing high carbon source concentrations appears to be less effective. In this case, the yeast cells prefer to use readily available carbon sources instead of using dyes as a carbon source (Saratale et al. 2009b). On the other hand, the supplementation of nitrogen sources to the medium (peptone, yeast extract, urea), can also regenerate NADH (Bras et al. 2001). However, similarly to carbon, high nitrogen concentrations may influence the decolorization efficiency. Tatarko and Bumpus (1998) reported that supplementation of high nitrogen concentrations to the medium inhibited Congo red decolorization. Conformingly, a study by Kaushik and Malik (2009), demonstrated that higher nitrogen concentrations (25–60 mM), suppressed ligninolytic enzyme

activity. It is therefore important to determine the appropriate concentration of carbon and nitrogen sources that improve the decolorization process (Pearce et al. 2003; Van der Zee et al. 2001).

Since several factors can influence the process of biodegradation of dyes by yeast cells, optimizing these factors is essential to limit losses, whether related to chemicals, growing conditions, or process time. Applying the design of the experiment can be a promising solution that can reduce treatment costs and time, making, therefore, the use of yeast more competitive than the other treatment processes.

Chemical characterization and toxicity assessment of dye biodegradation by-products

Irrespective of the technique used (physical, chemical, or biological) in the treatment of textile wastewater, the main concern is not only the dye removal, but mainly the guarantee of its effective detoxification after treatment. Hence, the ecotoxicological evaluation of post-treatment is crucial. The oxidation processes of synthetic dye using Fenton reactions, non-metallic oxidation catalysts based on hydroxyl radicals, and other chemical techniques, can ensure a successful decolorization (Javaid and Qazi 2019). However, these techniques can produce various oxidation by-products that may be more toxic than the original dye molecules (dos Santos et al. 2007; Sun et al. 2009). In order to highlight the biodegradation efficiency of dyes from a toxicological point of view, a detailed characterization of the metabolites produced during and after complete decolorization must be assessed. Particularly, the colorless aromatic amines resulting from the reduction of the cleavage of chromophore azo-bonds, because they are classified among the most hazardous compounds (Forss and Welander 2009; Puvaneswari et al. 2006). Based on the available literature, detailed characterization of dye by-product degradation can be carried out with different chromatography techniques such as thin-layer chromatography (TLC), high performance liquid chromatography (HPLC), high performance thin layer chromatography (HPTLC), liquid chromatography–mass spectrometry (LC–MS), gas chromatography-mass spectrometry (GC–MS), and spectroscopy techniques such as ultraviolet–visible spectroscopy (UV–VIS), Fourier transform infrared spectroscopy (FTIR) and nuclear magnetic resonance (NMR) spectroscopy. In addition, some studies (Saratale et al. 2009a, b; Tan et al. 2014b) reported that biodegradation could also be calculated by measuring the level of mineralization using total organic carbon (TOC), chemical oxygen demand (COD) and biochemical oxygen demand (BOD). Table 2 summarizes the analytical technique used for the identification of the by-products of dye biodegradation by yeast species. As showed in Fig. 4 and Table 2, the degradation of the same dye by different yeast strains produces different by-products. This suggests the need for ecotoxicological analyzes to ensure the safety of these metabolites. Indeed, a variety of ecotoxicological approaches can be used. Among the existing ecotoxicological bioassays, phytotoxicity tests are the most commonly used, because of their high sensitivity, low cost and easy use. Saratale et al. (2009a) studied the phytotoxicity of Navy Blue HER dye and its biodegradation by-products on two plant models, *Sorghum vulgare* and *Phaseolus mungo.* The results showed a higher germination percentage and significant growth of the plumule and radical in seedlings treated with degradation by-products compared to those treated with the original dye, confirming thus the detoxification of HER by *T. beigelii*. Similarly, Waghmode et al. (2012a) assessed the phytotoxicity of Remazol Red and its by-products on *S. vulgare* and *P. mungo* seeds, and demonstrated that the by-products produced were less toxic compared to the original dye. Likewise, Tan et al. (2014a) reported that the investigation of metabolites derived from Acid Orange G decolorization on *P. mungo* and *Oryza sativa* seeds, confirmed the biotransformation of this dye into less toxic by-products after complete decolorization using *C. tropicalis* TL-F strain. The other common bioassay used to estimate the acute toxicity of the dye and their biodegradation intermediates may be performed using the Microtox test. Tan et al. (2016) assessed the shift in acute toxicity before and after biodegradation of Acid Scarlet 3R using *Scheffersomyces spartinae* TLHS-SF1 strain, with the Microtox test, at the initial dye concentration of 20 mg $L^{-1}$and 50 mg L^{-1}. Moderate (IRs 60% within 30 min) and high (IRs 75% within 30 min) toxicity were recorded against *Vibrio fischeri*. The dye treatment toxicity sharply decreased to non-toxic levels. Similarly, Song et al. (2018a, b) studied the toxic effects of decolorization intermediates of ARB dye using a yeast strain of *P. occidentalis* G1 through Microtox test. It was shown that the IRs of 20 mg L^{-1} and 50 mg L^{-1} were respectively about 68% and 78%. After dye treatment, the toxicity of both dye solutions decreased to non-toxic levels as indicated by the IRs, which decreased to 8% and 11%, respectively. Likewise, Tan et al. (2019) assessed the toxicity of ARB (50 mg L^{-1}) and its decolorization by-products produced by *C. tropicalis* SYF-1 by using the Microtox test. The IR was about 75.4% after 5 min exposure, suggesting that the initial dye concentration possessed high acute toxicity. After a 6 h treatment, the dye displayed the 5 min IR of about 67.2%, slightly lower than initial IR. However, the 5 min IR of the dye solution sharply decreased to 9.4% after complete decolorization (12 h), suggesting a non-toxic level. Also, the combinations of different bioassays were used to assess the toxicological effects of synthetic dyes or their metabolites. Waghmode et al. (2012b) studied the toxicity of Rubine GFL

Table 2 By-products detected after the biodegradation of some azo dyes by yeast

Yeast strain	Dye name and chemical structure	Analyses	Biotransformation products	References
C. tropicalis SYF-1			4-hydrazinylnaphthalene-1- sulfonic acid 4-hydroxynaphthalene-1- sulfonic acid 4-aminonaphthalene-1-sulfonic acid 3,4-dihydroxynaphthalene-1-sulfonic acid 4-hydroxynaphthalene-1,2-dione	(Tan et al. 2019)
Pichia sp. TCL			4-aminonaphthalene-1-sulfonic acid naphthalene1,2,3,4-tetraol 3-7-dihydroxy-octahydronaphthalene-2,6-dione	(Qu et al. 2012)
M. ingens LH-F1.	Acid Red B 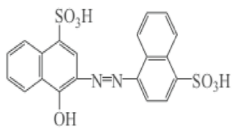		4-aminonaphthalene-1-sulfonic acid 3-amino-4-hydroxynaphthalene-1-sulfonic acid naphthalen-1-ol 3,7-dihydroxy-hexahydronaphthalene-2,6 (1H,7H)-dione	(Tan et al. 2014b)
P. occidentalis G1		UV–vis HPLC-MS	4-amino-naphthalene-1-sulfonic acid 3,4-dihy droxy-naphthalene-1-sulfonic acid naphthalene-1,2,4-triol	(L. Song et al. 2018)
S. cerevisiae ATCC 9763			4-Amino-1-naphthalene sulfonic acid sodium salt 3-amino-4-naphthol-1- sulfonic acid sodium salt Disodium 4-hydroxy-2-[(E)-(4-sulfonato-1-naphthyl) diazenyl]naphthalene-1-sulfonate Disodium 4-hydroxy-2-[(E)-(4-sulfonato-1-phenyl) diazenyl]naphthalene-1-sulfonate Disodium 4-hydroxy-2-[(E)-(4-sulfonato-1-naphthyl) diazenyl]benzene-1-sulfonate	(Kiayi et al. 2019)
S. spartinae TLHS-SF1	Acid Scarlet 3R 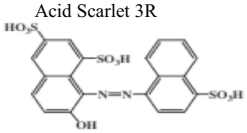		4-aminonaphthalene-1-sulfonic acid 7,8-dihydroxynaphthalene-1,3-disulfonic acid, 3,4-dihydroxynaphthalene-1-sulfonic acid naphthalene-1,2,6,8-tetraol naphthalene-1,2,4-triol	(Tan et al. 2016)
C. tropicalis	Monoazo disperse dye 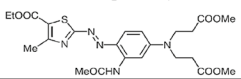	HNMR TLC HPLC LC-MS	2-amino-4-methyl- 5-ethoxycarbomylthiazole	(Arora et al. 2005)
C. rugopelliculosa HXL-2	Reactive blue 13 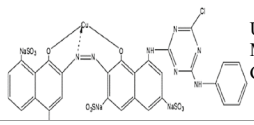	UV-Vis MS/MS GC-MS	1-chloro-3- aniline 2,4,6-triazine 2-chloro-1,3,5-triazine Phenol aniline	(Liu et al. 2011)
S. cerevisiae ATCC 9763	Methyl red 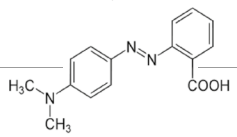	UV-Vis FTIR TLC ESI-MS	N, N-dimethyl-p-phenylene diamine (DMPD) 2-Aminobenzoic acid.	(Vatandoostar ani et al. 2017)
		UV-Vis FTIR HPLC	N, N'-dimethyl- p-phenylenediamine 2-authentic 2-aminobenzoic acid	(Jadhav et al. 2008b)
G. geotrichum MTCC 1360	Remazol Red 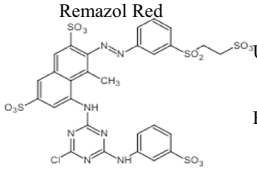	UV-Vis FTIR TLC HPTLC	3-amino [4, 5 (6-chloro-1, 3, 5 triazine-2yl) amino] naphthalene 2, 4, 7 benzene trisulfonic acid. 2[(3-aminophenyl) sulfonyl] ethane sulfonic acid. 2- amino naphthalene N-phenyl-1, 3, 5 triazine 2[(3-aminophenyl) sulfonyl] ethane sulfonic acid ethylsulfonyl-benzene 2-ethylphenyl sulfone	(Waghmode et al. 2012a)
	Rubine GFL 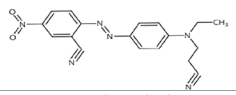	HPTLC HPLC FTIR GC-MS	2-(aminomethyl)-4-nitroaniline 1-(3-nitrophenyl)methana- mine N-(3-aminopropyl)benzene-1,4-diamine	(Waghmode et al. 2012b)
T. akiyoshidainum	Reactive Black 5 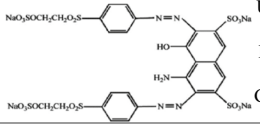	UV–vis FTIR HPLC-GPC GC–MS	4-((chlorodifluoromethyl)sulfonyl) aniline 4- ((diazenilfenil) sulfonyl) methyl hydrogen sulfate 5,7-dimethoxy-1-naphthol 5-amino-4-hydroxy-3,6-dioxo-2,3, 5,6-tetrahydronaphthalene2,7-sodium disulfonate.	(Martorell et al. 2017b)
Candida sp. VITJASS	Reactive green dye 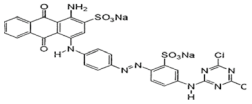	UV–Vis FTIR HPLC GC–MS	sodium 3-[(dichloro-1,3,5-triazin-2-yl) amino] benzene-1-sulfonate sodium 1-amino-4-[(4-aminophenyl) amino]-9,10-dioxo-9,10- dihydroanthracene-2-sulfonate 2-chloro-1,1-diphenyethane Diphenylmethane	(Sinha et al. 2018)

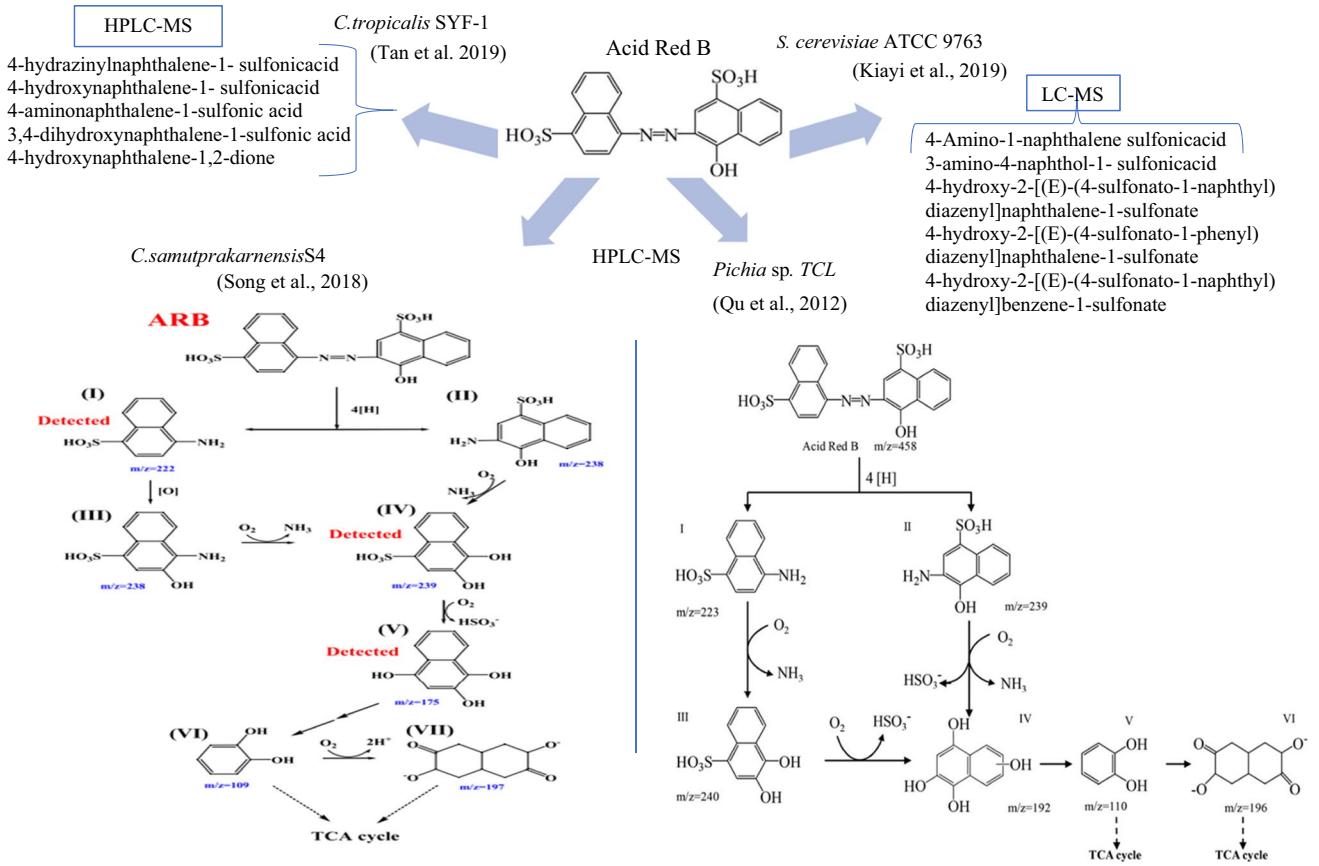

Fig. 4 Proposed partial biodegradation pathways of ARB by various yeasts using HPLC–MS and LC–MS analysis techniques

dye and its by-products produced from the biodegradation by *G. geotrichum* MTCC 1360 yeast strain. Analytical methods in this study included genotoxicity and cytotoxicity tests, oxidative stress, activity of antioxidant enzymes, lipid peroxidation and protein oxidation on root cells of *Allium cepa* as well as the phytotoxicity of the dye and dye by-products using *P. mungo* and *S. vulgare*. The outcomes showed that Rubine GFL dye exerted oxidative stress and subsequent toxic effects on the root cells, whereas its metabolites were less toxic. Likewise, Roșu et al. (2019) suggested that after treatment of BB41 dye by *Pichia kudriavzevii* CR-Y103, the degraded metabolites was found to be less toxic than the parent dye compound, by using phytotoxicity, cytotoxicity, and genotoxicity assays on *Trifolium pratense* and *Triticum aestivum* seedlings. This indicates the detoxification of this azo dye.

The chemical characterization of the by-products of dye biodegradation not only makes it possible to recognize the pathways of their biodegradation, but may also indicate the toxicity of the aromatic compounds formed during biodegradation. This will assess the performance of treatment from a toxicological point of view.

Molecular aspects of dye degradation by yeasts

In all areas of life sciences, the use of omics methods, namely metagenomics, transcriptomics, proteomics, and metabolomics, has recently become widespread. The integration of these approaches allows a holistic view of the biological systems. Understanding the molecular mechanisms of biodegradation of aromatic compounds such as synthetic dyes is essential for the development of successful bioremediation strategies. Numerous studies have been carried out on the molecular aspects of dye degradation by fungi (Mäkinen et al. 2019; Sun et al. 2015) and bacteria (Joshi et al. 2020; Ma et al. 2019). However, very little research has focused on the molecular mechanisms involved in the enzymatic biodegradation of synthetic dyes by yeast cells. María et al. (2018) unraveled the genetic basis of the enzymatic activities of Mnp, Lac, and Phenoloxidase after complete decolorization of Reactive Black 5 by *Trichosporon akiyoshidainum* HP-2023, their genome comprises 30 MB with a G + C content of 60.75% and 9019 gene models. Thus, thirty-three putative carbohydrate-active enzymes with auxiliary activity have been identified in the annotated

genome, nineteen hydrogen peroxide-producing enzymes, four benzoquinone oxidoreductases, four extracellular fungal heme-peroxidases, and two Lacs. For the decolorization of ARB at high osmotic environment, Wang et al. (2020) reported that the halotolerance enhancement through the detection of different genes expressed in *P. occidentalis* used for the decolorization of ARB was related to the upregulated genes encoding the enzymes or functional proteins related to intracellular synthesis of glycerol. Also based on the transcriptome sequencing, Tan et al. (2020) suggested that the halotolerance capacity of *C. tropicalis* SYF-1 yeast, used for the decolorization of ARB was enhanced by the regulation of the cell wall component. Some recent studies have focused on enhancing the biodegradation of dyes by improving enzyme activity through protein engineering. For example, Zhang et al. (2019) have reported that the recombinant enzyme rMnP3-BBP6 that resulted from cloning of new MnP gene (mnp3) of the white-rot fungus *Cerrena unicolor* BBP6 in *Pichia pastoris,* has shown a high decolorization activity of various dyes: Brilliant blue R, Methyl orange, Crystal Violet, Bromophenol Blue, and Remazol Brilliant Blue. Karla et al. (2020) have used saturation mutagenesis to alter two amino acids in the catalytic tryptophan environment positions V160 and A260, of Versatile peroxidase (VP) from *Pleurotus eryngii*. In order to effectively use VP and its variants for the degradation of azo dyes (Evans Blue, Amido Black 10B, and Guinea Green B), VP was immobilized on *S. cerevisiae* EBY100 cell surface and cell wall fragments were used after lysis. Thus, the embedded VP retained ~ 70% of its initial activity after 10 cycles of decolorization.

State-of-the-art technology in the biochemical characterization of dye biodegradation pathways coupled with further studies on genomic, proteomic, and metabolomic aspects, could improve fundamental knowledge in the mycoremediation field. This could offer a wide range of possibilities for improving the performance of yeasts or their enzymes for applications in the bioremoval of toxic dyes or other contaminants from wastewater.

Future perspectives

Despite the scientific and technical advancements that have been developed for the depollution of textile wastewater, there is no universal approach to achieve effective detoxification with low-cost investment. Each technique has its own advantages and limitations. Therefore, the use of hybrid and/or integrated processes may be a promising solution. In fact, mycoremediation can be an efficient approach to be combined with other chemical or physical processes (Akhtar et al. 2020). In order to promote such bioprocesses and make them more attractive, the first crucial concern is related to the choice of tolerant yeast strains. Furthermore, optimizing operating conditions such as agitation, temperature, and the use of low-cost substrates as carbon and nitrogen sources can significantly reduce the processing cost. From the point of view of environmental sustainability, the chemical characterization of the by-products of the enzymatic biodegradation of dyes by yeast cells and the evaluation of their toxicity after complete decolorization will highlight the environmental safety of this bioprocess compared to other chemical dye-degradation processes. Thus, the combination of characterization studies of biodegradation by-products with further studies based on omics approaches, notably transcriptomics, proteomics and metabolomics techniques, will greatly contribute to the understanding of dye biodegradation pathways by yeast cells (Wang et al. 2020; Zheng et al. 2020). Also, the use of yeast oxidoreductive enzymes in the bioremediation of dyes, and the improvement of their performance in terms of stability, selectivity, and catalytic activity, can be carried out with various genetic engineering techniques (Karla et al. 2020). Indeed, over the past decade, research has become increasingly interested in the application of genetic engineering techniques to develop enzyme formulation for bioremediation applications. Meanwhile, the fate of the biomass after the biodegradation of dyes is among the main questions that needs to be solved. The resulting biomass can be valued in several areas, mainly in the energy sector, for the production of biodiesel (Ali et al. 2021). The mycoremediation of synthetic dyes using yeast is simple, reliable, and cost-efficient at laboratory scales, however approval of this approach should be carried out on pilot schemes prior to large-scale industrial operations.

Conclusion

Based on the studies reviewed in this review, it can be concluded that mycoremediation using yeast cells can be an efficient and eco-friendly strategy for the treatment of toxic dyes. The biodegradation ability of yeasts has been related to the activity of oxidases (Lac, Tyr, LiP, and MnP), and reductases (AzoR, NADH-DCIP reductase and MG-reductase). The operating physicochemical parameters that influence the biodegradation process have to be optimized for successful decolorization. For most yeast strains, the highest bioremoval capacity is achieved at neutral or acidic pH ranges, in shaken cultures at 30 °C. The addition of appropriate supply of nitrogen or carbon sources significantly improves the dye-removal efficiency. Meanwhile, textile dyes can affect the biodegradation capacity of yeast, both by their chemical properties and/or concentration. During the process of dye biotransformation, the chemical characterization of the degradation intermediates using chromatography and spectroscopy techniques enables the identification of the dye degradation pathways. Besides, toxicological bioassays

revealed that the resulting intermediate metabolites of dye biodegradation using yeast are typically less toxic than the initial dye. We can therefore deduce that the biodegradation of synthetic dyes by yeasts does not only allow dye decolorization, but ensures the effective detoxification of these contaminants and their by-products. This makes the use of yeast cells or their enzymes in the biodegradation of synthetic dyes a promising future technology to ensure environmental sustainability.

Acknowledgements The authors gratefully acknowledge Moroccan Foundation for Advanced Science, Innovation and Research (MASCIR) for the financial and technical support. Authors wish also to thank Chanda Mutale Joan for reviewing the quality of the English language in this article.

Compliance with ethical standards

Conflict of interest On behalf of all authors, the corresponding author states that there is no conflict of interest.

References

Abiri F, Fallah N, Bonakdarpour B (2017) Sequential anaerobic-aerobic biological treatment of colored wastewaters: case study of a textile dyeing factory wastewater. Water Sci Technol 75(6):1261–1269. https://doi.org/10.2166/wst.2016.531

Akhtar N, Mannan MA (2020) Mycoremediation: Expunging environmental pollutants. Biotechnol Rep 26:e00452. https://doi.org/10.1016/j.btre.2020.e00452

Aksu Z (2003) Reactive dye bioaccumulation by *Saccharomyces cerevisiae*. Process Biochem 38(10):1437–1444. https://doi.org/10.1016/S0032-9592(03)00034-7

Ali H (2010) Biodegradation of synthetic dyes—a review. Water Air Soil Pollut 213(1–4):251–273. https://doi.org/10.1007/s11270-010-0382-4

Ali SS, Al-Tohamy R, Koutra E, El-Naggar AH, Kornaros M, Sun J (2021) Valorizing lignin-like dyes and textile dyeing wastewater by a newly constructed lipid-producing and lignin modifying oleaginous yeast consortium valued for biodiesel and bioremediation. J Hazard Mater 403:123575. https://doi.org/10.1016/j.jhazmat.2020.123575

Al-Tohamy R, Kenawy ER, Sun J, Ali SS (2020) Performance of a newly isolated salt-tolerant yeast strain *Sterigmatomyces halophilus* SSA-1575 for Azo Dye decolorization and detoxification. Front Microbiol 11:1–19. https://doi.org/10.3389/fmicb.2020.01163

Arora S, Saini HS, Singh K (2005) Decolorisation of a monoazo disperse dye with *Candida tropicalis*. Colorat Technol 121:298–303. https://doi.org/10.1111/j.1478-4408.2005.tb00372.x

Arregui L, Ayala M, Gómez-Gil X, Gutiérrez-Soto G, Hernández-Luna CE, De Los H, Santos M, Valdez-Cruz NA (2019) Laccases: structure, function, and potential application in water bioremediation. Microb Cell Fact 18(1):1–33. https://doi.org/10.1186/s12934-019-1248-0

Arslan S, Eyvaz M, Gürbulak E, Yüksel E (2016) A review of state-of-the-art technologies in dye-containing wastewater treatment—the textile industry case. In: Textile wastewater treatment, pp 1–28. https://doi.org/10.5772/64140

Ates S, Cortenlioglu E, Bayraktar E, Mehmetoglu U (2007) Production of l-DOPA using Cu-alginate gel immobilized tyrosinase in a batch and packed bed reactor. Enzyme Microb Technol 40(4):683–687. https://doi.org/10.1016/j.enzmictec.2006.05.031

Balapure K, Bhatt N, Madamwar D (2015) Mineralization of reactive azo dyes present in simulated textile waste water using down flow microaerophilic fixed film bioreactor. Biores Technol 175:1–7. https://doi.org/10.1016/j.biortech.2014.10.040

Bankole PO, Adekunle AA, Obidi OF, Olukanni OD, Govindwar SP (2017) Degradation of indigo dye by a newly isolated yeast, *Diutina rugosa* from dye wastewater polluted soil. J Environ Chem Eng 5(5):4639–4648. https://doi.org/10.1016/j.jece.2017.08.050

Bankole PO, Adekunle AA, Govindwar SP (2018) Enhanced decolorization and biodegradation of acid red 88 dye by newly isolated fungus, *Achaetomium strumarium*. J Environ Chem Eng 6(2):1589–1600. https://doi.org/10.1016/j.jece.2018.01.069

Barakat MA (2011) New trends in removing heavy metals from industrial wastewater. Arab J Chem 4(4):361–377. https://doi.org/10.1016/j.arabjc.2010.07.019

Biradar SP, Rane NR, Patil TS, Khandare RV, Govindwar SP, Pawar PK (2016) Herbal augmentation enhances malachite green biodegradation efficacy of *Saccharomyces cerevisiae*. Biologia (Poland) 71(5):475–483. https://doi.org/10.1515/biolog-2016-0069

Bras R, Ferra MIA, Pinheir HM, Goncalves IC (2001) Batch tests for assessing decolourisation of azo dyes by methanogenic and mixed cultures. J Biotechnol 89:155–162. https://doi.org/10.1016/s0168-1656(01)00312-1

Brijwani K, Rigdon A, Vadlani PV (2010) Fungal laccases: production, function, and applications in food processing. Enzyme Res. https://doi.org/10.4061/2010/149748

Brown MA, De Vito SC (1993) Predicting Azo Dye toxicity. Crit Rev Environ Sci Technol 23(3):249–324. https://doi.org/10.1080/10643389309388453

Carmen Z, Suteu D, Muresan A, Muresan R, Popescu A (2009) Textile wastewater treatment by homogeneous oxidation with hydrogen peroxide. Environ Eng Manag J 8(6):1359–1369. https://doi.org/10.30638/eemj.2009.199

Chang J, Kuo T, Chao Y, Ho J, Lin P (2000) Azo dye decolorization with a mutant *Escherichia coli* strain. Biotech Lett 22:807–812. https://doi.org/10.1023/A:1005624707777

Charumathi D, Das N (2011) Biodegradation of Basic Violet 3 by *Candida krusei* isolated from textile wastewater. Biodegradation 22(6):1169–1180. https://doi.org/10.1007/s10532-011-9472-2

Chen K-C, Wu J-Y, Liou D-J, Hwang S-CJ (2003) Decolorization of the textile Azo Dyes by newly isolated bacterial strains. J Biotechnol 101:57–68. https://doi.org/10.1016/S0168-1656(02)00303-6

Chen CY, Kuo JT, Cheng CY, Huang YT, Ho IH, Chung YC (2009) Biological decolorization of dye solution containing malachite green by *Pandoraea pulmonicola* YC32 using a batch and continuous system. J Hazard Mater 172(2–3):1439–1445. https://doi.org/10.1016/j.jhazmat.2009.08.009

Chia MA, Musa RI (2014) Effect of indigo dye effluent on the growth, biomass production and phenotypic plasticity of *Scenedesmus quadricauda* (Chlorococcales). Anais da Academia Brasileira de Ciencias 86(1):419–428. https://doi.org/10.1590/0001-3765201420130225

Chivukula M, Spadaro JT, Renganathan V (1995) Lignin peroxidase-catalyzed oxidation of sulfonated azo dyes generates novel sulfophenyl hydroperoxides. Biochemistry 34(23):7765–7772. https://doi.org/10.1021/bi00023a024

Choinowski T, Blodig W, Winterhalter KH, Piontek K (1999) The crystal structure of lignin peroxidase at 1.70 Å resolution reveals a hydroxy group on the C(β) of tryptophan 171: a novel radical site

formed during the redox cycle. J Mol Biol 286(3):809–827. https://doi.org/10.1006/jmbi.1998.2507
Chowdhary P, More N, Yadav A, Bharagava RN (2018) Ligninolytic enzymes: an introduction and applications in the food industry. In: Enzymes in food biotechnology: production, applications, and future prospects. Academic Press, pp 181–195. https://doi.org/10.1016/B978-0-12-813280-7.00012-8
Chung KT (2016) Azo dyes and human health: a review. J Environ Sci Health Part C Environ Carcinog Ecotoxicol Rev 34(4):233–261. https://doi.org/10.1080/10590501.2016.1236602
Das D, Charumathi D, Das N (2010) Combined effects of sugarcane bagasse extract and synthetic dyes on the growth and bioaccumulation properties of *Pichia fermentans* MTCC 189. J Hazard Mater 183(1–3):497–505. https://doi.org/10.1016/j.jhazmat.2010.07.051
Dave SR, Patel TL, Tipre DR (2015) Bacterial degradation of Azo Dye containing wastes. In: Microbial degradation of synthetic dyes in wastewaters, environmental science and engineering (Springer, or. 57–83). https://doi.org/10.1007/978-3-319-10942-8_3
Dil EA, Ghaedi M, Ghezelbash GR, Asfaram A (2017) Multi-responses optimization of simultaneous biosorption of cationic dyes by live yeast *Yarrowia lipolytica* 70562 from binary solution: Application of first order derivative spectrophotometry. Ecotoxicol Environ Saf 139:158–164. https://doi.org/10.1016/j.ecoenv.2017.01.030
dos Santos AB, Cervantes FJ, van Lier JB (2007) Review paper on current technologies for decolourisation of textile wastewaters: Perspectives for anaerobic biotechnology. Biores Technol 98(12):2369–2385. https://doi.org/10.1016/j.biortech.2006.11.013
Duckworth HW, Coleman JE (1970) Physicochemical and kinetic properties of mushroom tyrosinase. J Biol Chem 245(7):1613–1625. https://doi.org/10.1016/S0031-9422(00)82247-5
Elfarash A, Mawad AMM, Yousef NMM, Shoreit AAM (2017) Azoreductase kinetics and gene expression in the synthetic dyes-degrading *Pseudomonas*. Egypt J Basic Appl Sci 4(4):315–322. https://doi.org/10.1016/j.ejbas.2017.07.007
El-Sheekh MM, Gharieb MM, Abou-El-Souod GW (2009) Biodegradation of dyes by some green algae and cyanobacteria. Int Biodeterior Biodegrad 63(6):699–704. https://doi.org/10.1016/j.ibiod.2009.04.010
Forss J, Welander U (2009) Decolourization of reactive azo dyes with microorganisms growing on soft wood chips. Int Biodeterior Biodegrad 63(6):752–758. https://doi.org/10.1016/j.ibiod.2009.05.005
Franciscon E, Grossman M, Paschoal JA, Reyes FG, Durrant L (2012) Decolorization and biodegradation of reactive sulfonated azo dyes by a newly isolated *Brevibacterium* sp. strain VN-15. SpringerPlus 1(1):37. https://doi.org/10.1186/2193-1801-1-37
Fu Y, Viraraghavan T (2001) Fungal decolorization of dye wastewaters: a review. Biores Technol 79:251–262. https://doi.org/10.1556/034.58.2016.1-2.6
Fu F, Wang Q (2011) Removal of heavy metal ions from wastewaters: a review. J Environ Manag 92(3):407–418. https://doi.org/10.1016/j.jenvman.2010.11.011
Gita S, Shukla SP, Saharan N, Prakash C, Deshmukhe G (2019) Toxic effects of selected textile dyes on elemental composition, photosynthetic pigments, protein content and growth of a freshwater chlorophycean alga *Chlorella vulgaris*. Bull Environ Contam Toxicol 102(6):795–801. https://doi.org/10.1007/s00128-019-02599-w
Gönen F, Aksu Z (2009) Predictive expressions of growth and Remazol Turquoise Blue-G reactive dye bioaccumulation properties of *Candida utilis*. Enzyme Microb Technol 45(1):15–21. https://doi.org/10.1016/j.enzmictec.2009.03.006
Guo G, Tian F, Zhao Y, Tang M, Liu W, Liu C, Wang S (2019) Aerobic decolorization and detoxification of Acid Scarlet GR by a newly isolated salt-tolerant yeast strain *Galactomyces geotrichum* GG. Int Biodeterior Biodegrad 145(May):104818. https://doi.org/10.1016/j.ibiod.2019.104818
Hernández-Zamora M, Martínez-Jerónimo F, Cristiani-Urbina E, Cañizares-Villanueva RO (2016) Congo red dye affects survival and reproduction in the *cladoceran Ceriodaphnia* dubia. Effects of direct and dietary exposure. Ecotoxicology 25(10):1832–1840. https://doi.org/10.1007/s10646-016-1731-x
Hofrichter M (2002) Review: lignin conversion by manganese peroxidase (MnP). Enzyme Microb Technol 30(4):454–466. https://doi.org/10.1016/S0141-0229(01)00528-2
Hsueh CC, Chen BY, Yen CY (2009) Understanding effects of chemical structure on azo dye decolorization characteristics by *Aeromonas hydrophila*. J Hazard Mater 167(1–3):995–1001. https://doi.org/10.1016/j.jhazmat.2009.01.077
Hu TL (2001) Kinetics of azoreductase and assessment of toxicity of metabolic products from azo dyes by *Pseudomonas luteola*. Water Sci Technol 43(2):261–269. https://doi.org/10.2166/wst.2001.0098
Jadhav JP, Govindwar SP (2006) Biotransformation of malachite green *by Saccharomyces cerevisiae* MTCC 463. Yeast 23(4):315–323. https://doi.org/10.1002/yea.1356
Jadhav JP, Parshetti GK, Kalme SD, Govindwar SP (2007) Decolourization of azo dye methyl red by *Saccharomyces cerevisiae* MTCC 463. Chemosphere 68(2):394–400. https://doi.org/10.1016/j.chemosphere.2006.12.087
Jadhav SU, Jadhav MU, Kagalkar AN, Govindwar SP (2008a) Decolorization of brilliant blue G dye mediated by degradation of the microbial consortium of *Galactomyces geotrichum* and *Bacillus* sp. J Chin Inst Chem Eng 39(6):563–570. https://doi.org/10.1016/j.jcice.2008.06.003
Jadhav SU, Kalme SD, Govindwar SP (2008b) Biodegradation of Methyl red by *Galactomyces geotrichum* MTCC 1360. Int Biodeterior Biodegrad 62(2):135–142. https://doi.org/10.1016/j.ibiod.2007.12.010
Jafari N, Soudi MR, Kasra-Kermanshahi R (2014) Biodegradation perspectives of azo dyes by yeasts. Microbiology 83(5):484–497. https://doi.org/10.1134/s0026261714050130
Javaid R, Qazi UY (2019) Catalytic oxidation process for the degradation of synthetic dyes: an overview. Int J Environ Res Public Health 16(11):1–27. https://doi.org/10.3390/ijerph16112066
Jeon JR, Baldrian P, Murugesan K, Chang YS (2012) Laccase-catalysed oxidations of naturally occurring phenols: from in vivo biosynthetic pathways to green synthetic applications. Microb Biotechnol 5(3):318–332. https://doi.org/10.1111/j.1751-7915.2011.00273.x
Joshi AU, Hinsu AT, Kotadiya RJ, Rank JK, Andharia KN (2020) Decolorization and biodegradation of textile di-azo dye Acid Blue 113 by *Pseudomonas stutzeri* AK6. 3 Biotech. https://doi.org/10.1007/s13205-020-02205-5
Kakuta T, Tateno Y, Koizumi T, Kodama K, Yoshizawa K, Nojiro K (1992) Azo dye wastewater treatment with immobilized yeast. J Soc Ferment Technol 70:387–393. https://doi.org/10.1016/0922-338x(92)80018-e
Kalyani DC, Patil PS, Jadhav JP, Govindwar SP (2008) Biodegradation of reactive textile dye Red BLI by an isolated bacterium Pseudomonas sp. SUK1. Bioresour Technol 99(11):4635–4641. https://doi.org/10.1016/j.biortech.2007.06.058
Kandelbauer A, Guebitz GM (2005) Bioremediation for the decolorization of textile dyes—a review. In: Environmental chemistry: green chemistry and pollutants in ecosystems (or. 269–288). https://doi.org/10.1007/3-540-26531-7_26

Karla I, Ostafe R, ĐurđevićĐelmaš A, Popović N, Stefan S, Fischer R, Prodanović R (2020) Saturation mutagenesis to improve the degradation of azo dyes by versatile peroxidase and application in form of VP-coated yeast cell walls. Enzym Microb Technol J. https://doi.org/10.1016/j.enzmictec.2020.109509

Kaur K, Kaur A (2014) Fish erythrocytes as biomarkers for the toxicity of sublethal doses of an Azo Dye, basic violet-1 (CI: 42535). Microsc Microanal 21(1):264–273. https://doi.org/10.1017/S1431927614013609

Kaushik P, Malik A (2009) Fungal dye decolourization: recent advances and future potential. Environ Int 35(1):127–141. https://doi.org/10.1016/j.envint.2008.05.010

Khan R, Bhawana P, Fulekar MH (2013) Microbial decolorization and degradation of synthetic dyes: a review. Rev Environ Sci Biotechnol 12(1):75–97. https://doi.org/10.1007/s11157-012-9287-6

Kiayi Z, Lotfabad TB, Heidarinasab A, Shahcheraghi F (2019) Microbial degradation of azo dye carmoisine in aqueous medium using *Saccharomyces cerevisiae* ATCC 9763. J Hazard Mater 373(March):608–619. https://doi.org/10.1016/j.jhazmat.2019.03.111

Kim YJ, Uyama H (2005) Tyrosinase inhibitors from natural and synthetic sources: structure, inhibition mechanism and perspective for the future. Cell Mol Life Sci 62(15):1707–1723. https://doi.org/10.1007/s00018-005-5054-y

Kunamneni A, Ghazi I, Camarero S, Ballesteros A, Plou FJ, Alcalde M (2008) Decolorization of synthetic dyes by laccase immobilized on epoxy-activated carriers. Process Biochem 43(2):169–178. https://doi.org/10.1016/j.procbio.2007.11.009

Lellis B, Fávaro-Polonio CZ, Pamphile JA, Polonio JC (2019) Effects of textile dyes on health and the environment and bioremediation potential of living organisms. Biotechnol Res Innov 3(2):275–290. https://doi.org/10.1016/j.biori.2019.09.001

Li JG, Lalman JA, Biswas N (2004) Biodegradation of red B dye by *Bacillus* sp. OY1–2. Environ Technol 25(10):1167–1176. https://doi.org/10.1080/09593332508618384

Libra JA, Borchert M, Vigelahn L, Storm T (2004) Two stage biological treatment of a diazo reactive textile dye and the fate of the dye metabolites. Chemosphere 56(2):167–180. https://doi.org/10.1016/j.chemosphere.2004.02.012

Liu X, Zhang J, Jiang J, Li R, Xie Z, Li S (2011) Biochemical degradation pathway of reactive blue 13 by *Candida rugopelliculosa* HXL-2. Int Biodeterior Biodegrad 65(1):135–141. https://doi.org/10.1016/j.ibiod.2010.10.005

Lucas MS, Amaral C, Sampaio A, Peres JA, Dias AA (2006) Biodegradation of the diazo dye Reactive Black 5 by a wild isolate of *Candida oleophila*. Enzyme Microb Technol 39(1):51–55. https://doi.org/10.1016/j.enzmictec.2005.09.004

Ma Y, Li L, Tian H, Lu M, Megharaj M, He W (2019) Transcriptional analysis of the laccase-like gene from *Burkholderia cepacia* BNS and expression in *Escherichia coli*. Appl Microbiol Biotechnol 103(2):747–760. https://doi.org/10.1007/s00253-018-9468-5

Mahmoud MS (2016) Decolorization of certain reactive dye from aqueous solution using Baker's Yeast (*Saccharomyces cerevisiae*) strain. HBRC J 12(1):88–98. https://doi.org/10.1016/j.hbrcj.2014.07.005

Mäkinen M, Kuuskeri J, Laine P, Smolander OP, Kovalchuk A, Zeng Z, Lundell T (2019) Genome description of *Phlebia radiata* 79 with comparative genomics analysis on lignocellulose decomposition machinery of phlebioid fungi. BMC Genom 20(1):430. https://doi.org/10.1186/s12864-019-5817-8

María N, Gil B, Fernando H, María P, Soro R, Inés L, Figueroa CD, Kurth D (2018) Genome-wide overview of *Trichosporon akiyoshidainum* HP-2023, new insights into its mechanism of dye discoloration. 3 Biotech 8:1–5. https://doi.org/10.1007/s13205-018-1465-y

Martorell MM, Pajot HF, de Figueroa LIC (2012) Dye-decolourizing yeasts isolated from Las Yungas rainforest. Dye assimilation and removal used as selection criteria. Int Biodeterior Biodegrad 66(1):25–32. https://doi.org/10.1016/j.ibiod.2011.10.005

Martorell MM, Pajot HF, Ahmed PM, de Figueroa LIC (2017a) Biodecoloration of Reactive Black 5 by the methylotrophic yeast *Candida boidinii* MM 4035. J Environ Sci (China) 53:78–87. https://doi.org/10.1016/j.jes.2016.01.033

Martorell MM, Pajot HF, Figueroa LIC, d. (2017b) Biological degradation of Reactive Black 5 dye by yeast *Trichosporon akiyoshidainum*. J Environ Chem Eng 5(6):5987–5993. https://doi.org/10.1016/j.jece.2017.11.012

Martorell MM, del Rosales SoroPajot MHF, de Figueroa LIC (2018) Optimization and mechanisms for biodecoloration of a mixture of dyes by *Trichosporon akiyoshidainum* HP 2023. Environ Technol (UK) 39(24):3169–3180. https://doi.org/10.1080/09593330.2017.1375024

Mendes S, Farinha A, Ramos CG, Leitão JH, Viegas CA, Martins LO (2011) Synergistic action of azoreductase and laccase leads to maximal decolourization and detoxification of model dye-containing wastewaters. Biores Technol 102(21):9852–9859. https://doi.org/10.1016/j.biortech.2011.07.108

Miranda RCMD, Gomes EB, Pereira N, Marin-Morales MA, Machado KMG, Gusmão NB (2013) Biotreatment of textile effluent in static bioreactor by *Curvularia lunata* URM 6179 and *Phanerochaete chrysosporium* URM 6181. Bioresour Technol 142:361–367. https://doi.org/10.1016/j.biortech.2013.05.066

Misal SA, Gawai KR (2018) Azoreductase: a key player of xenobiotic metabolism. Bioresourc Bioprocess Libk. 5:2–9. https://doi.org/10.1186/s40643-018-0206-8

Moopantakath J, Kumavath R (2018) Bio-augmentation of actinobacteria and their role in dye decolorization. New Future Dev Microb Biotechnol Bioeng Actinobacteria Divers Biotechnol Appl. https://doi.org/10.1016/B978-0-444-63994-3.00020-5

Nishiya Y, Yamamoto Y (2007) Characterization of a NADH:dichloroindophenol oxidoreductase from *Bacillus subtilis*. Biosci Biotechnol Biochem 71(2):611–614. https://doi.org/10.1271/bbb.60548

Pajot HF, de Figueroa LIC, Fariña JI (2007) Dye-decolorizing activity in isolated yeasts from the ecoregion of Las Yungas (Tucumán, Argentina). Enzyme Microb Technol 40(6):1503–1511. https://doi.org/10.1016/j.enzmictec.2006.10.038

Pajot HF, Martorell MM, de Figueroa LIC (2014) Ecology of dye decolorizing yeasts. Bioremediation in Latin America. Springer, Cham, pp 223–240. https://doi.org/10.1007/978-3-319-05738-5_14

Pandey A, Singh P, Iyengar L (2007) Bacterial decolorization and degradation of azo dyes. Int Biodeterior Biodegrad 59(2):73–84. https://doi.org/10.1016/j.ibiod.2006.08.006

Pearce CI, Lloyd JR, Guthrie JT (2003) The removal of colour from textile wastewater using whole bacterial cells: a review. Dyes Pigm 58(3):179–196. https://doi.org/10.1016/S0143-7208(03)00064-0

Peña A, Sánchez NS, Álvarez H, Calahorra M, Ramírez J (2015) Effects of high medium pH on growth, metabolism and transport in *Saccharomyces cerevisiae*. FEMS Yeast Res 15(2):1–13. https://doi.org/10.1093/femsyr/fou005

Phale PS, Sharma A, Gautam K (2019) Microbial degradation of xenobiotics like aromatic pollutants from the terrestrial environments. In: Pharmaceuticals and personal care products: waste management and treatment technology emerging contaminants and micro pollutants. Butterworth-Heinemann, pp 259–278. https://doi.org/10.1016/B978-0-12-816189-0.00011-1

Puvaneswari N, Muthukrishnan J, Gunasekaran P (2006) Toxicity assessment and microbial degradation of azo dyes. Indian J Exp Biol 44(8):618–626 ((**Berreskuratua -(e)tik**))

Qu Y, Cao X, Ma Q, Shi S, Tan L, Li X, Zhou J (2012) Aerobic decolorization and degradation of Acid Red B by a newly isolated *Pichia* sp. TCL J Hazard Mater 223–224:31–38. https://doi.org/10.1016/j.jhazmat.2012.04.034

Rai HS, Bhattacharyya MS, Singh J, Bansal TK, Vats P, Banerjee UC (2005) Removal of dyes from the effluent of textile and dyestuff manufacturing industry: a review of emerging techniques with reference to biological treatment. Crit Rev Environ Sci Technol 35(3):219–238. https://doi.org/10.1080/10643380590917932

Ramalho PA, CardosoRamalho MHMT (2004) Characterization of Azo reduction activity in a novel ascomycete yeast strain. Appl Environ Microbiol 70(4):2279–2288. https://doi.org/10.1128/AEM.70.4.2279

Rau J, Knackmuss HJ, Stolz A (2002) Effects of different quinoid redox mediators on the anaerobic reduction of azo dyes by bacteria. Environ Sci Technol 36(7):1497–1504. https://doi.org/10.1021/es010227+

Rosu CM, Avadanei M, Gherghel D, Mihasan M, Mihai C, Trifan A, Vochita G (2018) Biodegradation and detoxification efficiency of Azo-Dye reactive orange 16 by *Pichia kudriavzevii* CR-Y103. Water Air Soil Pollut. https://doi.org/10.1007/s11270-017-3668-y

Roșu CM, Vochița G, Mihășan M, Avădanei M, Mihai CT, Gherghel D (2019) Performances of *Pichia kudriavzevii* in decolorization, biodegradation, and detoxification of C.I. Basic Blue 41 under optimized cultural conditions. Environ Sci Pollut Res 26(1):431–445. https://doi.org/10.1007/s11356-018-3651-1

Saratale RG, Saratale GD, Chang JS, Govindwar SP (2009a) Decolorization and biodegradation of textile dye Navy blue HER by *Trichosporon beigelii* NCIM-3326. J Hazard Mater 166(2–3):1421–1428. https://doi.org/10.1016/j.jhazmat.2008.12.068

Saratale RG, Saratale GD, Chang JS, Govindwar SP (2009b) Ecofriendly degradation of sulfonated diazo dye CI Reactive Green 19A using *Micrococcus glutamicus* NCIM-2168. Bioresour Technol 100(17):3897–3905. https://doi.org/10.1016/j.biortech.2009.03.051

Saratale RG, Saratale GD, Chang JS, Govindwar SP (2011) Bacterial decolorization and degradation of azo dyes: a review. J Taiwan Inst Chem Eng 42(1):138–157. https://doi.org/10.1016/j.jtice.2010.06.006

Sen SK, Raut S, Bandyopadhyay P, Raut S (2016) Fungal decolouration and degradation of azo dyes: a review. Fung Biol Rev 30(3):112–133. https://doi.org/10.1016/j.fbr.2016.06.003

Shahid M, Azeem K, Muhammad A, Tariq M, Crowley DE (2015) Detoxification of azo dyes by bacterial oxidoreductase enzymes. Crit Rev Biotechno. https://doi.org/10.3109/07388551.2015.1004518

Singh K, Arora S (2011) Removal of synthetic textile dyes from wastewaters: a critical review on present treatment technologies. Crit Rev Environ Sci Technol 41(9):807–878. https://doi.org/10.1080/10643380903218376

Sinha S, Singh R, Chaurasia AK, Nigam S (2016) Self-sustainable *Chlorella pyrenoidosa* strain NCIM 2738 based photobioreactor for removal of Direct Red-31 dye along with other industrial pollutants to improve the water-quality. J Hazard Mater 306:386–394. https://doi.org/10.1016/j.jhazmat.2015.12.011

Sinha A, Lulu S, Vino S, Banerjee S, Acharjee S, Jabez Osborne W (2018) Degradation of reactive green dye and textile effluent by *Candida* sp. VITJASS isolated from wetland paddy rhizosphere soil. J Environ Chem Eng 6(4):5150–5159. https://doi.org/10.1016/j.jece.2018.08.004

Soares EV, Soares HMVM (2012) Bioremediation of industrial effluents containing heavy metals using brewing cells of *Saccharomyces cerevisiae* as a green technology: a review. Environ Sci Pollut Res 19(4):1066–1083. https://doi.org/10.1007/s11356-011-0671-5

Solís M, Solís A, Pérez HI, Manjarrez N, Flores M (2012) Microbial decolouration of azo dyes: a review. Process Biochem 47(12):1723–1748. https://doi.org/10.1016/j.procbio.2012.08.014

Song L, Shao Y, Ning S, Tan L (2018a) Performance of a newly isolated salt-tolerant yeast strain *Pichia occidentalis* G1 for degrading and detoxifying azo dyes. Biores Technol 233:21–29. https://doi.org/10.1016/j.biortech.2017.02.065

Song Z, Song L, Shao Y, Tan L (2018b) Degradation and detoxification of azo dyes by a salt-tolerant yeast *Cyberlindnera samutprakarnensis* S4 under high-salt conditions. World J Microbiol Biotechnol. https://doi.org/10.1007/s11274-018-2515-7

Srinivasan A, Viraraghavan T (2010) Decolorization of dye wastewaters by biosorbents: a review. J Environ Manag 91(10):1915–1929. https://doi.org/10.1016/j.jenvman.2010.05.003

Srivastava A, Verma N, Mistri A, Ranjan B, Nigam AK, Kumari U, Mittal AK (2017) Alterations in the skin of *Labeo rohita* exposed to an azo dye, *Eriochrome black* T: a histopathological and enzyme biochemical investigation. Environ Sci Pollut Res 24(9):8671–8681. https://doi.org/10.1007/s11356-017-8517-4

Sun J, Hu Y, BiCao ZY (2009) Simultaneous decolorization of azo dye and bioelectricity generation using a microfiltration membrane air-cathode single-chamber microbial fuel cell. Bioresour Technol 100(13):3185–3192. https://doi.org/10.1016/j.biortech.2009.02.002

Sun S, Xie S, Chen H, Cheng Y, Shi Y, Qin X, Dai SY, Zhang X, Yuan JS (2015) Genomic and molecular mechanisms for efficient biodegradation of aromatic dye. Elsevier B.V. https://doi.org/10.1016/j.jhazmat.2015.09.071

Swamy J, Ramsay JA (1999) Effects of glucose and NH 4+ concentrations on sequential dye decoloration by *Trametes versicolor*. Enzyme Microb Technol 25:278–284. https://doi.org/10.1016/S0141-0229(99)00058-7

Tan L, Ning S, Zhang X, Shi S (2013) Aerobic decolorization and degradation of azo dyes by growing cells of a newly isolated yeast *Candida tropicalis* TL-F1. Bioresour Technol 138:307–313. https://doi.org/10.1016/j.biortech.2013.03.183

Tan L, Li H, Ning S, Hao J (2014a) Aerobic Decolorization and degradation of acid orange G (AOG) by suspended growing cells and immobilized cells of a yeast strain *Candida tropicalis* TL-F1. Appl Biochem Biotechnol 174:1651–1667. https://doi.org/10.1007/s12010-014-1086-9

Tan L, Li H, Ning S, Xu B (2014b) Aerobic decolorization and degradation of azo dyes by suspended growing cells and immobilized cells of a newly isolated yeast *Magnusiomyces ingens* LH-F1. Bioresour Technol 158:321–328. https://doi.org/10.1016/j.biortech.2014.02.063

Tan L, He M, Song L, Fu X, Shi S (2016) Bioresource Technology Aerobic decolorization, degradation and detoxification of azo dyes by a newly isolated salt-tolerant yeast *Scheffersomyces spartinae* TLHS-SF1. Bioresour Technol 203:287–294. https://doi.org/10.1016/j.biortech.2015.12.058

Tan L, Xu B, Hao J, Wang J, Shao Y, Mu G (2019) Biodegradation and detoxification of azo dyes by a newly isolated halotolerant yeast *Candida tropicalis* SYF-1. Environ Eng Sci 36:999–1010. https://doi.org/10.1089/ees.2018.0485

Tan L, Shao Y, Mu G, Ning S, Shi S (2020) Enhanced azo dye biodegradation performance and halotolerance of *Candida tropicalis* SYF-1 by static magnetic fi eld (SMF). Bioresour Technol 295:122283. https://doi.org/10.1016/j.biortech.2019.122283

Tatarko M, Bumpus JA (1998) Biodegradation of Congo Red by *Phanerochaete chrysosporium*. Water Res 32(5):1713–1717. https://doi.org/10.1016/S0043-1354(97)00378-3

Tkaczyk A, Mitrowska K, Posyniak A (2020) Synthetic organic dyes as contaminants of the aquatic environment and their implications

for ecosystems: a review. Sci Total Environ 717:137222. https://doi.org/10.1016/j.scitotenv.2020.137222
Upadhyay P, Shrivastava R, Agrawal PK (2016) Bioprospecting and biotechnological applications of fungal laccase. 3 Biotech 6(1):1–12. https://doi.org/10.1007/s13205-015-0316-3
Van der Zee FP, Bouwman RHM, Strik David PBT, Lettinga G, Field JA (2001) Application of redox mediators to accelerate the transformation of reactive azo dyes in anaerobic bioreactors. Biotechnol Bioeng 75(6):691–701. https://doi.org/10.1002/bit.10073
Vatandoostarani S, Bagheri Lotfabad T, Heidarinasab A, Yaghmaei S (2017) Degradation of azo dye methyl red by *Saccharomyces cerevisiae* ATCC 9763. Int Biodeterior Biodegrad 125:62–72. https://doi.org/10.1016/j.ibiod.2017.08.009
Viswanath B, Rajesh B, Janardhan A, Kumar AP, Narasimha G (2014) Fungal laccases and their applications in bioremediation. Enzyme Res. https://doi.org/10.1155/2014/163242
Waghmode TR, Kurade MB, Govindwar SP (2011) Time dependent degradation of mixture of structurally different azo and non azo dyes by using *Galactomyces geotrichum* MTCC 1360. Int Biodeterior Biodegrad 65(3):479–486. https://doi.org/10.1016/j.ibiod.2011.01.010
Waghmode TR, Kurade MB, Kabra AN, Govindwar SP (2012a) Biodegradation of Rubine GFL by *Galactomyces geotrichum* MTCC 1360 and subsequent toxicological analysis by using cytotoxicity, genotoxicity and oxidative stress studies. Microbiology (United Kingdom) 158(9):2344–2352. https://doi.org/10.1099/mic.0.060467-0
Waghmode TR, Kurade MB, Kabra AN, Govindwar SP (2012b) Degradation of remazol red dye by *Galactomyces geotrichum* MTCC 1360 leading to increased iron uptake in *Sorghum vulgare* and *Phaseolus mungo* from soil. Biotechnol Bioprocess Eng 17(1):117–126. https://doi.org/10.1007/s12257-011-0307-0
Walker R, Ryan AJ (1971) Some molecular parameters influencing rate of reduction of azo compounds by intestinal. Xenobiotica 1(4/5):483–486. https://doi.org/10.3109/00498257109041513
Wang X, Wang Y, Ning S, Shi S, Tan L (2020) Improving Azo Dye decolorization performance and halotolerance of *Pichia occidentalis* A2 by static magnetic field and possible mechanisms through comparative transcriptome analysis. Front Microbiol 11:1–10. https://doi.org/10.3389/fmicb.2020.00712
Yang Q, TaoYangZhang LMH (2008) Effects of glucose on the decolorization of Reactive Black 5 by yeast isolates. J Environ Sci 20:105–108. https://doi.org/10.1016/S1001-0742(08)60016-9
Yu Z, Wen X (2005) Screening and identification of yeasts for decolorizing synthetic dyes in industrial wastewater. Int Biodeterior Biodegrad 56(2):109–114. https://doi.org/10.1016/j.ibiod.2005.05.006
Zaidi KU, Ali AS, Ali SA, Naaz I (2014) Microbial tyrosinases: promising enzymes for pharmaceutical, food bioprocessing, and environmental industry. Biochem Res Int. https://doi.org/10.1155/2014/854687
Zhang H, Zhang X, Geng A (2019) Expression of a novel manganese peroxidase from *Cerrena unicolor* BBP6 in *Pichia pastoris* and its application in dye decolorization and PAH degradation. Biochem Eng J. https://doi.org/10.1016/j.bej.2019.107402
Zheng X, Xie X, Liu Y, Cong J, Fan J, Fang Y, Liu J (2020) Deciphering the mechanism of carbon sources inhibiting recolorization in the removal of refractory dye: Based on an untargeted LC–MS metabolomics approach. Biores Technol 307(March):123248. https://doi.org/10.1016/j.biortech.2020.123248
Zhou XW, Cong WR, Su KQ, Zhang YM (2013) Ligninolytic enzymes from *Ganoderma* spp: current status and potential applications. Crit Rev Microbiol 39(4):416–426. https://doi.org/10.3109/1040841X.2012.722606

Publisher's Note Springer Nature remains neutral with regard to jurisdictional claims in published maps and institutional affiliations.

Affiliations

M. Danouche[1,2] · H. EL Arroussi[1] · N. El Ghachtouli[2]

[1] Green Biotechnology Center, Moroccan Foundation for Advanced Science, Innovation and Research (MAScIR), Rue Mohamed Al Jazoulie Madinat Al Irfane, 10 100 Rabat, Morocco

[2] Microbial Biotechnology and Bioactive Molecules Laboratory, Faculty of Sciences and Technologies, Sidi Mohamed Ben Abdellah University, Route Immouzer, P. O. Box 2202, Fez, Morocco

Chapitre IV

An overview of the biosorption mechanism for the bioremediation of synthetic dyes using yeast cells

RÉSUMÉ

L'adsorption est une méthode universelle, rapide et efficace pour le traitement des polluants organiques et métalliques. Cette approche implique le plus souvent l'utilisation de charbon actif comme adsorbant. Cependant, le coût de leur production ainsi que son prétraitement chimique rendent ce type de procédé coûteux. L'utilisation de nouveaux adsorbants économiques, disponibles et efficaces est une exigence incontournable. Le terme “biosorption” désigne l'absorption au moyen de matériaux biologiques tels que des résidus naturels, des déchets agricoles ou des micro-organismes. Au cours des dernières décennies, l'utilisation des levures a fait l'objet d'une attention croissante en raison de leurs avantages en termes de coût, de disponibilité et de capacité à éliminer divers contaminants récalcitrants.

La présente revue se concentre d'abord sur les effets des colorants synthétiques sur les écosystèmes aquatiques et la santé publique. Par la suite, une synthèse bibliographiques détaillée portant sur l'utilisation des levure vivantes, mortes ou des biomasses modifiées comme adsorbants ont été abordé. En effet, une variété de souches telles que *S. cerevisiae, Y. lipolytica, T. lixii, S. pombe* ont montré une efficacité d’élimination par biosorption des colorants synthétiques. La performance d'élimination des colorants dépend non seulement des souches, mais aussi des conditions physico-chimiques dans lesquelles se déroule l'expérience, en particulier le pH, la concentration de colorant, la taille du biosorbant, le niveau d'agitation et la température. Par conséquent, l'optimisation de ces facteurs doit être envisagée afin d'améliorer les performances du processus de biosorption.

Les modèles cinétiques et les isothermes d'équilibre utilisés pour modéliser les systèmes de biosorption (colorant-levure), ainsi que des approches analytiques pour étudier les mécanismes de la biosorption sont discutés dans la troisième section de cette revue. La dernière section se concentre sur les méthodes physico-chimiques et moléculaires de prétraitement qui peuvent augmenter la capacité de biosorption des levures.

Bien que diverses méthodes analytiques de pointe aient été utilisées pour la caractérisation de l'interaction levure-colorant, le mécanisme de biosorption n'a pas encore été entièrement compris. Par conséquent, des études supplémentaires sont nécessaires pour une exploration à grande échelle des bioprocédés de biosorption utilisant la biomasse des levures.

ENVIRONMENTAL TECHNOLOGY REVIEWS
2021, VOL. 10, NO. 1, 58–76
https://doi.org/10.1080/21622515.2020.1869839

Taylor & Francis
Taylor & Francis Group

REVIEW

Check for updates

An overview of the biosorption mechanism for the bioremediation of synthetic dyes using yeast cells

M. Danouche [a,b], H. El Arroussi[a], W. Bahafid[b] and N. El Ghachtouli [b]

[a]Green Biotechnology Center, MAScIR (Moroccan Foundation for Advanced Science, Innovation and Research), Rabat, Morocco; [b]Microbial Biotechnology and Bioactive Molecules Laboratory, Sciences and Techniques Faculty, Sidi Mohamed Ben Abdellah University, Fez, Morocco

ABSTRACT

Dye effluents are among the most polluted wastewaters that require adequate treatment before their discharge into the environment. They have multiple chemical properties that allow them great resistance to environmental conditions, such as the persistence of coloured fabric against washing, exposure to light, chemicals, and biological attacks. However, these same particularities make them hardly degradable, thereby complicating their disposal using traditional methods. The use of biosorption for the removal of dye from wastewater has emerged as a simple, effective, and ecologically technique. Diverse biomaterials are known to bind such pollutants, including natural residues, agricultural wastes and various microorganisms like bacteria, fungi, microalgae, and yeast. In recent decades, the use of yeast cells has received increasing attention, due to their advantages such as low-cost price, availability, and ability to remove various recalcitrant contaminants. On the other hand, their autoaggregation properties can facilitate their recuperation after treatment. The present paper explores the state of the art in the field of biosorption of dye using living, dead, and modified yeast cells. Kinetic, equilibrium models as well as the analytical methods employed in biosorption studies are also discussed. The effects of physicochemical conditions on the biosorption efficiency, including physical, chemical, and biotechnological techniques that can be utilized to increase yeast's biosorption capacities are also highlighted.

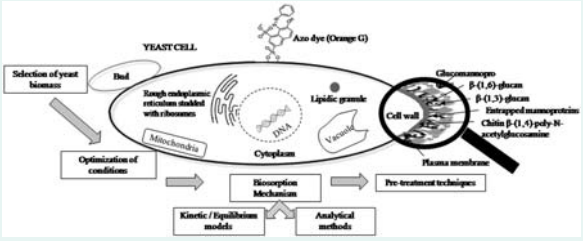

ARTICLE HISTORY
Received 1 April 2020
Accepted 14 December 2020

KEYWORDS
Yeast; dye; toxicity; biosorption; bioremediation

1. Introduction

The textile industry is one of the world's leading and fast-growing industries [1]. It is also one of the main producers of liquid effluents due to its high-water consumption, it requires about 200–500 L of water to produce 1 kg of a finished textile product [2,3]. Compared to other industrial wastewaters, textile effluents have a high concentration of diverse pollutants including suspended solids, surfactants, volatile organic compounds, and different synthetic dyes, in addition to pH fluctuation [4,5]. The total consumption of dyes in the textile sector is estimated at over 10 000 tons per year. However, during the dyeing processes about 10–15% of this amount is discarded as waste due to the low affinity of dyes molecules to the coloured surface [6,7]. The real quantity of dyes discharged into the environment through textile effluents is uncertain, but an estimated concentration of 1000–1300 (hazen unit) has been reported [8]. The release of contaminated effluents into the environment does not only negatively affect the appearance of water, but results into serious toxicity to exposed fauna and flora species [9]. To address this issue, laws have been implemented around the world on the management of textile effluent release into the environment. Also,

CONTACT N. El Ghachtouli naima.elghachtouli@usmba.ac.ma Laboratoire de Biotechnologie Microbienne, Faculté des Sciences et Techniques, Université Sidi Mohamed Ben Abdellah, Route Immouzer, P. O. Box 2202, Fez, Morocco

© 2021 Informa UK Limited, trading as Taylor & Francis Group

various physicochemical methods (membrane processes, photochemical oxidation processes, and electrochemical processes) have been proposed as solutions for the treatment of dye contaminated effluents [10]. Although these methods are effective, they require chemicals and energy-intensive equipment, which makes them expensive, thereby limiting their large-scale applications [11,12]. Thus, increasing attention has recently been focused on new effective, environmentally friendly and low-cost technologies, like Adsorption. In fact, this method is considered a rapid and universal method for wastewater treatment processes. It is used by several industries to reduce the hazardous effects of pollutants present in effluents. In adsorption using solid matter, the adsorbents can be of mineral, organic, or biological origin. Due to their versatility and effectiveness, activated carbon (GAC or PAC), are the most common adsorbent materials used. This is attributed to their pore volume, high surface area and pore size distribution [13,14]. However, the need for thermal or chemical regeneration of the carbon makes the process expensive and unsuitable at large scale. Also, the need for complexing agents to improve the removal performance of the synthetic adsorbent limits their application [15]. New inexpensive, readily available and highly effective adsorbents for the removal of these contaminants are therefore required. The term biosorption refers to the uptake of pollutants from aqueous solutions using biological materials [16,17]. It has been reported that cheap and efficient alternative biosorbents can be identified in nature [18,19] such as natural residues (sawdust, plant residues, tree barks …) [20,21], industrial food wastes (Eggshell waste, orange seeds …) [22,23], agricultural wastes [24], seaweeds (macroalgae) [25] and biomass of microorganisms belonging to different taxonomic classes like microalgae [26,27] cyanobacteria [28], or filamentous fungi [29–31]. However, the use of yeast cells as a biosorbent has not been thoroughly studied, despite the advantages that yeast has over other taxa, such as its fast growth compared to filamentous fungi or microalgae [32], as well as its ability to survive in harsh environments [33]. Furthermore, yeast have a special flocculating characteristic that allows them to aggregate into multicellular masses (flakes), facilitating, therefore, their recovery after treatment of coloured effluents [34]. The mycoremediation of synthetic dyes when using living yeast cells can be accomplished through: (i) the biosorption of the dye to the cell wall, followed by a specific bioaccumulation inside the cells and/or (ii) biodegradation of the dye by the action of different enzymes (oxidases and reductases) [35,36]. Regardless of the mechanism involved, the first interaction always occurs between the cell wall and the pollutants (biosorption), and it can be managed by electrostatic interaction, complexation, ion exchange, physical and chemical adsorption [37]. It is therefore necessary to study and model the process that manages this interaction. Although several reviews have been interested in the use of various biosorbents in the treatment of dyes, there is a lack of information on the effectiveness of biosorption of dyes using yeast cells. The present review will focus on the state-of-the-art of the biosorption mechanisms of synthetic dyes using yeast cells. It will provide (i) a complete, up-to-date and critical information on the environmental impact of synthetic dyes; (ii) the recent laboratory-scale biosorption studies of dyes using live, dead and modified yeast cells; (ii) the analytical methods used in the study of the biosorption mechanism; (iv) the widely used kinetic studies and equilibrium models in the biosorption of dye by yeast cells; (v) the efficiency of the biosorption in various physical-chemical conditions; and (vi) Finally, the physico-chemical and biological pre-treatment methods that can increase the yeast's biosorption capacity.

2. Synthetic dyes: industrial use and environmental impacts

Colour has always played a crucial role in human everyday life, and in many cultural events. Until the end of the nineteenth century, dyes were produced only from natural sources. The synthetic dye area is widely recognized as having begun in 1856, when W. H. Perkins (1838–1907) serendipitously discovered Mauveine. This discovery paved the way for the synthesis of new chemical colouring agents [38]. Since then, challenges have been and remain to be resolved on how to meet the growing demand for synthetic dyes for various industrial applications, in particular food processing, cosmetics, plastics, textile industries and tanning [39]. With the production of new dye molecules, a variety of classification schemes have been suggested. The most commonly used is based on chemical structure or on their method of

application to different substrates (plastics, paper, textile fibres, and leathers). On the basis of the chemical classification, different dye families can be distinguished, the largest class includes Azo dyes such as monoazo (Yellow reactive 4), diazo (Black reactive 5) and triazo dyes (Direct blue 71). They constitute 70% of the world's annual dyes production. Meanwhile, Anthraquinone dyes (Acid blue 62, Reactive blue 19 …) are also a large class of dyes after Azo dyes. Different other classes include Indigo dyes (Blue acid 74, and Indigo blue), Xanthene dyes (Erythrosine B, Fluorescein), Phthalocyanine dyes, Nitrated and Nitrosated dyes, Diphenylmethane, Triphenylmethane and Polymethinic dyes [40]. Synthetic dyes can also be classified in two families according to their application. Several dyes belonging to the class of water-soluble dyes are particularly Acid dyes (anionic dyes), Basic dyes (cationic dyes), Reactive dyes, Direct dyes and Metalliferous dyes [41]. Regarding water insoluble dyes, the main classes are Vat dyes, Sulfur dyes, and Disperse or dispersible dyes [40] (Figure 1).

Regardless of the class of dyes used, the stability and the durability of their colour on coloured surfaces are required criteria in different industrial fields. Consequently, complex chemical dyes that can withstand environmental, photochemical, and biological attacks are the most used. However, the same criteria conferring higher dyes resistance qualities, could complicate their removal using conventional methods [8]. Thus, the release of such dye effluents without prior treatment can cause considerable environmental pollution, and induce several signs of toxicity to living organisms, including humans, throughout the food chain [42]. In aquatic ecosystems, high concentrations of dyes inhibit the reoxygenation capacity of the receiving waters and reduce the penetration of sunlight, thereby inhibiting the photosynthetic activity of aquatic plants or algae [43]. Additionally, high concentrations of dye in water bodies can affect various microalgae parameters, including morphological, biochemical, as well genetic characteristics. A study by [44] provides a better understanding of the effects of synthetic dyes (Drimarene blue, Optilan yellow

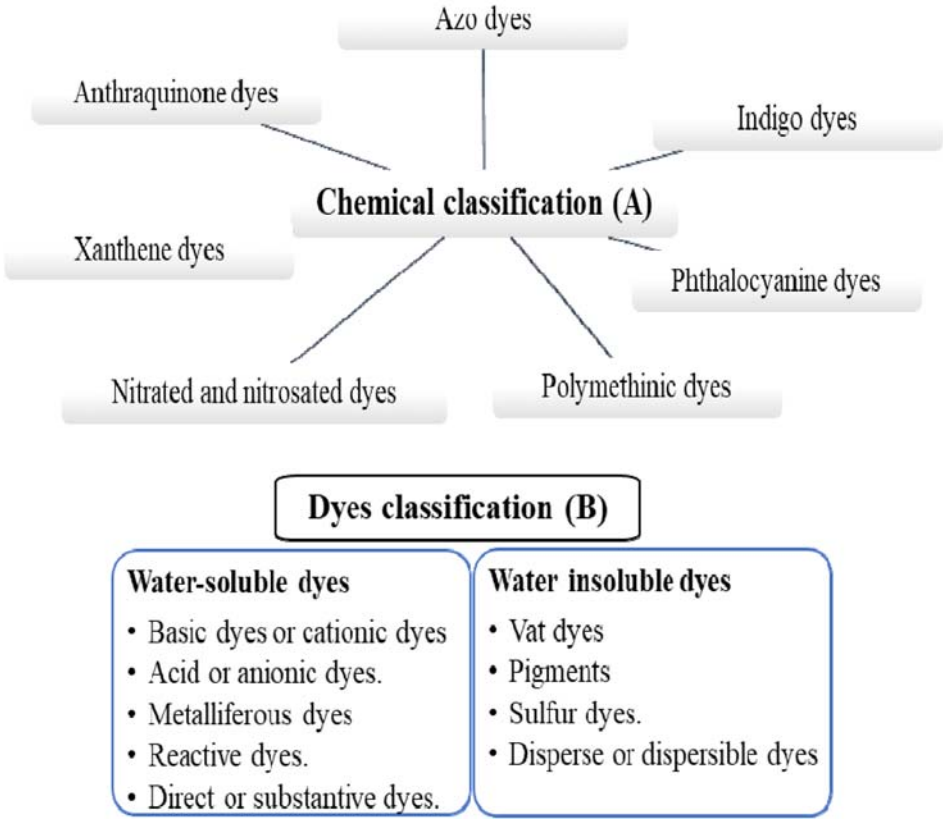

Figure 1. Classification of the textile dyes based on their chemical structure (**A**) or on their method of application to different substrates (**B**), adapted from [40].

and Lanasyn brown) on microalgae strain of *Chlorella vulgaris.* It showed a concentration-dependent decrease in the specific growth rate and pigments after exposure to increasing dye concentrations, and the elemental profile of the treated and untreated cells also showed a significant decrease in the quantity of some elements (C, H, N, S). The Indigo dye was also able to alter the morphological characteristics of the freshwater microalgae *Scenedesmus quadricauda*, and significantly reduced its growth and therefore its biomass production [45]. Similar results were obtained for the effects of synthetic dyes on cyanobacteria. For instance, azo dye RP2B affected the growth of *Anabaena* sp [46], the growth inhibition increased by 31% when the dye concentration was increased from 5 to 50 $mg.L^{-1}$. Synthetic dyes can also affect zooplankton either directly or by feeding on microalgae that have accumulated the dye. A study by [47] demonstrated that sub-lethal concentrations of Congo red in sub-chronic exposures inhibited the survival and fertility of *Ceriodaphnia dubia* fed with intoxicated algae (previously exposed to Congo red dye). Following the food chain, we can note that several physiological and biochemical disturbances caused by changes in water quality or consumption of contaminated organisms have been observed in different fish species [48]. Other studies [49,50] have reported Basic violet-1 dye as highly toxic for *Labeo rohita* (96 h LC_{50} as 0.45 $mg.L^{-1}$), causing poikilocytosis as an early indicator of stress before the appearance of other external symptoms, such as abnormal behaviour or mortality. Similarly, using a 24 h turnover bioassay, [51] noted that histopathological changes and alterations in the activity of specific metabolic and antioxidant enzymes in *Labeo rohita*, occurred after 4 days exposure to azo dye Eriochrome black T. Plants and terrestrial animals can be also impacted by the harmful effects of dyes resulting from the release of untreated effluents into the soil. Several studies have used different plant growth parameters, including percent germination, seedling survival, and plant height, as criteria to assess plant responses to synthetic dyes and their degradation metabolites [48,52]. In their study, [53] tested the toxicity of Methyl red and Red BS dyes on earthworms (*Pheretima phosthuma*), plants (*Phaseolus mungo* and *Triticum aestivum*), and microorganisms. The results indicated a change in the protein content of the head, clitella, and abdomen of earthworms (*P. posthuman)* after exposure to dye solutions. In the same study, microbial toxicity depended on the dye concentration. Whereas, a phytotoxicity test on *P. mungo* and *T. aestivum* indicated that percent germination and shoot and leaf lengths were negatively affected by exposure to dye solutions. On the other hand, different human health complications, such as nausea, hemorrhage, ulceration of the skin, and mucous membranes result from consuming contaminated food or water [54]. Moreover, such compounds can cause serious damage to the kidney, reproductive system, liver, brain, and central nervous system [55]. Many by-products of dye decolorization, particularly aromatic amines, can also be carcinogenic, mutagenic and allergenic [56]. The toxicity of dyes and their by-products of degradation is directly related to the low molecular weight of dyes and their lipophilic character, which facilitates their diffusion across the cell membrane. The genotoxic nature of these dyes is attributed to the binding of free amino groups of the dye that can occur with DNA / RNA molecules [57]. In order to avoid such problems, it is necessary to develop promising methods that allow effective treatment of these pollutants before they are released into natural ecosystems.

3. Biosorption for dye removal using yeast cells

3.1. Biosorption mechanisms

The use of microbial biomass in the biosorption of toxic dyes is a new, low-cost and effective strategy, compared to the use of synthetic adsorbents. This bioremoval mechanism is considered as a physico-chemical process that involves a number of metabolism-independent processes occurring naturally in some living or dead microbial cells. The interactions between the cell surface and dye molecules can be achieved by various mechanisms such as physical and chemical adsorption, electrostatic interaction, ion exchange, complexation, chelation, and microprecipitation [58]. It has been reported that serval biosorbents can be more selective and faster than traditional ion exchange resins and commercial active carbons [13]. The binding mechanism of dye molecules to biosorbents is explained by the strong attractive forces of cell wall components, particularly lipids and heteropolysaccharides, which contains

several functional groups such as carboxyl, hydroxyl, amino, phosphate, and other charged groups [17,59]. The Table 1 summarizes the major binding groups for biosorption.

The research on the biosorption of dyes using yeast cells showed that the cell wall of yeast strains contains numerous functional groups, such as protein and nitrogen-containing groups, mainly peptidomannan, peptidoglycan [61], other active groups like acidic polysaccharides, lipids and amino acids may also be involved (Figure 2) [62,63]. For example, it has been reported by [64] that the biosorption of synthetic dyes by the cell wall of *S. cerevisiae* can be performed in amide and amine groups (R–NH–C–O–CH3–C–NH, –C–NH), in (–C = O) and (–C–O) bonds, the chemical group belonging to a chitin structure and present in the sugars of the cell wall of yeast, as well as the –C–N–C group found in cell wall proteins of yeast.

Depending on the type of interaction between the surface of the adsorbent and the adsorbate, the biosorption process can be classified into two types: (i) chemisorption, which is an irreversible interaction, illustrated by the formation of strong chemical bonding, for example, between the dye molecules and the yeast cell surface; and (ii) physisorption, which is considered as a reversible process characterized in most cases by weak van der Waals forces, hydrogen bonds, polarity, and dipole-dipole interactions [62,66]. The biosorption capacity of yeast cells can be affected depending on the functional groups in the cell wall, like the number and the accessibility of reactive sites, the chemical state of the sites (i.e. availability), and the affinity between the sites and the pollutant of interest (i.e. binding strength). The nature of the dye molecule and the physiochemical conditions of treatment are also important factors affecting the biosorption capacity of yeast cells [67]. This therefore makes the comparison between the performance of yeasts and other microorganisms more difficult. In fact, the most studied yeast strain as biosorbent is *S. cerevisiae* [68–70]. However, studies whether based on the application of live or inactivated cells, are still at the laboratory level. The *S. cerevisiae* strains exhibit many advantages, including their availability: the biomass of yeast cells are readily available because they can be a by-product of large fermentation industries [71], their ability to remove various recalcitrant contaminants such as heavy metals, hydrocarbons and synthetic dyes [72,73]. Besides, they can be handled freely without any public concern: as they are commonly used in food manufacturing. Also, *S. cerevisiae* strains have generally been recognized as safe organisms by the U.S. food and drug administration [34]. Moreover, they are appropriate biological models to carry out fundamental and advanced research focusing on omics aspects, such as the application of cell surface designs by genetic manipulation, in order to improve the biosorption capacity, because they are eukaryotic organisms that can easily be cultured and manipulated, and have a completely sequenced genome [74]. For a large-scale application, other characteristics must be considered, such as the process feasibility and the cost-effectiveness. Regarding the price of the biomass, brass biomass received little attention as a profitable material, whereas Spent brewer's yeast is commonly sold as a low-cost product to the animal feed industry after heat inactivation [75]. The surplus yeast produced from fermentation industries can therefore be obtained at a low price. On the other hand, yeast cells can be easily and quickly separated from the treated effluent due to the autoaggregation properties of brewing yeast strains. This property avoids the requirement to additional solid-liquid separation processes or the use of immobilized cells, which can increase the cost of treatment [34]. Table 2 summarizes the reported information on the biosorption of dyes using yeast cells.

3.2. Analytical methods employed for biosorption studies

A number of analytical techniques can be used to understand the biosorption process. Among the most commonly used are: the image-based instrumental techniques like scanning or transmission electron microscopy coupled with energy dispersive X-ray spectroscopy (SEM/TEM–EDX). Spectroscopic analysis techniques are also very useful in the characterization of absorbents as well as the study of interactions between pollutants and biomass. The most useful tools are Fourier transform infrared spectroscopy (FTIR), X-ray photoelectron spectroscopy (XPS), atomic absorption spectrophotometry (AAS), electron paramagnetic resonance spectroscopy (EPR), spectroscopy and X-ray photoelectron spectroscopy-XPS (EDS). FTIR has proved to be a powerful tool for

Table 1. Major binding groups for biosorption [60].

Binding group Structural	Structural formula	pKa	HSAB classif	Ligand atom	Occurrence in selected biomolecules
Hydroxyl	−OH	9.5–13	Hard	O	PS, UA, SPS, AA
Ketone	>C = O	–	Hard	O	Peptide bond
Carboxyl	-C = O	1.7–4.7	Hard	O	UA, AA
Thiol	−SH	8.3–10.8	Soft	S	AA
Sulfonate		1.3	Hard	O	SPS
Thioether	>S	-	Soft	S	AA
Amine	−NH	8–11	Int	N	Cto, AA
Secondary Amine	>NH	13	Int	N	Cti, PG, peptide bond
Amide		-	Int	N	AA
Imine	=NH	11.6–12.6	Int	N	AA
Imidazole		6.0	Soft	N	AA
Phosphonate		0.9–2.1	Hard	O	PL
Phosphodiester		6.1–6.8 1.5	Hard	O	TA, LPS

(PS) Polysaccharides, (**UA)** Uronic acids, (**SPS)** Sulfated PS, (**Cto**) Chitosan, (**PG)** PeptidoGlycan, (**AA)** Amino Acids, (**TA**) Teichoic Acid, (**PL**) PhosphoLipids, (**LPS)** LipoPS.

studying biological molecules and is used in obtaining structural and bonding information on complex and large molecules [60,88]. The possibility of studying surface chemistry of the biomass in a non-destructive manner can be achieved by using XPS analysis. Moreover, the potentiometric titration can determine the active absorbent sites and their quantity. Other techniques such as thermogravimetric analysis (TGA) and differential scanning calorimetry (DSC) can be used in thermal studies. The monitoring of pollutants removal in aquatic medium can be carried out using different techniques, depending on the nature of these pollutants and their concentration in the solution. Due to the presence of chromophore groups, dyes can easily be quantified by UV-Vis spectrophotometry. Additional quantification methods include proxy measurements such as the percentage of mineralization by biochemical oxygen demand (BOD), chemical oxygen demand (COD) and total organic carbon (TOC). The latter can be a very helpful tool when studying real effluents and for the comparison of treatment efficiency with standards [89]. Metals and other ions that may be present in the dye molecules or in coloured effluents can be quantified by using selective electrodes (SSI), inductively coupled plasma (ICP) or transformer coupled plasma (TCP) and X-ray diffraction (XRD). The nuclear magnetic resonance (NMR) technique is also capable of revealing a great deal about molecular structures of biopolymers and mechanisms involved in selective binding [90]. All these techniques are able to complement each other in giving insights into the mechanisms of biosorption [91]. Figure 3 summarizes the most commonly analytical techniques used in biosorption studies and information provided from each technique.

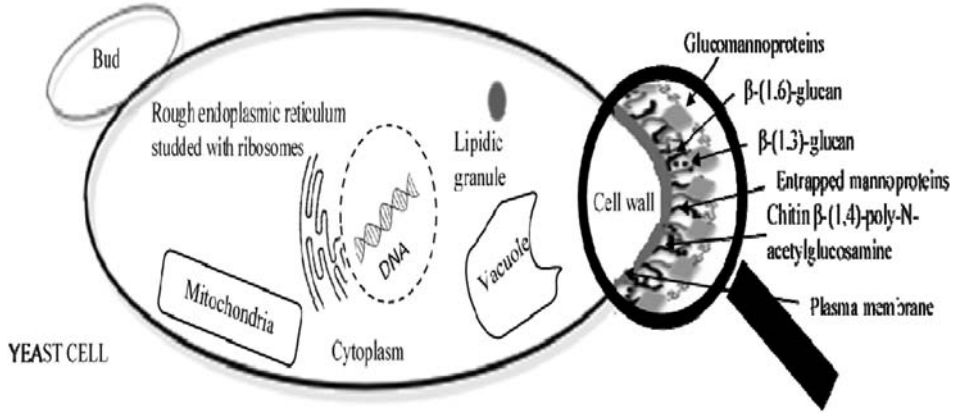

Figure 2. Schematic representation of the yeast cell wall, adapted from [65].

Table 2. Reported information on the biosorption of dyes using yeasts.

Yeast	Dye name	Conditions	Max biosorption	Isotherm model	Ref
S. cerevisiae	Acid Blue 161 (AB 161)	AB161:100 mg.L^{-1} 20°C /40 rpm pH 8.5	1.248 mg.g^{-1} 3 h	Langmuir & Freundlich	[64]
S. cerevisiae	Orange 2GL (O2GL)	O2GL:100 mg.L^{-1} 30°C /40 rpm pH 2.5–8.5	55.4 mg.g^{-1} 5 h	Langmuir & Freundlich	[76]
S. cerevisiae	Reactive Green 19 Reactive Blue (38 & 3) Reactive Black 8 Reactive Brown 9	Dyes: 50 mg.L^{-1} 30°C /120 rpm pH 6.0	112–204 mg.g^{-1} 4 h	Langmuir & Freundlich	[77]
S. cerevisiae	Direct Red 23 (DR23)	(DR23):100 mg.L^{-1} 37°C /40 rpm pH 2.5	6.192 mg.g^{-1} 4 h	Langmuir, Freundlich and Temkin	[78]
S. cerevisiae	Reactive Red 120 (RR 120)	RR120:16.25 mg.L^{-1} pH 4.75 8.25 g L^{-1}	99.97% 52.5 min	Langmuir	[68]
S. cerevisiae	Remazol Orange RR (RORR)	RORR: 200 mg L^{-1} pH 3.0 25°C 2 g.L^{-1}	84.9% 150 min	Langmuir	[69]
S. cerevisiae	Alizarin red-S removal (ARS)	ARS: 50 mg L^{-1} pH 3.0 28°C /120 rpm 0.4% w v^{-1}	68.51% 2 h	Langmuir	[70]
S. cerevisiae	Astrazone Blue (AB)	AB: 1000 mg.L^{-1} 30°C /150 rpm, pH 7.0	70 mg.g^{-1} 4 h	Langmuir	[79]
S. cerevisiae	Alizarin red-S (ARS)	ARS: 50 mg.L^{-1} pH 3.0	29.41 mg.g^{-1} 2 h	Langmuir	[70]
Yarrowia lipolytica 70562	Crystal Violet (CV) Brilliant Green (BG)	CV:8 mg.L^{-1} BG:10 mg.L^{-1} 25°C /180 rpm pH 7.0–8.0	56.497 mg.g^{-1} 65.359 mg.g^{-1}	Langmuir	[80]
Brewery yeast	Reactive Orange 16	RO16: 200 cm^3 35°C /400 rpm pH 3.0	0.56 mol.kg^{-1} 48 h	Langmuir	[81]
S. cerevisiae	Ramazole Blue (RB)	RB: 100 mg.L^{-1} 25°C /180 rpm pH 2.02	54.17 mg.g^{-1} 1 h	Freundlich	[82]
Brewery yeast	Methylene blue (MB) Malachite green (MG) Safranin O (SO)	MB: 30 mg.L^{-1} MG: 30 mg.L^{-1} SO: 60 mg.L^{-1}	212.05 mg.g^{-1} 212.05 mg.g^{-1} 76.77 mg.g^{-1}	Langmuir Freundlich Redlich-Peterson	[83]
Waste beer yeast slurry	Reactive Red 239 (RR239) Reactive Black B (RBB) Direct Blue 85 (DB85)	100 mg.L^{-1} pH 2.0	152.9 mg.g^{-1} 162.7 mg.g^{-1} 139.2 mg.g–^{1}	Langmuir	[84]
Yeast-treated peat	Crystal violet (CV)	CV: 5–100 mg.L^{-1}	17.95 mg.g^{-1}	Langmuir, Freundlich, Temkin, Dubinin–Radushkevich, Sips	[85]
S. cerevisiae *Schizosaccharomyces pombe* *Kluyveromycesmarxianus* *Candida* sp.	Remazol Blue (RB)	RB: 100 mg.L^{-1} 25°C /150 rpm pH: 2.0	Decolorization (%): >90	Langmuir & Freundlich	[16]
Trichoderma lixii F21	Alizarin Red S (AR S) Quinizarine Green SS (QGSS)	ARS: 50 mg.L^{-1} QGSS: 50 mg.L^{-1}	Decolorization (%): 33.7% Decolorization (%): 74.7%	[86]	
Kluyveromyces marxianus	Remazol Black-B (RB-B)	RB-B 100 mg.L^{-1} 37°C /150 rpm pH 4.0	Decolorization (%): >98; 24h	[87]	

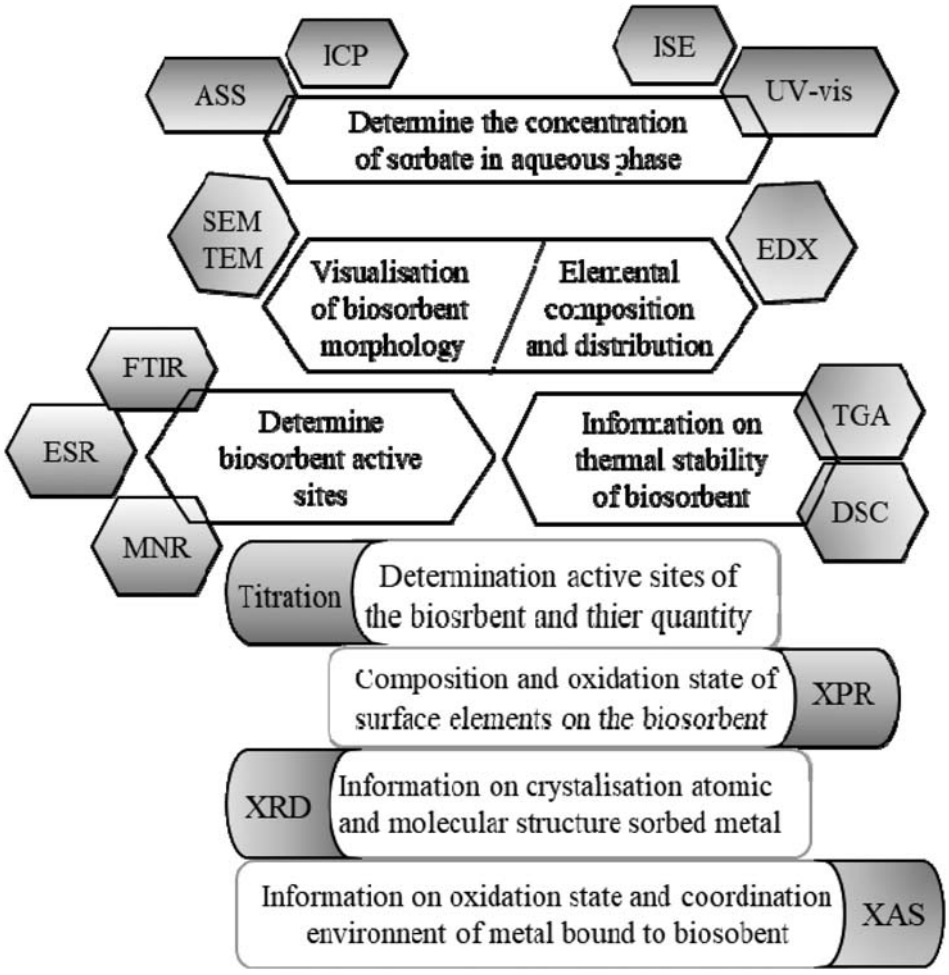

Figure 3. Analytical techniques in biosorption research, adapted from [58].

3.3. Kinetic study and equilibrium biosorption models

Understanding the biosorption mechanism and modelling the reactions involved in the process is not only a matter of academic interest, but can also generate practical benefits for industrial interests [92]. Studies on the biosorption mechanisms are not readily available, as dyes are not simple and clearly defined chemical pollutants. Indeed, they present a wide structural variety and a large difference in their physicochemical properties. In addition, the complexity of the microbial cell wall, which includes a variety of different molecules that may have several binding sites, makes the comparison of pollutant-cell interactions even more complicated [93]. Thus, there is a need for theoretical models to simulate and explain these interactions. Kinetic studies are usually performed using different concentrations of the dye/chemical, while maintaining the adsorbent dose at a constant level [94]. The conventional method used to construct isothermal curves quantifies only the total amount of dye adsorbed without distinguishing the nature of the dye-solid bond. In fact, the concentration of the dye in the solid phase is obtained by a mass balance in the system as the difference between the initial concentration and the final concentration of the dye in the liquid phase [58] (Equation 1). Varying the initial dye concentration allows to obtain the final dye concentrations in the solid phase for different values of the equilibrium concentration in the liquid phase and then what is called the isotherm [84].

$$Qt = ((C_i - C_t)V / W) \quad (1)$$

Where $\mathbf{C_i}$ and $\mathbf{C_t}$ are the initial and the equilibrium dye concentrations ($mg.L^{-1}$); V is the volume of solution (mL); and W is the weight of the biomass (g.L-1).and **b** is the biosorbent concentration in the solution ($g.L^{-1}$). To explain and predict the kinetics of the

liquid-solid biosorption process, several mathematical kinetic and isothermal models have been proposed to study the adsorption mechanism, estimate the rate of adsorption, and test the experimental data [13]. Lagergren developed the pseudo first-order kinetic equation, the pseudo–second order kinetic equation, and the intraparticle diffusion model [95]. The pseudo-first-order and pseudo-second-order define the type of interactions (physisorption or chemisorption), while the intra-particle diffusion model defines the internal diffusion that establishes the rate of adsorption in most liquid systems. Kinetic isotherms are applied to define the adsorption efficiency and to understand the relationship between the adsorbed dye concentrations at its equilibrium concentration in the biosorbent solution [96]. The linear equations of kinetic and isotherm models commonly applied in the study of dye biosorption using yeast cells are presented in Table 3.

Table 3. Linear equations of the kinetic and isothermal models used in yeast dye biosorption studies.

		Linear equation	Representation plot
Kinetic model	Pseudo first order	$\log(q_e\text{-}q_t)=\log(q_e)-(k_1/2.303)t$	$\log(q_e - q_t)$ vs t
	Pseudo second order	$(t/qt)=(k_2/k_2qe^{2})+(t/q_e)$	(t/q_t) vs t
	Intra particle diffusion	$qt = K_{id}t^{0.5}+C$	q_t vs $t^{0.5}$
Isotherm model	Freundlich	$\log qe = \log K_F + 1/n \log C_e$	$\log q_e vs \log C_e$
	Langmuir	$C_e/q_e = C_e/q_m + 1/K_L q_m$	$C_e/q_e vs C_e$
	Temkin	$q_e=(R_T/b_t)\ln k_T+(R_T/b_t)\ln C_e$	$q_e vs \ln C_e$
	Dubinin-Radushkevich (D–R)	$\ln q_e = \ln q_m - \beta\varepsilon^2$ $\varepsilon = R_T \ln(1 + 1/C_e)$ $Ea = 1/\sqrt{2_\beta}$	$\ln q_e vs \ln C_e$
	Sips (Langmuir-Freundlich)	$\ln(q_e/q_m\text{-}q_e)=n\ln C_e + \ln K_s^n$	$\ln(qmq\text{-}eqe)$ *vs* $\ln Ksn$
	Redlich–Peterson	$\ln(K_R C_e/q_e - 1) = n\ln C_e + \ln_b$	$\ln(K_R C_e/qe - 1)$ *vs* $\ln C_e$

Where, $\mathbf{q_e}$ is the sorption capacity at equilibrium (mg.g^{-1}); $\mathbf{C_e}$ (mg.L^{-1}) is the equilibrium concentration of biosorbent; $\mathbf{q_m}$ is the maximum sorption capacity (mg.g^{-1}); $\mathbf{K_L}$ is the Langmuir constant (L.mg^{-1}); $\mathbf{K_F}$ is the Freundlich constants of the adsorption capacity and exponent n is the adsorption intensity which varies with heterogeneity of the material. $\mathbf{K_s}$ is the affinity constant for adsorption in Sips model (L.g^{-1}); $\mathbf{K_R}$ (L.g^{-1}) and b (L.mg^{-1}) are the Redlich–Peterson constants of adsorption. $\mathbf{K_T}$ is the Temkin's equilibrium binding constant corresponding to the maximum binding energy (L.mg^{-1}); $\mathbf{b_t}$ is the Temkin isotherm constant (J.mol^{-1}); **R** is the gas constant (8.314 JK^{-1}mol^{-1}); **T** is the temperature in Kelvin; **ε** is the Polanyi potential for adsorption; $\mathbf{E_a}$ is the change in free energy when 1 mol of ion is transported to the surface of the solid in solution. It is calculated from **β**, which is the D-R constant. If the magnitude of **Ea** is between 8 and 16 kJ.mol^{-1}, then chemisorption process takes place and if the values of **Ea** are less than 8 kJ.mol^{-1}, then physisorption process occurs.

4. Factors affecting the biosorption of dyes

The biosorption is controlled by several operating factors, including physicochemical factors such as pH, temperature, adsorbent-adsorbate ratio, adsorbent surface area, ionic strength, as well as biological factors such as the type of biomass and its mode of application (freely suspended cells or immobilized cells) [17,91].

pH effect: the pH of the solutions is one of the main regulatory factors of the biosorption process. It can affect the chemistry of dye molecules, the physicochemical properties of yeast biomass, and can also control the magnitude of electrostatic charges imparted by the ionized dye molecules [97]. It has been reported that the optimal pH for the biosorption of dyes depends closely on their chemical characteristics. For example, biosorption of reactive dyes requires an acidic medium. However, biosorption of basic dyes requires neutral or alkaline conditions [79,98]. In addition, the net charge of the biosorbent is pH dependent, because of the functional groups (amino, carboxyl, hydroxyl, and phosphate) present in the surface of yeast biomass [99]. At a low pH, the biomass surface becomes protonated and acquires a net positive charge increasing thereby the binding of anionic dyes to the surface. However, at high pH values, the increase of the net negative charge on the biomass surface leads to an electrostatic attraction of cation dyes [100] (Figure 4).

Temperature effect: The change in the temperature of the biosorption system can significantly influence the biosorption efficiency. If the biosorption capacity increases with increasing the temperature of the system, the biosorption process is considered endothermic. As shown in the Table 3, it is the case of yeast cells within the temperature range from 25 to 37°C. In such case, the increase in the biosorption can be associated to the activation of chemical groups on the surface of the biomass (surface activity), or to an increased mobility of the dye molecules (kinetic energy of the solute). In turn, at high temperatures, the reduced viscosity of the dye solution, can increase thereby the diffusion of the dye molecules throughout the external boundary layer and in the inner pores of the biosorbent particles [18,100–102]. On the other hand, the biosorption is considered exothermic when the biosorption capacity decreases with increasing the temperature as a result

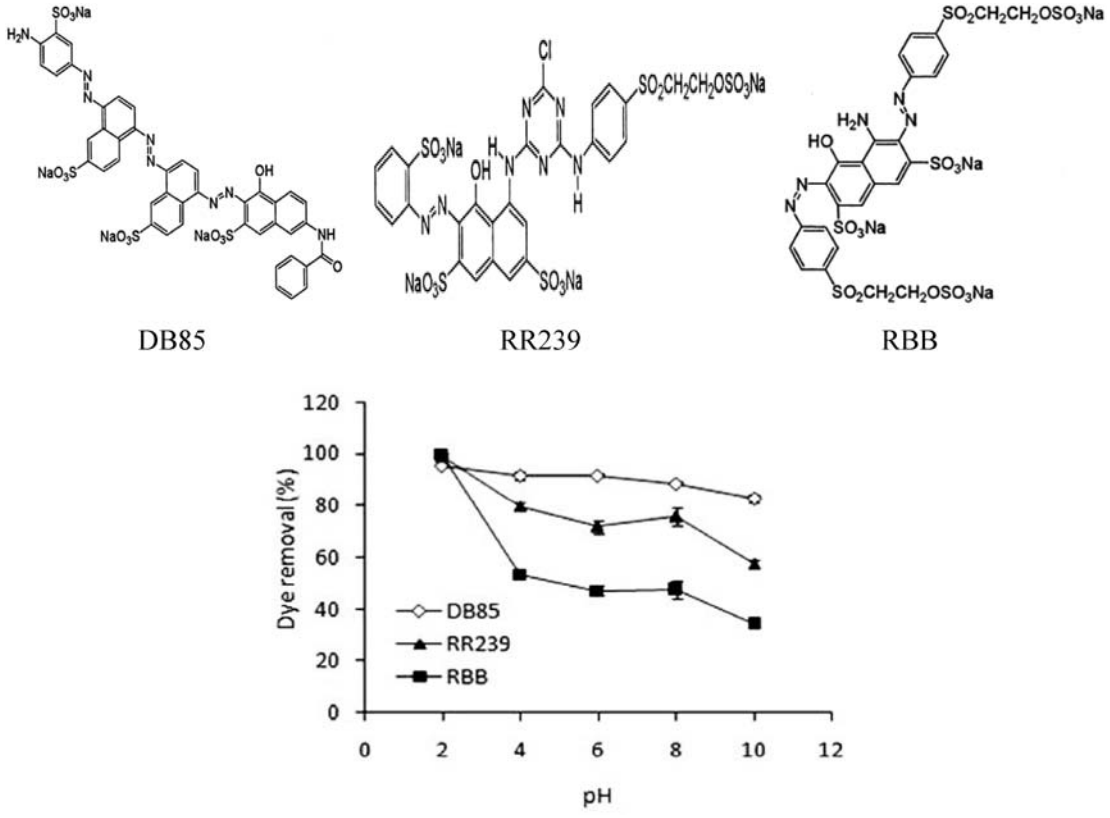

Figure 4. Effect of pH on the removal efficiency of dyes (Direct blue 85 (DB85), Reactive red 239 (RR239), Reactive black B (RBB)) by using waste beer yeast slurry (biosorbent dosage = 3.12 g.L^{-1}, dye concentration = 100 mg.L^{-1}, contact time = 60 min, temperature = 30 °C) [84].

of the decrease in the adsorptive forces between the active sites on the adsorbent surface and the dye molecules [103]. Therefore, it is always desirable to conduct biosorption at room temperature, as this condition is economical and easily reproducible at a large scale [3].

Dye concentration effect: Depending on the binding sites available on the biomass surface, a high initial concentration of dye appears to influence its removal capacity. It could be assessed at varying time intervals by preparing adsorbate/adsorbent solutions with a fixed amount of the biomass but various dye concentrations, then shaken until the equilibrium state is obtained [13]. It has been reported that a higher dye solute uptake can be obtained at a high initial dye concentration, this is linked to the high driving force for mass transfer [104,105]. However, at lower initial dye concentrations, the biosorption becomes independent of the initial dye concentration, because the ratio of the initial moles of the solute to the available area becomes low [3]. It is therefore necessary to determine the maximum saturation potential of a biosorbent, for which experiments may be conducted at the highest initial dye concentration.

Dye chemical structure Effect: As described above, there is a variety of synthetic dyes with very complex chemical structures. The biosorption efficiency of yeast cells vary depending on the chemical structure of the dyes in question. It has been reported that the biosorption of dyes with various chemical structures using the yeast *S. cerevisiae* was of 66% for Reactive brown, 69% for Reactive black, 83% for Reactive green, 83% for Reactive blue 38 and 91% for Reactive blue 3 [77]. Similarly, [84] reported that high biosorption of Bromophenol blue compared to Eriochrome black T. was explained by the difference in their structures. In the case of BPB, there are four Bromo substituent groups on the benzene rings. These electron-withdrawing groups deactivate the benzene rings by decreasing the electron density on the rings through a resonance-withdrawing effect. Consequently, the density of electrons on the bromine atoms increases and becomes more active in

binding with the H atom of the hydroxyl groups on the cell surface by forming H bonds. In addition, the aromatic cycle of the dye molecule could determine its ability to have hydrophobic interactions.

Biosorbent effect: The amount of the biosorbent and its size can strongly influence the biosorption capacity. Commonly, the biosorption capacity increases with the concentration of the biosorbent, because of the increase in the quantity of exchangeable sites of the biomass. It has been reported that with a lower amount of biosorbent, higher uptakes and lower removal efficiencies were noticed [106,107]. Concerning the impact of biosorbent size on dye biosorption, it has been demonstrated that the size of adsorbents is also a fundamental influencing factor. [108] found that biosorption kinetics were directly related to the area of activated sludge particles (Figure 5). In fact, a smaller size biosorbent has a higher surface area, which in turn favours the biosorption process expressed by a shorter equilibration time [109]. Preliminary experiments are therefore required to decide the appropriate size of the biosorbent, in order to recognize its remediation capability from an economic perspective [18]. So far, available studies have not highlighted the effect of the size of yeast particles on the biosorption efficiency. Hence, future research should include this effect in order to optimize the treatment effectiveness.

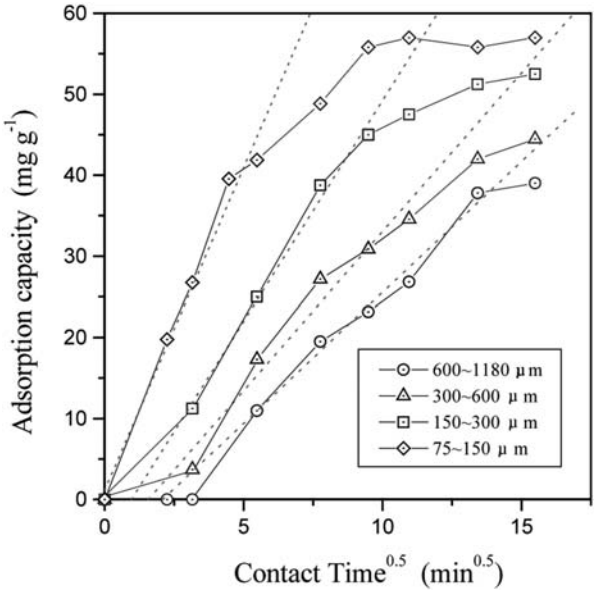

Figure 5. Adsorption capacity against the square root of contact time for various particle sizes of activated sludge biomass [108].

Shaking rate Effect: At a lab-scale biosorption study, the effect of agitation on the biosorption efficiency is usually ignored. However, only a few studies have shown the effect of the rotational speed of shakers on the performance of yeast biosorption. As shown in Table 3, there is no standard agitation level that allows optimum removal efficiency for all studies. The agitation ranges from 40 rpm up to 200 rpm in most reports [70,76,82], except for some studies such as [81] who reported that an optimized biosorption of Reactive orange 16 by using Brewery yeast was achieved at 400 rpm. Agitation enhances the turbulence and therefore decreases the thickness of the liquid boundary layer. Additionally, a strong agitation can lead to the fragmentation of adsorbent particles, thus forming particles of finer size [110]. On the other hand, when using live yeast cells, the agitation allows medium aeration and equal distribution of oxygen and nutrients [111–114].

Ionic strength effect: Unlike controlled laboratory conditions, textile effluents contain various impurities like metal ions, salts, acids or alkalis. The presence of such ions contribute to the high ionic strength, which influences the biosorption of a target pollutant to the biomass [115]. As suggested by [116], adsorption decreases with increasing ionic strength. This effect might be related to the competition between dyes and ions for the binding sites, by changing its activity or by forming complexes with it [3]. Thus, ionic strength can influence the biosorption by affecting the surface charge and the double-layer properties of cells [117]. A few reports have described the affectation of ionic strength on dye removal by yeast biomass. For instance, [118] demonstrated that the biosorption of Rhodamine B on *Phellinus igniarius* was decreased by the presence of 7% of Na^+ ions. This suggests the possibility of competition between Na^+ ions and positively charged dye ions for the same binding sites on the biosorbent.

5. Methods to improve the biosorption capacity of yeast cells

Since dye biosorption occurs mainly on the surface of the yeast cell, surface modification by different physical, chemical and biomolecular techniques can significantly increase the biosorption efficiency. In scientific literature, various modification methods

have been used for this purpose. Table 4 outlines a number of these methods, such as physicochemical pretreatments, immobilization and advanced biomolecular techniques like cell surface engineering [58,119].

Physical pre-treatment like drying, boiling, autoclaving, and mechanical disruption can affect the biosorbent properties [120]. Whereas chemical treatments, such as alkalic treatment can often improve the biosorption capacity, especially in fungal systems, because of the deacetylation of chitin to form Chitosan-glucan complexes with higher affinities to various pollutants [73]. For example, [121] reported that ethylenediaminetetraacetic dianhydride (EDTAD) modified magnetic baker's yeast (EMB) showed higher biosorption of methylene blue (223.66 $mg.g^{-1}$) compared to baker's yeast (62.7 $mg.g^{-1}$). Nevertheless, its capacity was less compared to the polymer-modified baker's yeast (869.6 $mg.g^{-1}$). Moreover, the biosorption of Rhodamine B and Congo red in single and binary systems by using polyallylamine modified yeast showed that the amine groups improved the adsorption capacity. It also increased the affinity of modified yeast to Congo red and Rhodamine B in both systems, revealing, therefore, the implications of the electrostatic adsorption mechanism [122]. Similarly, [123] demonstrated that the application of baker's yeast modified with Nano-polyaniline for the removal of anionic sulfonated dyes, such as acid red was very promising. According to [124], the modification of *S. cerevisiae* subsp with perchloric acid stabilized ferro-fluid, leads to the formation of a magnetic material, which can be used as an efficient biosorbent for the removal of various water-soluble dyes. Likewise, [125] studied the biosorption of Malachite green from an aqueous solution by using modified baker's yeast with $KMnO_4$, produced by a direct oxidation of yeast with $KMnO_4$ under acidic conditions. The results of this study showed that the modification of baker's yeast significantly increased the biosorption capacity of MG compared to unmodified yeast. In addition, the results from the study of the immobilization of *S. cerevisiae* cells on *Luffa cylindrica* to form a novel biosorbent for the removal of Direct Red 23 has shown that the removal efficiency of the immobilized cells was significantly increased [78]. The main drawback of using these methods is the loss of gross mass of the biomass during the pretreatment. Researchers studying the modification of yeast cells evaluated the methods of modification in terms of the biosorptive capacity of gross biomass and modified biosorbent, without taking into account its overall mass yield. Hence, researchers must also measure biomass weights before and after modification methods. In recent years, advanced studies have been oriented towards the use of genetic and biomolecular techniques for the generation of microorganisms with different properties. The cell surface engineering (CSE) is a new strategy that has attracted an interest, particularly in biomedical science [126] and recovery of rare metal elements [127]. Indeed, CSE can be used as an effective approach for building an innovation biosorbent, for example by adaptation of the metallosorption properties of cell surfaces trough the anchoring of various proteins and functional peptides on the cell surface [119]. To date, no studies have focused on the generation of surfaces for the targeted removal of dyes. Studies available in the literature have focused much attention on the design of yeast cell surfaces for targeted absorption of rare earth elements or for improving the biosorption capacity of various heavy metals. For instance, [128] built new yeast cells by using CSE, for selective recovery of Molybdenum as a rare metal. The cell surface display of target proteins is achieved by mingling them with the anchoring motifs. It is a synchronized expression of two or more proteins in a unicellular system [129]. The target protein is fuzed to the anchor protein into

Table 4 Modification methods of biomass to improve biosorptive capacity [58].

Modification Methods	Detailed methods
Immobilization	Immobilization on inert support (Sand, beads fibres, active carbon)
Entrapment	Within polymeric matrix like Alginate, Polyacrylamide, Polyethylene
Cross-linking	Chemical linker with Formaldehyde, Glutaraldehyde, Divinylesulfone.
Physical or mechanical	Modification by autoclaving thermal drying, lyophilization, steam etc.
Magnetic modification	Introducing ferro-, ferri or superparamagnetic materials into biopolymers
Combining with mineral sorbents	Enhancing biosorption by cultivating microorganisms with clay minerals
Chemical modification	Acidic/alkalis washing, pretreatment with organic solvents or other chemicals
Biological modification	Enhancing biosorption by optimizing condition of cell cultivation
Genetical modification	Over-expression of cysteine-rich peptides (glutathione, phytochelatins, metallothioneins); and expression of hybrid proteins on the surface of cells

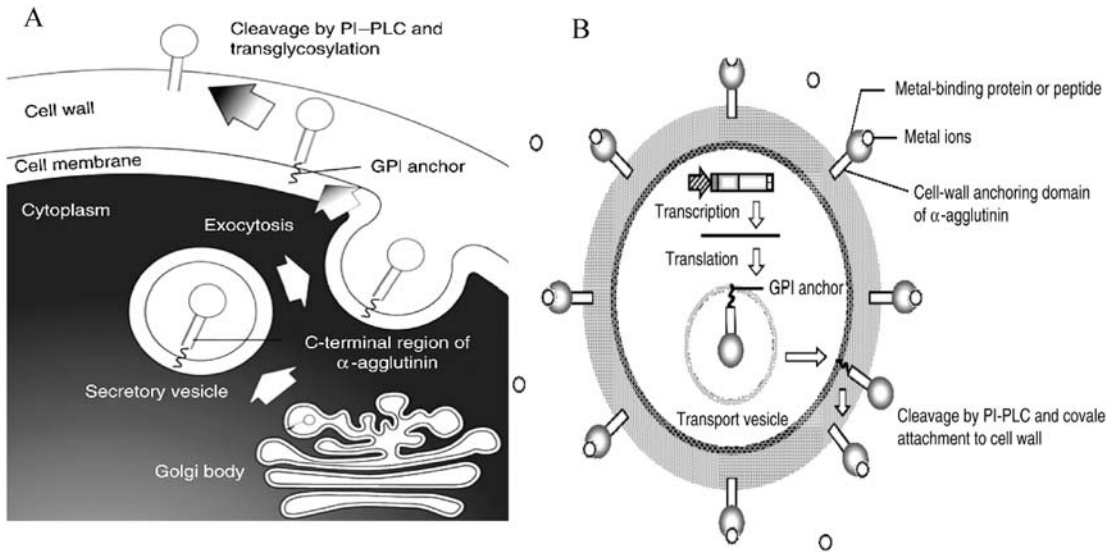

Figure 6. Cell surface display system using the cell wall-anchoring domain of α-agglutinin (**A**), and the yeast biosorbent constructed by cell surface engineering (**B**) [119].

the cell wall, and expressed thereby in a host cell. Thus, the target protein's orientation toward the anchor protein is crucial to its function. For instance, in C-terminal fusion, the C-terminus of an anchor protein is fuzed to the N-terminus of a target protein. Whereas, in the N-terminal fusion, the N-terminus of an anchor protein is fuzed to the C-terminus of a target protein [130]. In the yeast cell system of *S. cerevisiae*, the α-agglutinin is a mannoprotein of the cell surface, generally involved in the sexual adhesion of mating-type A and α cells [131]. Many functional heterologous proteins were successfully displayed using the N-terminal signal sequence targeting the fusion to the endoplasmic reticulum and ultimately at the cell wall and the C-terminal cell wall-anchoring domain of α-agglutinin. This domain contains the glycosylphosphatidylinositol (GPI) anchor attachment signal as illustrated in the Figure 6 [119,132–135]. The α-agglutinin based system allowed the successful display of many functional peptides and proteins of relatively large molecular masses in their functional forms [136,137].

6. Conclusion

The use of yeast cells for the biosorption of textile dyes is a promising solution to complement the physicochemical methods currently used. The literature examined in this review indicates that a variety of yeast strains such as *S. cerevisiae, Y. lipolytica*, *T. lixii*, *S. pombe* have been used in the biosorption of dyes at laboratory scale. Moreover, some research highlights the use of waste beer yeast slurry, brewery yeast, and other fermentation wastes as biosorbents. The performance of dye removal depends not only on the yeast strains, but also on the physicochemical experimental conditions, including the pH of the solution, the initial concentration of the dye, the dosage and the size of the biosorbent as well as the level of agitation and temperature of the system. Therefore, optimization of these factors should be considered in order to improve the performance of the biosorption process. Despite the various isotherms that have been used to simulate and model the biosorption equilibrium and kinetics, as well as the advanced analytical methods employed in the biosorbent characterization, he biosorption mechanism has not been fully understood. Further knowledge is therefore needed for the effective use of yeast cells in wastewater treatment, and for a more practical exploration of this full-scale treatment method. In fact, like many biotechnology approaches, the first challenge is to move the process to an industrial scale. On the other hand, the current challenge facing researchers is how to improve the biosorption performance of yeast cells. Indeed, despite the use of various approaches of chemical and physical pretreatment for improving their uptake capacity, there is a considerable loss of biomass during these pretreatments. The orientation of research towards the

improvement of genes, particularly through the bioengineering of surface cells, can address this matter. Also, the mismatch between scientific progress in research on biosorbent capacity and the stagnation of industrial biotechnology innovation need to be corrected by translational research with an effort to commercialize research.

Acknowledgments

The authors gratefully acknowledge Moroccan Foundation for Advanced Science, Innovation and Research (MAScIR) for the financial support. Authors wish to thank Chanda Mutale Joan for reviewing the quality of the English language in this article.

Disclosure statement

No potential conflict of interest was reported by the author(s).

Notes on contributors

Mr. Mohammed DANOUCHE is a PhD student, at Green Biotechnology Laboratory of Moroccan Foundation for Advanced Science, Innovation & Research, and Microbial Biotechnology and Bioactive Molecules Laboratory, Sciences and Techniques Faculty, Sidi Mohamed Ben Abdellah University. He has a master's degree in biodiversity management and conservation. He is preparing his PhD on microbial diversity applications for the development of a low-cost bioprocess for the treatment of organic and inorganic pollutants in the aquatic environment. Author or co-author of many scientific articles. He also participated in several international congresses on biological management of organic and metallic waste.

Dr. Hicham EL ARROUSSI is Senior Scientist, R&D Manager of Physiology and Biotechnology of microalgae at Moroccan fondation for advanced science, innovation and research (MAScIR), Rabat Morocco. He is a researcher for the last 13 years of microalgae biotechnology and valorization in agriculture, energy and environment fields. His research focuses on based microalgae plant biostimulant for sustainable agriculture and uses of microalgae for wastewater treatment and heavy metals remediation and biosequestration of carbo dioxide by microalgae for biodiesel production. Dr EL ARROUSSI has set up and led several national and international research projects and has important contributions including several international patents and publications in microalgae biotechnology for bioproducts and new process development in different fields. Author or co-author of many JCR scientific articles, book chapters and 9 international patents.

Pr. Wikak BAHAFID is a Teacher-Researcher of Microbiology at the Faculty of Sciences and Techniques, University of Sidi Mohammed Ben Abdellah. She has 10 years experience in environmental microbiology and bioremediation research. Her research focuses on bioremediation of polluted sites, with an emphasis on heavy metals and azo dyes pollution. Relevant recent results include the bacterial and yeast mechanisms involved in the detoxification of Cr (VI), the characterization of bacteria and yeast with high potential in azo dyes removal, phytotoxic effect of Cr(VI) and azo dyes. Author or co-author of many scientific articles and book chapters.

Pr. Naïma EL GHACHTOULI is professor in Microbiology at the Faculty of Sciences and Techniques, University of Sidi Mohammed Ben Abdellah. She has more than 23 years experience in environmental microbiology and bioremediation research. Her research focuses on soil and water microbiology, with an emphasis on polluted ecosystems. Relevant recent results include the characterization of bacteria and yeast with high potential in pollutants removal, cell surface characterization and Biofilm formation, wastewater treatment. She participated in several reserch projects including 5 international projects. Author of publications in peer-reviewed journals, book chapters and communications at scientific meetings.

ORCID

M. Danouche http://orcid.org/0000-0003-1654-8372
N. El Ghachtouli http://orcid.org/0000-0002-5452-5406

References

[1] Singh S, Khajuria R. Penicillium enzymes for the textile industry. In: *New and future developments in microbial biotechnology and bioengineering*; 2018. p. 201–215. doi:10.1016/B978-0-444-63501-3.00011-9.

[2] Waghmode TR, Kurade MB, Kabra AN, et al. Degradation of remazol red dye by *galactomyces geotrichum* MTCC 1360 leading to increased iron uptake in *sorghum vulgare* and *phaseolus mungo* from soil. Biotechnol Bioprocess Eng. 2012;17:117–126. doi:10.1007/s12257-011-0307-0.

[3] Vijayaraghavan K, Yun YS. Bacterial biosorbents and biosorption. Biotechnol Adv. 2008;26:266–291. doi:10.1016/j.biotechadv.2008.02.002.

[4] Balapure K, Bhatt N, Madamwar D. Mineralization of reactive azo dyes present in simulated textile waste water using down flow microaerophilic fixed film bioreactor. Bioresour Technol. 2015;175:1–7. doi:10.1016/j.biortech.2014.10.040.

[5] Chen CY, Kuo JT, Cheng CY, et al. Biological decolorization of dye solution containing malachite green by *pandoraea pulmonicola* YC32 using a batch and continuous system. J Hazard Mater. 2009;172:1439–1445. doi:10.1016/j.jhazmat.2009.08.009.

[6] Kunamneni A, Ghazi I, Camarero S, et al. Decolorization of synthetic dyes by laccase immobilized on epoxy-activated carriers. Process Biochem. 2008;43:169–178. doi:10.1016/j.procbio.2007.11.009.

[7] Saratale RG, Saratale GD, Chang JS, et al. Bacterial decolorization and degradation of azo dyes: a review. J Taiwan Inst Chem Eng. 2011;42:138–157. doi:10.1016/j.jtice.2010.06.006.

[8] Pereira L, Alves M. Dyes-environmental impact and remediation. In: *Environmental protection strategies for sustainable development*; 2012. p. 111–162. doi:10.1007/978-94-007-1591-2_4.

[9] Fu Y, Viraraghavan T. Fungal decolorization of dye wastewaters: a review. Bioresour Technol. 2001;79:251–262. doi:10.1556/034.58.2016.1-2.6.

[10] Arslan S, Eyvaz M, Gürbulak E, et al. A review of state-of-the-Art technologies in Dye- containing wastewater treatment – The textile industry case. In: *Textile wastewater treatment*. InTech; 2016. p. 3–28. doi:10.5772/64140.

[11] Fu F, Wang Q. Removal of heavy metal ions from wastewaters: a review. J Environ Manage. 2011;92:407–418. doi:10.1016/j.jenvman.2010.11.011.

[12] Srinivasan A, Viraraghavan T. Decolorization of dye wastewaters by biosorbents: a review. J Environ Manage. 2010;91:1915–1929. doi:10.1016/j.jenvman.2010.05.003.

[13] Yagub MT, Sen TK, Afroze S, et al. Dye and its removal from aqueous solution by adsorption: a review. Adv Colloid Interface Sci. 2014;209:172–184. doi:10.1016/j.cis.2014.04.002.

[14] Moreno-Castilla C. Adsorption of organic molecules from aqueous solutions on carbon materials. Carbon N Y. 2004;42:83–94. doi:10.1016/j.carbon.2003.09.022.

[15] Crini G, Lichtfouse E, Wilson LD, et al. Conventional and non-conventional adsorbents for wastewater treatment. Environ Chem Lett. 2019;17:195–213. doi:10.1007/s10311-018-0786-8.

[16] Aksu Z, Dönmez G. A comparative study on the biosorption characteristics of some yeasts for remazol blue reactive dye. Chemosphere. 2003;50:1075–1083. doi:10.1016/S0045-6535(02)00623-9.

[17] Gadd GM. Biosorption: critical review of scientific rationale, environmental importance and significance for pollution treatment. J Chem Technol Biotechnol. 2009;84:13–28. doi:10.1002/jctb.1999.

[18] Salleh MAM, Mahmoud DK, Karim WAWA, et al. Cationic and anionic dye adsorption by agricultural solid wastes: a comprehensive review. Desalination. 2011;280:1–13. doi:10.1016/j.desal.2011.07.019.

[19] Dąbrowski A. Adsorption from theory to practice. Adv Colloid Interface Sci. 2001;93:135–224. doi:10.1016/S0001-8686(00)00082-8.

[20] Chaudhari UE, Somwanshi AR. Evaluation of adsorption efficiency of *alangium salvifolium* tree bark for methylene blue retrieval from aqueous solution. Biomed Pharmacol J. 2010;3:439–442.

[21] Garg VK, Gupta R, Yadav AB, et al. Dye removal from aqueous solution by adsorption on treated sawdust. Bioresour Technol. 2003;89:121–124. doi:10.1016/S0960-8524(03)00058-0.

[22] Rápó E, Aradi LE, Szabó Á, et al. Adsorption of remazol brilliant violet-5R textile Dye from aqueous solutions by using eggshell waste biosorbent. Sci Rep. 2020;10:1–12. doi:10.1038/s41598-020-65334-0.

[23] Suteu D, Badeanu M, Malutan T, et al. Valorization of food wastes (orange seeds) as adsorbent for dye retention from aqueous medium. Desalin Water Treat. 2016;57:29070–29081. doi:10.1080/19443994.2016.1196392.

[24] Kahraman S, Yalcin P. Removal of dyes from aqueous solution using various agricultural wastes as biosorbent. Fresenius Environ Bull. 2005;14:1196–1201.

[25] Daneshvar E, Vazirzadeh A, Bhatnagar A. Biosorption of methylene blue Dye onto three different marine macroalgae: effects of different parameters on isotherm, kinetic and thermodynamic. Iran J Sci Technol Trans A Sci. 2019;43:2743–2754. doi:10.1007/s40995-019-00764-8.

[26] Chin JY, Chng LM, Leong SS, et al. Removal of synthetic Dye by *chlorella vulgaris* microalgae as natural adsorbent. Arab J Sci Eng. 2020;45:7385–7395. doi:10.1007/s13369-020-04557-9.

[27] Aksu Z, Tezer S. Biosorption of reactive dyes on the green alga *chlorella vulgaris*. Process Biochem. 2005;40:1347–1361. doi:10.1016/j.procbio.2004.06.007.

[28] Dotto GL, Lima EC, Pinto LAA. Bioresource technology biosorption of food dyes onto *spirulina platensis* nanoparticles : equilibrium isotherm and thermodynamic analysis. Bioresour Technol. 2012;103:123–130. doi:10.1016/j.biortech.2011.10.038.

[29] Abd El-Rahim WM, El-Ardy OAM. Direct-dyes bioremoval using *aspergillus Niger* in pilot scale bioreactor. Desalin Water Treat. 2011;25:39–46. doi:10.5004/dwt.2011.1194.

[30] Abd El-Rahim WM, Mostafa EM, Moawad H. High cell density cultivation of six fungal strains ef fi cient in azo dye bioremediation. Biotechnol Reports. 2016;12:1–5. doi:10.1016/j.btre.2016.08.001.

[31] Abd El-Rahim WM, Moawad H, Abdel Azeiz AZ, et al. Optimization of conditions for decolorization of azo-based textile dyes by multiple fungal species. J Biotechnol. 2017;260:11–17. doi:10.1016/j.jbiotec.2017.08.022.

[32] Singh K, Arora S. Removal of synthetic textile dyes from wastewaters: a critical review on present treatment technologies. Crit Rev Environ Sci Technol. 2011;41:807–878. doi:10.1080/10643380903218376.

[33] Sen SK, Raut S, Bandyopadhyay P, et al. Fungal decolouration and degradation of azo dyes: A review. Fungal Biol Rev. 2016;30:112–133. doi:10.1016/j.fbr.2016.06.003.

[34] Soares EV, Soares HMVM. Bioremediation of industrial effluents containing heavy metals using brewing cells of *saccharomyces cerevisiae* as a green technology: A review. Environ Sci Pollut Res. 2012;19:1066–1083. doi:10.1007/s11356-011-0671-5.

[35] Wu Y, Li T, Yang L. Mechanisms of removing pollutants from aqueous solutions by microorganisms and their

aggregates: A review. Bioresour Technol. 2012;107:10–18. doi:10.1016/j.biortech.2011.12.088.

[36] Jadhav JP, Govindwar SP. Biotransformation of malachite green by *saccharomyces cerevisiae* MTCC 463. Yeast. 2006;23:315–323. doi:10.1002/yea.1356.

[37] Asgher M. Biosorption of reactive dyes: A review. Water Air Soil Pollut. 2012;223:2417–2435. doi:10.1007/s11270-011-1034-z.

[38] Rai HS, Bhattacharyya MS, Singh J, et al. Removal of dyes from the effluent of textile and dyestuff manufacturing industry: a review of emerging techniques with reference to biological treatment. Crit Rev Environ Sci Technol. 2005;35:219–238. doi:10.1080/10643380590917932.

[39] Telke A, Kalyani D, Jadhav J, et al. Kinetics and mechanism of reactive Red 141 degradation by a bacterial isolate *rhizobium radiobacter* MTCC 8161. Acta Chim Slov. 2008;55(2).

[40] Berradi M, Hsissou R, Khudhair M, et al. Textile finishing dyes and their impact on aquatic environs. Heliyon. 2019;5:e02711. doi:10.1016/j.heliyon.2019.e02711.

[41] Yang XQ, Zhao XX, Liu CY, et al. Decolorization of azo, triphenylmethane and anthraquinone dyes by a newly isolated *trametes sp*. SQ01 and its laccase. Process Biochem. 2009;44:1185–1189. doi:10.1016/j.procbio.2009.06.015.

[42] Moopantakath J, Kumavath R. Bio-Augmentation of actinobacteria and their role in Dye decolorization. In: *New and future developments in microbial biotechnology and bioengineering*. Elsevier; 2018. p. 297–304. doi:10.1016/B978-0-444-63994-3.00020-5.

[43] Carmen Z, Suteu D, Muresan A, et al. Textile wastewater treatment by homogeneous oxidation with hydrogen peroxide. Environ Eng Manag J. 2009;8:1359–1369.

[44] Gita S, Shukla SP, Saharan N, et al. Toxic effects of selected textile dyes on elemental composition, photosynthetic pigments, protein content and growth of a freshwater chlorophycean alga *chlorella vulgaris*. Bull Environ Contam Toxicol. 2019;102:795–801. doi:10.1007/s00128-019-02599-w.

[45] Chia MA, Musa RI. Effect of indigo dye effluent on the growth, biomass production and phenotypic plasticity of *scenedesmus quadricauda* (chlorococcales). Anais da Academia Brasileira de Ciências. 2014;86:419–428. doi:10.1590/0001-3765201420130225.

[46] Hu TL, Wu SC. Assessment of the effect of azo dye RP2B on the growth of a nitrogen fixing cyanobacterium - *anabaena* sp. Bioresour Technol. 2001;77:93–95. doi:10.1016/S0960-8524(00)00124-3.

[47] Hernández-Zamora M, Martínez-Jerónimo F, Cristiani-Urbina E, et al. Congo red dye affects survival and reproduction in the cladoceran *ceriodaphnia dubia*. effects of direct and dietary exposure. Ecotoxicology. 2016;25:1832–1840. doi:10.1007/s10646-016-1731-x.

[48] Puvaneswari N, Muthukrishnan J, Gunasekaran P. Toxicity assessment and microbial degradation of azo dyes. Indian J Exp Biol. 2006;44:618–626. doi:16924831.

[49] Kaur K, Kaur A. Fish erythrocytes as biomarkers for the toxicity of sublethal doses of an Azo Dye, basic violet-1 (CI: 42535). Microsc Microanal. 2015;21:264–273. doi:10.1017/S1431927614013609.

[50] Kaur K, Kaur S, Kaur A. Scanning electron microscopic observations of basic violet-1 induced changes in the gill morphology of *labeo rohita*. Environ Sci Pollut Res. 2016;23:16579–16588. doi:10.1007/s11356-016-6764-4.

[51] Srivastava A, Verma N, Mistri A, et al. Alterations in the skin of *labeo rohita* exposed to an azo dye, eriochrome black T: a histopathological and enzyme biochemical investigation. Environ Sci Pollut Res. 2017;24:8671–8681. doi:10.1007/s11356-017-8517-4.

[52] Anbuselvam J, Sridhar A, Anbuselvam M, et al. Effect of textile waste water irrigation on seed germination, plant growth, biomass, and crop yield in green gram seeds (*vigna radiate* (L)wilczez) under plating technique and Pot experiment. J Environ Sci Toxicol Food Technol. 2016;10:86–89. doi:10.9790/2402-1005018689.

[53] Gupte S, Keharia H, Gupte A. Toxicity analysis of azo Red BS and methyl Red dye solutions on earthworm (*pheretima phosthuma*), micro-organisms, and plants. Desalin Water Treat. 2013;51:4556–4565. doi:10.1080/19443994.2012.748637.

[54] Mendes S, Farinha A, Ramos CG, et al. Synergistic action of azoreductase and laccase leads to maximal decolourization and detoxification of model dye-containing wastewaters. Bioresour Technol. 2011;102:9852–9859. doi:10.1016/j.biortech.2011.07.108.

[55] Zhang W, Liu W, Zhang J, et al. Characterisation of acute toxicity, genotoxicity and oxidative stress posed by textile effluent on zebrafish. J Environ Sci. 2012;24:2019–2027. doi:10.1016/S1001-0742(11)61030-9.

[56] Chung KT. Azo dyes and human health: a review. J Environ Sci Health, Part C. 2016;34:233–261. doi:10.1080/10590501.2016.1236602.

[57] Rawat D, Mishra V, Sharma RS. Detoxification of azo dyes in the context of environmental processes. Chemosphere. 2016;155:591–605. doi:10.1016/j.chemosphere.2016.04.068.

[58] Fomina M, Gadd GM. Biosorption: current perspectives on concept, definition and application. Bioresour Technol. 2014;160:3–14. doi:10.1016/j.biortech.2013.12.102.

[59] Vitor V, Corso CR. Decolorization of textile dye by *candida albicans* isolated from industrial effluents. J Ind Microbiol Biotechnol. 2008;35:1353–1357. doi:10.1007/s10295-008-0435-5.

[60] Naja G, Volesky B. The mechanism of metal cation and anion biosorption. In: Microbial biosorption of metals. Dordrecht: Springer; 2011. p. 19–58. doi:10.1007/978-94-007-0443-5.

[61] Ashkenazy R, Gottlieb L, Yannai S. Characterization of acetone-washed yeast biomass functional groups involved in lead biosorption. Biotechnol Bioeng. 1997;55:1–10.

[62] Brady D, Stoll A, Duncan JR. Biosorptton of heavy metal cations by non-viable yeast biomass. Environ Technol (United Kingdom). 1994;15:429–438. doi:10.1080/09593339409385447.

[63] Aksu Z. Application of biosorption for the removal of organic pollutants: a review. Process Biochem. 2005;40:997–1026. doi:10.1016/j.procbio.2004.04.008.

[64] Dilarri G, de Almeida ÉJR, Pecora HB, et al. Removal of Dye toxicity from an aqueous solution using an industrial strain of *saccharomyces cerevisiae* (meyen). Water Air Soil Pollut. 2016;227; doi:10.1007/s11270-016-2973-1.

[65] Feldmann H. Yeast molecular and cell biology. Germany: John Wiley & Sons; 2011. p. 5–24.

[66] Ali H. Biodegradation of synthetic dyes - A review. Water Air Soil Pollut. 2010;213:251–273. doi:10.1007/s11270-010-0382-4.

[67] Vieira RHSF, Volesky B. Biosorption: a solution to pollution? Int Microbiol. 2000;3:17–24.

[68] Navaei A, Yazdani M, Alidadi H, et al. Biosorption of reactive red 120 dye from aqueous solution using *saccharomyces cerevisiae*: Rsm analysis, isotherms and kinetic studies. Desalin Water Treat. 2019;171:418–427. doi:10.5004/dwt.2019.24780.

[69] Ulas B, Ergun M. Biosorption of remazol orange RR from aqueous solution: kinetic, equilibrium and thermodynamic studies. Desalin Water Treat. 2019;163:366–375. doi:10.5004/dwt.2019.24420.

[70] Ramavandi B, Najafpoor AA, Alidadi H, et al. Alizarin Red S removal from aqueous solutions using *saccharomyces cerevisiae:* kinetic and equilibrium study. Desalin Water Treat. 2019;144:286–291. doi:10.5004/dwt.2019.23556.

[71] Parapouli M, Vasileiadis A, Afendra AS, et al. *Saccharomyces cerevisiae* and its industrial applications. AIMS Microbiol. 2020;6:1–32. doi:10.3934/microbiol.2020001.

[72] Bahafid W, Joutey NT, Asri M, et al. Yeast biomass: an alternative for bioremediation of heavy metals. In: *Yeast-Industrial applications*; 2017. doi:10.5772/intechopen.70559.

[73] Wang J, Chen C. Biosorption of heavy metals by *saccharomyces cerevisiae*: a review. Biotechnol Adv. 2006;24:427–451. doi:10.1016/j.biotechadv.2006.03.001.

[74] Goffeau A, Barrell BG, Bussey H, et al. Life with 6000 genes. Science. 1996;274:546–567.

[75] Ferreira IMPLVO, Pinho O, Vieira E, et al. Brewer's *saccharomyces* yeast biomass: characteristics and potential applications. Trends Food Sci Technol. 2010;21:77–84. doi:10.1016/j.tifs.2009.10.008.

[76] Dilarri G, Corso CR. *Saccharomyces cerevisiae* immobilized onto cross-linked chitosan beads: application of a novel material for the removal of dye toxicity. Environ Technol (United Kingdom). 2018;39:1851–1867. doi:10.1080/09593330.2017.1340351.

[77] Kumari K, Abraham TE. Biosorption of anionic textile dyes by nonviable biomass of fungi and yeast. Bioresour Technol. 2007;98:1704–1710. doi:10.1016/j.biortech.2006.07.030.

[78] Morão LG, Dilarri G, Corso CR. Immobilization of *saccharomyces cerevisiae* cells on luffa cylindrica: a study of a novel material for the adsorption of textile Dye. Water Air Soil Pollut. 2017;228:228–248. doi:10.1007/s11270-017-3433-2.

[79] Farah JY, El-Gendy NS, Farahat LA. Biosorption of astrazone blue basic dye from an aqueous solution using dried biomass of baker's yeast. J Hazard Mater. 2007;148:402–408. doi:10.1016/j.jhazmat.2007.02.053.

[80] Dil EA, Ghaedi M, Ghezelbash GR, et al. Multi-responses optimization of simultaneous biosorption of cationic dyes by live yeast *yarrowia lipolytica* 70562 from binary solution: application of first order derivative spectrophotometry. Ecotoxicol Environ Saf. 2017;139:158–164. doi:10.1016/j.ecoenv.2017.01.030.

[81] Kim TY, Lee JW, Cho SY. Application of residual brewery yeast for adsorption removal of reactive orange 16 from aqueous solution. Adv Powder Technol. 2015;26:267–274. doi:10.1016/j.apt.2014.10.006.

[82] Mahmoud MS. Decolorization of certain reactive dye from aqueous solution using baker's yeast (*saccharomyces cerevisiae*) strain. HBRC J. 2016;12:88–98. doi:10.1016/j.hbrcj.2014.07.005.

[83] Lin HH, Stephen Inbaraj B, Kao TH. Removal potential of basic dyes and lead from water by brewer's yeast biomass. J Am Soc Brew Chem. 2019;77:30–39. doi:10.1080/03610470.2018.1561794.

[84] de Castro KC, Cossolin AS, Oliveira dos Reis HC, et al. Biosorption of anionic textile dyes from aqueous solution by yeast slurry from brewery. Brazilian Arch Biol Technol. 2017;60:1–13. doi:10.1590/1678-4324-2017160101.

[85] Zehra T, Priyantha N, Lim LBL. Removal of crystal violet dye from aqueous solution using yeast-treated peat as adsorbent: thermodynamics, kinetics, and equilibrium studies. Environ Earth Sci. 2016;75:1–15. doi:10.1007/s12665-016-5255-8.

[86] Adnan LA, Sathishkumar P, Yusoff ARM, et al. Rapid bioremediation of alizarin Red S and quinizarine green SS dyes using *trichoderma lixii* F21 mediated by biosorption and enzymatic processes. Bioprocess Biosyst Eng. 2017;40:85–97. doi:10.1007/s00449-016-1677-7.

[87] Meehan C, Banat I, McMullan G, et al. Decolorization of remazol black-B using a thermotolerant yeast, *kluyveromyces marxianus* IMB3. Environ Int. 2000;26:75–79. doi:10.1016/S0160-4120(00)00084-2.

[88] Nakamoto K. Infrared and Raman spectra of inorganic and coordination compounds. handbook of vibrational spectroscopy. In: *Handbook of vibrational spectroscopy*; 2006. p. 1872–1892. doi:10.1002/9780470027325.s4104.

[89] Waghmode TR, Kurade MB, Govindwar SP. Time dependent degradation of mixture of structurally different azo and non azo dyes by using *galactomyces geotrichum* MTCC 1360. Int Biodeterior Biodegrad. 2011;65:479–486. doi:10.1016/j.ibiod.2011.01.010.

[90] Davis TA, Llanes F, Volesky B, et al. 1H-NMR study of Na alginates extracted from *sargassum* spp. in relation to

metal biosorption. Appl Biochem Biotechnol. 2003;110:75–90. doi:10.1385/ABAB:110:2:75.

[91] Park D, Yun YS, Park JM. The past, present, and future trends of biosorption. Biotechnol Bioprocess Eng. 2010;15:86–102. doi:10.1007/s12257-009-0199-4.

[92] Michalak I, Chojnacka K, Witek-Krowiak A. State of the art for the biosorption process - A review. Appl Biochem Biotechnol. 2013;170:1389–1416. doi:10.1007/s12010-013-0269-0.

[93] Adewuyi A. Chemically modified biosorbents and their role in the removal of emerging pharmaceutical waste in the water system. Water (Switzerland). 2020;12:1–31. doi:10.3390/W12061551.

[94] Das N, Vimala R, Karthika P. Biosorption of heavy metals - An overview. Indian J Biotechnol. 2008;7:159–169.

[95] Ho YS, Ng JCY, McKay G. Kinetics of pollutant sorption by biosorbents: review. Sep Purif Rev. 2000;29:89–232. doi:10.1081/SPM-100100009.

[96] Morosanu I, Teodosiu C, Paduraru C, et al. Biosorption of lead ions from aqueous ef fl uents by rapeseed biomass. N Biotechnol. 2017;39:110–124. doi:10.1016/j.nbt.2016.08.002.

[97] Fu Y, Viraraghavan T. Removal of Congo Red from an aqueous solution by fungus *aspergillus Niger*. Adv Environ Res. 2002;7:239–247. doi:10.1016/S1093-0191(01)00123-X.

[98] O'Mahony T, Guibal E, Tobin JM. Reactive dye biosorption by *rhizopus arrhizus* biomass. Enzyme Microb Technol. 2002;31:456–463. doi:10.1016/S0141-0229(02)00110-2.

[99] Kaushik P, Malik A. Fungal dye decolourization: recent advances and future potential. Environ Int. 2009;35:127–141. doi:10.1016/j.envint.2008.05.010.

[100] Charumathi D, Das N. Packed bed column studies for the removal of synthetic dyes from textile wastewater using immobilised dead *C. tropicalis*. Desalination. 2012;285:22–30. doi:10.1016/j.desal.2011.09.023.

[101] Sağ Y, Kutsal T. Determination of the biosorption heats of heavy metal ions on *zoogloea ramigera* and *rhizopus arrhizus*. Biochem Eng J. 2000;6:145–151. doi:10.1016/S1369-703X(00)00083-8.

[102] Vijayaraghavan K, Yun YS. Utilization of fermentation waste (*corynebacterium glutamicum*) for biosorption of reactive black 5 from aqueous solution. J Hazard Mater. 2007;141:45–52. doi:10.1016/j.jhazmat.2006.06.081.

[103] Ofomaja AE, Ho YS. Equilibrium sorption of anionic dye from aqueous solution by palm kernel fibre as sorbent. Dye Pigment. 2006;74:60–66. doi:10.1016/j.dyepig.2006.01.014.

[104] Binupriya AR, Sathishkumar M, Kavitha D, et al. Aerated and rotated mode decolorization of a textile dye solution by native and modified mycelial biomass of *trametes versicolor*. J Chem Technol Biotechnol. 2007;82:350–359. doi:10.1002/jctb.

[105] Bulut Y, Aydin H. A kinetics and thermodynamics study of methylene blue adsorption on wheat shells. Desalination. 2006;194:259–267. doi:10.1016/j.desal.2005.10.032.

[106] Aksu Z, Çağatay ŞŞ. Investigation of biosorption of gemazol turquise blue-G reactive dye by dried *rhizopus arrhizus* in batch and continuous systems. Sep Purif Technol. 2006;48:24–35. doi:10.1016/j.seppur.2005.07.017.

[107] Esposito A, Pagnanelli F, Lodi A, et al. Biosorption of heavy metals by *sphaerotilus natans*: an equilibrium study at different pH and biomass concentrations. Hydrometallurgy. 2001;60:129–141. doi:10.1016/S0304-386X(00)00195-X.

[108] Chu HC, Chen KM. Reuse of activated sludge biomass: II. The rate processes for the adsorption of basic dyes on biomass. Process Biochem. 2002;37:1129–1134. doi:10.1016/S0032-9592(01)00326-0.

[109] Yeddou-Mezenner N. Kinetics and mechanism of dye biosorption onto an untreated antibiotic waste. Desalination. 2010;262:251–259. doi:10.1016/j.desal.2010.06.023.

[110] Kuśmierek K, Świątkowski A. The influence of different agitation techniques on the adsorption kinetics of 4-chlorophenol on granular activated carbon. React Kinet, Mech Catal. 2015;116:261–271. doi:10.1007/s11144-015-0889-1.

[111] Martorell MM, Pajot HF, de Figueroa LI. Biological degradation of reactive black 5 dye by yeast *trichosporon akiyoshidainum*. J Environ Chem Eng. 2017;5:5987–5993. doi:10.1016/j.jece.2017.11.012.

[112] Qingxiang Y, Lingxia T, Min Y, et al. Effects of glucose on the decolorization of reactive black 5 by yeast isolates. J Environ Sci. 2008;20:105–108.

[113] Pajot HF, de Figueroa LIC, Fariña JI. Dye-decolorizing activity in isolated yeasts from the ecoregion of Las yungas (tucumán, Argentina). Enzyme Microb Technol. 2007;40:1503–1511. doi:10.1016/j.enzmictec.2006.10.038.

[114] Yu Z, Wen X. Screening and identification of yeasts for decolorizing synthetic dyes in industrial wastewater. Int Biodeterior Biodegrad. 2005;56:109–114. doi:10.1016/j.ibiod.2005.05.006.

[115] Borrok DM, Fein JB. The impact of ionic strength on the adsorption of protons, Pb, Cd, and Sr onto the surfaces of gram negative bacteria: testing non-electrostatic, diffuse, and triple-layer models. J Colloid Interface Sci. 2005;286:110–126. doi:10.1016/j.jcis.2005.01.015.

[116] Dönmez G, Aksu Z. Removal of chromium(VI) from saline wastewaters by *dunaliella* species. Process Biochem. 2002;38:751–762. doi:10.1016/S0032-9592(02)00204-2.

[117] Ju YH, Chen TC, Liu JC. A study on the biosorption of lindane. Colloids Surf B. 1997;9:187–196. doi:10.1016/S0927-7765(97)00019-2.

[118] Maurya NS, Mittal AK, Cornel P, et al. Biosorption of dyes using dead macro fungi: effect of dye structure, ionic strength and pH. Bioresour Technol. 2006;97:512–521. doi:10.1016/j.biortech.2005.02.045.

[119] Kuroda K, Ueda M. Yeast biosorption and recycling of metal ions by cell surface engineering. In: Microbial biosorption of metals. Dordrecht: Springer. p. 235–247. doi:10.1007/978-94-007-0443-5.

[120] Li H, Yu C, Chen R, et al. Novel ionic liquid-type gemini surfactants: synthesis, surface property and antimicrobial activity. Colloids Surf, A. 2012;395:116–124. doi:10.1016/j.colsurfa.2011.12.014.

[121] Xia Y, Yao Q, Zhang W, et al. Comparative adsorption of methylene blue by magnetic baker's yeast and EDTAD-modified magnetic baker's yeast: equilibrium and kinetic study. Arab J Chem. 2015. doi:10.1016/j.arabjc.2015.03.010.

[122] Yu JX, Li BH, Sun XM, et al. Poly(amic acid)-modified biomass of baker's yeast for enhancement adsorption of methylene blue and basic magenta. Appl Biochem Biotechnol. 2010;160:1394–1406. doi:10.1007/s12010-009-8601-4.

[123] Ahmed SM, El-Dib FI, El-Gendy NS, et al. A kinetic study for the removal of anionic sulphonated dye from aqueous solution using nano-polyaniline and baker's yeast. Arabian J Chem. 2016;9:S1721–S1728. doi:10.1016/j.arabjc.2012.04.049.

[124] Safarikova M, Ptáčková L, Kibriková I, et al. Biosorption of water-soluble dyes on magnetically modified *saccharomyces cerevisiae* subsp. uvarum cells. Chemosphere. 2005;59:831–835. doi:10.1016/j.chemosphere.2004.10.062.

[125] dos Santos BAP, Cossolin AS, Reis HCOD, et al. Baker's yeast-MnO2 composites as biosorbent for malachite green: an ecofriendly approach for dye removal from aqueous solution. Rev Ambient e Agua. 2018;14:22–54. doi:10.4136/1980-993X.

[126] Lee DY, Cha BH, Jung M, et al. Cell surface engineering and application in cell delivery to heart diseases 09 engineering 0903 biomedical engineering. J Biol Eng. 2018;12:1–11. doi:10.1186/s13036-018-0123-6.

[127] Kuroda K, Ueda M. Engineering of microorganisms towards recovery of rare metal ions. Appl Microbiol Biotechnol. 2010;87:53–60. doi:10.1007/s00253-010-2581-8.

[128] Chien MF, Ikeda N, Kubota K, et al. Construction of a cell surface engineered yeast aims to selectively recover molybdenum, a rare metal. Solid State Phenom. 2017;262:421–424. doi:10.4028/www.scientific.net/SSP.262.421.

[129] Tanaka T, Kondo A. Cell surface engineering of industrial microorganisms for biorefining applications. Biotechnol Adv. 2015;33:1403–1411. doi:10.1016/j.biotechadv.2015.06.002.

[130] Devasia VLA, Kanchana R, Vashist P, et al. Technological advancements in industrial enzyme research. In: *Advances in biological science research*. Academic Press; 2019. p. 85–102. doi:10.1016/B978-0-12-817497-5.00006-9

[131] Lipkel PN, Kurjan J. Sexual agglutination in budding yeasts: structure, function, and regulation of adhesion glycoproteins. Microbiol Mol Biol Rev. 1992;96:180–194.

[132] Nishitani T, Shimada M, Kuroda K, et al. Molecular design of yeast cell surface for adsorption and recovery of molybdenum, one of rare metals. Appl Microbiol Biotechnol. 2010;86:641–648. doi:10.1007/s00253-009-2304-1.

[133] Kuroda K, Ueda M. Bioadsorption of cadmium ion by cell surface-engineered yeasts displaying metallothionein and hexa-His. Appl Microbiol Biotechnol. 2003;63:182–186. doi:10.1007/s00253-003-1399-z.

[134] Kuroda K, Shibasaki S, Ueda M, et al. Cell surface-engineered yeast displaying a histidine oligopeptide (hexa-His) has enhanced adsorption of and tolerance to heavy metal ions. Appl Microbiol Biotechnol. 2001;57:697–701. doi:10.1007/s002530100813.

[135] Kuroda K, Ueda M, Shibasaki S, et al. Cell surface-engineered yeast with ability to bind, and self-aggregate in response to, copper ion. Appl Microbiol Biotechnol. 2002;59:259–264. doi:10.1007/s00253-002-1014-8.

[136] Kondo A, Ueda M. Yeast cell-surface display - applications of molecular display. Appl Microbiol Biotechnol. 2004;64:28–40. doi:10.1007/s00253-003-1492-3.

[137] Ueda M, Tanaka A. Genetic immobilization of proteins on the yeast cell surface. Biotechnol Adv. 2000;18:121–140. doi:10.1016/S0734-9750(00)00031-8.

Partie Pratique

“ La connaissance s 'acquiert par l 'expérience, tout le reste n 'est que de l 'information “

Albert Einstein

Mathématicien, Physicien, Scientifique (1879 - 1955)

Chapitre I

Heavy metals phycoremediation using tolerant green microalgae: Enzymatic and non-enzymatic antioxidant systems for the management of oxidative stress

RÉSUMÉ

Afin d'évaluer le potentiel des microalgues à éliminer les MLs, huit souches algales d'eau douce dont *Chlorella vulgaris, C. ellipsoidea, C. sorokiniana, C. pyrenoidosa, Scenedesmus dimorphus, S. obliquus, Chlamydomonas reinhardtii*, et une cyanobactérie *Aphanothece* sp. ont été testées vis-à-vis de quatre MLs (cuivre (Cu (II)), chrome (Cr(VI)), plomb (Pb(II)) et cadmium (Cd(II)).

Les objectifs spécifiques de la présente recherche étaient d'abord de cribler les microalgues en fonction de leur tolérance aux quatre MLs, ensuite évaluer la capacité de phycoremédiation de la souche la plus tolérante, et finalement déterminer les mécanismes biochimiques et enzymatiques impliqués dans la gestion du stress oxydatif généré par les ions métalliques pendant le processus de phycoremédiation.

La souche *S. obliquus* a pu surmonter des niveaux élevés de contamination par Pb (II) allant jusqu'à 141 ppm (EC_{50}). Son utilisation dans la phycoremédiation du Pb (II) a montré une efficacité de traitement de plus de 50% de la concentration initiale (EC_{50}).

La mesure des teneurs des marqueurs du stress oxydatif dans les cellules de *S. obliquus* après la phycoremédiation du Pb(II) a montré une augmentation significative des niveaux de peroxyde d'hydrogène (H_2O_2) et de peroxydation lipidique (MDA). De même, l'évaluation des systèmes antioxydants non enzymatiques, à savoir l'estimation de l'activité antioxydants par la DPPH, La mesure des teneurs de proline, l'ascorbate et les polyphénols ont aussi connu une augmentation significative.

En outre, les enzymes de piégeage des ROS, y compris les activités de la superoxyde dismutase, de la catalase, de la guaiacol peroxydase, de l'ascorbate peroxydase et de la glutathion réductase, étaient significativement plus élevées dans la biomasse provenant du milieu dopé au Pb(II) par rapport à la biomasse issue du milieu témoin.

Ces résultats témoignent de la manière dont le stress oxydatif causé par les ions Pb(II) dans les cellules de *S. obliquus* pourrait être atténuée par des voies non enzymatiques et enzymatiques.

Journal of Environmental Chemical Engineering 8 (2020) 104460

Contents lists available at ScienceDirect

Journal of Environmental Chemical Engineering

journal homepage: www.elsevier.com/locate/jece

Heavy metals phycoremediation using tolerant green microalgae: Enzymatic and non-enzymatic antioxidant systems for the management of oxidative stress

M. Danouche [a,b,*], N. El Ghachtouli [b], A. El Baouchi [c], H. El Arroussi [a]

[a] Green Biotechnology Center, MAScIR (Moroccan Foundation for Advanced Science, Innovation and Research), Rabat, Morocco
[b] Microbial Biotechnology and Bioactive Molecules Laboratory, Faculty of Sciences and Technologies, Sidi Mohamed Ben Abdellah University, Fez, Morocco
[c] International Center for Agriculture Research in the Dry Area (ICARDA), Rabat, Morocco

ARTICLE INFO

Editor: G. Palmisano

Keywords:
Microalgae
Heavy-metal
Phycoremediation
Antioxidants
ROS-Enzymes

ABSTRACT

Heavy metal pollution is one of the most serious problems facing the world today. Given their toxicity and persistence in the environment, the treatment of these pollutants is of great concern. The use of microalgae is a promising solution for the remediation of metal-contaminated wastewater. In the present work, eight microalgae strains: *Chlorella vulgaris*, *C. ellipsoidea*, *C. sorokiniana*, *C. pyrenoidosa*, *Scenedesmus dimorphus*, *S. obliquus*, *Chlamydomonas reinhardtii*, and *Aphanothece* sp. were screened for their tolerance against heavy metals: copper (Cu (II)), chromium (Cr(VI)), lead (Pb(II)) and cadmium (Cd(II)). The outcomes revealed that *S. obliquus* was the most tolerant strain to Pb(II), with an EC_{50} value of 141 ppm. The phycoremediation potential of Pb(II) by this strain was carried out in scaling-up culture conditions. The Pb(II)-removal efficiency reached over fifty percent after 18 days of culture. The measurement of oxidative stress markers in *S. obliquus* cells after Pb(II) phycoremediation, showed a significant increase in the level of hydrogen peroxide (H_2O_2) and lipid peroxidation (MDA). Interestingly, non-enzymatic antioxidant systems, including α,α-diphenyl-β-picrylhydrazyl (DPPH) radical scavenging activity, proline, ascorbate, and polyphenol production. Besides, the ROS-scavenging enzymes including superoxide dismutase, catalase, guaiacol peroxidase, ascorbate peroxidase and glutathione reductase activities were significantly higher in the biomass from Pb(II)-medium compared to the control medium. This indicates that the oxidative stress caused by Pb(II) ions in *S. obliquus* cells could be attenuated via these non-enzymatic and enzymatic pathways. Our study highlights *S. obliquus* as a promising strain for the phycoremediation of polluted effluents on a large-scale.

1. Introduction

Water pollution is considered today, as one of the greatest challenges facing the world, especially in developing countries. Hence, increasingly scientists and environmentalists pay attention to environmental contamination by heavy metals (HMs) [1]. Indeed, since the formation of the Earth, nearly all HMs have been recycled biogeochemically, and therefore are present naturally in trace amounts. However, the global expansion of industrialization and other anthropogenic actions, including mining activities, irrational use of fertilizers in agriculture, and non-hazardous waste management, have introduced processes that increased the redistribution level of metals between environmental compartments [2]. Several HMs are known to be water contaminants, prominently Cu(II), Cr(VI), Cd(II), and Pb(II) [3]. They are also considered to be harmful, even at very low exposure doses, and can be accumulated into food chains [4,5]. Consequently, their release into the environment without appropriate treatment remains a serious problem. In order to deal with this issue, a variety of physicochemical methods such as adsorption, electro-coagulation, chemical precipitation, reverse osmosis, ultra-filtration and electrochemical methods have been applied to remove HMs from wastewater, prior to their release into ecosystems [6–8]. Although these methods are effective, they unfortunately require a considerable amount of chemical reagents such as sacrificial reagents in photocatalysis process [9], and energy-intensive equipment [10]. This makes the processing cost of such processes overpriced, restricting thereby their large-scale applications [11]. Alternatively,

* Corresponding author at: Green Biotechnology Center, MAScIR (Moroccan Foundation for Advanced Science, Innovation and Research), Rue Mohamed Al Jazouli, Madinat Al Irfane, 10 100 Rabat, Morocco.
E-mail address: mohammed.danouche@usmba.ac.ma (M. Danouche).

https://doi.org/10.1016/j.jece.2020.104460
Received 26 June 2020; Received in revised form 27 August 2020; Accepted 28 August 2020
Available online 6 September 2020
2213-3437/© 2020 Elsevier Ltd. All rights reserved.

biotechnological approaches involving microorganisms (bioremediation) and plants (phytoremediation), are promising options, because they are eco-friendly and cost-effective process, as well they require low investment [12]. Recently, wastewater treatment using microalgae has aroused the interest of the scientific community, because of their countless advantages. In addition to their excellent potential for pollutants removal, microalgae have the advantage of producing value-added products like lipids and pigments [13]. To distinguish the use of microalgae from the other bioremediation and phytoremediation methods, this process is called phycoremediation [14]. Studies on HMs phycoremediation date back to the 1990s [15]. However, microalgae were used mainly as inactive biomass, and the removal mechanism was therefore mediated by an extracellular biosorption, such as the biosorption of Pb (II) [16], Cd (II) [17], Cr(VI) [18], and Cu(II) [19]. There are only a few studies that focused on the use of viable microalgae cells in the phycoremediation of HMs [20,21], despite the fact that the use of microalgae cultures has many advantages, including avoiding processes related to biomass harvesting, drying, pre-treatment, and storage, which are generally required when the process is based on biosorption [22]. On the other hand, the use of HMs tolerant microalgae species will further increase the bioremoval capacity through active (bioaccumulation) and/or passive (biosorption) mechanisms [3]. Also, under metal-stressed environments, living microalgae produce various extracellular polymeric substances (EPS) (polysaccharides, proteins, uronic acids, lipids, and non-polymeric substances). In association with the properties of the cell surface and its functional groups, EPS can be involved in the sorption of metal ions, enhancing thereby the microalgae potential for the remediation of metallic pollution [23]. Other strategies can also be used by living microalgae for the removal metal ions, for instance the extracellular complexation, exclusion and chelation with phytochelatins, metallothioneins and polyphosphates [24]. When the phycoremediation process is based on living cells, the choice of metal-tolerant microalgae is the first determinant step. Thereafter, the factors that can influence the growth and physiology of microalgae should be investigated, especially the inhibitory effect of metal ions, by assessing the physiological and the ultrastructural changes that can occur in the microalgae cells after metal exposure [25,26]. It is also very important to investigate the antioxidant defense mechanisms adopted by microalgae for the management of oxidative stress, specially non-enzymatic antioxidant systems and reactive oxygen species (ROS)-scavenging enzymes [27]. Hence, with the aim to evaluate the potential application of living freshwater microalgae in the removal of HMs, the specific objectives of the present research were to: (i) screen microalgae for HMs tolerance, (ii) assess their phycoremediation ability, and (iii) identify the biochemical and enzymatic mechanisms involved in the management of the oxidative stress generated during the phycoremediation process.

2. Material and methods

2.1. Potential use of freshwater microalgae in phycoremediation

2.1.1. Screening of metal tolerant microalgae candidates

In the present study, the screening of eight species of microalgae was performed on the basis of their metal sensitivity, by monitoring their growth inhibition. The studied microalgae belong to the following genera: Chlorella (*C. vulgaris, C. ellipsoidea, C. sorokiniana and C. pyrenoidosa*), Scenedesmus (*S. dimorphus and S. obliquus*), Chlamydomonas (*C. reinhardtii*) and one cyanobacteria Aphanothece (*Aphanothece* sp.). The screening test was carried out in 250 mL Erlenmeyer flasks containing a standard BG-11 medium containing 1.5 g $NaNO_3$, 40 mg K_2HPO_4, 36 mg $CaCl_2$ $2H_2O$, 6 mg ammonium citrate monohydrate, 6 mg ammonium ferric citrate, 1 mg EDTA, 2.86 mg H_3BO_3, 1.81 mg $MnCl_2$ $4H_2O$, 0.22 mg $ZnSO_4$ $7H_2O$, 0.39 mg $NaMoO_4$ $5H_2O$, 0.079 mg $CuSO_4$ $5H_2O$, 0.050 mg $CoCl_2$ $6H_2O$ in 1 L sterile distilled water [28]. Medium was then doped with 10 ppm of a mono-metal solution of Cu (II), Cr (VI), Pb (II) and Cd (II), respectively, in the following chemical forms: $CuSO_4$, $K_2Cr_2O_7$, $Pb(NO_3)_2$ and $Cd(NO_3)_2$. All chemicals were of analytical grade and obtained from Sigma-Aldrich (USA). The pH of the tested solutions was adjusted with 0.1 M HCl or 0.1 M NaOH. The media were inoculated with microalgae at the initial density equivalent to 0.35 $\pm$ 0.025 at $A_{680\ nm}$. All experiments were carried out in triplicate, and the cultures were maintained in a constant orbital shaking (120 rpm) at 25 $\pm$ 2 °C and 10 h: 14 h light–dark cycle for 15 days. The cell density was determined spectrophotometrically using Ultrospec™ 3100 pro UV-Visible instrument. The screening of heavy-metal-tolerant microalgae was performed using principal component analysis (PCA) on the data of growth inhibition (Gi) as the following:

$$(\mathbf{Gi}) = (OD_{680c} - OD_{680s})/\ OD_{680c} \quad (1)$$

Where OD_{680s} means optical density of the analyzed experiment and OD_{680c} is the control optical density. Thereafter, the choice of the strain that could be used in phycoremediation of the target metal was performed by using one-way ANOVA multiple comparisons on the basis of metal tolerance.

2.1.2. Half maximal effective concentration

Half maximal effective concentration (EC_{50}) test is widely used as an index of toxicity; it indicates the concentration of metal that reduces population growth to 50 % compared to the control [29]. However, it can also be used as a range finder test for metal concentration, which should not be exceeded in order to prevent high cell mortality during the phycoremediation process [25]. The selected microalgae strain was grown in a wide range of metal concentrations to determine the EC_{50} value. The experiment was performed in multiple well plate size 12 wells (CellBIND, Sigma) containing contaminated BG-11medium with concentrations ranging from 0 to 10.5 ppm for Cu (II) and Cr (VI), and from 0 to 350 ppm for Cd (II) and Pb (II). The difference in the concentration range of the four metals used in this study was based on the results of previous studies, which showed a significant difference in the toxicity of each heavy metal [30,31]. The experiments were carried out in triplicate. Thus, the EC_{50} was calculated by applying a nonlinear regression to the log of metal concentration relative to the mean percentage reduction in cell density at 7 days of culture.

2.1.3. Lead phycoremediation at scaling up microalgal cultures

Based on EC_{50} tests, Pb (II) was selected as a model pollutant in order to determine the potential application of the selected microalgae in phycoremediation of polluted water. The experiment was conducted at scaling up conditions in 10 L flat bottom flask containing BG-11 culture media contaminated with Pb (II) at the EC_{50} concentration (141 ppm). The inoculation was performed using pre-culture of the selected microalgae. The biomass was recovered by centrifugation (4700x*g* for 10 min) from a preculture in exponential growth phase, and the pellet was diluted to the optical density of 0.350 $\pm$ 0.025 at $A_{680\ nm}$. Then, the culture was grown under the same conditions as described above for 18 days. The agitation was achieved by bubbling air through spargers located at the base of the reactors. The growth kinetic was performed spectrophotometrically every 4 days, and the concentration of Pb (II) in the medium before and after treatment was established as described by Oyebamiji et al. [32]: after culture centrifugation at 4700xg of 10 min, the supernatant was filtered by 0.45 µm cellulose acetate filters, then digested with nitric acid HNO_3 and 30% H_2O_2 at 120 °C during 12 h. Finally, prior to measurement, samples were diluted to 10% HNO_3 by adding 10 mL of deionized water. Thus, the content of Pb (II) in solution was determined using Thermofisher 7000 series inductively coupled plasma optical emission spectrometer. In order to verify the effects of the test conditions on metal removal, the abiotic control (Pb (II)-medium without microalgae inoculation) was prepared and maintained under the same conditions as described above.

2.2. Management of oxidative stress

2.2.1. Oxidative stress markers

The assessment of oxidative stress markers in *S. obliquus* cells after Pb (II) phycoremediation was estimated by examining the levels of H_2O_2 and MDA.

2.2.1.1. Determination of hydrogen peroxide. H_2O_2 was extracted using the protocol from [33], by homogenizing 0.5 g of fresh biomass in 5 mL of iced trichloroacetic acid (TCA). After 10 minutes of centrifugation at 12 000xg, 0.5 mL of the supernatant was added to 1.5 mL of potassium phosphate buffer (50 mM, pH 7.0) and 1 mL of 1 M potassium iodide (KI). The reaction mixture was incubated for 1 h in the dark at room temperature. Thus, the absorbance was measured at A_{390nm}. The results were calculated using a H_2O_2 standard curve [34].

2.2.1.2. Measurement of lipid peroxidation. It was determined according to the method provided by Heath and Packer [35]. Harvested cells (0.5 g) were resuspended in 5 mL of (1 % w/v) TCA. Then, they were disrupted by sonification using ultrasonic homogenizer SONOPULS mini20. The mixture was centrifuged at 6300xg for 10 min at 10 °C, 0.5 mL of supernatant was mixed with 2 mL of TCA (20% w/v) containing (0.5 % w/v) of thiobarbutric acid (TBA). The mixture was heated at 96 °C for 25 min, and quickly transferred in ice, then centrifuged at 10 000xg for 10 min. The determination of thiobarbituric acid-reactive substances (TBARS), mostly malondialdehyde (MDA), was performed on supernatants by spectrophotometry at A_{532nm}, using an extinction coefficient of 159.2 mM^{-1} cm^{-1} [36].

2.2.2. Non-enzymatic scavenging pathways

2.2.2.1. Radical scavenging activity. DPPH radical-scavenging activity was carried out in flat bottom polystyrene 96-well microtiter plates as described by Maadane et al. [37]. The microalgae extract was prepared in methanol at the concentration of 20 $mg.mL^{-1}$. 20 µL of the extract was added to 180 µL of DPPH radical solution (60 µM). The absorbance of the mixture was read at $A_{517\ nm}$, using SpectraMax Plus 384 Microplate Reader (Molecular Devices), and the Ascorbic acid was used as standard. The percentage of scavenging (SE %) of DPPH radical from a sample at a given concentration was calculated from the absorbance readings as shown in Eq. (2).

$$SE\ \% = [1-(A_{\text{sample}} - A_{\text{sample blank}})/A_{\text{control}}] \times 100 \quad (2)$$

Where A_{sample}: is the absorbance of methanolic DPPH solution with extract samples or standard, $A_{\text{sample blank}}$: is the absorbance of extracts sample in methanol, and A_{control}: is the absorbance of the methanolic DPPH solution.

2.2.2.2. Proline content. The proline assay was conducted as describe by Cervantes-García et al. [38], 50 mg of microalgae biomass was homogenized in 3 mL of sulfosalicylic acid (3%) followed by centrifugation at 4000xg for 15 min. 2 mL of glacial acetic acid and 2.5 % acid ninhydrin solution were added to 2 mL of the filtrate. The mixture was incubated for 45 min in a boiling water bath. The reaction was stopped by placing the filtrate mixture on ice. In the next step, equal volumes of toluene were added, then the absorbance of the upper pink layer was read at A_{520nm}. The concentration of proline was calculated from a calibration curve using L-proline as a standard [39].

2.2.2.3. Ascorbate content. The estimation of ascorbate (ASC) content was conducted based on the stochiometric reduction of phosphomolybdenum as described by Sahu and Sabat [40]. Briefly, 50 mg of microalgae biomass was homogenized with 5% metaphosphoric acid, and the homogenate was centrifuged at 14000xg for 10 min at 4 °C. To 0.5 mL of the supernatant, 0.2 mL of sodium molybdate (0.66 %), 0.2 mL H_2SO_4 (0.05 N) and 0.1 sodium phosphate (0.025 mM) were added. The reaction mixture was incubated at 60 °C in water bath for 40 min., then the reaction mixture was cooled under running water. The absorbance was measured at $A_{660\ nm}$, and the concentration of ASC was calculate using a standard curve with L-ascorbate [41].

2.2.2.4. Phenolic compounds. Total polyphenols in the microalgae biomass was determined according to the Folin-Ciocalteu method as illustrated by Li et al. [42]. The microalgal biomass was homogenized with 5 mL of 80 % ethanol and centrifuged at 10000xg for 10 min. To the supernatant, 1 mL of Folin-Ciocalteu's reagent and 5 mL of distilled water were added, and mixed together followed by incubation at room temperature in the dark for 5 min. Thereafter, 2 mL of sodium carbonate (20 % w/v) was added and incubated for 1 h in the dark at room temperature. The absorbance of the solution was measured at $A_{650\ nm}$ against a blank. Gallic acid was used as a standard, and the total phenolic content of algal samples was expressed in mM of gallic acid equivalent (GAE) [43].

2.2.3. Enzymatic scavenging pathways

The ROS-scavenging enzymes including; superoxide dismutase (SOD), catalase (CAT), guaiacol peroxidase (GPX), ascorbate peroxidase (APX) and glutathione reductase (GR) were extracted by homogenizing 500 mg of fresh algal cells using ultrasonic homogenizer (Sonopuls mini20) in an ice bath assisted by freezing cycles thawing at −80 °C. Microscopic evaluation of cell disturbance was performed to ensure enzyme extraction. The extraction buffer contained 50 mM of potassium phosphate buffer (pH 7.0), 2 mM EDTA, 5 mM β-mercaptoethanol, 1 % polyvinyl pyrrolidone, 1 % glycerol, 1 mM polymethyl sulfonyl fluoride (PMSF) and 50 mM NaCl. The extraction procedure for all enzymes was the same except that for APX, for which the extraction buffer contained also 5 mM ascorbate. The homogenate was centrifuged at 12 000xg for 15 min at 4 °C. The supernatant was used for analyzing the enzymatic activities [44,45], and for the estimation of soluble proteins, by using the Bradford method with bovine serum albumin (BSA) as a standard [46]. SOD activity was determined by measuring the inhibition of the photochemical reduction of NBT at $A_{560\ nm}$ [47]. One unit of SOD per mg of soluble protein was identified as the amount that causes 50 % inhibition of the photochemical reduction of NBT. The CAT activity was estimated by measuring the decrease in H_2O_2 absorbance at $A_{240\ nm}$. A unit of CAT (U) activity was assumed to be the amount of enzymes that breaks down 1 mM of H_2O_2 per minute per mg soluble protein [48]. GPX activity was measured according to the method of Hemeda and Klein [49], using phosphate buffer (100 mM, pH 7.0) containing 10 mM of guaiacol and 10 mM H_2O_2. The increase in absorbance due to oxidation of guaiacol (extinction coefficient 26.6 mM^{-1} cm^{-1}) was recorded at A_{470} nm. Enzyme activity was expressed as micromoles of guaiacol oxidized min^{-1}. g^{-1}. GR activity was measured as the reduction of GSSG at $A_{340\ nm}$ using phosphate buffer 100 mM, pH 7.0 containing 7.5 nM $MgCl_2$, 3.6 nM NADPH and 15 mM GSSG. For the determination of APX activity, the cytosolic fraction was mixed with 0.6 mM L-ascorbate, 0.12 mM EDTA and 1.5 mM of H_2O_2 in 100 mM phosphate buffer pH 7.0, the reduction of H_2O_2 absorbance was measured at $A_{290\ nm}$. The decrease in NADPH ($A_{340\ nm} = 6.22\ mM^{-1}.\ cm^{-1}$) and in ascorbic acid ($A_{290\ nm} = 2.8\ mM^{-1}.\ cm^{-1}$) were used to measure the activities of GR and APX, respectively [50].

2.2.4. Statistical analysis

The PCA data analysis of the screening step was generated using RStudio, and the visualization by FactoMineR package, integrated into the R software. The choice between strains was based on one-way ANOVA with Dunnett's multiple comparisons test. The normalization of data for the EC_{50} calculation was performed by using a log dose-response curve using GraphPad Prism software version 8.0. All experiments were performed in triplicate, and data was expressed as the mean

± standard deviation. The statistical analysis of differences between control and stressed microalgae cells was performed with unpaired T-test. P-value of < 0.05 were considered to be statistically significant.

3. Results and Discussion

3.1. Potential use of microalgae in phycoremediation

3.1.1. Screening of metal tolerant microalgae candidates

Growth inhibition is one of the most important ways of examining the ecological performance of microalgae species in relation to the environmental or experimental conditions. The PCA statistical analysis enables the evaluation and visualization of the data set containing the strains described by the four metals to which they are exposed. As shown in the Fig. 1, the first two principal components PC_1 and PC_2 accounted for 91.3 % of the data variance. PC_1 and PC_2 explained 75.5 % and 15.8 %, respectively, of total data variability. The main factors involved in the construction of the PC_1 are Cd (II), Cr (VI) and Cu (II), whereas microalgae tolerance to Pb (II) is the descriptive factor of the PC_2 (Fig. 1C). The PCA-biplot (Fig. 1A) shows the arrangement of microalgae strains according to the two principal dimensions PC_1 and PC_2, in which microalgal strains were represented by dots and HMs with vectors. At first glance, the projection of the two strains *C. sorokiniana* and *S. obliquus* is positioned in the middle of the right side of the biplot. This means that they have a strong positive correlation with the PC_1, and are slightly influenced by the PC_2, which is mainly constructed by the effect of Pb (II) (Fig. 1C). *C. pyrenoidosa* and *Aphanothece* sp. Also showed a slight positive correlation with the first component. These distinctions between species of the same genus can be explained by the defense mechanisms that have been evolved in the various locations where they have been isolated. It was reported that microalgae belonging to the same genus but varying in their species, respond differently to HMs [51]. The microalgae tolerance can also be either genetic or physiological, although the difference between these two mechanisms is not clearly defined [52].

In order to distinguish the most metal-tolerant strain between the selected strain of *C. sorokiniana* and *S. obliquus,* one-way ANOVA multiple comparisons was performed, and the results are presented in Fig. 2. From the obtained results, *S. obliquus* was much more resistant to both metals Pb (II) and Cd (II) compared to *C. sorokiniana*. There was no significant difference between the growth of *S. obliquus* cultivated in media artificially contaminated with Pb (II) or Cd (II) and that of the control culture. However, the growth rate in Cu (II) or Cr (VI)-contaminated media differed significantly from the control (CTR). The differences between means (CTR-Cu) ± SEM and (CTR-Cr) were recorded as 0.779 ± 0.113 ($p = 0.002$, $t = 6.877$, $df = 4$), and -1.212 ± 0.044 ($p < 0.0001$, $t = 27.10$, $df = 4$) respectively. Indicating the harmful effect of these hazardous metals on the growth and survival of *S. obliquus*. Conformingly *C. sorokiniana*, was sensitive to exposure to all four tested metals; their growth was significantly different from that of the control

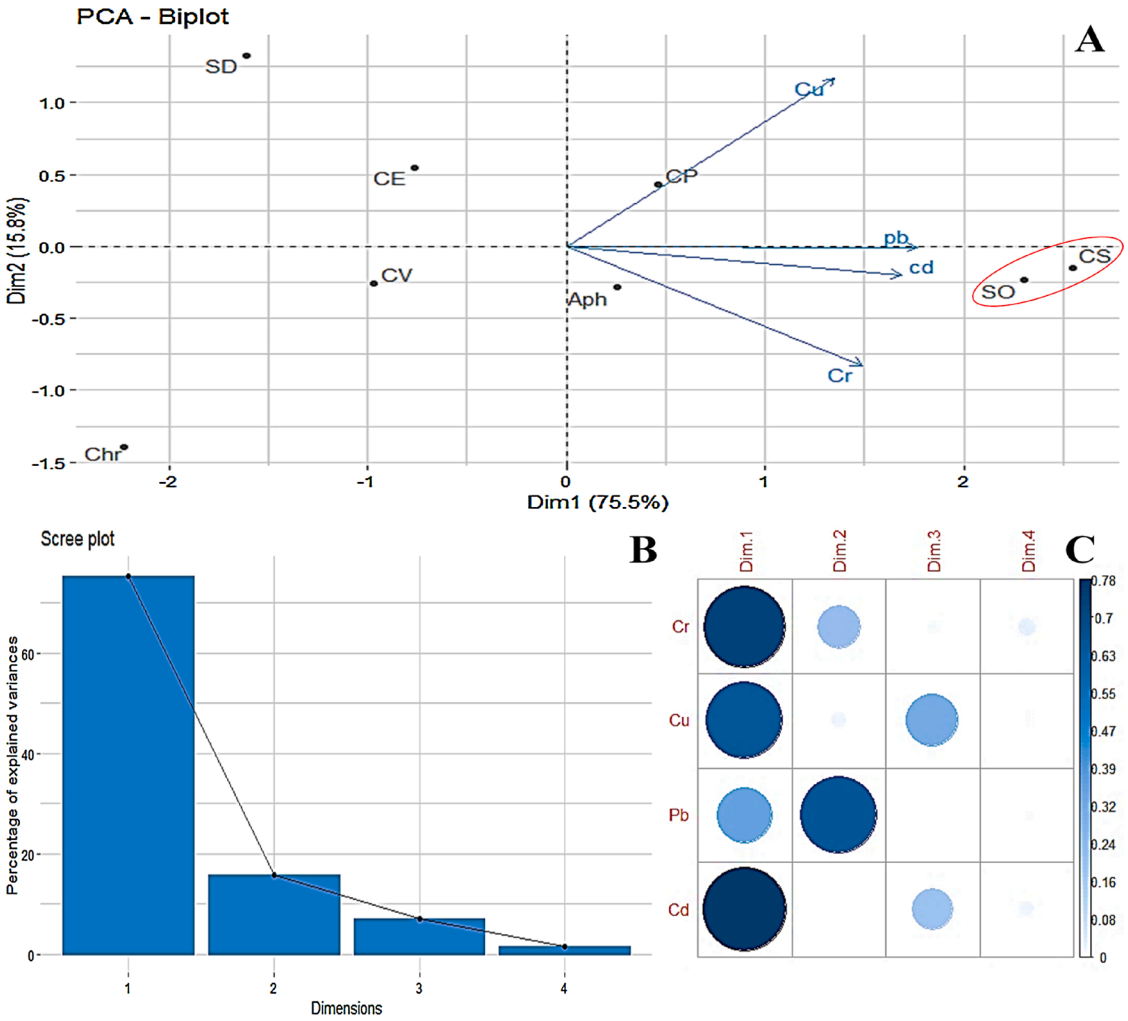

Fig. 1. Screening of metal tolerant microalgae strains (*C. vulgaris* (CV), *C. ellipsoidea* (CE), *C. sorokiniana* (CS), *C. pyrenoidosa* (CP), *Scenedesmus dimorphus* (SD), *S. obliquus* (SO), *Chlamydomonas reinhardtii* (ChR), and *Aphanothece*sp (Aph)), exposed to 10 ppm of single metal solution for 15 days: (A) 2-D biplots correlation based on the first two principal components axes, (B) Bar-plot of the contribution of the variables, (C) Scree plot.

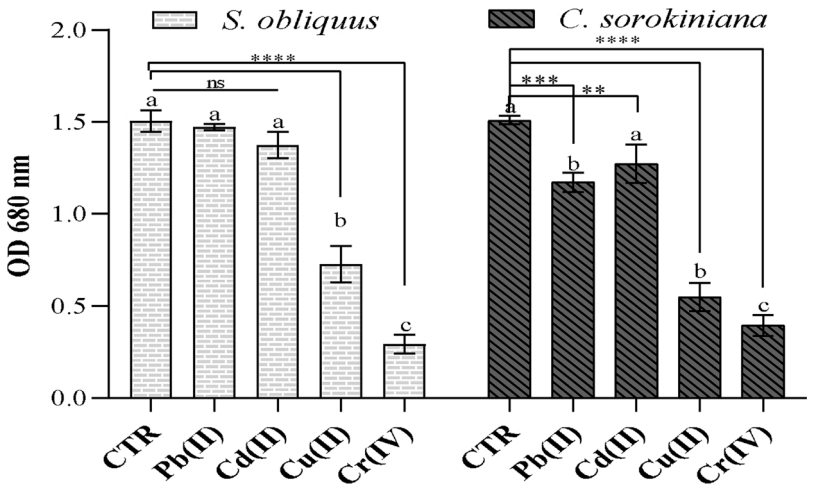

Fig. 2. One-way ANOVA multiple comparison of *C. sorokiniana* Vs *S. obliquus* based on the rate of the growth inhibition after 15 days exposure to 10 ppm of single metal solution. Values are mean of three experiments ± SEM. Significantly different from control cells at *P ≤ 0.05< **P < 0.01 by one-way ANOVA with Dunnett's multiple comparisons test.

culture. In accordance with this outcome, Shanab et al. [53] examined the tolerance of three microalgae strains, and showed that a strain of *S. quadricauda* was Pb (II)-tolerant even at high concentrations up to 100 $mg.L^{-1}$. Likewise, Ajayan et al. [12] affirmed the potential application of *Scenedesmus* sp. in phycoremediation of tannery wastewater. Indeed, there is growing interest in research on the possibilities of using strains of *S. obliquus* for the removal of metal from wastewater [54,55]. Multiple researchers suggest that the affinity of the microalgae strain to a specific metal may contribute to the determination of its potential usage in target phycoremediation [56,57].

3.1.2. Half maximal effective concentration

There is lacking information on the resistance margin of *S. obliquus* towards the tested HMs. Hence, its tolerance ability was evaluated using the EC_{50} value. As shown in Fig. 3, the tested metal ions have varying concentration-response relationships due to the difference in their level of toxicity. The growth rate of *S. obliquus* decreased with increasing doses of HMs. Thus, the following order of toxicity was established; Cr (VI)> Cu (II)> Cd (II)> Pb (II). Indeed, *S. obliquus* was more resistant to Pb (II) compared to the other metals, with the highest EC_{50} value of 141.4 ppm (Fig. 3D), followed by Cd (II) that induces a moderate toxicity with EC_{50} value of 59.43 ppm (Fig. 3C). However, exposure to Cr (VI) and Cu (II) induced growth inhibition even at very low concentrations, with EC_{50} values of 4.526 ppm and 5.838 ppm, respectively (Fig. 3B, A). It has been reported that increased concentrations of HMs can significantly impact the growth of microalgae. Debelius et al. [30] demonstrated that the EC_{50} (Pb (II)) value was at 2600 ppm for the seawater microalgae *Tetraselmis chuii*. In addition, the calculated EC_{50} (Cd(II)) values, were 0.058 ppm and 1.92 ppm, respectively for the *S. obliquus* and *D. pleiomorphus* [58]. Various reports elucidate the high toxicity of Cu (II) and Cr (VI) against microalgae. For example, Anderson and Morel [59] stated that 1 ppm of Cu (II) was enough to interfere with some of the cellular processes of *Gonyaulax tamarensis*, causing thereby the inhibition of their motility. Likewise, Franklin et al. [60] obtained an EC_{50}(Cu(II)) value of 10 ppm for *Chlorella* sp. and *Selenastrum capricornutum*. Contrarily, Debelius et al. [30] reported that the seawater microalgae *Tetraselmis chuii* can withstand very high concentrations of Cu (II), that can reach up to an EC_{50} value of 330 ppm. On the other hand, Cr(VI) significantly inhibited the growth of *Chlorella vulgaris*, with an EC_{50} (Cr(VI)) value of 1.76 ppm [61]. The toxicity mechanism of Cr (VI) is mainly related to its easy diffusion across the cell membrane, followed by its reduction in cells giving rise to free radicals that may directly cause DNA alterations, and other damages like the Fenton-type mechanism, that can reduce the activity of certain antioxidant enzymes [62,63].

In industrial wastewater, concentrations of Pb (II) can be close to 200-500 ppm, which is very high in relation to water quality standards. Therefore, an adequate treatment is required before release into the aquatic ecosystems. From this perspective, we hypothesized that the tolerance of the selected strain *S. obliquus* to this high value of EC_{50} Pb (II) may make it a promising candidate for a targeted bioremoval of Pb (II) at this high concentration.

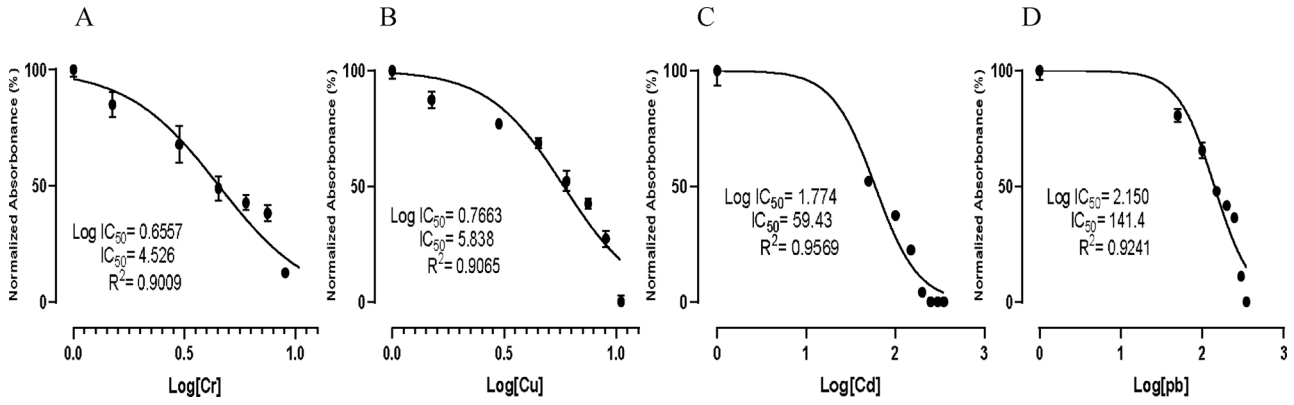

Fig. 3. Growth inhibition curves at increasing concentrations (0 to 10.5 ppm) of Cr (VI) (A) and Cu (II) (B), and 0 to 350 ppm of Cd (II) (C) and Pb (II) (D) for *S. obliquus* culture at one-week HMs exposure.

3.1.3. Lead phycoremediation at scaling up microalgal cultures

The simulation of the phycoremediation of highly toxic effluent was achieved at Pb (II) concentrations around EC_{50} (141 ppm) using the selected strain *S. obliquus,* the growth kinetics and the removal capacity are illustrated in Fig. 4.

S. obliquus strain was slightly sensitive to Pb (II) with a continuous decline in growth rate vs free Pb (II) medium. After 18 days of cultivation, the growth decreased by 20.7 % compared to the control (Fig. 4A). This provides an overall indication of the influence of Pb (II)-induced cell toxicity. Significant growth inhibition of *S. acutus* YaA6 was reported by Dao et Beardall [64], after exposure to lower Pb(II) concentrations (0.03-0.87 $\times$ 10^{-9} M). On the other hand, the ability of the selected strain to remove Pb (II) ions was determined by measuring their concentration in the solution after 18 days of culture at scaling up conditions. The results demonstrate a high bioremoval capacity of Pb (II), it was 58.42 % of the EC_{50} initial concentration (141 ppm) (Fig. 4B). Compared with previous literature studies, the bioremoval capacity of Pb (II) by the selected strain was more efficient. For example, Nacorda et al. [62] reported that the bioremoval percentage of Pb (II) by two *Chlorella vulgaris* strains, at the initial concentration of 0.1 ppm was 32.15 % and 46.01 %. Similarly, Pham et al. [65] found that the removal efficiency of Pb (II) at the initial concentration of 1 and 2 ppm by *Scenedesmus* sp. was at 83.5 % and 84.2 %, respectively. According to a study by Shanab et al. [53], *Pseudochlorococcum typicum* removed 70 % of Pb (II) in the culture medium with initial concentration of 3.31 ppm. In fact, microalgae like all living organisms, have various defense mechanisms against toxic substances, including HMs, to maintain their survival in extreme conditions [66]. These mechanisms can be classified into three types: extracellular adsorption, intracellular complexation and ROS detoxification [13]. The detoxification can also be accomplished by binding metal to particular intracellular compounds and/or transferring them to specific cellular compartments [17,67]. As seen in the freshwater *S. vacuolatus* and the seawater *Tetraselmis suecica*, the formation of metal-binding peptides or proteins, namely, phytochelatins or metallothioneins (class III), are the most common intracellular metal detoxification mechanisms [68,69].

3.2. Management of oxidative stress by S. obliquus

3.2.1. Oxidative stress markers

3.2.1.1. Hydrogen peroxide and lipid peroxidation. The measurement of oxidative stress in biomass after Pb (II) removal was investigated using the levels of H_2O_2 and MDA as indicators. The concentration of H_2O_2 was determined to be representative of the ROS. A significant increase in H_2O_2 production was noticed in *S. obliquus* cells after exposure to Pb (II) (Fig. 5A). The difference between the means of the control and test cultures was 142.9 $\pm$ 8.420 µM ($p < 0.0001$). It is known that the level of H_2O_2 in microalgae cells usually increases under stress conditions. In line with the present findings, a significant increase in H_2O_2 content was observed in the cells of *A. obliquus* exposed to Pb (II) ions, compared to non-stressed cells [70]. One of the main effects of Pb (II) is the increase in ROS production, it is known that the binding of Pb (II) ions to thiols can disrupt the redox status of the cell, enhancing thereby the production of ROS [50], causing thus cell membrane damage, protein denaturation, DNA mutations, and oxidation of lipids [71].

The lipid peroxidation is a natural metabolic process under normal conditions, but it is also one of the most studied consequences of ROS reaction on membrane structure and function [72]. In the present assays, the level of lipid peroxidation in *S. obliquus* cells was determined by the estimation of MDA content. The obtained results show that Pb (II) at EC_{50} concentration enhanced lipid peroxidation (Fig. 5B). The level of MDA increased significantly after Pb (II) accumulation, the difference between the means of control and Pb (II)-exposure biomass was 129.0 $\pm$ 40.19 nMol.g^{-1} FW ($p < 0.05$). Many previous studies have highlighted the increase in the MDA content after exposure to HMs [33,44,73].

3.2.2. Non-enzymatic antioxidants pathways

After Pb (II) phycoremediation, the total antioxidant capacity was significantly increased. The free radical scavenging activity of the methanolic extract was achieved by using DPPH. The obtained results show that the mean DPPH radical scavenging activity in *S. obliquus* cells cultivated in Pb (II)-medium reached 33.71 % compared to the control 23.87 % (Fig. 6A). Similar findings were indicated by [74] in the halophilic microalga *Dunaliella salina,* exposed to various concentrations of Cd (II). The increase in the total antioxidant capacity could be attributed to the enhancement of the activity of biological components involved in defense mechanisms against free oxidative radicals [75]. More details on antioxidant compounds that act in the non-enzymatic pathways against Pb (II) stress were investigated in this study. The results presented in Fig. 6B, C and D, indicate clearly that the concentration of proline, ascorbate, and polyphenol in *S. obliquus* cells after Pb (II) phycoremediation was higher than in cells from the control culture. A statistically significant effect on the level of both proline and polyphenol contents was obtained; the difference between means of control and treated biomass were 128.7 $\pm$ 29.85 ($p = 0.012$, $t = 4.310$, $df = 4$), and 3.700 $\pm$ 0.237 ($P < 0.0001$, $t = 15.59$, $df = 4$), respectively. However, the ascorbate concentration was not significantly affected. These results are in line with previous observations. For instance, a study by Tripathi et al. [50] suggested that the accumulation of proline in *S. acuminatus* cells can be an effective strategy for reducing metal-induced oxidative stress. Indeed, the production of proline is one of the mechanisms by which plants and microalgae face the adverse effects of HMs [76]. During the oxidative stress, proline performs three key roles: as a metal chelator, as an antioxidant resistance molecule, and as a signaling

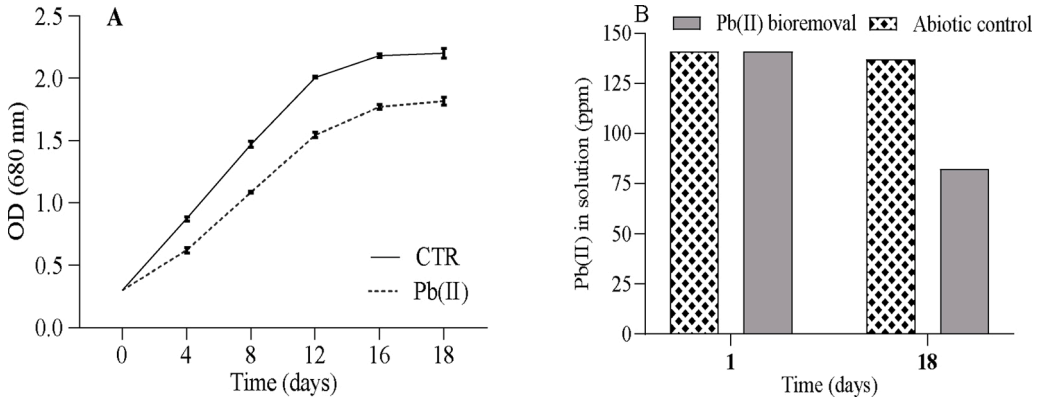

Fig. 4. Growth kinetics (A), and Pb (II) bioremoval capacity (B) at the initial concentration of 141 ppm using *S. obliquus* after 18 days at scaling up culture's conditions.

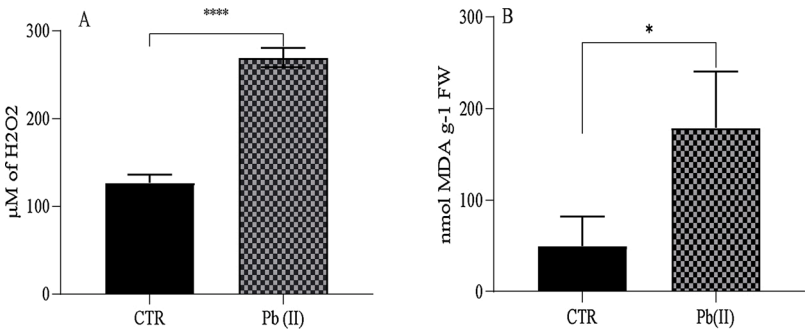

Fig. 5. The level of (A) hydrogen peroxide (H2O2) and (B) lipid peroxidation in control (CTR) and Pb (II)-exposure biomass (Pb (II)) after 18 days of cultures at scaling up condition.

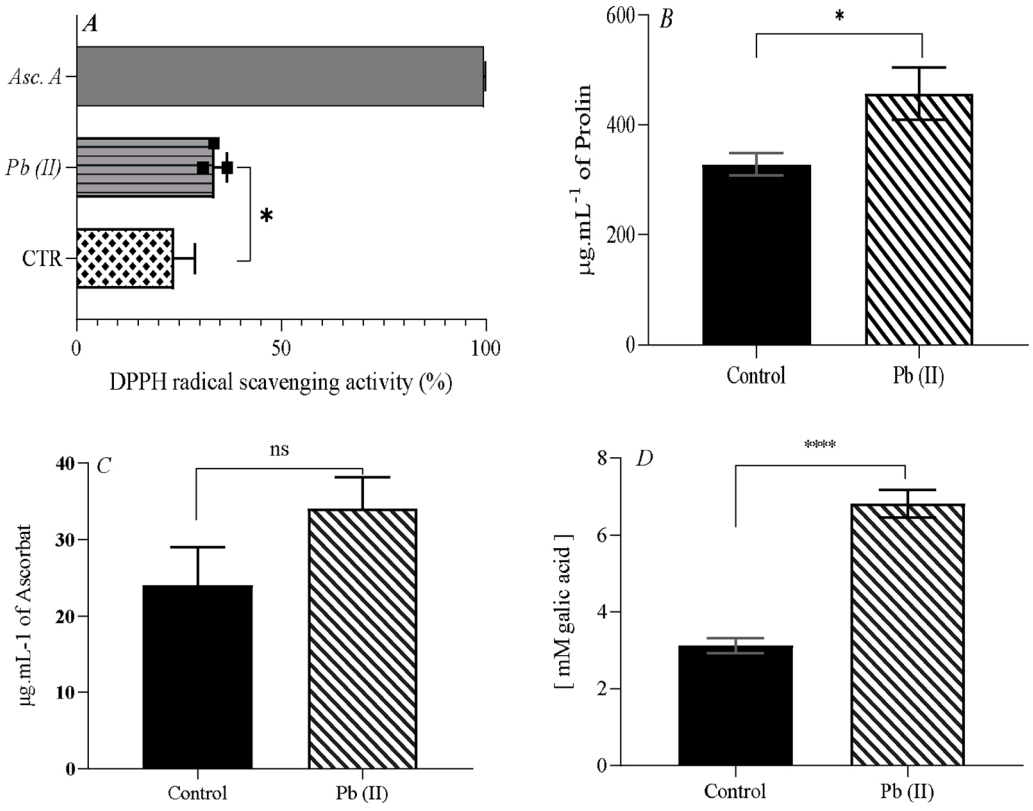

Fig. 6. Level of antioxidant compounds: DPPH radical scavenging activity (A), Proline (B), Ascorbate (C) and Polyphenol (D). In the biomass from control vs Pb (II) processing medium (Pb (II)), after 18 days at scaling up cultures' conditions.

molecule [77]. Ascorbate is also one of the most studied antioxidants in ROS detoxification. The obtained results are consistent with those of numerous literature reports. Piotrowska-Niczyporuk et al. [70] showed that an increase in ascorbate content, reaching up to 25% was observed in *A. obliquus* cells treated with Pb (II) compared to unstressed cells. Several other studies have confirmed that Pb (II) stimulates the accumulation of ascorbate as a mechanism for improving cell tolerance against metal stress [78–80]. The main function of ascorbate in protecting cells against oxidative stress, is their potential to donate electrons to a variety of enzymatic and non-enzymatic reactions against ROS [72]. It may also directly trap superoxide, hydroxyl radicals, and singlet oxygen and reduce H_2O_2 to H_2O through an ascorbate peroxidase reaction [81]. In the chloroplasts, Ascorbate acts as a cofactor of violaxantin de-epoxidase, sustaining thus the dissipation of excess excitation energy [82]. Moreover, it can regenerate tocopherols from tocopheroxyl radicals providing membrane protection [83].

Regarding the increase in polyphenol content and its relationship with ROS induced by HMs, it has been demonstrated that the cells protection against oxidative stress with polyphenols may take different pathways and mechanisms [84,85]. The antioxidative properties of polyphenols arise from their high reactivity as hydrogen or electron donors [72]. They may chelate transition metal ions, directly scavenge reactive oxygen species or reduce lipid peroxidation by trapping the radical lipid alkoxyl [86].

3.2.3. *Enzymatic scavenging pathways*

As photosynthetic organisms, microalgae involve enzymatic and non-enzymatic mechanisms for ROS scavenging pathways under oxidative stress conditions. This is consistent with the results on the analysis of oxidative stress markers and the variations in the production of antioxidant compounds in *S. obliquus* after remediation of Pb (II). The antioxidant enzymes activities in Pb (II)-treated biomass was significantly higher than the control cells (Fig. 7). The difference between the means SOD activity of Pb (II) treated biomass and the control was

0.009155 ± 5.589e-005 ($p < 0.0001$, $t = 163.8$, $df = 4$), for the CAT activity, and 0.3106 ± 0.06859 ($p = 0.0106$, $t = 4.529$, $df = 4$) and of 0.001825 ± 0.0005359 ($P = 0.0272$, $t = 3.405$, $df = 4$) for APX activity. Whereas, it was of 0.0004814 ± 8.779e-005 ($p = 0.0054$, $t = 5.484$, $df = 4$) for GPX activity, and of 0.007809 ± 0.001787 ($p = 0.0120$, $t = 4.369$, $df = 4$) for GR activity. In previous studies, the activity of these antioxidant enzymes was also increased with increasing the metal concentrations [87,88], as well as the duration of stress exposure [89]. SOD is one of the most important antioxidant enzyme, ubiquitous in all subcellular compartments of aerobic organisms prone to ROS-mediated oxidative stress [90]. It provides the first line of defense against toxic effects of ROS by catalyzing the neutralization of 2 superoxide radicals, by the addition of 2 hydrogen ions to form H_2O_2 and O_2 at a very fast rate [91]. The increase in SOD activity observed in this study, is consistent with previous reports, in which a variety of microalgae species were treated with different HMs [89,92,93]. Likewise, a significant increase in CAT, POX and APX activities was evident in stressed cultures compared to the control. Similar findings were reported in *C. vulgaris*

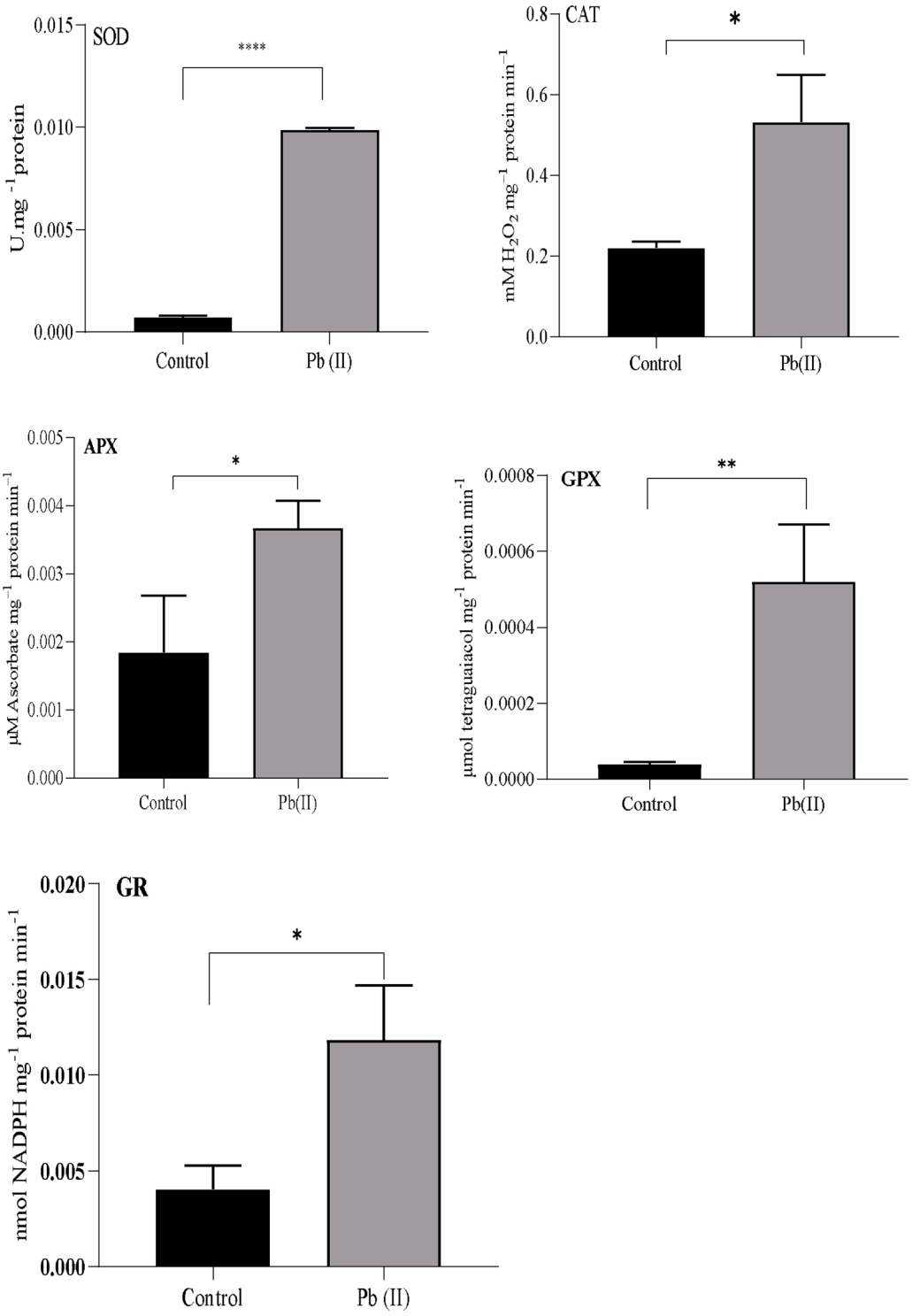

Fig. 7. Effect of Pb (II) exposure on the activity of the antioxidant enzyme of *S. obliquus*, the asterisk presents the significant difference between Pb (II)-exposed group and the control ($p < 0.05$). Data are presented as mean ± SD ($n = 3$).

under Cu (II) exposure [94], and in *Pavlova viridis* under Cobalt and Manganese stress condition [88]. CATs are tetrameric heme containing enzyme, with the potential to directly dismutate H_2O_2 into H_2O and O_2, and is indispensable for ROS detoxification during stressed conditions [95]. CAT is important in the removal of H_2O_2 generated in peroxisomes by oxidases involved in b-oxidation of fatty acids, photorespiration and purine catabolism [90]. Peroxidases are a class of enzymes that catalyze the oxidation of a substrate with H_2O_2, the substrates for some of the peroxidase enzymes include APX, cytochrome c (CcP), pyrogallol (PPX), and glutathione (GPX) [90,95]. Overall, the increase in the activity of these enzymes during the remediation of Pb (II) may reduce the concentrations of superoxyde and H_2O_2, minimizing therefore the risk of oxidative stress [92]. The glutathione reductase (GR) is a flavo-protein oxidoreductase, responsible for the reduction of GSSG to GSH, found in both prokaryotes and eukaryotes [96]. In the present study, its activity increased significantly in the presence of Pb (II) compared to the control. Previous reports also showed an increase by 92.38 % in the enzyme activity of GR in the freshwater microalgae *C. vulgaris* after exposure to Cd (II) ion at a concentration 1 ppm [97].

4. Conclusions

The current study provided new insights into the potential application, as well as the self-defense mechanisms of freshwater microalgae against oxidative stress generated during the phycoremediation of HMs. The screening of eight strains of freshwater microalgae for the tolerance to HMs Cu (II), Cr (VI), Pb (II), and Cd (II) showed that green microalgae *Scenedesmus obliquus* might withstand high Pb (II) contamination of 141 ppm (EC_{50}). The use of living cells of the chosen strain for the phycoremediation of Pb (II) in scaling-up culture conditions resulted in a bioremoval yield of more than 50 % from the EC_{50} concentration (141 ppm). The oxidative stress in Pb (II)-medium, highlighted by the increased oxidative stress markers H_2O_2 and MDA relative to the control was attenuated in *S. obliquus* cells through a combination of biochemical and enzymatic pathways. Indeed, a significant increase in the free radical scavenging activity, the content of proline, and polyphenol, as well as the enzymatic activities of SOD, CAT, POD, POX, and GR was achieved in cells grown in Pb (II)-medium compared to control medium. These results provide useful and relevant information that can be used to closely examine strategies for a targeted phycoremediation purpose.

CRediT authorship contribution statement

M. Danouche: Conceptualization, Methodology, Formal analysis, Writing - original draft, Visualization. **N. El Ghachtouli:** Supervision, Writing - review & editing, Project administration. **A. El Baouchi:** Formal analysis. **H. El Arroussi:** Supervision, Writing - review & editing, Validation, Resources, Funding acquisition, Project administration.

Declaration of Competing Interest

The authors reported no declarations of interest.

Acknowledgements

The authors gratefully acknowledge Moroccan Foundation for Advanced Science, Innovation and Research (MAScIR) for the financial and technical support. Authors wish to thank Chanda Mutale Joan for reviewing the quality of the English language in this article.

References

[1] V. Masindi, K.L. Muedi, Environmental contamination by heavy metals. Heavy metals, IntechOpen, London, 2018, pp. 115–132, https://doi.org/10.5772/intechopen.76082.
[2] R.G. Garrett, Natural sources of metals to the environment, Hum. Ecol. Risk Assess. 6 (6) (2000) 945–963, https://doi.org/10.1080/10807030091124383.
[3] K.S. Kumar, H.U. Dahms, E.J. Won, J.S. Lee, K.H. Shin, Microalgae - A promising tool for heavy metal remediation, Ecotoxicol. Environ. Saf. 113 (2015) 329–352, https://doi.org/10.1016/j.ecoenv.2014.12.019.
[4] C. Sanfeliu, J. Sebastià, R. Cristàfol, E. Rodríguez-Farré, Neurotoxicity of organomercurial compounds, Neurotox. Res. 5 (4) (2003) 283–305, https://doi.org/10.1007/BF03033386.
[5] P.B. Tchounwou, C.G. Yedjou, A.K. Patlolla, D.J. Sutton, Heavy metal toxicity and the environment, in: Molecular, Clinical and Environmental Toxicology, 101, Springer, Basel, 2012, pp. 133–164, https://doi.org/10.1007/978-3-7643-8340-4_6.
[6] N. Bouchelkia, L. Mouni, L. Belkhiri, A. Bouzaza, J.C. Bollinger, K. Madani, F. Dahmoune, Removal of lead (II) from water using activated carbon developed from jujube stones, a low-cost sorbent, Sep. Sci. Technol. 51 (10) (2016) 1645–1653, https://doi.org/10.1080/01496395.2016.1178289.
[7] E. Bazrafshan, L. Mohammadi, A. Ansari-Moghaddam, A.H. Mahvi, Heavy metals removal from aqueous environments by electrocoagulation process - A systematic review, J. Environ. Health Sci. Eng. 13 (1) (2015) 13–74, https://doi.org/10.1186/s40201-015-0233-8.
[8] N. Pugazhenthiran, S. Anandan, M. Ashokkuma, Removal of heavy metal from wastewater. Handbook of Ultrasonics and Sonochemistry, Springer, Singapore, 2016, pp. 1–27, https://doi.org/10.1007/978-981-287-278-4_58.
[9] J. Schneider, D.W. Bahnemann, Undesired role of sacrificial reagents in photocatalysis, J. Phys. Chem. Lett. 4 (20) (2013) 3479–3483, https://doi.org/10.1021/jz4018199.
[10] M.A. Barakat, New trends in removing heavy metals from industrial wastewater, Arab. J. Chem. 4 (4) (2011) 361–377, https://doi.org/10.1016/j.arabjc.2010.07.019.
[11] F. Fu, Q. Wang, Removal of heavy metal ions from wastewaters: A review, J. Environ. Manage. 92 (3) (2011) 407–418, https://doi.org/10.1016/j.jenvman.2010.11.011.
[12] K.V. Ajayan, M. Selvaraju, P. Unnikannan, P. Sruthi, Phycoremediation of Tannery Wastewater Using Microalgae *Scenedesmus* Species, Int. J. Phytoremed. 17 (10) (2015) 907–916, https://doi.org/10.1080/15226514.2014.989313.
[13] Y.K. Leong, J.S. Chang, Bioremediation of heavy metals using microalgae: Recent advances and mechanisms, Bioresour. Technol. 303 (2020) 122886, https://doi.org/10.1016/j.biortech.2020.122886.
[14] N.M. Jais, R.M.S.R. Mohamed, A.A. Al-Gheethi, M.K.A. Hashim, The dual roles of phycoremediation of wet market wastewater for nutrients and heavy metals removal and microalgae biomass production, Clean Technol. Environ. Policy 19 (1) (2017) 37–52, https://doi.org/10.1007/s10098-016-1235-7.
[15] E.W. Wilde, J.R. Benemann, Bioremoval of heavy metals by the use of microalgae, Biotechnol. Adv. 11 (4) (1993) 781–812, https://doi.org/10.1016/0734-9750(93)90003-6.
[16] E. Chmielewská, J. Medved', Bioaccumulation of heavy metals by green algae *Cladophora glomerata* in a refinery sewage lagoon, Croat. Chem. Acta 74 (1) (2001) 135–145. https://hrcak.srce.hr/131783.
[17] C.M. Monteiro, P.M.L. Castro, F.X. Malcata, Cadmium Removal by Two Strains of *Desmodesmus pleiomorphus* Cells, Water Air Soil Pollut. 208 (1–4) (2010) 17–27, https://doi.org/10.1007/s11270-009-0146-1.
[18] G. Dönmez, Z. Aksu, Removal of chromium (VI) from saline wastewaters by *Dunaliella species*, Process Biochem. 38 (5) (2002) 751–762, https://doi.org/10.1016/S0032-9592(02)00204-2.
[19] D. Kumar, A. Singh, J.P. Gaur, Mono-component versus binary isotherm models for Cu (II) and Pb (II) sorption from binary metal solution by the green alga *Pithophora oedogonia*, Bioresour. Technol. 99 (17) (2008) 8280–8287, https://doi.org/10.1016/j.biortech.2008.03.008.
[20] K. Verma, P.K. Kumar, S.V. Krishna, V. Himabindu, Phycoremediation of Sewage-Contaminated Lake Water Using Microalgae–Bacteria Co-Culture, Water Air Soil Pollut. 231 (2020) 1–16, https://doi.org/10.1007/s11270-020-04652-5.
[21] P.K. Kumar, S. Vijaya Krishna, K. Verma, K. Pooja, D. Bhagawan, V. Himabindu, Phycoremediation of sewage wastewater and industrial flue gases for biomass generation from microalgae, S. Afr. J. Chem. Eng. 25 (2018) 133–146, https://doi.org/10.1016/j.sajce.2018.04.006.
[22] A. Malik, Metal bioremediation through growing cells, Environ. Int. 30 (2) (2004) 261–278, https://doi.org/10.1016/j.envint.2003.08.001.
[23] S. Naveed, C. Li, X. Lu, S. Chen, B. Yin, C. Zhang, Y. Ge, Microalgal extracellular polymeric substances and their interactions with metal(loid)s: A review, Crit. Rev. Environ. Sci. Technol. 49 (19) (2019) 1769–1802, https://doi.org/10.1080/10643389.2019.1583052.
[24] J.D. García-García, R. Sánchez-Thomas, R. Moreno-Sánchez, Bio-recovery of non-essential heavy metals by intra- and extracellular mechanisms in free-living microorganisms, Biotechnol. Adv. 34 (5) (2016) 859–873, https://doi.org/10.1016/j.biotechadv.2016.05.003.
[25] H. Yan, G. Pan, Toxicity and bioaccumulation of copper in three green microalgal species, Chemosphere 49 (5) (2002) 471–476, https://doi.org/10.1016/S0045-6535(02)00285-0.
[26] S. Carfagna, N. Lanza, G. Salbitani, A. Basile, S. Sorbo, V. Vona, Physiological and morphological responses of Lead or Cadmium exposed *Chlorella sorokiniana* 211-8K (Chlorophyceae), SpringerPlus 2 (1) (2013) 1–7, https://doi.org/10.1186/2193-1801-2-147.
[27] J.T. Cirulis, J.A. Scott, G.M. Ross, Management of oxidative stress by microalgae, Can. J. Physiol. Pharmacol. 91 (1) (2013) 15–21, https://doi.org/10.1139/cjpp-2012-0249.
[28] R.Y. Stanier, R. Kunisawa, M. Mandel, G. Cohen-Bazire, Purification and properties of unicellular blue-green algae (order *Chroococcales*), Bacteriol. Rev. 35 (2) (1971) 171–205, https://doi.org/10.1128/mmbr.35.2.171-205.1971.

[29] E. Torres, A. Cid, C.H. A, J. Abalde, Effect of cadmium on growth, ATP content, carbon fixation and ultrastructure in the marine diatom *Phaeodactylum tricornutum* Bohlin, Water Air Soil Pollut. 117 (1–4) (2000) 1–14, https://doi.org/10.1023/A:1005121012697.
[30] B. Debelius, J.M. Forja, Á. DelValls, L.M. Lubián, Toxicity and bioaccumulation of copper and lead in five marine microalgae, Ecotoxicol. Environ. Saf. 72 (5) (2009) 1503–1513, https://doi.org/10.1016/j.ecoenv.2009.04.006.
[31] L. Lu, Y. Wu, H. Ding, W. Zhang, The combined and second exposure effect of copper (II) and chlortetracycline on fresh water algae, *Chlorella pyrenoidosa* and *Microcystis aeruginosa*, Environ. Toxicol. Pharmacol. 40 (1) (2015) 140–148, https://doi.org/10.1016/j.etap.2015.06.006.
[32] O.O. Oyebamiji, W.J. Boeing, F.O. Holguin, O. Ilori, O. Amund, Green microalgae cultured in textile wastewater for biomass generation and biodetoxification of heavy metals and chromogenic substances, Bioresour. Technol. Rep. 7 (2019) 100247, https://doi.org/10.1016/j.biteb.2019.100247.
[33] S. Tahira, S. Khan, S. Samrana, L. Shahi, I. Ali, W. Murad, Z. ur Rehman, A. Azizullah, Bio-assessment and remediation of arsenic (arsenite As-III) in water by *Euglena gracilis*, J. Appl. Phycol. 31 (1) (2019) 423–433, https://doi.org/10.1007/s10811-018-1593-0.
[34] V. Velikova, I. Yordanov, A. Edreva, Oxidative stress and some antioxidant systems in acid rain-treated bean plants protective role of exogenous polyamines, Plant Sci. 151 (1) (2000) 59–66, https://doi.org/10.1016/S0168-9452(99)00197-1.
[35] R.L. Heath, L. Packer, Photoperoxidation in isolated chloroplasts: I. Kinetics and stoichiometry of fatty acid peroxidation, Arch. Biochem. Biophys. 125 (1) (1968) 189–198, https://doi.org/10.1016/0003-9861(68)90654-1.
[36] H. Esterbauer, K.H. Cheeseman, Determination of aldehydic lipid peroxidation products: Malonaldehyde and 4-hydroxynonenal, in: Methods in Enzymology, 186, Academic Press, 1990, pp. 407–421, https://doi.org/10.1016/0076-6879(90)86134-H.
[37] A. Maadane, N. Merghoub, T. Ainane, H. El Arroussi, R. Benhima, S. Amzazi, Y. Bakri, I. Wahby, Antioxidant activity of some Moroccan marine microalgae: Pufa profiles, carotenoids and phenolic content, J. Biotechnol. 215 (2015) 13–19, https://doi.org/10.1016/j.jbiotec.2015.06.400.
[38] D. Cervantes-García, D. González-Mendoza, O. Grimaldo-Juárez, S. Aviles-Marin, Changes on proline, phenolics compounds and antioxidants status in *Euglena gracilis* exposed to copper, Afr. J. Microbiol. Res. 5 (28) (2011) 5127–5131, https://doi.org/10.5897/AJMR11.1096.
[39] L.S. Bates, R.P. Waldren, I.D. Teare, Rapid determination of free proline for water-stress studies, Plant Soil 39 (1) (1973) 205–207, https://doi.org/10.1007/BF00018060.
[40] G.K. Sahu, S.C. Sabat, Changes in growth, pigment content and antioxidants in the root and leaf tissues of wheat plants under the influence of exogenous salicylic acid, Braz. J. Plant Physiol. 23 (3) (2011) 209–218, https://doi.org/10.1590/S1677-04202011000300005.
[41] A. Mitsui, T. Ohta, Photooxidative consumption and photoreductive formation of ascorbic acid in green leaves, Plant Cell Physiol. 2 (1) (1961) 31–44, https://doi.org/10.1093/oxfordjournals.pcp.a077661.
[42] H. Bin Li, K.W. Cheng, C.C. Wong, K.W. Fan, F. Chen, Y. Jiang, Evaluation of antioxidant capacity and total phenolic content of different fractions of selected microalgae, Food Chem. 102 (3) (2007) 771–776, https://doi.org/10.1016/j.foodchem.2006.06.022.
[43] J.A. Vinson, Y. Hao, X. Su, L. Zubik, Phenol Antioxidant Quantity and Quality in Foods: Vegetables, J. Agric. Food Chem. 46 (9) (1998) 3630–3634, https://doi.org/10.1021/jf980295o.
[44] U.N. Rai, N.K. Singh, A.K. Upadhyay, S. Verma, Chromate tolerance and accumulation in *Chlorella vulgaris* L.: Role of antioxidant enzymes and biochemical changes in detoxification of metals, Bioresour. Technol. 136 (2013) 604–609, https://doi.org/10.1016/j.biortech.2013.03.043.
[45] A. Piotrowska-Niczyporuk, A. Bajguz, E. Zambrzycka, B. Godlewska-Żyłkiewicz, Phytohormones as regulators of heavy metal biosorption and toxicity in green alga *Chlorella vulgaris* (Chlorophyceae), Plant Physiol. Biochem. 52 (2012) 52–65, https://doi.org/10.1016/j.plaphy.2011.11.009.
[46] M.M.B. Bradford, Rapid and Sensitive Method for quantitation of microgram quantities of protein utilizing principle of protein-dye binding, Anal. Biochem. 72 (1–2) (1976) 248–254, https://doi.org/10.1016/j.sbi.2014.10.005.
[47] H.P. Misra, I. Fridovich, The role of superoxide anion in the autoxidation of epinephrine and a simple assay for superoxide dismutase, J. Biol. Chem. 247 (10) (1972) 3170–3175.
[48] H. Aebi, Catalase in Vitro, Methods Enzymol. 105 (1984) 121–126, https://doi.org/10.1016/S0076-6879(84)05016-3.
[49] H.M. Hemeda, B.P. Klein, Effects of naturally occurring antioxidants on peroxidase activity of vegetable extracts, J. Food Sci. 55 (1) (1990) 184–185, https://doi.org/10.1111/j.1365-2621.1990.tb06048.x.
[50] B.N. Tripathi, S.K. Mehta, A. Amar, J.P. Gaur, Oxidative stress in *Scenedesmus* sp. during short- and long-term exposure to Cu2+ and Zn2+, Chemosphere 62 (4) (2006) 538–544, https://doi.org/10.1016/j.chemosphere.2005.06.031.
[51] F. González, E. Romera, A. Ballester, M.L. Blázquez, J.Á. Muñoz, C. García-Balboa, Algal biosorption and biosorbents. Microbial Biosorption of Metals, Springer, Dordrecht, 2011, pp. 159–178, https://doi.org/10.1007/978-94-007-0443-5.
[52] J.P. Gaur, L.C. Rai, Heavy metal tolerance in algae. Algal Adaptation to Environmental Stresses, Springer, Berlin, 2001, pp. 363–388, https://doi.org/10.1007/978-3-642-59491-5_12.
[53] S. Shanab, A. Essa, E. Shalaby, Bioremoval capacity of three heavy metals by some microalgae species (Egyptian isolates), Plant Signal. Behav. 7 (3) (2012) 392–399, https://doi.org/10.4161/psb.19173.
[54] K.V. Ajayan, M. Selvaraju, Heavy metal induced antioxidant defense system of green microalgae and its effective role in phycoremediation of tannery effluent, Pak. J. Biol. Sci. 15 (22) (2012) 1056–1062, https://doi.org/10.3923/pjbs.2012.1056.1062.
[55] J. Jena, N. Pradhan, V. Aishvarya, R.R. Nayak, B.P. Dash, L.B. Sukla, P.K. Panda, B. K. Mishra, Biological sequestration and retention of cadmium as CdS nanoparticles by the microalga *Scenedesmus*-24, J. Appl. Phycol. 27 (6) (2015) 2251–2260, https://doi.org/10.1007/s10811-014-0499-8.
[56] L.E. de-Bashan, Y. Bashan, Immobilized microalgae for removing pollutants: Review of practical aspects, Bioresour. Technol. 101 (6) (2010) 1611–1627, https://doi.org/10.1016/j.biortech.2009.09.043.
[57] H. Cameron, M.T. Mata, C. Riquelme, The effect of heavy metals on the viability of *Tetraselmis marina* AC16- MESO and an evaluation of the potential use of this microalga in bioremediation, PeerJ (2018), https://doi.org/10.7717/peerj.5295.
[58] C.M. Monteiro, S.C. Fonseca, P.M.L. Castro, F.X. Malcata, Toxicity of cadmium and zinc on two microalgae, *Scenedesmus obliquus* and *Desmodesmus pleiomorphus*, from Northern Portugal, J. Appl. Phycol. 23 (1) (2011) 97–103, https://doi.org/10.1007/s10811-010-9542-6.
[59] D.M. Anderson, F.M.M. Morel, Copper sensitivity of *Gonyaulax tamarensis*1, Limnol. Oceanogr. 23 (2) (1978) 283–295, https://doi.org/10.4319/lo.1978.23.2.0283.
[60] N.M. Franklin, J.L. Stauber, R.P. Lim, Development of flow cytometry-based algal bioassays for assessing toxicity of copper in natural waters, Environ. Toxicol. Chem. 20 (1) (2001) 160–170, https://doi.org/10.1002/etc.5620200118.
[61] J.O.O. Nacorda, M.R. Martinez-Goss, N.K. Torreta, Bioremoval and bioreduction of chromium (VI) by the green microalga, *Chlorella vulgaris* Beij., isolated from laguna de bay, Philippines, Philippine J. Sci. 139 (2) (2010) 181–188.
[62] J.O. Nacorda, M.R. Martinez-Goss, N.K. Torreta, F.E. Merca, Metal resistance and removal by two strains of the green alga, *Chlorella vulgaris* Beijerinck, isolated from Laguna de Bay, Philippines, J. Appl. Phycol. 19 (6) (2007) 701–710, https://doi.org/10.1007/s10811-007-9216-1.
[63] R. Jobby, P. Jha, A.K. Yadav, N. Desai, Biosorption and biotransformation of hexavalent chromium [Cr(VI)]: A comprehensive review, Chemosphere 207 (2018) 255–266, https://doi.org/10.1016/j.chemosphere.2018.05.050.
[64] L.H.T. Dao, J. Beardall, Effects of lead on growth, photosynthetic characteristics and production of reactive oxygen species of two freshwater green algae, Chemosphere 147 (2016) 420–429, https://doi.org/10.1016/j.chemosphere.2015.12.117.
[65] T.-L. Pham, T.-S. Dao, H. Bui, T. Pham, T. Ngo, H. Bui, Lipid Production Combined with Removal and Bioaccumulation of Pb by *Scenedesmus* sp. Green Alga, Pol. J. Environ. Stud. 29 (2) (2020) 1785–1791, https://doi.org/10.15244/pjoes/109277.
[66] E.R.S. Dewi, R. Nuravivah, Potential of Microalgae *Chlorella vulgaris* As Bioremediation Agents of Heavy Metal Pb (Lead) On Culture Media, In E3S Web of Conferences 31 (2018) 3–6, https://doi.org/10.1051/e3sconf/20183105010.
[67] B. Pawlik-Skowrońska, When adapted to high zinc concentrations the periphytic green alga *Stigeoclonium tenue* produces high amounts of novel phytochelatin-related peptides, Aquat. Toxicol. 62 (2) (2003) 155–163, https://doi.org/10.1016/S0166-445X(02)00080-2.
[68] S. Le Faucheur, R. Behra, L. Sigg, Phytochelatin induction, cadmium accumulation, and algal sensitivity to free cadmium ion in *Scenedesmus vacuolatus*, Environ. Toxicol. Chem. 24 (7) (2005) 1731–1737, https://doi.org/10.1897/04-394R.1.
[69] M. Pérez-Rama, C.H. López, J.A. Alonso, E.T. Vaamonde, Class III metallothioneins in response to cadmium toxicity in the marine microalga *Tetraselmis suecica* (Kylin) Butch, Environ. Toxicol. Chem. 20 (9) (2001) 2061–2066, https://doi.org/10.1002/etc.5620200927.
[70] A. Piotrowska-Niczyporuk, A. Bajguz, M. Talarek, M. Bralska, E. Zambrzycka, The effect of lead on the growth, content of primary metabolites, and antioxidant response of green alga *Acutodesmus obliquus* (Chlorophyceae), Environ. Sci. Pollut. Res. 22 (23) (2015) 19112–19123, https://doi.org/10.1007/s11356-015-5118-y.
[71] V. Alexieva, I. Sergiev, S. Mapelli, E. Karanov, The effect of drought and ultraviolet radiation on growth and stress markers in pea and wheat, Plant Cell Environ. 24 (12) (2001) 1337–1344, https://doi.org/10.1046/j.1365-3040.2001.00778.x.
[72] O. Blokhina, E. Virolainen, K.V. Fagerstedt, Antioxidants, oxidative damage and oxygen deprivation stress: A review, Ann. Bot. 91 (2) (2003) 179–194, https://doi.org/10.1093/aob/mcf118.
[73] M. Choudhary, U.K. Jetley, M. Abash Khan, S. Zutshi, T. Fatma, Effect of heavy metal stress on proline, malondialdehyde, and superoxide dismutase activity in the cyanobacterium *Spirulina platensis*-S5, Ecotoxicol. Environ. Saf. 66 (2) (2007) 204–209, https://doi.org/10.1016/j.ecoenv.2006.02.002.
[74] T. Belghith, K. Athmouni, K. Bellassoued, A. El Feki, H. Ayadi, Physiological and biochemical response of *Dunaliella salina to* cadmium pollution, J. Appl. Phycol. 28 (2) (2016) 991–999, https://doi.org/10.1007/s10811-015-0630-5.
[75] P. Siddhuraju, K. Becker, Antioxidant properties of various solvent extracts of total phenolic constituents from three different agroclimatic origins of drumstick tree (*Moringa oleifera Lam.*) leaves, J. Agric. Food Chem. 51 (8) (2003) 2144–2155, https://doi.org/10.1021/jf020444+.
[76] S. Siripornadulsil, S. Traina, D.P.S. Verma, R.T. Sayre, Molecular mechanisms of proline-mediated tolerance to toxic heavy metals in transgenic microalgae, Plant Cell 14 (11) (2002) 2837–2847, https://doi.org/10.1105/tpc.004853.
[77] S. Hayat, Q. Hayat, M.N. Alyemeni, A.S. Wani, J. Pichtel, A. Ahmad, Role of proline under changing environments: A review, Plant Signal. Behav. 7 (11) (2012) 1456–1466, https://doi.org/10.4161/psb.21949.
[78] A. Strejckova, M. Dvorak, B. Klejdus, O. Krystofova, J. Hedbavny, V. Adam, D. Huska, The strong reaction of simple phenolic acids during oxidative stress caused by nickel, cadmium and copper in the microalga *Scenedesmus quadricauda*, New Biotechnol. 48 (2019) 66–75, https://doi.org/10.1016/j.nbt.2018.07.004.

[79] R. Ruciska-Sobkowiak, P.M. Pukacki, Antioxidative de fense sys tem in lu pin roots ex posed to in creas ing con cen tra tions of lead, Acta Physiol. Plant. 28 (4) (2006) 357–364, https://doi.org/10.1007/s11738-006-0032-z.
[80] S. Singh, S. Eapen, S.F. D'Souza, Cadmium accumulation and its influence on lipid peroxidation and antioxidative system in an aquatic plant, *Bacopa monnieri* L, Chemosphere 62 (2) (2006) 233–246, https://doi.org/10.1016/j.chemosphere.2005.05.017.
[81] G. Noctor, C.H. Foyer, Ascorbate and glutathione: keeping active oxygen under control, Ann. Rev. Plant Biol. 49 (1) (1998) 249–279, https://doi.org/10.1146/annurev.arplant.49.1.249.
[82] N. Smirnoff, Ascorbic acid: metabolism and functions of a multi-facetted molecule, Curr. Opin. Plant Biol. 3 (3) (2000) 229–235, https://doi.org/10.1016/s1369-5266(00)80070-9.
[83] C.E. Thomas, L.R. McLean, R.A. Parker, D.F. Ohlweiler, Ascorbate and phenolic antioxidant interactions in prevention of liposomal oxidation, Lipids 27 (7) (1992) 543–550, https://doi.org/10.1007/BF02536138.
[84] S.M. Hamed, S. Selim, G. Klöck, H. AbdElgawad, Sensitivity of two green microalgae to copper stress: Growth, oxidative and antioxidants analyses, Ecotoxicol. Environ. Saf. 144 (2017) 19–25, https://doi.org/10.1016/j.ecoenv.2017.05.048.
[85] J. Kováčik, B. Klejdus, J. Hedbavny, M. Bačkor, Effect of copper and salicylic acid on phenolic metabolites and free amino acids in *Scenedesmus quadricauda* (Chlorophyceae), Plant Sci. 178 (3) (2010) 307–311, https://doi.org/10.1016/j.plantsci.2010.01.009.
[86] R. Rodrigo, M. Libuy, Modulation of plant endogenous antioxidant systems by polyphenols. Polyphenols in Plants, Academic Press, 2014, pp. 65–85, https://doi.org/10.1016/B978-0-12-397934-6.00005-X.
[87] J. Cheng, H. Qiu, Z. Chang, Z. Jiang, W. Yin, The effect of cadmium on the growth and antioxidant response for freshwater algae *Chlorella vulgaris*, SpringerPlus 5 (1) (2016) 1–8, https://doi.org/10.1186/s40064-016-2963-1.
[88] M. Li, Q. Zhu, C. Wei Hu, L. Chen, Z. Li Liu, Z. Ming Kong, Cobalt and manganese stress in the microalga *Pavlova viridis* (Prymnesiophyceae): effects on lipid peroxidation and antioxidant enzymes, J. Environ. Sci. 19 (11) (2007) 1330–1335, https://doi.org/10.1016/S1001-0742(07)60217-4.
[89] Q.L. Zhu, S.N. Guo, F. Wen, X.L. Zhang, C.C. Wang, L.F. Si, J.L. Zheng, J. Liu, Transcriptional and physiological responses of *Dunaliella salina* to cadmium reveals time-dependent turnover of ribosome, photosystem, and ROS-scavenging pathways, Aquat. Toxicol. 207 (2019) 153–162, https://doi.org/10.1016/j.aquatox.2018.12.007.
[90] S.S. Gill, N. Tuteja, Reactive oxygen species and antioxidant machinery in abiotic stress tolerance in crop plants, Plant Physiol. Biochem. 48 (12) (2010) 909–930, https://doi.org/10.1016/j.plaphy.2010.08.016.
[91] J.F. Gonçalves, A.G. Becker, D. Cargnelutti, L.A. Tabaldi, L.B. Pereira, V. Battisti, R. M. Spanevello, V.M. Morsch, F.T. Nicoloso, M.R.C. Schetinger, Cadmium toxicity causes oxidative stress and induces response of the antioxidant system in cucumber seedlings, Braz. J. Plant Physiol. 19 (3) (2007) 223–232, https://doi.org/10.1590/S1677-04202007000300006.
[92] S.M. Hamed, G. Zinta, G. Klöck, H. Asard, S. Selim, H. AbdElgawad, Zinc-induced differential oxidative stress and antioxidant responses in *Chlorella sorokiniana* and *Scenedesmus acuminatus*, Ecotoxicol. Environ. Saf. 140 (2017) 256–263, https://doi.org/10.1016/j.ecoenv.2017.02.055.
[93] S. Mahjouri, A. Movafeghi, B. Divband, M. Kosari-Nasab, Toxicity impacts of chemically and biologically synthesized CuO nanoparticles on cell suspension cultures of *Nicotiana tabacum*, Plant Cell Tissue Organ Culture (PCTOC) 135 (2) (2018) 223–234, https://doi.org/10.1007/s11240-018-1458-x.
[94] R. Kebeish, Y. El-Ayouty, A. Husain, Effect of copper on growth, bioactive metabolites, antioxidant enzymes and photosynthesis-related gene transcription in *Chlorella vulgaris*, World J. Biol. Biol. Sci. 2 (2) (2014) 34–43. http://wsrjournals.org/journal/wjbbs.
[95] N. Garg, G. Manchanda, ROS generation in plants: Boon or bane? Plant Biosyst. 143 (1) (2009) 81–96, https://doi.org/10.1080/11263500802633626.
[96] M.C. Romero-Puertas, F.J. Corpas, L.M. Sandalio, M. Leterrier, M. Rodríguez-Serrano, L.A. Del Río, J.M. Palma, Glutathione reductase from pea leaves: Response to abiotic stress and characterization of the peroxisomal isozyme, New Phytol. 170 (1) (2006) 43–52, https://doi.org/10.1111/j.1469-8137.2006.01643.x.
[97] V.K. Randhawa, F. Zhou, X. Jin, C. Nalewajko, D.J. Kushner, Role of oxidative stress and thiol antioxidant enzymes in nickel toxicity and resistance in strains of the green alga *Scenedesmus acutus* f. alternans, Can. J. Microbial. 47 (11) (2001) 987–993, https://doi.org/10.1139/cjm-47-11-987.

Chapitre II

Mechanisms of lead (II) phycoremediation using Scenedesmus obliquus: Cells physicochemical properties, biochemical composition and metabolomic profiling

RÉSUMÉ

L'objectif de la présente étude était d'étudier les mécanismes impliqués dans la phycoremédiation de Pb(II) par la microalgue présélectionnée *S. obliquus*, et d'examiner les propriétés physico-chimiques et les réponses physiologiques, biochimiques et métaboliques de cette souche au stress métallique.

Tout d'abord, l'influence des ions Pb(II) sur la croissance, la viabilité et la taille des cellules ont été analysée en utilisant respectivement l'hémocytomètre, la cytométrie de flux et le zétasizer. Les résultats ont montré une inhibition significative du taux de croissance. Néanmoins, il n'y avait pas de différence significative en termes de viabilité et de la taille des cellules. Afin d'évaluer la récupération du Pb(II) dans les cellules de *S. obliquus*, une analyse thermogravimétrique des cellules témoins et des cellules chargées en Pb(II) a été réalisée à la fin du processus de phycoremédiation. Pour la discrimination entre l'élimination intracellulaire et extracellulaire, une extractions chimiques des ions adsorbée a la surface cellulaire a été effectuer, puis la mesure de la concentration de Pb(II) intracellulaire a été analysé par ICP après digestion de la biomasse. Les poids résiduels des cellules témoins et des cellules chargées en Pb(II), analysé par l'ATG, étaient respectivement de 31,34 % et 57,8 %, ce qui indique la prise des ions de Pb(II) par les cellules. Ensuite, le résultat de l'analyse par ICP a indiqué l'implication de deux mécanismes : biosorption (85,5%) et bioaccumulation (14,5%). L'interaction des ions Pb(II) avec la paroi cellulaire a été ainsi caractérisée par des techniques d'imagerie (MEB), des techniques d'analyse spectroscopique (EDX et FTIR), et que des mesures du potentiel zêta, de la charge au point zéro et des analyses des caractéristiques physicochimiques de la surface des cellules par l'angle de contact. Les résultats obtenus ont confirmé l'implication des interactions chimiques et électrostatiques entre les macromolécules qui composent la surface cellulaire et les ions de Pb(II) en solution.

En ce qui concerne l'impact de la bioaccumulation de Pb(II) sur la composition biochimique de *S. obliquus*, une augmentation significative de la teneur en caroténoïdes et en lipides a été montrée. Alors que, la teneur en chlorophylle, en carbohydrates, et en protéines a diminué. Enfin, l'analyse du profil métabolomique par GC-MS, a révélé une augmentation de l'abondance relative des esters méthyliques d'acides gras, des alcanes, des composés aromatiques et des stérols. En revanche, le contenu en alcènes et d'acides gras monoinsaturés a diminué.

Sur la base de ces résultats, nous avons pu déduire que *S. obliquus* a modifié son métabolisme biochimique, en particulier la biosynthèse des lipides, afin d'adapter ses propriétés membranaires, empêchant ainsi l'effet toxique de la bioaccumulation intracellulaire des ions Pb (II) qui pourraient causer divers dommages.



Mechanisms of lead (II) phytoremediation using Scenedesmus obliquus: Cells physicochemical properties, biochemical composition and metabolomic profiling

Journal:	*International Journal of Phytoremediation*
Manuscript ID	Draft
Manuscript Type:	Original Article
Date Submitted by the Author:	n/a
Complete List of Authors:	Danouche, Mohammed; MASCIR, green Biotechnology; USMBA FSTF, Ghachtouli, N EL; USMBA FSTF a.aasfar@mascir.ma, A; MASCIR bennis, I; MASCIR ELARROUSSI, Hicham; MASCIR,
Keywords:	Scenedesmus obliquus; Pb(II)-phycoremediation; Physicochemical properties; Biochemical composition; Metabolomic profiling

SCHOLARONE™
Manuscripts

Mechanisms of lead (II) phycoremediation using *Scenedesmus obliquus*: Cells physicochemical properties, biochemical composition and metabolomic profiling

Danouche M.[a,b]*, El Ghachtouli N.[b], Aasfar A.[a], Bennis I.[a], El Arroussi H.[a,c]

[a] *Green Biotechnology Center, Moroccan Foundation for Advanced Science, Innovation and Research (MAScIR), Rabat, Morocco.*

[b] *Microbial Biotechnology and Bioactive Molecules Laboratory, Sciences and Technologies Faculty, Sidi Mohamed Ben Abdellah University, Fez, Morocco.*

[c] *AgroBioScience (AgBS), Mohammed VI Polytechnic University (UM6P), Ben Guerir, Morocco.*

***Corresponding author**: Danouche Mohammed

Address: Microbial Biotechnology and Bioactive Molecules Laboratory, Faculty of Sciences and Techniques,

Sidi Mohamed Ben Abdellah University, Route Immouzer, P. O. Box 2202, Fez, Morocco

E-mail: mohammed.danouche@usmba.ac.ma

Abstract

This study highlights the mechanisms of Pb(II)-phycoremediation using the Pb(II) tolerant strain of *Scenedesmus obliquus*. First, monitoring of cell growth kinetics in control and Pb(II)-doped medium revealed significant growth inhibition, while the analyses through flow cytometry and Zetasizer revealed no difference in cell viability and size. Residual weights of control and Pb(II)-loaded cells assessed by thermogravimetric analysis, were 31.34% and 57.8%, respectively, indicating the uptake of Pb(II) into *S. obliquus* cells. Next, the use of chemical extraction to distinguish between the intracellular and extracellular uptake indicated the involvement of both biosorption (85.5%) and bioaccumulation (14.5%) mechanisms. Biosorption interaction of Pb(II) ions and the cell wall was confirmed using SEM-EDX, FTIR, zeta potential, zero-charge pH, and contact angle analyses. Besides, the biochemical characterization of control and Pb(II)-loaded cells revealed that the bioaccumulation of Pb(II) induces significant increases in the carotenoids and lipids content, although decreases in the chlorophyll, carbohydrates, and proteins content. Finally, the metabolomic analysis indicated an increase in the relative abundance of fatty acid methyl esters, alkanes, aromatic compounds, and sterols. However, the alkenes and monounsaturated fatty acids decreased. Such metabolic adjustment may represent an adaptive strategy, that preventing high Pb(II)-bioaccumulation in cellular compartments.

Graphical Abstract

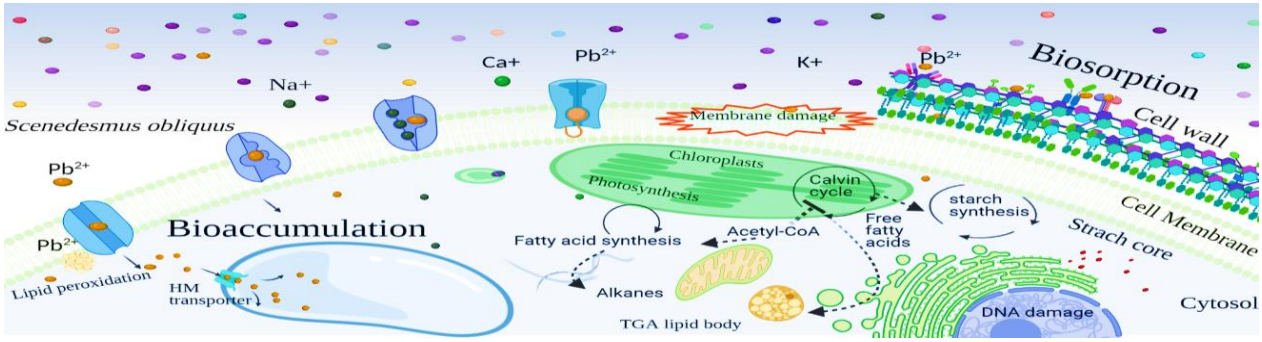

Keywords: *Scenedesmus obliquus*; Pb(II)-phycoremediation; Physicochemical properties; Biochemical composition; Metabolomic profiling.

1. Introduction

Since the Earth formation, nearly all of the heavy metals (HMs) that we know today have been naturally present in trace amounts and have been recycled biogeochemically between the environmental compartments, through several biotic and abiotic biogeochemical processes (Garrett, 2000). However, with global expansion, anthropogenic activities including mining, excessive use of fertilizers in agriculture, and mismanagement of hazardous wastes have increased the redistribution of HMs among environmental compartments, resulting in increased inorganic pollution of water and soil (Ashraf *et al.*, 2014). Indeed, because they are not biodegradable, HMs can persist in ecosystems and can bioaccumulate into organisms of different trophic levels, causing various signs of toxicity to all life forms(Yan *et al.*, 2018). In fact, Mercury (Hg(II)), cadmium (Cd(II)), lead (Pb(II)), arsenic (As(III)), and chromium (Cr(VI) are among the most harmful pollutants (Kumar *et al.*, 2015). According to the regulations of the U.S. Environmental Protection Agency (EPA), the maximum contamination limits of these HMs are 0.002, 0.005, 0.015, 0.01, and 0.1 mg L^{-1}, respectively (USEPA, 2016). Unfortunately, their actual concentrations in effluents from various industries are generally higher than these standards requiring, therefore, an adequate treatment before their release into the environment (Selvi *et al.*, 2019). For example, the presence of Pb(II)ions in aquatic ecosystems, even at low concentrations causes a wide range of toxic effects on the physiological, biochemical, and metabolic functions of the exposed organism (microorganisms, aquatic plant, and animal), as well as complications for human health due to direct exposure or the consumption of contaminated food or water (Lee *et al.*, 2019).

Worldwide, water pollution with HMs has recently piqued the interest of scientists, conservationists, and politicians. Indeed, various techniques, including precipitation, adsorption, nanofiltration, ultrafiltration, reverse osmosis, electrochemical technologies, and biological approaches have been applied to remove HMs from contaminated water bodies (Kumar *et al.*, 2015). Because bioremediation approaches are effective, environmentally friendly, and inexpensive, they appear to be competitive to the conventional physicochemical procedures (Chibueze *et al.*, 2016). The application of microalgae in wastewater treatment has recently emerged as a promising solution due to its advantages over the other conventional methods (Wollmann *et al.*, 2019). To differentiate the use of microalgae from the other biological approaches, this (bio)procedure is called phycoremediation (Jais *et al.*, 2017). It has been documented in the literature that phycoremediation has been applied to remove Pb(II) ions from contaminated waters. Nevertheless, a number of these studies only highlight the potential application of inactive biomass of microalgae species as biosorbents (Flouty and Estephane, 2012; Kumar *et al.*, 2008), while only a few researchers have described the potential application of living microalgae in the bioremoval of Pb(II) ions (Liyanage *et al.*, 2020; Pham *et al.*, 2020; Piotrowska-Niczyporuk *et al.*, 2015). although the use of growing cells is more advantageous because it avoids the steps of cultivation, harvesting, drying, pre-treatment and conservation of biomass before their use as biosorbents (Danouche *et al.*, 2021a). In addition, the use of growing microalgae will improve removal efficiency through both metabolism-independent (biosorption) and metabolism-dependent (bioaccumulation) mechanisms (Kumar *et al.*, 2015). On the other hand, under metal-stressed conductions, living cells of microalgae can produce various high-value substances such as polymeric substances, as well as proteins, pigments, and lipids (Liu *et al.*, 2016). Thus, they offer a real possibility of exploitation in various industrial sectors, mainly in the field of renewable energies (Ansari *et al.*, 2019; Liu *et al.*, 2016). Hence, understanding the influence of HMs on the biochemical composition of green microalgae is critical for a targeted valorization of the biomass and/or the metabolites produced during the phycoremediation process. Several studies have investigated the economic aspects of combining wastewater treatment and the

valorization of the biomass into value-added products, especially lipids, as a source of third-generation biofuels (Ansari *et al.*, 2019; Randrianarison and Ashraf, 2017). The use of omics approaches such as metabolomics approaches can help to advance the insight of the phycoremediation mechanism (Danouche *et al.*, 2021b). As well as the valorization of high-value-added metabolites produced under metallic stress (Jamers *et al.*, 2009; Salama *et al.*, 2019). The present study aims to investigate the phycoremediation mechanism of Pb(II) ions using living cells of Pb(II)-tolerant strain of *S. obliquus*. Firstly, the physicochemical properties of the cells before and after Pb(II) phycoremediation were evaluated to investigate the extracellular elimination mechanisms between the cell surface and Pb(II) ions in solution. Thereafter, the changes in biochemical composition and the metabolomic profiling of cells were examined after Pb(II) bioaccumulation in order to identify the resistance strategies of this strain to Pb(II) ions.

2. Material and methods

2.1 Microalgae strain and culture condition

The green microalgae *S. obliquus* used in this study has been previously selected as a Pb(II)-tolerant strain (Danouche *et al.*, 2020). Its pure culture was sub-cultured at regular times in BG_{11} medium (1.5 g $NaNO_3$, 40 mg K_2HPO_4, 36 mg $CaCl_2$ $2H_2O$, 6 mg ammonium citrate monohydrate, 6 mg ammonium ferric citrate, 1 mg ethylenediaminetetraacetic acid (EDTA), 2.86 mg H_3BO_3, 1.81 mg $MnCl_2$ $4H_2O$, 0.22 mg $ZnSO_4$ $7H_2O$, 0.39 mg $NaMoO_4$ $5H_2O$, 0.079 mg $CuSO_4$ $5H_2O$, 0.050 mg $CoCl_2$ $6H_2O$ in 1 L of distilled water) (Allen 1968). The experiments were performed with a pre-culture of *S. obliquus* obtained at the exponential phase. The biomass was firstly recovered by centrifugation at 4700 rpm for 10 min. Then, the pellet was diluted in Erlenmeyer flasks containing 100 mL of BG_{11} medium for negative control and Pb(II)-doped medium at the concentration of EC_{50} = 141 mg L^{-1} corresponding to the half-maximal effective concentration (Danouche *et al.*, 2020). The initial optical density (OD) of all experiments was adjusted to 0.350 ± 0.025 at A_{680nm} using Ultrospec™ 3100 pro UV-Visible spectrophotometer, corresponding to 2 x 10^6 cells mL^{-1} equivalent. Flasks were incubated for 23 days under controlled conditions at 25 ± 2 ºC, under rotary shaking conditions at 150 rpm, and 10 h:14 h light-dark cycle.

2.2 Growth monitoring, membrane integrity and cells size

***Growth monitoring*:** the growth kinetics of *S. obliquus* in control and Pb(II)-doped medium were monitored spectrophotometrically at two-day intervals. The linear relationship between microalgal density (N, in cells per milliliter) and OD_{680} was determined as reported by Zhou *et al.*, (2012) using a CKX41 Olympus light microscope and a Malassez counting chamber with a depth of 0.2 mm. The calibration curve was as eq (1):

$Y = 7.\ 10^6\ X + 2083$ ($R^2 = 0.98$) eq (1)

Where Y is the number of cells (C mL^{-1}) and X denotes the OD at 680 nm. The specific growth rate (SGR) (μ, in day^{-1}) was calculated in the exponential phase using eq (2), as described by Aguilar-Ruiz *et al.*, (2020).

$$\mu = \frac{\text{Ln X2} - \text{Ln X1}}{t2 - t1} \quad \text{eq (2)}$$

Where μ is the growth rate and X_2, X_1 represents the microalgal biomass concentration at t_2 and t_1 (time), respectively.

Membrane integrity: Membrane integrity of *S. obliquus* cells grown in BG11 control medium and Pb(II)-doped medium was performed as described below da Silva *et al.*, (2009). An amount of 10^6 cells were centrifuged at 4700 rpm for 10 min. The pellet was then washed with

phosphate buffer solution (PBS, pH 7.0). Then, cells were exposed to 10 µg mL^{-1} of propidium iodide (PI, Ref 81845 FLUKA). The reaction was maintained in the dark for 10 min and directly analyzed by BD FACSCalibur Flow Cytometry (FCM) System (BD Biosciences). PI is a fluorescent intercalating agent that intersperses with double-stranded nucleic acids to produce red fluorescence when excited by blue light. Undamaged membranes of living microalgae are impermeable to PI. While, due to the loss in the membrane integrity, the dye can be input to the intracellular compartment of stressed cells (Suman *et al.*, 2015). Heat-inactivated cells were primed for positive control and processed under the same conditions. The fluorescent emission of PI was collected from ~ 3000 events per sample. The PI was excited at 488 nm and measured at 585 nm (FL_2 channel) using the FACSCalibur optical system. Parameter settings were adjusted to place the non-stained population in the negative area FL_2/FL_1 as an autofluorescence control. Data were processed with CELLQuest Pro software (Becton Dickinson) and expressed as fluorescence arbitrary units. The cell viability was expressed as the percentage of cells viable versus the total number of cells acquired (Asghari *et al.*, 2019; Urrutia *et al.*, 2019).

***Cells size**:* effect of Pb(II) ions on the osmotic state of *S. obliquus* cultured in control and Pb(II)-doped medium was carried out based on the change in cell size, using the Malvern Zetasizer Zeta-Nano (England), working with laser doppler electrophoresis technique. The method of dynamic light scattering (DLS) was used to determine the changes in cells size after Pb(II)-phycoremediation (Xia *et al.*, 2017).

2.3 Pb(II)-phycoremediation mechanism by *S. obliquus*

Pb(II)-uptake (biosorption and/or bioaccumulation) was firstly evaluated using thermogravimetric analysis (TGA). The changes in weight of samples while heated to a constant temperature under an inert atmosphere was measured using TGA Q500 - Emballage - TA Instruments - USA. Equal weight of biomass samples was first placed in a platinum pan, then heated up to 600 ºC under nitrogen-controlled atmosphere, at a heating rate of 10 ºC min^{-1} (Sudhakar and Premalatha, 2015). Finally, the TGA, as well as the difference thermogravimetry ratio (DTG) profiles of the control and Pb(II)-loaded cells was plotted using excel software.

Furthermore, the discrimination between the intracellular biosorption and the extracellular bioaccumulation of Pb(II) ions was carried out using chemical extractions as reported by Hassler *et al.*, (2004). In fact, after the phycoremediation process, the biomass was recovered by centrifugation (4700 rpm for 10 min). and the pellet samples were washed with EDTA solution (5.10^{-3} M; pH 6.0). Dried biomass samples (washed and unwashed) were then digested with 65% HNO_3 and 30% H_2O_2 in ACCblock digital dry bath (Labnet) for 40 min at 140 ºC. The concentration of Pb(II) ions in the mineralized samples was measured using a Thermofisher 7000 series inductively coupled plasma optical emission spectrometer (ICP-AES). Thus, the Pb(II)-bioadsorbed onto the cells' surface was determined by subtracting the intracellular Pb(II) concentration from the total Pb(II) removed (Huang *et al.*, 2004).

For further insight into the Pb(II)-bioremoval mechanism using living cells of *S. obliquus*, the intracellular concentration of Na^+, K^+, and their ratios were thereby analyzed. The decomposition of samples and the measurement of Na^+, K^+ concentration was performed as previously described for the determination of Pb(II) concentration in the resulting biomass.

2.4 Physicochemical characterization of *S. obliquus* cells and metal interaction

Scanning electron microscope coupled with Energy-dispersive X-ray spectroscopy (SEM-EDX): SEM (JSM-IT500 InTouchScope™) was used to visualize the cells' surface morphology of

S. obliquus before and after Pb(II)-biosorption, while the EDX was employed to analyze the elemental composition from the imaged area. The analytical conditions were as follows: Signal SED, magnification of x1 000 - x55 000, landing voltage of 3.0 kV, work distance of 10.1 mm, at high vacuum mode.

Fourier Transform InfraRed spectroscopy (FTIR) analysis*:* in order to predict the functional groups on the cell wall of *S. obliquus.* The biomass from the control and Pb(II)-doped medium were analyzed using FTIR spectroscopy. Salt pellets were firstly prepared using 1 mg of dried biomass and 149 mg of KBr and then compressed at 40 kN for 5 min to form pellets. Finally, thirty-two scans were performed at a range of 400 to 4000 cm^{-1}, with 4 cm^{-1} of resolution for each sample, using the ABB Bomem FTLA 2000 spectrometer analyzer (Das et al., 2016).

Zeta potential and Zero-point charge measurement*:* in order to determine the zeta potentials of the biosorbents as a function of pH from 3 to 10. A volume of 100 mL of microalgae suspension was harvested by centrifugation (4700 rpm for 10 min), and then the pellet was resuspended in 10 mL of NaCl (0.1 M). The pH of the suspensions was adjusted from 3 to 10 with 0.1 M of HCl or NaOH solutions. The zeta potential was evaluated in the electrophoresis cell at 25 ºC using Nanosizer Nano (Malvern). For each pH value, triplicate measurements were taken, and approximately 30 readings were done for each data (Hadjoudja *et al.*, 2010). The electrical state of the microalgae surface in solution was characterized using a zero-charge point (pHzc). Briefly, NaCl solutions (0.1 M) with pH ranging from 3 to 10 were prepared, then aliquots of 10 mL of each pH-adjusted NaCl solution were mixed with 50 mg of the biomass, shaken for 24 h at 25 ºC, and the final pH values were measured. The difference in ΔpH was plotted against the initial pH_i to determine the pHzc (Zehra *et al.*, 2016).

Contact angle measurements: measurement of the contact angle of *S. obliquus* cells from the control and Pb(II)-doped medium was carried out at 25 ºC as described by Asri *et al.*, (2018) using a digital optical contact angle (Data Physics OCA 40), via the sessile drop method, using water, formamide, and diiodomethane (Table 1). Both the left and the right contact angle measurements of both biomasses were automatically calculated from the digitalized image using SCA 20 software for OCA and PCA operated under Windows 7. The degree of hydrophobicity of the control and Pb(II)-loaded cells were then estimated according to Vogler's and Van Oss approach (Van Oss *et al.*, 1988; Vogler, 1998).

Table 1. Energy characteristics [Lifshitz–van der Waals (Υ^{LW}), electron-donor (Υ^{-}), and electron-acceptor (Υ^{+}) parameters ($mJ.m^{-2}$)] of the liquids used

Liquids	**Surface energy parameters (mJ m^{-2})**		
	Υ^{LW}	Υ^{+}	Υ^{-}
Water (θ_W)	21.8	25.5	25.5
Formamide (θ_F)	38.7	2.3	39.4
Diiodomethane (θ_D)	50.5	0.7	0

2.5 Effect of Pb(II) on the biochemical composition of *S. obliquus*

Photosynthetic pigments analysis*:* given that the main component of endogenous fluorescence (autofluorescence) is associated with the concentration of cellular pigments as reported by Yentsch and Yentsch (2008). The impact of Pb(II) on the photosynthetic system was firstly evaluated based on the autofluorescence using the FCM system. In fact, when cells are excited by

red (635 nm) and blue (488 nm) diode lasers, the chlorophyll can be observed in both orange (FL_2: 585/42 nm) and red (FL_3: 530/30 nm) fluorescence emission. The phycoerythrin (PE) is excited with the argon laser (488 nm) and emits in the orange region, the fluorescence can be measured at the FL_2 channel. Regarding the phycocyanin (PC), it's generally excited with diode laser and emits at the FL_4 (661/16 nm) channel. On the other hand, the content of the pigment was also assayed spectrophotometrically using the method of Tahira *et al.*, (2019). For the preparation of the pigments extract, the biomass resulting from both conditions was prepared at a concentration of 1 mg mL^{-1} in ethanol 95%. Cells were then homogenized by a SONOPULSmini20 ultrasonic homogenizer at 4 ºC and kept overnight in the dark at 4 ºC. Thus, the homogenate was centrifuged for 10 min at 4700 rpm. Finally, the absorbance of both samples was measured spectrophotometrically at 470 nm, 649 nm, and 664 nm. The pigments contents of chlorophyll a (Ch-a), chlorophyll b (Ch-b), and the total carotenoids (C $x_{+}c$) were calculated based on Lichtenthaler and Buschmann (2001) equations:

- ✓ Ch-a =13.36 A_{664} - 5.19 A_{649} eq (3)
- ✓ Ch-b =27.43 A_{649} - 8.12 A_{664} eq (4)
- ✓ C $x_{+}c$ = (1000 A_{470} - 2.13 Ch-a - 97.63 Ch-b) / 209 eq (5)

***Proteins, lipids, and carbohydrates determination*:** extraction of total lipid and quantification were achieved with a solvent mixture: water: chloroform: methanol (1:2:1) as reported by El Arroussi *et al.*, (2017). The biomass mixture (1 mg mL^{-1}) was centrifuged for 5 min at 4700 rpm, the chloroform layer was recovered and evaporated using nitrogen gas, and the total lipids were then weighed. The estimation of neutral and polar lipid content in cells of *S. obliquus* from control and Pb(II)-doped medium was also evaluated employing the multi-parameter FCM with the fluorescent stain Nile Red (NR) as reported by da Silva *et al.*, (2009). Lipids' straining with NR is traduced to different fluorescence emissions after excitation with the argon laser at 488 nm. When NR is dissolved in neutral lipids it emits an intense yellow fluorescence collected in the FL_2 channel, and when dissolved in polar lipids it exhibits red fluorescence collected in the FL_3 channel (Jara *et al.*, 2003). For the protein's extraction, 50 mg of lyophilized microalgal biomass was homogenized using the ultrasonic homogenizer (Sonopuls mini20) in the ice bath assisted by freezing cycles thawing at -80 ºC. The homogenate was next centrifuged at 4700 rpm for 15 min at 4 ºC. The supernatant was used for the estimation of the total soluble proteins using the Bradford method and bovine serum albumin (BSA) as standard (Bradford, 1976). Total soluble sugars were estimated using the protocol described by Wychen and Laurens (2017). First, the biomass was hydrolyzed by two-step sulfuric acid hydrolysis first in 72% (w/w) sulfuric acid for 1 h at 30 ºC. Then place in an autoclave for 1 h at 121 ºC with 4% (w/w) sulfuric acid. Finally, the total soluble carbohydrate content was assessed via the phenol-sulfuric acid colorimetric method (Dubois *et al.*, 1956).

2.6 Metabolomics profiling of control and Pb(II)-loaded cells

Lipidomic extraction: metabolomics profiling of *S. obliquus* cultivated in control and Pb(II)-doped medium were analyzed using a Gas chromatography-mass spectrometry (GC-MS) (Agilent 7890A Series GC). Firstly, 50 mg of both biomasses were recovered by centrifugation. Thus, the pellets were washed and transferred in 15 mL conical centrifuge tubes prepared in a dewar filled with liquid nitrogen. Non-polar metabolites were secondly extracted using a solvent mixture: water: chloroform: methanol (1:2:1) (El Arroussi *et al.*, 2017).

Non-polar metabolites determination: the transesterification reaction was performed using 6% H_2SO_4-methanol at 80 ºC, and atmospheric pressure during 3 h, assisted by ultrasonication in Branson ultrasonic (Soniffier 450) bath at 40 kHz as described by Chanda *et al.*, (2020). 2 mL aliquots of chloroform-solubilized metabolites were analyzed by GC using split mode (1:4) with the

helium at 1.5 mL min^{-1} as carrier gas. The ion source and quadruple temperatures were 230 ºC and 150 ºC respectively. The oven temperature program started at 30 ºC, then it was increased by 10 ºC min^{-1} to 120 ºC, increased until 200 ºC by 30 ºC min^{-1}, increased to 250 ºC by 10 ºC min^{-1}, temperature and hold for 1 min at the end of each phase. Finally, the temperature was increased to 270 ºC by 5 ºC min^{-1} and kept constant for 5 min. The detection was achieved by full scan mode between 30 and 1000 m/z, with a gain factor of 5 (El Arroussi *et al.*, 2015).

Metabolite identification, data mining, normalization, and statistical analysis*:* metabolites detected by GC-MS were identified with MS NIST 2014 library, as having predictability greater than 90%. The classification of these metabolites was carried out by PubChem® and LIPID MAPS® structure database. To correct heteroscedasticity and pseudo-scaling, the power transformation was carried out on the obtained data (van den Berg *et al.*, 2006). The quantities of individual fatty acids were calculated from the peak areas using dodecane as an internal standard.

2.7 Statistical analysis

The experiments were carried out in triplicate, and data were expressed as the mean ± standard deviation. The statistical analysis of the differences between cells of *S. obliquus* from the control and Pb(II)-doped medium was performed with unpaired T-test, and two-way ANOVA by Sidak's multiple comparisons test using GraphPad Prism software version 8.0. The P-values of < 0.05 were considered to be statistically significant. The heat map generation was performed using RStudio, and the visualization by FactoMineR package, integrated into the R software.

3. Results and discussion

3.1 S. obliquus growth inhibition, cells viability and size

The kinetic of growth and the SGR of *S. obliquus* cultured in control and Pb(II)-doped medium are illustrated in Figure 1A. The growth inhibition of *S. obliquus* was monitored throughout the exponential phase to assess the influence of Pb(II) ions on the growth, not to be confused with growth inhibition related to decreased nutrient availability. During the first week of culture, the growth kinetics of *S. obliquus* in Pb(II)-doped medium showed no significant inhibition compared with control cells. However, from the 7th day of culture, significant growth inhibition was observed and continued until the beginning of the stationary phase. As shown in Figure 1B, the SGR of *S. obliquus* in both media decreased considerably during the first week. Though, from the 13th day of culture, it was maintained at a stationary level. This finding is consistent with previous research reporting the inhibitory effect of Pb(II) ions against green microalgae (Li *et al.*, 2021).

Furthermore, the cell membrane integrity assay was used to evaluate the viability of *S. obliquus* cells grown in control or Pb(II)-doped medium. As depicted in the cytogram (Figure 1C), the viability of the negative control (cells from the control medium) was at 96.07%. However, the rate of living cells versus the negative control was decreased by 6.3% after exposure to Pb(II) ions. The viability of heat-inactivated cells used as a positive control was 0.07%. Generally, the membrane of living cells excludes the penetration of intercalary agents, while this type of molecule can achieve the intracellular compartment across the cell membrane of dead or damaged cells (Johnson *et al.*, 2013). From the obtained results, we can conclude that the Pb(II) at the EC_{50} concentration of 141 mg L^{-1} has a low impact on the integrity of the cell membrane. To our knowledge, there is very little research that has focused on assessing cells viability after Pb(II)-phycoremediation using FCM system. For example, Nazari *et al.*, (2018) reported a significant reduction in viability of *C. vulgaris* treated with reduced graphene-silver oxide nanocomposites. A similar effect was also observed in *C. vulgaris* exposed to zinc oxide nanoparticles {Formatting Citation}.

The effect of Pb(II) ions on the size of the cells, revealed that Pb(II) ions at EC_{50} concentration induced a decrease in the diameter and volume of *S. obliquus* cells (Figure 1D). This change can be attributed to the decrease of cells density, compensated by the decrease of cells biovolume. In line with this finding, Kim *et al.*, (2016) indicated a reduction in the biovolume of *Chlorella* cells exposed to a high dosage of magnesium aminoclay (MgAC) compared to the control cells. In contrast, Luis et al., (2006) showed a progressive size increase of *C. reinhardtii* exposed to Cu(II) with a concentration ranging from 0 to 200 µM. Romero *et al.*, (2020) reported also that the diameter and the volume of *C. vulgaris* had been enhanced following exposure to silver nanoparticles (AgNPs). It is noteworthy that biovolume is an important parameter in studies of microalgal population dynamics, phytoplankton physiology, ecosystem energy, etc. However, this parameter is not commonly considered in ecotoxicological research (Thomas *et al.*, 2018).

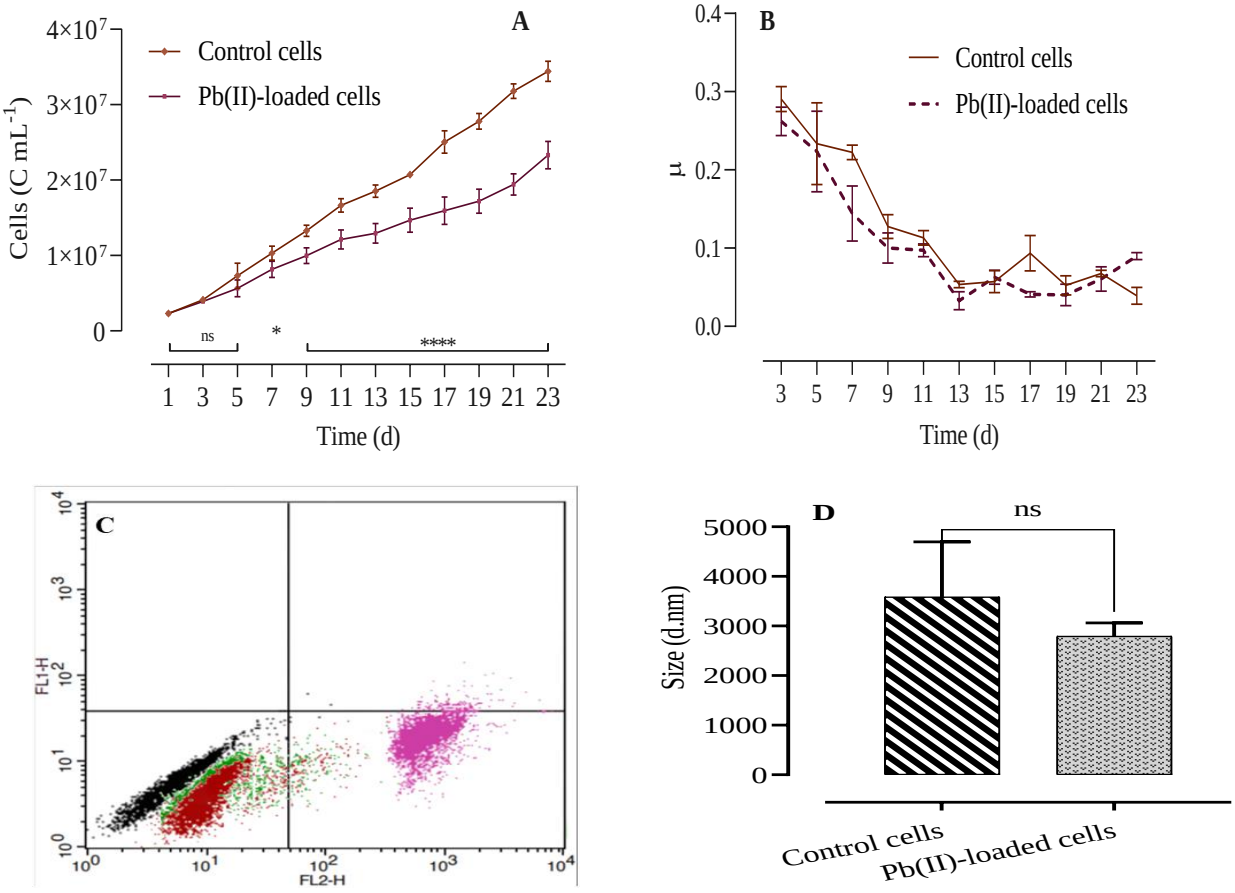

Figure 1 Shows growth kinetics (mean ± S.D, n=3) (**A**), specific growth rate (**B**) of *S. obliquus* cultures in control and Pb(II)-doped medium. **Figure 1C** illustrate the cytogram of the cells viability: (black) cells auto-fluorescence canceled (green) the negative control (96.07%), (red) after Pb(II)-phycoremediation (90.10 %) and (pink) heat-inactivated cells. The population moved in the FL_2 channel corresponding to the positive control (0.07 %). UL: Upper Left, UR: Upper Right, LL: Lower Left, LR: Lower Right. **Figure 1D** displays the effect of Pb(II) ions on the intensity particle size distribution of *S. obliquus* cells.

3.2 Pb(II)-phycoremediation mechanism with *S. obliquus*

As illustrated in Figure 2A, the TGA and DTG profiles of control and Pb(II)-loaded biomass have indicated that there are three phases of decomposition of *S .obliquus* biomass. The first stage (from 25 to 250 ºC), corresponding to the weight losing process of volatile compounds, the second stage (from 250 to 445 ºC) belongs to the devolatilization process, and the third stage (more than 445 ºC) consistent with the slow decomposition of the inorganic residue of ash, resulting from the previous step. In agreement with these findings, Marcilla *et al.*, (2009) noted that the TGA and the DTG of the thermal pyrolysis of *Nannochloropsis* sp., have also three main decomposition steps (<180 ºC, 180 - 540 ºC, and > 540 ºC). It is also clearly illustrated in Figure 2A that the rate of residue weight of cells after Pb(II)-biosorption (57.8%) was higher than that of cells from the control medium (31.34%). Moreover, the DTG showed that the weight loss at 315 ºC was 0.588% for control biomass and 0.346% for Pb(II)-loaded cells. This difference in weight loss would be related to the composition of the cells after biosorption or bioaccumulation of Pb(II) ions. In this way, Venkata Mohan *et al.*, (2007) stated that the heat required for thermal degradation of *Spirogyra* sp. was higher after biosorption of fluoride, compared to the control cells, which could be the result of the ionic bond formed after biosorption.

Afterward, the discrimination between extracellular biosorption and intracellular bioaccumulation was examined. As presented in the pie chart of Figure 2B, Pb(II) concentration in washed and unwashed cells was 9.2 mg L^{-1} and 54.2 mg L^{-1}, respectively. This indicates that both mechanisms: bioaccumulation (14.5%) and biosorption (85.5%) are implicated in the process of Pb(II)-phycoremediation by *S. obliquus.* Various studies have demonstrated the potential application of green microalgae biomass as a biosorbent for the removal of Pb(II) ions from wastewater. However, very little research has been conducted to demonstrate the potential application of living microalgae in the phycoremediation of Pb(II) contaminants (Kumar *et al.*, 2015). Among the few types of research that have been focused on the discrimination between intracellular bioaccumulation, and the extra-cellular biosorption, Pérez-Rama *et al.*, (2002) reported that the bioremoval of Cd(II) into living cells of *Tetraselmis suecica* involves both mechanisms, intracellular bioaccumulation, and extra-cellular biosorption.

Regarding the analysis of the concentration of Na^+, K^+, and their ratios in cells of *S. obliquus* from the control and Pb(II)-dopped medium, the findings illustrated in Figure 2C indicate a significant decrease in the concentration of Na^+ ions in Pb(II)-loaded cells, compared to control cells. However, no significant change was noticed in the concentration of the K^+ ions. It has been reported that Na^+ can play several functions in the process of the phycoremediation. The cell surface of microalgae incorporates many ions (K^+, Ca^{2+}, and Mg^{2+}) of which Na^+ constitutes the major part; such ions can be reversibly replaced by other toxic ions via a process called ion exchange (Navakoudis and Ververidis, 2018). On the other hand, we can also hypothesize that Pb(II) bioaccumulation can be managed by the flow of Na^+ ions to establish cellular homeostasis. It has been indicated by Bartolommei *et al.*, (2010) that Pb(II) ions can reversibly bind to the phosphoenzyme. These results are in agreement with the results of the cells size. In general, the maintenance of cells size is related to the regulation of sodium pumps, which is accomplished through the pump-leak mechanism (Kay, 2017).

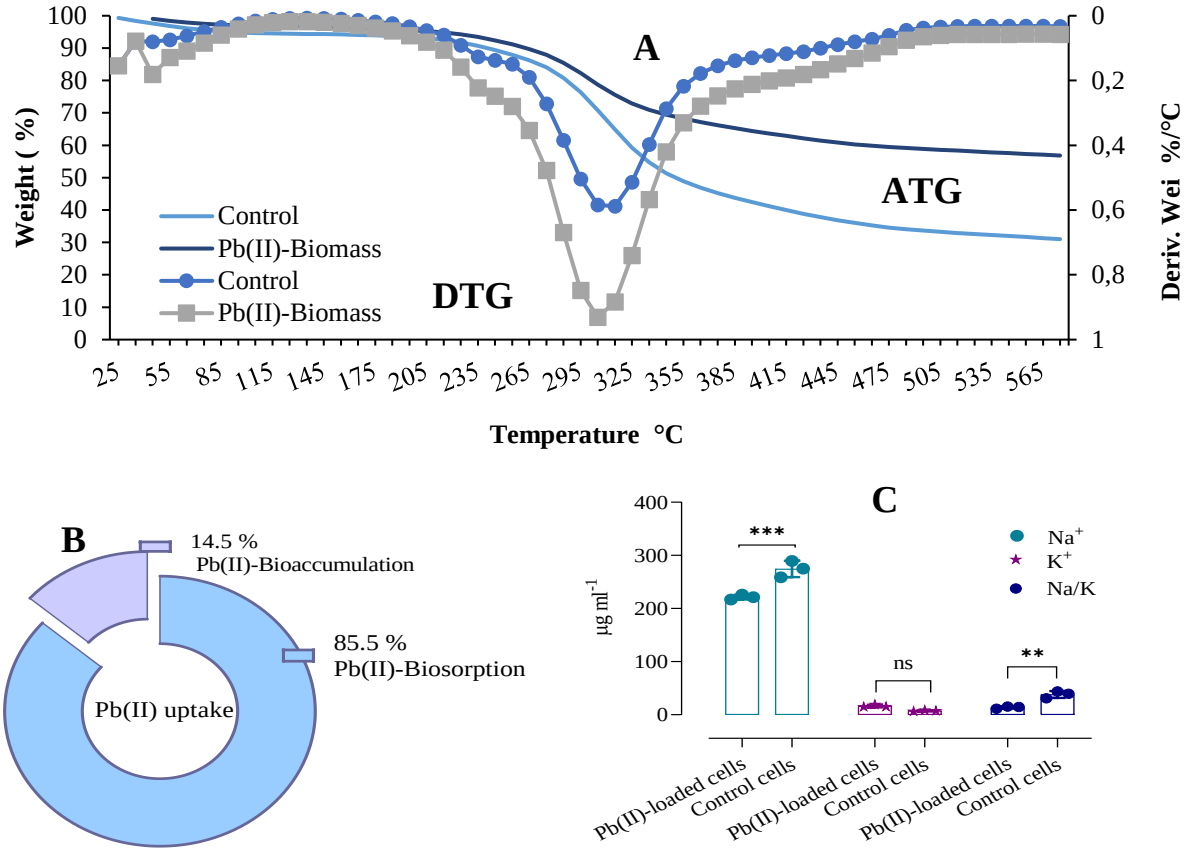

Figure 2A plots the TGA and DTG profile of the decomposition of controlled and Pb(II)-loaded cells. **Figure 2B** illustrates the rate of bioaccumulation and biosorption of Pb (II) ions by living cells of *S. obliquus*. **Figure 2C** displays the contents of Na^+, K^+ and the ratios of Na/K in control and Pb(II)-loaded cells, the error bar indicates the standard error of the mean (n = 3).

3.3 Physicochemical characterization of *S. obliquus* biomass

Regardless of the mechanism involved in HMs-phycoremediation, the first interaction usually occurs between the cell wall and ions in the solution. Both SEM and EDX analyses were firstly carried out to determine the morphological and elemental compositional variations in the cells' surface of *S. obliquus* cultured in Pb(II)-doped medium versus cells from the control medium. Figure 3A and B display respectively the SEM images of control and cells of *S. obliquus* after Pb(II)-biosorption at 8000× magnification. Notable differences in cells appearance were observed in Pb(II)-loaded cells compared to control cells. Indeed, a white appearance appears on the cells after Pb(II) biosorption, which reflects the absorption of Pb(II) ions by the cell walls.

The findings of the X-ray analysis confirmed these observations. As shown in Figure 3C, the presence of X-ray peaks representing C, P, O, S, K, Mg, Ca, and Si in control cells may be attributed to the biological components of the cell wall. Whereas a notable change was observed in the elemental composition of Pb(II)-loaded cells, with a disappearance of the peaks corresponding to Si and S in the region 2.2 - 2.3 KeV, and this peaks was substituted by a Pb corresponding peak. Moreover, there was a variation in the intensity level of the other elements detected. Based on our results, there were two peaks region related to the presence of Pb in cells, the first was on the low-energy region (2.2 KeV) and five other peaks related to the presence of Pb were detected on the

high-energy region of the EDX spectrum (Figure 3D), confirming, therefore, the variation in the distribution of Pb accumulation onto *S. obliquus.* Indeed, Pb(II) ions are able to pass from the cell wall to the biological membrane of *S. obliquus* and be bioaccumulated in the intracellular environment, whereas a large quantity of Pb was accumulated within the cell wall. This finding is agreeing with the results of ICP and TGA analyses.

The FTIR spectra (Figure 3E) of *S. obliquus* revealed a heterogeneous composition of the cell wall, evidenced by different peaks characteristic of lipids, proteins, and carbohydrates. Significant changes in the functional groups were demonstrated in the cell wall after Pb(II) biosorption. The absorption peaks at the region between 3200 and 3600 cm^{-1} indicated the existence of stretching vibration of hydroxyl (-OH) and amino ($-NH_2$) groups, which are among the functional groupings of chitosan and amino acids. The peaks around the region 3000 - 2800 cm^{-1} showed the stretching vibration functional of Methyl, and Methylene groups ($-CH_3$, $-CH_2-$). The peaks at 1650 and 1542 cm^{-1} would be caused by the bending and stretching of amine ($-R_2-NH$) groups of the proteins. The peaks around 1400 and 1200 cm^{-1} may be caused by sulfur group (-SO-), and phosphorous group (-PO-) that compose the phospholipid membrane. The peaks at 1026 cm^{-1} elongation of bonds C-C, C-O, and C-N, correspond to the polysaccharides (He and Chen, 2014). After Pb(II)-biosorption, a significant decrease in the transmittance of the surface peaks was recorded, which may be attributed to its occupation by Pb(II) ions. Furthermore, the comparison of FTIR spectra of *S. obliquus* biomass before and after Pb(II) biosorption showed a shift in functional groups of cells loaded to Pb(II) ions. The main shifts were detected in the absorption bands of hydroxyl, carboxylic acid, amine and amino groups. These functional groups have been previously identified on the cell wall of various microalgae species (Zheng *et al.,* 2016). This finding suggests that the biosorption of Pb(II) involves π-cation interactions between the cells' surface and cations in the solution (Tran *et al.*, 2017). Furthermore, some previous studies also indicated that biosorption process was accomplished by chelation and formation of ionic bridges between HMs and functional groups (Gupta and Rastogi 2008; Jena *et al.,* 2015).

The electrical state of the cells' surface is also one of the critical parameters in biosorption studies. Thus, the measurement of zeta potential, as well as the pHzc of *S. obliquus* cells are among the keys parameters related to the external loads of the adsorbent (Akar *et al.,* 2009). As shown in Figure 3F, the zeta potential of *S. obliquus* was maintained at a negative charge, regardless of the initial pH value. Indeed, it varied from -8.17 mV at pH 3 to -36.13 at pH 6.5. This result testifies the anionic characteristics and the high concentration of acid functional groups on the cell wall surface. Furthermore, at pHi, the zeta potentials of control cells were more negatively charged (-36.13 mV) than the Pb(II)-loaded microalgae cells (-32.5 mV) (Figure 3F and G). The value of pHz at which the $\Delta pH = 0$ was at 6.45 (Figure 3H), confirming the dominance of anion groups over cation groups on the cells surface. These negatively charged groups permit the binding of ions from the surrounding environment, making the outer layer of the cell wall the first participator in the removal of HMs (Leong and Chang, 2020; Saavedra *et al.*, 2018; Singh *et al.*, 2021). These findings are consistent with previous research that evaluated the zeta potential of different microalgae strains. For instance, Li *et al.*, (2017) had shown that the zeta potential was charged negatively at all growth phases of the oleaginous microalgae strains of *Desmodesmus bijugatus*, *Botryococcus* sp, and *Chlorella* sp. Also, Samadani *et al.*, (2018) reported that the average of the zeta potential of *Chlamydomonas* was at - 41 mV, - 4mV respectively at pH 7 and pH 4, they propose that at low pH, the zeta potential around to zero can reduce the electrostatic interactions between the metal cations and the cell wall surface, thereby reducing the cationic fluxes into the cells.

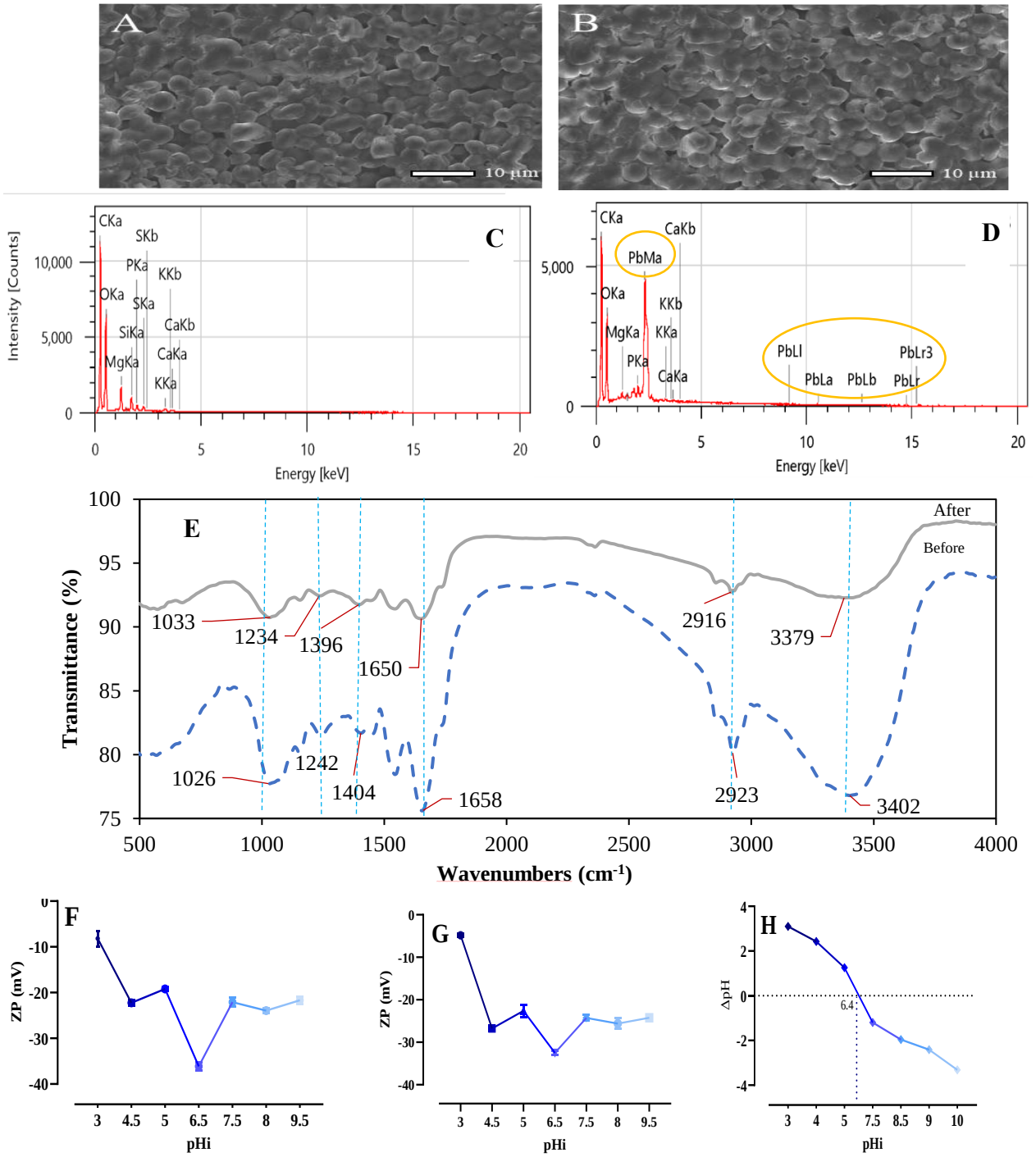

Figure 3 Displays SEM image of (**A**) control cells; (**B**) Pb(II)-loaded cells at x8000 magnification. as well as the selected X-ray spectra of control (**C**), Pb(II)-loaded cells (**D**), FTIR spectra of control and Pb(II)-loaded cells (**E**), zeta potential of control (**F**) and Pb(II)-loaded cells (**G**), as well as zero pH loading (**H**) of *S. obliquus* biomass in the pHi range of 3-10.

Based on both Vogler's and Van Oss approaches, *S. obliquus* exhibited a hydrophilic character, the θ_w value (34.9° ± 0.4) was less than 65° (Table 2), and the ΔGiwi had a positive value (37.23 ± 1.13 mJ m^{-2}). These findings agree with previous results reporting the hydrophilic character

of various microalgae strains (Ozkan and Berberoglu, 2013). It has been reported that the hydrophobicity of the surface of microbial cells can be attributed to proteins present in the cell wall (Vichi *et al.*, 2010). Additionally, cells of *S. obliquus* appear to behave predominantly as electron donors/Lewis bases with high values of γ^- = 52.57 ± 0.6 mJ m^{-2}. These results indicate that *S. obliquus* strain exhibit a weak electron acceptor character with γ^+ = 0.24 ± 0.07 mJ m^{-2}. Previous studies have also demonstrated the electron donor character of several microorganisms, which has been correlated with the presence of various phosphate groups in the cell wall (Vichi *et al.*, 2010). These findings are consistent with the FTIR analyses that confirm the presence of phosphate groups on its cells surface. On the other hand, the θ_w of *S. obliquus* significantly decreased from 34.9° ± 0.4 to 31.6° ± 0.9 after Pb(II) biosorption (Table 2). This can be attributed to an increase in the density of polar functional groups on the biomass surfaces after the biosorption process (Yalçin *et al.*, 2010). Additionally, a significant variation was noted in the electron donor and acceptor character after Pb(II)-biosorption (γ^+ from 0.24 ± 0.07 to 0.08 ± 0.02 mJ m^{-2}; and γ^- from 52.57 ± 0.6 to 59.79 ± 0.5 mJ m^{-2}) because of the interaction of functional groups in the cells' surface with the Pb(II) ions.

Table 2. Contact angle values of control (CTR) and Pb(II)-loaded cells (Pb-C), using water (θ_w), formamide (θ_F) and diiodomethane (θ_D), Lifshitz-vander Waals (γ^{LW}), electron-donor (γ^-), electron-acceptor (γ^+) parameters, and surface energies (ΔGiwi).

	Contact angles (°)			**Surface tension: components and parameters (mJ m^{-2})**			**Surface energies**
	θ_w	θ_F	θ_D	γ^{LW}	γ^+	γ^-	ΔGiwi (mJ m^{-2})
CTR	34.9±0.4	42.2±0.6	49.5±1.6	34.45±0.9	0.24±0.07	52.57±0.6	37.23±1.13
Pb-c	31.6±0.9*	44.1±0.5^{ns}	36.3±0.6***	41.33±0.3***	0.08±0.02*	59.79±0.5***	44.9±1.2**

*Statistical significance p value < 0.05

3.4 Pb (II) impact on the biochemical composition of *S. obliquus*

Influence on photosynthetic pigments: cells of green microalgae are autofluorescent, their signature can be observed in the red, the orange, and the green channel using FCM system. As shown in Figure 4, Pb(II) ions cause an alteration in the autofluorescence of *S. obliquus* pigments. Indeed, a shift in autofluorescence of native pigments of Pb(II)-loaded cells (B, D, F, and H) was observed in comparison with cells from the control medium (A, C, E, and G). The orange fluorescence is much lower than the chlorophyll autofluorescence, as detected in the red channel. The intensity of orange, green, and red autofluorescence can vary in response to changes in the physiological state of the algae due to oxidative stress (Ying and Dobbs, 2007). In line with our findings, Cheloni and Slaveykova (2013) also reported a change in the autofluorescence of *C. reinhardtii* exposed to metallic (copper, mercury, and nanoparticulate copper oxide).

Thereafter, spectrophotometric measurements of the pigment content were performed. As indicated in Figure 4I, the concentration of Ch-a and Chl-b decreased significantly in cells extract of *S. obliquus* grown in Pb(II)-doped medium compared to cells from the control medium. The total Chl-a and Chl-b were reduced from 54.08% to 52.5% and from 30.99% to 20.1%, respectively. In contrast, total C x+c increased from 14.93% to 27.3% in Pb(II)-loaded cells. Only a few research has examined how chlorophylls and carotenoids are expressed in microalgae cells in response to Pb(II) stress. In keeping with this finding, Piotrowska-Niczyporuk *et al.*, (2015) has reported that the total C x+c in *Acutodesmus obliquus* strain was less influenced by Pb(II) ions as compared to the chlorophyll pigments. According to Nazari *et al.*, (2018), the decrease in chlorophyll content is one of the main indicators of oxidative stress in microalgae. The reduction in chlorophyll content can be

explained by the inhibition of their biosynthesis, by eventual degradation of these pigments or their predecessors, or by the alteration of the thylakoid system as a consequence of the binding of metals to proteins, perturbing therefore its normal function (Carfagna *et al.*, 2013; Piotrowska-Niczyporuk *et al.*, 2015). Regarding the increase of C x+c levels in Pb(II)-loaded cells, it has been reported that this class of pigments provides protection to photosynthetic membranes against free radicals generated following the accumulation of HMs in intracellular compartments (Piotrowska-Niczyporuk *et al.*, 2015; Rai *et al.*, 2013).

Pb(II)-influence on the proteins, lipids, and carbohydrates content*:* the biochemical characterization of *S. obliquus* biomass from control and Pb(II)-doped medium is presented in Figure 4J. Results revealed that Pb(II) stimulates the production of lipids, a significant increase in lipids content, which increases from 14.58% in control cells to 22.14% in Pb(II)-loaded cells. Several previous studies support this finding. For example, Nanda *et al.*, (2021) has showed an increase in lipid content in *Chlorella sorokiniana* grown under Pb(II) stress. Next, neutral and polar lipids were examined with the FCM system using the NR dye for the characterization of the lipids accumulated in the Pb(II)-loaded cells. As shown in the cytograms (Figure 4K and L), the signal collected in the FL_2 channel is stronger for Pb(II)-loaded cells compared to cells from the control medium, meaning that an increase in neutral lipids fluorescence was apparent in stressed cells of *S. obliquus.* Several microalgae species have been reported to have a strong capacity to accumulate lipid bodies (energy reserves) under various stress conditions. Moreover, neutral lipids are part of the essential components of membranes such as glycol and phospholipids (Benhima *et al.*, 2018). In this study, the enhancement of natural lipids content in Pb(II)-loaded cells might be an adaptation mechanism against the oxidative stress caused by Pb(II) ions in the intracellular compartment.

Regarding the carbohydrates and proteins content, a significant decrease was noticed in Pb(II)-loaded cells compared to the control cells. It was from 14.35% to 10.6%. and from 15.68% to 11.6% for the content of carbohydrates and proteins, respectively. These results are consistent with previous research. For example, Napan *et al.*, (2015) reported that lipid yield was higher in *S. obliquus* grown in the presence of different metals (As, Cd, Co, Cr, Cu, Hg, Ni, Pb, Se, and Zn). Similarly, Han *et al.*, (2019) showed that lipid productivity in *S. obliquus* was significantly increased by 27.95%, 19.21%, and 18.63% respectively after supplementation with trace metals of Fe, Mn, and Mo. In contrast, Pham *et al.*, (2020) found that Pb(II) concentration around 0.5 and 1 mg L^{-1}, significantly increased the production of the total lipids content, but the increase in Pb(II) concentration to 10 mg L^{-1} shows a reverse effect. Concerning the influence of Pb(II) ions on total carbohydrates, our findings are in agreement with some previous study. For instance, Belghith *et al.*, (2016) reported that soluble and insoluble carbohydrates in *Dunaliella salina* significantly decrease with increasing Cd(II) concentration. However, Tahira *et al.*, (2019) noticed an increase in total sugar content in *Euglena gracilis* cells in response to As(III) ions. The obtained results of the effects of Pb(II) ions on the proteins content are consistent with the outcomes reported by Piotrowska-Niczyporuk *et al.*, (2015), who noticed a gradual decrease in the contents of soluble and insoluble proteins of *A. obliquus* exposed to Pb(II) ions. Under stress conditions, it was reported downregulation of genes involved in primary metabolism and proteins synthesis, as well as activation of genes related to autophagy and proteins degradation (Dittami *et al.*, 2009). In the context of biorefineries, the results of the present study are very promising since the selected strain can accumulate lipids after Pb(II)-phycoremediation, even at very high concentrations. Consequently, it is possible to use these lipids for the production of third-generation biofuels or their use in other kinds of applications.

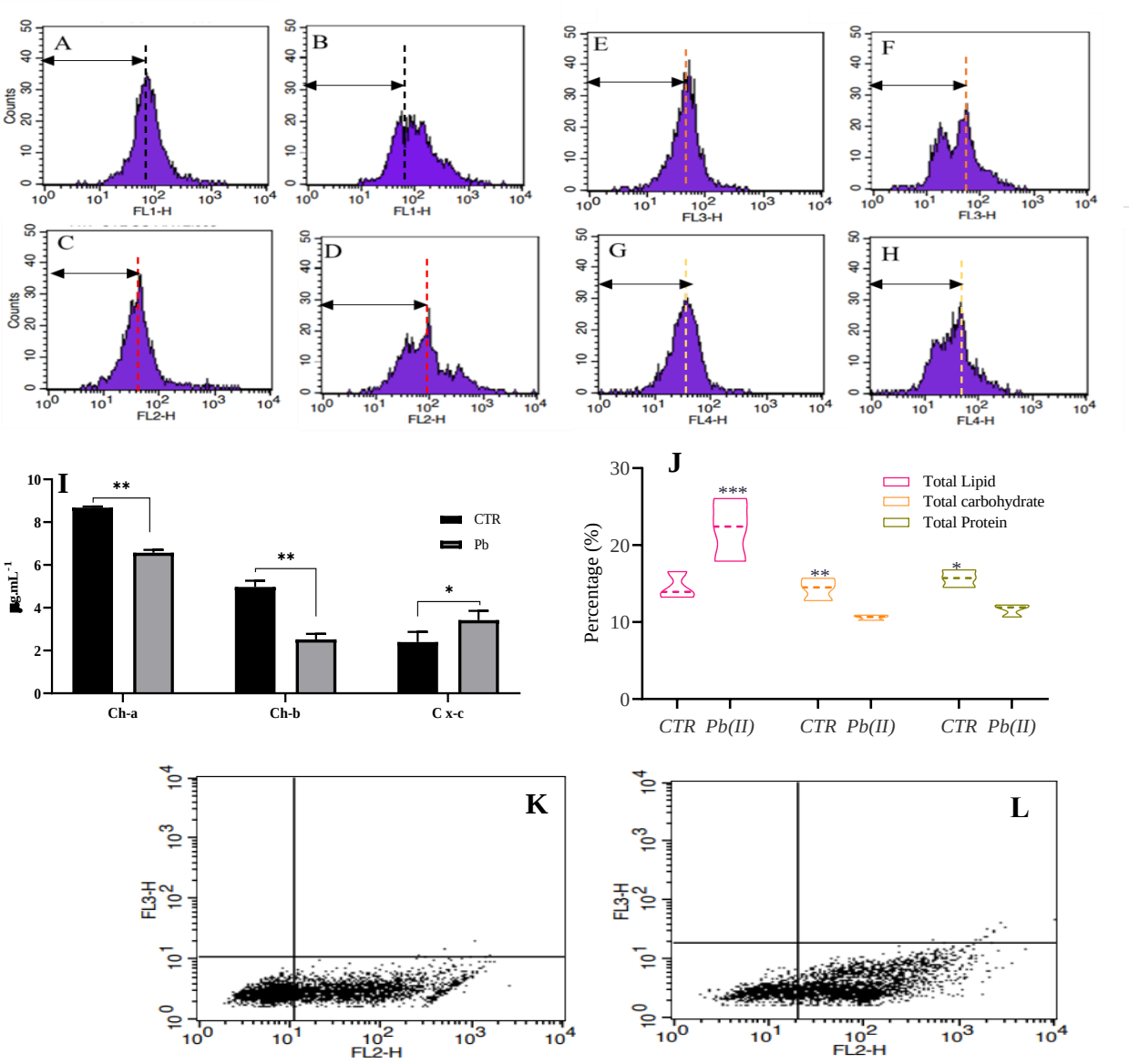

Figure 4 shows the autofluorescence of native pigments of control cells (**A, C, E** and **G**) and (**B, D, F** and **H**) and Pb(II)-loaded cells. **Fig 4I** illustrate the concentration of chlorophyll a (Ch-a), b (Ch-b), and total carotenoids (C x+c) in control (CTR) and Pb(II)-loaded cells. Fig 4 (J) shows the the compositions of the total lipid, carbohydrate and protein in control and Pb(II)-loaded cells. Fig 4 (K) and (L) present NR staining dot plots of control and Pb(II)-loaded cells.

3.5 Metabolomics profiling of control and Pb(II)-loaded cells

In this section, the metabolomic profiling of (i) fatty acids, (ii) alkanes and alkenes, (iii) sterols and other compounds detected in *S. obliquus* cells grown in control, and Pb(II)-doped medium was analyzed. Figure 5 summarizes the metabolite profile of control (A) and Pb(II)-loaded cells of *S. obliquus* (B). Indeed, a total of 54 and 59 putative compounds were detected respectively in the resulting biomasses. In Pb(II)-loaded cells, relative to control cells, a notable increase in the relative abundance of fatty acid methyl esters (FAME) (15% to 18%), Alkanes (3% to 8%), aromatic compounds (2% to 13%) and sterols (1% to 2%). However, the amount of monounsaturated fatty acids (MUFA) was decreased from 22% in control to 5% in Pb(II)-loaded cells, and also, alkenes

were reduced from 3% to 2%. Regarding the amount of saturated fatty acids (SFA), no clear variations were noted, and the polyunsaturated fatty acids (PUFA) were only detected in the control biomass. Previous metabolomic studies on microalgae have mainly focused on the identification and valorization of algal metabolites in the agri-food (polysaccharides, fatty acids...), pharmaceutical (carotenoids, steroids...), and public health (algal toxins) fields (Richmond, 2004). A very limited number of research studies have been focused on the metabolomics analysis of microalgae after the phycoremediation of HMs.

***Fatty acid composition**:* composition and degree of saturation of fatty acids are among the main characteristics examined in lipidomic studies. As shown in Figure 5C. The composition and concentration of fatty acids identified in cells from the control and Pb(II)-doped medium were significantly different. A set of 28 fatty acids was detected, belonging to 4 sub-classes including SFA (12), MUFA (7), PUFA (1), and FAME (8). The most abundant SFAs in both biomasses are palmitic acid ($C_{16:0}$), pentadecanoic acid ($C_{15:0}$) and stearic acid ($C_{18:0}$). However, Pelargonic acid ($C_{9:0}$) and Cerotic acid ($C_{26:0}$) were present only in the control cells of *S. obliquus*. Nevertheless, the Myristic acid ($C_{14:0}$) and Margaric acid ($C_{17:0}$) were detected only in the Pb(II)-loaded cells. The concentrations of Lauric acid ($C_{12:0}$), Pentadecanoic acid ($C_{15:0}$), Stearic acid ($C_{18:0}$), Lignoceric acid ($C_{24:0}$), and Montanic acid ($C_{28:0}$) were higher in the control cells compared to Pb(II)-loaded cells. Conversely, the concentration of Palmitic acid ($C_{16:0}$) was higher in Pb(II)-loaded cells. The concentrations of Behenic acid ($C_{22:0}$) and Melissic acid ($C_{30:0}$) were almost equal in both biomasses. Except for oleic acid ($C_{18:1\omega 9}$), all MUFAs were found only in the biomass from the control medium. As regards the PUFA, linoleic acid ($C_{18:2:9.12}$) was detected only in the control biomass. The following FAME: Methyl tetradecanoate ($C_{15}H_{30}O_2$), Methyl 13-methyltetradecanoate ($C_{16}H_{32}O_2$), and Methyl octadecanoate ($C_{19}H_{38}O_2$) were present in both biomasses. Whereas, Methyl 20-methyl-heneicosanoate ($C_{23}H_{46}O_2$), Methyl 11-(3-pentyl-2-oxiranyl) undecanoate ($C_{19}H_{36}O_3$), Methyl 2-hydroxy-tetracosanoate ($C_{25}H_{50}O_3$), and Methyl 5,9-hexadecadienoate ($C_{17}H_{30}O_2$) were detected only in Pb(II)-loaded cells. Oppositely, Methyl 2-octylcyclopropene-1-heptanoate ($C_{19}H_{34}O_2$) was detected in the control cells. To our knowledge, no previous study has examined the effect of Pb(II) ions on the metabolic profiling of *S. obliquus* following the phycoremediation process. Only a few studies have been conducted on the lipidomic profiling of some microalgae strains exposed to HMs.

The results of the present study indicate that a number of changes can occur in the overall lipids content, and in their saturation profile. Among all lipid classes, fatty acids (FAs) are the most abundant in microalgae and are generally the most influenced by metal stress (Guschina and Harwood 2006). Consistent with the result obtained, similar observations have also been reported in the literature regarding the influence of HMs on the lipidomic profile of some microalgal strains (Rocchetta *et al.*, 2012, 2006; Sibi *et al.*, 2014). For instance, the lipid profiles of *C. sorokiniana* under Pb(II) stress increased the levels of C_{14}, C_{16}, and $C_{18:1}$, however, the levels of $C_{16:1}$, C_{18}, $C_{18:2}$, $C_{18:3}$, and C_{20} were reduced as compared to control cells (Nanda *et al.*, 2021). It has been reported that the FAs can play several roles in various physiological functions, like a key bioindicator of the adaptation of the cell membranes to the environmental conditions (Filimonova *et al.*, 2016; Gonçalves *et al.*, 2016). Also, under stress conditions cells of microalgae stimulate the synthesize and the accumulation of energy reserves, mainly in the form of TAG (Minhas *et al.*, 2016). It is known that PUFAs are the lipid fraction involved in the maintenance of structural functions. Whereas, SFA and MUFA constitute among others the energy reserves (Olofsson *et al.*, 2012). These findings can be explained by the biochemical adaptation mechanism. Indeed, under metal stress conditions, cells of microalgae change their metabolism via an adjustment of the ratio between unsaturated and saturated fatty acids, in order to reduce the permeability and or fluidity of the cell

membrane prevent, therefore, the intracellular bioaccumulation of metal ions across the cell membrane (Lu *et al.*, 2012).

***Alkanes and Alkenes*:** As illustrated in Figure 5D, a large variation in alkane and alkene composition between *S. obliquus* biomass grown in control and Pb(II)-doped media. the relative abundance of saturated hydrocarbons (alkane) was higher than unsaturated hydrocarbons (alkenes). The diversity of the saturated hydrocarbons showed that the content of n-alkanes ranging from n-C_{17} to n-C_{36}, and they are dominated by very long-chain alkanes. A total of 15 alkane metabolites were detected in Pb(II)-loaded cells, compared with 11 in control cells.
The long-chain (L.C) alkanes are present in both groups, the content of n-C_{17}, n-C_{18}, and n-C_{20} decrease mildly in the Pb(II)-loaded cells. However, a remarkable increase was recorded for n-C_{21} and n-C_{22}. The distribution patterns of very-long-chain alkanes (V.L.C) varied from 10 in Pb(II)-loaded cells to 6 control cells. One branched long-chain alkanes (2-Methyltriacontane ($C_{31}H_{64}$)) was at an equal amount in both biomasses. Though four V.L.C alkanes: Hexacosane ($C_{26}H_{54}$), Heptacosane ($C_{27}H_{56}$), Pentatriacontane ($C_{35}H_{72}$), and Hexatriacontane ($C_{36}H_{74}$) have been detected only in Pb(II)-loaded cells. Regarding the analysis of the alkene profile, 8 alkenes were detected, they are distributed as follows: in the cells from the control medium, four L.C and one V.L.C alkenes, while, two L.C, and two V.L.C alkene was detected in Pb(II)-loaded cells. The analysis of alkene data showed that the position of the double bond "C=C", in the alkene from cells grown in the control medium, was located in the first position (1-Heptadecene, 1-Octadecene, 1-Eicosene, 1-Heptacosene), while a change in this position to 9 and 10 (10-Heneicosene ($C_{21}H_{42}$), 9-Tricosene ($C_{23}H_{46}$) and 9-Hexacosene ($C_{26}H_{52}$)) was found in Pb(II)-loaded cells. In the available literature, no previous studies have been investigated the effect of Pb(II) ions on the alkane and alkene profiles of green microalgae. It has been reported that hydrocarbons can play several roles in microalgal cells. Due to their high hydrophobicity, they contribute to the regulation of the fluidity of photosynthetic membranes and also act in intercellular signaling (Sorigué *et al.*, 2016). It is evident that additional omics research is needed to identify the biochemical pathways responsible for the synthesis of alkanes and long-chain alkenes in microalgal cells under metal ion stress conditions, in order to identify the mechanisms by which they are involved in managing such oxidative stress.

Sterol and aromatics: after lipids transesterification, sterol and some aromatic compounds were also identified in the organic phase. Two sterols were detected in *S. obliquus* cells from the control and Pb(II)-doped medium: (20.Xi.-Lanosta-7,9(11)-diene-3.b...) and (Lanost-8-en-7-one). However, (9,19-Cyclocholest-24-en-3-ol) was detected only in control cells, and (Cholestan-3-ol) was detected only in Pb(II)-loaded cells. On the other hand, 11 aromatic molecules were detected in Pb(II)-loaded cells and 3 in control cells (data not shown). In fact, the common feature of aromatic compounds detected in Pb(II)-loaded cells is the presence of radical ketone groups such as 2H-pyrrol-2-one, 2H-Inden-2-one, 2(3H)-Furanone, and 2H-pyrrol-2-one. Sterols are usually good chemotaxonomic tools for studying microalgal biochemistry. In contrast to fatty acid compositions, the differences in the relative proportions of sterols with varying environmental conditions were minorly investigated (Volkman, 2016). The published literature on sterol composition of microalgae continues to grow however is still far from complete in terms of implications for resistance to possible oxidative stress generated by HMs.

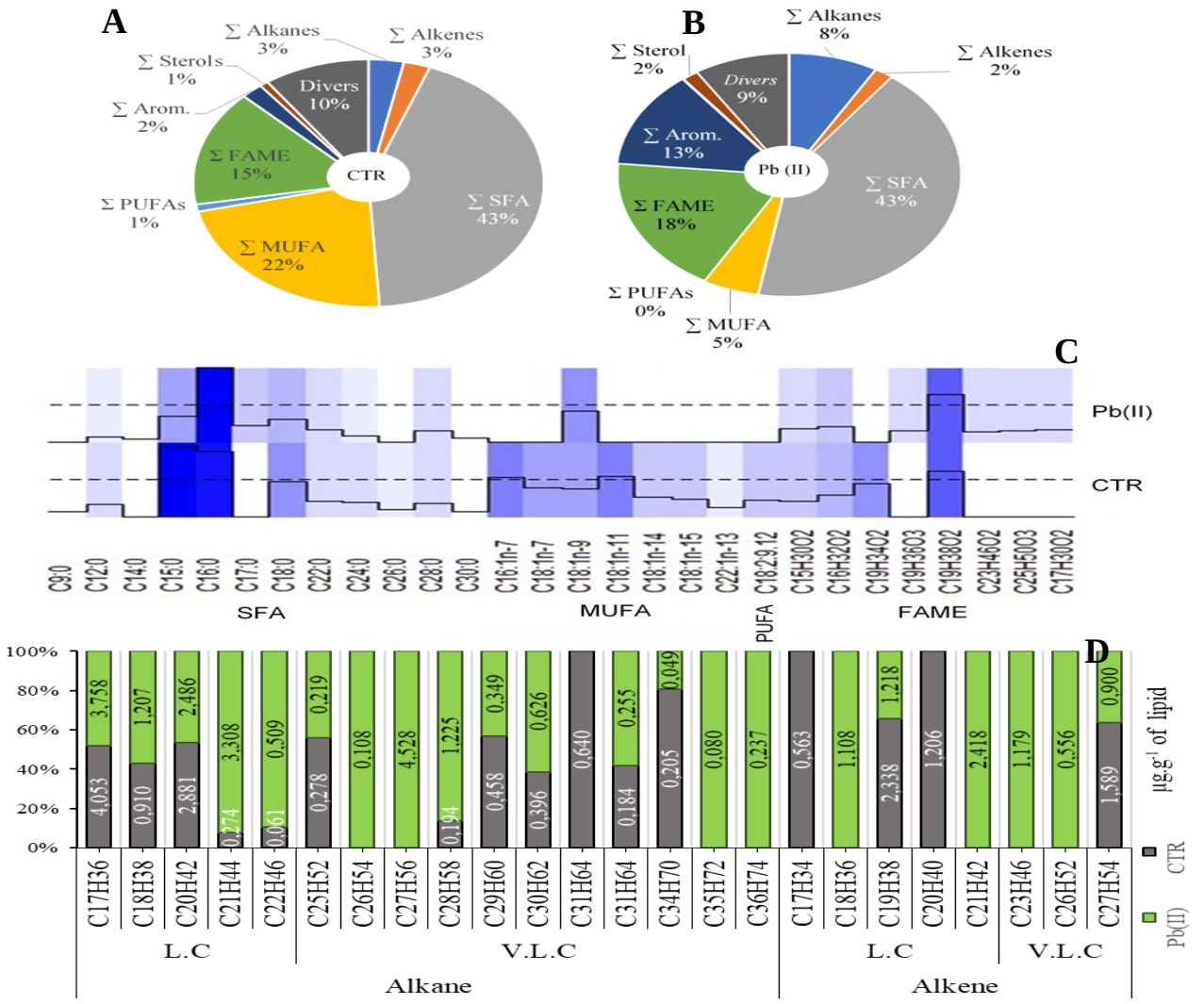

Figure 5 indicates the level of the metabolite classes (Σ alkanes, Σ alkenes, Σ sterols, Fatty acid methyl ester (FAME); monounsaturated fatty acids (MUFA); saturated fatty acids (SFA); Polyunsaturated fatty acids (PUFA); Aromatic compounds (Arom.); divers compounds (Divers)) in control (**A**) and Pb(II)-loaded (**B**) cells. **Figure 5C** shows the distribution of the fatty acid profile (fatty acid methyl ester (FAME); monounsaturated fatty acids (MUFA); saturated fatty acids (SFA); polyunsaturated fatty acids (PUFA)), and **Figure 5D** illustrates the metabolomic profiling of alkanes and alkenes (very long-chain alkanes (V.L.C); long-chain alkanes (L.C)) in control and Pb(II)-loaded cells

4. Conclusion

Based on the above considerations, we can deduce that the phycoremediation of Pb(II) ions using living cells of *S. obliquus* involves both extracellular biosorption and intracellular bioaccumulation. The physicochemical characterization of the control and Pb(II)-loaded cells using a range of physicochemical characterization analyses (SEM-EDX, FTIR, zeta potential, zero-point charge, and contact angle measurements) has confirmed the involvement of several chemical and electrostatic interactions between the macromolecules constituting the cell surface and the Pb(II) ions in solution. The comparison of the biochemical and metabolomic profile of *S. obliquus* grown in the control and

Pb(II)-doped medium revealed that cells subjected to Pb(II) exposure conditions adjust their metabolism, particularly lipid biosynthesis, in order to reduce the permeability and fluidity of cell membranes. Therefore, preventing the intracellular accumulation of Pb(II) ions that might cause a variety of damage.

Acknowledgements

Authors gratefully acknowledge the Moroccan Foundation for Advanced Science, Innovation and Research (MAScIR), and Regional University Centre of Interface (CURI), Sidi Mohamed Ben Abdellah University for their financial and technical support.

References

Aguilar-Ruiz RJ, Martínez-Macias M del R, Sánchez-Machado DI, et al., 2020. Removal of copper improves the lipid content in *Nannochloropsis oculata* culture. Environ. Sci. Pollut. Res. 27(35): 44195–44204. https://doi.org/10.1007/s11356-020-10283-4

Akar T, Anilan B, Gorgulu A, Tunali S. 2009. Assessment of cationic dye biosorption characteristics of untreated and non-conventional biomass: *Pyracantha coccinea berries*. J. Hazard. Mater. 168: 1302–1309. https://doi.org/10.1016/j.jhazmat.2009.03.011

Allen MM. 1968. Simple Conditions for Growth of Unicellular Blue-Green Algae on Plates. J. Phycol. 4(1): 1–4. https://doi.org/10.1111/j.1529-8817.1968.tb04667.x

Ansari FA, Gupta S K, Bux F. 2019. Microalgae: A Biorefinary Approach to the Treatment of Aquaculture Wastewater. In Application of Microalgae in Wastewater Treatment (Vol. 2). https://doi.org/https://doi.org/10.1007/978-3-030-13909-4_4

Asghari S, Rajabi F, Tarrahi R, Salehi-Lisar SY, Asnaashari S, Omidi Y, Movafeghi A. 2019. Potential of the green microalga *Chlorella vulgaris* to fight against fluorene contamination: evaluation of antioxidant systems and identification of intermediate biodegradation compounds. J. Appl. Phycol. https://doi.org/10.1007/s10811-019-01921-7

Ashraf MA, Maah MJ, Yusoff I. 2014 Soil contamination, risk assessment and remediation. In Environmental Risk Assessment of Soil Contamination: Vol. i (3–56). https://doi.org/10.1016/j.colsurfa.2011.12.014

Asri M, El Ghachtouli N, Elabed S, Ibnsouda S, Elabed A, Silva B, Tavares T. 2018. *Wicherhamomyces anomalus* biofilm supported on wood husk for chromium wastewater treatment. J. Hazard. Mater. 359(May): 554–562. https://doi.org/10.1016/j.jhazmat.2018.05.050

Bartolommei G, Gramigni E, Tadini-Buoninsegni F, Santini G, Moncelli MR. 2010. Confining the sodium pump in a phosphoenzyme form: The effect of lead(II) ions. Biophys. J. 99(7): 2087–2096. https://doi.org/10.1016/j.bpj.2010.07.050

Belghith T, Athmouni K, Bellassoued K, El Feki A, Ayadi H. 2016. Physiological and biochemical response of *Dunaliella salina* to cadmium pollution. J. Appl. Phycol. 28(2): 991–999. https://doi.org/10.1007/s10811-015-0630-5

Benhima, R, El Arroussi, H, Kadmiri IM, El Mernissi N, Wahby I, et al., 2018. Nitrate reductase inhibition induces lipid enhancement of *Dunaliella tertiolecta* for biodiesel production. Sci. World J. https://doi.org/10.1155/2018/6834725

Bradford MMB. 1976. Rapid and Sensitive Method for quantitation of microgram quantities of protein utilizing principle of protein-dye binding. Anal., Biochem. 72: 248–254. https://doi.org/10.1016/j.sbi.2014.10.005

Carfagna S, Lanza N, Salbitani G, Basile A, Sorbo S, Vona V. 2013. Physiological and morphological responses of Lead or Cadmium exposed *Chlorella sorokiniana* 211-8K (Chlorophyceae). SpringerPlus, 2(1): 1–7. https://doi.org/10.1186/2193-1801-2-147

Chanda MJ, Benhima R, Elmernissi N, et al., 2020. Screening of microalgae liquid extracts for their bio stimulant properties on plant growth, nutrient uptake and metabolite profile of *Solanum lycopersicum* L. Sci. 10(1): 1–12. https://doi.org/10.1038/s41598-020-59840-4

Cheloni, G, Slaveykova VI. 2013. Optimization of the C11-BODIPY581/591 dye for the determination of lipid oxidation in *Chlamydomonas reinhardtii* by flow cytometry. Cytometry A. 83(10): 952–961. https://doi.org/10.1002/cyto.a.22338

Chibueze C, Chioma A, Chikere B. 2016. Bioremediation techniques – classification based on site of application: principles, advantages, limitations and prospects. World J. Microbiol. Biotechnol. 32(11): 1–18. https://doi.org/10.1007/s11274-016-2137-x

da Silva TL, Santos CA, Reis A. 2009. Multi-parameter flow cytometry as a tool to monitor heterotrophic microalgal batch fermentations for oil production towards biodiesel. Biotechnol. Bioprocess Eng. 14(3): 330–337. https://doi.org/10.1007/s12257-008-0228-8

Danouche M, EL Arroussi, H, El Ghachtouli N. 2021a. Mycoremediation of synthetic dyes by yeast cells: a sustainable biodegradation approach. Environmental Sustainability, 1-18. https://doi.org/10.1007/s42398-020-00150-w

Danouche M, El Ghachtouli N, El Arroussi H. 2021b. Phycoremediation mechanisms of heavy metals using living green microalgae: physicochemical and molecular approaches for enhancing selectivity and removal capacity. Heliyon 7, e07609. https://doi.org/10.1016/j.heliyon.2021.e07609

Danouche M, El Ghachtouli N, El Baouchi A, El Arroussi H. 2020. Heavy metals phycoremediation using tolerant green microalgae: Enzymatic and non-enzymatic antioxidant systems for the management of oxidative stress. J. Environ. Chem. Eng. 8(5): 104460. https://doi.org/10.1016/j.jece.2020.104460

Das, D., Chakraborty, S., Bhattacharjee, C., Chowdhury, R. 2016. Biosorption of lead ions (Pb2+) from simulated wastewater using residual biomass of microalgae. Desalination and Water Treatment, 57(10), 4576-4586. https://doi.org/10.1080/19443994.2014.994105

Dittami SM, Scornet D, Petit JL, Ségurens B, Da Silva C, Corre E, et al., 2009. Global expression analysis of the brown alga *Ectocarpus siliculosus* (Phaeophyceae) reveals large-scale reprogramming of the transcriptome in response to abiotic stress. Genome Biol. 10(6). https://doi.org/10.1186/gb-2009-10-6-r66

Dubois M, Gilles KA, Hamilton JK, Rebers PA, Smith F. 1956. Colorimetric Method for Determination of Sugars and Related Substances. Anal., Chem. 28(3): 350–356. https://doi.org/10.1021/ac60111a017

El Arroussi H, Benhima R, Bennis I, El Mernissi N, Wahby I. 2015. Improvement of the potential of *Dunaliella tertiolecta* as a source of biodiesel by auxin treatment coupled to salt stress. Renew. Energ. 77: 15–19. https://doi.org/10.1016/j.renene.2014.12.010

El Arroussi H, Benhima R, El Mernissi N, Bouhfid R, Tilsaghani C, Bennis I, Wahby I. 2017. Screening of marine microalgae strains from Moroccan coasts for biodiesel production. Renew. Energ. 113: 1515–1522. https://doi.org/10.1016/j.renene.2017.07.035

Filimonova V, Gonçalves F, Marques JC, De Troch M, Gonçalves AMM. 2016. Fatty acid profiling as bioindicator of chemical stress in marine organisms: A review. Ecol. Indic. 67: 657–672. https://doi.org/10.1016/j.ecolind.2016.03.044

Flouty R, Estephane G. 2012. Bioaccumulation and biosorption of copper and lead by a unicellular algae *Chlamydomonas reinhardtii* in single and binary metal systems: A comparative study. J. Environ. Manage. 111: 106–114. https://doi.org/10.1016/j.jenvman.2012.06.042

Garrett RG. 2000. Natural sources of metals to the environment. Human and Ecological Risk Assessment (HERA). 6(6): 945–963. https://doi.org/10.1080/10807030091124383

Gonçalves AMM, Marques JC, Gonçalves F. 2016. Fatty Acids' Profiles of Aquatic Organisms: Revealing the Impacts of Environmental and Anthropogenic Stressors. In Intech: Vol. i (p. 13). https://doi.org/http://dx.doi.org/10.5772/intechopen.68544

Gupta VK, Rastogi A. 2008. Biosorption of lead from aqueous solutions by green algae Spirogyra species: Kinetics and equilibrium studies. J. Hazard. Mater. 152(1): 407–414. https://doi.org/10.1016/j.jhazmat.2007.07.028

Guschina IA, Harwood J L. 2006. Lead and copper effects on lipid metabolism in cultured lichen photobionts with different phosphorus status. Phytochemistry. 67(16): 1731–1739. https://doi.org/10.1016/j.phytochem.2006.01.023

Hadjoudja S, Deluchat V, Baudu M. 2010. Cell surface characterisation of *Microcystis aeruginosa* and *Chlorella vulgaris*. J. Colloid Interface Sci. 342(2): 293–299. https://doi.org/10.1016/j.jcis.2009.10.078

Han, SF, Jin W, Abomohra AEF, Tu R, Zhou X, He Z, Chen C, Xie GJ. 2019. Municipal Wastewater Enriched with Trace Metals for Enhanced Lipid Production of the Biodiesel-Promising Microalga *Scenedesmus obliquus*. Bioenergy Res. 12(4): 1127–1133. https://doi.org/10.1007/s12155-019-10042-5

Hassler CS, Slaveykova VI, Wilkinson, K. J. 2004. Discriminating between intra- and extracellular metals using chemical extractions. LIMNOL OCEANOGR-METH, 2(7): 237–247. https://doi.org/10.4319/lom.2004.2.237

He J, Chen JP. 2014. A comprehensive review on biosorption of heavy metals by algal biomass: Materials, performances, chemistry, and modeling simulation tools. Bioresour. Technol. 160: 67–78. https://doi.org/10.1016/j.biortech.2014.01.068

Huang L, Bell RW. Dell B. Woodward J. (2004). Rapid nitric acid digestion of plant material with an open-vessel microwave system. Communications in Soil Science and plant analysis, 35(3-4), 427-440. https://doi.org/10.1081/CSS-120029723

Jais NM, Mohamed RMSR, Al-Gheethi AA, Hashim MKA. 2017. The dual roles of phycoremediation of wet market wastewater for nutrients and heavy metals removal and microalgae biomass production. Clean Technol Environ Policy. 19(1): 37–52. https://doi.org/10.1007/s10098-016-1235-7

Jamers A, Blust R, De Coen W. 2009. Omics in algae: Paving the way for a systems biological understanding of algal stress phenomena? Aquat. Toxicol. 92(3): 114–121. https://doi.org/10.1016/j.aquatox.2009.02.012

Jara AD, Martel A, Molina C, Nordström L, Rosa VD, Ricardo D. 2003. Flow cytometric determination of lipid content in a marine dinoflagellate, *Crypthecodinium cohnii*. J. Appl. Phycol. 15: 433–438. https://doi.org/10.1023/A:1026007902078

Jena J, Pradhan N, Aishvarya V, Nayak RR, Dash BP, Sukla LB, Panda PK, Mishra BK. 2015. Biological sequestration and retention of cadmium as CdS nanoparticles by the microalga Scenedesmus-24. J. Appl. Phycol., 27(6): 2251–2260. https://doi.org/10.1007/s10811-014-0499-8

Johnson S, Nguyen V, Coder D. 2013. Assessment of cell viability. Curr Protoc Cytom. 15(1): 1–26. https://doi.org/10.1002/0471142956.cy0902s64

Kay AR. 2017. How cells can control their size by pumping ions. Front. Cell Dev. Biol, 5(May), 1–14. https://doi.org/10.3389/fcell.2017.00041

Kim B, Praveenkumar R, Lee J, Nam B, Kim DM, Lee K., Lee YC, Oh YK. 2016. Magnesium aminoclay enhances lipid production of mixotrophic *Chlorella* sp. KR-1 while reducing bacterial populations. Bioresour. Technol. 219: 608–613. https://doi.org/10.1016/j.biortech.2016.08.034

Kumar D, Singh A, Gaur JP. 2008. Mono-component versus binary isotherm models for Cu(II) and Pb(II) sorption from binary metal solution by the green alga *Pithophora oedogonia*. Bioresour. Technol. 99(17): 8280–8287. https://doi.org/10.1016/j.biortech.2008.03.008

Kumar KS, Dahms HU, Won EJ, Lee JS, Shin KH. 2015. Microalgae - A promising tool for heavy metal remediation. Ecotoxicol. Environ. Saf. 113: 329–352. https://doi.org/10.1016/j.ecoenv.2014.12.019

Lee J, Choi H, Hwang U, Kang J, Jai Y, Il K, Kim J. 2019. Toxic effects of lead exposure on bioaccumulation, oxidative stress, neurotoxicity, and immune responses in fish: A review. Environmental Toxicol. Appl. Pharmacol. 68(March): 101–108. https://doi.org/10.1016/j.etap.2019.03.010

Leong YK, Chang J S. 2020. Bioremediation of heavy metals using microalgae: Recent advances and mechanisms. Bioresour. Technol. 303(December): 122886. https://doi.org/10.1016/j.biortech.2020.122886

Li C, Zheng C, Fu H, Zhai S, Hu F, Naveed S, et al., 2021. Contrasting detoxification mechanisms of *Chlamydomonas reinhardtii* under Cd and Pb stress. Chemosphere, 274: 129771. https://doi.org/10.1016/j.chemosphere.2021.129771

Li Y, Xia L, Huang R, Xia C, Song S. 2017. Algal biomass from the stable growth phase as a potential biosorbent for Pb(II) removal from water. RSC Adv. 7(55): 34600–34608. https://doi.org/10.1039/c7ra06749f

Lichtenthaler HK, Buschmann C. 2001. Chlorophylls and Carotenoids: Measurement and Characterization by UV-VIS Spectroscopy. Curr. protoc. food anal., chem. 1(1): F4.3.1-F4.3.8. https://doi.org/10.1002/0471709085.ch21

Liu L, Pohnert G, Wei D. 2016. Extracellular metabolites from industrial microalgae and their biotechnological potential, Mar. Drugs 14(10): 191. https://doi.org/10.3390/md14100191

Liyanage LMM, Lakmali WGM, Athukorala SNP, Jayasundera KB. 2020. Application of live *Chlorococcum aquaticum* biomass for the removal of Pb(II) from aqueous solutions. J. Appl. Phycol. 32(6): 4069–4080. https://doi.org/10.1007/s10811-020-02242-w

Lu N, Wei D, Jiang XL, Chen F, Yang ST. 2012. Fatty Acids Profiling and Biomarker Identification in Snow Alga *Chlamydomonas Nivalis* by NaCl Stress Using GC/MS and Multivariate Statistical Analysis. Anal., Lett., 45(10): 1172–1183. https://doi.org/10.1080/00032719.2012.673094

Luis P, Behnke K, Toepel J, Wilhelm C, 2006. Parallel analysis of transcript levels and physiological key parameters allows the identification of stress phase gene markers in *Chlamydomonas reinhardtii* under copper excess. Plant, Cell Environ. 29: 2043–2054. https://doi.org/10.1111/j.1365-3040.2006.01579.x

Marcilla A, Gómez-Siurana A, Gomis C, Chápuli E, Catalá MC, Valdés FJ. 2009. Characterization of microalgal species through TGA/FTIR analysis: Application to nannochloropsis sp. Thermochim Acta., 484(1–2): 41–47. https://doi.org/10.1016/j.tca.2008.12.005

Minhas AK, Hodgson P, Barrow C J, Adholeya A. 2016. A review on the assessment of stress conditions for simultaneous production of microalgal lipids and carotenoids. Front. Microbiol. 7, 546. https://doi.org/10.3389/fmicb.2016.00546

Nanda M, Kumar K, Kumar V. 2021. Micro-pollutant Pb(II) mitigation and lipid induction in oleaginous microalgae *Chlorella sorokiniana* UUIND6. Environ. Technol. Innov., 23: 101613. https://doi.org/10.1016/j.eti.2021.101613

Napan K, Teng L, Quinn JC, Wood BD. 2015. Impact of heavy metals from flue gas integration with microalgae production. Algal Res. 8: 83–88. https://doi.org/10.1016/j.algal., 2015.01.003

Navakoudis AME, Ververidis KPF. 2018. Microalgae: a potential tool for remediating aquatic environments from toxic metals. Int J Environ Sci Technol (Tehran). (0123456789). https://doi.org/10.1007/s13762-018-1783-y

Nazari F, Movafeghi A, Jafarirad S, Kosari-Nasab M, Divband B. 2018. Synthesis of Reduced Graphene Oxide-Silver Nanocomposites and Assessing Their Toxicity on the Green Microalga *Chlorella vulgaris.* BioNanoScience, 8(4): 997–1007. https://doi.org/10.1007/s12668-018-0561-0

Olofsson M, Lamela T, Nilsson E, Bergé JP, del Pino V, Uronen P, Legrand C. 2012. Seasonal variation of lipids and fatty acids of the microalgae *Nannochloropsis oculata* grown in outdoor large-scale photobioreactors. Energies, 5(5): 1577–1592. https://doi.org/10.3390/en5051577

Ozkan A, Berberoglu H. 2013. Physico-chemical surface properties of microalgae. Colloids Surf. B. 112: 287–293. https://doi.org/10.1016/j.colsurfb.2013.08.001

Pérez-Rama M, Abalde Alonso J, Herrero López C, Torres Vaamonde E. 2002. Cadmium removal by living cells of the marine microalga *Tetraselmis suecica.* Bioresour. Technol. 84(3): 265–270. https://doi.org/10.1016/S0960-8524(02)00045-7

Pham T-L, Dao T-S, Bui H, Pham T, Ngo T, Bui H. 2020. Lipid Production Combined with Removal and Bioaccumulation of Pb by Scenedesmus sp. Green Alga. Pol J Environ Stud. 29(2): 1785–1791. https://doi.org/10.15244/pjoes/109277

Piotrowska-Niczyporuk A, Bajguz A, Talarek M, Bralska M, Zambrzycka E. 2015. The effect of lead on the growth, content of primary metabolites, and antioxidant response of green alga *Acutodesmus obliquus* (Chlorophyceae). Environ. Sci. Pollut. Res. 22(23): 19112–19123. https://doi.org/10.1007/s11356-015-5118-y

Rai UN, Singh NK, Upadhyay AK, Verma S. 2013. Chromate tolerance and accumulation in *Chlorella vulgaris L.*: Role of antioxidant enzymes and biochemical changes in detoxification of metals. Bioresour. Technol. 136: 604–609. https://doi.org/10.1016/j.biortech.2013.03.043

Randrianarison G, Ashraf MA. 2017. Microalgae: a potential plant for energy production. Geology, Ecology, and Landscapes, 1(2): 104–120. https://doi.org/10.1080/24749508.2017.1332853

Richmond A. 2004. Economic Applications of Microalgae. In Handbook of Microalgal Culture: Applied Phycology and Biotechnology (pp. 255–353). https://doi.org/10.1002/9781118567166.ch1

Rocchetta I, Mazzuca M, Conforti V, Balzaretti V, de Molina MDCR. 2012. Chromium induced stress conditions in heterotrophic and auxotrophic strains of *Euglena gracilis.* Ecotoxicol. Environ. Saf. 84: 147–154. https://doi.org/10.1016/j.ecoenv.2012.07.020

Rocchetta, I, Mazzuca M, Conforti V, Ruiz L, Balzaretti V, De Molina MDCR. 2006. Effect of chromium on the fatty acid composition of two strains of *Euglena gracilis.* Environ. Pollut. 141(2): 353–358. https://doi.org/10.1016/j.envpol.2005.08.035

Romero N, Visentini FF, Márquez VE, Santiago LG, Castro GR, Gagneten AM. 2020. Physiological and morphological responses of green microalgae *Chlorella vulgaris* to silver nanoparticles. Environ. Res. 189(April). https://doi.org/10.1016/j.envres.2020.109857

Saavedra R, Muñoz R, Taboada ME, Vega M, Bolado S. 2018. Comparative uptake study of arsenic, boron, copper, manganese and zinc from water by different green microalgae. Bioresour. Technol. 263(April): 49–57. https://doi.org/10.1016/j.biortech.2018.04.101

Salama ES, Govindwar SP, Khandare RV, Roh HS, Jeon BH, Li X. 2019. Can Omics Approaches Improve Microalgal Biofuels under Abiotic Stress? Trends Plant Sci. 24(7): 611–624. https://doi.org/10.1016/j.tplants.2019.04.001

Samadani M, Perreault F, Oukarroum A, Dewez D. 2018. Effect of cadmium accumulation on green algae *Chlamydomonas reinhardtii* and acid-tolerant Chlamydomonas CPCC 121. Chemosphere, 191, 174–182. https://doi.org/10.1016/j.chemosphere.2017.10.017

Selvi A, Rajasekar A, Theerthagiri J, Ananthaselvam A, Sathishkumar K, Madhavan J, Rahman PKSM. 2019. Integrated remediation processes toward heavy metal removal/recovery from various environments-A review. Front. Environ. Sci. 7(May). https://doi.org/10.3389/fenvs.2019.00066

Sibi G, Anuraag T S, Bafila G. 2014. Copper stress on cellular contents and fatty acid profiles in Chlorella species. Online J Biol Sci., 14(3): 209–217. https://doi.org/10.3844/ojbsci.2014.209.217

Singh DV, Bhat RA, Upadhyay AK, Singh R, Singh DP. 2021. Microalgae in aquatic environs: A sustainable approach for remediation of heavy metals and emerging contaminants. Environ. Technol. Innov. 21: 101340. https://doi.org/10.1016/j.eti.2020.101340

Sorigué D, Légeret B, Cuiné S, Morales P, Mirabella B, Guédeney G, et al., 2016. Microalgae synthesize hydrocarbons from long-chain fatty acids via a light-dependent pathway. Plant Physiol. 171(4): 2393–2405. https://doi.org/10.1104/pp.16.00462

Sudhakar K, Premalatha M. 2015. Characterization of micro algal biomass through FTIR/TGA /CHN analysis: Application to *Scenedesmus* sp. ENERG SOURCE PART A, 37(21): 2330–2337. https://doi.org/10.1080/15567036.2013.825661

Suman TY, Radhika Rajasree SR, Kirubagaran R. 2015. Evaluation of zinc oxide nanoparticles toxicity on marine algae *Chlorella vulgaris* through flow cytometric, cytotoxicity and oxidative stress analysis. Ecotoxicol. Environ. Saf.113: 23–30. https://doi.org/10.1016/j.ecoenv.2014.11.015

Tahira S, Khan S, Samrana S, Shahi L, Ali I, Murad W, et al., 2019. Bio-assessment and remediation of arsenic (arsenite As-III) in water by *Euglena gracilis*. J. Appl. Phycol. 31(1): 423–433. https://doi.org/10.1007/s10811-018-1593-0

Thomas MK, Fontana S, Reyes M, Pomati, F. 2018. Quantifying cell densities and biovolumes of phytoplankton communities and functional groups using scanning flow cytometry, machine learning and unsupervised clustering. PLoS ONE, 13(5): 1–22. https://doi.org/10.1371/journal., pone.0196225

Tran NH, You S, Hosseini-bandegharaei A. 2017. Mistakes and inconsistencies regarding adsorption of contaminants from aqueous solutions: A critical review. Water Res. 120: 88–116. https://doi.org/10.1016/j.watres.2017.04.014

Urrutia C, Yañez-Mansilla E, Jeison D. 2019. Bioremoval of heavy metals from metal mine tailings water using microalgae biomass. Algal Res. 43(September): 101659. https://doi.org/10.1016/j.algal., 2019.101659

USEPA. 2016. National Primary Drinking Water Regulations. in: EPA 816-F-09-004, (Ed.) U.S.E.P. Agency, United State Environmental Protection Agency. United State. Drinking Water Contaminants, 141–142. https://doi.org/EPA 816-F-09-004

van den Berg RA, Hoefsloot HCJ, Westerhuis JA, Smilde A K, et al., 2006. Centering, scaling, and transformations: Improving the biological information content of metabolomics data. BMC Genom. 7: 1–15. https://doi.org/10.1186/1471-2164-7-142

Van Oss CJ, Chaudhury MK, Good RJ. 1988. Interfacial Lifshitz-van der Waals and polar interactions in macroscopic systems. Chem. Rev. 88(6): 927–941. https://doi.org/10.1021/cr00088a006

Venkata Mohan, S., Ramanaiah, S. V., Rajkumar, B., Sarma, P. N. (2007). Removal of fluoride from aqueous phase by biosorption onto algal biosorbent Spirogyra sp.-IO2: Sorption mechanism elucidation. J. Hazard. Mater. 141(3): 465–474. https://doi.org/10.1016/j.jhazmat.2006.07.008

Vichi S, Gallardo-chacón JJ, Pradelles R, Chassagne D, López-tamames E, Buxaderas S. 2010. Surface properties of *Saccharomyces cerevisiae* lees during sparkling wine ageing and their effect on flocculation. Int. J. Food Microbiol. 140(2–3): 125–130. https://doi.org/10.1016/j.ijfoodmicro.2010.04.009

Vogler EA. 1998. Structure and reactivity of water at biomaterial surfaces. Adv. Colloid Interface Sci. 74, 69–117. https://doi.org/10.1016/S0001-8686(97)00040-7

Volkman JK. 2016. Sterols in Microalgae. The Physiology of Microalgae. In Developments in Applied Phycology 6 (pp. 485–505). https://doi.org/DOI 10.1007/978-3-319-24945-2_19

Wollmann, F., Dietze, S., Ackermann, J. U., Bley, T., Walther, T., Steingroewer, J., Krujatz, F. (2019). Microalgae wastewater treatment: Biological and technological approaches. Engineering in Life Sciences, 19(12), 860–871. https://doi.org/10.1002/elsc.201900071

Wychen SV, Laurens LML. 2017. Total Carbohydrate Content Determination of Microalgal Biomass by Acid Hydrolysis Followed by Spectrophotometry or Liquid Chromatography. In Methods in Molecular Biology (pp. 257–284). https://doi.org/10.1007/7651_2017_106

Xia L, Huang R, Li Y, Song S. 2017. The effect of growth phase on the surface properties of three oleaginous microalgae (Botryococcus sp. FACGB-762, *Chlorella* sp. XJ-445 and *Desmodesmus bijugatus* XJ-231). PLoS ONE, 12(10). https://doi.org/10.1371/journal., pone.0186434

Yalçin E, Çavuşoğlu K, Kinalioğlu K. 2010. Biosorption of Cu2+ and Zn2+ by raw and autoclaved *Rocella phycopsis*. J Environ Sci (China). 22(3): 367–373. https://doi.org/10.1016/S1001-0742(09)60117-0

Yan X, Liu M, Zhong J, Guo J, Wu W. 2018. How human activities affect heavy metal contamination of soil and sediment in a long-term reclaimed area of the Liaohe River Delta, North China. Sustainability (Switzerland), 10(2): 1–19. https://doi.org/10.3390/su10020338

Yentsch CS, Yentsch CM. 2008. Single cell analysis in biological oceanography and its evolutionary implications. J. Plankton Res. 30. https://doi.org/10.1093/plankt/fbm092

Ying ZT, Dobbs FC. 2007. Green autofluorescence in dinoflagellates, diatoms, and other microalgae and its implications for vital staining and morphological studies. Appl. Environ. Microbiol. 73(7): 2306–2313. https://doi.org/10.1128/AEM.01741-06

Zehra T, Priyantha N, Lim LBL. 2016. Removal of crystal violet dye from aqueous solution using yeast-treated peat as adsorbent: thermodynamics, kinetics, and equilibrium studies. Environ. Earth Sci. 75(4): 1–15. https://doi.org/10.1007/s12665-016-5255-8

Zheng H, Guo W, Li S, Wu Q, Yin R, Feng X, et al., 2016. Biosorption of cadmium by a lipid extraction residue of lipid-rich microalgae. RSC Adv. 6(24): 20051–20057. https://doi.org/10.1039/c5ra27264e

Zhou GJ, Peng FQ, Zhang LJ, Ying GG. 2012. Biosorption of zinc and copper from aqueous solutions by two freshwater green microalgae *Chlorella pyrenoidosa* and *Scenedesmus obliquus*. Environ. Sci. Pollut. Res. 19(7): 2918–2929. https://doi.org/10.1007/s11356-012-0800-9

Les microalgues présentent un réel potentiel de bioremédiation des contaminants organiques et inorganiques. Toutefois, l'une des difficultés qui limiteraient leur utilisation dans le traitement des effluents industrielles chargés en métaux lourds réside dans le fait que ces rejets peuvent être fortement troubles ou colorés, en raison de la présence des polluants organiques, en particulier les colorants synthétiques. La présence de ces derniers limiterait ainsi la pénétration de la lumière indispensable à l'activité photosynthétique des microalgues, ce qui aurait un effet négatif aussi bien sur leur croissance que sur leur activité épuratrice.

L'application d'une étape préalable en vue de la décoloration de ces rejets, grâce à l'action des micro-organismes capables d'éliminer de tels polluants organiques permettrait de surmonter ce défi. Les levures, microorganismes hétérotrophes, connues pour leur habilité de dégradation de nombreux substrats carbonés, ont été étudiées pour leur potentiel de mycoremédiation des colorants synthétiques, comme model de polluants organiques. Ainsi, l'évaluation de souches de levures dans la décoloration de ces composés, l'étude du mécanisme et l'optimisation des facteurs qui influencent cette décoloration ont fait l'objet du deuxième axe de recherche abordé dans cette thèse.

Chapitre III

Mycoremediation of azo dyes using *Cyberlindnera fabianii* yeast strain: Application of designs of experiments for decolorization optimization

RÉSUMÉ

Dans ce troisième axe de recherche, nous avons commencé par évaluer la capacité de décoloration d'un colorant azoïque (AR_{14}) par trois souches de levure préalablement isolées d'un site contaminé. La souche *Cyberlindnera fabianii* a été retenue en raison de sa grande capacité de décoloration. Afin de prouver sa performance, cette souche a été ensuite testée vis-à-vis d'autres colorants ayant des structures chimiques différentes. Sur la base de la couleur de la biomasse après décoloration, les mécanismes d'élimination des colorants pourraient être déduits. Les cellules deviennent colorées dans le cas de la biosorption ou de la bioaccumulation, alors que les cellules exerçant la biodégradation des colorants conservent leur couleur originale. Sur la base de la couleur du culot et l'analyse UV-Vis du surnagent, le colorant AR_{14} a été choisi comme colorant modèle pour examiner les mécanismes enzymatiques impliqués dans sa biodégradation. Les activités des oxydases et réductases, intra et extracellulaires ont été ainsi mesurées. Les résultats indiquent une augmentation significative des activités intra et extracellulaires de la laccase, la tyrosinase, la manganèse peroxydase et de l'azoréductase. Pour évaluer l'efficacité de la biodégradation de point de vue éco-toxicologique, un test de phytotoxicité des sous-produits de la biodégradation de l'AR14 vis à vis de *Medicago sativa* a été effectué. D'après les résultats obtenus au regard du pourcentage de la germination, de la longueur des plumules et des radicules, la biodégradation enzymatique de l'AR14 par *W. anomalus* a permis une détoxification efficace de ce polluant.

Dans la dernière partie de ce travail, l'approche statistique par plan d'expériences a été utilisée pour l'optimisation de la capacité de décoloration de AR_{14} par *C. fabianii*. Le criblage des facteurs a été effectué selon le plan de Plackett-Burman. Cinq variables (Température, pH, Taille de l'inoculum, Concentration initiale du colorant et Vitesse d'agitation) ont été examinées. En outre, l'optimisation de la décoloration et les éventuelles interactions synergiques ou antagonistes entre les facteurs ont été évaluées avec le plan de Box-Behnken. Le criblage des facteurs a montré que le pH, la concentration du colorant et la vitesse d'agitation avaient des effets significatifs. Ces facteurs et leur effet combiné ont été évalués en utilisant la méthodologie de surface de réponse. Le pH était le facteur le plus significatif, suivi par la concentration de colorant. L'analyse du tracé de contour et du diagramme de surface de réponse 3D a montré que la décoloration était inversement proportionnelle à la concentration initiale de colorant, mais proportionnelle au pH initial et à la vitesse d'agitation. Dans des conditions optimales (pH = 5,15 et AR14 = 50 mg L^{-1}), *C. fabianii* a pu décolorer plus de 97% en moins de 12 H. Les résultats de cette étude nous ont permis de conclure que la souche *C. fabianii* a le potentiel d'être exploitée dans la mycorémédiation des colorants synthétiques

Water Environment Federation
the water quality people™

Mycoremediation of azo dyes using *Cyberlindnera fabianii* yeast strain: Application of designs of experiments for decolorization optimization

Mohammed Danouche ,[1,2,*] Mohamed Ferioun ,[2] Wifak Bahafid ,[2] Naima El Ghachtouli [2]

[1] Green Biotechnology Center, MAScIR (Moroccan Foundation for Advanced Science, Innovation and Research), Rabat, Morocco

[2] Microbial Biotechnology and Bioactive Molecules Laboratory, Faculty of Sciences and Technology, Sidi Mohamed Ben Abdellah University, Fez, Morocco

Received 18 July 2020; Revised 7 October 2020; Accepted 11 December 2020

Correspondence to: Mohammed Danouche, Green Biotechnology Center, MAScIR (Moroccan Foundation for Advanced Science, Innovation and Research), Rabat, Morocco.
Email: mohammed.danouche@usmba.ac.ma

DOI: 10.1002/wer.1499

© 2020 Water Environment Federation

Abstract

This study investigated the dye decolorization capacity of three yeast strains. *Cyberlindnera fabianii* was shortlisted for its high decolorization capacity and was further tested on various azo dyes. Based on the color of the biomass, and the UV–Vis analysis, Acid Red 14 was selected as a model dye, to examine the enzymatic biodegradation. The results showed significant increase in the intracellular and extracellular activities of laccase, tyrosinase, manganese peroxidase, and azoreductase. Phytotoxicity assessment indicated that the AR14 biodegradation by-products were not phytotoxic compared to the original dye molecules. Regarding the decolorization optimization, the screening of factors using the Plackett–Burman design showed that pH, dye concentration, and shaking speed had significant effects. These factors and their combined effect were evaluated using response surface methodology with the Box–Behnken model. The pH was the most significant factor, followed by dye concentration. The analysis of the contour plot and the 3D response surface diagram showed that the decolorization was inversely proportional to the increase in the initial dye concentration, but proportional to the initial pH and shaking speed. At optimal conditions (pH = 5.154, AR14 = 50 mg/L), *C. fabianii* could decolorize more than 97% of AR14 within 12 hr. © 2020 Water Environment Federation

Practitioner points

- *Cyberlindnera fabianii* is a successful candidate for dye mycoremediation.
- Oxidase and reductase are the key enzymes involved in the biodegradation of azo dyes.
- By-products of Acid red 14 biodegradation are not phytoxic compared to the original dye.
- Design of experience tools enables to determine optimum conditions for efficient decolorization.

Key words

Box–Behnken design; decolorization; enzymatic activity; optimization; Plackett–Burman design; yeast

Introduction

Since the beginning of the industrial revolution in the nineteenth century, the balanced equation of economic growth while protecting the environment has not yet been solved. Indeed, our planet faces an array of challenges, especially water pollution, which is considered as one of the critical issues emerging from anthropogenic activities. In recent decades, scientists, environmentalists, and legislators are increasingly interested in finding solutions that can help to address this challenge. Particular interest has been projected toward the treatment of industrial effluents. Compared to

other industrial sectors, the textile industry is one the major consumers of water. It was estimated that about 200–500 litter of water is required to produce 1 kg of a finished textile product (Vijayaraghavan & Yun, 2008; Waghmode et al., 2012b). It, therefore, generates high volumes of wastewater, composed of heterogeneous substances including suspended solids, surfactants, heavy metals, and various synthetic dyes (Balapure et al., 2015; Chen et al., 2009). The exact quantity of dyes released to the environment is uncertain, but it is well known that more than 10,000 tons of dye is utilized in the textile industry per year, and about 10%–15% of it is liberated through effluents during the dyeing process (Kunamneni et al., 2008; Saratale et al., 2011). Moreover, textile industries are highly demanding. Physicochemical requirements including resistance of dyes to changing environmental conditions such as washing, exposure to light, chemicals, and biological attacks are considered essential (Khan et al., 2013). These same requirements make the degradability of such synthetic dyes more difficult and complicated, thereby making their treatment too complex for conventional methods. On the other hand, releasing wastewater effluents contaminated with such toxic dyes into aqueous systems can be deleterious to exposed living organisms, including humans (Moopantakath & Kumavath, 2018). Therefore, laws and regulations have been adopted worldwide for the management and treatment of dye contaminants prior to their release into the environment. Several single or hybrid/combined physical and chemical processes have been applied for the treatment of textile effluents, such as membrane processes, ultrasonic and photochemical oxidation processes, as well as electrochemical processes (Arslan et al., 2016). Although these methods are effective, they require a considerable amount of chemicals that can lead to secondary pollution. Likewise, the physical methods necessitate an energy consuming facility, which makes the processing costs overpriced, thereby restricting the large-scale applications of these methods (Fu & Wang, 2011; Srinivasan & Viraraghavan, 2010). The exploitation of ecological principles of bacteria, fungi, and microalgae in the treatment of synthetic dyes has emerged as a promising alternative solution (Chen et al., 2009; Jafari et al., 2014; Miranda et al., 2013). In fact, mycoremediation or the bioremediation using fungi has increasingly been used for the biodegradation of recalcitrant xenobiotics, including polycyclic aromatic pollutants like synthetic dyes (Rhodes, 2014). Nevertheless, the application of mycoremediation using filamentous fungi is limited by their slow growth and acid environment requirement. Contamination by bacteria is also highly probable, due to the long period of time required for a complete decolorization (Singh & Arora, 2011). Much attention has recently been drawn to the use of yeast in the bioremoval of synthetic dyes, because of the many advantages that they have over other microorganisms, including their rapid growth, great plasticity and ability to adapt to unfavorable growth conditions (Jafari et al., 2014; Sen et al., 2016). Research focusing on the decolorization mechanisms of ascomycete and basidiomycete yeast strains demonstrated the involvement of active and/or passive metabolism processes, namely extracellular biosorption (Dil et al., 2017; Mahmoud, 2016), intracellular bioaccumulation (Das et al., 2010; Gönen & Aksu, 2009), and an intracellular/extracellular biodegradation (Martorell et al., 2018; Tan et al., 2019). In the present study, the azo dye C. I. Acid Red 14 (AR14) (disodium;4-hydroxy-3-[(4-sulfonatonaphthalen-1-yl)diazenyl]naphthalene-1-sulfonate) was used to evaluate the biodegradation of sulfonated azo dyes using yeast, due to its wide range of applications in several industries such as the textile, leather (C. I. 14720; Acid Red B) (Daneshvar et al., 2006), and food industries (Carmoisine, Azorubin, Food red 3 or E122) (Kiayi et al., 2019). Therefore, it is one of the main contaminants present in the effluents released by these industries. On the other hand, AR14 dye has particular chemical properties, such as water solubility, anionic characteristics, and a sulfonated (SO3Na), monoazoic (-N = N-) chemical structure. It contains two naphthalene groups in its structure, which are difficult to break down (Zhu et al., 2012). Several researchers have focused on the removal of synthetic dyes by means of various methods such as Fenton reaction (Daneshvar et al., 2006; Idel-aouad et al., 2011), photocatalytic degradation (Akerdi et al., 2016; Samarghandi et al., 2020), or electrocoagulation processes (Daneshvar et al., 2004). Despite their elimination effectiveness, the majority of these approaches are costly, environmentally destructive, and time-consuming. As a result, financial and technical limitations have made wastewater treatment using such techniques a difficult task (Khalid et al., 2017). The use of bacteria (Franca et al., 2020; Liu et al., 2007; Uddin et al., 2007) or fungi (Kiayi et al., 2019; Qu et al., 2012) in the treatment of colored wastewater has recently emerged as a promising solution due to its advantages over other conventional methods (Rai et al., 2005). To the best of our knowledge, this is the first report of utilizing yeast strain of *Cyberlindnera fabianii* for the decolorization of azo dyes. In this study, we have first evaluated the decolorization capacity of three metal-tolerant yeast strains previously isolated from a contaminated location in Fez city (Morocco). Then, the decolorization ability of different azo dyes with varied chemical structures was achieved by the selected strain of *C. fabianii*. It is known that fungal biodegradation was generally associated with their ligninolytic enzyme system (Kumar & Chandra, 2020). Hence, intra- and extracellular oxidase and reductase activities were measured after complete decolorization of the azo dye AR14. On the other hand, the azo dye AR14 has been reported as harmful against microorganisms (Song et al., 2018), plants (Journal, 2018), animals (Amin et al., 2010), and humans (Osman et al., 2004). To evaluate the effectiveness of the treatment from a toxicological point of view, phytotoxicity assessments of AR14 before and after complete decolorization were evaluated with plant seeds of *Medicago sativa*. In the last section of this work, the statistical approach of the design of experiments (DoE) was used for the optimization of prime parameters influencing the decolorization capacity of *C. fabianii*. DoE is a useful method for improving the decolorization efficiency and reducing process variability, time, as well as the overall cost (Papadopoulou et al., 2013). For screening factors, the Plackett–Burman design was used due to its capacity to substantially reduce the number

of repeated experiments for further optimization analysis (Karlapudi et al., 2018). Additionally, the optimization of the decolorization and the possible synergistic or antagonistic interactions between significant factors were evaluated with Box–Behnken design, which is well suited for fitting a quadratic surface and usually works well for the optimization process (Kousha et al., 2012). The data were analyzed by fitting toa second-order polynomialmodel, which was statistically validated by performing analysis of variance (ANOVA) and lack of fittest to evaluate the significance of the model (Mona et al., 2011). Thereafter, the predicted optimum conditions, using the RSM method, were validated experimentally.

Material and methods

Chemicals

The AR14 (chemical formula: $C_{20}H_{12}N_2Na_2O_7S_2$, molecular weight: 502.42 g/mol) was used in this study as a model of azo dye. The decolorization performance of the selected strain was also tested against other azo dyes: Mordant Black 17 (MB17) (C.I.-15705), Acid Red 18 (AR18) (C.I.16255), Food Red 17 (FR17) (C.I.16035), Direct Red 28 (DR28) (C.I.22120), Acid Orange 52 (AO52) (C.I.13025), and Acid Yellow 23 (AY23) (C.I.19140). The chemical structure of these dyes is given in Table 3. Stock solutions of the dyes were prepared at 5 g/L in distilled water. The dye solutions were sterilized by membrane filtration (Millipore Millex ® - GS, 0.22 Mm filter unit). All other chemicals are analytical-grade reagents purchased from Sigma and Merck.

Yeast source and culture medium

The ascomycetous yeast strains of *Cyberlindnera fabianii* (HE650139), *Wickerhamomyces anomalus* (HE648168), and *Candida tropicalis* (HE650140) used in this study were previously isolated from a contaminated site in the region of Fez (Morocco)(Bahafid et al., 2013). Pure cultures of yeast strains were maintained at 4°C on YPD medium containing (g/L): Difco peptone: 20, yeast extract: 10, glucose to 2% (Liu et al., 2011), and subcultured at regular intervals.

Screening of yeast strains for dye decolorization

The screening of yeast strains for dye decolorization was performed in 250-ml Erlenmeyer flasks containing 100 ml of liquid YPD-modified medium, as previously suggested by Bahafid et al. (2013). Sterilized mediums were inoculated with pure culture of yeast strains. Appropriate volume was then added to the culture mediums from the dye stock solution, to have a final concentration of 50 mg/L. This concentration was systematically used in all subsequent experiments, which were conducted at 30 ± 2°C under rotary shaking (120 rpm), unless otherwise stated. Flasks containing doped YPD medium with 50 mg/L of AR 14 without inoculum were used as abiotic control under the same operation conditions. The decolorization performance was monitored with a Prim Light SECOMAM spectrophotometer, using culture supernatants obtained after centrifugation at 10,000 g for 10 min. The color removal was reported as percentage decolorization (D%):

$$D\% = \left(A_i - A_f\right) / A_i \times 100 \quad (1)$$

where $A_{(i)}$ and $A_{(t)}$ are the absorbance of dye-amended medium at the start point (i) and at a cultivation time (t), respectively.

Growth measurement and biomass determination

The biomass concentration was estimated based on the calibration curve of the optical density at 600 nm and the dry cell weight. Dilution series of the cell suspension were made, and optical density was measured. Then, the cell suspension was filtered through a preweighed Whatman GF/C glass fiber filter and dried at 90°C for 24 hr. The optical values were converted to dry weight by the following formula:

$$\text{Dry cell weight (DCW)} = 0.2418 \times \text{OD600} + 0.2609 \quad \left(R^2 = 0.989\right) \quad (2)$$

Yeast decolorization performance of various synthetic dyes

The decolorization performance of the selected yeast strain (*C. fabianii*) was examined against five other azo dyes, namely MB17, AR18, FR17, DR28, and AY23. The experiment was carried out as previously described, and 100 ml of YPD-modified mediums containing 50 mg/L of the different single dye solutions was inoculated with cells of *C. fabianii*. Thereafter, the cultures were incubated at 30°C under orbital shaking condition (120 rpm) for 12 hr. The decolorization performance was carried out spectrophotometrically at λ max for each dye (Table 3), using culture supernatants obtained after centrifugation at 10,000 g for 10 min. Then, the confirmation of biodegradation of the targeted dye was determined spectrophotometrically (200–800 nm) using Ultrospec™ 3100 pro UV–Vis instrument.

Determination of yeast enzyme activities

Preparation of cell extracts. Cell-free extracts were prepared as reported by Jadhav and Govindwar (2006). Briefly, after complete decolorization, cells of *C. fabianii* cultivated in the YPD-modified medium as negative control and cells from the test medium containing 50 mg/L of AR14 were collected by centrifugation at 10,000 g for 20 min at 4°C. The supernatants were used to assess the extracellular enzymatic activities. For the determination of the intracellular enzymatic activities, the pellets were washed with 10 mM potassium phosphate buffer (pH 7.2), then homogenized using a mortar and pestle at 4°C in the same buffer containing 1 mM polymethyl sulfonyl fluoride (PMSF), 1 mM EDTA, 5 mM β-mercaptoethanol, 1% glycerol, and 50 mM NaCl. The intracellular extract was collected by centrifugation at 10,000 g for 20 min at 4°C.

Enzymatic activities. The activities of laccase (Lac), tyrosinase (Tyr), manganese peroxidase (Mnp), and azoreductase (AzoR) were spectrophotometrically evaluated in intracellular and extracellular extracts. Lac activity was determined as described by Arora and Sandhu (1985), the reaction mixture contained

10 mM acetate buffer (pH 5.0), 1.76 mM guaiacol, and samples of the enzyme extract. The reaction was incubated at 25°C for 2 hr, and the absorbance was measured at 450 nm. The Tyr activity was assayed by following the procedures stated by Duckworth and Coleman (1970). The reaction mixture contained 50 mM of potassium phosphate buffer (pH 6.5) and 1 mM of L-tyrosine as a substrate. The reaction was incubated at 25°C for 10 min, and the absorbance was measured at 280 nm. The Mnp activity was assayed as reported by Paszczyński et al. (1988), the reaction mixture containing 0.2 M sodium tartrate buffer (pH 5.0), 0.1 mM $MnSO_4$, 0.1 mM H_2O_2 was incubated at 25°C for 1 min, and the absorbance wavelength was measured at 238 nm. The AzoR activity was analyzed using the protocol from Saratale et al. (2009a), by monitoring the decrease in the AR14 concentration at 518 nm in a reaction mixture of 2.2 mL containing 152 μM AR14, 50 mM sodium phosphate buffer (pH 5.5) and 20 μM NADH. All enzyme assays were conducted in triplicate, and the average rates were calculated to represent the enzyme activity. One unit of enzyme activity is defined as the change in absorbance unit min^{-1} mg^{-1} of the enzyme. The estimation of the soluble proteins was performed by Bradford method using bovine serum albumin (BSA) as a standard (Bradford, 1976).

Phytotoxicity assessment

Phytotoxicity of the untreated and treated dye was evaluated with plant seeds of *M. sativa*. Seeds were sterilized by dipping into ethanol solution (95%) for 5 min and sodium hypochlorite (5%) for 10 min, and then rinsed with sterile water. Thirty seeds were germinated in Petri dishes containing 7% Agar (w/v) watered with 5 ml of dye solution before and after treatment. The control set was carried out by distilled water (DW) at the same time. Seed germination (%) and lengths (cm) of plumule and radicle were recorded after 5 days of growth at room temperature. The germination % was calculated by using the following formula (Waghmode et al., 2012a):

$$\text{Germination}\,(\%) = \left(\text{No. of seeds germinated}/\text{No. of seeds sowed}\right) \times 100 \quad (3)$$

Statistical analysis

All experiments were conducted in triplicate, and the data were expressed as the mean ± standard deviation. The statistical analysis was performed with *t*-test and the one-way ANOVA using GraphPad Prism software version 8.0. The *p*-values < 0.05 were considered statistically significant.

Optimization of decolorization by using the design of experiments

Factors screening using Plackett–Burman design. The first step of the optimization consists of the screening of factors that significantly influence the decolorization process of AR14 by *C. fabianii*. This step was performed with the Plackett–Burman design (PBD). Five variables were screened using MINITAB 18.1 software, including temperature (°C), initial pH of the medium, inoculum size (g/L), initial dye concentration (mg/L), and the shaking speed (rpm), at two levels: maximum (−1) and minimum (+1) (Table 1). These variables were selected by means of a bibliographic analysis of previous work on the one-factor-at-a-time method. According to the adopted method, it was presumed that there is no interaction between the various operating parameters. Therefore, a first-order multiple regression (Equation 4) can model the data properly. The experiments were carried out in duplicate (2k-factorial PBDs for a total of 24 experiments):

$$Y = \beta_0 + \sum \beta_i X_i \;\; (i = 1, \ldots, k) \quad (4)$$

where Y is the decolorization response, β_0 is the model intercept and β_i is the variable estimates (Plackett & Burman, 1946). In the next step, the statistical significance of the first-order model was identified using ANOVA and the lack of fit, while effective parameters were selected by the Fisher variation ratio (F) and the significant probability value (p) and judgment in this regard were undertaken based on their comparison with tabulated value.

Optimization of process parameters using Box–Behnken model. On the basis of preliminary experimental results of the Plackett–Burman design, three variables were found to have an effect on the decolorization process. Thereafter, the decolorization was optimized using the response surface methodology (RSM) to determine the relationship between a set of controllable experimental parameters and the observed results. Such design is capable of fitting a second-order prediction equation for the response (Myers & Montgomery, 1995). The optimization method by RSM consists of three steps: first conducting statistically designed experiments, then estimating the coefficients in a mathematical model, and finally predicting the response and confirming the adequacy of the model (Box & Hunter, 1957). A class of three levels (low (−1), central point (0) and high (+1)) complete factorial design for the estimation of the parameters in a second-order model was established based on the Box Behnken design model (BBD) (Box & Behnken, 1960) (Table 2). The RSM represents independent process variables in the following quantitative form:

TABLE 1. Variables and levels used in screening design for factors affecting decolorization

TEST VARIABLES	TEMPERATURE (°C) (*A*)	PH (*B*)	INOCULUM SIZE (G/L) (*C*)	DYE (MG/L) (*D*)	SHAKING SPEED (RPM) (*E*)
Low level (−)	25	3	0.04	50	0
High level (+)	37	7	0.004	200	120

TABLE 2. Process variables used in Box–Behnken design, with three design factors and one optimization parameters (decolorization responses)

NAME	UNITS	TYPE	−1	0	+1
pH (*A*)	–	Factor	3	5	7
Dye concentration (*B*)	mg/L	Factor	50	125	200
Shaking speed (*C*)	rpm	Factor	0	60	120
Decolorization	(%)	Response			

$$Y = f\left(X_1;\ X_2;\ X_3;\ X_4;\ldots X_n\right) \pm \varepsilon \tag{5}$$

where (Y) is the decolorization rate, (f) is the response function, ($X_1, X_2, X_3, X_4,\ldots,X_n$) are the independent variables, and (ε) is the experimental error. The surface response is constructed by plotting the predicted response. When the response varies linearly, the linear function equation can be represented as:

$$Y = \beta_0 + \beta_1 x_1 + \beta_2 x_2 + \beta_3 x_3 + \beta_4 x_4 \cdots + \beta_n x_n \tag{6}$$

On the other hand, if the curvature is there in the system, a higher-order polynomial like a quadratic model is used which can be stated in the form of the following equation:

$$Y = \beta_0 + \Sigma\beta_i x_i + \Sigma\beta_{ii} x_{ii}^2 + \Sigma\beta_{ij} x_{iXj} + \varepsilon \tag{7}$$

where Y is the decolorization response, β_0 is the constant coefficient, β_i is the slope or linear effect of the input factor x_i, and β_{ij} is the linear by linear interaction effect between the input factor x_i and x_j, and β_{ii} is the quadratic effect of the input factor x_i. The model significance is derived from the test of goodness of fit, mostly expressed as the coefficient of determination (R^2), which is the proportion of variations in response that can be explained by independent factors and their interactions. The p-value below to 0.05 was considered statistically significant. Further, the correlation between the experimental and the predicted values was determined by the coefficient of determination (R^2). Illustration of the 3D response surface plot and the contour plot was displayed to analyze the synergistic effects of different variables toward the decolorization of AB 14 dye (Mona et al., 2011; Papadopoulou et al., 2013). The validation of the optimization model was performed by the comparison between the experimental and the predicted results.

Results and discussion

Decolorization screening of the yeast strains

In this study, three metal-resistant yeast strains were screened based on their dye removal efficiency. The three strains showed varying decolorization efficiencies. The highest rate of decolorization was achieved by *C. fabianii* (97%), followed by *W. anomaly* (69.73%), and finally *C. tropicalis* (32.69%). The studies on the mycoremediation of azo dyes using viable yeast cells were mainly focused on the use of *Candida* species such as *C. tropicalis*(Tan et al., 2019; Yang et al., 2008), *C. krusei* (Charumathi & Das, 2011; Yu & Wen, 2005), *C. boidinii* (Martorell et al., 2017), *C. oleophila* (Lucas et al., 2006), as well as *Saccharomyces cerevisiae* species (Biradar et al., 2016; Jadhav et al., 2007; Kiayi et al., 2019; Vatandoostarani et al., 2017). To our knowledge, only two previous studies were conducted with yeasts of the *Cyberlindnera* genus. The study by Martorell et al. (2012)was the first report on the decolorization capacity of the yeast strain *Cyberlindnera satwnus* MM 4034, using a mixture dye of Yellow 4R-HE, Blue RR-BB, Black B-V, and Red 7B-HE. Recently, Song et al. (2018) also have highlighted the capacity of *Cyberlindnera samutprakarnensis* for the bioremoval of AR14.

Yeast decolorization performance of various synthetic dyes

There are a variety of dyes in industrial effluents with different chemical structures. Hence, the yeast strain that can be considered useful for mycoremediation of such pollutants must be able to remove a wide range of synthetic dyes. As shown in Table 3, the selected *C. fabianii* strain removed synthetic dyes of different chemical structures (mono- and diazo dyes), with the exception of AY23 dye. The selected yeast strain can successfully remove the monoazo dye AR14, MB17, AO52, and AR 18. However, a moderate decolorization efficiency was obtained for FR17 and for the diazoic dye DR28. In fact, several previous studies have reported that the chemical structure of dyes can directly influence the decolorization efficiency. Simple structure (monoazo) dyes with low molecular weight are easily removable compared to complex synthetic dyes (diazo or triazo…) (Franciscon et al., 2012). Additionally, the number of azo bonds, as well as the chemical conformation of dyes, can strongly influence the biodegradation efficiency. Indeed, the azo bond is more susceptible to be broken when the substituent is in the para-position of the phenyl ring relative to the ortho and meta position (Hsueh et al., 2009). The substitution of electron withdrawal groups ($-SO_3H$) by ($-SO_2NH_2$) in the phenyl ring para position relative to the azo bond increases the reduction rate (Walker & Ryan, 1971). Nevertheless, amino- and hydroxyl-based dyes are more resistant to degradation than nitro, methyl, sulfo, and methoxy groups. This can be explained by the mechanism of reduction of azo dyes, which involves two steps: A fast one-electron transfer reaction occurs to the radical anion, followed by a second, slower electron transfer process to create a stable dianion. The functional group of azo dyes with a higher electronic density may not be suitable for this second electron transfer forming the dianion, thus resulting in low decolorization capability (Pearce et al., 2003; Rau et al., 2002; Zimmermann et al., 1982). Therefore, the decolorization of AR14 with the chemical formula $C_{20}H_{12}N_2Na_2O_7S_2$, and the molar mass 502.44 g/mol was less than that of MB17 with the chemical formula: $C_{20}H_{13}N_2NaO_5S$ and a molar mass of 416.39 g/mol. The structural difference between the two azo dyes is only the substitution of the "4-sulfonato" of the AR14 (disodium 4-hydroxy-2-[(E)-(4-sulfonato-1-naphthyl)diazenyl]naphthalene-1-sulfonate) with "2-hydroxy" in naphthyl group of MB17 (sodium 3-hydroxy-4-(2-hydroxy-1-naphthylazo)-1-naphthalenesulfonate). Just this difference

TABLE 3. Decolorization of various azo dyes by yeast strain of *C. fabianii*

DYES	Λ MAX	ABIOTIC CONTROL	AFTER DECOLORIZATION OF AZO DYES			*D* (%)
			SUSPENSION	SUPERNATANT	PELLETS	
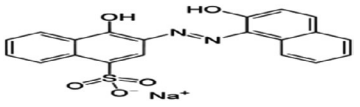 Mb 17	520					99
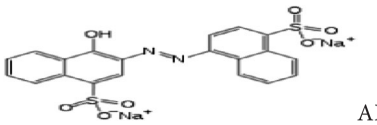 AR 14	518				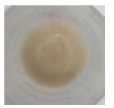	93.95
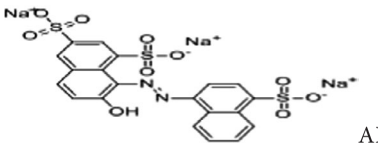 AR 18	507				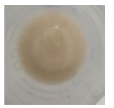	99
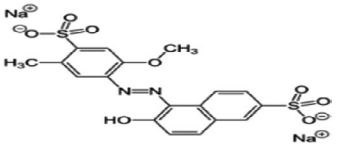 FR 17	500		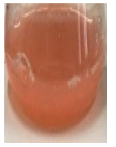			63.38
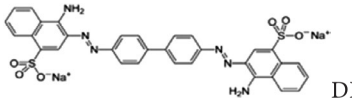 DR 28	490		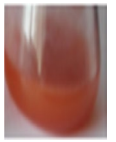		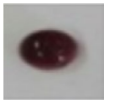	81.02
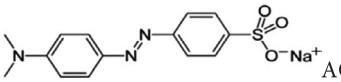 AO 52	440					96.21
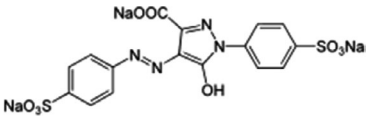 AY 23	430				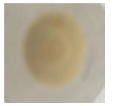	25.27

Note. Decolorization percentage (*D*%).

can induce a remarkable variation on their decolorization efficiency. Despite that the SO_3Na group is in the para position relative to the azo bond in the azo dye FR17, its removal was not successful. It has been indicated that the overall complexity of dye molecules alone is not an indication of the complexity of its decolorization, even minor structural differences may influence the decolorization process and the pathway of their degradation by the oxidoreductase enzymes (Eichlerová et al., 2007; Paszczynski et al., 1992). Another important point to draw from the obtained results is the color of the biomass after decolorization of the medium. The biomass color may give an indication of the involved mechanism during the mycoremediation of dyes. Indeed, yeast cells become colored in the case of dye biosorption or bioaccumulation, whereas they maintain their original color when the bioremoval process is achieved by enzymatical biodegradation (Yu & Wen, 2005). As shown in Table 3, the biomass of *C. fabianii* from the decolorization assay of MB17, FR17 and DR28 took the color of the dye, indicating the involvement of combined mechanisms of biosorption or bioaccumulation. On the other hand, the pellets after complete decolorization of AR14, AR18, AO52, AY23 were colorless. Therefore, the removal of these dyes would be managed by enzymatic biodegradation. In addition to the prediction based on the biomass color, the hypothesis of biodegradation as a dye degradation mechanism was also confirmed by UV–Vis analysis of dye pre- and post-treatment. The UV – Vis spectra of the azo dye AR14 (Figure 1) is characterized by a main band in the visible region, with maximum absorption at 518 nm, and two bands in the ultraviolet region at 218 nm and 317 nm. The band in the visible region was assigned to the chromophore-containing bond (-N = N-) of the dye molecules (Lin et al., 2008), and the peaks at the ultraviolet region were ascribed to the absorption of the π–π^* transition related to the naphthalene rings bonded to the azo group in the dye molecule (Wang et al., 2005). The disappearance of these peaks testifies of a biodegradation of the dye molecule. Hence, in the follow-up to the current study, we focused on the enzymatic biodegradation of AR14 as a model dye for further investigation.

Determination of enzyme activities

To have additional insight into the predictions of the decolorization mechanisms based on the color of the biomass as shown above, the enzyme activities were investigated to study the changes that occur in the enzymatic status of *C. fabianii* that might be responsible of the biodegradation of AR14. Table 4 depicts the extracellular and intracellular enzymatic activities from control YPD and AR14-doped YPD medium. A significant induction of the intracellular activities of Mnp (69.94%), Tyr (263.63%), and AzoR (34.08%) was observed in cells from the test medium compared to control cells from the YPD medium. Likewise, the extracellular activities showed an increase in the activities of Lac (118.52%) and Tyr (550%) as compared to control medium. It is known that the biodegradation of synthetic dyes by yeast cells can be catalyzed by redox reactions carried out through enzymes belonging to the classes of oxidases and reductases. Many researchers have studied the role of oxidases in the biodegradation of synthetic dyes by yeast cells. For instance, Martorell, Pajot, Ahmed, et al. (2017), Martorell et al. (2018) found that the biodegradation of the Reactive Black 5 by *C. boidinii* MM 4035 and *T. kiyoshidainum* HP2023 was achieved mainly by MnP, Lac, and peroxidase. Similarly, the biodegradation of Reactive Black 5 with *Debaryomyces polymorphus* and *C. tropicalis* was also involved the activation of MnP (Yang et al., 2008). Other reports describe only the involvement of reductases mainly the AzoR and NADH-DCIP reductase during the biodegradation of some azo dyes in basidiomycete yeast strain of *T. beigelii* NCIM-3326 (Saratale et al., 2009b) as well as the Ascomycetes yeast strains of *P. kudriavzevii* CR-Y103 (Rosu et al., 2018). The biodegradation of dyes by yeast can also be carried out in a combined pathway involving both oxidases and reductases. NADH-DCIP reductase has been considered as the major enzyme involved in the biodegradation of AR14 by *P. occidentalis* G1 in intracellular and extracellular compartments. Thus, lignin peroxidase, manganese peroxidase, and Lac have been found to be the main oxidases involved in the biodegradation of by-products resulting from the biodegradation of reductase (Song, Shao, et al., 2018). In the same way, Guo et al. (2019) showed that NADH-DCIP reductase, lignin peroxidase, and Lac are the catalyzers of the biodegradation of Acid Scarlet GR by *Galactomyces geotrichum* GG. Also, Sinha et al. (2018) found that the reductive enzyme AzoR, DCIP-NADH reductase, and the oxidative enzyme Lac are enhanced during the decolorization of reactive green dye using *Candida* sp. VITJASS. In addition, Waghmode et al. (2012a), Waghmode

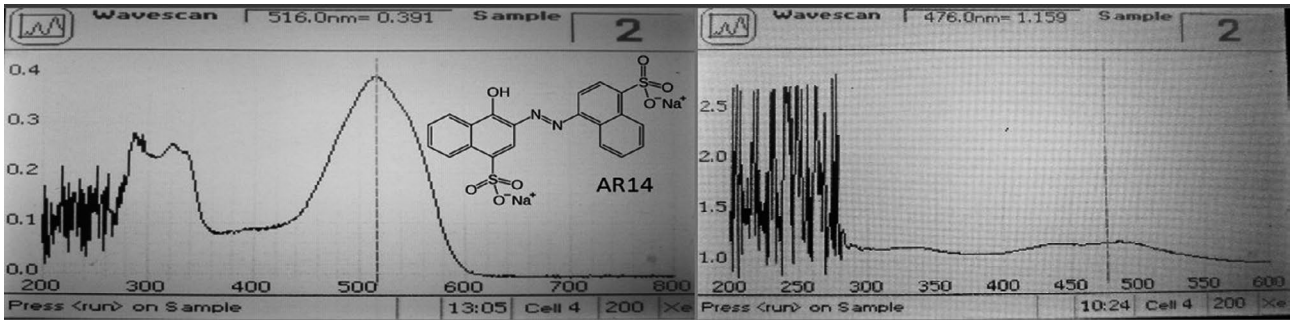

FIGURE 1. UV–Vis spectra of AR14 before (a) and after (b) decolorization (50 mg/L, 120 rpm, 30°C).

TABLE 4. Enzymatic activities of *C. fabianii* in control cells and after decolorization of AR14

	INTRACELLULAR ACTIVITY		EXTRACELLULAR ACTIVITY	
ENZYMES	CONTROL CELLS	CELLS AFTER DECOLORIZATION	CONTROL CELLS	CELLS AFTER DECOLORIZATION
Lac[a]	0.0013 ± 0.001	0.0037 ± 0.001	0.0027 ± 0.001	0.0059 ± 0.001*
Mnp[a]	0.0173 ± 0.007	0.0294 ± 0.007*	0.0062 ± 0.002	0.0054 ± 0.004
Tyr[a]	0.0011 ± 0.001	0.0040 ± 0.001*	0.0020 ± 0.002	0.0130 ± 0.005*
AzoR[b]	0.2230 ± 0.002	0.2990 ± 0.004*	0.2510 ± 0.007	0.3120 ± 0.002

Note. Values are the mean of three experiments ± *SEM*. Significantly different from control cells at $^{*}p \leq 0.05$ $^{**}p < 0.01$ using *t*-test. Significantly different from control cells at $^{*}p \leq 0.05$ $^{**}p < 0.01$ by one-way ANOVA with Tukey–Kramer multiple comparisons test.

[a]Enzyme unit's/min/mg protein (U min^{-1} mg^{-1}).

[b]μM of AR14 reduced min^{-1} mg $protein^{-1}$.

et al. (2012b) showed that the biodegradation of Remazol red and Rubine GFL by *G. geotrichum* MTCC 1360 was carried out by two oxidases, Tyr and Lac, as well as three reductases, NADH-DCIP reductase, AzoR, and Riboflavin reductase. Other studies focusing on pathways of dye degradation have shown that AzoR and NADH-DCIP reductase were the primarily responsible for the biodegradation of the azo bonds of synthetic azo dyes, whereas LiP, MnP, and Lac are the oxidases that may be involved in the further degradation of by-products of the decolorization (Jadhav & Govindwar, 2006; Jadhav et al., 2007, 2008).

Phytotoxicity assessment

The phytotoxicity tests were applied to evaluate the toxicity of the azo dye AR14 and the by-products resulting from its biodegradation by *C. fabianii* (Table 5). From the results, a significant difference was revealed for both seed germination and growth of plumule and radicle. The germination (%) of the control seeds irrigated with DW, treated solution of AR14 with *C. fabianii*, and the untreated dye solutions were 96.6%, 92.3%, and 74.5%, respectively. Indeed, there is no significant difference between the seeds irrigated with distilled water and those irrigated with the dye solution after complete decolorization. However, there was significant inhibition of *M. sativa* germination irrigated with AR14 dye solution compared to control DW. Similar investigations were documented in previous research. For instance, Roşu et al. (2019) showed that the seed germination of *Triticum aestivum* and *Trifolium pratense* treated with biodegraded products of Basic blue 41 had similar germination rates with the control. However, treatment with the dye solution inhibited the germination of both plants by 20% and 30%, respectively. In line with our findings, Jadhav et al. (2008) also reported that Brilliant blue G (4,000 ppm) had shown 70% inhibition on the germination of *T. aestivum* and *Sorghum bicolor* compared with the control DW, and the metabolites formed did not show any inhibition on the germination. In this study, it was noticed that a significant enhancement in the plumule and radicle growth of *M. sativa* treated with metabolites of AR14, thus confirming their nontoxic nature. These results were similar to previous studies, in which the metabolites of azo dyes exhibited lower toxicity compared with the original dyes (Guo et al., 2019; Sinha et al., 2018).

Optimization of decolorization by using the design of experiments

Screening of factors affecting decolorization by Plackett–Burman design. In the first step of optimization, the screening of factors influencing the decolorization was achieved with the Plackett–Burman design; then, the equation was expressed by the coefficient of R^2. The statistical analysis of regression coefficients, the *t*-test, and the *p*-values of five independent variables is given in Table 6. When excluding the insignificant factors ($\alpha = 0.05$), the model equation for decolorization in coded units can be represented as:

$$D\ (\%) = 113.2 - 0.356A - 2.547B + 4.05C - 0.0950D + 0.1426E \quad (8)$$

The multiple correlation coefficient R^2 of the first-order model indicates that 77.45% of the data variance could be estimated by the model. But, the difference between the adjusted R^2 (71.19%) and the predicted R^2 (59.91%) indicted that it is impossible to evaluate the relationship between the significant independent variables and the response with the first-order equation. As shown in Table 6, the *p*-value for lack of fit and curvature is below a significant level; therefore, the first-order model is not appropriate for predicting the response. Thus, further investigation could be carried

TABLE 5. Phytotoxicity assessment of AR 14 and its by-product degradation with *C. fabianii*

PARAMETERS	DISTILLED WATER	AR14 DYE	DYE BY-PRODUCT
Germination (%)	46.33	26.67	39.00
Plumule (cm)	5.93 ± 0.57	3.9 ± 0.2*	5.36 ± 0.68[ns]
Radicle (cm)	4.7 ± 0.66	0.53 ± 0.44***	3.73 ± 0.511[ns]

Note. Values are mean of three experiments ± *SEM*. Significantly different from control cells at $^{*}p \leq 0.05$ $^{**}p < 0.01$ by one-way ANOVA with Tukey–Kramer multiple comparisons test.

TABLE 6. ANOVA for process variables

SOURCE	*DF*	ADJ SS	ADJ MS	*F*-VALUE	*P*-VALUE
Model	5	3,785.88	757.18	12.37	0.000
Linear	5	3,785.88	757.18	12.37	0.000
T (°C)	1	109.70	109.70	1.79	0.197
pH	1	622.71	622.71	10.17	0.005*
Inoculum (g/L)	1	79.75	79.75	1.30	0.269
AR14 (mg/L)	1	1,217.38	1,217.38	19.88	0.000*
Shaking (rpm)	1	1,756.34	1,756.34	28.68	0.000*
Error	18	1,102.21	61.23		
Lack of fit	6	1,043.49	173.92	35.54	0.000*
Pure error	12	58.72	4.89		
Total	23	4,888.09			

Note. R^2 77.45; Adjusted R^2 71.19; Predicted R^2 59.91%.

df: degrees of freedom; MS: mean sum of squares; SS, sum of squares.

*Significance (α = 0.05).

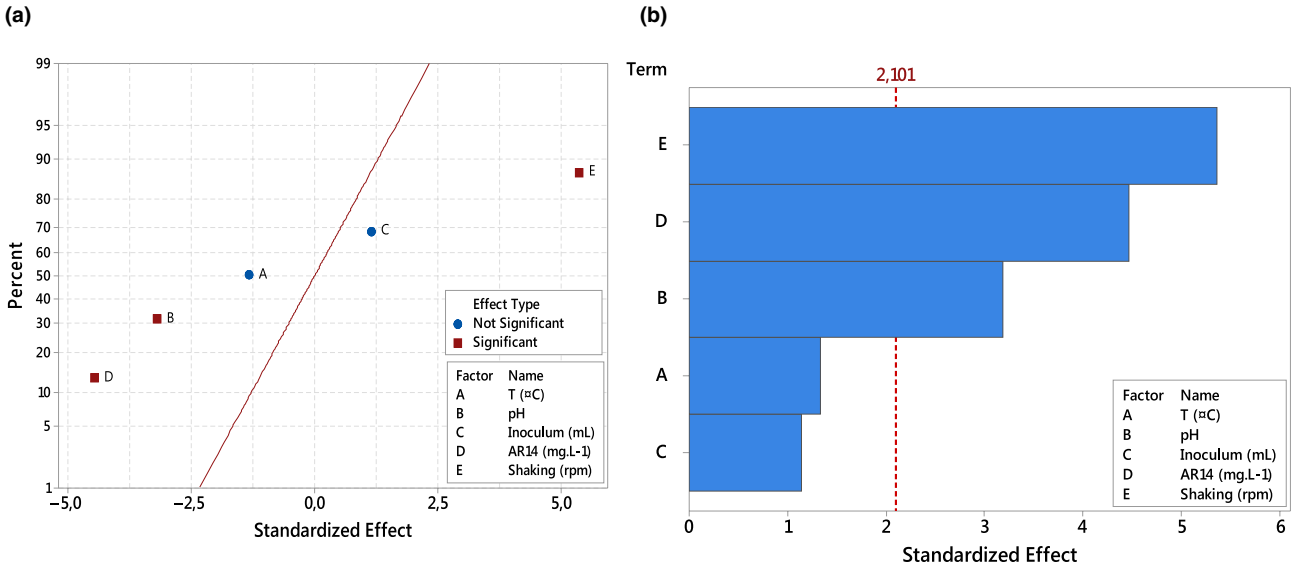

FIGURE 2. Main effect of variables on the decolorization of AR14 by *C. fabianii*. (a) Normal plot of standardized effects and (b) Pareto chart of standard effect.

out using a second-order model. Furthermore, based on the results graphically presented in Figure 2, the tested factors that showed a high percentage of contribution to the decolorization are the shaking speed (87.03%), pH (31.48%), and the initial dye concentration (12.97%). Moreover, the variable coefficient value indicates that the increase in the shaking speed showed a positive influence, while increasing dye concentration and pH have a negative influence on the decolorization of AR14 by *C. fabianii* (Figure 2a). There are differing views on the effect of agitation on the decolorization efficiency. In line with our findings, several studies have indicated the improvement of the decolorization capacity under shaking cultures compared to static cultures. As a matter of fact, the agitation of the medium during the biodegradation process allows an equal distribution of oxygen, nutrients, and facilitates the gas exchange of the fermentation products from yeast cells (Martorell et al., 2017; Pajot et al., 2007; Yang et al., 2008; Yu & Wen, 2005). Moreover, oxidative enzymes require oxygen. For example, Lac oxidizes aromatic compounds in the presence of oxygen. In such reactions, phenoxy radicals are produced from their corresponding substrates, which in turn create a phenolic polymer for polymerization or quinine by additional Lac oxidation (Shahid et al., 2015; Thurston, 1994). On the other hand, some authors documented the best decolorization results under static conditions (Al-Tohamy et al., 2020; Bankole et al., 2017). The negative effect of agitation on the decolorization efficiency is supported by the interpretation that oxygen acts as an electron acceptor with high redox potential, thereby preventing dye reduction (Al-Tohamy et al., 2020; Kalyani et al., 2008; Li et al., 2004). Strain et al. (2006) reported that oxygen can inhibit the enzymatic activity of oxygen-insensitive AzoR

TABLE 7. Analysis of variance table (ANOVA) for response surface quadratic model

SOURCE	*DF*	ADJ SS	ADJ MS	*F*-VALUE	*P*-VALUE
Model	9	2,927.68	325.30	16.48	0.003
Linear	3	2,575.45	858.48	43.50	0.001
pH (*A*)	1	1,598.10	1,598.10	80.99	0.000*
AR14 (*B*)	1	951.13	951.13	48.20	0.001*
Shaking (*C*)	1	26.21	26.21	1.33	0.301
Square	3	82.31	27.44	1.39	0.348
A^2	1	0.42	0.42	0.02	0.890
B^2	1	67.15	67.15	3.40	0.124
C^2	1	9.73	9.73	0.49	0.514
Two-way interaction	3	269.92	89.97	4.56	0.068
A * *B*	1	251.70	251.70	12.76	0.016*
A * *C*	1	5.48	5.48	0.28	0.621
B * *C*	1	12.74	12.74	0.65	0.458
Error	5	98.67	19.73		
Lack of fit	3	79.42	26.47	2.75	0.278
Pure error	2	19.25	9.62		
Total	14	3,026.34			

Note. R^2 96.74; Adjusted R^2 90.87; Predicted R^2 56.58%. Significantly different from control cells at $^*p \leq 0.05$ $^{**}p < 0.01$ by one-way ANOVA with Tukey–Kramer multiple comparisons test.

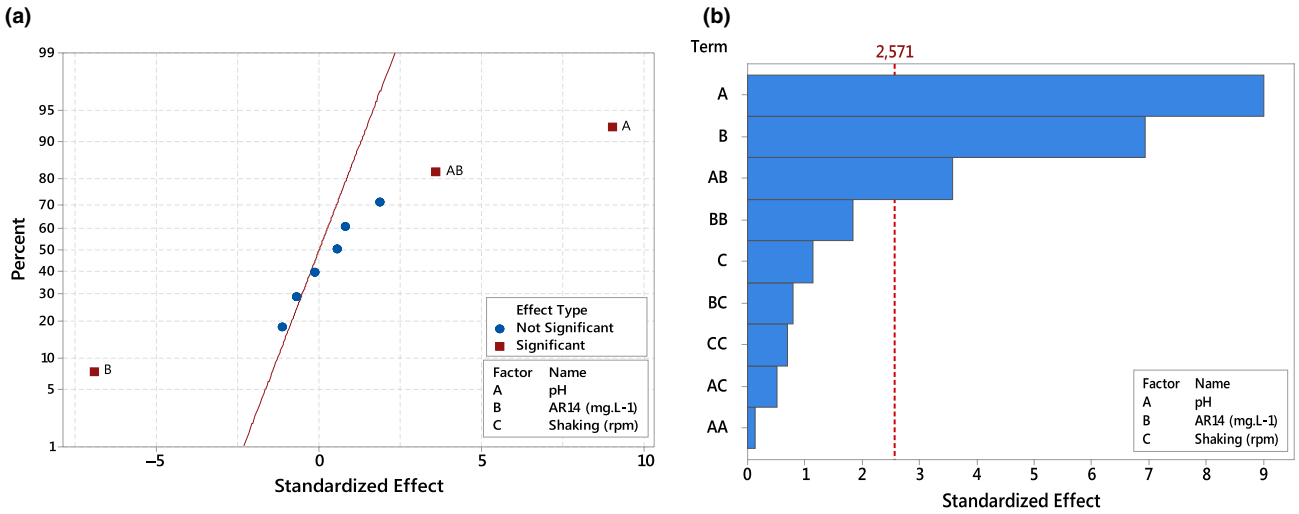

FIGURE 3. Normal plot of the standardized effects (a) and Pareto chart of the standardized effects (response is decolorization (%); α = 0.05) (b).

from anaerobic microorganisms, while AzoR from aerobic microorganisms are usually oxygen-insensitive (Misal & Gawai, 2018). Several reports highlighted the intervention of AzoR in the first step of degradation of azo dyes (Charumathi & Das, 2011; Jadhav et al., 2007; Sinha et al., 2018).This can explain the dominance of their activity during the biodegradation of AR14 dye by the selected strain *C. fabanii* (Table 4). Concerning the effects of pH on the decolorization, it is known that fungi, including yeast species, show a greater biodegradation behavior at acidic or neutral pH setting (Ali, 2010). Almost all studies of decolorization using yeast indicate that the rate of dye removal is higher at optimum neutral or acidic conditions (Bankole et al., 2017; Jadhav, Kalme, et al., 2008; Ramalho et al., 2004), and tend to decrease rapidly when the pH of the medium is within the alkaline range. The effects of pH may be related to cell viability. Peña et al. (2015) reported that the cell cycle of *S. cerevisiae* was interrupted at pH 9.0, due to the adaptation needed by the yeast cells to cope with changes in pH conditions. In the same study, it was suggested that the growth inhibition might be attributed to the decrease in cell transport of amino acids or the incorporation of proteins. On the other hand, higher pH levels may inhibit the transport of dye molecules through the cell membrane, which is considered as a limiting step for intracellular

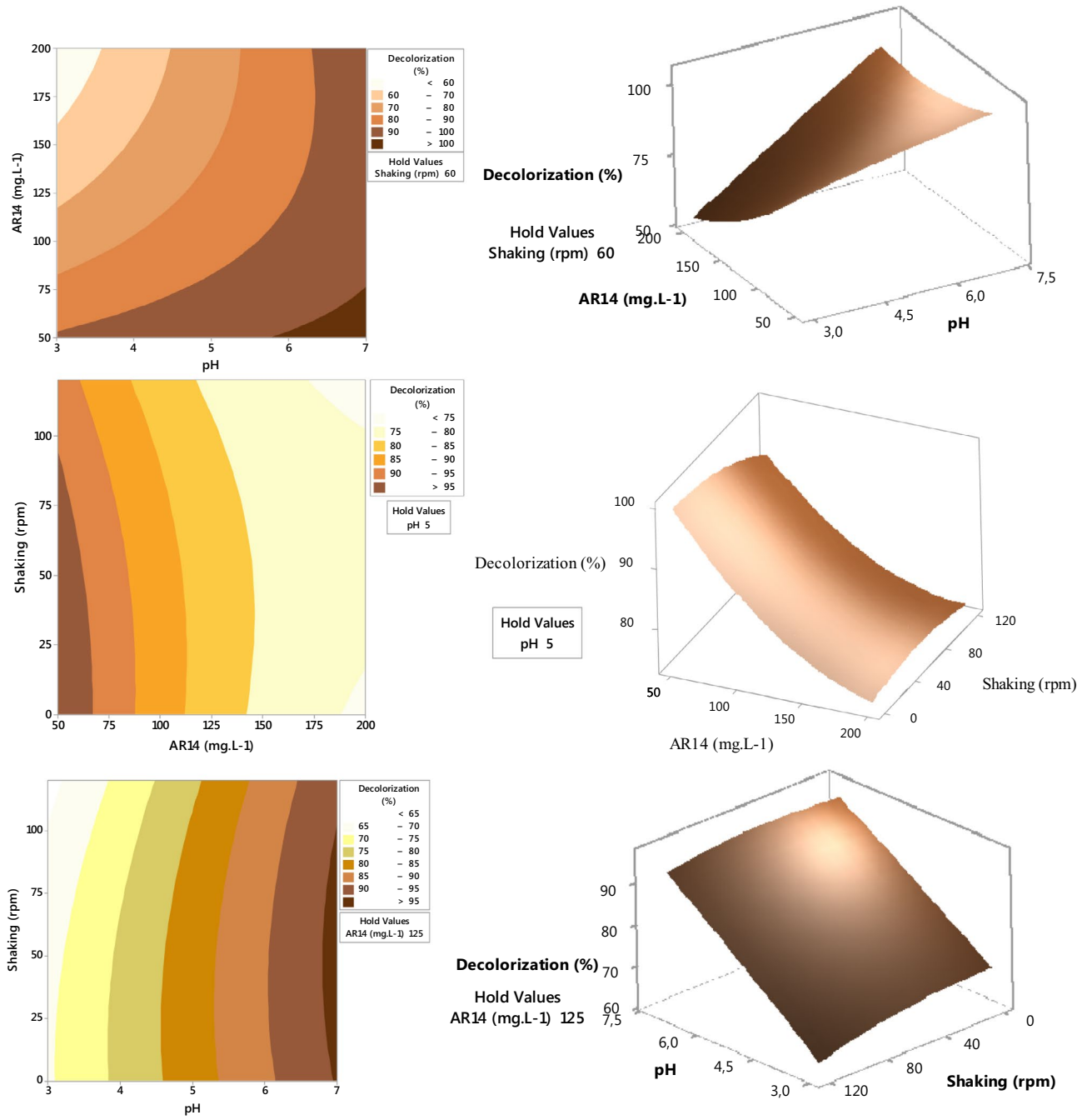

FIGURE 4. Effect of selected factors pH, shaking speed and dye concentration on the decolorization of AR14 by *C. fabianii*.

decolorization (Khan et al., 2013). Regarding the effect of dye concentration, several researchers suggest that increasing dye concentration gradually reduces decolorization levels (Aksu, 2003; Jadhav et al., 2007; Martorell et al., 2018). This could be due to the dye molecule's toxicity toward the yeast cells, which makes effective decolorization not possible (Saratale et al., 2011). Another cause of this toxicity is the binding of the dye molecule to the active site of enzymes, especially for AzoR, which therefore prevents their activity (Cruz & Buitrón, 2001; Jadhav, Jadhav, et al., 2008; Saratale et al., 2009b).

Box–Behnken design for decolorization optimization. Based on the results of the Plackett–Burman design, three variables, including the shaking speed, the initial pH of the medium, and the initial dye concentration, were the most influential factors on the decolorization of AR14 by *C. fabianii*. Thereafter, the experiments were planned following the Box–Behnken design

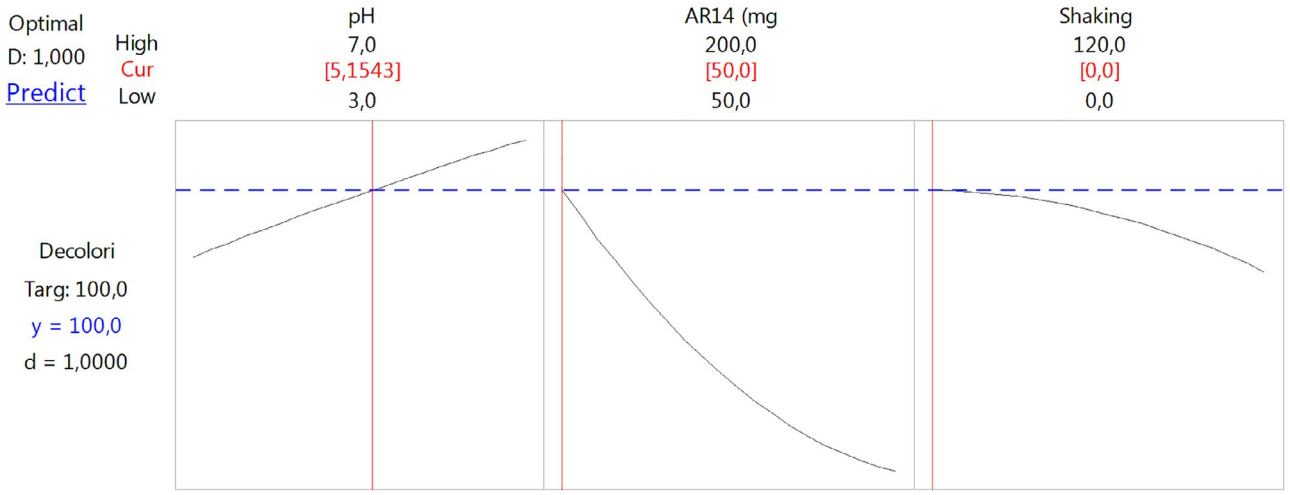

FIGURE 5. Profiles of predicated values (*y*) and desirability function (*d*) for the biodegradation of AR14 with *C. fabianii*.

to obtain a quadratic model consisting of 12 trials plus 3-center points. The removal rate of AR14 by *C. fabianii* varied from 57.47% to 100%. The relationship between the predicted response, *D*% (decolorization rate of AR14 dye), and the process parameters is represented by the second-order polynomial equation as:

$$D(\%) = 114.2 + 0.71A - 0.623B - 0.074C - 0.084A * A + 0.000758B * B - 0.000451C * C + 0.0529A * B + 0.0097A * C + 0.000397B * C \quad (9)$$

The coherence of the design model can be examined by the coefficient of determination (R^2). In the present analysis, the regression model of the decolorization was statistically significant (F = 16.48; p = 0.003). As described in Table 7, the R^2 indicates that the model as fitted explains 96.73% of the variability, suggesting a significant correlation between the experimental and predicted effects of the variables on decolorization. Furthermore, the predicted R^2 (0.5658) value was in line with the founded value of the adjusted R^2 (0.9087), thereby indicating that only 3.27% of the variability in the response is not explainable by the model. Hence, such design model could be successfully applied for modeling the design space. The lack of fit F test measures the lack of performance of the design model in generating data in the experimental area, which is not part of the regression. Thus, the test must be nonsignificant to indicate the design model. In the current analysis, the value of the lack of fit F was 2.75, indicating that it is not significant proportionate to the pure error. There is a 27.8% chance that a lack of adjustment value F that could arise on account of noise. Additionally, the F values for A, B, and C are, respectively, 80.99, 48.20, and 12.76, showing that the initial pH of the medium was most significantly different from zero at the 95.0% confidence level followed by dye concentration and shaking speed (Figure 3). The contour plots displaying the variation on the decolorization of AR14, with respect to the simultaneous shift in two factors, indicated the relationship and interaction impact of two variables with varying concentrations on decolorization, while the third variable was apprehended at the central point. The plots of the response surface region were made to learn about changes in RSM and to predict the decolorization capacity with various concentrations of the test variables. As described in Figure 4a, when the agitation was maintained at 60 rpm, the decolorization rate was inversely proportional to the increase in the initial dyes concentration and proportional to the initial pH of the medium. If the pH is maintained at 5 (Figure 4b), the decolorization was optimum at the shaking speed of 120 rpm, with dye concentration of 50 mg/L. Similarly, when the initial dye concentration is maintained at a concentration of 125 mg/L (Figure 4c), the optimum of the decolorization was proportional to the initial pH of the medium; this was achieved between 6 and 7.*Model validation.* The optimum values of the predicted variables are pH (5.154), agitation (0 rpm), and AR14 concentration (50 mg/L). As shown in the optimization plot (Figure 5), the decolorization percentage of experiments (N = 3) shows that the experimental response at predicted conditions was at 99.2%, whereas the targeted predicted value was 100%. From the results, it was concluded that the model developed could accurately predict the optimum decolorization of AR14 using the yeast strain of *C. fabianii,* which show a good agreement among experimental and prediction data.

Conclusion

From this study, we can conclude that *C. fabianii* could be a potential alternative for the bioremediation of various synthetic dyes. The bioremoval mechanisms involved are shown to be dependent on the chemical structure of dye molecules. In addition, the bioremoval of azo dye AR14 was achieved by enzymatic biodegradation, by increased intracellular and extracellular enzyme activities of Lac, Tyr, Mnp, and AzoR. Furthermore, *C. fabianii* detoxified AR14 to nontoxic by-products. With respect to the optimization of the process, factor screening using the Plackett–Burman plan suggested that the

contribution of the high percentage variables on decolorization was attributed to the shaking speed (87.3%), pH (31.48%) and initial dye concentration (12.97%). Moreover, the RSM analysis confirmed the positive interactive effect of pH and shaking speed. However, the initial dye concentration was inversely proportional to the rate of decolorization. Under optimal conditions (pH = 5.154, AR14 concentration = 50 mg/L), the selected strain could decolorize more than 97% of the targeted dye after 12 h of treatment. Hence, *C. fabianii* can be successfully utilized in mycoremediation of synthetic dyes and may be employed as a practical solution for the treatment of such pollutants.

Author contributions

Mohammed Danouche: Conceptualization (equal); data curation (equal); formal analysis (equal); funding acquisition (equal); investigation (equal); methodology (equal); project administration (equal); resources (equal); software (equal); validation (equal); visualization (equal); writing-original draft (equal); writing-review & editing (equal). **Mohamed Ferioun**: Methodology (supporting). **Wifak Bahafid**: Supervision (supporting). **Naima El Ghachtouli**: Supervision (supporting); validation (equal); visualization (lead); writing-original draft (supporting); writing-review & editing (lead).

References

Akerdi, A. G., Bahrami, S. H., Arami, M., & Pajootan, E. (2016). Photocatalytic discoloration of Acid Red 14 aqueous solution using titania nanoparticles immobilized on graphene oxide fabricated plate. *Chemosphere*, *159*, 293–299. https://doi.org/10.1016/j.chemosphere.2016.06.020

Aksu, Z. (2003). Reactive dye bioaccumulation by *Saccharomyces cerevisiae*. *Process Biochemistry*, *38*, 1437–1444. https://doi.org/10.1016/S0032-9592(03)00034-7

Ali, H. (2010). Biodegradation of synthetic dyes - A review. *Water, Air, & Soil Pollution*, *213*, 251–273. https://doi.org/10.1007/s11270-010-0382-4

Al-Tohamy, R., Kenawy, E. R., Sun, J., & Ali, S. S. (2020). Performance of a newly isolated salt-tolerant yeast strain *Sterigmatomyces halophilus* SSA-1575 for azo dye decolorization and detoxification. *Frontiers in Microbiology*, *11*, 1–19. https://doi.org/10.3389/fmicb.2020.01163

Amin, K. A., Hameid, H. A. II, & Abd Elsttar, A. H. (2010). Effect of food azo dyes tartrazine and carmoisine on biochemical parameters related to renal, hepatic function and oxidative stress biomarkers in young male rats. *Food and Chemical Toxicology*, *48*(10), 2994–2999.

Arora, D. S., & Sandhu, D. K. (1985). Laccase production and wood degradation by a white-rot fungus *Daedalea flavida*. *Enzyme and Microbial Technology*, *7*, 405–408. https://doi.org/10.1016/0141-0229(85)90131-0

Arslan, S., Eyvaz, M., Gürbulak, E., & Yüksel, E. (2016). A review of state-of-the-art technologies in dye- containing wastewater treatment – The textile industry case. In E. Perrin Akçakoca Kumbasar& Ayşegül Ekmekci Körlü*Textile wastewater treatment* (pp. 3–28). IntechOpen. https://doi.org/10.5772/64140. https://www.intechopen.com/books/textile-wastewater-treatment/a-review-of-state-of-the-art-technologies-in-dye-containing-wastewater-treatment-the-textile-industr.

Bahafid, W., Joutey, N. T., Sayel, H., Iraqui-Houssaini, M., & El Ghachtouli, N. (2013). Chromium adsorption by three yeast strains isolated from sediments in Morocco. *Geomicrobiology Journal*, *30*, 422–429. https://doi.org/10.1080/01490451.2012.705228

Balapure, K., Bhatt, N., & Madamwar, D. (2015). Mineralization of reactive azo dyes present in simulated textile waste water using down flow microaerophilic fixed film bioreactor. *Bioresource Technology*, *175*, 1–7. https://doi.org/10.1016/j.biortech.2014.10.040

Bankole, P. O., Adekunle, A. A., Obidi, O. F., Olukanni, O. D., & Govindwar, S. P. (2017). Degradation of indigo dye by a newly isolated yeast, *Diutina rugosa* from dye wastewater polluted soil. *Journal of Environmental Chemical Engineering*, *5*, 4639–4648. https://doi.org/10.1016/j.jece.2017.08.050

Biradar, S. P., Rane, N. R., Patil, T. S., Khandare, R. V., Govindwar, S. P., & Pawar, P. K. (2016). Herbal augmentation enhances malachite green biodegradation efficacy of *Saccharomyces cerevisiae*. *Biologia*, *71*, 475–483. https://doi.org/10.1515/biolog-2016-0069

Box, G. E. P., & Behnken, D. W. (1960). Some new three level design for study of quantitative variables. *Technometrics*, *2*, 455–475.

Box, G., & Hunter, J. (1957). *Multifactor experimental design for exploring the response surfaces*.

Bradford, M. M. B. (1976). Rapid and sensitive method for quantitation of microgram quantities of protein utilizing principle of protein-dye binding. *Analytical Biochemistry*, *72*, 248–254. https://doi.org/10.1016/j.sbi.2014.10.005

Charumathi, D., & Das, N. (2011). Biodegradation of Basic Violet 3 by *Candida krusei* isolated from textile wastewater. *Biodegradation*, *22*, 1169–1180. https://doi.org/10.1007/s10532-011-9472-2

Chen, C. Y., Kuo, J. T., Cheng, C. Y., Huang, Y. T., Ho, I. H., & Chung, Y. C. (2009). Biological decolorization of dye solution containing malachite green by *Pandoraea pulmonicola* YC32 using a batch and continuous system. *Journal of Hazardous Materials*, *172*, 1439–1445. https://doi.org/10.1016/j.jhazmat.2009.08.009

Cruz, A., & Buitrón, G. (2001). Biodegradation of disperse blue 79 using sequenced anaerobic/aerobic biofilters. *Water Science and Technology*, *44*(4), 159–166. https://doi.org/10.2166/wst.2001.0209

Daneshvar, N., AshassiSorkhabi, H., & Kasiri, M. B. (2004). Decolorization of dye solution containing Acid Red 14 by electrocoagulation with a comparative investigation of different electrode connections. *Journal of Hazardous Materials*, *112*, 55–62. https://doi.org/10.1016/j.jhazmat.2004.03.021

Daneshvar, N., Khataee, A. R., & Treatment, W. (2006). Removal of azo dye C.I. Acid Red 14 from contaminated water using Fenton, UV/H2O2, UV/H2O2/Fe(II), UV/H2O2/Fe(III) and UV/H2O2/Fe(III)/oxalate processes: A comparative study. *Journal of Environmental Science and Health, Part A: Toxic/hazardous Substances and Environmental Engineering*, *41*, 315–328. https://doi.org/10.1080/10934520500423196

Das, D., Charumathi, D., & Das, N. (2010). Combined effects of sugarcane bagasse extract and synthetic dyes on the growth and bioaccumulation properties of *Pichia fermentans* MTCC 189. *Journal of Hazardous Materials*, *183*, 497–505. https://doi.org/10.1016/j.jhazmat.2010.07.051

de Miranda, R., Gomes, E. D. B., Pereira, N., Marin-Morales, M. A., Machado, K. M. G., & Gusmão, N. B. D. (2013). Biotreatment of textile effluent in static bioreactor by *Curvularia lunata* URM 6179 and *Phanerochaete chrysosporium* URM 6181. *Bioresource Technology*, *142*, 361–367. https://doi.org/10.1016/j.biortech.2013.05.066

Dil, E. A., Ghaedi, M., Ghezelbash, G. R., & Asfaram, A. (2017). Multi-responses optimization of simultaneous biosorption of cationic dyes by live yeast *Yarrowialipolytica* 70562 from binary solution: Application of first order derivative spectrophotometry. *Ecotoxicology and Environmental Safety*, *139*, 158–164. https://doi.org/10.1016/j.ecoenv.2017.01.030

Duckworth, H. W., & Coleman, J. E. (1970). Physicochemical and kinetic properties of mushroom tyrosinase. *Journal of Biological Chemistry*, *245*, 1613–1625. https://doi.org/10.1016/S0031-9422(00)82247-5

Eichlerová, I., Homolka, L., & Nerud, F. (2007). Decolorization of high concentrations of synthetic dyes by the white rot fungus *Bjerkandera adusta* strain CCBAS 232. *Dyes and Pigments*, *75*, 38–44. https://doi.org/10.1016/j.dyepig.2006.05.008

Franca, R. D. G., Vieira, A., Carvalho, G., Oehmen, A., Pinheiro, H. M., Barreto Crespo, M. T., & Lourenço, N. D. (2020). *Oerskovia paurometabola* can efficiently decolorize azo dye Acid Red 14 and remove its recalcitrant metabolite. *Ecotoxicology and Environmental Safety*, *191*, 110007. https://doi.org/10.1016/j.ecoenv.2019.110007

Franciscon, E., Grossman, M., Paschoal, J. A., Reyes, F. G., & Durrant, L. (2012). Decolorization and biodegradation of reactive sulfonated azo dyes by a newly isolated *Brevibacterium* sp. strain VN-15. *SpringerPlus*, *1*(1), 37. https://doi.org/10.1186/2193-1801-1-37

Fu, F., & Wang, Q. (2011). Removal of heavy metal ions from wastewaters: A review. *Journal of Environmental Management*, *92*, 407–418. https://doi.org/10.1016/j.jenvman.2010.11.011

Gönen, F., & Aksu, Z. (2009). Predictive expressions of growth and Remazol Turquoise Blue-G reactive dye bioaccumulation properties of *Candida utilis*. *Enzyme and Microbial Technology*, *45*, 15–21. https://doi.org/10.1016/j.enzmictec.2009.03.006

Guo, G., Tian, F., Zhao, Y., Tang, M., Liu, W., Liu, C., Xue, S., Kong, W., Sun, Y., & Wang, S. (2019). Aerobic decolorization and detoxification of Acid Scarlet GR by a newly isolated salt-tolerant yeast strain *Galactomyces geotrichum* GG. *International Biodeterioration & Biodegradation*, *145*, 104818. https://doi.org/10.1016/j.ibiod.2019.104818

Hsueh, C. C., Chen, B. Y., & Yen, C. Y. (2009). Understanding effects of chemical structure on azo dye decolorization characteristics by *Aeromonas hydrophila*. *Journal of Hazardous Materials*, *167*, 995–1001. https://doi.org/10.1016/j.jhazmat.2009.01.077

Idel-aouad, R., Valiente, M., Yaacoubi, A., Tanouti, B., & López-Mesas, M. (2011). Rapid decolourization and mineralization of the azo dye C.I. Acid Red 14 by heterogeneous Fenton reaction. *Journal of Hazardous Materials*, *186*, 745–750. https://doi.org/10.1016/j.jhazmat.2010.11.056

Jadhav, J. P., & Govindwar, S. P. (2006). Biotransformation of malachite green by *Saccharomyces cerevisiae* MTCC 463. *Yeast*, *23*, 315–323. https://doi.org/10.1002/yea.1356

Jadhav, J. P., Parshetti, G. K., Kalme, S. D., & Govindwar, S. P. (2007). Decolourization of azo dye methyl red by *Saccharomyces cerevisiae* MTCC 463. *Chemosphere*, *68*, 394–400. https://doi.org/10.1016/j.chemosphere.2006.12.087

Jadhav, S. U., Jadhav, M. U., Kagalkar, A. N., & Govindwar, S. P. (2008). Decolorization of brilliant blue G dye mediated by degradation of the microbial consortium *of Galactomyces geotrichum* and *Bacillus* sp. *Journal of the Chinese Institute of Chemical Engineers*, *39*, 563–570. https://doi.org/10.1016/j.jcice.2008.06.003

Jadhav, S. U., Kalme, S. D., & Govindwar, S. P. (2008). Biodegradation of Methyl red by *Galactomyces geotrichum* MTCC 1360. *International Biodeterioration & Biodegradation*, *62*, 135–142. https://doi.org/10.1016/j.ibiod.2007.12.010

Jafari, N., Soudi, M. R., & Kasra-Kermanshahi, R. (2014). Biodegradation perspectives of azo dyes by yeasts. *Microbiology*, *83*, 484–497. https://doi.org/10.1134/s0026261714050130

Kalyani, D. C., Patil, P. S., Jadhav, J. P., & Govindwar, S. P. (2008). Biodegradation of reactive textile dye Red BLI by an isolated bacterium *Pseudomonas* sp. SUK1. *Bioresource Technology*, *99*, 4635–4641. https://doi.org/10.1016/j.biortech.2007.06.058

Karlapudi, A. P., Krupanidhi, S., Rajeswara Reddy, E., Indira, M., Bobby, M. N., & Venkateswarulu, T. C. (2018). Plackett-Burman design for screening of process components and their effects on production of lactase by newly isolated *Bacillus* sp. VUVD101 strain from Dairy effluent. *Beni-Suef University Journal of Basic and Applied Sciences*, *7*, 543–546. https://doi.org/10.1016/j.bjbas.2018.06.006

Khalid, S., Shahid, M., Niazi, N. K., Murtaza, B., Bibi, I., & Dumat, C. (2017). A comparison of technologies for remediation of heavy metal contaminated soils. *Journal of Geochemical Exploration*, *182*, 247–268. https://doi.org/10.1016/j.gexplo.2016.11.021

Khan, R., Bhawana, P., & Fulekar, M. H. (2013). Microbial decolorization and degradation of synthetic dyes: A review. *Reviews in Environmental Science and Bio/Technology*, *12*, 75–97. https://doi.org/10.1007/s11157-012-9287-6

Kiayi, Z., Lotfabad, T. B., Heidarinasab, A., & Shahcheraghi, F. (2019). Microbial degradation of azo dye carmoisine in aqueous medium using *Saccharomyces cerevisiae* ATCC 9763. *Journal of Hazardous Materials*, *373*, 608–619. https://doi.org/10.1016/j.jhazmat.2019.03.111

Kousha, M., Daneshvar, E., Dopeikar, H., Taghavi, D., & Bhatnagar, A. (2012). Box-Behnken design optimization of Acid Black 1 dye biosorption by different brown macroalgae. *Chemical Engineering Journal*, *179*, 158–168. https://doi.org/10.1016/j.cej.2011.10.073

Kumar, A., & Chandra, R. (2020). Ligninolytic enzymes and its mechanisms for degradation of lignocellulosic waste in environment. *Heliyon*, *6*, e03170. https://doi.org/10.1016/j.heliyon.2020.e03170

Kunamneni, A., Ghazi, I., Camarero, S., Ballesteros, A., Plou, F. J., & Alcalde, M. (2008). Decolorization of synthetic dyes by laccase immobilized on epoxy-activated carriers. *Process Biochemistry*, *43*, 169–178. https://doi.org/10.1016/j.procbio.2007.11.009

Li, J. G., Lalman, J. A., & Biswas, N. (2004). Biodegradation of red B dye by *Bacillus* sp. OY1-2. *Environmental Technology*, *25*, 1167–1176. https://doi.org/10.1080/09593332508618384

Lin, J. J., Zhao, X.-S., Liu, D., Yu, Z.-G., Zhang, Y., & Xu, H. (2008). The decoloration and mineralization of azo dye C.I. Acid Red 14 by sonochemical process: Rate improvement via Fenton's reactions. *Journal of Hazardous Materials*, *157*, 541–546. https://doi.org/10.1016/j.jhazmat.2008.01.050

Liu, G. F., Zhou, J. T., Qu, Y. Y., & Ma, X. (2007). Decolorization of sulfonated azo dyes with two photosynthetic bacterial strains and a genetically engineered *Escherichia coli* strain. *World Journal of Microbiology and Biotechnology*, *23*, 931–937. https://doi.org/10.1007/s11274-006-9316-0

Liu, X., Zhang, J., Jiang, J., Li, R., Xie, Z., & Li, S. (2011). Biochemical degradation pathway of reactive blue 13 by *Candida rugopelliculosa* HXL-2. *International Biodeterioration & Biodegradation*, *65*, 135–141. https://doi.org/10.1016/j.ibiod.2010.10.005

Lucas, M. S., Amaral, C., Sampaio, A., Peres, J. A., & Dias, A. A. (2006). Biodegradation of the diazo dye Reactive Black 5 by a wild isolate of *Candida oleophila*. *Enzyme and Microbial Technology*, *39*, 51–55. https://doi.org/10.1016/j.enzmictec.2005.09.004

Mahmoud, M. S. (2016). Decolorization of certain reactive dye from aqueous solution using Baker's Yeast (*Saccharomyces cerevisiae*) strain. *HBRC Journal*, *12*, 88–98. https://doi.org/10.1016/j.hbrcj.2014.07.005

Martorell, M. M., del Rosales Soro, M. M., Pajot, H. F., de Figueroa, L. I. C. (2018). Optimization and mechanisms for biodecoloration of a mixture of dyes by *Trichosporona kiyoshidainum* HP 2023. *Environmental Technology (United Kingdom)*, *39*, 3169–3180. https://doi.org/10.1080/09593330.2017.1375024

Martorell, M. M., Pajot, H. F., Ahmed, P. M., & de Figueroa, L. I. C. (2017). Biodecoloration of Reactive Black 5 by the methylotrophic yeast *Candida boidinii* MM 4035. *Journal of Environmental Sciences (China)*, *53*, 78–87. https://doi.org/10.1016/j.jes.2016.01.033

Martorell, M. M., Pajot, H. F., & de Figueroa, L. I. C. (2012). Dye-decolourizing yeasts isolated from Las Yungas rainforest. Dye assimilation and removal used as selection criteria. *International Biodeterioration & Biodegradation*, *66*, 25–32. https://doi.org/10.1016/j.ibiod.2011.10.005

Martorell, M. M., Pajot, H. F., & Figueroa, L. I. C., (2017). Biological degradation of Reactive Black 5 dye by yeast *Trichosporona kiyoshidainum*. *Journal of Environmental Chemical Engineering*, *5*, 5987–5993. https://doi.org/10.1016/j.jece.2017.11.012

Misal, S. A., Gawai, K. R. (2018). Azoreductase: a key player of xenobiotic metabolism. *Bioresources and Bioprocessing*, *5*, (1), 1–9. http://dx.doi.org/10.1186/s40643-018-0206-8.

Mona, S., Kaushik, A., & Kaushik, C. P. (2011). Biosorption of chromium (VI) by spent cyanobacterial biomass from a hydrogen fermentor using Box-Behnken model. *International Biodeterioration & Biodegradation*, *65*, 656–663. https://doi.org/10.1016/j.ibiod.2011.04.002

Moopantakath, J., & Kumavath, R. (2018). *Bio-augmentation of actinobacteria and their role in dye decolorization, new and future developments in microbial biotechnology and bioengineering: Actinobacteria: Diversity and biotechnological applications*. Elsevier B.V. https://doi.org/10.1016/B978-0-444-63994-3.00020-5

Myers, R. H., & Montgomery, D. C. (1995). *Response surface methodology: Process and product in optimization using designed experiments* (1st ed.).

Pajot, H. F., de Figueroa, L. I. C., & Fariña, J. I. (2007). Dye-decolorizing activity in isolated yeasts from the ecoregion of Las Yungas (Tucumán, Argentina). *Enzyme and Microbial Technology*, *40*, 1503–1511. https://doi.org/10.1016/j.enzmictec.2006.10.038

Osman, M. Y., Sharaf, I. A., Osman, H. M. Y., El-Khouly, Z. A., & Ahmed, E. I. (2004). Synthetic organic food colouring agents and their degraded products: effects on human and rat cholinesterases. *British journal of biomedical science*, *61*(3), 128–132.

Papadopoulou, K., Kalagona, I. M., Philippoussis, A., & Rigas, F. (2013). Optimization of fungal decolorization of azo and anthraquinone dyes via Box-Behnken design. *International Biodeterioration & Biodegradation*, *77*, 31–38. https://doi.org/10.1016/j.ibiod.2012.10.008

Paszczyński, A., Crawford, R. L., & Huynh, V. B. (1988). Manganese peroxidase of *Phanerochaete chrysosporium*: Purification. *Methods Enzymology*, *161*, 264–270. https://doi.org/10.1016/0076-6879(88)61028-7

Paszczynski, A., Pasti-Grigsby, M. B., Goszczynski, S., Crawford, R. L., & Crawford, D. L. (1992). Mineralization of sulfonated azo dyes and sulfanilic acid by *Phanerochaete chrysosporium* and *Streptomyces chromofuscus*. *Applied and Environmental Microbiology*, *58*, 3598–3604. https://doi.org/10.1128/aem.58.11.3598-3604.1992

Pearce, C. I., Lloyd, J. R., & Guthrie, J. T. (2003). The removal of colour from textile wastewater using whole bacterial cells: A review. *Dyes and Pigments*, *58*, 179–196. https://doi.org/10.1016/S0143-7208(03)00064-0

Peña, A., Sánchez, N. S., Álvarez, H., Calahorra, M., & Ramírez, J. (2015). Effects of high medium pH on growth, metabolism and transport in *Saccharomyces cerevisiae*. *FEMS Yeast Research*, *15*, 1–13. https://doi.org/10.1093/femsyr/fou005

Plackett, R., & Burman, J. (1946). The design of optimum multifactorial experiments. *Biometrika*, *33*(4), 305–325. https://doi.org/10.2307/2332195

Qu, Y., Cao, X., Ma, Q., Shi, S., Tan, L., Li, X., Zhou, H., Zhang, X., & Zhou, J. (2012). Aerobic decolorization and degradation of Acid Red B by a newly isolated *Pichia* sp. TCL. *Journal of Hazardous Materials*, *223–224*, 31–38. https://doi.org/10.1016/j.jhazmat.2012.04.034

Rai, H. S., Bhattacharyya, M. S., Singh, J., Bansal, T. K., Vats, P., & Banerjee, U. C. (2005). Removal of dyes from the effluent of textile and dyestuff manufacturing industry: A review of emerging techniques with reference to biological treatment. *Critical Reviews in Environmental Science and Technology*, *35*, 219–238. https://doi.org/10.1080/10643380590917932

Ramalho, P. A.,Cardoso, M. H., & Ramalho, M. T. (2004). Characterization of azo reduction activity in a novel ascomycete yeast strain characterization of azo reduction activity in a novel ascomycete yeast strain. *Applied and Environmental Microbiology*, *70*, 2279–2288. https://doi.org/10.1128/AEM.70.4.2279

Rau, J., Knackmuss, H. J., & Stolz, A. (2002). Effects of different quinoid redox mediators on the anaerobic reduction of azo dyes by bacteria. *Environmental Science & Technology*, *36*, 1497–1504. https://doi.org/10.1021/es010227+

Rhodes, C. J. (2014). Mycoremediation (bioremediation with fungi) - growing mushrooms to clean the earth. *Chemical Speciation & Bioavailability*, *26*, 196–198. https://doi.org/10.3184/095422914X14047407349335

Rosu, C. M., Avadanei, M., Gherghel, D., Mihasan, M., Mihai, C., Trifan, A., Miron, A. & Vochita, G. (2018). Biodegradation and Detoxification Efficiency of Azo-Dye Reactive Orange 16 by Pichia kudriavzevii CR-Y103. *Water, Air, & Soil Pollution*, *229*, (1), 1–18. http://dx.doi.org/10.1007/s11270-017-3668-y.

Roșu, C. M., Vochița, G., Mihășan, M., Avădanei, M., Mihai, C. T., & Gherghel, D. (2019). Performances of *Pichia kudriavzevii* in decolorization, biodegradation, and detoxification of C.I. Basic Blue 41 under optimized cultural conditions. *Environmental Science and Pollution Research*, *26*, 431–445. https://doi.org/10.1007/s11356-018-3651-1

Samarghandi, M. R., Dargahi, A., ZolghadrNasab, H., Ghahramani, E., & Salehi, S. (2020). Degradation of azo dye Acid Red 14 (AR14) from aqueous solution using H2O2/nZVI and S2O82−/nZVI processes in the presence of UV irradiation. *Water Environment Research*, *92*, 1173–1183. https://doi.org/10.1002/wer.1312

Saratale, R. G., Saratale, G. D., Chang, J. S., & Govindwar, S. P. (2009a). Ecofriendly degradation of sulfonated diazo dye C.I. Reactive Green 19A using *Micrococcus glutamicus* NCIM-2168. *Bioresource Technology*, *100*, 3897–3905. https://doi.org/10.1016/j.biortech.2009.03.051

Saratale, R. G., Saratale, G. D., Chang, J. S., & Govindwar, S. P. (2009b). Decolorization and biodegradation of textile dye Navy blue HER by *Trichosporonbeigelii* NCIM-3326. *Journal of Hazardous Materials*, *166*, 1421–1428. https://doi.org/10.1016/j.jhazmat.2008.12.068

Saratale, R. G., Saratale, G. D., Chang, J. S., & Govindwar, S. P. (2011). Bacterial decolorization and degradation of azo dyes: A review. *Journal of the Taiwan Institute of Chemical Engineers*, *42*, 138–157. https://doi.org/10.1016/j.jtice.2010.06.006

Sen, S. K., Raut, S., Bandyopadhyay, P., & Raut, S. (2016). Fungal decolouration and degradation of azo dyes: A review. *Fungal Biology Reviews*, *30*, 112–133. https://doi.org/10.1016/j.fbr.2016.06.003

Shahid, M., Azeem, K., Muhammad, A., Tariq, M., & Crowley, D. E. (2015). Detoxification of azo dyes by bacterial oxidoreductase enzymes. *Critical Reviews in Biotechnology*, *36*(4), 639–651. https://doi.org/10.3109/07388551.2015.1004518

Singh, K., & Arora, S. (2011). Removal of synthetic textile dyes from wastewaters: A critical review on present treatment technologies. *Critical Reviews in Environmental Science and Technology*, *41*, 807–878. https://doi.org/10.1080/10643380903218376

Sinha, A., Lulu, S., Vino, S., Banerjee, S., Acharjee, S., & Jabez Osborne, W. (2018). Degradation of reactive green dye and textile effluent by *Candida sp*. VITJASS isolated from wetland paddy rhizosphere soil. *Journal of Environmental Chemical Engineering*, *6*, 5150–5159. https://doi.org/10.1016/j.jece.2018.08.004

Song, L., Shao, Y., Ning, S., & Tan, L. (2018). Performance of a newly isolated salt-tolerant yeast strain *Pichia occidentalis* G1 for degrading and detoxifying azo dyes. *Bioresource Technology*, *233*, 21–29. https://doi.org/10.1016/j.biortech.2017.02.065

Song, Z., Song, L., Shao, Y., & Tan, L. (2018). Degradation and detoxification of azo dyes by a salt-tolerant yeast Cyberlindnera samutprakarnensis S4 under high-salt conditions. *World Journal of Microbiology and Biotechnology*, *34*, (9), 1–13. http://dx.doi.org/10.1007/s11274-018-2515-7.

Srinivasan, A., & Viraraghavan, T. (2010). Decolorization of dye wastewaters by biosorbents: A review. *Journal of Environmental Management*, *91*, 1915–1929. https://doi.org/10.1016/j.jenvman.2010.05.003

Strain, J., Pearce, C. I., Christie, R., Boothman, C., Canstein, H. V., Guthrie, J. T., & Lloyd, J. R. (2006). Reactive Azo Dye reduction by ShewanellaJ18 143. *Biotechnology and Bioengineering*, *95*(4), 692–703. https://doi.org/10.1002/bit.21021

Tan, L., Xu, B., Hao, J., Wang, J., Shao, Y., & Mu, G. (2019). Biodegradation and detoxification of azo dyes by a newly isolated halotolerant yeast *Candida tropicalis* SYF-1. *Environmental Engineering Science*, *36*, 999–1010. https://doi.org/10.1089/ees.2018.0485

Thurston, C. F. (1994). The structure and function of fungal laccases. *Microbiology*, *140*(1), 19–26. https://doi.org/10.1099/13500872-140-1-19

Uddin, M. S., Zhou, J., Qu, Y., Guo, J., Wang, P., & Zhao, L. H. (2007). Biodecolorization of azo dye acid red B under high salinity condition. *Bulletin of Environmental Contamination and Toxicology*, *79*, 440–444. https://doi.org/10.1007/s00128-007-9260-1

Vatandoostarani, S., Bagheri Lotfabad, T., Heidarinasab, A., & Yaghmaei, S. (2017). Degradation of azo dye methyl red by *Saccharomyces cerevisiae* ATCC 9763. *International Biodeterioration & Biodegradation*, *125*, 62–72. https://doi.org/10.1016/j.ibiod.2017.08.009

Vijayaraghavan, K., & Yun, Y. S. (2008). Bacterial biosorbents and biosorption. *Biotechnology Advances*, *26*, 266–291. https://doi.org/10.1016/j.biotechadv.2008.02.002

Waghmode, T. R., Kurade, M. B., Kabra, A. N., & Govindwar, S. P. (2012a). Degradation of remazol red dye by *Galactomyces geotrichum* MTCC 1360 leading to increased iron uptake in *Sorghum vulgare* and *Phaseolus mungo* from soil. *Biotechnology and Bioprocess Engineering*, *17*, 117–126. https://doi.org/10.1007/s12257-011-0307-0

Waghmode, T. R., Kurade, M. B., Kabra, A. N., & Govindwar, S. P. (2012b). Biodegradation of Rubine GFL by *Galactomyces geotrichum* MTCC 1360 and subsequent toxicological analysis by using cytotoxicity, genotoxicity and oxidative stress studies. *Microbiology (United Kingdom)*, *158*, 2344–2352. https://doi.org/10.1099/mic.0.060467-0

Walker, R., & Ryan, A. J. (1971). Some molecular parameters influencing rate of reduction of azo compounds by intestinal. *Xenobiotica*, *1*, 483–486. https://doi.org/10.3109/00498257109041513

Wang, A., Qu, J., Ru, J., Liu, H., & Ge, J. (2005). Mineralization of an azo dye Acid Red 14 by electro-Fenton's reagent using an activated carbon fiber cathode. *Dyes and Pigments*, *65*, 227–233. https://doi.org/10.1016/j.dyepig.2004.07.019

Yang, Q., Tao, L., Yang, M., & Zhang, H. (2008). Effects of glucose on the decolorization of Reactive Black 5 by yeast isolates. *Journal of Environmental Sciences*, *20*(1), 105–108. https://doi.org/10.1016/S1001-0742(08)60016-9

Yu, Z., & Wen, X. (2005). Screening and identification of yeasts for decolorizing synthetic dyes in industrial wastewater. *International Biodeterioration & Biodegradation*, *56*, 109–114. https://doi.org/10.1016/j.ibiod.2005.05.006

Zhu, N., Gu, L., Yuan, H., Lou, Z., Wang, L., & Zhang, X. (2012). Degradation pathway of the naphthalene azo dye intermediate 1-diazo-2- naphthol-4-sulfonic acid using Fenton's reagent. *Water Research*, *46*, 3859–3867. https://doi.org/10.1016/j.watres.2012.04.038

Zimmermann, T., Kulla, H. G., & Leisinger, T. (1982). Properties of purified orange II azoreductase, the enzyme initiating azo dye degradation by *Pseudomonas* KF46. *European Journal of Biochemistry*, *129*, 197–203. https://doi.org/10.1111/j.1432-1033.1982.tb07040.x

Chapitre IV

Mycoremediation of the azo dye Acid Red_{14} by *Wickerhamomyces anomalus*: Physicochemical characterization, equilibrium, and kinetics studies

.

RÉSUMÉ

Cette dernière partie se concentre plus particulièrement à évaluer la performance de la biomasse inactivée de la souche *W. anomalus* en tant que biosorbant naturel destiné à l'élimination du colorant AR_{14}, et à examiner en profondeur les interactions phytochimiques responsables du mécanisme de la biosorption.

D'abord, l'étude de la cinétique, et la modélisation des isothermes de biosorption a montré que les modèles de pseudo-second ordre et de diffusion intra-particulaire étaient plus adaptés aux données expérimentales. En outre, le modèle de Langmuir était l'isotherme le plus approprié pour expliquer le système de biosorption AR_{14}-*W. anomalus.* Au début du processus de biosorption, une décoloration rapide se produit, puis évolue progressivement pour atteindre l'état d'équilibre. D'après ces résultats, il a été déduit que la biosorption du colorant AR_{14} par la biomasse de *W. anomalus* correspond à une chimiosorption sur une monocouche de sites homogènes à la surface. Par la suite, la biomasse de levure a été caractérisée, avant et après la biosorption des colorants, par SEM-EDX, FTIR, le potentiel zêta, le pH zéro charge (pHzc), et la mesure de l'angle de contact. Les résultats ont indiqué que l'élimination du colorant était attribuée à la présence de divers groupes actifs sur la surface cellulaire. En plus, le potentiel zêta des cellules de *W. anomalus* avait une charge négative et la valeur du pHzc se trouvait dans la plage acide, ce qui confirme la présence de groupes anioniques à la surface de la cellule

Enfin, le plan de Plackett-Burman a été utilisé pour déterminer les facteurs qui influence le processus de biosorption, dont la concentration de colorant et de la biomasse, la température, la vitesse d'agitation et le temps de contact. La concentration de l'adsorbat et le ratio de dosage de l'adsorbant ainsi que le pH initial ont affecté de manière significative l'efficacité de la biosorption. Cette dernière a été optimisée selon le plan Box-Behnken et la biosorption optimale de l'AR_{14} a été atteinte à pH 3-4, avec des concentrations initiales de colorant plus faibles de 50 à 75 mg L^{-1} et une biomasse autour 1.25 g L^{-1}.

Ces résultats suggèrent que la biomasse de *W. anomalus* pourrait être utilisée comme un biosorbant efficace, peu coûteux et écologique pour l'élimination des colorants toxiques de l'environnement aqueux. Jusqu'à aujourd'hui, très peu d'études ont été menées sur l'utilisation des levures comme biosorbant. D'où l'importance d'approfondir les études sur cette approche qui pourrait faire partie des futures solutions à proposer pour le traitement des effluents colorés.

Antonie van Leeuwenhoek

Mycoremediation of the azo dye Acid Red 14 by Wickerhamomyces anomalus: Physicochemical characterization, equilibrium, and kinetics studies

--Manuscript Draft--

Manuscript Number:	
Full Title:	Mycoremediation of the azo dye Acid Red 14 by Wickerhamomyces anomalus: Physicochemical characterization, equilibrium, and kinetics studies
Article Type:	Original Article
Section/Category:	Fungi and yeast microbiology
Keywords:	Wickerhamomyces anomalus; Azo dye, Biosorption; Kinetic and Isotherms model; Biomass characterization; Optimization.
Corresponding Author:	Mohammed Danouche Université Sidi Mohamed Ben Abdellah Rabat, MOROCCO
Corresponding Author Secondary Information:	
Corresponding Author's Institution:	Université Sidi Mohamed Ben Abdellah
Corresponding Author's Secondary Institution:	
First Author:	Mohammed Danouche
First Author Secondary Information:	
Order of Authors:	Mohammed Danouche
	Hicham El Arroussi
	Naima El Ghachtouli
Order of Authors Secondary Information:	
Funding Information:	
Abstract:	This study aimed to evaluate the potential application, and the involved mechanism in the biosorption of Acid Red 14 (AR 14) by the biomass of Wickerhamomyces anomalus. Kinetics and biosorption isotherms were first examined. Then, the physicochemical characterization of cells-AR 14 interactions was determined using scanning electron microscopy coupled with energy dispersive X-ray spectroscopy, Fourier transforms infrared spectroscopy, zeta potential, zero-point charge, and contact angle measurements. Finally, the Plackett-Burman and the Box-Behnken designs were used respectively to identify the most influential factors on the biosorption process and their optimization. The pseudo-second-order and the intra-particle diffusion models best fit the experimental data. Furthermore, the Langmuir model was the appropriate isotherm to explain the biosorption system, suggesting the involvement of chemisorption on a monolayer of homogeneous sites. Biomass characterizations supported these theoretical predictions. A change in the transmittance of the functional groups present was noticed after AR14-biosorption, the analysis of the zeta potential confirms the presence of anionic groups, and the contact angle measurement indicates a significant variation of the electron donor and acceptor character. Hence, it can be concluded that both chemical and electrostatic interactions of AR14 onto the macromolecular structures composing the cell surface. The most influential factors on biosorption efficiency were dye and biomass concentration, and the pH of the medium. Optimal biosorption was achieved at pH 3-4, with AR14 concentrations around 50 - 75 mg L -1 and a biomass concentration at 1.25 g L -1 . These results suggest that W. anomalus might be exploited as an effective, inexpensive, and environmentally friendly biosorbent.

Powered by Editorial Manager® and ProduXion Manager® from Aries Systems Corporation

Mycoremediation of the azo dye Acid Red 14 by *Wickerhamomyces anomalus:* Physicochemical characterization, equilibrium, and kinetics studies

Danouche M.[1,2 *], El Arroussi H.[1,3], El Ghachtouli N. [2]

[1] *Green Biotechnology Center, Moroccan Foundation for Advanced Science, Innovation and Research (MAScIR), Rabat, Morocco.*
[2] *Microbial Biotechnology and Bioactive Molecules Laboratory, Sciences and Technologies Faculty, Sidi Mohamed Ben Abdellah University, Fez, Morocco.*
[3] *AgroBioScience (AgBS), Mohammed VI Polytechnic University (UM6P), Ben Guerir, Morocco.*
[*]Correspondence: mohammed.danouche@usmba.ac.ma

Abstract

Biosorption processes have recently become an economic and eco-friendly solution for the treatment of industrial wastewater. The purpose of this study was to evaluate the potential application of the biomass of the yeast strain *Wickerhamomyces anomalus* as a natural biosorbent for the removal of the synthetic dye Acid Red 14 (AR14). Modeling of biosorption kinetics suggested that pseudo-second-order and intraparticle diffusion models were the best fit for the experimental data. In addition, the Langmuir model was the most appropriate isotherm to explain the AR14- *W. anomalus* biosorption system. Next, the physicochemical properties of *W. anomalus* before and after dye biosorption were characterized by scanning electron microscopy with energy dispersive X-Ray analysis, Fourier-transform infrared spectroscopy, zeta potential, zero-point charge, and contact angle measurement. The functional groups such as hydroxyl, carboxyl, amide, and amine present on the yeast wall surface can be responsible for AR14 biosorption. Finally, the Plackett-Burman design was used to screen the most influencing factors on the biosorption process, including dye concentration, yeast biomass, temperature, shaking speed, and contact time. The latter was optimized according to the Box-Behnken design and the optimum AR14-biosorption was attained at pH 3-4, with lower initial dye concentrations (50 - 75 mg L^{-1}) and yeast biomass (1.25 g L^{-1}). These findings suggest that the biomass of *W. anomalus* could be used as an efficient, low-cost, and eco-friendly biosorbent for the removal of toxic dyes from the aqueous environment.

Keywords: *Wickerhamomyces anomalus*; Azo dye, Biosorption; Kinetic and Isotherms model; Biomass characterization; Optimization.

Graphical abstract

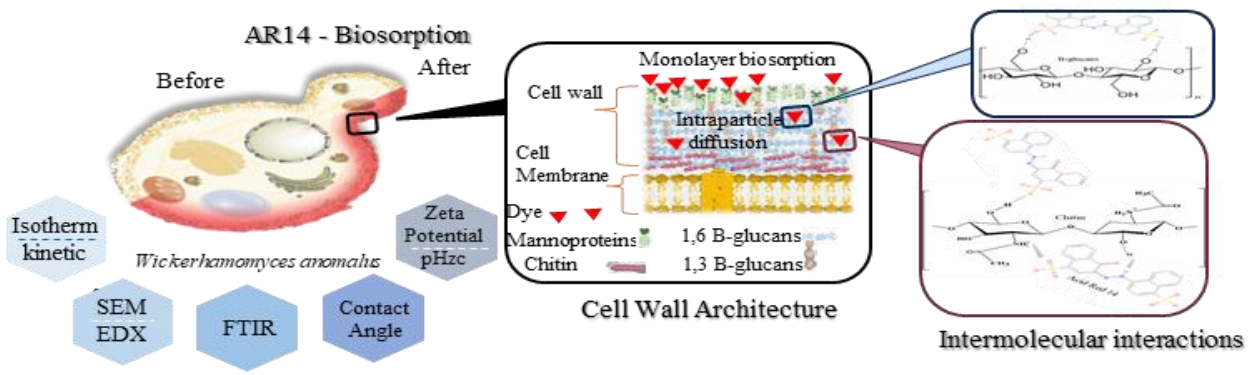

1. Introduction

Worldwide, the textile industry is one of the leading fast-growing businesses. However, for the production of 1 kg of finished textile products, this manufacturing requires between 200 to 500 L of water, which makes this sector one of the largest producers of liquid effluents (Waghmode et al. 2012). It has also been estimated that approximately 10 000 tons per year of synthetic dyes are used in this sector, of which 10-15% are rejected during the dyeing process as waste (Saratale et al. 2011). Unfortunately, the release of these effluents into the aquatic environment does not only affect the color of the water, also it has adverse effects on exposed organisms, including humans (Fu and Viraraghavan 2001). To deal with this issue, strict regulations have been implemented to manage the release of such xenobiotics into the environment. Also, several approaches have been proposed as solutions for their treatment, such as membrane, photochemical oxidation, and electrochemical processes. Although these methods are effective, they require chemicals, energy-intensive equipment, and require high maintenance costs. Which makes them expensive, thereby limiting their large-scale applications (Arslan et al. 2016).

Recently, there has been a particular interest in new technologies that are environmentally friendly, efficient, and inexpensive such as adsorption techniques. Activated carbon is the most commonly used adsorbent material (Yagub et al. 2014). However, their thermal or chemical regeneration as well as the need for complexing agents to improve their performance make the use of activated carbon-based processes an expensive proposition (Crini et al. 2019). New economical, readily available and effective adsorbents are in high demand today. Hence, the use of biological materials (biosorbents) such as natural residues, industrial food wastes, agricultural wastes, and biomass of various microorganisms has been reported as a cheap and effective alternative (Srinivasan and Viraraghavan 2010). Several studies have been reported the potential application of microalgae, cyanobacteria, and filamentous fungi in the biosorption of toxic dyes (Aksu and Tezer 2005; Jafari et al. 2014; Rita de Cássia et al. 2013). However, only a few studies have focused on yeast cells, despite their advantages over other taxa. Particularly their fast growth compared to filamentous fungi or microalgae (Singh and Arora 2011), their ability to survive in harsh environments (Sen et al. 2016), and the special flocculating characteristic that allows them to aggregate into multicellular masses (flakes), facilitating, therefore, their recovery after the treatment process (Soares and Soares 2012).

The purpose of this study was to evaluate the potential application of inactivated cells of *Wickerhamomyces anomalus* (*W. anomalus*) in the biosorption of the dye Acid red 14 (AR14). The specific objectives of this research were: (i) to study the kinetics and equilibrium isotherms of the biosorption of the AR14 dye by yeast cells. (ii) to investigate the physicochemical interaction between the yeast biomass and the dye, and (iii) to optimize the biosorption process using the design of the experiments.

2. Material and methods

2.1 Chemicals

The monoazo dye AR14 (1-Naphthalenesulfonic acid, 4-hydroxy-3-((4-sulfo-1-naphthalenyl) azo)-, disodium salt), commonly employed in many different industries such as textile, paper, food, etc..., was used as a model pollutant. The dye solution was prepared at a concentration of 5 g L^{-1} in distilled water, then sterilized by filtration and store at 4 ºC. All other chemicals used for this study were of analytical grade reagents and were purchased from Sigma and Merck.

2.2 Yeast source, culture medium, and biosorbent preparation

This study was conducted with the heat-kill cells of *W. anomalus* yeast strain, previously isolated from a contaminated site located in Fez (Morocco). Its pure culture was maintained on Yeast Extract–Peptone–Glucose (YPG) medium (2% Difco peptone, 1% yeast extract, and 2% glucose) (Bahafid et al. 2013). The biomass was recovered by centrifugation at 10,000xg. and inactivated by autoclaving (121ºC for 45 min). The regression equation of OD_{600nm} and the dry cell weight (DCW) was calculated based on the standard curve according to eq (1).

$DCW = 0.2418 \times OD_{600nm} + 0.2609$ ($R^2 = 0.989$) eq (1).

2.3 Biosorption: kinetics and equilibrium study

Kinetic studies were carried out in Erlenmeyer flasks containing 150 mL of the dye solution at a concentration of 50 mg L^{-1} and 0.5 g L^{-1} of biomass. The flasks were placed on orbital shakers at a constant speed (120 rpm) at 25 ºC. Aliquots were collected at a regular time, centrifuged (10 000xg for 10 min) to remove the biosorbent, and the dye concentration was measured using the spectrophotometer Prim Light SECOMAM at λ = 515 nm. The biosorption was reported as decolorization rate (D%) (eq 2), and the biosorption capacity was calculated according to eq 3.

$D\% = (A(i) - A(t)) / A(i) \times 100$ eq (2).

$Qt = ((C(i)-C(t)) V / W)$ eq (3).

Where, (Qt) is the biosorption capacity, A(i) and A(t) are the absorbance of dye dopped medium at the start point (i) and at a regular time (t); C(i) and C(t) are the initial and the equilibrium dye concentrations (mg L^{-1}); V is the volume of the solution (mL); W is the biomass weight (g L^{-1}).

To explain and predict the kinetics of the yeast-dye biosorption interaction, various mathematical kinetic and isotherm models can be employed (Danouche et al. 2021). In this study, Lagergren's Pseudo-first-order and pseudo-second-order were applied to define the type of interactions (physisorption or chemisorption), while the intra-particle diffusion model was used to describe the internal diffusion of dye in the cell wall. The isotherms were next employed to describe the biosorption efficiency and to understand the relationship between the dye concentrations at its equilibrium concentration in the biosorbent solution (Morosanu et al. 2016). The linear equations of kinetic and isotherm models used in the present study are summarized in Table 1.

Table 1. Linear equations of the kinetic and isothermal models used in the biosorption of AR14 by yeast biomass

		Linear Equation	Representation Plot
Isotherm Model	*Freundlich*	Log qe = Log K_F+ 1/n Log C_e	Log $q_e vs$ Log C_e
	Langmuir	$C_e/q_e = C_e/q_m + 1/K_L q_m$	$C_e/q_e vs C_e$
Kinetic Model	*Pseudo first order*	Log(q_e-q_t)=Log(q_e) - (k_1/2.303)t	Log (q_e - q_t) vs t
	Pseudo second order	$(t/qt) = (k_2/k_2 qe^2) + (t/q_e)$	(t/q_t) vs t
	Intra particle diffusion	$qt = K_{id} t^{0.5} + C$	q_t vs $t^{0.5}$

Where, q_t is the sorption capacity (mg g^{-1});, q_e is the sorption capacity at equilibrium (mg g^{-1}); q_m is the maximum sorption capacity (mg g^{-1}); C_e (mg L^{-1}) is the equilibrium concentration of the biosorbent; K_L is the Langmuir constant (L mg^{-1}); K_F is the Freundlich constant of the adsorption capacity and exponent n is the adsorption intensity which varies with the heterogeneity of the material.

2.4 Physicochemical characterization of W. anomalus / dye interaction

2.4.1 Scanning electron microscopy with energy dispersive X-Ray analysis

SEM (JSM-IT500 InTouchScope™) was used to visualize the surface morphology of cells from control and AR14 dopped medium, while EDX was used to analyze the elemental composition of control and AR14-loaded cells in the imaged area. The SEM analytical settings were as follows: Signal SED, magnification of x1 000-x55 000 landing voltage of 3.0 kV, operation distance distance of 10.1 mm, at high vacuum mode.

2.4.2 Fourier-transform infrared spectroscopy analysis

In order to determine the functional groups on the surface of *W. anomalus* and their participation in the biosorption of AR14. Control and AR14-loaded cells were analyzed by ABB Bomem FTLA 2000 spectrometer analyzer. Salt pellets were prepared using 1 mg of biomass and 149 mg of KBr. Samples were dried at 85 ºC for 24 h and compressed at 40 kN for 5 min to form pellets. Thirty-two scans were performed at a range of 400 to 4000 cm^{-1}, with 4 cm^{-1} of resolution for each sample.

2.4.3 Zeta potential and Zero-point charge measurement

The zeta potential measurement was performed to determine the zeta potentials of the yeast cell as a function of pH from 3 to 10. Indeed, a volume of 100 mL of yeast suspension (0.05 g L^{-1}) was harvested by centrifugation at 10 000xg for 10 min, then the biomass was resuspended in 10 mL of 0.1 M NaCl. The initial pH of the suspensions was adjusted from 3 to 10 with 0.1 M of HCl or NaOH solutions. Next, the zeta potential was evaluated in the electrophoresis cell at 25 ºC with Nanosizer Nano (Malvern). For each pH value, triplicate measurements were taken, and for each data, approximately 30 readings were taken (Hadjoudja et al. 2010). The electrical state of the yeast surface in the solution was also characterized using the zero-charge point (pHzc). Indeed, NaCl solutions (0.1 M) with pH ranging from 3 to 10 were prepared, before being mixed with 0.05 g of the fungal biomass, and then were shaken for 24 h at 25 ºC. Finally, the final pH values were measured and the difference in ΔpH was plotted against the initial pHi to determine the pHzc (Zehra, et al. 2016).

2.4.4 Contact angle measurement

Measurement of the contact angle was carried out at 25 ºC as described by Asri et al. (2018), using a digital optical contact angle (Data Physics OCA 40), via the sessile drop method, using water, formamide, and diiodomethane (Table S1). Both the left and the right contact angles measurements of algal biomasses were automatically calculated from the digitalized image using SCA 20 software. The degree of hydrophobicity of control and dye-leaded to cells of *W. anomalus* was then estimated according to Van Oss, et al (1988) and Vogler (1998).

2.5 Statistical analysis

Experiments were carried out in triplicate, and the results were recorded as the mean ± standard deviation. The statistical analysis of obtained data was performed using GraphPad Prism software version 8.0, with an unpaired T-test. P-value of < 0.05 was perceived as statistically.

2.6 Optimization of biosorption using the design of experiments

2.6.1 Screening of factors using Plackett–Burman design (PBD)

Factors screening was performed using PBD (Plackett and Burman 1946) via MINITAB 18.1 software. The selection of the most influential factors on the biosorption process was based on previous research addressing biosorption optimization using a "one factor at a time" approach. Indeed, six variables were selected including temperature (ºC), pH, yeast biomass (g L^{-1}), dye concentration (mg L^{-1}), shaking speed (rpm), and contact time (min) at two levels (max (+1) and min (-1)) (Table S2). According to the adopted method, it was presumed that there is no parameters interaction. The data were therefore modeled using first-order multiple regression (eq 7).

$$Y = \beta_0 + \sum \beta_i X_{i\ (i = 1, \ldots, k)} \quad \text{eq (7).}$$

Where, (Y) is the biosorption response, (β_0) is the model intercept, and (β_i) is the variable estimates. Thus, ANOVA and lack of fit were used for statistical significance. While the Fisher variation ratio (F), and the P-value (P) were used to select the effective parameters.

2.6.2 Optimization of biosorption parameters using Box-Behnken design (PBD)

In order to optimize the biosorption of AR14 by the biomass of *W. anomalus*, the PBD model was applied (Box and Behnken 1960). The eq (8) was used to calculate the coded values of variables.

$$Xi = (x_i - x_0 / \Delta x),\ i = 1, 2, 3, \ldots k \quad \text{eq (8).}$$

Where, (Xi) is the dimensionless value of a process variable; (x_i) is the real value of an independent variable; (x_0) is the value of (x_i) at the center point; (Δx) is the step change. The second-order equation (eq (9)) was used to correlate the dependent and independent variables:

$$Y = b_0 + b_1A + b_2B + b_3C + b_{12}AB + b_{13}AC + b_{23}BC + b_{11}A^2 + b_{22}B^2 + b_{33}C^2 \quad \text{eq (9).}$$

Where, (Y) is the biosorption efficiency response; (b_0) is constant, (b_1, b_2, and b_3) are linear coefficients; (b_{12}, b_{13}, and b_{23}) are cross-product coefficients, and (b_{11}, b_{22}, and b_{33}) are quadratic coefficients; (A, B, and C) are coded experimental levels of the selected variables of the screening phase. It was represented in terms of three class levels (low (-1), central point (0), and high (+1)) (Table S3). The optimum values of each factor were calculated by solving the regression equation, evaluating the contour map, and setting up constraints on the variable levels (Kousha et al. 2012). The significance of the model is derived from the test of goodness-of-fit, mostly expressed as the coefficient of determination (R^2). A P-value below 0.05 was considered statistically significant (Papadopoulou et al. 2013).

3. Results and discussion

3.1 Biosorption: kinetics and equilibrium study

The result of AR14 biosorption kinetics in *W. anomalus* biomass at four initial dye concentrations (50, 100, 150, and 200 mg L^{-1}) indicates that the rate of biosorption increased with increasing the contact time up to 10 min, after that, an equilibrium was reached (Fig. 1). Indeed, three phases were recorded in this biosorption process. The initial phase (5 min), a rapid biosorption rate occurred. Afterward, the dye is gradually biosorbed until the maximum biosorption capacity of the biosorbents is reached. The initial phase can be attributed to the availability of a large surface area and many vacant macropores for the dye uptake. Also, the fast dye biosorption at this phase suggesting the involvement of a passive interaction like physical adsorption or ion exchange interaction. The second stage (5 to 10 min), was characterized by a gradual and slow absorption, explained by the saturation of active functions groups on the cell surface (Daneshvar et al. 2019).

As well as, by the repulsive forces among adsorbed dye molecules and those present in the solution (Smaranda et al. 2009). At the third stage, the biosorption reached the equilibrium state. Similar findings were reported previously on the biosorption of Strazone blue (Farah et al. 2007), Acid blue 161 (Dilarri et al. 2016), and Direct red 23 (Morão et al. 2017) using various *S. cerevisiae* biomass.

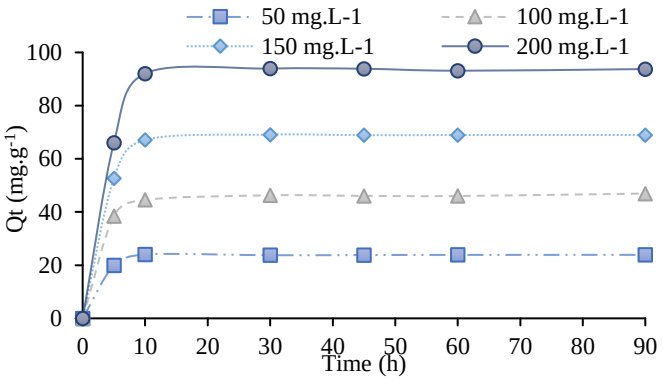

Fig 1. Kinetics of AR14 uptake by *W. anomalus* biomass at various initial dye concentrations.

The pseudo-second-order model was more applicable for the AR14-yeast biosorption system fit. Indeed, there was a linearization of the experimental data (Fig. 2A), and the R2 of all studied concentrations was relatively close to 1 (Table 2). Moreover, the calculated values of Qe (cal) were closer to the experimental values Qe (exp), confirming the goodness-of-fit of the model. The distinguishing features of this model are related to the biosorption capacity of the solid phase, which is in agreement with chemosorption (Davranche et al. 2019). However, the pseudo-second-order model did not identify the potential mechanism of diffusion into the pores. The kinetics were then analyzed through the intraparticle diffusion model. It has been shown that if biosorption follows an intraparticle diffusion model, the plot of (Qt) versus ($\sqrt{t}$) should be linear, and if the plot passes through the origin (C = 0). However, if (C # 0), this point to some degree of boundary layer control. The intraparticle diffusion model is not the rate control step of the biosorption process, but it can work simultaneously with other diffusion models (Wu et al. 2009).

Table 2. Kinetic parameters of AR14 biosorption on yeast biomass

Models	kinetics parameters	Initial dye concentrations (mg L^{-1})			
		50	100	150	200
Pseudo first order	K_1 (min^{-1})	0.205	0.194	0.215	0.195
	R^2	0.857	0.477	0.609	0.524
Pseudo second order	K_2 (g mg^{-1} min^{-1})	0.126	0.051	0.022	0.014
	R^2	0.999	0.999	0.999	0.998
	Qe (cal)	23.980	46.510	69.930	95.230
	Qe (exp)	24.038	50.000	67.129	92.082
Intra-particle diffusion	K_{i1}	7.847	14.66	21.65	29.190
	C_1	0.549	1.277	0.955	0.179
	R_1^2	0.983	0.974	0.993	0.999
	K_{i2}	0.030	0.083	0.022	0.028
	C_2	23.59	45.657	68.835	93.527
	R_2^2	0.920	0.254	0.148	0.035

As shown in Fig. 2B, two linear regions are representing the diffusion boundary layer, followed by intraparticle diffusion in macropore (Ho and McKay 1998). This result highlights that the yeast biomass reaches biosorption equilibrium when diffusion occurs in the macropore layer, and the resistance to mass transfer is not involved in the dye uptake kinetics (Ka Yee et al. 2003). Also, Kismir and Aroguz (2011) reported that the process of mass transfer of dye onto the biosorbents can take place in general through four steps: (i) bulk diffusion (transfer from the bulk solution to the surface of the biosorbent), (ii) film diffusion (transfer through the boundary layer to the biosorbent surface), (iii) intra-particle diffusion (transfer from the surface to the interior pores of the particle), (iv) chemical reaction via ion-exchange, complexation, chelation; the adsorption of dye at an active site on the biosorbent surface.

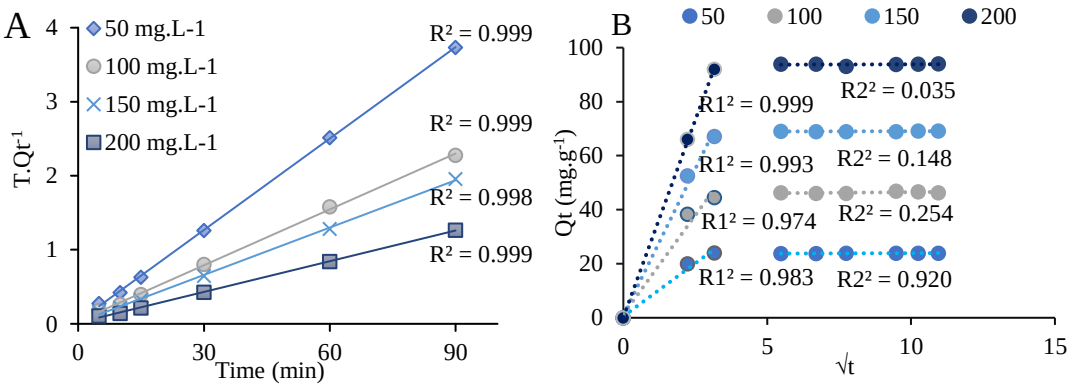

Fig 2. Plot of pseudo-second order model (A), and intra-particle diffusion model (B) of AR14 biosorption onto *W. anomalus* at various initial concentrations.

According to the graphical representation of Langmuir and Freundlich isotherms (Fig 3), and the corresponding models' constants listed in Table 3, the R^2 was respectively at 0.954 and 0.849. Which means that Langmuir isotherms provide an appropriate fit for AR14 biosorption onto *W. anomalus* compared to Freundlich isotherms. Langmuir isotherms predict that the biosorption is based on monolayer adsorption on a homogeneous site, without any interaction between biosorbed dye molecules on neighboring sites, it also assumes that the energy is equal for all sites and that there are multiple biosorption sites for a specific surface. When these sites are fully saturated, no further biosorption can take place (de Castro et al. 2017; Daneshvar et al. 2019). Aksu and Dönmez (2003) reported the applicability of both Langmuir and Freundlich models to the biosorption system of Remazol Blue reactive dye into dried cells of *Candida* strains.

Table 3. Biosorption isotherm models and their corresponding parameters for the biosorption AR14 by *W. anomalus* biomass

Langmuir			Freundlich		
Q_{max} (mg g^{-1})	K_L (L mg^{-1})	R^2	1/n	K_f	R^2
126.58	0.107	0.954	0.5	15.87	0.849

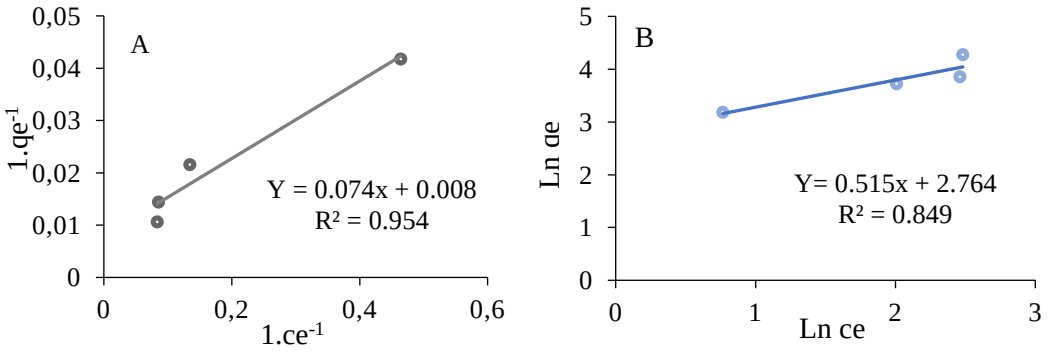

Fig 3. Langmuir (A) and Freundlich (B) isotherm plot and fitted models of AR14 biosorption by *W. anomalus* biomass.

3.2 Characterization of yeast biomass

3.2.1 SEM coupled with EDX analysis

SEM and EDX analysis were used to establish the changes in morphology and the elemental composition of the yeast biomass before AR14 biosorption, in order to establish the binding mechanism of the dye to the cell wall. Fig. 4A shows the SEM images of colorless yeast cells, and Fig. 4B shows *W. anomalus* after AR14 biosorption. There was a difference in cellular morphology between the control and AR14-loaded cells. The yeast cells before biosorption of AR14 had a normal shape and a transparent outer layer outside the cell surface. However, after dye biosorption, the cell becomes smooth and presents hazy textures. Furthermore, the X-ray spectra showed a difference in the intensity of elementary peaks of C, O, P, and K after dye biosorption.

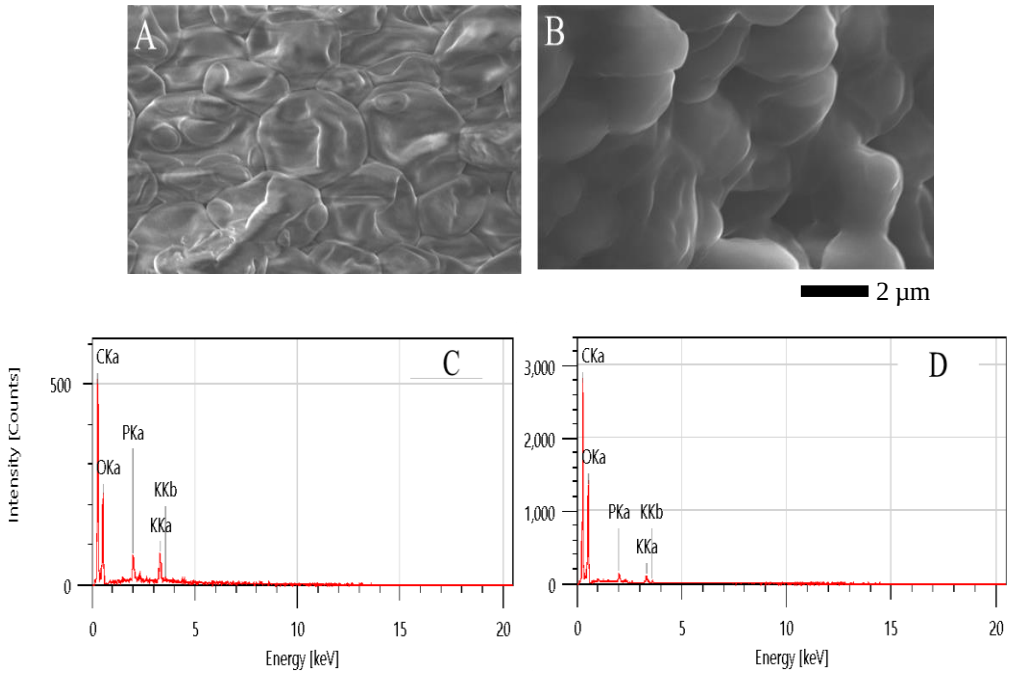

Fig 4. SEM of *W. anomalus* (x8000): (A) control yeast cells; (B) dye loaded, and the selected X-ray spectra of control (C) and dye loaded cells (D).

3.2.2 FTIR spectroscopy analysis

The FTIR spectra (Fig. 5) of *W. anomalus* biomass before and after AR14 biosorption were used to identify the involved functional groups of the cell wall in the dye-biosorption process (Pugazhenthi 2009). The strong vibration around 3000–3500 cm^{-1} illustrates the existence of stretching vibration of hydroxyl (-OH) and/or amino ($-NH_2$) groups, which are among the functional groups of chitosan and amino acids on the cell wall of *W. anomalus* (Paula et al. 2016). The peaks at 2854 – 2923 cm^{-1} are in the region of the absorption of lipid acyl chains (3050-2800 cm^{-1}) that correspond to symmetric and asymmetric stretching of methylene and methyl groups in the membrane phospholipids (Ami et al. 2014). The strong peaks at 1642 cm^{-1} detected in the region between 1700 and 1500 cm^{-1} indicate the presence of amide (I and II) bands, mainly from protein peptide bonds (C=O stretching and N-H bending), corresponding to several uronic acids and amino acids present in the cell wall (Zhang et al. 2010). The infrared absorption in the spectral at 1406 cm^{-1} may be caused by the sulfur (-SO-) and phosphorous (-PO-) groups, which range between 1500 and 1300 cm^{-1} corresponding to vibrations of fatty acids and proteins (Paula et al. 2016). The bands observed at 1073 cm^{-1} are assigned to C-O stretching vibration of alcohols and carboxylic acids which are mainly related to complex vibrations from carbohydrates (Naja and Volesky 2011). Based on the comparison of the spectra before and after biosorption, a significant change was noticed in the transmittance of these functional groups which may be attributed to its occupation by dye molecule. There was also a shift in various bands, which represented the groups involved in the biosorption corresponding to hydroxyl, carboxylic acid, amine, and amino groups. Some previous studies indicated that the biosorption process is accomplished by chelation and formation of ionic bridges between dye and functional groups. The binding mechanism of dye molecules to the yeast cell is explained by the strong attractive forces of peptidomannan, peptidoglycan, lipids, and heteropolysaccharides…, which contains several functional groups such as carboxyl, hydroxyl, amino, phosphate, and other charged groups (Gadd 2009; Vitor and Corso 2008). In line with our findings, it has been reported by Dilarri et al. (2016) that the biosorption of synthetic dyes by the cell wall of *S. cerevisiae* involved some amide and amine groups, and demonstrated that the vibration of (-C=O) and (-C-O) can be another linking group in the chitin structure. Moreover, it can be predicted according to the FTIR analysis that Yoshida H-binding, dipole-dipole H-binding, π-π, and n-π interactions play an indispensable role in the AR14 biosorption onto yeast cell (Tran et al. 2017).

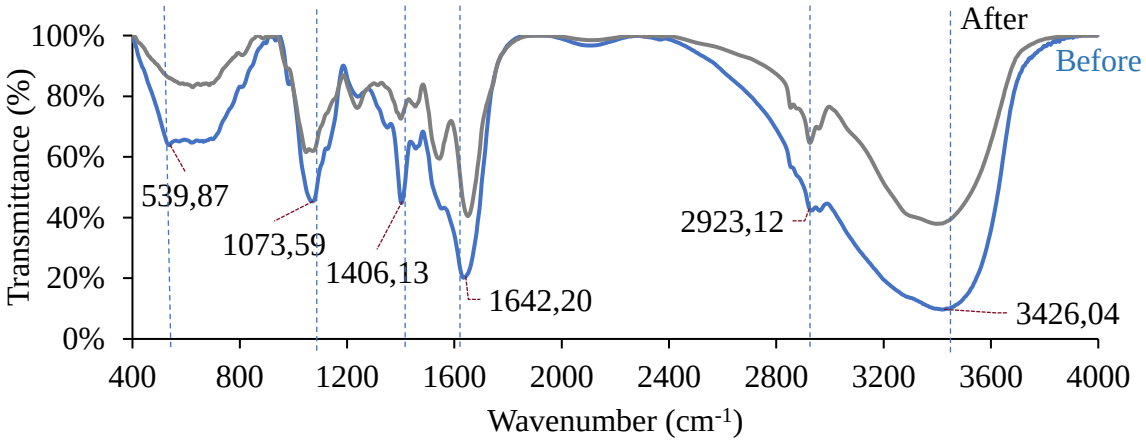

Fig 5. FTIR spectra of *W. anomalus* cells before and after AR14 biosorption.

The cell wall architecture and the proposed mechanisms of AR14 biosorption are illustrated in Fig. 6. In fact, the major components of the *S. cerevisiae* cell wall are β-glucans (formed by 1,3-β- and 1,6-linkages) and mannoproteins (proteins highly N- or O-glycosylated mannose residues linked by 1,2,-1,3-, 1,4- and 1,6-α-linkages), which represent about 50-60% and 40-50%, respectively of the cell wall mass, as well as 1-3% for the chitin, which is manufactured by 1,4-β-N-acetylglucosamine (Stewart 2017). These complex macromolecular structures present potential binding sites for diverse pollutants including toxic dye molecules (Fomina and Gadd 2014).

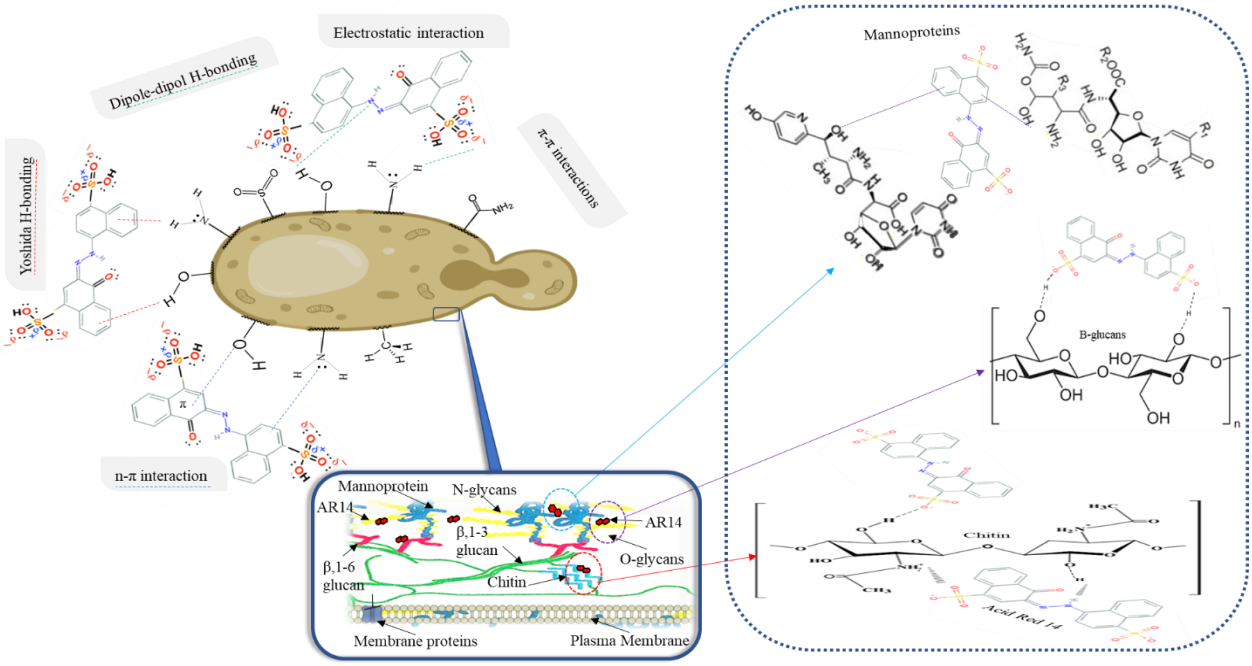

Fig 6. Architecture of yeast cell wall and proposed interaction mechanisms of AR14 biosorption.

3.2.3 Zeta potential and Zero-point charge measurement

The electrical state of the cell surface is one of the critical parameters in biosorption studies. Thus, the measurement of zeta potential can be one of the key parameters related to the external loads of the adsorbent (Akar et al. 2009). As shown in Fig. 7A, the zeta potential of *W. anomalus* biomass was maintained at a negative charge, regardless of the initial pH value, and it varied from –4.6 mV at pH 3 to -9.28 at pH 10. This can testify to the anionic characteristics and the high concentration of acid functional groups on the surface of *W. anomalus*. These results are consistent with previous studies that evaluated the zeta potential of different yeast strains (Lin et al. 2003; Tazhibaeva et al. 2003). It is known that there was a close relationship between the zeta potential of biomaterials and their biosorption capacity (Dundar et al. 2008). On the other hand, the value of pHzc at which ΔpH = 0 was found at 5.25 (Fig. 7B) confirmed thus the presence of anionic groups on the cell surface that dominate over the cationic groups. Zehra et al. (2016) reported that the acidic value of pHzc of baker's yeast, was attributed to the presence of various biopolymers on the yeast cell wall, mainly β-glucan and chitosan, that may have caused a substantial load on the external surface of the cells and given a net charge on the surface that depending on the pH caused by deprotonation of functional groups in the cell wall (Garcia-rubio et al. 2020; Klis et al. 2002). The number of positively charged sites decreases when the pH of the solution increases.

The decrease in the biosorption of AR14 anions is a result of the electrostatic repulsion forces of the negatively charged cell surface at acidic pH conditions (Akar et al. 2009).

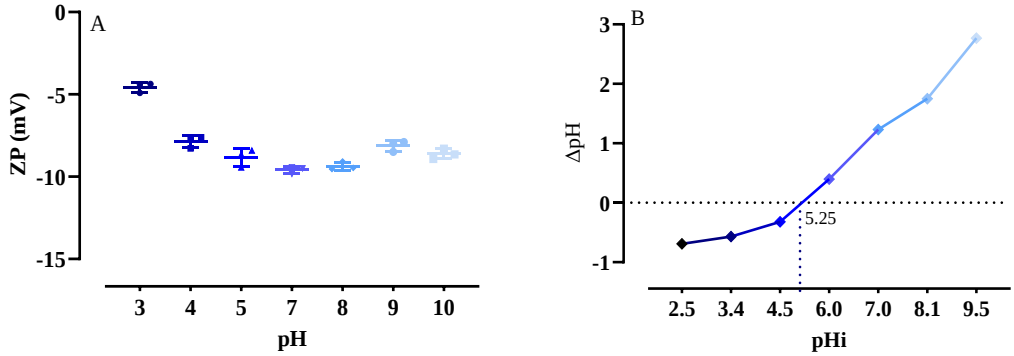

Fig 7. Zeta potential of (A) and pH zero charge (B) of *W. anomalus* yeast cells

3.2.4 Contact angle measurements

Based on both Vogler's and Van Oss approaches, *W. anomalus* exhibited a hydrophilic character, the θ_w value (34.9 ° ± 0.4) was less than 65 °, and the ΔGiwi had a positive value (37.23 ± 1.13 mJ m^{-2}). These findings agree with previous results reporting the hydrophilic character of various yeast strains (Lucas et al. 2006; Guillemot et al. 2006). The hydrophobicity of the yeast surface has been attributed to the proteins forming the cell wall (Suzzi et al. 1994; Vichi et al. 2010). In addition, *W. anomalus* appear to behave predominantly as electron donors/Lewis bases with high values of γ^- = 52.57 ± 0.6 mJ m^{-2} (Table 4). These results also indicate that this strain exhibits weak electron acceptor characters with γ^+ = 0.24 ± 0.07 mJ m^{-2}. Some previous research reported also that the microbial cell surfaces are mainly electron-donating, while electron-accepting cell surfaces are rarely found (Mei et al. 1998), which may be due to the presence of phosphate groups in the cell wall (Vichi et al. 2010). These findings are consistent with the FTIR analyses of *W. anomalus*, which confirm the presence of phosphate groups on its cell surface. On the other hand, the θ_w of *W. anomalus* significantly decreased from 34.9 º ± 0.4 to 31.6 º ± 0.9 after dye biosorption (Table 4). This may be attributed to an increase in the density of polar functional groups on the biomass surfaces after the biosorption process (Legorreta-Castañeda et al. 2020). In addition, a significant variation was noted in the electron donor and acceptor character after dye biosorption (γ^+ from 0.24 ± 0.07 to 0.08 ± 0.02 mJ m^{-2}; and γ^- from 52 57 ± 0.6 to 59.79 ± 0.5 mJ m^{-2}) which can be attributed to the interaction of cell surface functional groups with dye molecules.

Table 4. Contact angle values using water (θ_w), formamide (θ_F) and diiodomethane (θ_D), Lifshitz-vander Waals (γ^{LW}), electron-donor (γ^-) and electron-acceptor (γ^+) parameters, surface energies (ΔGiwi) of *W. anomalus* cells before and after AR14 biosorption

	Contact angles (°)			Surface tension: components and parameters (mJ m^{-2})			Surface energies
	θ_w	θ_F	θ_D	γ^{LW}	γ^+	γ^-	ΔGiwi (mJ m^{-2})
Raw Biomass	34.9±0.4	42.2±0.6	49.5±1.6	34.45±0.9	0.24±0.07	52.57±0.6	37.23±1.13
AR14-Biomass	31.6±0.9*	44.1±0.5^{ns}	36.3±0.6***	41.33±0.3***	0.08±0.02*	59.79±0.5***	44.9±1.2**

3.3 Optimization of the biosorption by using the design of experiments

3.3.1 Factor's screening using Plackett–Burman design

Based on the positive or negative values of the factors modeled on the eq 10, both factors A and C have positive values, indicating their synergistic effect on the biosorption, while the other negative factors indicate an antagonistic effect.

$$D\ \% = 11.0 + 0.933\ A - 3.64\ B + 12.89\ C - 0.003\ D - 0.207\ E + 0.774\ F \qquad \text{eq (10).}$$

Table 5 represents the value of the regression coefficients, the t-tests, and the p-values of six independent variables. The multiple correlation coefficient R^2 of the first-order model indicates that 75.82% of the data variance could be estimated by this model. Moreover, the difference between the predicted R2 (51.80%) and the adjusted R2 (67.28%), indicates that the relationship between the independent variables and the response cannot be evaluated based on the first-order model. As illustrated in Fig. 8A, the significant influence factors on biosorption capacity are the biomass (89.06%), pH (26.57%), and the dye concentration (10.94%). Indeed, the increase in the yeast dosage showed a positive influence, while increasing dye concentration and pH had a negative influence on the efficiency of AR14 biosorption (Fig. 8B).

Table 5. ANOVA for process variables of the PBD

Source	DF	Adj SS	Adj MS	F-Value	P-Value
Model	6	10216.7	1702.79	8.88***	0.000
Linear	6	10216.7	1702.79	8.88***	0.000
Temperature (ºC) (A)	1	751.4	751.39	3.92NS	0.064
pH (B)	1	1272.1	1272.06	6.64**	0.02
Biomass dosage ($g.L^{-1}$) (C)	1	2241.6	2241.58	11.69**	0.003
Agitation (rpm) (D)	1	0.8	0.82	0.00 NS	0.949
Dye ($mg\ L^{-1}$) (E)	1	5821.6	5821.58	30.37***	0.000
Contact time (min) (F)	1	129.3	129.30	0.67 NS	0.423
Error	17	3258.8	191.69		
Lack-of-Fit	5	1860.8	372.16	3.19*	0.046
Pure Error	12	1398.0	116.50		
Total	23	13475.5			

R^2 75.82; Adjusted R^2 67.28; Predicted R^2 51.80%.
DF: degrees of freedom; SS: sum of squares; MS: mean sum of squares,
*Significance (α = 0.05)

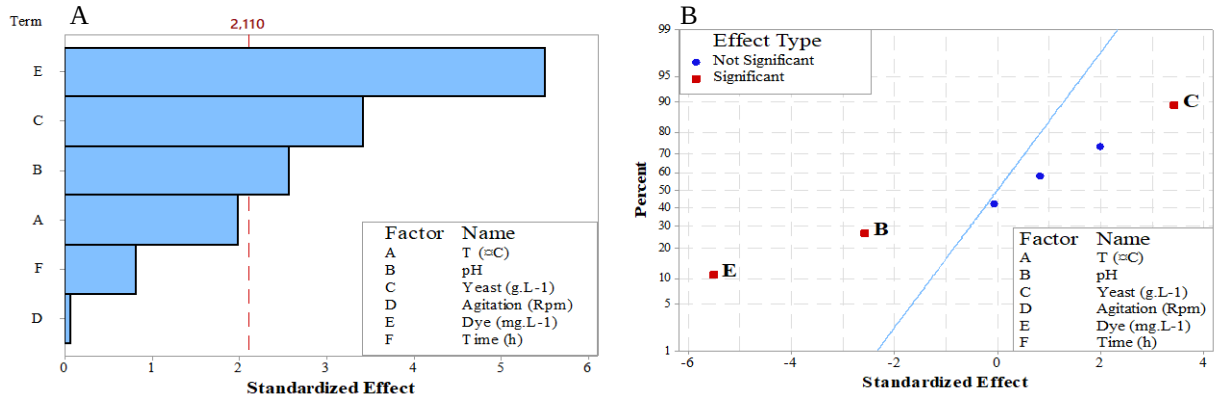

Fig 8. Main effect of variables on the biosorption capacity of AR14 using *W. anomalus*: Pareto chart of standard effect (A), and normal plot of standardized effects (B).

Several studies reported that an increase in biomass dosage significantly improves the biosorption capacity, due to the increase of exchangeable sites present in the cell wall (Kousha et al. 2012). pH is also one of the factors controlling the biosorption process. In fact it can affect the chemistry of dye molecules, the physicochemical properties of the yeast surface, and the magnitude of electrostatic charges imparted by the ionized dye molecules (Fu and Viraraghavan 2002). It has been documented that the optimal biosorption pH of particular dyes depends closely on their chemical properties. For instance, the biosorption of reactive dyes require acidic conditions, whereas basic dyes biosorption require neutral or alkaline conditions (Farah et al. 2007). In addition, the net charge of the biosorbent is also pH-dependent, at a low pH value, the functional group on the cell surface becomes protonated and acquires a net positive charge increasing thereby the binding of anionic dyes. Regarding the effect of the initial dye concentration on the biosorption capacity, its closely depending on the binding sites available on the biomass surface. Moreover, it has been reported that a high dye solute uptake can be obtained at a high initial dye concentration, which is linked to the high driving force for mass transfer (Binupriya et al. 2007; Bulut and Aydin 2006). However, at lower initial dye concentrations, the biosorption becomes independent of the initial dye concentration, because the ratio of the initial moles of the solute to the available area becomes low (Vijayaraghavan and Yun 2008).

3.3.2 Optimization of process parameters using Box-Behnken model

The eq (11) models the relationship between the predicted biosorption response and the process parameters with the second-order polynomial equation. In fact, the negative values of both factors (A) and (C) indicate that a high biosorption efficiency occurs at lower dye concentration and at acidic pH solution.

$$D\% = 70.8 - 0.243\ A + 48.99\ B - 23.18\ C - 0.00015\ A*A - 10.50\ B*B + 1.625\ C*C + 0.0001\ A*B + 0.0419\ A*C - 2.61\ B*C \quad \text{eq (11).}$$

As illustrated in Table 6, the regression of the quadratic model was statistically significant (F=21.48; P=0.00), at 95% confidence limits. The R^2 indicate that the model as fitted explains 90.62% of the variability, suggesting a significant correlation between the predicted and experimental effects of the selected variables. Furthermore, the predicted R^2 value (76.27%) was in line with the founded R^2value (86.41%) of the adjusted, indicating that 10.14% of the variability in the response was not explainable by this model. Also, the F value was significantly proportional to the pure error, and the F values for the factors A, B and C were at 17.44, 42.69, and 79.62, respectively, showing consequently that the pH of the solution was most significantly different from zero at the 95.0% confidence level followed by the biomass dosage and dye concentration (Fig. 9A). Consistent with the results of the factor selection step, the normalized effects indicate that increasing the yeast dose had a positive influence, whereas a negative influence on biosorption efficiency was observed when increasing the dye concentration or initial pH of the medium (Fig. 9B). As described in Fig. 10A, the contours illustrating the change in AR14 biosorption, relative to the simultaneous change in two factors. while the third is included at the midpoint. When the initial pH was maintained at 5, the biosorption rate was proportional to the increase in the biomass dosage, but inversely proportional to the increase in the initial dye concentration. Meanwhile, when the initial dye concentration was maintained at 125 mg L^{-1} (Fig. 10B), the rate of biosorption was proportional to the increase in the biomass dosage, and the optimum biosorption was achieved at a lower pH level. Similarly, when the biomass dosage was maintained at 1.125 mg L^{-1} (Fig. 10C), the optimum biosorption level was proportional to the initial pH of the medium and the initial dye

concentration. Higher biosorption was achieved at acidic conditions with lower dye concentration. El-Naggar and El-Malkey (2020) reported that the dye biosorption system depended on protonation or deprotonation of the functional groups on the cell surface. At pH 3-4, the protonation of amino groups on the yeast cell wall increases the net positive charge and enhances the biosorption of negatively charged dye ions by electrostatic binding.

Table 6. Analysis of variance for response surface quadratic model.

Source	DF	Adj SS	Adj MS	F-Value	P-Value
Model	9	3821.96	424.66	21.48***	0.000
Linear	3	2762.70	920.90	46.58***	0.000
Dye (mg L^{-1})(A)	1	344.76	344.76	17.44***	0.000
Biomass (g L^{-1}) (B)	1	843.87	843.87	42.69***	0.000
pH (C)	1	1574.06	1574.06	79.62***	0.000
Square	3	620.61	206.87	10.46***	0.000
A * A	1	3.03	3.03	0.15NS	0.700
B * B	1	257.68	257.68	13.03**	0.002
C * C	1	312.17	312.17	15.79***	0.001
2-Way Interaction	3	438.65	146.22	7.40**	0.002
A * B	1	0.00	0.00	0.00 NS	0.997
A * C	1	315.76	315.76	15.97***	0.001
B * C	1	122.89	122.89	6.22**	0.022
Error	20	395.38	19.77		
Lack-of-Fit	3	361.66	120.55	60.77***	0.000
Pure Error	17	33.72	1.98		
Total	29	4217.34			

R^2 90.62; Adjusted R^2 86.41; Predicted R^2 76.27%.

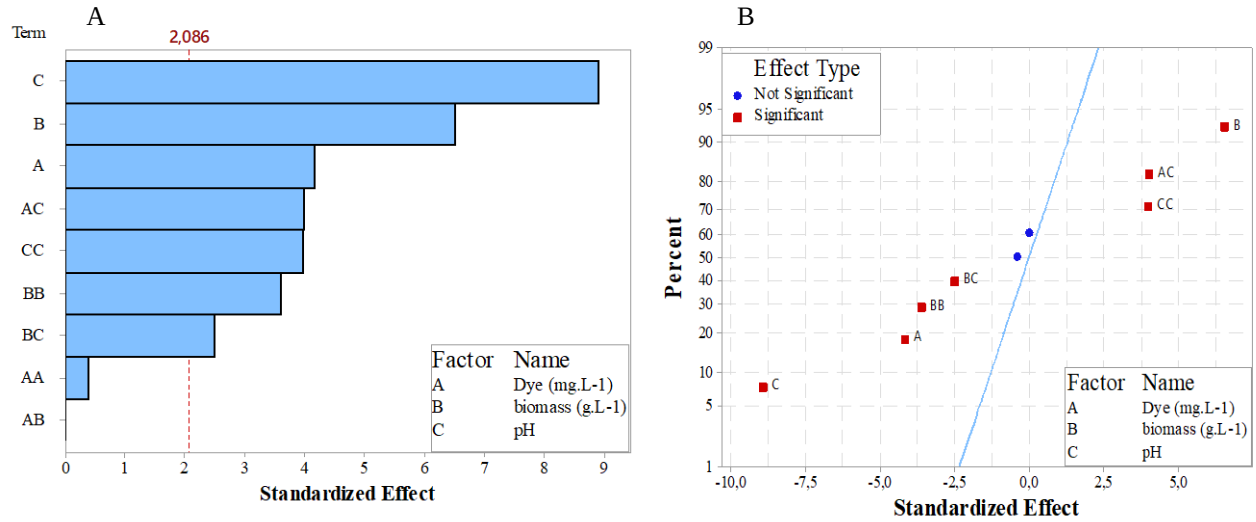

Fig 9. Effect of variables and 2-Way interaction on the biosorption capacity of AR14 using *W. anomalus*: pareto-chart of standardized effects (A), and normal plot of standardized effects (B).

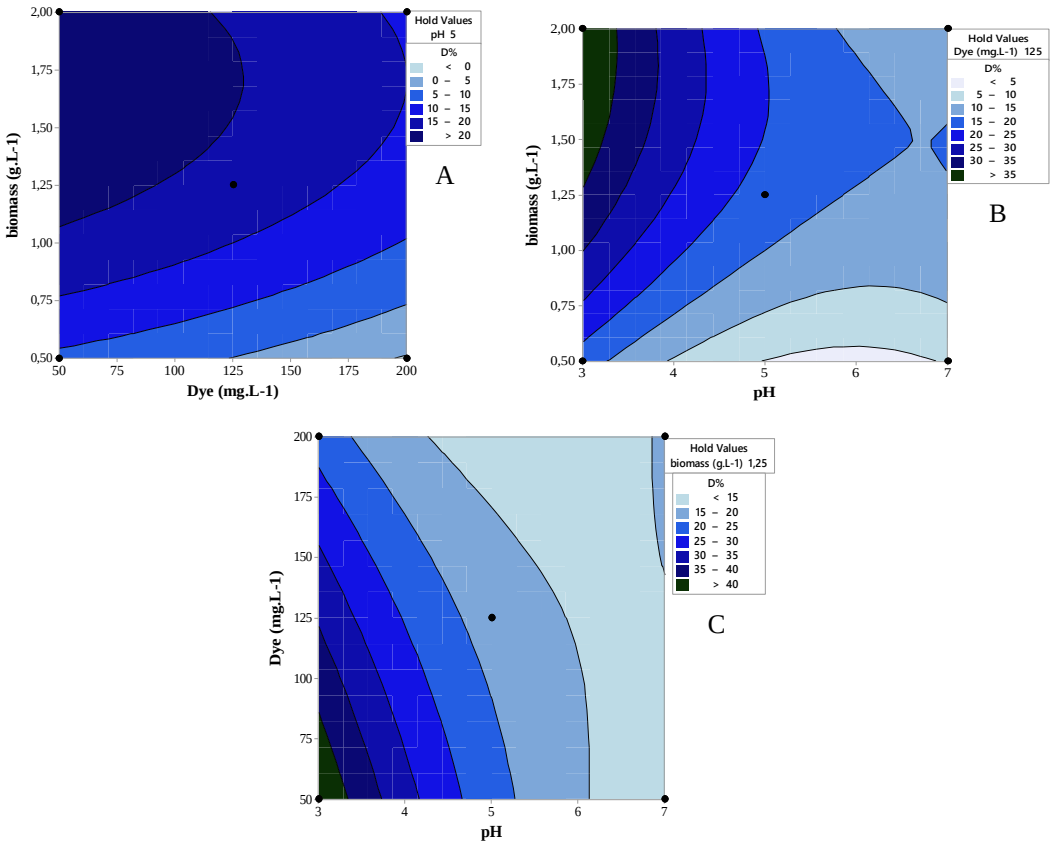

Fig 10. Effect of selected factors (pH, dye concentration and yeast biomass) on the biosorption capacity of AR14 onto *W. anomalus.*

4. Conclusion

Based on the above considerations, it can be concluded that the biomass of *W. anomalus* could be used as an effective, inexpensive and environmentally friendly biosorbent for the removal of toxic dyes. The study of the kinetics of biosoprtopn indicated that at the beginning of the biosorption process, the bioremoval occurred rapidly, then proceeded gradually to reach the equilibrium state. The studied isotherm model indicated a monolayer adsorption of AR14 molecules at homogeneous sites on the cell wall surface of *W. anomalus*. Furthermore, biosorption kinetic modelling followed both the pseudo-second-order as well as the intraparticle diffusion model. The characterization of yeast biomass before and after dye biosorption indicated that the bioremoval was attributed to the presence of various active groups on the cell surface, the zeta potential of *W. anomalus* was at a negative charge, and the acidic value of pHzc confirmed the presence of anionic groups on the cell surface that dominate over the cationic groups. The adsorbate concentration and the adsorbent dosage ratio as well as the initial pH have significantly affected the biosorption efficiency. The optimum condition for maximum dye biosorption was achieved at pH 3-4, with lower initial dye concentrations (50 - 75 mg L^{-1}) and yeast biomass greater than 1.25 g L^{-1}. Until today, very few studies have been conducted on the use of yeasts as biosorbent. To our knowledge, most of these researches are limited to the laboratory scale. Hence the emergence of this new research topic which may be part of the future solutions proposed for the treatment of colored effluents.

Acknowledgements

The authors gratefully acknowledge the Moroccan Foundation for Advanced Science, Innovation and Research (MAScIR), and Regional University Centre of Interface (CURI), Sidi Mohamed Ben Abdellah University for their financial and technical support.

Conflicts of interest

The authors declare no conflicts of interest related to this work

Data Availability

All data generated or analyzed during this study are available from the corresponding author.

Funding

Not Applicable

References

Akar, Tamer, Burcu Anilan, Asli Gorgulu, and Sibel Tunali. 2009. Assessment of Cationic Dye Biosorption Characteristics of Untreated and Non-Conventional Biomass : *Pyracantha Coccinea Berries*. *Journal of Hazardous Materials* 168: 1302–9. https://doi.org/10.1016/j.jhazmat.2009.03.011.

Akar, S. T., Gorgulu, A., Kaynak, Z., Anilan, B., and Akar, T. 2009. Biosorption of Reactive Blue 49 Dye under Batch and Continuous Mode Using a Mixed Biosorbent of Macro-Fungus *Agaricus Bisporus* and *Thuja Orientalis* Cones. *Chemical Engineering Journal* 148: 26–34. https://doi.org/10.1016/j.cej.2008.07.027.

Aksu, Zümriye, and Gönül Dönmez. 2003. A Comparative Study on the Biosorption Characteristics of Some Yeasts for Remazol Blue Reactive Dye. *Chemosphere* 50(8): 1075–83. https://doi.org/10.1016/S0045-6535(02)00623-9.

Aksu, Zümriye, and Sevilay Tezer. 2005. Biosorption of Reactive Dyes on the Green Alga *Chlorella vulgaris*. *Process Biochemistry* 40(3–4): 1347–61. https://doi.org/10.1016/j.procbio.2004.06.007.

Ami, D., Posteri, R., Mereghetti, P., Porro, D., Doglia, S. M., and Branduardi, P. 2014. Fourier Transform Infrared Spectroscopy as a Method to Study Lipid Accumulation in Oleaginous Yeasts. *Biotechnology for Biofuels*: 7–12. https://doi.org/https://doi.org/10.1186/1754-6834-7-12.

Arslan, Serkan, Murat Eyvaz, Ercan Gürbulak, and Ebubekir Yüksel. 2016. A Review of State-of-the-Art Technologies in Dye- Containing Wastewater Treatment – The Textile Industry Case. In *Textile Wastewater Treatment*, InTech, 3–28. https://doi.org/http://dx.doi.org/10.5772/64140.

Asri, M., El Ghachtouli, N., Elabed, S., Koraichi, S. I., Elabed, A., Silva, B., and Tavares, T. 2018. *Wicherhamomyces Anomalus* Biofilm Supported on Wood Husk for Chromium Wastewater Treatment. *Journal of Hazardous Materials* 359(May): 554–62. https://doi.org/10.1016/j.jhazmat.2018.05.050.

Bahafid, W., Joutey, N. T., Sayel, H., Iraqui-Houssaini, M., and El Ghachtouli, N. 2013. Chromium Adsorption by Three Yeast Strains Isolated from Sediments in Morocco. *Geomicrobiology Journal* 30(5): 422–29. https://doi.org/10.1080/01490451.2012.705228.

Binupriya, A. R., Sathishkumar, M., Kavitha, D., Swaminathan, K., and Yun, S. E. 2007. Aerated and Rotated Mode Decolorization of a Textile Dye Solution by Native and Modified Mycelial Biomass of *Trametes Versicolor*. *Journal of Chemical Technology and Biotechnology* 82(4):

350–359. https://doi.org/10.1002/jctb.
Box, G.E.P., and D.W. Behnken. 1960. Some New Three Level Design for Study of Quantitative Variables. *Technometrics* 2: 455-475. https://doi.org/10.2307/1266454
Bulut, Yasemin, and Haluk Aydin. 2006. A Kinetics and Thermodynamics Study of Methylene Blue Adsorption on Wheat Shells. *Desalination* 194(1–3): 259–67. https://doi.org/10.1016/j.desal.2005.10.032.
de Castro, Ketinny Camargo, Aline Silva Cossolin, Hélen Cristina Oliveira dos Reis, and Eduardo Beraldo de Morais. 2017. Biosorption of Anionic Textile Dyes from Aqueous Solution by Yeast Slurry from Brewery. *Brazilian Archives of Biology and Technology* 60(December): 1–13. https://doi.org/10.1590/1678-4324-2017160101.
Crini, Grégorio, Eric Lichtfouse, Lee D. Wilson, and Nadia Morin-Crini. 2019. Conventional and Non-Conventional Adsorbents for Wastewater Treatment. *Environmental Chemistry Letters* 17(1): 195–213. https://doi.org/10.1007/s10311-018-0786-8.
Daneshvar, Ehsan, Arya Vazirzadeh, and Amit Bhatnagar. 2019. Biosorption of Methylene Blue Dye onto Three Different Marine Macroalgae: Effects of Different Parameters on Isotherm, Kinetic and Thermodynamic. *Iranian Journal of Science and Technology, Transaction A: Science* 43(6): 2743–54. https://doi.org/10.1007/s40995-019-00764-8.
Danouche, M., El Arroussi, H., Bahafid, W., and El Ghachtouli, N. 2021. An Overview of the Biosorption Mechanism for the Bioremediation of Synthetic Dyes Using Yeast Cells. *Environmental Technology Reviews* 10(1): 58–76. https://doi.org/10.1080/21622515.2020.1869839.
Davranche, M., Veclin, C., Pierson-Wickmann, A. C., El Hadri, H., Grassl, B., Rowenczyk,L., Dia, A., Halle, A.T. Blancho, F., Reynaud, S., and Gigault, J. 2019. Are Nanoplastics Able to Bind Significant Amount of Metals? The Lead Example. *Environmental Pollution* 249: 940–48. https://doi.org/10.1016/j.envpol.2019.03.087.
Dilarri, Guilherme, Érica Janaina Rodrigues de Almeida, Hengli Barbosa Pecora, and Carlos Renato Corso. 2016. Removal of Dye Toxicity from an Aqueous Solution Using an Industrial Strain of *Saccharomyces Cerevisiae* (Meyen). *Water, Air, and Soil Pollution* 227(8). http://dx.doi.org/10.1007/s11270-016-2973-1.
Dundar, Murat, Cigdem Nuhoglu, and Yasar Nuhoglu. 2008. Biosorption of Cu (II) Ions onto the Litter of Natural Trembling Poplar Forest. *J. Hazard. Mater*. 151 (2008) 86–95. https://doi.org/10.1016/j.jhazmat.2007.05.055.
El-Naggar, N. E. A., Rabei, N. H., and El-Malkey, S. E. 2020. Eco - Friendly Approach for Biosorption of - Pb 2 + and Carcinogenic Congo Red Dye from Binary Solution onto Sustainable *Ulva Lactuca* Biomass. *Scientific Reports* (0123456789): 1–22. https://doi.org/10.1038/s41598-020-73031-1.
Farah, Joseph Y, Nour Sh El-Gendy, and Laila A Farahat. 2007. Biosorption of Astrazone Blue Basic Dye from an Aqueous Solution Using Dried Biomass of Baker's Yeast. *Journal of hazardous materials* 148(1–2): 402–8. https://doi.org/10.1016/j.jhazmat.2007.02.053.
Fomina, Marina, and Geoffrey Michael Gadd. 2014. Biosorption: Current Perspectives on Concept, Definition and Application. *Bioresource Technology* 160: 3–14. http://dx.doi.org/10.1016/j.biortech.2013.12.102.
Fu, Yuzhu, and T. Viraraghavan. 2001. Fungal Decolorization of Dye Wastewaters: A Review. *Bioresource Technology* 79: 251–62. https://doi.org/10.1556/034.58.2016.1-2.6.
———. 2002. Removal of Congo Red from an Aqueous Solution by Fungus Aspergillus Niger. *Advances in Environmental Research* 7(1): 239–47. https://doi.org/10.1016/S1093-

0191(01)00123-X.
Gadd, Geoffrey Michael. 2009. Biosorption: Critical Review of Scientific Rationale, Environmental Importance and Significance for Pollution Treatment. *Journal of Chemical Technology and Biotechnology* 84(1): 13–28. https://doi.org/10.1002/jctb.1999.
Garcia-Rubio, R., de Oliveira, H. C., Rivera, J., and Trevijano-Contador, N. 2020. The Fungal Cell Wall : *Candida* , *Cryptococcus* , and *Aspergillus* Species. 10(January): 1–13. https://doi.org/10.3389/fmicb.2019.02993.
Hadjoudja, S, V Deluchat, and M Baudu. 2010. Journal of Colloid and Interface Science Cell Surface Characterisation of *Microcystis Aeruginosa* and *Chlorella Vulgaris*. *Journal of Colloid And Interface Science* 342(2): 293–99. http://dx.doi.org/10.1016/j.jcis.2009.10.078.
Ho, Y. S., and G. McKay. 1998. Kinetic Models for the Sorption of Dye from Aqueous Solution by Wood. *Process Safety and Environmental Protection* 76(2): 183–91. https://doi.org/10.1205/095758298529326.
Jafari, Narjes, Mohammad Reza Soudi, and Rouha Kasra-Kermanshahi. 2014. Biodecolorization of Textile Azo Dyes by Isolated Yeast from Activated Sludge: *Issatchenkia Orientalis* JKS6. *Annals of Microbiology* 64(2): 475–82. https://doi.org/10.1007/s13213-013-0677-y
Ka Yee, Ho, Gordon McKay, and Yeung King Lun. 2003. Selective Adsorbents from Chemically Modified Ordered Mesoporous Silica. *Langmuir* 19(7): 3019–24. https://doi.org/10.1016/s0167-2991(04)80581-0.
Kismir, Yasemin, and Ayse Z. Aroguz. 2011. Adsorption Characteristics of the Hazardous Dye Brilliant Green on Sakli{dotless}kent Mud. *Chemical Engineering Journal* 172(1): 199–206. https://doi.org/10.1016/j.cej.2011.05.090.
Klis, F. M., P. Mol, K. Hellingwerf, and S. Brul. 2002. Dynamics of Cell Wall Structure in *Saccharomyces cerevisiae*. *FEMS Microbiology Reviews* 26. https://doi.org/10.1111/j.1574-6976.2002.tb00613.x
Kousha, M., Daneshvar, E., Dopeikar, H., Taghavi, D., and Bhatnagar, A. 2012. Box-Behnken Design Optimization of Acid Black 1 Dye Biosorption by Different Brown Macroalgae. *Chemical Engineering Journal* 179: 158–68. http://dx.doi.org/10.1016/j.cej.2011.10.073.
Legorreta-Castañeda, A. J., Lucho-Constantino, C. A., Beltrán-Hernández, R. I., Coronel-Olivares, C., and Vázquez-Rodríguez, G. A. 2020. Biosorption of Water Pollutants by Fungal Pellets. *Water*, 12(4), 1155. doi:10.3390/w12041155
Lin, D. Q., Brixius, P. J., Hubbuch, J. J., Thömmes, J., and Kula, M. R. 2003. Biomass/Adsorbent Electrostatic Interactions in Expanded Bed Adsorption: A Zeta Potential Study. *Biotechnology and bioengineering* 83(2): 149-157. https://doi.org/10.1002/bit.10654.
Lucas, M. S., Amaral, C., Sampaio, A., Peres, J. A., and Dias, A. A. 2006. Biodegradation of the Diazo Dye Reactive Black 5 by a Wild Isolate of *Candida Oleophila*. *Enzyme and Microbial Technology* 39(1): 51–55. https://doi.org/10.1016/j.enzmictec.2005.09.004.
Mei, H C Van Der, R Bos, and H J Busscher. 1998. A Reference Guide to Microbial Cell Surface Hydrophobicity Based on Contact Angles. *Colloids and Surfaces B: Biointerfaces* 11(4): 213–21. https://doi.org/doi:10.1016/s0927-7765(98)00037-x.
Rita de Cássia, M., de Barros Gomes, E., Pereira Jr, N., Marin-Morales, M. A., Machado, K. M. G., and de Gusmão, N. B. 2013. Biotreatment of Textile Effluent in Static Bioreactor by Curvularia Lunata URM 6179 and *Phanerochaete Chrysosporium* URM 6181. *Bioresource Technology* 142: 361–67. http://dx.doi.org/10.1016/j.biortech.2013.05.066.
Morão, Luana Galvão, Guilherme Dilarri, and Carlos Renato Corso. 2017. Immobilization of *Saccharomyces Cerevisiae* Cells on *Luffa Cylindrica*: A Study of a Novel Material for the

Adsorption of Textile Dye. *Water, Air, and Soil Pollution* 228(7): 228–48. https://doi.org/10.1007/s11270-017-3433-2.

Morosanu, I., Teodosiu, C., Paduraru, C., Ibanescu, D., and Tofan, L. 2016. Biosorption of Lead Ions from Aqueous Ef Fl Uents by Rapeseed Biomass. *New Biotechnology*. http://dx.doi.org/10.1016/j.nbt.2016.08.002.

Naja, Ghinwa, and Bohumil Volesky. 2011. *The Mechanism of Metal Cation and Anion Biosorption. In Microbial Biosorption of Metals (Pp. 19-58).* Dordrecht: Springer.

Van Oss, C. J., M. K. Chaudhury, and R. J. Good. 1988. Interfacial Lifshitz-van Der Waals and Polar Interactions in Macroscopic Systems. *Chemical reviews* 88(6): 927–41. https://doi.org/10.1021/cr00088a006.

Papadopoulou, Konstantina, Iphigeneia Maria Kalagona, Antonios Philippoussis, and Fotis Rigas. 2013. Optimization of Fungal Decolorization of Azo and Anthraquinone Dyes via Box-Behnken Design. *International Biodeterioration and Biodegradation* 77: 31–38. http://dx.doi.org/10.1016/j.ibiod.2012.10.008.

A. Paula, G. Maria, A. Gabriela, F. Zielinski, M. Vieira, C. Windson, I. Haminiuk. 2016. Biosorption of Anthocyanins from Grape Pomace Extracts by Waste Yeast : Kinetic and Isotherm Studies. *Journal of Food Engineering* 169: 53–60. https://doi.org/10.1016/j.jfoodeng.2015.08.016.

Plackett, R. L, and J. P. Burman. 1946. The Design of Optimum Multifactorial Experiments: R. L. Plackett , and J. P. Burman. Published by : Biometrika Stable URL : http://www.jstor.org/stable/2, Biometrika. 33. 305–325. https://doi.org/doi:10.2307/2332195.

Pugazhenthi, P Monash G. 2009. Adsorption of Crystal Violet Dye from Aqueous Solution Using Mesoporous Materials Synthesized at Room Temperature. : 390–405. https://doi.org/10.1007/s10450-009-9156-y

Saratale, R. G., G. D. Saratale, J. S. Chang, and S. P. Govindwar. 2011. Bacterial Decolorization and Degradation of Azo Dyes: A Review. *Journal of the Taiwan Institute of Chemical Engineers* 42(1): 138–57. https://doi.org/10.1016/j.jtice.2010.06.006

Sen, Sudip Kumar, Smita Raut, Partha Bandyopadhyay, and Sangeeta Raut. 2016. Fungal Decolouration and Degradation of Azo Dyes: A Review. *Fungal Biology Reviews* 30(3): 112–33. http://dx.doi.org/10.1016/j.fbr.2016.06.003.

Singh, Kamaljit, and Sucharita Arora. 2011. Removal of Synthetic Textile Dyes from Wastewaters: A Critical Review on Present Treatment Technologies. *Critical Reviews in Environmental Science and Technology* 41(9): 807–78. https://doi.org/10.1080/10643380903218376

Smaranda, Camelia, Dumitru Bulgariu, and Maria Gavrilescu. 2009. An Investigation of the Sorption of Acid Orange 7 from Aqueous Solution onto Soil. *Environmental Engineering and Management Journal* 8(6): 1391–1402. https://doi.org/10.30638/eemj.2009.203

Soares, Eduardo V., and Helena M.V.M. Soares. 2012. Bioremediation of Industrial Effluents Containing Heavy Metals Using Brewing Cells of *Saccharomyces Cerevisiae* as a Green Technology: A Review. *Environmental Science and Pollution Research* 19(4): 1066–83.

Srinivasan, Asha, and Thiruvenkatachari Viraraghavan. 2010. Decolorization of Dye Wastewaters by Biosorbents: A Review. *Journal of Environmental Management* 91(10): 1915–29. http://dx.doi.org/10.1016/j.jenvman.2010.05.003.

Stewart, G. G. 2017. The Structure and Function of the Yeast Cell Wall , Plasma Membrane and Periplasm. In *Brewing and Distilling Yeasts*, Springer, Cham., 55–75. https://doi.org/https://doi.org/10.1007/978-3-319-69126-8_5.

Suzzi, Giovanna, Patrizia Romano, and Lucia Vannini. 1994. Cell Surface Hydrophobicity and

Flocculence in *Saccharomyces Cerevisiae* Wine Yeasts '. *Colloids and Surfaces B: Biointerfaces* 2: 505–10. https://doi.org/10.1016/0927-7765(94)80058-8

Tazhibaeva, S M, K B Musabekov, A B Orazymbetova, and A A Zhubanova. 2003. Surface Properties of Yeast Cells. *Colloid Journal* 65(1): 122–24. https://doi.org/https://doi.org/10.1023/A:1022391613491.

Tran, Nguyen Hai, Sheng-jie You, and Ahmad Hosseini-bandegharaei. 2017. Mistakes and Inconsistencies Regarding Adsorption of Contaminants from Aqueous Solutions : A Critical Review. *Water Research* 120: 88–116. http://dx.doi.org/10.1016/j.watres.2017.04.014.

Guillemot, G., Vaca-Medina, G., Martin-Yken, H., Vernhet, A., Schmitz, P., and Mercier-Bonin, M. 2006. Shear-Flow Induced Detachment of *Saccharomyces Cerevisiae* from Stainless Steel : Influence of Yeast and Solid Surface Properties. *Colloids and Surfaces B: Biointerfaces* 49: 126–35. https://doi.org/10.1016/j.colsurfb.2006.03.001.

Vichi, S., Gallardo-Chacón, J. J., Pradelles, R., Chassagne, D., López-Tamames, E., and Buxaderas, S. 2010. Surface Properties of *Saccharomyces Cerevisiae* Lees during Sparkling Wine Ageing and Their Effect on Flocculation. *International Journal of Food Microbiology* 140(2–3): 125–30. http://dx.doi.org/10.1016/j.ijfoodmicro.2010.04.009.

Vijayaraghavan, K., and Yeoung Sang Yun. 2008. Bacterial Biosorbents and Biosorption. *Biotechnology Advances* 26(3): 266–91. https://doi.org/10.1016/j.biotechadv.2008.02.002.

Vitor, Vivian, and Carlos Renato Corso. 2008. Decolorization of Textile Dye by *Candida Albicans* Isolated from Industrial Effluents. *Journal of Industrial Microbiology and Biotechnology* 35(11): 1353–57. https://doi.org/10.1007/s10295-008-0435-5.

Vogler, Erwin A. 1998. Structure and Reactivity of Water at Biomaterial Surfaces. *Advances in Colloid and Interface Science* 74: 69–117. https://doi.org/10.1016/S0001-8686(97)00040-7

Waghmode, Tatoba R., Mayur B. Kurade, Akhil N. Kabra, and Sanjay P. Govindwar. 2012. Degradation of Remazol Red Dye by *Galactomyces Geotrichum* MTCC 1360 Leading to Increased Iron Uptake in Sorghum Vulgare and Phaseolus Mungo from Soil. *Biotechnology and Bioprocess Engineering* 17(1): 117–26. https://doi.org/10.1007/s12257-011-0307-0.

Wu, Feng Chin, Ru Ling Tseng, and Ruey Shin Juang. 2009. Initial Behavior of Intraparticle Diffusion Model Used in the Description of Adsorption Kinetics. *Chemical Engineering Journal* 153(1–3): 1–8. https://doi.org/10.1016/j.cej.2009.04.042.

Yagub, Mustafa T, Tushar Kanti Sen, Sharmeen Afroze, and H M Ang. 2014. Dye and Its Removal from Aqueous Solution by Adsorption: A Review. *Advances in colloid and interface science* 209: 172–84. https://doi.org/10.1016/j.cis.2014.04.002.

Zehra, Tasneem, Namal Priyantha, and Linda B.L. Lim. 2016. Removal of Crystal Violet Dye from Aqueous Solution Using Yeast-Treated Peat as Adsorbent: Thermodynamics, Kinetics, and Equilibrium Studies. *Environmental Earth Sciences* 75(4): 1–15. https://doi.org/10.1007/s12665-016-5255-8.

Zhang, Y., Liu, W., Xu, M., Zheng, F., and Zhao, M. 2010. Study of the Mechanisms of Cu 2 + Biosorption by Ethanol / Caustic-Pretreated Baker ' s Yeast Biomass. *Journal of Hazardous Materials* 178(1–3): 1085–93. http://dx.doi.org/10.1016/j.jhazmat.2010.02.051.

DISCUSSION GÉNÉRALE

La pollution de l'eau est l'un des défis les plus graves auxquels le monde est confronté. Compte tenu de leur toxicité et de leur persistance dans l'environnement, le traitement des MLs et des polluants organiques persistants, tels que les colorants synthétiques, est une préoccupation majeure. La bioremédiation de tels contaminants à l'aide de levures ou de microalgues est parmi les stratégies écologiques les plus prometteuses à envisager pour faire face à ces problèmes (Ahmad et al., 2020; Connell et al., 2005).

Dans la première section de cette étude, huit souches de microalgues (*Chlorella vulgaris*, *C. ellipsoidea*, *C. sorokiniana*, *C. pyrenoidosa*, *Scenedesmus dimorphus*, *S. obliquus*, *Chlamydomonas reinhardtii*, et *Aphanothece* sp) ont été examinées pour évaluer leur tolérance vis-à-vis de quatre MLs: Cu(II), Cr(VI), Pb(II) et Cd(II). Les résultats de ce criblage nous a permis de sélectionner la souche de *S. obliquus*, qui a montré une tolérance élevée aux ions Pb(II), avec une EC_{50} de 141 ppm. La forte tolérance de cette souche serait liée à la nature de paroi cellulaire du genre *Scenedesmus*, qui a généralement une paroi composée par une architecture complexe des couches de pectine, d'algénane, et de microfibrilles. Cette barrière physique empêcherait la pénétration d'ions ou de tout autre type de xénobiotiques au niveau intracellulaire (Baudelet et al., 2017). C'est la raison pour laquelle plusieurs recherches ont signalé la grande capacité des souches de ce genre dans le traitement des MLs (Jena et al., 2015; Oliveira et al., 2019; Zhang et al., 2016). La souche sélectionnée a montré des performances intéressantes en termes d'élimination du Pb(II) en comparaison avec les travaux existants. L'analyse de la concentration d'ions Pb(II) restant dans le surnageant par ICP après la phycoremédiation a montré une réduction de 58,42% de la concentration initiale (EC_{50}). De plus, l'analyse thermogravimétrique des biomasses algales résultantes a révélé que les poids résiduels des cellules témoins et des cellules chargées en Pb(II) après la phycoremédiation du Pb(II) étaient respectivement de 31,34 % et 57,8 %, indiquant alors que les cellules de *S. obliquus* ont pu récupérer les ions Pb(II) de la solution.

Pour examiner les mécanismes extracellulaires et intracellulaires impliqués dans l'élimination du Pb(II) par la souche *S. obliquus*, un relargage chimique des ions adsorbés à la surface des cellules a été effectué par le biais d'une extraction par l'EDTA. Puis, les teneurs de

Pb(II) au niveau extra et intracellulaires ont été analysées par ICP. Les résultats de ce teste ont révélé l'implication de deux mécanismes, la biosorption et la bioaccumulation avec une participation à l'élimination du Pb(II) respectivement de 85,5% et 14,5%. L'implication simultanée de ces deux mécanismes dans l'élimination des MLs par certaines microalgues a été rapportée dans la littérature. Par exemple, Pérez-Rama et al. (2002) ont rapporté que la phycoremédiation de Cd(II) par *Tetraselmis suecica* implique à la fois la bioaccumulation intracellulaire et la biosorption extracellulaire.

Pour une compréhension détaillée des interactions gérant le phénomène de biosorption des ions Pb(II) avec les composants de la paroi cellulaire de la souche *S. obliquus*, nous avons procédé à une caractérisation physicochimique de la surface cellulaire au moyen de techniques d'imagerie (SEM), d'analyses spectroscopiques (EDX et FTIR), par la mesure du potentiel zêta, du pH de charge nulle (pHzc), ainsi que par la mesure de l'angle de contact. En effet, des différences dans l'aspect des cellules ont été observées par SEM après biosorption des ions Pb(II). De plus, des changements dans la composition élémentaire de la surface des cellules analysée par EDX montrant la disparition des pics correspondant au (S) et (Si) et leur remplacement par des pics correspondant à (Pb). Après la biosorption des ions Pb(II), l'analyse par la FTIR des cellules témoins et celles chargées en Pb(II) a montré une diminution de la transmittance des groupements fonctionnels (hydroxyle, amine, méthylène, soufre et phosphore) de la paroi cellulaire, ce qui signifie que les ions Pb(II) ont été chélatés par ces groupement via une chimiosorption (Leong and Chang, 2020). Le résultat de la mesure du potentiel zêta témoigne également des caractéristiques anioniques dues à la présence de groupements fonctionnels acides à la surface de *S. obliquus*. Selon les approches de Vogler (1998), la mesure de l'angle de contact montre que la surface de *S. obliquus* a un caractère hydrophile et cette hydrophobocité a diminué après la biosorption des ions Pb(II). En outre, une variation significative a été notée dans le caractère donneur et accepteur d'électrons après la biosorption de Pb(II) en raison de l'interaction des groupements fonctionnels de la surface des cellules avec les ions de Pb(II). Ces résultats indiquent que la biosorption de Pb(II) implique plusieurs interactions de type chimique et électrostatique, qui se produiraient entre les macromolécules qui composent la surface cellulaire et les ions Pb(II) en solution (Tran et al., 2017).

Concernant la proportion de Pb(II) accumulée par *S. obliquus*, le suivi de la souche durant le processus de phycoremédiation a montré que les ions de Pb(II) ont provoqué une diminution de

la croissance de cette souche. Cependant, le taux de la viabilité analysé par Cytométrie en flux (FCM) n'a été réduit que par 6,3 % après exposition au Pb(II), en comparaison avec les cellules témoins. Cela indique que la souche *S. obliquus* est capable de maintenir son intégrité membranaire dans de telles conditions de stress métallique, bien qu'il est connu que la membrane plasmique est l'une des cibles des ions Pb(II) ou des ROS résultantes de leur accumulation (Machado and Soares, 2015).

Par la suite, l'effet de la bioaccumulation du Pb(II) sur l'état osmotique des cellules a été analysé en se basant sur le changement de la taille cellulaire. Le Zetasizer a été utilisé pour analyser la taille des cellules témoins et celles résultantes du processus de la phycoremédiation. Les résultats obtenus ont indiqué une diminution statistiquement non significative de la taille de *S. obliquus* après bioaccumulation de Pb(II). Il est donc probable que la résistance osmotique de cette souche soit liée aux mécanismes d'osmorégulation, telle que la régulation des flux d'eau, des ions, des métabolites, ainsi que l'accumulation des osmorégulateurs, ou par la régulation de l'équilibre entre synthèse et dégradation des composants cellulaires (Chen, 2009; Kay, 2017). Ces hypothèses ont ensuite été vérifiées. En mesurant d'abord la concentration intracellulaire de Na^+, K^+ dans les cellules chargées de Pb(II), les résultats ont montré une diminution significative de la concentration de Na^+ avec une légère augmentation de K^+. Ceci peut être attribué au flux d'ions du compartiment intracellulaire vers le milieu extracellulaire ou vice-versa. En plus, la bioaccumulation du Pb(II) a provoqué une augmentation significative de la concentration de proline au niveau intracellulaire. Ce dernier peut agir simultanément comme osmolytes, chaperons chimiques et piégeurs de ROS (Hayat et al., 2012; Liang et al., 2013). Pour évaluer l'équilibre entre la synthèse et la dégradation des constituants cellulaires, une caractérisation biochimique des cellules a révélé que les teneurs en lipides et en caroténoïdes ont augmenté significativement après accumulation de Pb(II). En revanche, leurs teneurs en chlorophylle, en glucides, et en protéines ont diminué significativement. Le résultat le plus remarquable de la caractérisation biochimique des cellules réside dans le fait que le Pb(II) stimule de manière importante la production de lipides. Ainsi, l'estimation des lipides neutres parmi les lipides accumulés peut donner une indication sur les mécanismes impliqués dans la résistance au stress métallique. Le marquage des lipides neutres dans les cellules a été effectué par le colorant rouge du Nil, puis analysé par le système FCM. Le résultat a montré que la fluorescence des lipides neutres mesurée dans les cellules après accumulation de Pb(II) était apparente par rapport aux témoins. Il est admis que les lipides neutres font partie des composants

essentiels des membranes cellulaires, en particulier les triglycérides (Benhima *et al.* 2018). En combinant ces résultats avec ceux de l'intégrité de la membrane, nous pouvons alors émettre l'hypothèse que les cellules de *S. obliquus* auraient orienté leur métabolisme vers la production des lipides neutres tels que les triglycérides afin de renforcer la bicouche phospholipidique de la membrane qui est souvent soumise aux réactions de la peroxydation lipidique engendrées par les ROS. Les résultats de cette étude sont également intéressants dans le contexte des bioraffineries car la souche sélectionnée peut accumuler des lipides neutres après la phycoremédiation du Pb(II). Ces lipides peuvent être utilisés pour la production de biocarburants de troisième génération ou pour d'autres types d'applications (Mehariya et al., 2021).

La réponse des cellules de microalgues aux MLs conduit souvent à la production des ROS dont principalement l'oxygène singulet ($^1O_2$), le radical anionique superoxyde (O_2•), le radical hydroxyle (OH•), le radical perhydroxy (HO_2•) et le peroxyde d'hydrogène (H_2O_2) (Pinto et al., 2003). Dans notre étude, l'évaluation de la production des ROS suite à l'accumulation des ions de Pb(II) par *S. obliquus* a été effectuée en mesurent le niveau de H_2O_2 au niveau intracellulaire. Le H_2O_2 a des propriétés relativement stables par rapport aux autre ROS. En outre, il peut facilement traverser les membranes cellulaires et cliver divers sites après sa conversion en HO (Rezayian et al., 2019). Le résultat obtenu montre qu'une augmentation significative des teneurs en H_2O_2 dans les cellules stressées par rapport aux cellules témoins. Une telle augmentation des niveaux de ROS peut perturber plusieurs fonctions vitales dans les cellules des microalgues, en particulier la peroxydation des lipides, l'oxydation des protéines et des sucres et la détérioration des acides nucléiques (Blokhina et al., 2003). Ainsi, la peroxydation des lipides a été estimée par la mesure des teneurs en MDA. Les résultats obtenus ont montré une augmentation de leurs teneurs suite à l'exposition aux ions de Pb(II).

Pour faire face aux effets nocifs des ions métalliques, des ROS, et les sous-produits de la peroxydation des lipides, plusieurs stratégies d'autodéfense peuvent été impliquées par les microalgues, et ceci grâce à l'action des antioxydants non enzymatique et/ou enzymatique (Cirulis et al., 2013). La comparaison de l'activité antioxydante totale entre les cellules témoins et celles ayant accumulé le Pb(II) a été réalisée en utilisant le test de piégeage des radicaux libres par le DPPH. Ce dernier a montré que l'activité antioxydante moyenne chez les cellules de *S. obliquus* ayant accumulé le Pb(II) été plus élevée que chez les cellules témoins. De même, les résultats de

l'évaluation des systèmes antioxydants non enzymatiques après la phycoremédiation du Pb(II) ont montré l'intervention des caroténoïdes, de la proline, de l'ascorbate et des polyphénols. En effet, leurs teneurs étaient significativement plus élevées dans les cellules exposées au Pb(II) par rapport aux témoins. Il est connu que la plupart des caroténoïdes ont des caractéristiques antioxydantes qui leurs permettent d'inhiber les réactions de la peroxydation des lipides, ainsi renforcer la stabilité de l'appareil photosynthétique et de protéger l'intégrité des membranes (Pérez-Gálvez et al., 2020). En outre, de nombreuses études ont mis l'accent sur la stimulation de la production d'ascorbate après une exposition au Pb(II) et leur rôle dans le renforcement de la tolérance cellulaire (Piotrowska-Niczyporuk et al., 2015; Ruciska-Sobkowiak and Pukacki, 2006; Singh et al., 2006; Strejckova et al., 2019). De même, il a été signalé que l'ascorbate participe à la défense contre le stress oxydatif induit par les MLs en tant que donneur d'électrons pour les radicaux hydroxyles, et aussi comme agent antioxydant en raison de son potentiel à donner des électrons à diverses réactions enzymatiques et non enzymatiques contre les ROS (Blokhina et al., 2003). Les composés phénoliques comptent parmi les antioxydants naturels les plus puissants en raison de leur capacité à transférer des électrons et des atomes d'hydrogène aux radicaux libres, et à réduire également la peroxydation des lipides (Blokhina et al., 2003; Rezayian et al., 2019; Rodrigo and Libuy, 2014).

Par ailleurs, le système enzymatique contre les ROS, notamment SOD, CAT, GPX, APX et GR, était significativement plus élevé dans les cellules exposées au Pb(II) que dans les cellules témoins. La SOD catalyse la réaction de dismutation de $\bullet O_2^-$, via l'addition de 2 ions H^+, donnant lieu à deux composés, l'un avec un état d'oxydation supérieur (O_2), et l'autre avec un état d'oxydation inférieur (H_2O_2) (Rajput et al., 2021). La CAT est située dans la plupart des sites de production de H_2O_2, elle catalyse la dismutation de deux molécules de H_2O_2 en eau et O2 (Mhamdi et al., 2010). En raison de leur large distribution dans le cytosol, les chloroplastes et les mitochondries, ainsi que de leur forte affinité pour H_2O_2, les peroxydases (APX) et (GPX) catalysent également l'oxydation de l'H_2O_2 par un substrat tels que l'ascorbate ou la gaïacol (Cirulis et al., 2013). La GR est une enzyme clé du cycle de l'ascorbate et du glutathion. Elle catalyse la réduction du GSSG en GSH en utilisant le NAD(P)H comme donneur d'électrons (Chisla and Massey, 1989). Sur la base de ces résultats, on peut suggérer que des voies enzymatiques et non enzymatiques sont impliquées dans l'atténuation du stress oxydatif causé par les ions Pb(II) chez *S. obliquus* (Rezayian et al., 2019).

Après avoir évalué les effets du Pb(II) sur les paramètres physiologiques (croissance, taille des cellules et intégrité de la membrane), la composition des cellules (lipides, sucres, protéines) et les réponses biochimiques (polyphénols, ascorbate...) et enzymatiques (SOD CAT, APX,....) au stress oxydatif provoqué par le Pb(II), nous avons cherché à approfondir notre recherche à l'échelle métabolomique pour une compréhension approfondie des phénomènes impliqués dans la gestion du stress métalliques chez les microalgues. À cette fin, une analyse par GC-MS des fractions lipidiques après leur transestérification a été réalisée. Les résultats ont indiqué une augmentation de l'abondance relative des esters méthyliques d'acides gras, des alcanes, des aromatiques et des stérols dans les cellules après accumulation de Pb (II) en comparaison avec des cellules témoins. En revanche, les alcènes et les acides gras monoinsaturés ont diminué. Ces résultats concordent avec les observations précédentes. En effet, les cellules de *S. obliquus* modifient leur métabolisme via un ajustement du ratio entre les acides gras insaturés et saturés, afin de réduire la perméabilité et/ou la fluidité membranaire, empêchant ainsi la bioaccumulation intracellulaire des ions de Pb(II).

Les résultats de ces premières sections confirment les deux premières hypothèses de cette thèse, qui ont été formulées autour de l'application potentielle des microalgues résistantes aux ML dans le traitement des polluants inorganiques et les mécanismes qui y sont associés.

Dans la deuxième section de cette étude, trois souches de levures (*Cyberlindnera fabianii*, *Wickerhamomyces anomalus*, et *Candida tropicalis*) précédemment isolées d'un site contaminé dans la région de Fès (Bahafid et al., 2013), ont été proposés comme candidats à la décoloration des colorants synthétiques. Le taux de décoloration le plus élevé a été atteint par la souche *C. fabianii*, qui a été donc sélectionnée pour la suite des études de ce travail. Les études sur la mycoremédiation des colorants azoïques par les levures sont principalement portées sur les espèces du genre *Candida* telle que *C. tropicalis* (Tan et al., 2019; Yang et al., 2008), *C. krusei* (Charumathi et Das, 2011; Yu et Wen, 2005), *C. boidinii* (Martorell et al., 2017), *C. oleophila* (Lucas et al., 2006), et des souche de *Saccharomyces cerevisiae* (Biradar et al., 2016; Jadhav et al., 2007; Kiayi et al., 2019; Vatandoostarani et al., 2017). Par contre, peu des études ont été menées avec des levures du genre *Cyberlindnera* (Martorell et al., 2012; Z. Song et al., 2018).

Les effluents industriels contiennent une grande variété de colorants possédant des structures chimiques très différentes. Par conséquent, la souche de levure envisagée pour la mycoremédiation des effluents colorés doit être capable d'éliminer une large gamme de colorants

synthétiques. De ce fait, la performance de la souche sélectionnée a été examinée contre sept autres colorants azoïques (MB_{17}, AR_{18}, AR_{14}, FR_{17}, AO_{52}, DR_{28} et AY_{23}). La souche *C. fabianii* a pu éliminer à des taux variables ces colorants synthétiques tant mono que diazoïques. Après la décoloration du milieu, la couleur de la biomasse peut donner une indication sur le mécanisme impliqué. En effet, les cellules de levure deviennent colorées en cas de biosorption ou de bioaccumulation du colorant, alors qu'elles conservent leur couleur d'origine lorsque le processus de la mycoremédiation est médié par une biodégradation enzymatique (Yu et Wen, 2005). D'après l'observation des biomasses issues de la décoloration, il a été déduit que les deux mécanismes d'élimination (biosorption et la biodégradation) sont impliqués, et ceci en fonction de la structure chimique du colorant examiné. A titre d'exemple, la différence structurelle entre le colorant AR14 et MB17, réside principalement dans la substitution du "4-sulfonato" de l'AR14 (disodium 4-hydroxy-2-[(E)-(4-sulfonato-1-naphtyl)diazényl]naphtalène-1-sulfonate) par le "2-hydroxy" du groupe naphtyle du MB17 (sodium 3-hydroxy-4-(2-hydroxy1-naphtylazo)-1-naphtalène sulfonate). Les biomasses issues de l'essai de décoloration de MB17 a pris la couleur de ce colorant, indiquant alors l'implication des mécanismes combinés de biosorption et de bioaccumulation. En revanche, le culot après décoloration complète du milieu contenant AR14 était incolore, indiquant alors que l'élimination de ce dernier est faite par une biodégradation enzymatique. Selon (Hsueh et al., 2009), la liaison azoïque des colorants est plus susceptible d'être rompue lorsque le substituant se trouve en position para du cycle phényle par rapport aux positions ortho et méta. la substitution des groupes de retrait d'électrons (-SO3H) par (-SO2NH2) en position para du cycle phényle par rapport à la liaison azoïque, augmente la vitesse de réduction (Walker and Ryan, 1971). De même, les colorants à base d'amino et d'hydroxyle sont plus résistants à la dégradation que les colorants comportant des groupes nitro, méthyle, sulfo et méthoxy.

En plus des prédictions basées sur la couleur de la biomasse, l'hypothèse de la biodégradation comme mécanisme de dégradation du colorant a été également confirmée par l'analyse UV-Vis du colorant AR14 avant et après traitement. Leur spectre est caractérisé par la présence d'une bande principale dans la région visible, avec une absorption maximale à 518 nm, et de deux bandes dans la région ultraviolette à 218 nm et 317 nm. La bande dans la région visible a été attribuée à la liaison (-N=N-) contenant le chromophore des molécules de colorant (Lin et al., 2008), et des pics dans la région ultraviolette ont été attribués à l'absorption de la transition π-π*

liée aux cycles naphtalènes de la molécule de colorant (Wang et al., 2005). La disparition de ces pics témoigne d'une biodégradation de la molécule de colorant. Par conséquent, dans la suite de cette étude, nous nous sommes concentrés sur la biodégradation enzymatique de l'AR14 comme colorant modèle pour une étude plus approfondie. Les oxydases sont les principales enzymes fongiques impliquées dans la dégradation de différentes matières organiques (Chakraborty et al., 2020). Nous avons alors mesuré l'activité enzymatique intracellulaires et extracellulaires de la laccase, de la tyrosinase, de la manganèse peroxydase, et l'activité d'une réductase (l'azoreductase) qui est impliquée également par certaines souches de levure dans le clivage de la bande azoïque des colorants azoïques (Jafari et al., 2014; Ramalho et al., 2004). Les résultats obtenus ont montré une augmentation significative de l'activité extracellulaire et intracellulaire de ces enzymes dans les cellules issues du traitement du colorant AR14. De nombreuses études ont documenté le rôle de la laccase dans la biodégradation des colorants synthétiques (Al-Tohamy et al., 2020; Guo et al., 2019). Cette enzyme permet la dégradation des colorants ou d'autres xénobiotiques organiques par des mécanismes radicalaires non spécifiques. Cela évite la génération de sous-produits toxiques, tels que les amines aromatiques, produites par le clivage spécifique de la liaison azoïque du colorant azoïque (Dave et al., 2015). L'implication de la tyrosinase dans la biodégradation des colorants synthétiques par les levures n'a été documentée que chez quelques souche de levures, telle que *Galactomyces geotrichum* MTCC (Waghmode et al., 2012), *S. cerevisiae* MTCC 463 (Jadhav et al., 2007), et *Candida krusei* (Charumathi and Das, 2011). De même que pour l'implication du manganèse peroxydase qui n'a été rapporté que chez *P. occidentalis* (Song et al., 2018), *Debaryomyces polymorphus*, *Candida tropicalis* (Yang et al., 2008), *T. multisporum*, et *T. laibachii* (Pajot et al., 2007). Le clivage de la liaison azoïque des colorants par l'Azoreductase est une étape critique dans les mécanismes de biotransformation des colorants (Elfarash et al., 2017). L'implication de l'Azoreductase pour la biodégradation des colorants par les souches de levures a été rapportée chez *S. cerevisiae* MTCC 463 (Jadhav et al., 2007), *C. krusei* (Charumathi and Das, 2011), *Issatchenkia occidentalis* (Ramalho et al., 2004), et *Trichosporon beigelii* NCIM-3326 (Saratale et al., 2009).

Indépendamment de la technique utilisée (physique, chimique ou biologique) dans le traitement des eaux usées de l'industrie de textiles, la principale préoccupation n'est pas seulement l'élimination des colorants, mais surtout la garantie d'une détoxification efficace après le traitement. L'évaluation écotoxicologique du post-traitement est donc cruciale. Les processus

d'oxydation des colorants synthétiques utilisant des réactions de Fenton, des catalyseurs d'oxydation non métalliques basés sur les radicaux hydroxyles et d'autres techniques chimiques, peuvent assurer une décoloration réussie (Javaid and Qazi, 2019). Cependant, ces techniques peuvent produire des sous-produits d'oxydation qui peuvent être plus toxiques que les molécules de colorant (dos Santos et al., 2007; Yu et al., 2009). Afin de mettre en évidence l'efficacité de la biodégradation des colorants AR14 par *C. fabianii* de point de vue eco-toxicologique, un test de phytotoxicité a été appliqué en utilisant les sous-produits résultants de la biodégradation de l'AR14. D'après les résultats obtenus concernant le pourcentage de germination, la longueur des plumules et des radicules de *Medicago sativa* utilisée comme plante modèle, on peut dire que la biodégradation enzymatique de l'AR14 par *C. fabianii* a permis non seulement une décoloration de ce colorant mais aussi une détoxification efficace de ce polluant. Ces résultats concordent avec des études antérieures dans lesquelles les métabolites des colorants azoïques présentaient une toxicité moindre que les colorants originaux après traitement par les levures (Guo et al., 2019; Sinha et al., 2018).

Comme nous l'avons déjà souligné, la biosorption est l'un des mécanismes impliqués dans l'élimination des colorants par la levure. Afin d'étudier en détail ce mécanisme et la manière dont les colorants interagissent avec la surface des cellules, une biomasse inactivée a été utilisée comme biosorbant. Des tests préliminaires ont révélé que la biomasse inactivée de *W. anomalus* et de *C. fabianii* présentent presque la même capacité d'adsorption. Ainsi, la biomasse inactivée de *W. anomalus* a été sélectionnée pour la suite de la présente recherche.

Tout d'abord, l'étude de la cinétique et la modélisation des isothermes de biosorption a montré que la biosorption de colorant AR14 par les cellules inactivées de *W. anomalus* suit un modèle de pseudo-second ordre. Les caractéristiques distinctives de ce modèle indiquent que le taux de biosorption est déterminé par la capacité d'adsorption plutôt que par la concentration de l'adsorbat, est en accord avec le fait que la chimiosorption est l'étape limitante du taux d'adsorption (Davranche et al., 2019). Cependant, ce même modèle n'a pas été adapté pour identifier le mécanisme de biosorption intra-particulaire. La cinétique a été ainsi analysée par le modèle de diffusion intra-particulaire. Le résultat obtenu démontre l'apparition de ce modèle de diffusion intra-particulaire, qui indique que la biomasse de levure atteint l'équilibre de biosorption lorsque la diffusion se produit dans la couche de macro-pores et que la résistance au transfert de masse n'est

pas impliquée dans la cinétique d'absorption du colorant (Ka Yee et al. 2003). Par la suite, les isothermes Langmuir et Freundlich ont été appliqués. Le modèle de Langmuir était plus approprié pour expliquer le système de biosorption de AR14-*W. anomalus.* Cet isotherme prédit que la biosorption est basée sur l'adsorption monocouche sur des sites homogènes sans aucune interaction entre les molécules du colorant biosorbées sur les sites voisins. Il suppose également que l'énergie est égale dans tous les sites de biosorption pour une surface spécifique. Lorsque ces derniers sont entièrement saturés, aucune autre biosorption ne peut avoir lieu (de Castro et al. 2017; Daneshvar et al. 2019). Ceci explique pourquoi au début du processus de biosorption, la décoloration se produit rapidement, puis évolue progressivement pour atteindre l'état d'équilibre. D'après ces résultats, il a été déduit que la biosorption du colorant AR14 par *W. anomalus* correspond à une chimiosorption sur une monocouche des sites homogènes à la surface cellulaire.

Ces prédictions ont été vérifiées en se basant sur une caractérisation physico-chimique de la biomasse de levure, avant et après la biosorption de colorant, par le biais de SEM-EDX, FTIR, le potentiel zêta, le pHzc, et l'angle de contact. Les résultats des observations SEM ont montré qu'il y avait des différences remarquables dans l'apparence des cellules chargées en AR14 par rapport aux cellules témoins. De même un changement notable a été constaté dans la transmittance des groupements fonctionnels analysés par FTIR après la biosorption d'AR14, ce qui peut être attribué à l'occupation de ces derniers par le colorant. Il a également été noté un déplacement des bandes correspondant aux groupements hydroxyle, acide carboxylique, amine et amino, indiquant leur implication dans la biosorption du colorant sur la surface cellulaire. Le mécanisme de liaison des molécules de colorant au composant de la surface cellulaire de la levure s'explique par les forces d'attraction du peptidomannane, du peptidoglycane, des lipides et des hétéropolysaccharides..., qui contient plusieurs groupes fonctionnels tels que des groupes carboxyle, hydroxyle, amino, phosphate et d'autres groupes chargés (Gadd, 2009; Vitor and Corso, 2008). En outre, l'analyse FTIR ont permis de prédire que les interactions Yoshida H-binding, dipole-dipole H-binding, π-π et n-π jouent un rôle indispensable dans la biosorption de l'AR14 sur la surface des cellules de levure (Tran et al. 2017). L'analyse du zêta potentiel a montré que les cellules de *W. anomalus* ont une charge négative et la valeur du pHzc se trouve dans la plage acide, ce qui confirme la présence de groupements anioniques à la surface de la cellule (Dundar et al. 2008). En outre, la mesure de l'angle de contact a montré que le caractère hydrophile de *W. anomalus* a diminué de manière

significative après la biosorption du colorant. Ceci peut être attribué à une augmentation de la densité des groupements fonctionnels polaires sur les surfaces de la biomasse après le processus de biosorption. De plus, une variation significative du caractère donneur et accepteur d'électrons a été notée après la biosorption du colorant. Ce phénomène peut être expliqué par les interactions électrostatiques des groupement fonctionnels avec le colorant en solution (Legorreta-Castañeda et al. 2020). En s'appuyant sur ces résultats, on peut dire que la biosorption du colorant AR14 sur la surface de *W. anomalus* implique à la fois plusieurs interactions de type chimique et électrostatique, qui se produisentt entre les structures macromoléculaires qui composent la surface cellulaire et les molécules de colorant en solution. Dans un concept de bioraffinerie, la biomasse de levure résultant du processus de biodégradation pourrait également être utilisée comme un biosorbant efficace, peu coûteux et respectueux de l'environnement.

Dans la dernière partie de ce travail, l'approche statistique du plan d'expériences a été utilisée pour l'optimisation du processus de la biodégradation de colorant AR14 par *C. fabianii* et leur biosorption par *W. anomalus.* Le criblage des facteurs les plus influençant a été mené au moyen du plan de Plackett-Burman, car il permet de réduire considérablement le nombre d'expériences répétées en vue d'une analyse d'optimisation ultérieure (Karlapudi et al., 2018). Les éventuelles interactions synergiques ou antagonistes entre les facteurs significatifs ont été analysées et optimisées à l'aide du plan de Box-Behnken (Kousha et al., 2012). Les résultats de cette analyse ont montré que dans des conditions optimales de biodégradation (pH = 5,154, AR14 = 50 mg L^{-1}), la souche *C. fabianii* a pu décolorer plus de 97% en moins de 12 heures. Alors que, la biosorption optimale de l'AR14 par la biomasse de *W. anomalus* a été atteinte à pH 3-4, avec une concentration initiale de colorant allant de 50 à 75 mg L^{-1} et une biomasse de 1.25 g L^{-1}.

De ces résultats, nous pouvons retenir les hypothèses proposées concernant la capacité de la levure à décomposer les colorants synthétiques, de même que la valorisation de la biomasse de levure comme biosorbant économique.

CONCLUSION ET PERSPECTIVES

La pollution des eaux par les contaminants organiques et métalliques est une préoccupation environnementale de premier ordre. Dans l'objectif de développer de nouvelles approches à la fois efficaces, économiques et écologiques pour résoudre ce problème, ce travail s'est focalisé sur l'exploration des potentialités biotechnologiques des microalgues et des levures dans la bioremédiation des contaminants organiques (colorants synthétiques) et métalliques (Pb(II)) communément présents dans les rejets industriels.

La microalgue *S. obliquus* a pu supporter le Pb(II) avec une EC50 de 141 ppm, l'emploi de cette souche pour la phycoremédiation du Pb(II) a permis un abattement de 58,42% de la concentration initiale à la valeur EC50. Cette forte capacité d'élimination est due à la combinaison de mécanisme de la bioaccumulation dans les compartiments intracellulaires et de la biosorption extracellulaire gérée par des interactions chimiques et électrostatiques entre les ions Pb(II) en solution et les groupements fonctionnels composant la parois cellulaire.

Au cours du processus de phycoremédiation, le Pb(II) accumulé a provoqué une diminution de la croissance de *S. obliquus*. Cependant, cette souche a pu maintenir sa taille cellulaire et son intégrité membranaire via l'activation des processus de l'osmorégulation et la re-modulation des lipides membranaires. La régulation de la pression osmotique est contrôlée par les flux ioniques (Na^+, K^+ et H^+), l'accumulation d'osmorégulateurs (Proline), et la régulation de l'équilibre entre la synthèse et la dégradation des composants cellulaires (Pigments, lipides, protéines et glucides). En outre, la production de H_2O_2 induite par l'accumulation d'ions Pb(II) a amplifié la peroxydation lipidique, comme en témoignent les taux élevés de MDA dans les cellules après le processus de phycoremédiation. La synthèse et l'accumulation de lipides neutres tels que les triglycérides participent à la formation de la bicouche phospholipidique, permettant la reconstruction des dommages qu'elle pourrait subir.

Par ailleurs, le contrôle de l'équilibre redox est assuré grâce à l'engagement des systèmes antioxydants enzymatiques (SOD, CAT, GPX, APX et GR), et non-enzymatiques (les caroténoïdes, l'ascorbate, les polyphénols). À l'échelle métabolomique, l'évaluation du profilage lipidique des cellules stressées a montré que ces dernier modifient leur métabolisme via un

ajustement du rapport entre les acides gras insaturés et saturés, afin de réduire la perméabilité et/ou la fluidité membranaire, empêchant ainsi la bioaccumulation des ions Pb(II).

La mycoremédiation des colorants synthétiques par la souche de levure *C. fabianii* a été envisagé pour comprendre les mécanismes de biodégradation enzymatique et/ou une biosorption extracellulaire, et ceci selon les propriétés physicochimiques du colorant considéré. D'un côté, la biodégradation du colorant AR14, se produit principalement via l'action des oxydases (Laccase, Tyrosinase et Manganèse peroxydase) et d'azoréductase. La mycoremédiation de ce colorant par la souche *C. fabianii* a permis non seulement un taux de décoloration élevé, mais aussi une détoxification efficace. Effectivement, le test de phytotoxicité des sous-produits issus de leur biodégradation n'a montré aucun signe de toxicité envers *Medicago sativa* utilisée comme plante modèle.

De l'autre côté, l'étude théorique et expérimentale de la biosorption du colorant AR14 par la biomasse inactive de *W. anomalus* était corrélée aux constats d'une chimisorption sur une monocouche de sites homogènes ayant une énergie égale. La caractérisation des interactions entre le colorant et la surface cellulaire par les techniques SEM-EDX, FTIR, potentiel zêta, pHzc, et angle de contact ont confirmé les prédictions théoriques évoquées. En effet, la biosorption du colorant AR14 implique à la fois des interactions de type chimique et électrostatiques entre les structures macromoléculaires de la surface cellulaire et les molécules de colorant en solution. L'optimisation du processus de la biodégradation du colorant AR14 par *C. fabianii* et sa biosorption par *W. anomalus* a été déterminé au moyen de l'approche statistique du plan d'expériences. Les conditions optimales de biodégradation de AR14 par *C. fabianii* se produisent à un pH initial de milieu de 5,154 avec une concentration initiale de colorant de 50 mg L^{-1}. Alors que leur biosorption optimale par la biomasse inactivée de *W. anomalus* a été atteinte à pH 3-4, avec une concentration initiale de colorant allant de 50 à 75 mg L^{-1} et une biomasse de 1.25 g L^{-1}.

Les recherches menées dans le cadre de cette thèse ouvrent de larges perspectives. Les principaux axes à poursuivre dans les travaux futurs concernent :

- ✓ Poursuite des recherches dans l'évaluation de la capacité des microalgues dans la biotransformation des métaux de transition comme la transformation du Cr(VI) en Cr(III),

tout en précisant les mécanismes engagés. S'agirait-il d'une photoréduction ou d'une réduction enzymatique, comme c'est le cas chez les bactéries ?

- ✓ Mettre en évidence le rôle des substances polymères extracellulaires dans les interactions avec les MLs (complexation extracellulaire) et rechercher des voies de détoxification intracellulaire en répondant aux questions sur le rôle des transporteurs membranaires dans l'accumulation des MLs, le rôle des métallothionéines et des polyphosphates dans la complexation intracellulaire, ainsi que localiser la compartimentation des MLs dans les organites cellulaires.

- ✓ Mettre en évidence le rôle des phytohormones dans la régulation du stress métallique chez les microalgues et la mise en œuvre d'approches omiques pour une compréhension approfondie des phénomènes de stress oxydatif induit par les MLs.

- ✓ Poursuivre les travaux de caractérisation chimique des sous-produits de la biodégradation du colorant AR14 par *C. fabianii* via les techniques LC-MS, RMN.... et proposition les voies de leur biodégradation.

- ✓ Etudier la toxicité des sous-produits de dégradation de AR14 par *C. fabianii* via les différentes méthodes : microtoxicité, cytotoxicité, génotoxicité ….

- ✓ Exploiter les domaines du génie génétique, de la bio-ingénierie, les techniques de prétraitement et d'immobilisation en vue d'améliorer la capacité et la sélectivité de ces bioprocédés.

- ✓ Évaluer l'efficacité des souches sélectionnées à l'échelle pilote et dans des conditions naturelles, tout en évaluant la faisabilité technique et économique de ces bioprocédés dans une optique d'application à grande échelle.

- ✓ Valorisation de la biomasse algale issue de la phycoremédiation des MLs en produits à haute valeur ajoutée en particulier les biocarburants.

REFERENCES

Ahmad, S., Pandey, A., Pathak, V. V., Tyagi, V. V., Kothari, R., 2020. Phycoremediation : Algae as Eco-friendly Tools for the Removal of Heavy Metals from Wastewaters, in: Bioremediation of Industrial Waste for Environmental Safety. Springer Singapore, pp. 53–76. https://doi.org/10.1007/978-981-13-3426-9_3

Al-Tohamy, R., Kenawy, E.R., Sun, J., Ali, S.S., 2020. Performance of a Newly Isolated Salt-Tolerant Yeast Strain *Sterigmatomyces halophilus* SSA-1575 for Azo Dye Decolorization and Detoxification. Front. Microbiol. 11, 1–19. https://doi.org/10.3389/fmicb.2020.01163

Aksu, Z., 2005. Application of biosorption for the removal of organic pollutants: A review. Process Biochem. 40, 997–1026. https://doi.org/10.1016/j.procbio.2004.04.008

Bahafid, W., Joutey, N.T., Sayel, H., Iraqui-Houssaini, M., El Ghachtouli, N., 2013. Chromium Adsorption by Three Yeast Strains Isolated from Sediments in Morocco. Geomicrobiol. J. 30, 422–429. https://doi.org/10.1080/01490451.2012.705228

Baudelet, P.H., Ricochon, G., Linder, M., Muniglia, L., 2017. A new insight into cell walls of Chlorophyta. Algal Res. 25, 333–371. https://doi.org/10.1016/j.algal.2017.04.008

Benhima, R, El Arroussi, H, Kadmiri IM, El Mernissi N, Wahby I, et al. 2018. Nitrate reductase inhibition induces lipid enhancement of *Dunaliella tertiolecta* for biodiesel production. Sci. World J. https://doi.org/10.1155/2018/6834725

Biradar, S.P., Rane, N.R., Patil, T.S., Khandare, R. V., Govindwar, S.P., Pawar, P.K., 2016. Herbal augmentation enhances malachite green biodegradation efficacy of *Saccharomyces cerevisiae*. Biol. 71, 475–483. https://doi.org/10.1515/biolog-2016-0069

Blokhina, O., Virolainen, E., Fagerstedt, K. V., 2003. Antioxidants, oxidative damage and oxygen deprivation stress: A review. Ann. Bot. 91, 179–194. https://doi.org/10.1093/aob/mcf118

Bosco, F., Chiara, M., 2016. Mycoremediation in Soil, in: Intech. p. 13. https://doi.org/http://dx.doi.org/10.5772/57353

Chakraborty, T., Nosanchuk, J.D., Attila, G., 2020. Multicopper Oxidases in *Saccharomyces cerevisiae* and Human Pathogenic Fungi. J. fungi 1, 1–11. https://doi.org/10.3390/jof6020056.

Charumathi, D., Das, N., 2011. Biodegradation of Basic Violet 3 by *Candida krusei* isolated from textile wastewater. Biodegradation 22, 1169–1180. https://doi.org/10.1007/s10532-011-9472-2

Chen, H.U.I., 2009. Osmotic Responses of *Dunaliella* to the Changes of Salinity. J. Cell. Physiol. 251–258. https://doi.org/10.1002/jcp.21715

Chisla, S., Massey, V., 1989. Mechanisms of flavoprotein-catalyzed reactions. Eur. J. Biochem. 181, 1–17. https://doi.org/https://doi.org/10.1111/j.1432-1033.1989.tb14688.x

Cirulis, J.T., Scott, J.A., Ross, G.M., 2013. Management of oxidative stress by microalgae. Can. J. Physiol. Pharmacol. 91, 15–21. https://doi.org/10.1139/cjpp-2012-0249

Connell, D. W., Connell, D. W., Vowles, P. D., Warne, M. S. J., & Hawker, D. W. (2005). Basic concepts of environmental chemistry (pp. 480-480). CRC/Taylor & Francis.

Daneshvar, E., Vazirzadeh, A., Bhatnagar, A., 2019. Biosorption of Methylene Blue Dye onto Three Different Marine Macroalgae: Effects of Different Parameters on Isotherm, Kinetic and Thermodynamic. Iran. J. Sci. Technol. Trans. A Sci. 43, 2743–2754. https://doi.org/10.1007/s40995-019-00764-8

Dave, S.R., Patel, T.L., Tipre, D.R., 2015. Bacterial Degradation of Azo Dye Containing Wastes, in: Microbial Degradation of Synthetic Dyes in Wastewaters,Environmental Science and Engineering. Cham., pp. 57–83. https://doi.org/DOI 10.1007/978-3-319-10942-8_3

Davranche, M., Veclin, C., Pierson-Wickmann, A.C., El Hadri, H., Grassl, B., Rowenczyk, L., Dia, A., Ter Halle, A., Blancho, F., Reynaud, S., Gigault, J., 2019. Are nanoplastics able to bind

significant amount of metals? The lead example. Environ. Pollut. 249, 940–948. https://doi.org/10.1016/j.envpol.2019.03.087
de Castro, K.C., Cossolin, A.S., Oliveira dos Reis, H.C., de Morais, E.B., 2017. Biosorption of anionic textile dyes from aqueous solution by yeast slurry from brewery. Brazilian Arch. Biol. Technol. 60, 1–13. https://doi.org/10.1590/1678-4324-2017160101
dos Santos, A.B., Cervantes, F.J., van Lier, J.B., 2007. Review paper on current technologies for decolourisation of textile wastewaters: Perspectives for anaerobic biotechnology. Bioresour. Technol. 98, 2369–2385. https://doi.org/10.1016/j.biortech.2006.11.013
Dundar, M., Nuhoglu, C., Nuhoglu, Y., 2008. Biosorption of Cu (II) ions onto the litter of natural trembling poplar forest 151, 86–95. https://doi.org/10.1016/j.jhazmat.2007.05.055
Elfarash, A., Mawad, A.M.M., Yousef, N.M.M., Shoreit, A.A.M., 2017. Azoreductase kinetics and gene expression in the synthetic dyes-degrading Pseudomonas . Egypt. J. Basic Appl. Sci. 4, 315–322. https://doi.org/10.1016/j.ejbas.2017.07.007
Gadd, G.M., 2009. Biosorption: Critical review of scientific rationale, environmental importance and significance for pollution treatment. J. Chem. Technol. Biotechnol. 84, 13–28. https://doi.org/10.1002/jctb.1999
Guo, G., Tian, F., Zhao, Y., Tang, M., Liu, W., Liu, C., Xue, S., Kong, W., Sun, Y., Wang, S., 2019. Aerobic decolorization and detoxification of Acid Scarlet GR by a newly isolated salt-tolerant yeast strain *Galactomyces geotrichum* GG. Int. Biodeterior. Biodegrad. 145, 104818. https://doi.org/10.1016/j.ibiod.2019.104818
Hayat, S., Hayat, Q., Alyemeni, M.N., Wani, A.S., Pichtel, J., Ahmad, A., 2012. Role of proline under changing environments: A review. Plant Signal. Behav. 7, 1456–1466. https://doi.org/10.4161/psb.21949
Hsueh, C.C., Chen, B.Y., Yen, C.Y., 2009. Understanding effects of chemical structure on azo dye decolorization characteristics by *Aeromonas hydrophila*. J. Hazard. Mater. 167, 995–1001. https://doi.org/10.1016/j.jhazmat.2009.01.077
Jadhav, J.P., Parshetti, G.K., Kalme, S.D., Govindwar, S.P., 2007. Decolourization of azo dye methyl red by *Saccharomyces cerevisiae* MTCC 463. Chemosphere 68, 394–400. https://doi.org/10.1016/j.chemosphere.2006.12.087
Jafari, N., Soudi, M.R., Kasra-Kermanshahi, R., 2014. Biodegradation perspectives of azo dyes by yeasts. Microbiology 83, 484–497. https://doi.org/10.1134/s0026261714050130
Javaid, R., Qazi, U.Y., 2019. Catalytic oxidation process for the degradation of synthetic dyes: An overview. Int. J. Environ. Res. Public Health 16, 1–27. https://doi.org/10.3390/ijerph16112066
Legorreta-Castañeda, A. J., Lucho-Constantino, C. A., Beltrán-Hernández, R. I., Coronel-Olivares, C., & Vázquez-Rodríguez, G. A. 2020. Biosorption of water pollutants by fungal pellets. Water, *12*(4), 1155. https://doi.org/10.3390/w12041155
Jena, J., Pradhan, N., Aishvarya, V., Nayak, R.R., Dash, B.P., Sukla, L.B., Panda, P.K., Mishra, B.K., 2015. Biological sequestration and retention of cadmium as CdS nanoparticles by the microalga Scenedesmus-24. J. Appl. Phycol. 27, 2251–2260. https://doi.org/10.1007/s10811-014-0499-8
Ka Yee, H., McKay, G., King Lun, Y., 2003. Selective adsorbents from chemically modified ordered mesoporous silica. Langmuir 19, 3019–3024. https://doi.org/10.1016/s0167-2991(04)80581-0
Karlapudi, A.P., Krupanidhi, S., E., R.R., M., I., Md., N.B., T.C., V., 2018. Plackett-Burman design for screening of process components and their effects on production of lactase by newly isolated Bacillus sp. VUVD101 strain from Dairy effluent. Beni-Suef Univ. J. Basic Appl. Sci. 7, 543–546. https://doi.org/10.1016/j.bjbas.2018.06.006
Kay, A.R., 2017. How cells can control their size by pumping ions. Front. Cell Dev. Biol. 5, 1–14. https://doi.org/10.3389/fcell.2017.00041

Kiayi, Z., Lotfabad, T.B., Heidarinasab, A., Shahcheraghi, F., 2019. Microbial degradation of azo dye carmoisine in aqueous medium using *Saccharomyces cerevisiae* ATCC 9763. J. Hazard. Mater. 373, 608–619. https://doi.org/10.1016/j.jhazmat.2019.03.111

Kousha, M., Daneshvar, E., Dopeikar, H., Taghavi, D., Bhatnagar, A., 2012. Box-Behnken design optimization of Acid Black 1 dye biosorption by different brown macroalgae. Chem. Eng. J. 179, 158–168. https://doi.org/10.1016/j.cej.2011.10.073

Kutty, S.N., Philip, R., 2008. Marine yeasts a review. Yeast 465–483. https://doi.org/10.1002/yea

Leong, Y.K., Chang, J.S., 2020. Bioremediation of heavy metals using microalgae: Recent advances and mechanisms. Bioresour. Technol. 303, 122886. https://doi.org/10.1016/j.biortech.2020.122886

Liang, X., Zhang, L., Natarajan, S.K., Becker, D.F., 2013. Proline Mechanisms of Stress Survival. Antioxid. Redox Signal. 19, 998–1011. https://doi.org/10.1089/ars.2012.5074

Lin, J. jie, Zhao, X. song, Liu, D., Yu, Z. guo, Zhang, Y., Xu, H., 2008. The decoloration and mineralization of azo dye C.I. Acid Red 14 by sonochemical process: Rate improvement via Fenton's reactions. J. Hazard. Mater. 157, 541–546. https://doi.org/10.1016/j.jhazmat.2008.01.050

Lucas, M.S., Amaral, C., Sampaio, A., Peres, J.A., Dias, A.A., 2006. Biodegradation of the diazo dye Reactive Black 5 by a wild isolate of *Candida oleophila*. Enzyme Microb. Technol. 39, 51–55. https://doi.org/10.1016/j.enzmictec.2005.09.004

Machado, M.D., Soares, E. V., 2015. Use of a fluorescence-based approach to assess short-term responses of the alga *Pseudokirchneriella subcapitata* to metal stress. J. Appl. Phycol. 27, 805–813. https://doi.org/10.1007/s10811-014-0351-1

Martorell, M.M., Pajot, H.F., Ahmed, P.M., de Figueroa, L.I.C., 2017. Biodecoloration of Reactive Black 5 by the methylotrophic yeast *Candida boidinii* MM 4035. J. Environ. Sci. (China) 53, 78–87. https://doi.org/10.1016/j.jes.2016.01.033

Martorell, M.M., Pajot, H.F., de Figueroa, L.I.C., 2012. Dye-decolourizing yeasts isolated from Las Yungas rainforest. Dye assimilation and removal used as selection criteria. Int. Biodeterior. Biodegrad. 66, 25–32. https://doi.org/10.1016/j.ibiod.2011.10.005

Mehariya, S., Goswami, R.K., Verma, P., Lavecchia, R., Zuorro, A., 2021. Integrated Approach Mehariya, S., Goswami, R. K., Verma, P., Lavecchia, R., & Zuorro, A. (2021). Integrated Approach for Wastewater Treatment and Biofuel Production in Microalgae Biorefineries. Energies, 14(8), 2282. https://doi.org/10.3390/en14082282

Mhamdi, A., Queval, G., Chaouch, S., Vanderauwera, S., Breusegem, F. Van, Noctor, G., 2010. Catalase function in plants : a focus on Arabidopsis mutants as stress-mimic models 61, 4197–4220. https://doi.org/10.1093/jxb/erq282

Miranda, R. de C.M. d., Gomes, E. de B., Pereira, N., Marin-Morales, M.A., Machado, K.M.G., Gusmão, N.B. de, 2013. Biotreatment of textile effluent in static bioreactor by *Curvularia lunata* URM 6179 and *Phanerochaete chrysosporium* URM 6181. Bioresour. Technol. 142, 361–367. https://doi.org/10.1016/j.biortech.2013.05.066

Oliveira, A.C., Barata, A., Batista, A.P., Gouveia, L., 2019. *Scenedesmus obliquus* in poultry wastewater bioremediation. Environ. Technol. (United Kingdom) 40, 3735–3744. https://doi.org/10.1080/09593330.2018.1488003

Pajot, H.F., de Figueroa, L.I.C., Fariña, J.I., 2007. Dye-decolorizing activity in isolated yeasts from the ecoregion of Las Yungas (Tucumán, Argentina). Enzyme Microb. Technol. 40, 1503–1511. https://doi.org/10.1016/j.enzmictec.2006.10.038

Pérez-Gálvez, A., Viera, I., Roca, M., 2020. Carotenoids and Chlorophylls as Antioxidants. antioxidants 9, 1–34. https://doi.org/doi:10.3390/antiox9060505

Pérez-Rama, M., Abalde Alonso, J., Herrero López, C., Torres Vaamonde, E., 2002. Cadmium removal by living cells of the marine microalga *Tetraselmis suecica*. Bioresour. Technol. 84, 265–270. https://doi.org/10.1016/S0960-8524(02)00045-7

Pinto, E., Sigaud-kutner, T.C., Leitao, M.A., Okamoto, O.K., Morse, D., Colepicolo, P., 2003. Heavy metal-induced oxidative stress in algae. J. Phycol. 39, 1008–1018. https://doi.org/10.1111/j.0022-3646.2003.02-193.x

Piotrowska-Niczyporuk, A., Bajguz, A., Talarek, M., Bralska, M., Zambrzycka, E., 2015. The effect of lead on the growth, content of primary metabolites, and antioxidant response of green alga *Acutodesmus obliquus* (Chlorophyceae). Environ. Sci. Pollut. Res. 22, 19112–19123. https://doi.org/10.1007/s11356-015-5118-y

Rajput, V.D., Singh, R.K., Verma, K.K., Sharma, L., Sushkova, S., Mandzhieva, S., 2021. Recent Developments in Enzymatic Antioxidant Defence Mechanism in Plants with Special Reference to Abiotic Stress. Biology (Basel). 10, 1--28. https://doi.org/10.3390/biology10040267

Ramalho, P. a, Cardoso, M.H., Ramalho, M.T., 2004. Characterization of Azo Reduction Activity in a Novel Ascomycete Yeast Strain Characterization of Azo Reduction Activity in a Novel Ascomycete Yeast Strain. Appl. Environ. Microbiol. 70, 2279–2288. https://doi.org/10.1128/AEM.70.4.2279

Rezayian, M., Niknam, V., Ebrahimzadeh, H., 2019. Oxidative damage and antioxidative system in algae. Toxicol. Reports 6, 1309–1313. https://doi.org/10.1016/j.toxrep.2019.10.001

Rodrigo, R., Libuy, M., 2014. Modulation of Plant Endogenous Antioxidant Systems by Polyphenols, Polyphenols in Plants: Isolation, Purification and Extract Preparation. Elsevier. https://doi.org/10.1016/B978-0-12-397934-6.00005-X

Ruciska-Sobkowiak, R., & Pukacki, P. M. (2006). Antioxidative defense system in lupin roots exposed to increasing concentrations of lead. Acta Physiologiae Plantarum, 28(4), 357-364. https://doi.org/10.1007/s11738-006-0032-z

Saratale, R.G., Saratale, G.D., Chang, J.S., Govindwar, S.P., 2009. Decolorization and biodegradation of textile dye Navy blue HER by Trichosporon beigelii NCIM-3326. J. Hazard. Mater. 166, 1421–1428. https://doi.org/10.1016/j.jhazmat.2008.12.068

Saratale, R.G., Saratale, G.D., Chang, J.S., Govindwar, S.P., 2011. Bacterial decolorization and degradation of azo dyes: A review. J. Taiwan Inst. Chem. Eng. 42, 138–157. https://doi.org/10.1016/j.jtice.2010.06.006

Singh, S., Eapen, S., D'Souza, S.F., 2006. Cadmium accumulation and its influence on lipid peroxidation and antioxidative system in an aquatic plant, *Bacopa monnieri* L. Chemosphere 62, 233–246. https://doi.org/10.1016/j.chemosphere.2005.05.017

Sinha, A., Lulu, S., Vino, S., Banerjee, S., Acharjee, S., Jabez Osborne, W., 2018. Degradation of reactive green dye and textile effluent by Candida sp. VITJASS isolated from wetland paddy rhizosphere soil. J. Environ. Chem. Eng. 6, 5150–5159. https://doi.org/10.1016/j.jece.2018.08.004

Srinivasan, A., Viraraghavan, T., 2010. Decolorization of dye wastewaters by biosorbents: A review. J. Environ. Manage. 91, 1915–1929. https://doi.org/10.1016/j.jenvman.2010.05.003

Song, L., Shao, Y., Ning, S., Tan, L., 2018. Performance of a newly isolated salt-tolerant yeast strain *Pichia occidentalis* G1 for degrading and detoxifying azo dyes. Bioresour. Technol. 233, 21–29. https://doi.org/10.1016/j.biortech.2017.02.065

Song, Z., Song, L., Shao, Y., Tan, L., 2018. Degradation and detoxification of azo dyes by a salt-tolerant yeast *Cyberlindnera samutprakarnensis* S4 under high-salt conditions. World J. Microbiol. Biotechnol. 34, 0. https://doi.org/10.1007/s11274-018-2515-7

Strejckova, A., Dvorak, M., Klejdus, B., Krystofova, O., Hedbavny, J., Adam, V., Huska, D., 2019. The strong reaction of simple phenolic acids during oxidative stress caused by nickel, cadmium and copper in the microalga *Scenedesmus quadricauda*. N. Biotechnol. 48, 66–75. https://doi.org/10.1016/j.nbt.2018.07.004

Tan, L., Xu, B., Hao, J., Wang, J., Shao, Y., Mu, G., 2019. Biodegradation and detoxification of azo dyes by a newly isolated halotolerant yeast *Candida tropicalis* SYF-1. Environ. Eng. Sci. 36, 999–1010. https://doi.org/10.1089/ees.2018.0485

Tran, N.H., You, S., Hosseini-bandegharaei, A., 2017. Mistakes and inconsistencies regarding adsorption of contaminants from aqueous solutions : A critical review. Water Res. 120, 88–116. https://doi.org/10.1016/j.watres.2017.04.014

Vatandoostarani, S., Bagheri Lotfabad, T., Heidarinasab, A., Yaghmaei, S., 2017. Degradation of azo dye methyl red by *Saccharomyces cerevisiae* ATCC 9763. Int. Biodeterior. Biodegrad. 125, 62–72. https://doi.org/10.1016/j.ibiod.2017.08.009

Vitor, V., Corso, C.R., 2008. Decolorization of textile dye by *Candida albicans* isolated from industrial effluents. J. Ind. Microbiol. Biotechnol. 35, 1353–1357. https://doi.org/10.1007/s10295-008-0435-5

Vogler, E.A., 1998. Structure and reactivity of water at biomaterial surfaces. Adv. Colloid Interface Sci. 74, 69–117. https://doi.org/10.1016/S0001-8686(97)00040-7

Waghmode, T.R., Kurade, M.B., Kabra, A.N., Govindwar, S.P., 2012. Degradation of remazol red dye by *Galactomyces geotrichum* MTCC 1360 leading to increased iron uptake in Sorghum vulgare and Phaseolus mungo from soil. Biotechnol. Bioprocess Eng. 17, 117–126. https://doi.org/10.1007/s12257-011-0307-0

Walker, R., Ryan, A.J., 1971. Some Molecular Parameters Influencing Rate of Reduction of Azo Compounds by Intestinal. XENOBIOTICA 1, 483–486. https://doi.org/10.3109/00498257109041513

Wang, A., Qu, J., Ru, J., Liu, H., Ge, J., 2005. Mineralization of an azo dye Acid Red 14 by electro-Fenton's reagent using an activated carbon fiber cathode. Dye. Pigment. 65, 227–233. https://doi.org/10.1016/j.dyepig.2004.07.019

Yang, Q., TAO, L., Yang, M., Zhang, H., 2008. Effects of glucose on the decolorization of Reactive Black 5 by yeast isolates. J. Environ. Sci. 20, 105–108. https://doi.org/10.1016/S1001-0742(08)60016-9

Yu, J. xia, Li, B. hai, Sun, X. mei, Jun, Y., Chi, R. an, 2009. Adsorption of methylene blue and rhodamine B on baker's yeast and photocatalytic regeneration of the biosorbent. Biochem. Eng. J. 45, 145–151. https://doi.org/10.1016/j.bej.2009.03.007

Yu, Z., Wen, X., 2005. Screening and identification of yeasts for decolorizing synthetic dyes in industrial wastewater. Int. Biodeterior. Biodegrad. 56, 109–114. https://doi.org/10.1016/j.ibiod.2005.05.006

Zhang, X., Zhao, X., Wan, C., Chen, B., Bai, F., 2016. Efficient biosorption of cadmium by the self-flocculating microalga *Scenedesmus obliquus* AS-6-1. Algal Res. 16, 427–433. https://doi.org/10.1016/j.algal.2016.04.002

Centre d'Etudes Doctorales : Sciences et Techniques de l'Ingénieur

Résumé de la thèse

Le sujet de recherche abordé dans cette thèse vise à mettre en évidence l'application potentielle de nouvelles stratégies de la phycoremédiation des métaux lourds (MLs) et de la mycoremédiation des contaminants organiques (colorants synthétiques), à travers l'étude de la performance de dépollution des souches des microalgues et des levures, ainsi que de la mise en évidence des mécanismes impliqués dans l'élimination de ces polluants par ces micro-organismes.

Huit souches de microalgues ont été criblées en vue de leur utilisation dans la phycoremédiation des MLs (Pb(II), Cd(II), Cu(II) et Cr(VI)). La souche *Scenedesmus obliquus* a fait preuve d'une forte tolérance aux ions de Pb(II), avec une EC50 de 141 ppm. Elle a été ainsi retenue pour l'étude des mécanismes impliqués. Lors de la phycoremédiation, les ions de Pb(II) à la concentration EC50 ont impacté la croissance de *S. obliquus*. Toutefois, la viabilité et la taille des cellules analysées respectivement par le cyrtométrie en flux et le Zetasizer n'ont montré aucune différence significative. Après traitement, la concentration de Pb(II) en solution, analysée par ICP-AES, a diminué de 58,42 % et l'analyse par thermogravimétrie des poids résiduels des cellules a montré une récupération des ions Pb(II) par *S. obliquus*. La discrimination entre les mécanismes de récupération extra et intracellulaires, via l'analyse des digests des cellules chargées en Pb(II) a révélé l'implication de la biosorption et de la bioaccumulation avec respectivement une contribution de 85,5% et 14,5%. La caractérisation physicochimique des interactions contrôlant la biosorption par le biais du MEB-EDX, de la FTIR, du potentiel zêta, du pH zéro charge, et de l'angle de contact ont confirmé l'implication des interactions de type chimiques et électrostatiques. Par ailleurs, la bioaccumulation du Pb(II) a induit des modifications biochimiques notamment l'augmentation des contenus en peroxyde d'hydrogène, malondialdéhyde, caroténoïdes et lipides. Cependant, les teneurs en chlorophylle, carbohydrates et protéines ont diminué sensiblement. Le profilage métabolomique des cellules stressées analysée par GS-MS a révélé une augmentation des esters méthyliques d'acides gras, des alcanes, des aromatiques et des stérols. En revanche, les alcènes et les acides gras monoinsaturés ont diminué par rapport au témoin. L'évaluation des systèmes antioxydants enzymatiques et non enzymatiques dans la gestion du stress oxydatif a montré une augmentation significative de l'activité de piégeage des radicaux libres, des teneurs en proline et polyphénols, de même qu'une induction des activités de la superoxyde dismutase, catalase, guaiacol peroxydase, ascorbate peroxydase et glutathion réductase.

Au regard de la mycoremédiation des colorants azoïques, trois levures ont été examinées. Le taux de décoloration le plus élevé a été atteint par la souche *Cyberlindnera fabianii* (97%). Ensuite, la couleur de la biomasse après décoloration du milieu a été évaluée pour anticiper les mécanismes impliqués dans la mycoremédiation de divers colorants synthétiques. Les résultats ont montré un couplage entre la structure chimique du colorant et la voie de son élimination. En effet, l'élimination du colorant AR14 a été accomplie principalement par des voies enzymatiques. Une augmentation significative de l'activité intracellulaire et extracellulaire de laccase, de tyrosinase, de peroxydase de manganèse et d'azoréductase a été enregistrée dans la biomasse incolore ainsi obtenue. Sur le plan éco-toxicologique, la dégradation enzymatique de l'AR14 par *C. fabianii* a permis une détoxification efficace. En effet, les sous-produits résultants n'ont montré aucun signe de phytotoxicité. En autre, le mécanisme de biosorption du colorant AR14 a également été abordé en utilisant des cellules inactivées. L'étude cinétique de la biosorption et sa modélisation ont montré que la biosorption de AR14 par la biomasse fongique répond à une chimiosorption sur une monocouche de sites homogènes. Ces prédictions ont été vérifiées en appliquant les mêmes techniques de caractérisation décrites ci-dessus. La biosorption de l'AR14 est médiée par des interactions chimiques avec les groupes fonctionnels de la paroi cellulaire ainsi que par des interactions électrostatiques.

Ces résultats ouvrent la voie au développement de bioprocédés de traitement des eaux usées basés sur des stratégies de phycoremédiation et de mycoremédiation en vue de répondre aux démarches de développement durable.

Mots clés: Levures; microalgues; colorants azoïques; métaux lourds; biosorption; bioaccumulation; biotransformation; phytotoxicité; systèmes antioxydants; caractérisation biochimique; profilage métabolomique.